The Role of Polymers in Cosmetics Formulations

SOCIETY OF COSMETIC CHEMISTS

Robert Lochhead, Professor Emeritus of Polymer Science

March 12th, 2019 | SCC Twin Cities Chapter - Holistic Cosmetic Symposium

Polymer?

- *Poly* = many
- *Mer* = member
- Polymers are formed by linking many small molecules together into very large molecules
  - This gives rise to new physical properties
    - Ethylene is a gas : polyethylene is a tough solid
    - Glucose is water-soluble: cellulose is water-insoluble
- *Copolymer* is a polymer made of two different monomers in the same molecular chain.
- *Terpolymer* is a polymer consisting of 3 different monomers in the same molecular chain.

Polymer Product Forms

- Polymer solids
  - Powder,flakes, prills, pellets, foils, chunks,
  - Amorphous, crystalline or semi-crystalline
  - Porous particles
- Polymer solutions
- Polymer latices
- Regular and Inverse emulsions and micro emulsions
- Dispersions
- Self assembled ordered structures

Polymer Classification

- Solubility
  - Which solvents?
- Ionic charge :
  - Anionic.nonionic, cationic.
- Polymerization method
  - Condensation (step-growth)
  - Addition (chain growth -free radical or ionic polymerization
- Natural or synthetic

Polymer Functions in Cosmetic Formulations

- Film-formers
  - Hair fixatives, Mascara, Nail enamels,Transfer-resistant color cosmetics
- Thickeners and Rheology-modifiers.
  - Emulsion-stabilizers, Gels, Binders, Hair colorants, Hair-relaxers
- Emulsifiers
  - Lotions, Sunscreen, Hair-Color
- Conditioners
- Moisturizers
- Emollients
- Dispersers
- Waterproofers
- Micropore sponges

Film Formers

- Nonionic
  - PVP [Poly(vinyl pyrolidone)], PVP/VA Copolymer
  - Polyvinylcaprolactam
  - Poly(vinyl alcohol), Poly (vinyl alcohol-*co*-vinylacetate)
  - Polyurethane-2,Polyurethane-5
  - PPG-17/IPDI/DMPA Copolymer
  - PVP/Dimethiconylacrylate/Polycarbamyl Polyglycol Ester
  - PEG-200 Hydrogenated Castor Oil/IPDI Copolymer
  - Polyglyceryl-2 Diisostearate/IPDI Copolymer
  - Vinylcaprolactam/PVP/Dimethylaminoethylmethacrylate Copolymer [poly-(vinylpyrrolidone-vinylcaprolactam-dimethylaminoethyl-methacrylate)]
  - VP/Vinyl Caprolactam/DMAPA Acrylates Copolymer
  - Cellulose Acetate, Cellulose Acetate Butyrate, Cellulose Acetate Propionate
  - Nitrocellulose

Film Formers

- Anionic
  - Shellac
  - Acrylates Copolymer
  - Acrylates/C_{1-2}Succinates/Hydroxyacrylates Copolymer
  - Acrylic Esters (and) Methacrylic Esters Copolymer
  - AMP-Acrylates/Allyl Methacrylate Copolymer
  - Diglycol/Cyclohexanedimethanol/Isophtalates/Sulfoisophtalates Copolymer Diglycol/Isophtalates/Sulfoisophtalates Copolymer
  - Isobutylene Ethylmaleimide/Hydroxyethylmaleimide Copolymer
  - Glycerin and Diglycol/Cyclohexanedimethanol/Isophtalates/Sulfoisophtalates Copolymer
  - Methacrylate Acid/Sodium Acrylamidomethyl Propane Sulfonate Copolymer
  - Octylacrylamide/Acrylates/Butylaminoethylmethacrylate Copolymer
  - Polyurethane (and) Acrylates Copolymer
  - PVM/MA Copolymer
  - PVP/Ethyl Methacrylate/Methacrylic Acid Terpolymer
  - PVP/Polycarbamyl Polyglycol Ester

Film Formers

- Amphoteric
  - Acrylates/Lauryl Acrylate/Stearyl Acrylate/Ethylamine Oxide Methacrylate
  - Methacryloyl Ethyl Betaine/Acrylates Copolymer

Film Formers

- Anionic
  - VA/Crotonates Copolymer
  - VA/Crotonates/Vinyl Neodecanoate Copolymer
    VP/Acrylates/Lauryl Methacrylate Copolymer

Thickeners

- Nonionic
  - Hydroxyethylcellulose, Hydroxymethylcellulose
  - Methylhydroxyethylcellulose, Hydroxypropylcellulose
  - Hydroxypropylmethylcellulose
  - Cetyl Hydroxyethylcellulose
  - Corn Starch, Hydroxypropyl Starch Phosphate
  - Distarch Phosphate, Distarch dimethylene urea
  - Aluminum Starch Octenyl Succinate
  - Guar gum, Hydroxypropyl Guar
  - Locust Bean Gum
  - Rosin, Sclerotium Gum
  - Maltodextrin, Dextran
  - Poly(acrylamide)
  - PEG-150 Distearate, PEG-150/DecylAlcohol/SMDI Copolymer
  - PEG-150/StearylAlcohol/SMDICopolymer,
  - PEG-180/Laureth-50/TMMG Copolymer, Polyether-1

Thickeners

- Anionic
  - Acrylic Acid/Acrylamidomethyl Propane Sulfonic Acid Copolymer
  - Acrylates/C_{10-30} Alkyl Acrylate Crosspolymer
  - Acrylates/Beheneth-25 Methacrylate Copolymer
  - Acrylates/Steareth-20 Methacrylate Copolymer
  - Acrylates Copolymer (and) Steareth-20
  - Acrylates/VA Crosspolymer
  - Acrylic Acid/Acrylonitrogens Copolymer
  - Ammonium Acryloyldimethyltaurate/Beheneth-25 Methacrylate Copolymer
  - Ammonium Acryloyldimethyltaurate/VP Copolymer
  - Caprylic/Capric Triglyceride (and) Sodium Acrylates Copolymer
  - Carbomer
  - PVM/MA Decadiene Crosspolymer

Thickeners

- Anionic
  - Alginic acid
  - Propylene Glycol Alginate
  - Carageenan gum (Kappa, Iota, Lambda)
  - Cellulose Gum (Carboxymethylcellulose)
  - Gum Arabic/ Gum Acacia
  - Karaya gum
  - Xanthan gum

Emulsifiers and Emulsion Stabilizers

- Tragacanth gum
- Poly (acrylamide-b-acrylic acid)
- Acrylates C10-30 Alkyl Acrylate Crosspolymer
- Acrylates/Beheneth-25Methacrylate/HEMA Crosspolymer
- Acrylates/Ceteareth-20 Methacrylate Crosspolymer
- Carbomer
- Acrylates Crosspolymer-4
- Acrylates/Steareth-20 Methacrylate Crosspolymer
- Acrylates/Vinyl Isodecanoate Crosspolymer
- AmmoniumAcryloyldimethyltaurate/Beheneth-25 Methacrylate Crosspolymer

Conditioners

- Chitosan
- Cocodimonium Hydroxypropyl Hydrolyzed Collagen
- Cocodimonium Hydroxypropyl Hydrolyzed Hair Keratin
- Cocodimonium Hydroxypropyl Hydrolyzed Keratin
- Cocodimonium Hydroxypropyl Hydrolyzed Wheat Protein
- Cocodimonium Hydroxypropyl Oxyethyl Cellulose
- Steardimonium Hydroxyethyl Cellulose
- Stearyldimonium Hydroxypropyl Hydrolyzed Oxyethyl Cellulose
- Guar Hydroxypropyltrimonium Chloride
- Starch Hydroxypropyltrimonium Chloride
- Lauryldimonium Hydroxypropyl Hydrolyzed Collagen
- Lauryldimonium Hydroxypropyl Hydrolyzed Wheat protein
- Stearyldimonium Hydroxypropyl Hydrolyzed Wheat Protein
- Polyquaternium-4, Polyquaternium-10,Polyquaternium-24

Conditioners

- Acrylamide/Ammonium Acrylate Copolymer
- Poly(methacryloxyethyltrimethylammonium methosulfate)
- Poly(N-methylvinylpyridinium chloride)
- Onamer M (polyquaternium-1), PEI-1500 (Poly(ethylenimine)
- Polyquaternium-2
- Polyquaternium-5-poly(acrylamide-*co*-methacryloxyethyltrimethyl ammonium ethosulfate)]
- Polyquaternium-6 poly(dimethyldiallylammonium chloride)
- Polyquaternium-7
  - poly(acrylamide-*co*-dimethyldiallylammonium chloride)
- Polyquaternium-8
- Polyquaternium-11
  - [poly-(N-vinyl-2-pyrrolidone-methacryloxyethyltrimethylammonium ethosulfate)]
- Polyquaternium-16 [Co(vinyl pyrrolidone-vinyl methylimidazolinium chloride)
- Polyquaternium-17
- Polyquaternium-18
- Polyquaternium-22
  - poly(sodium acrylate – dimethyldiallyl ammonium chloride)

SOCIETY OF COSMETIC CHEMISTS

Conditioners

- Polyquaternium–27
- Polyquaternium-28
  - polyvinylpyrolidone-methacrylamidopropyltrimethylammonium chloride)
- Polyquaternium-31
  - Poly(N,N-dimethylaminopropylacrylate-N-acrylamidine-acrylamide-acrylamidine-acrylic acid-acrylonitrile) ethosulfate
- Polyquaternium-39
  - poly(dimethyldiallylammonium chloride – sodium acrylate – acrylamide)
- Polyquaternium-43
  - poly(acrylamide-acrylamidopropyltrimoniumchloride-2-acrylamidopropyl sulfonate-DMAPA)
- Polyquaternium-44
  - Poly (vinyl pyrrolidone-*co*-imidazolinium methosulfate)
- Polyquaternium-46
  - Poly (vinylcaprolactam-vinylpyrrolidone-imidazolinium methosulfate)
- Polyquaternium-47
  - poly (acrylic acid-methacrylamidopropyltrimethyl ammonium chloride – methyl acrylate)

Conditioners

- Polyquaternium-53
- Polyquaternium-55
  - poly(vinylpyrrolidone-dimethylaminopropylmethacrylamide-lauryldimethylpropylmethacrylamido ammonium chloride)
- PVP/Dimethylaminoethyl Methacrylate Copolymer
- VP/DMAPA Acrylate Copolymer
- PVP/Dimethylaminoethylmethacrylate Polycarbamyl Polyglycol Ester
- PVP/Dimethiconylacrylate/Polycarbamyl Polyglycol Ester
- Quaternium-80 (Diquaternary polydimethylsiloxane)
- Poly(vinylpyrrolidone-*co*-dimethylamidopropylmethacrylamide)
- VP/Vinyl Caprolactam/DMAPA Acrylates Copolymer
- Amodimethicone
- PEG-7 Amodimethicone
- Trimethylsiloxyamodimethicone

Conditioners

- Ionenes
  - Poly(adipic acid-dimethylaminohydroxypropyldiethylenetriamine)
  - Poly (adipic acid-epoxypropyldiethylenetriamine) (Delsette 101)
  - Silicone Quaternium-8
  - Silicone Quaternium-12

Humectants

- PEG - poly(ethylene oxide)
- PPG - poly(propylene oxide)
- Poly(ethylene oxide-*co*-propylene oxide)
- Hyaluronic acid
- Polyglycerylmethacrylate
- Glyceryl Polymethacrylate
- Glyceryl polymethacrylate and Propylene glycol
- Glyceryl polymethacrylate and propylene glycol and PVM/MA Copolymer
- Glyceryl polymethacrylate (and) Cyclopentasiloxane (and) Cyclotetrasiloxane (and) Polysorbate 81 (and) PEG-51 Cocoamine (and) Dimethiconol (and) Laureth-9
- Glyceryl Polymethacrylate (and) Butylene Glycol (and) PVM/MA Copolymer
- Polyperfluoroethoxymethoxy Difluoroethyl PEG Phosphate

Humectants

- Amphoteric and Zwitterionic Polymers
  - Hydrolyzed Collagen, Soluble Collagen
  - Hydrolyzed Elastin
  - Soluble Keratin, Hydrolized Keratin PG-Propylmethylsilanediol
  - Hydrolized Milk Protein, Hydrolized Protein (and) Hyaluronic Acid
  - Hydrolized Silk, Hydrolized Silk PG-Propylmethylsilanediol
  - Hydrolized Soy Protein/Dimethicone PEG-7 Acetate
  - Hydrolized Soy ProteinPG-Propylmethylsilanediol
  - Soluble Wheat Protein
  - Hydrolized Wheat Protein/Dimethicone PEG-7 Acetate
  - Hydrolized Wheat Protein/PEG-20 Acetate Copolymer
  - Hydrolized Wheat Protein PG-Propylmethylsilanediol
  - Hydrolized Wheat Protein (and) Wheat Oligosaccharides
  - Hydrolized Wheat Protein Polysiloxane Copolymer
  - Hydrolized Whole Oats
  - Isostearoyl Hydrolized collagen
  - Sodium Lauroyl Hydrolyzed Silk

Emollients

- Bis-PEG-15 Methyl Ether Dimethicone, Bis-PEG/PPG-20/20 Dimethicone
- Dimethicone Copolyol, Dimethicone Copolyol Acetate
- Dimethicone Copolyol N-Acetate Taurate (and) Sodium Salt
- Dimethicone Copolyol Phosphate, Dimethicone PEG-7 Phosphate
- Dimethicone PEG/PPG-7/4 Phosphate
- Dimethicone PEG-7 Phthalate, Dimethicone Propyl PG-Betaine
- Methoxy PEG/PPG-7/3 Aminopropyl Dimethicone
- PEG-12 Dimethicone, PEG/PPG-17/18 Dimethicone
- PEG/PPG-20/6 Dimethicone, PEG/PPG-25/25 Dimethicone
- PVP/Eicosene Copolymer
- Behenoxy Dimethicone
- Bis-PEG/PPG-14/14 Dimethicone (and) Cyclopenta-Siloxane
- Bis-PEG/PPG-16/16 PEG/PPG-16/16 Dimethicone (and) Caprylic/Capric Triglyceride

Emollients

- C_{24-28} Alkyl Methicone, C_{30-45} Alkyl Methicone, C_{24-28} Methicone
- Cetyl Dimethicone
- Cetyl Dimethicone Copolyol
- Cetyl Methicone
- Cetyl PEG/PPG-10/1 Dimethicone
- Cetyl PEG/PPG-15/15 Butyl Ether Dimethicone
- Cyclohexasiloxane
- Cyclomethicone
- Cyclomethicone (and) Dimethicone Crosspolymer
- Cyclomethicone (and) Trimethylsiloxysilicate
- Cyclopentasiloxane
- Cyclopentasiloxane (and) Caprylyl Dimethicone Ethoxy Glucoside
- Cyclopentasiloxane (and) Dimethicone/Vinyltrimethylsiloxysilicate Crosspolymer
- Cyclopentasiloxane (and) Dimethiconol
- Cyclopentasiloxane (and) PEG-12 Dimethicone Crosspolymer
- Cyclopentasiloxane (and) PEG/PPG-18/18 Dimethicone
- Dimethicone
- Dimethicone (and) Trimethylsiloxysilicate
- Dimethicone Copolyol
- Dimethicone (and) Dimethiconol
- Dimethicone NF
- Dimethicone PEG-6 Acetate
- Dimethicone PEG-1 Isostearate
- Dimethicone PEG-7 Cocoate
- Dimethicone PEG-7 Olivate
- Dimethicone PEG-8 Beeswax
- Dimethicone (and) Trimethylsiloxysilicate
- Dimethicone/Vinyldimethicone Crosspolymer
- Dimethiconol (and) Cyclomethicone (and) Dimethicone
- Dimethiconol (and) Cyclopentasiloxane
- Dimethiconol (and) Dimethicone
- Dimethiconol Fluoroalcohol Dilinoleic Acid
- Dimethiconol/IPDI Copolymer
- Disiloxane
- Lauryl Dimethicone
- Lauryl PEG/PPG-18/18 Methicone
- PEG-7 Dimethicone Avocadoate
- Phenyl Dimethicone
- Phenyl Trimethicone
- Polymethylsilsesquioxane
- Stearoxy Dimethicone
- Stearoxy Dimethicone (and) Dimethicone
- Stearoxy Trimethylsilane (and) Stearyl Alcohol
- Stearyl Dimethicone
- Stearyl Methicone
- Graft-copoly(dimethylsiloxane/i-butyl methacrylate)

Emollients

- Dimethicone, Dimethicone (and) Trimethylsiloxysilicate
- Dimethicone Copolyol, Dimethicone (and) Dimethiconol
- Dimethicone NF
- Dimethicone PEG-6 Acetate, Dimethicone PEG-1 Isostearate
- Dimethicone PEG-7 Cocoate, Dimethicone PEG-7 Olivate
- Dimethicone PEG-8 Beeswax
- Dimethicone (and) Trimethylsiloxysilicate
- Dimethicone/Vinyldimethicone Crosspolymer
- Dimethiconol (and) Cyclomethicone (and) Dimethicone
- Dimethiconol (and) Cyclopentasiloxane, Dimethiconol (and) Dimethicone
- Dimethiconol Fluoroalcohol Dilinoleic Acid, Dimethiconol/IPDI Copolymer
- Copolymer
- Disiloxane
- Lauryl Dimethicone
- Lauryl PEG/PPG-18/18 Methicone, PEG-7 Dimethicone Avocadoate
- Phenyl Dimethicone, Phenyl Trimethicone
- Polymethylsilsesquioxane
- Stearoxy Dimethicone
- Stearoxy Dimethicone (and) Dimethicone
- Stearoxy Trimethylsilane (and) Stearyl Alcohol
- Stearyl Dimethicone
- Stearyl Methicone
- Graft-copoly(dimethylsiloxane/i-butyl methacrylate)

Emollients

- Stearoxy Dimethicone
- Stearoxy Dimethicone (and) Dimethicone
- Stearoxy Trimethylsilane (and) Stearyl Alcohol
- Stearyl Dimethicone
- Stearyl Methicone
- Graft-copoly(dimethylsiloxane/i-butyl methacrylate)
- Graft-copoly (IBMA; MeFOSEA/PDMS) Perfluorononyl Dimethicone
- Perfluoroethers
- Polyperfluoroethoxymethoxy Difluorohydroxyethyl Ether
- Polyperfluoroethoxymethoxy Difluoromethyl Distearamide
- Hydrogenated Polydecene, Hydrogenated Poyisobutene
- Polydecene/Polybutene Copolymer

Emollient Powders

- Silk Powder
- Nylon –6, Nylon-6/12, Nylon-12
- Polyethylene, Oxidized Polyethylene
- Trimethylsiloxysilicate

Dispersing Agents

- Sodium polystyrene sulfonate
- Sodium polymethacrylate
- Sodium polynaphthalenesulphonate

Waterproofers

- Acrylates/Octylacrylamide Copolymer
- Acrylic/Acrylate Copolymer
- Acrylates/$C_{12\text{-}22}$ Alkylmethacrylate Copolymer
- Ethylene/Acrylate Copolymer, Ethylene/Vinyl Acetate Copolymer
- PVP/Eicosene Copolymer, PVP/Hexadecane Copolymer

Poly(vinylpyrrolidone) the world's first synthetic water-soluble polymer

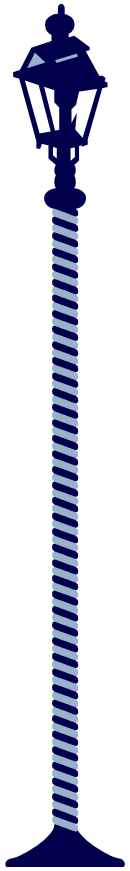

- Invention of the electric light
  - devastated the acetylene industry
  - I.G. Farbenfabriken scientists sought other uses for acetylene
  - I.G. Farbenfabriken possessed the Haber Process for the synthesis of ammonia from nitrogen and hydrogen
  - In 1938 Paul Reppe synthesized N-2-vinylpyrrolidone from acetylene and ammonia

Poly(vinylpyrrolidone) [PVP]

- Reppe went home and left the flask with the vinylpyrrolidone on the windowsill
- On his return he found a white solid in the flask
- The sunlight had polymerized vinylpyrrolidone to PVP

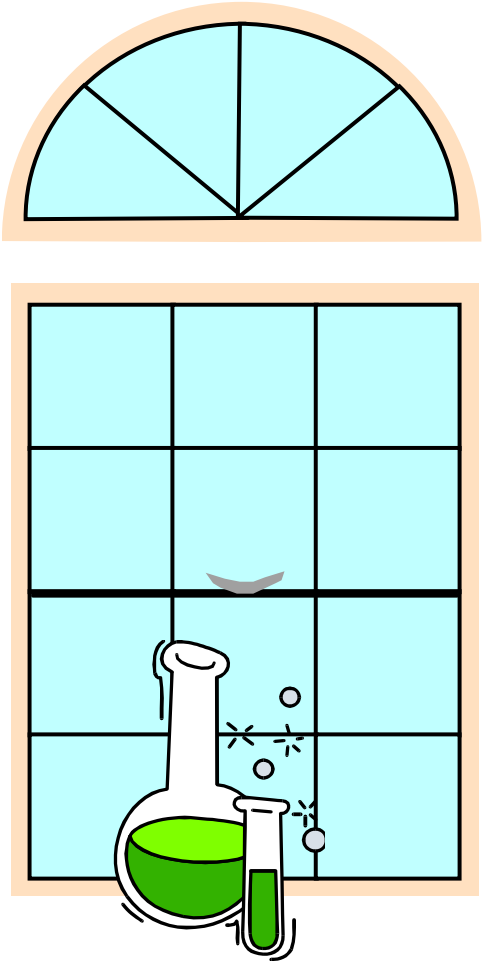

Poly(vinylpyrrolidone) [PVP]

- This amazing polymer dissolved in water and the solution was very viscous

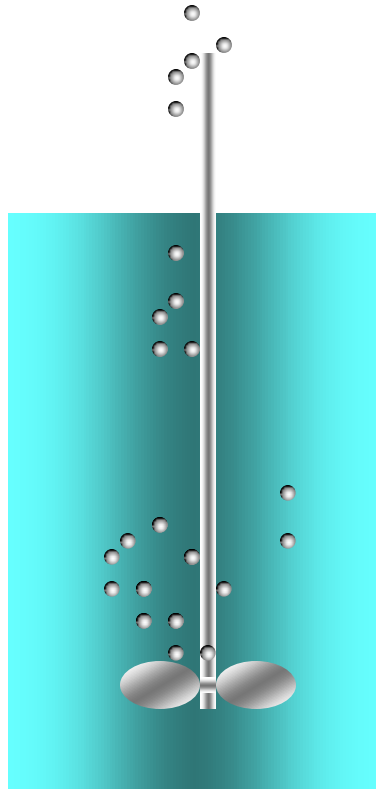

Poly(vinylpyrrolidone) [PVP]

- This amazing polymer dissolved in water and the solution was very viscous

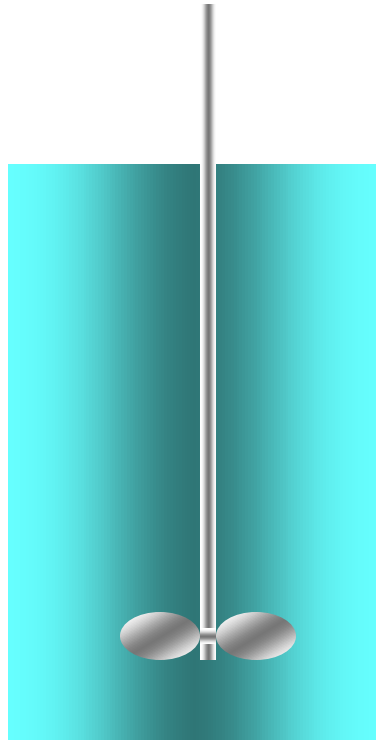

Poly(vinylpyrrolidone) [PVP]

- This amazing polymer dissolved in water and the solution was very viscous
- Unlike natural gums this polymer had a wide range of solubility in organic solvents

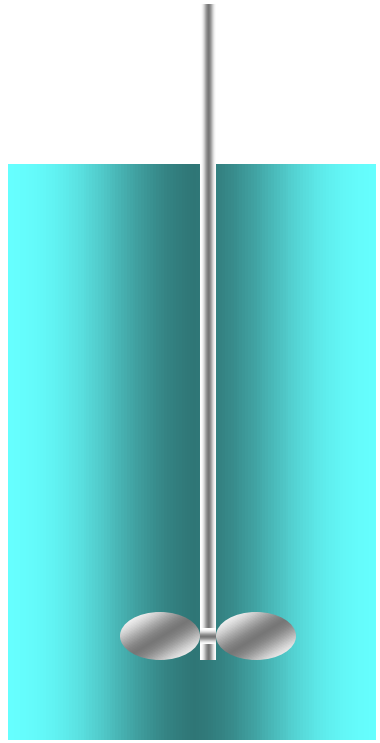

Poly(vinylpyrrolidone) [PVP]

- This amazing polymer was found to be safe in the body
- it could be added to the blood without any observable ill effects

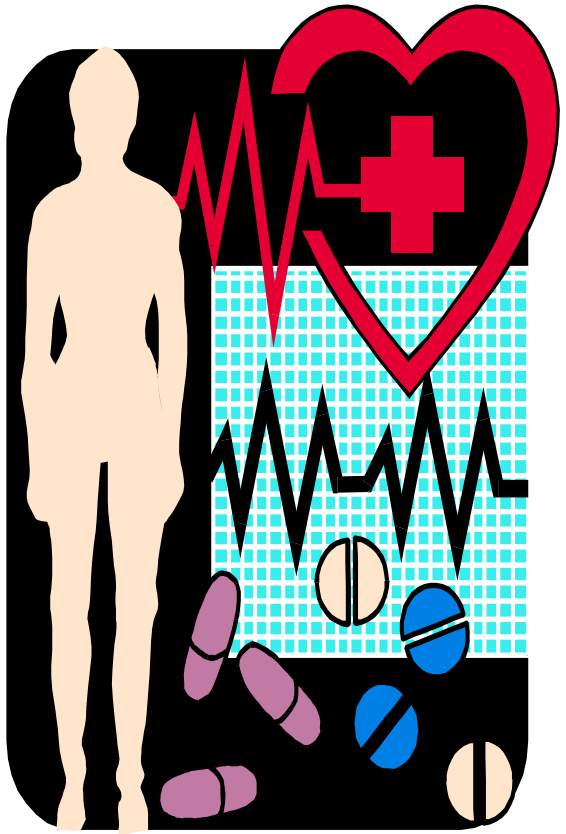

Poly(vinylpyrrolidone) [PVP]

- During World War II
- German Russian Front
- PVP used as a blood plasma substitute to save many German soldiers' lives

Poly(vinylpyrrolidone) [PVP]

- 1945 GAF received the rights to PVP upon cessation of hostilities
- They built a production facility in Calvert City KY - to provide PVP for Korean War

Poly(vinylpyrrolidone) [PVP]

- Korean War ceased
  - Market for PVP dried up
  - What to do?

Poly(vinylpyrrolidone) [PVP]

- 1950's -Hairstyles ascend
- Hairspray becomes necessary
- Shellac is used as the fixative polymer
  - but shellac is insoluble in water
  - cannot be removed by shampoos

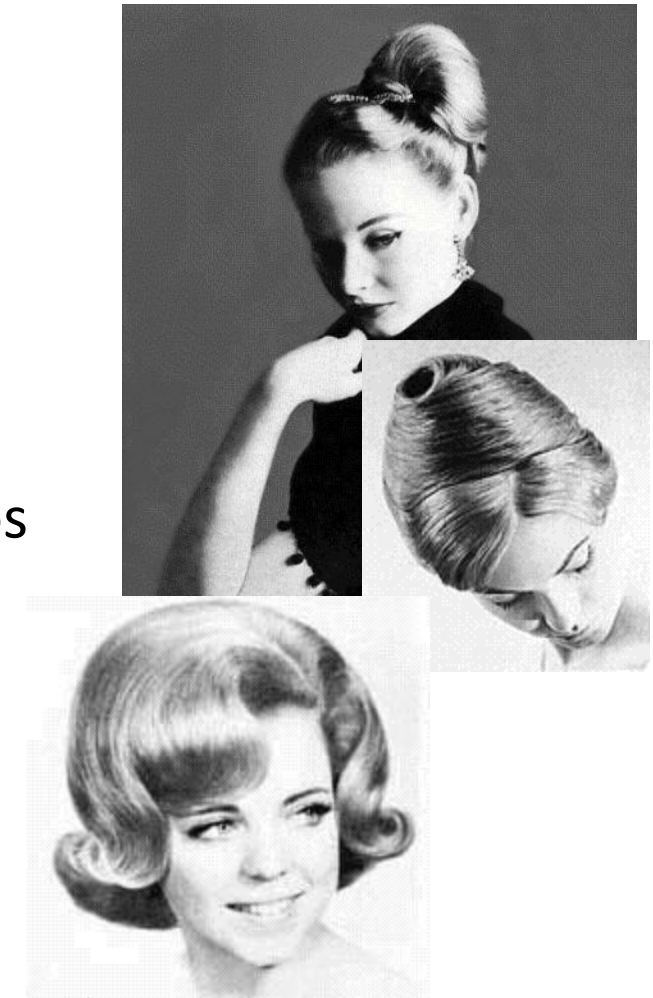

Polymer Solubility

Polymer solubility and insolubility are often not absolute

Phase Separation: Binodals and Spinodals

Polymer Solution Theory

Flory Huggins

and

Solubility Parameter

Solubility Parameter

- On the basis of “like dissolves like”, Hildebrand hypothesized that solvents dissolved solutes when the forces between the molecules matched
- How to compare the ‘cohesive forces’ between liquids
  - Compare their heats of vaporization
    - On the basis of energy per unit volume
      - Not molecular size

.

Solubility Parameter

- Hildebrand Introduced the concept that spontaneous molecular mixing occurs when the cohesive energy densities matched.
  - Energy per unit volume
  - Joules/cubic metre or joules/cubic cm.

- Hildebrand defined the solubility parameter as the square root of the cohesive energy density.
  - $\delta = c^{1/2} = (U/V)^{½} = (\Delta^{g}_{l} U/V)^{½}$
    - $= [(\Delta^{g}_{l} H - RT)/V^{½}]$
- This works well for materials with only dispersion forces
  - Such as alkanes.

Solubility Parameter

- Hildebrand Solubility does not work so well for substances that are polar or Lewis acids and Lewis bases
  - Because it does not account for the entropy loss due to orientational ordering in these materials
  - $\Delta G = \Delta H - T\Delta S$
  - To account for this Hansen introduced three components of the solubility parameter:
    - Dispersion
    - Polar
    - H-bonding

Solubility Parameter

- Hoy introduced the Idea of fractional solubility parameters
  - $f_{dispersign} = \delta_{dispersign} / \delta_{total}$
  - $f_{polar} = \delta_{polar} / \delta_{total}$
  - $f_{H\text{-}bonding} = \delta_{H\text{-}bonding} / \delta_{total}$

- He showed that molecular mixing was spontaneous when the three fractional ratios matched
- Solubilities of polymers could be mapped
- Matching could even be achieved by mixing two non-solvents
- Raising the molecular weight of the solute
  - Restricts the solubility scope

Hansen-Hoy Solubility Parameters

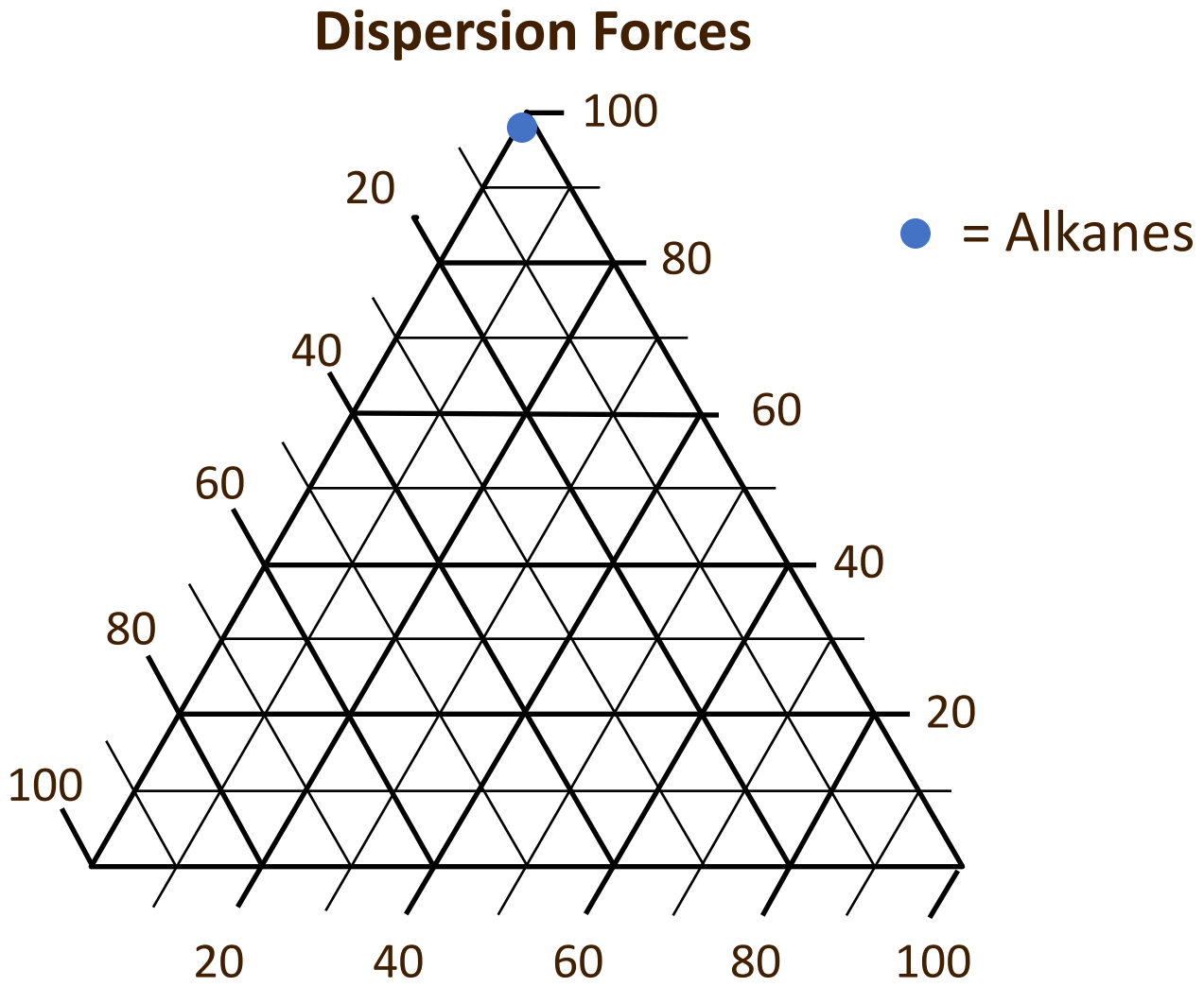

Solubility Diagrams

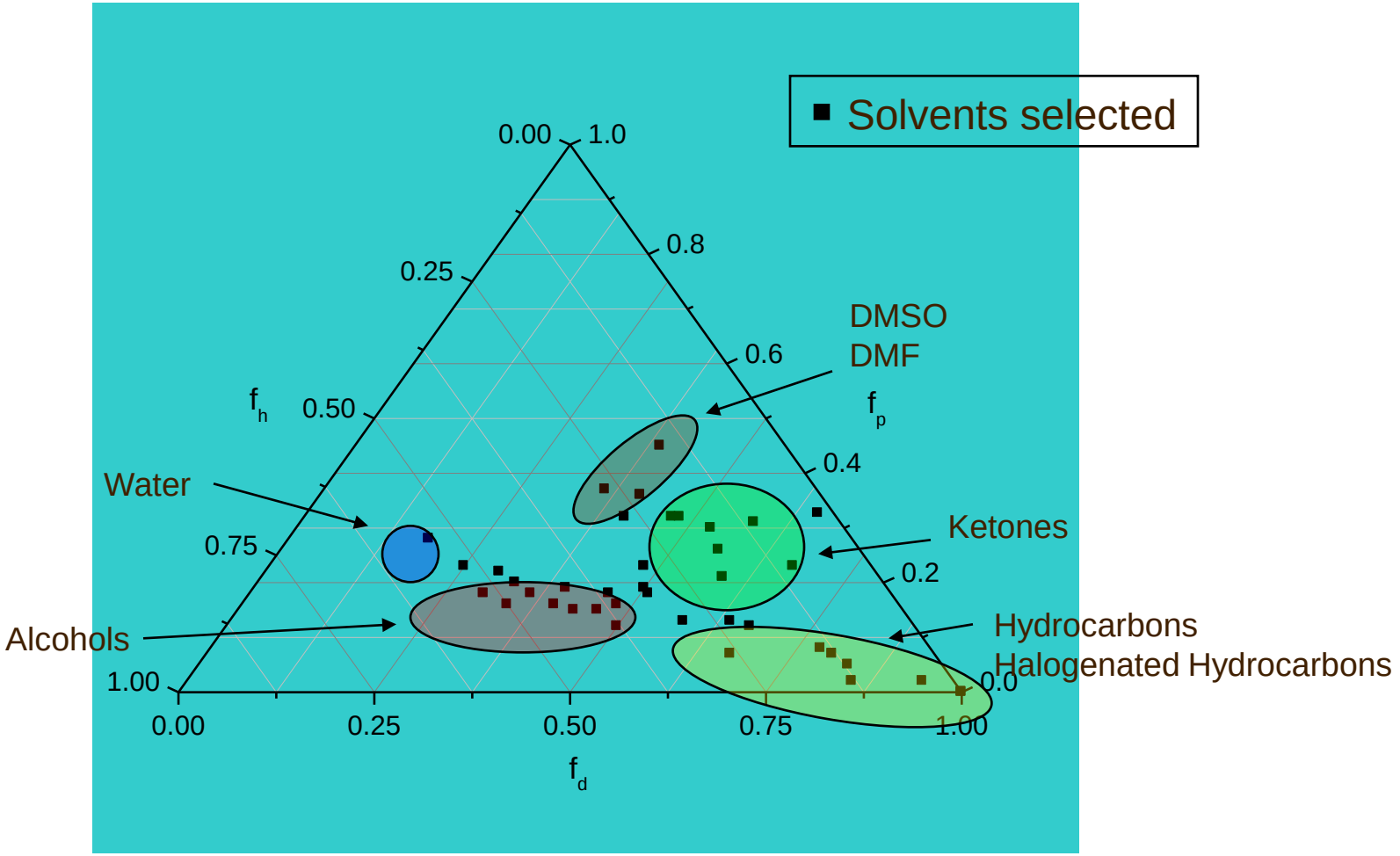

Barton, A.F.M. *Handbook of Solubility Parameters and Other Cohesion Parameters*. CRC Press: Boca Raton, Florida (1983).

PCL Solubility in Pure Solvents

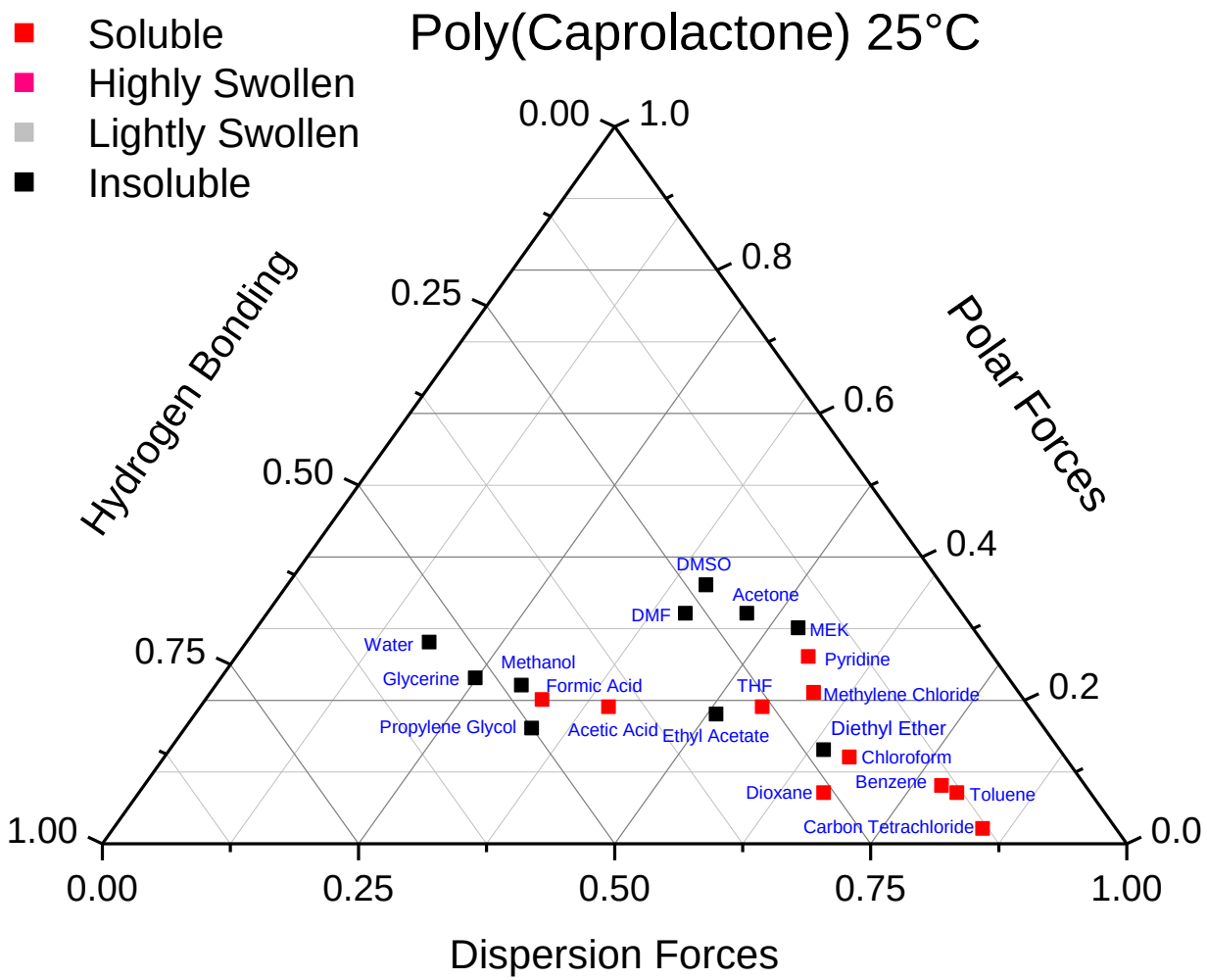

PVAm-11 Solubility in Pure Solvents

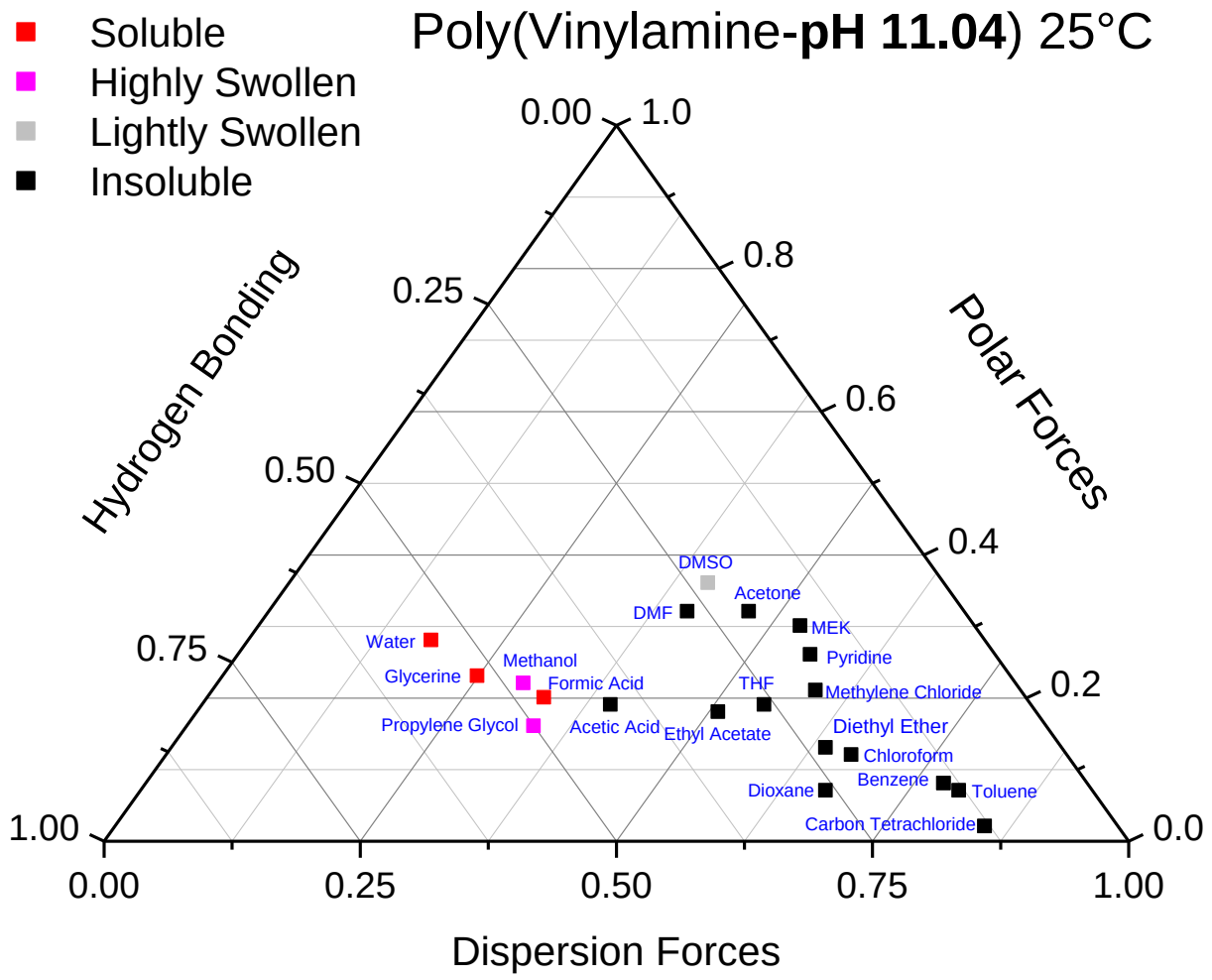

Poly(ε-Caprolactone) Solubility Diagram

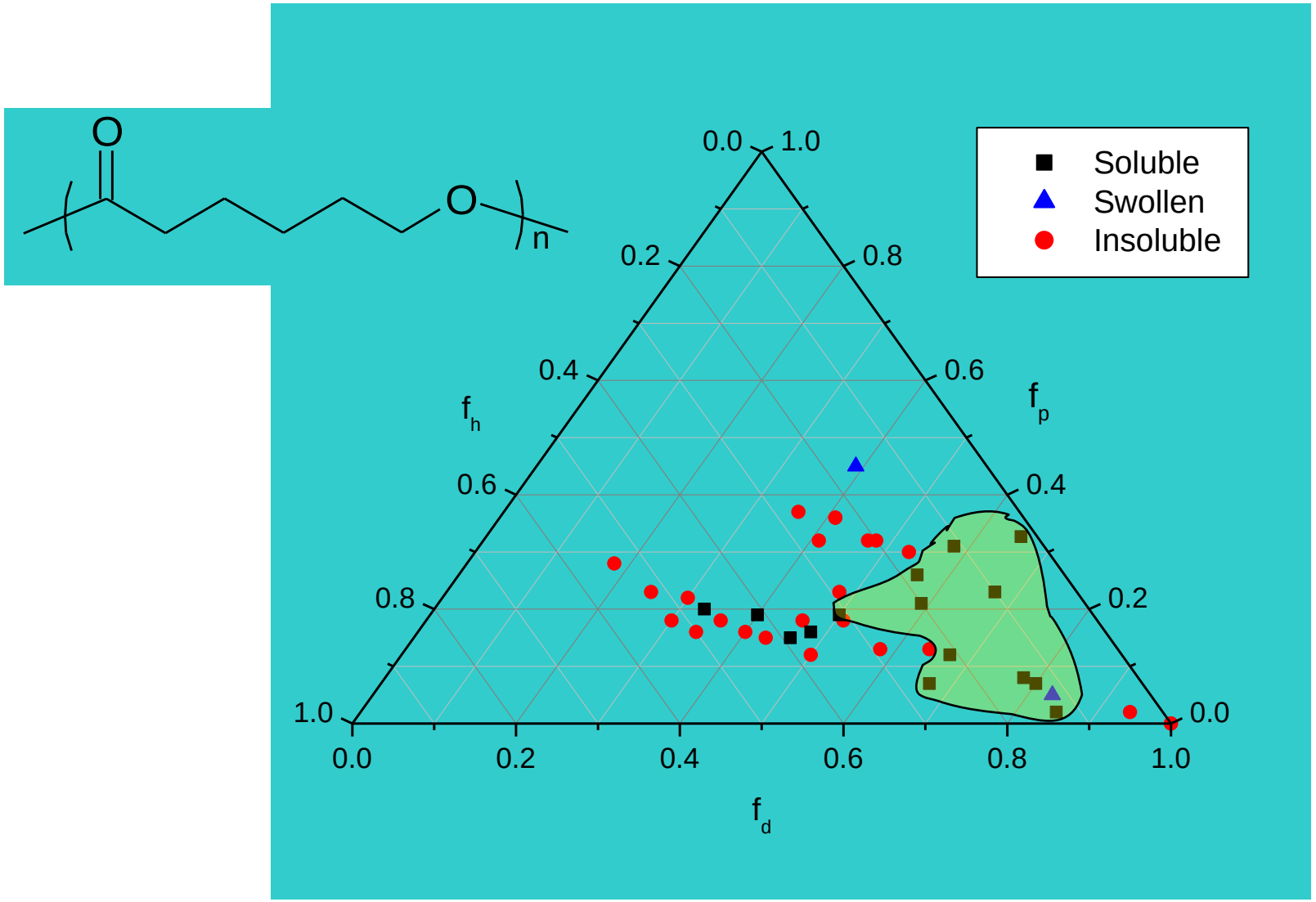

Poly(4-Vinylphenol) Solubility Diagram

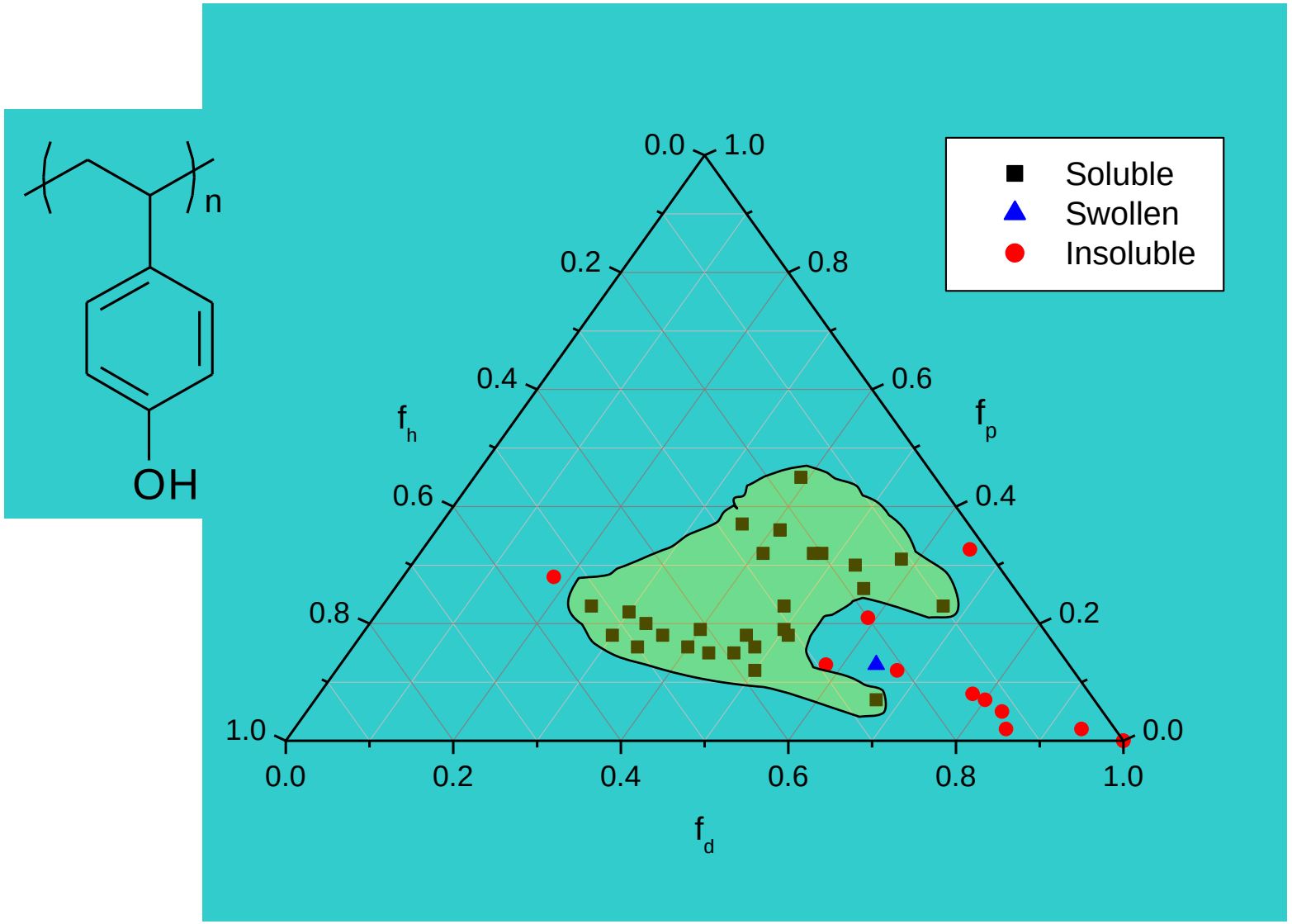

Poly(Ethylene oxide) Solubility Diagram

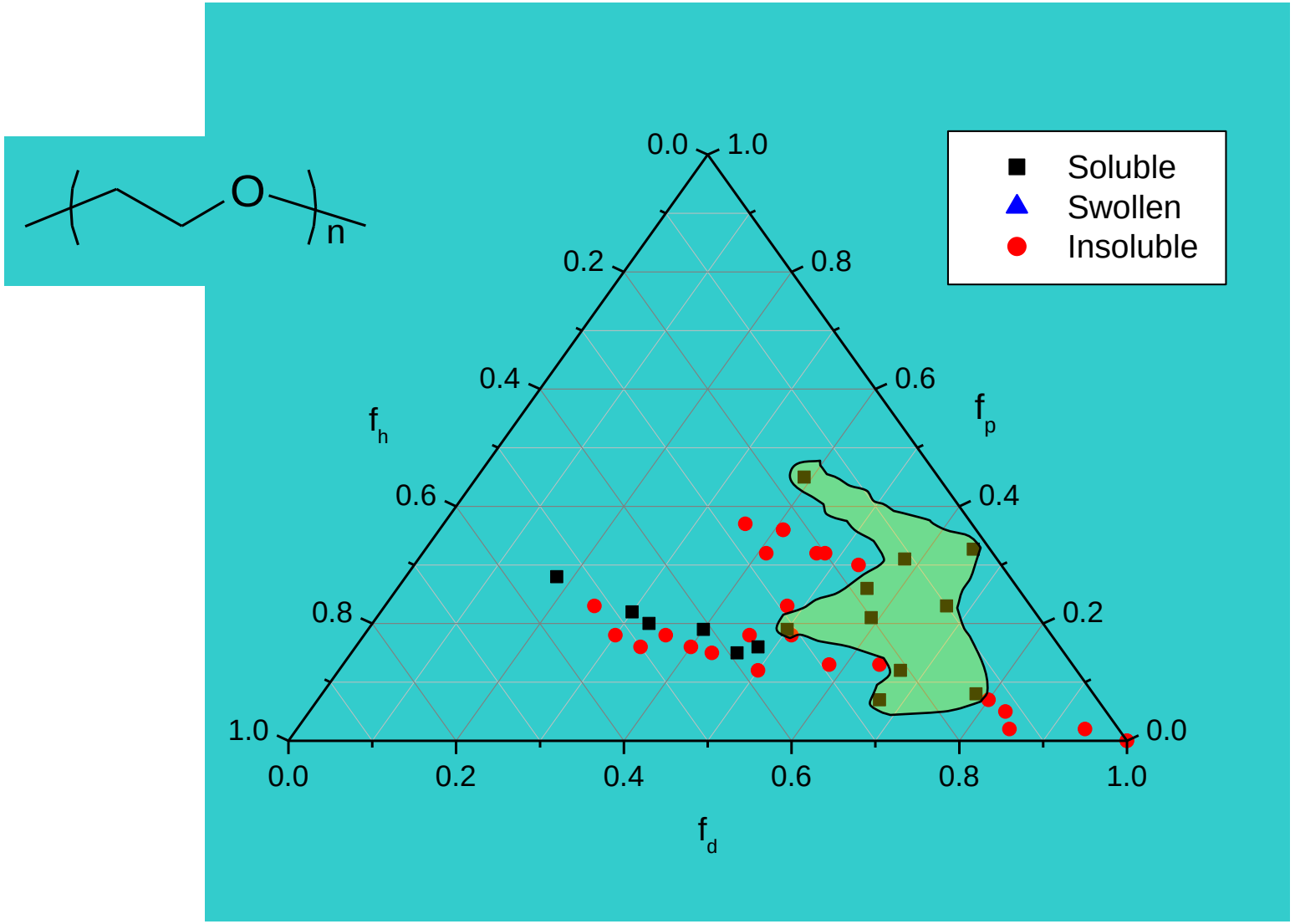

Poly(Vinylpyrrolidone) Solubility Diagram

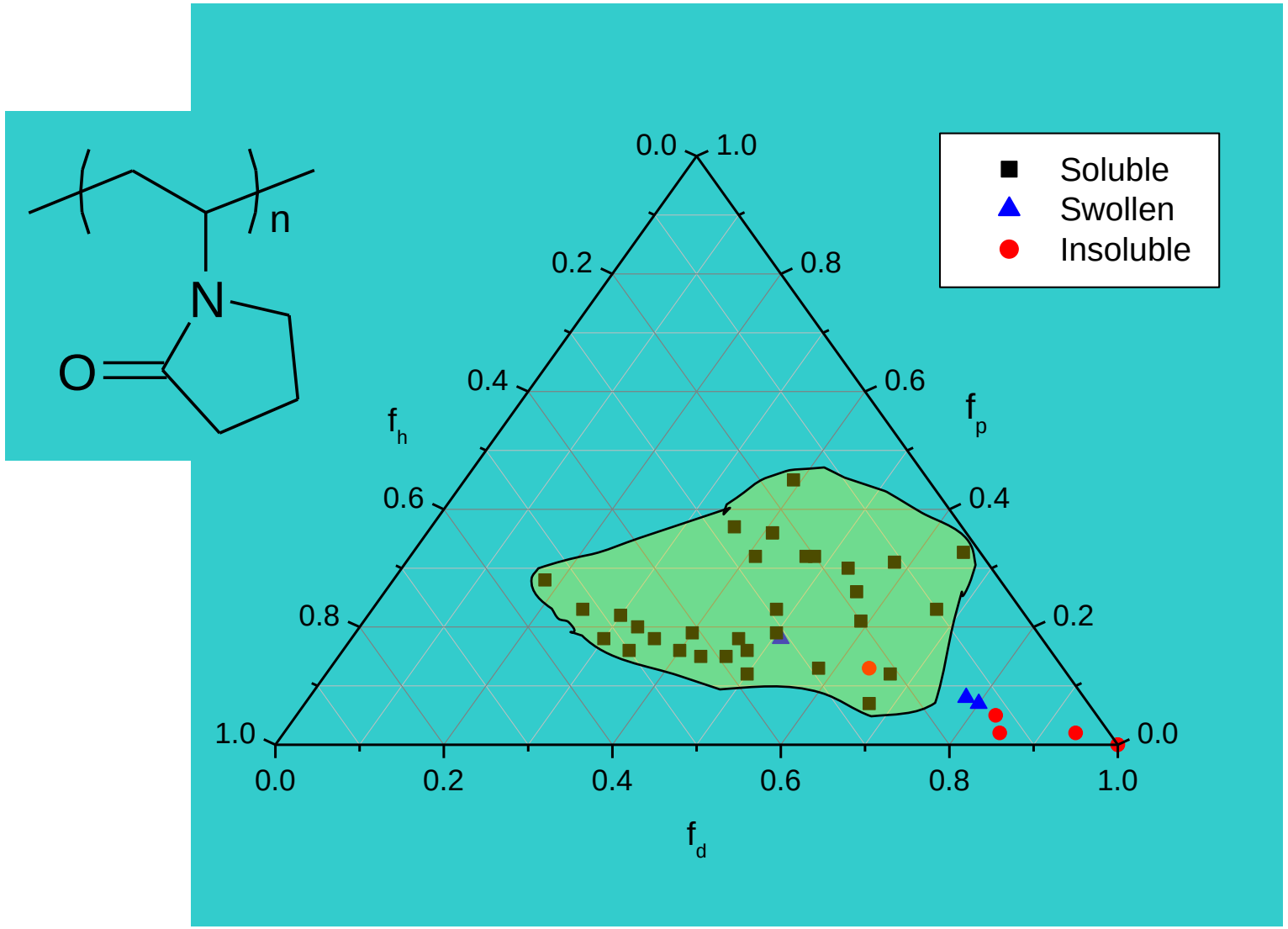

Composite Solubility Diagram

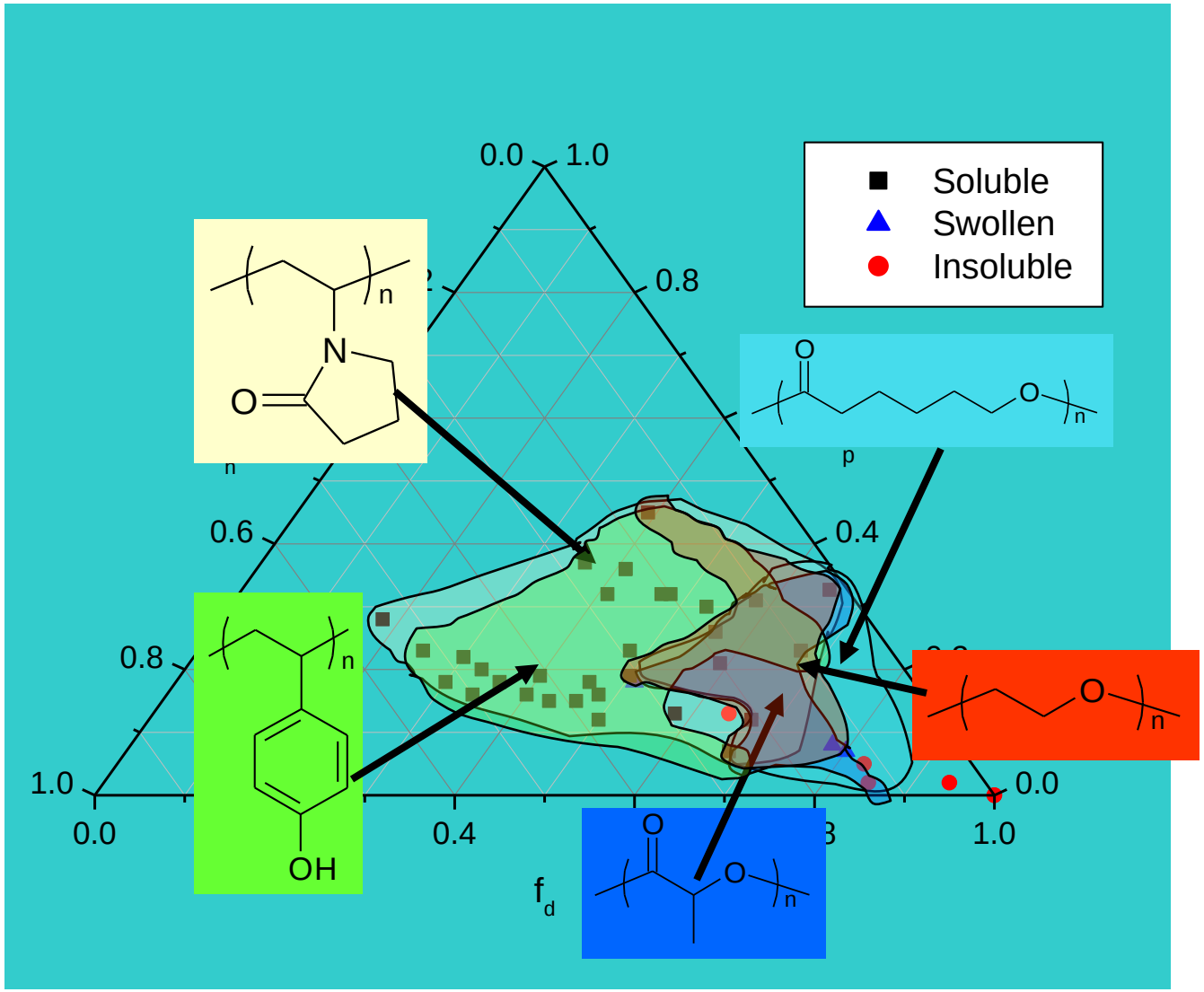

Hydrogen Bonding Parameter (γ_C)

- Spectrum of CH_3OD in sample liquid compared with reference spectrum
  - CH_3OD in benzene
  - OD stretch: 2681 cm^{-1}
- $\Delta\nu$ is the OD stretch absorption shift (cm^{-1})
- Nitrobenzene:
  - 2653 cm^{-1}
  - $\gamma_C = 2.8$

$$\gamma_C = \frac{\Delta\nu}{10}$$

Barton, A.F.M. *Handbook of Solubility Parameters and Other Cohesion Parameters*. CRC Press: Boca Raton, Florida (1983).

H-Bonding Parameter (γ_C) Diagram

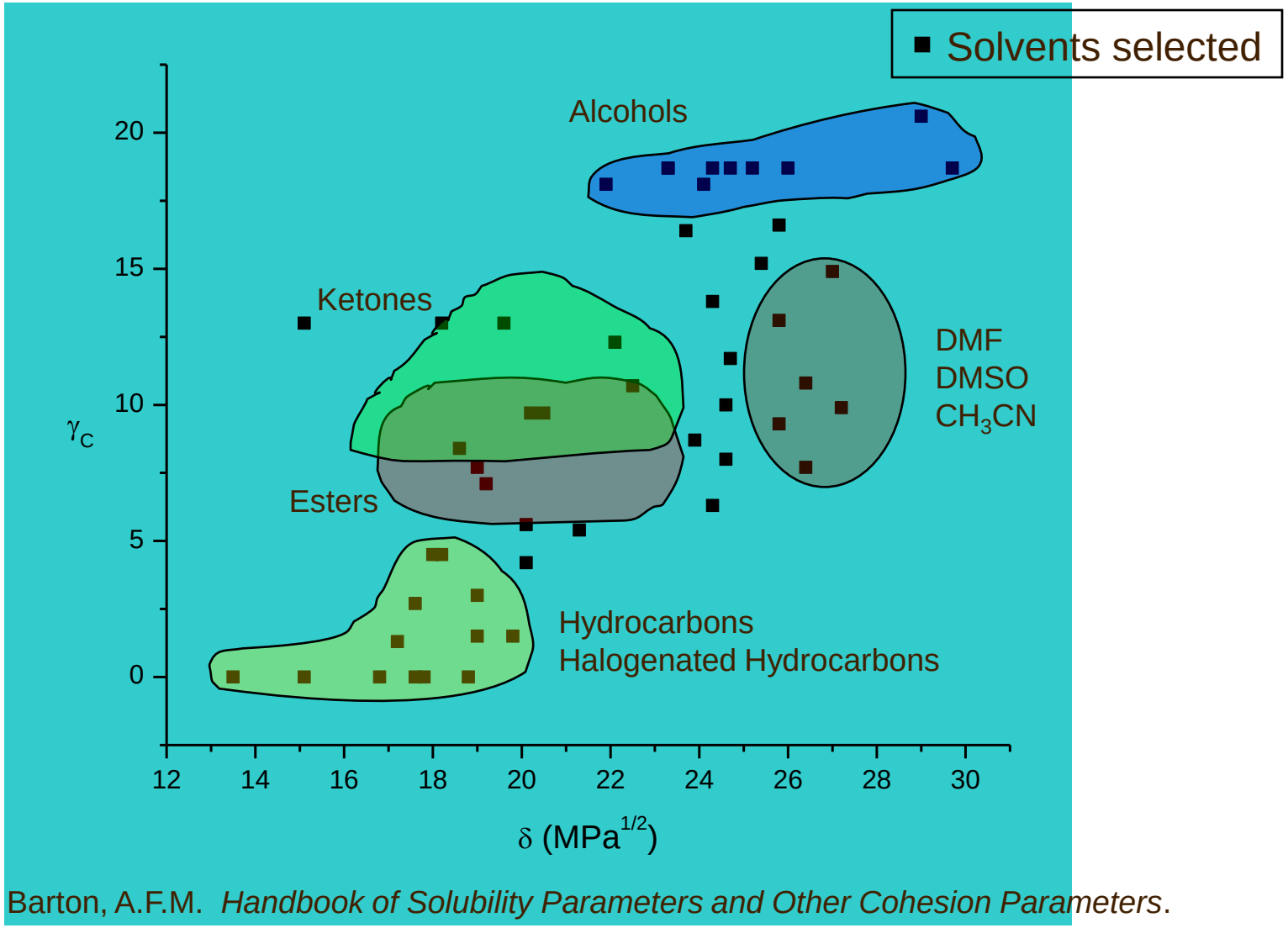

Barton, A.F.M. *Handbook of Solubility Parameters and Other Cohesion Parameters*. CRC Press: Boca Raton, Florida (1983).

Poly(ε-Caprolactone) H-bonding Interaction Diagram

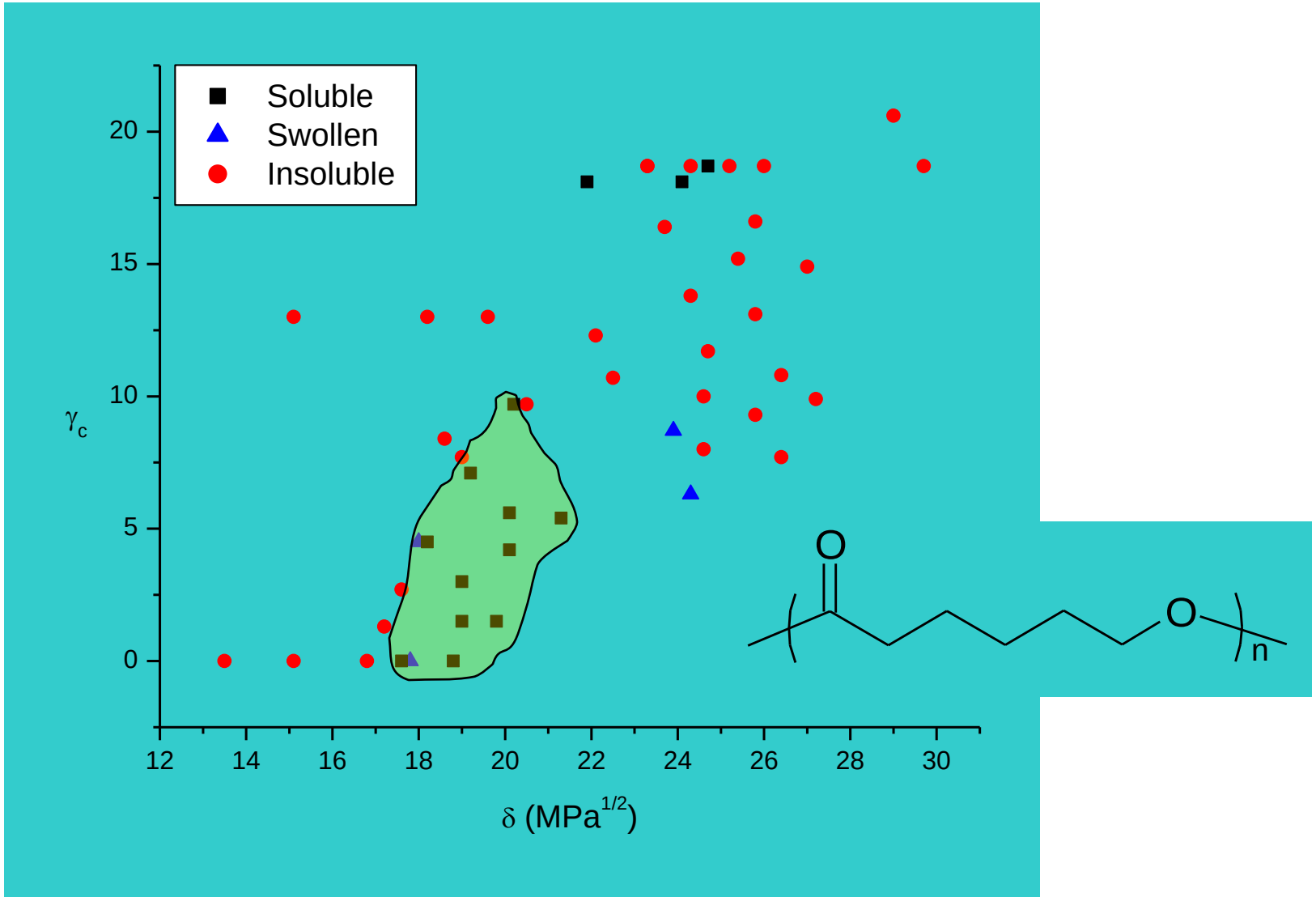

Poly(Lactic acid)
H-bonding Interaction Diagram

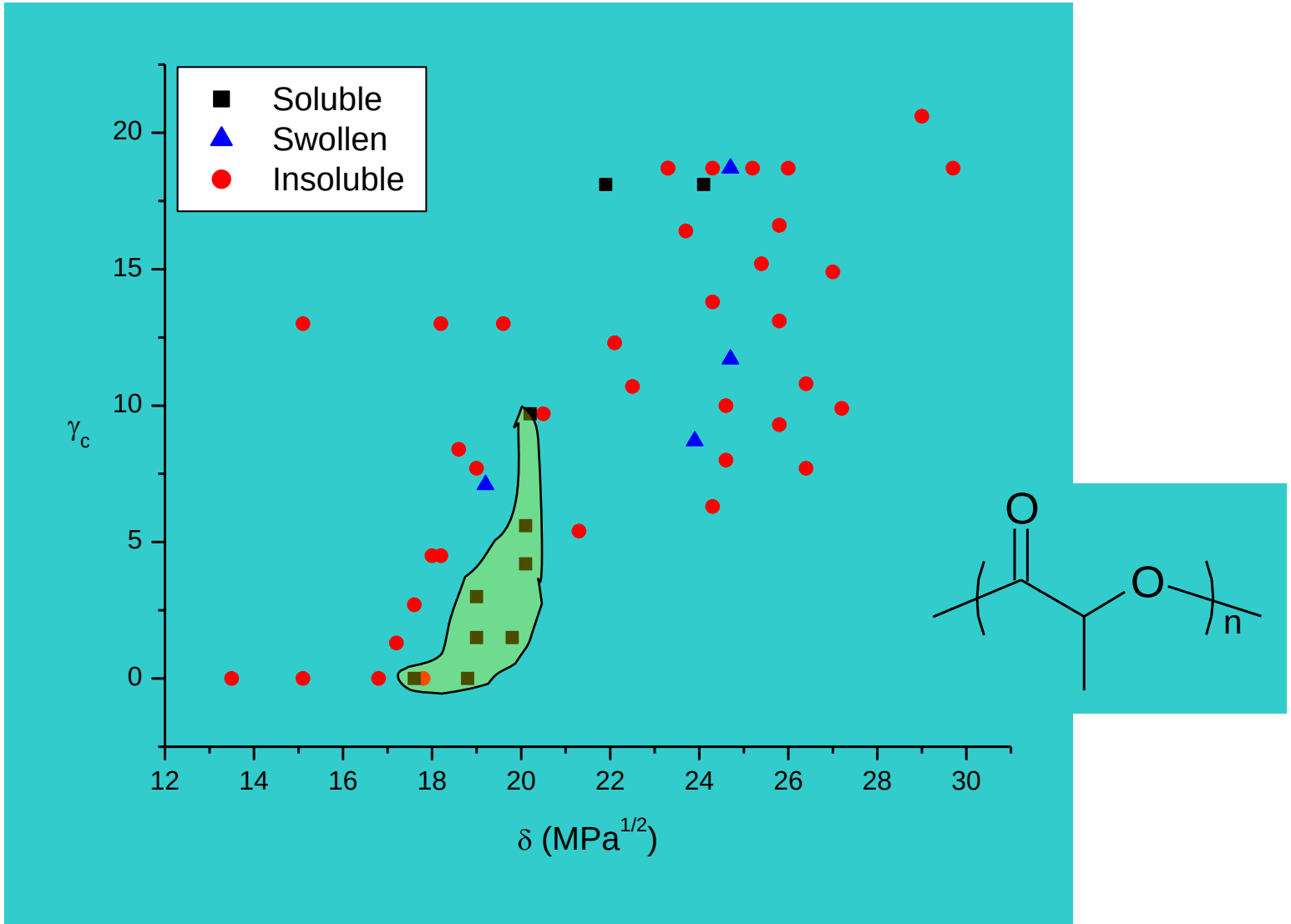

…but we also must consider the entropy of mixing……

Statistical Entropy of Mixing

Consider a container with four gold particles on the right of a partition and 4 Black particles on the left of the partition. **THIS IS THE UNMIXED STATE**

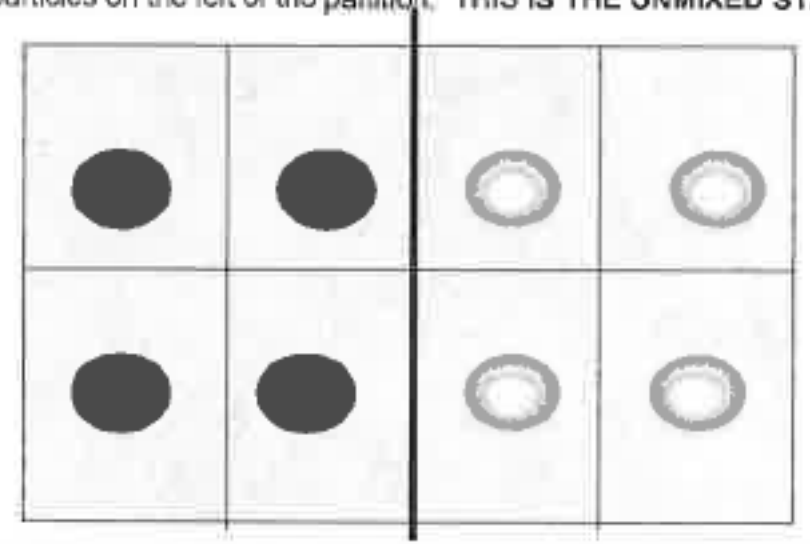

If the A's are indistinguishable and the B's are indistinguishable, there is only one possible way that this arrangement can exist

Statistical Entropy of Mixing

Now remove the partition and allow the particles to mix

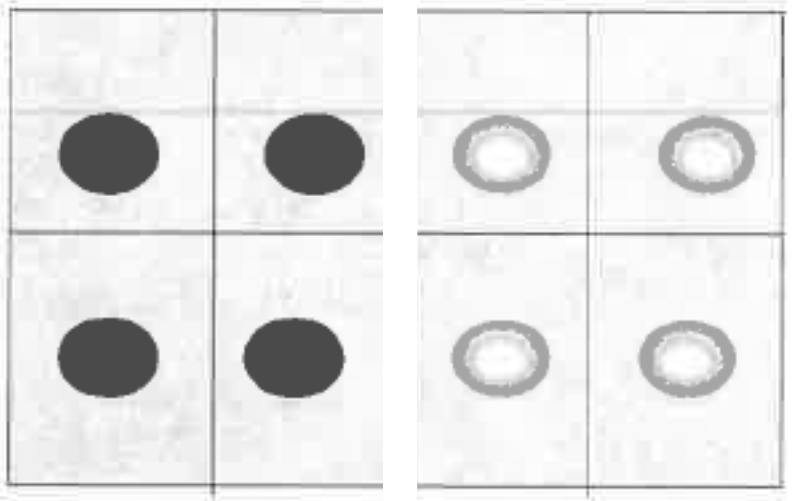

Statistical Entropy of Mixing

IF ONE BLACK PARTICLE IS EXCHANGED FOR ONE GOLD PARTICLE

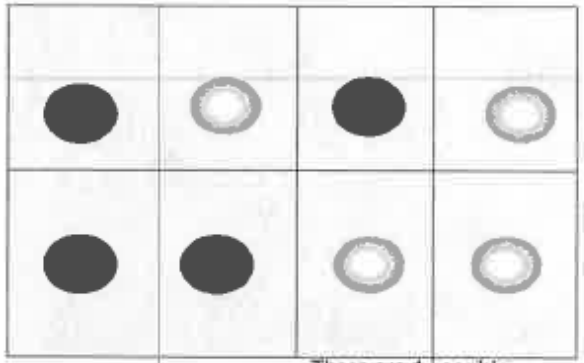

There are 4 possible arrangements on the left

There are 4 possible arrangements on the right

TOTAL POSSIBLE ARRANGEMENTS = 4X4 =16

Statistical Entropy of Mixing

IF TWO BLACK PARTICLES ARE EXCHANGED FOR TWO GOLD PARTICLES

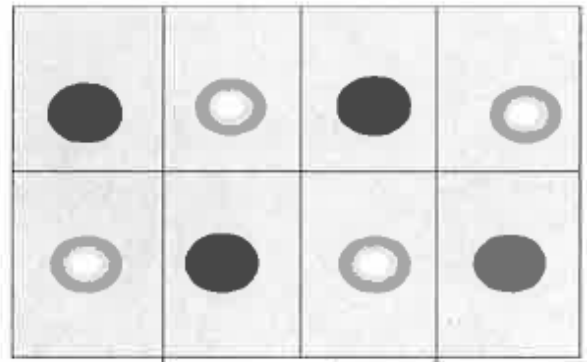

For the 4 possible arrangements of placing the first particle there are three ways of placing the second particle

But the gold particles are indistinguishable – so we have double counted –need to divide by 2

Statistical Entropy of Mixing

IF TWO BLACK PARTICLES ARE EXCHANGED FOR TWO GOLD PARTICLES

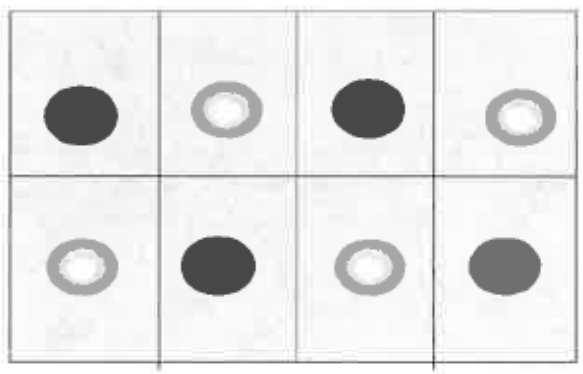

TOTAL NUMBER OF ARRANGEMENTS FOR 2+2 ON EACH SIDE = 6x6 =36

Total Number of Arrangements

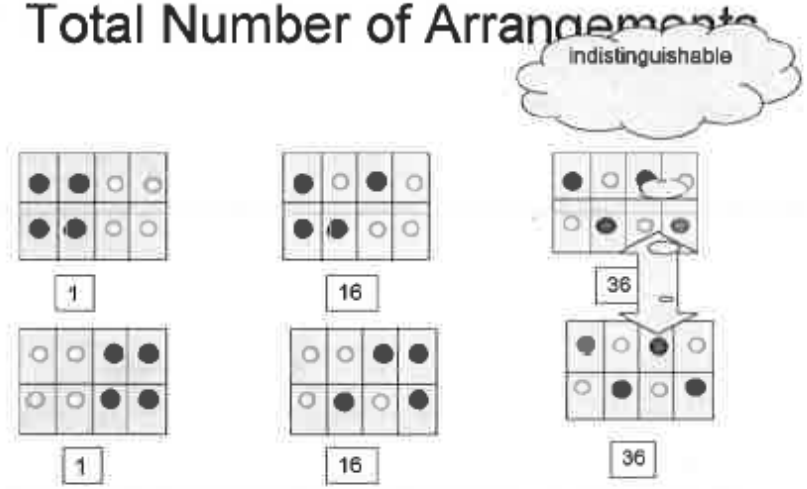

TOTAL NUMBER OF POSSIBLE ARRANGEMENTS = 1+1+16+16+36 =70

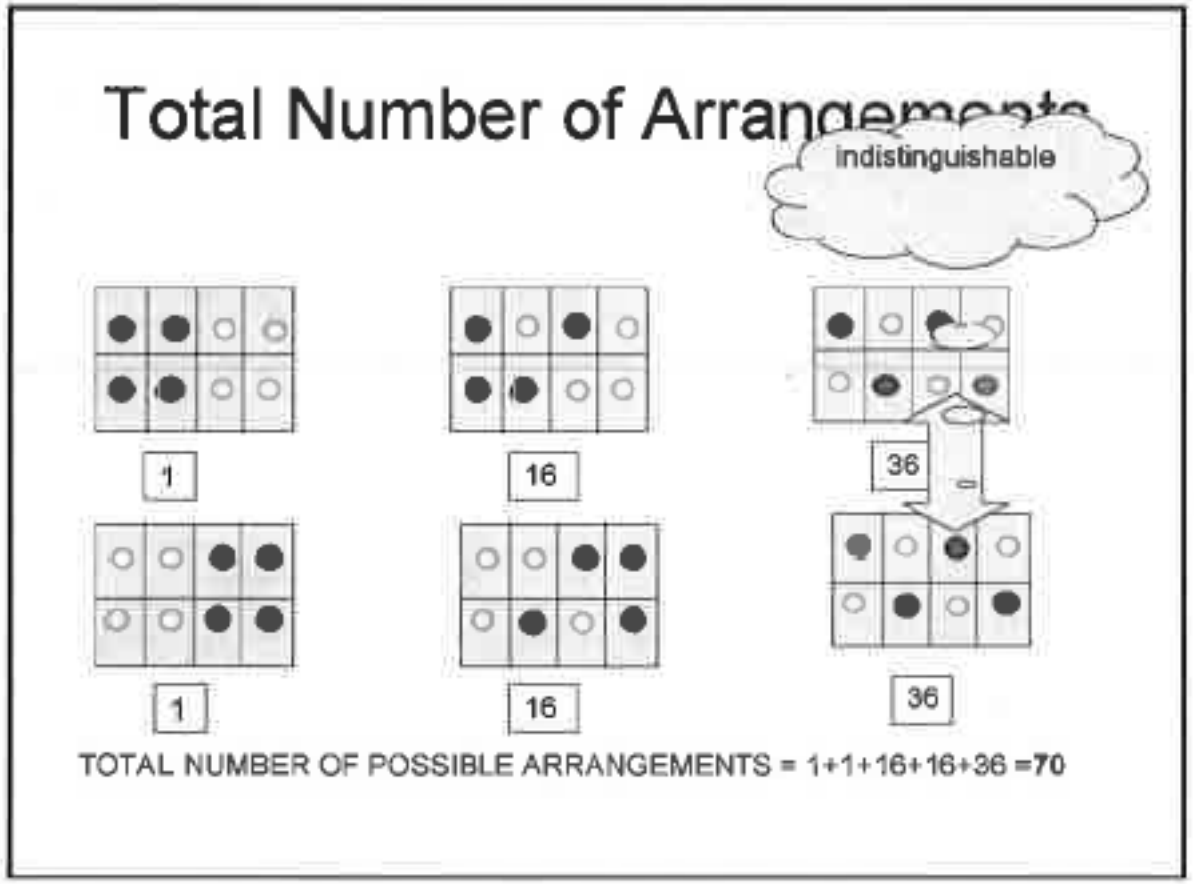

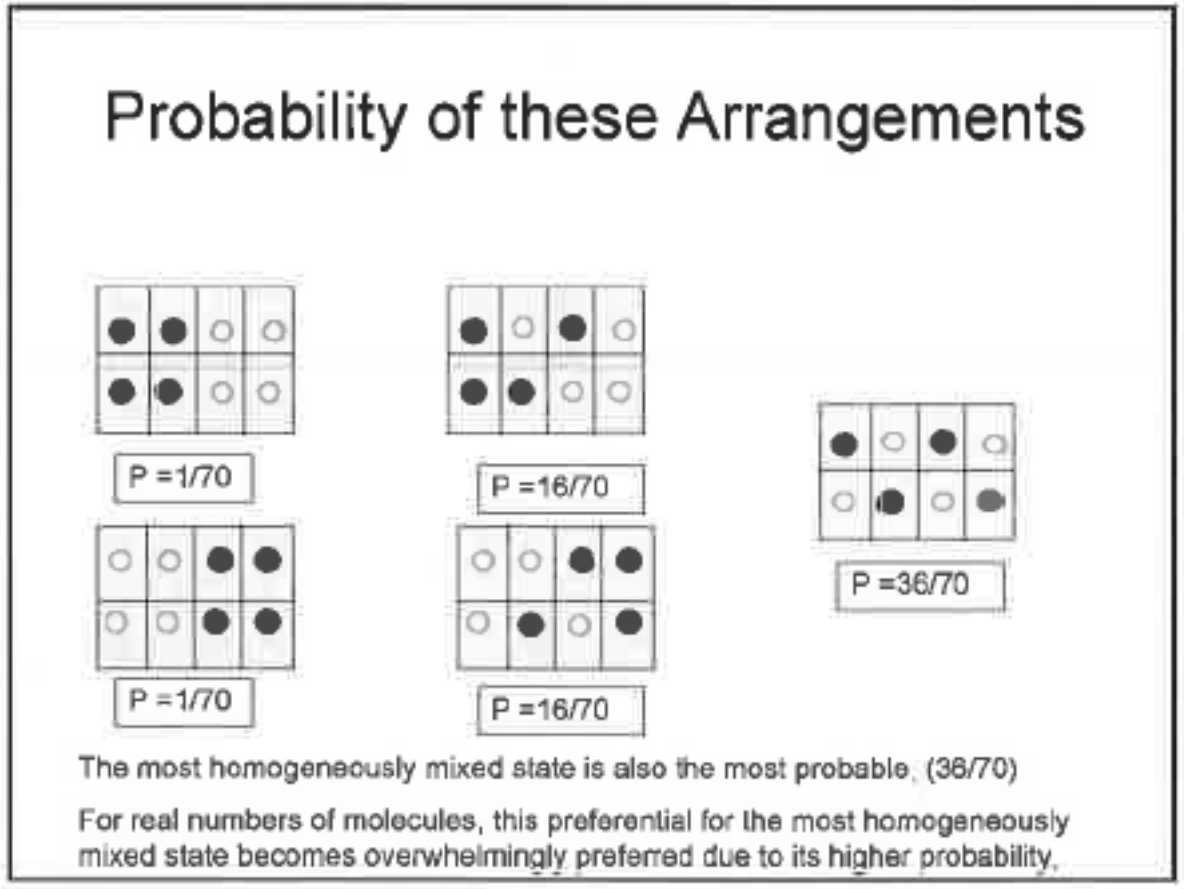

Configurations

The Flory-Huggins Interaction Parameter

- Flory-Huggins calculates the configurational entropy of placing the polymers in solution (on a lattice)
- Then F-H determines the enthalpic contribution required for molecular mixing
  - This Enthalpy is the Flory-Huggins Interaction Parameter, χ
    - $\chi = {}^{i}V({}^{i}\delta - {}^{j}\delta)^2/RT$
    - If $\chi<0.5$, the system will be compatible
    - If $\chi>2.0$ the system will be incompatible

The Flory-Huggins Interaction Parameter

- Flory-Huggins calculates the configurational entropy of placing the polymers in solution (on a lattice)
- Then F-H determines the enthalpic contribution required for molecular mixing
  - This H is the Flory-Huggins Interaction Parameter, χ
    - $\chi = {}^{i}V({}^{i}\delta - {}^{j}\delta)^2/RT$
    - If $\chi<0.5$, the system will be compatible
    - If $\chi>2.0$ the system will be incompatible

Flory Huggins Theory

- The thermodynamics of polymer solubility are classically described by the Flory- Huggins equation:

$$\Delta G_{mix}/RT = x_{solvent} \ln \Phi_{solvent} + x_{polymer} \ln \Phi_{polymer} + \chi x_{solvent} \Phi_{polymer}$$

- *where;* **Δ** Gmix is the free energy of mixing of the polymer and solvent
- xsolvent is the mole fraction of solvent in the solution
- xpolymer is the mole fraction of polymer in the solution
- **Φ**solvent is the volume fraction of solvent in the solution
- **Φ** polymer is the volume fraction of polymer in the solution
- **χ** is the Flory-Huggins interaction parameter for polymer-solvent interaction.

Flory-Huggins Theory

$$\Delta G_{mix}/RT = x_{solvent} \ln\Phi_{solvent} + x_{polymer} \ln \Phi_{polymer} + \chi x_{solvent} \Phi_{polymer}$$

Mixing Enthalpy contribution

Mixing Entropy contribution: Always favorable to mixing

Flory-Huggins Theory

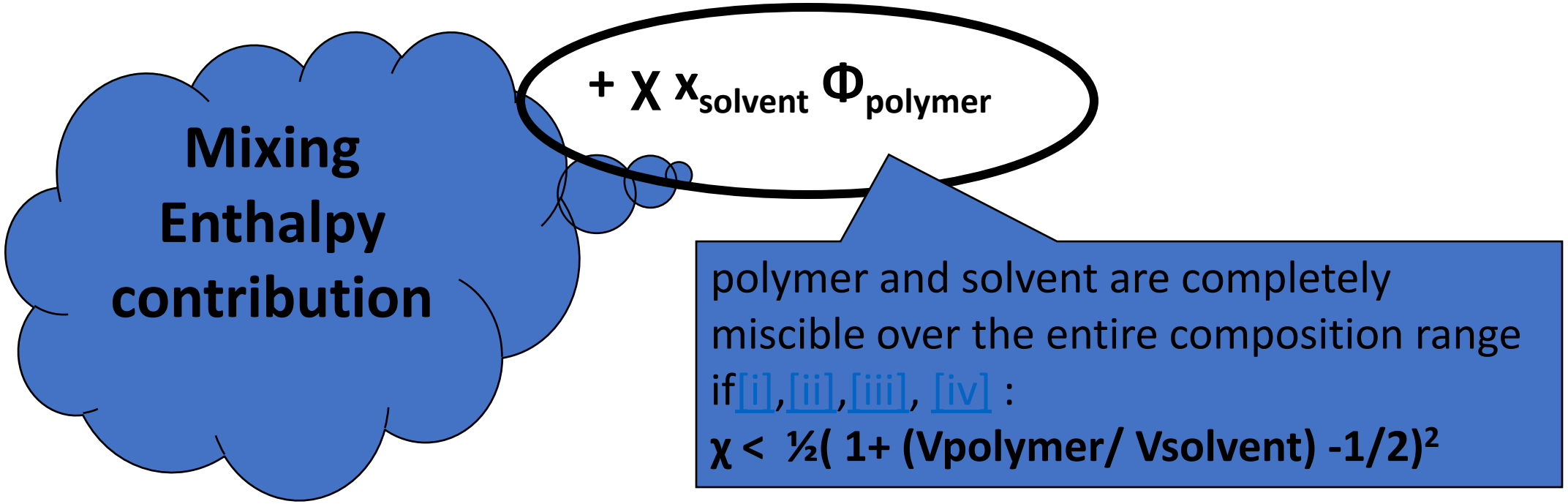

[i] Flory, P. J. "Thermodynamics of high polymer solutions", J.Chem. Phys., **1942**, *10*, 51.

[ii] Flory, P.J.; "*Principles of Polymer Chemistry*," Cornell University Press, Ithaca, N.Y., **1953**.

[iii] Patterson, D; *Macromolecules*, **1969**, *2*, 672

[iv] Barton, Allan, F. M.; "Handbook of Solubility Parameters and Other Cohesion Parameters; CRC Press, Boca Raton, Florida, **1983**.

Flory-Huggins Theory

- A polymer and solvent should be completely miscible if the value of the Flory-Huggins interaction parameter, **χ ,** is less than **0.5**

Drawbacks of the Flory-Huggins Theory

- **χ** is not a constant; it varies with polymer concentration and temperature.
- **χ** can not be easily found experimentally.
- **χ** is characteristic of only a polymer-solvent pair and it is not easily extended to multicomponent formulations.
- **χ** is not a simple term; it has to be modified to include terms for molecular orientation and specific binding such as hydrogen bonding.
- If the system becomes more ordered when a solution is formed, **χ** can have anomalous large positive values.
- Finally, classical Flory-Huggins theory can not explain the fact that polymer solutions can separate into two phases upon heating or cooling beyond certain critical temperatures.[3][i] [ii]
- This is especially pertinent for thermo-associative polymers.
- [i] Patterson, D.; "Thermodynamics of non-dilutee polymer solutions"; *Rubber Chem. Technol*., **1967**, 40, 1.
- [ii] Patterson, D., Delmas, G.; Somcynsky, T; "A Comparison of lower critical solution temperatures of some polymer solutions", *Polymer*, **1967**, *8*, 503.

Generalized Phase Diagram for a Polymer in Solution

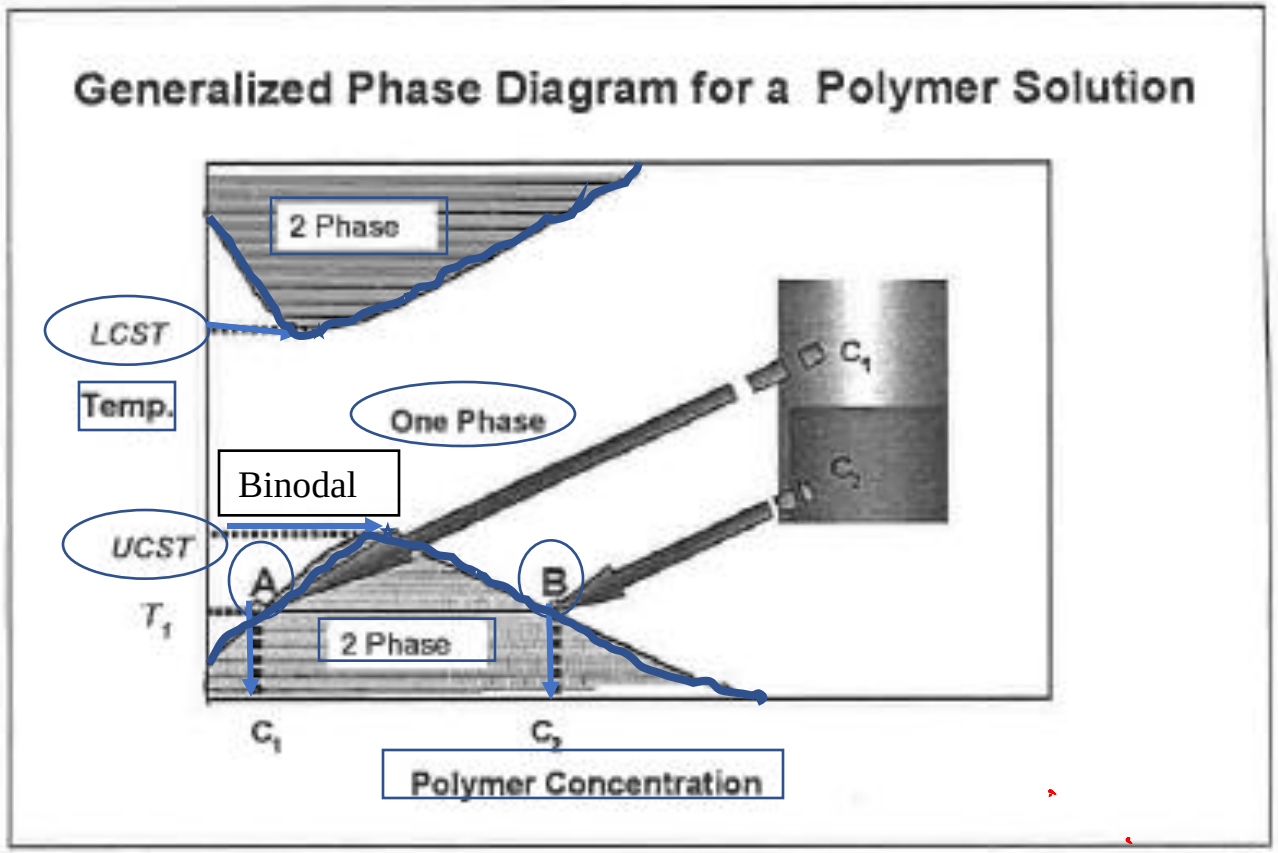

Figure 2. A generalized phase diagram for polymer solution as a function of temperature and polymer concentration. The miscible polymer solution separates into two phases upon cooling below the UCST or heating above the LCST. The compositions of the separated phases can be determined by the intersection points of the tie lines on the two-phase envelope.

Tie Lines

$$\text{C1 Relative Amount} = \frac{Y}{(X+Y)}$$

$$\text{C2 Relative Amount} = \frac{X}{(X+Y)}$$

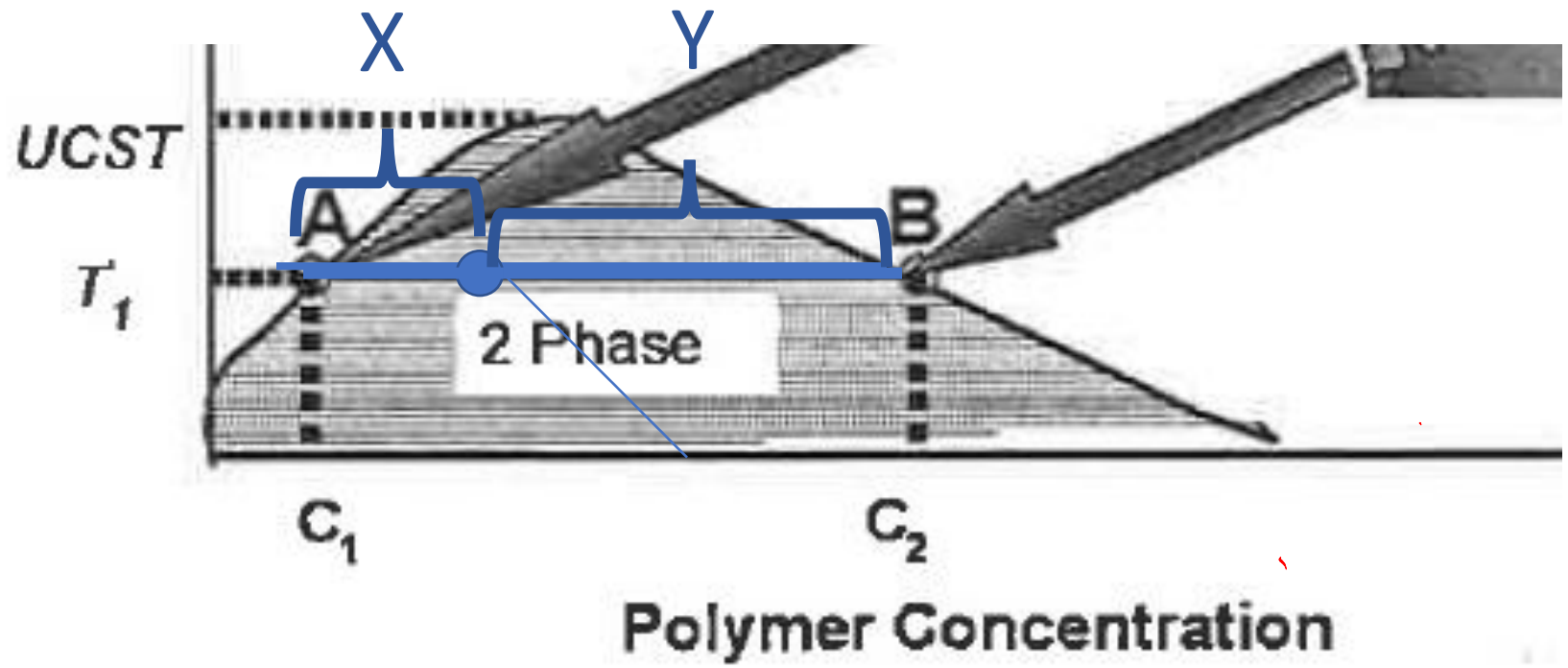

Free Energy of Mixing

- A system reaches chemical equilibrium (and this includes phase equilibria) when the free energy of the system reaches a minimum.
- The change in Gibbs free energy (ΔG) is related to the changes in enthalpy (Δ H) and entropy (Δ S) of a process at temperature, T, by the familiar equation:

$$\Delta G = \Delta H - T\,\Delta S$$

- **Phase separation below the UCST requires a significant negative enthalpy of mixing, and phase separation above the LCST requires both a negative enthalpy and entropy of mixing.**

Conditions for Miscibility and Phase Separation

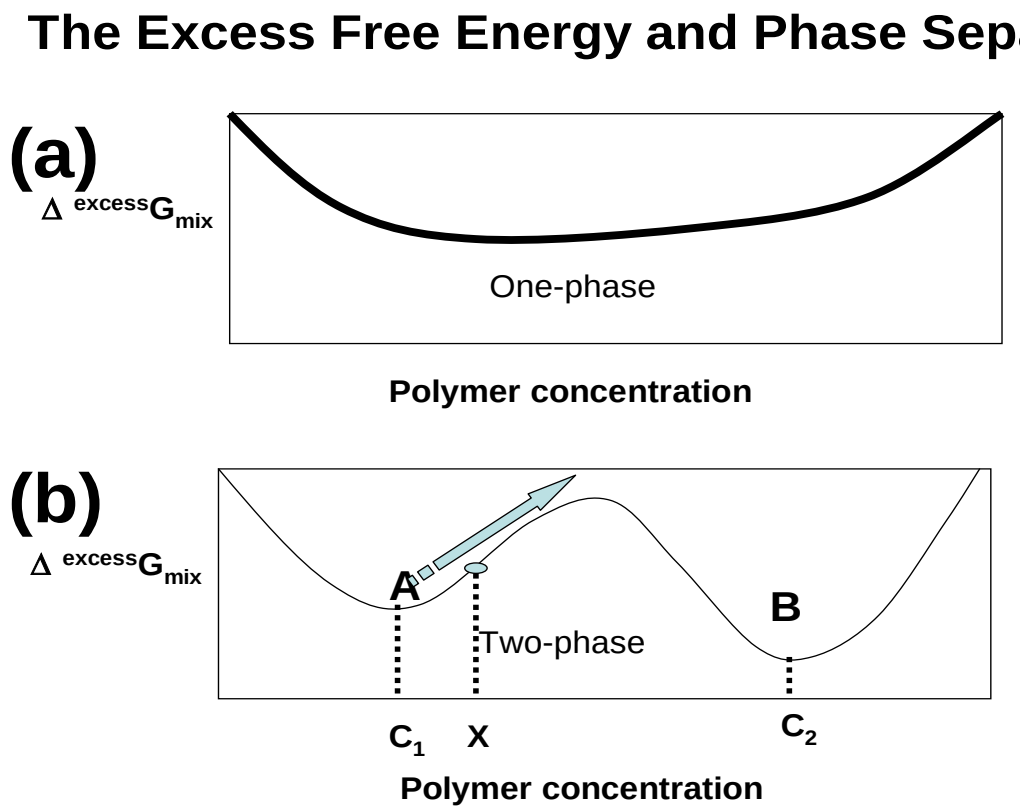

The excess free energy as a function of polymer concentration for (a) a miscible solution and (b) a phase-separated system

Metastable Equilibria and Thermal Gelling

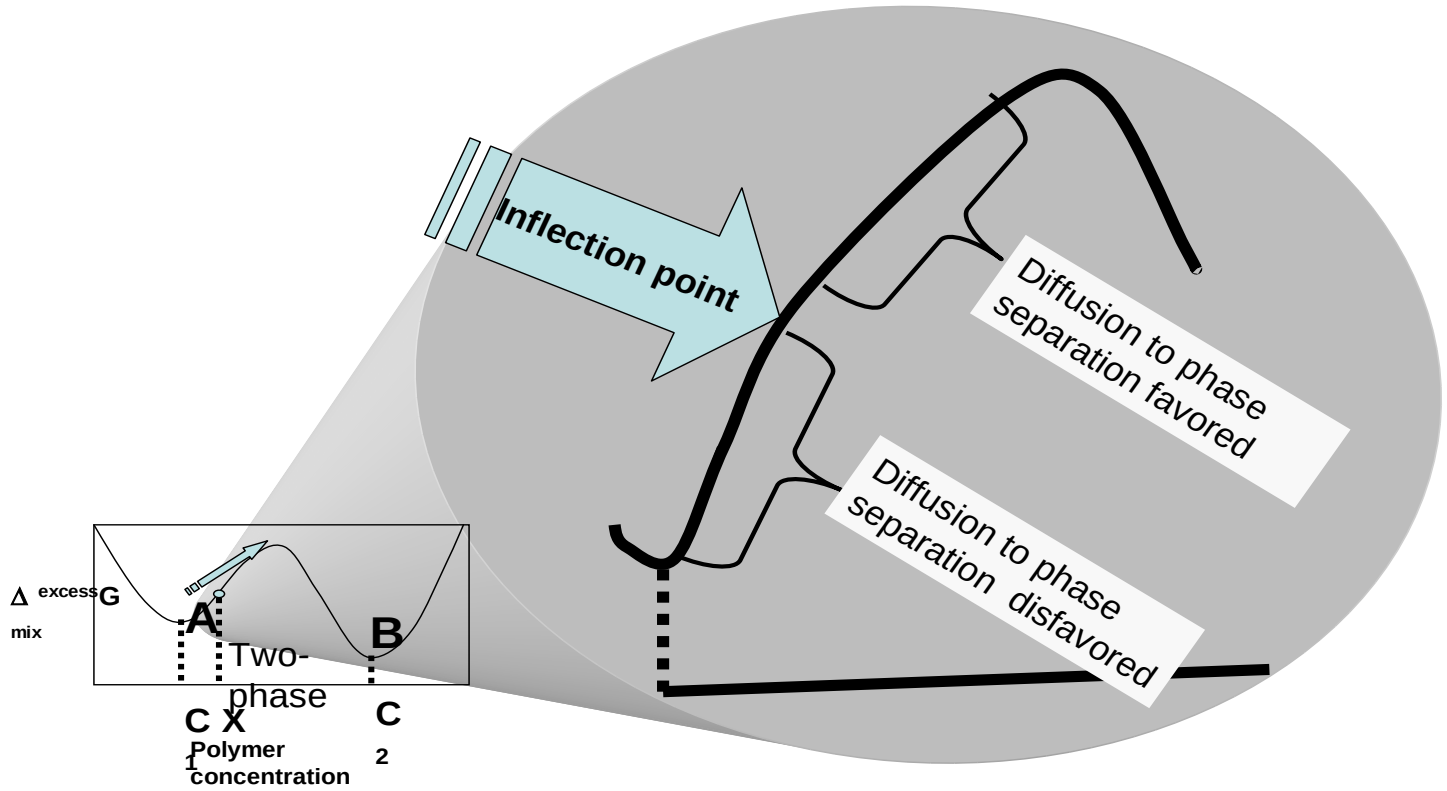

Exploded view of a segment of the free energy curve showing the inflection point.

Spinodals and Binodals

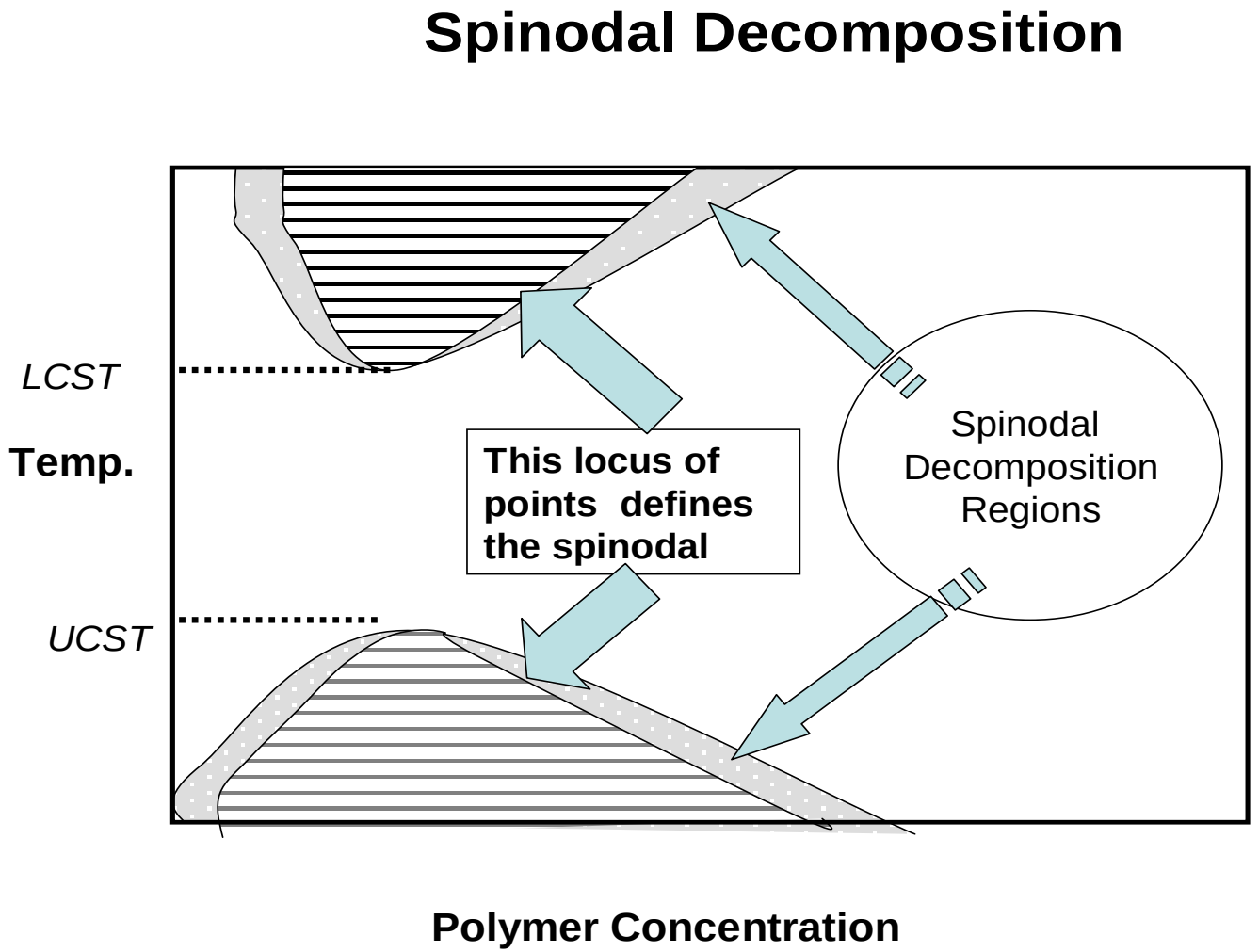

Spinodals and Binodals

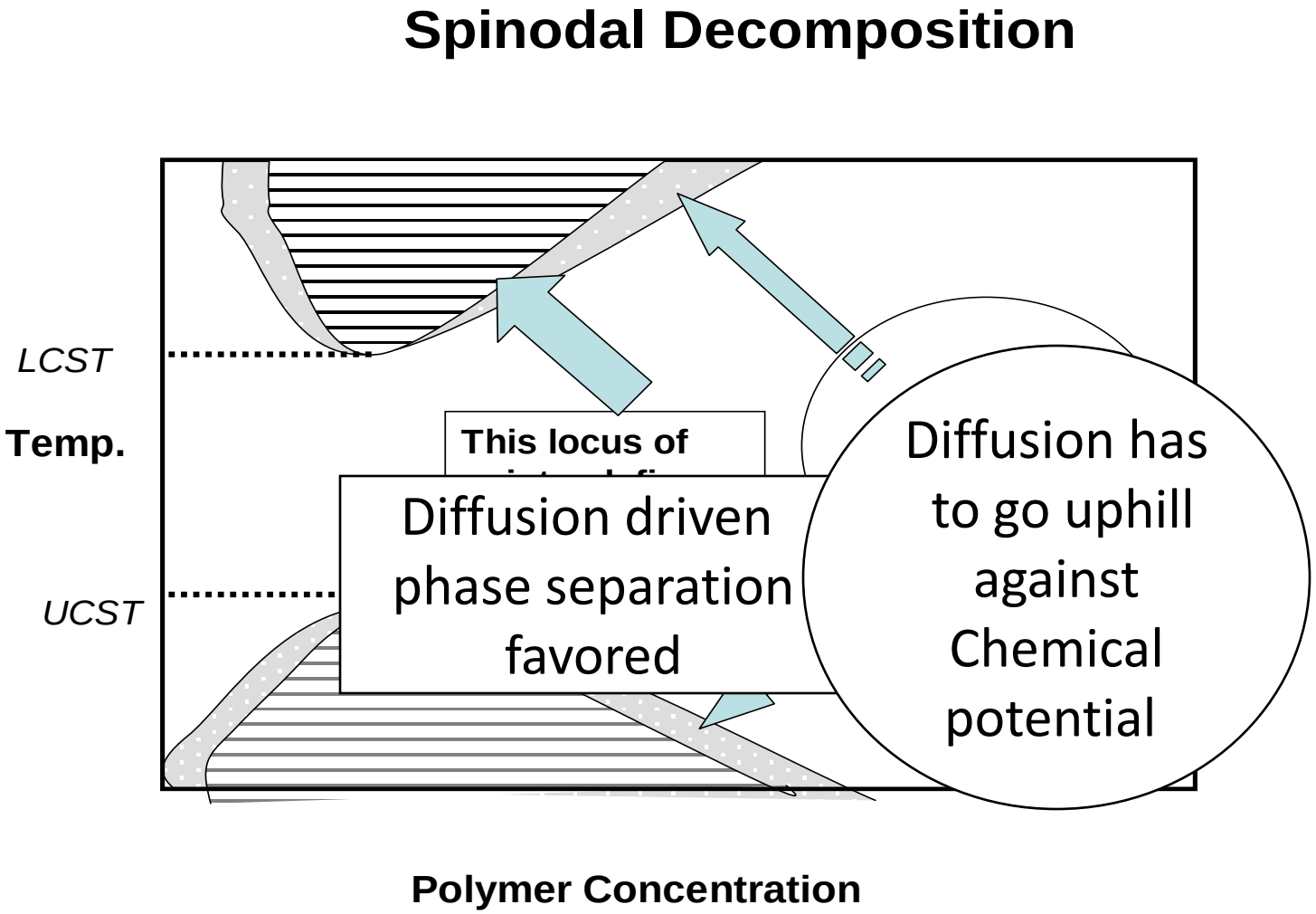

Summary of Polymer Solubility Theories

- Flory –Huggins attempts to include entropy of mixing
  - It is difficult to calculate the total entropy of mixing for polymer solutions and blends
    - But Flory-Huggins Theory is useful for conceptual understanding
- Solubility Parameter theory considers only enthalpy of mixing
  - But it is useful practically and relatively easy to use
  - if the interactions are divided into dispersion, polar and hydrogen bonding

Polymer Chains

The Basics

The Fundamental Parameters

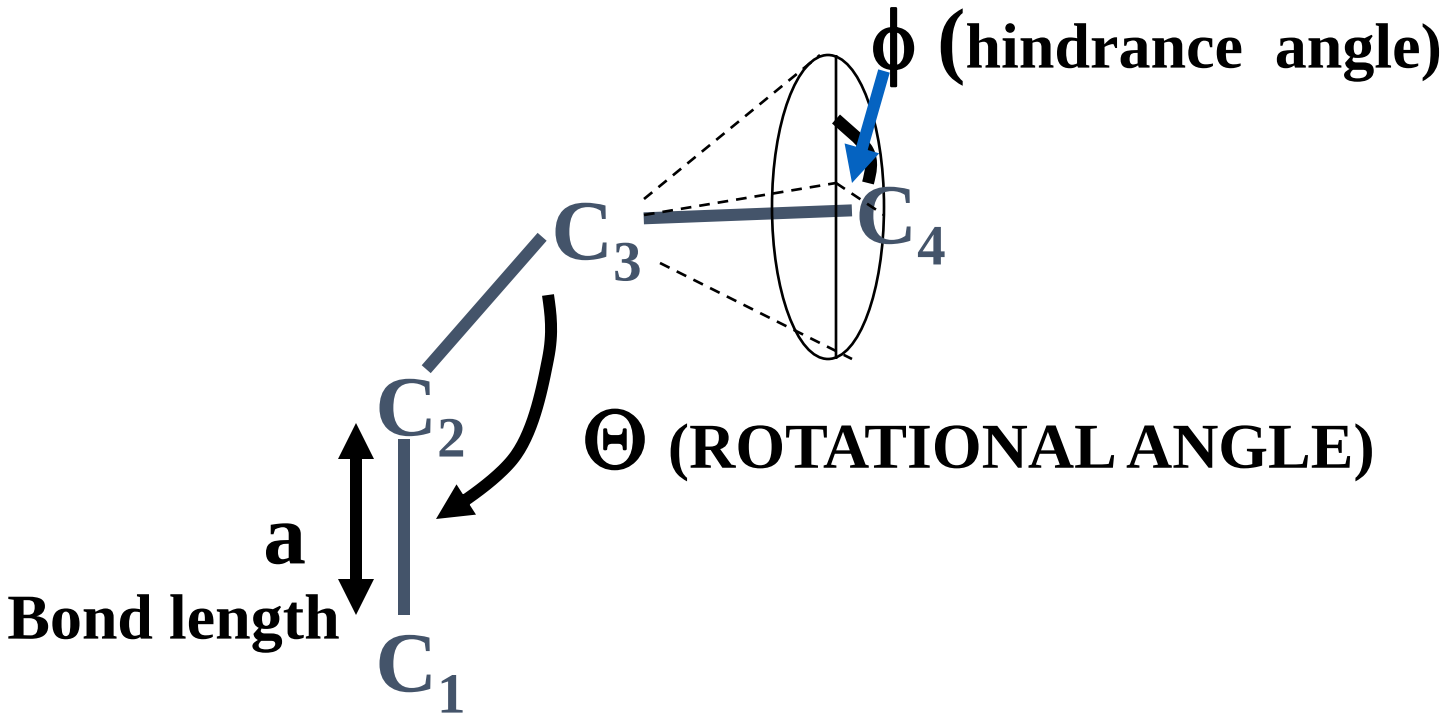

The Fundamental Parameters

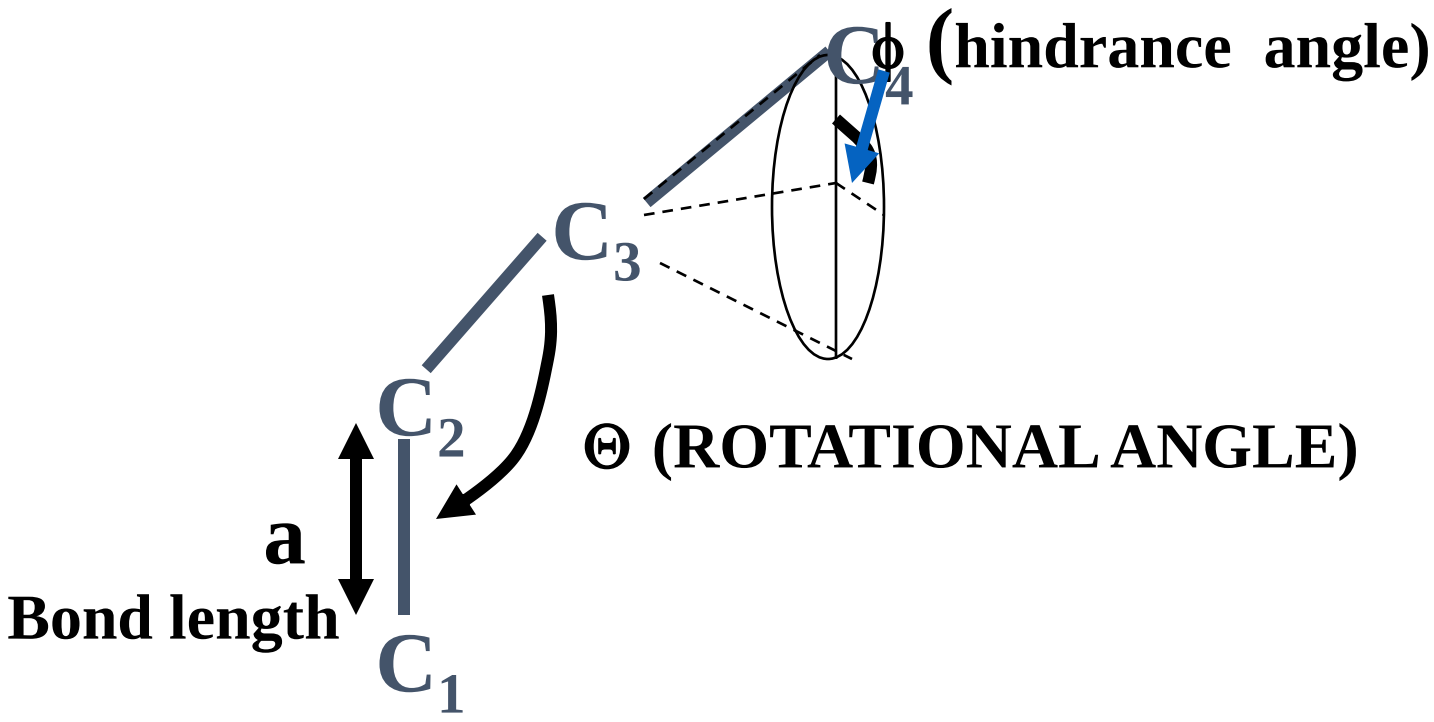

The Fundamental Parameters

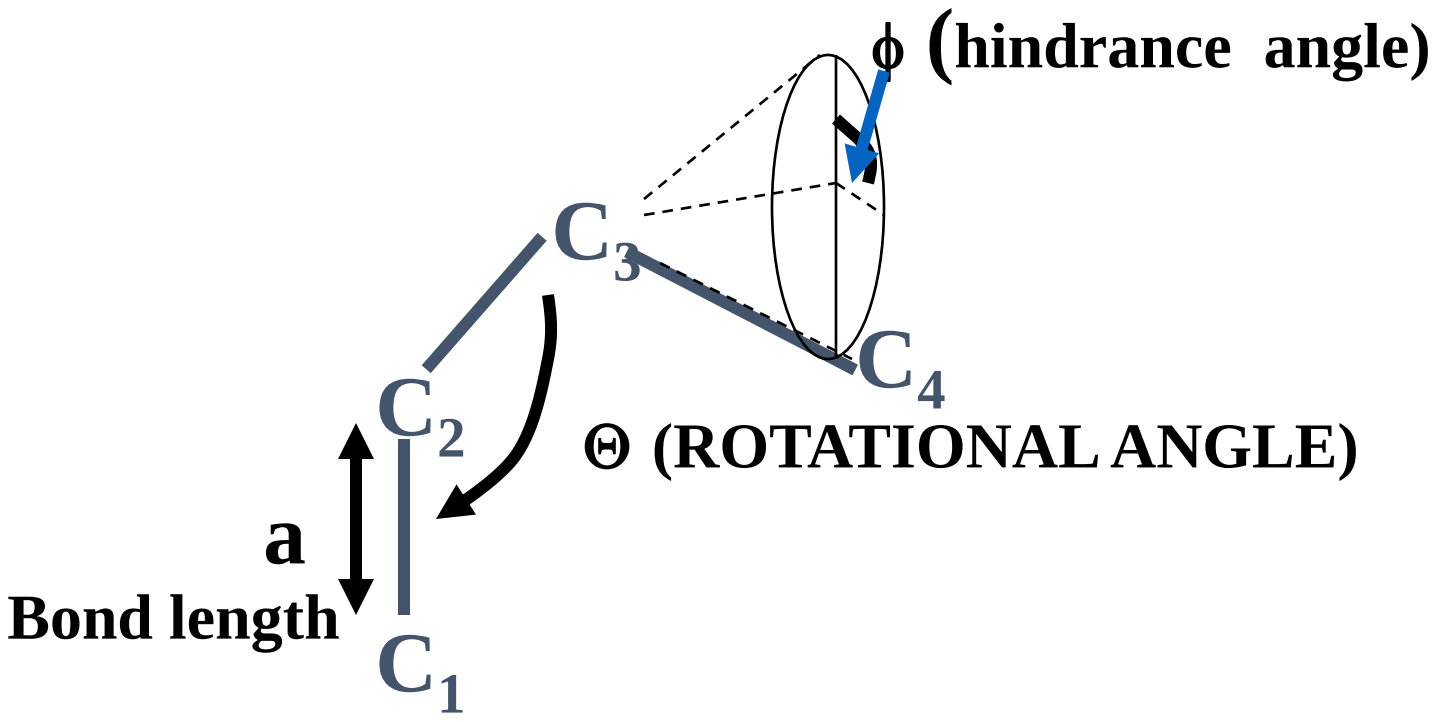

Dilute Solutions, c’

- The polymer chain behaves as a small sphere
  - a single blob, with radius, r
- Example:
    - Each polymer chain is an isolated chain at c’
    - The length scale L is represented by the radius r and is equal to the correlation length, ξ
    - therefore, $r = \xi$
  - the coils are separate from one another

Semidilute Solutions

- As concentration increases
  - blobs overlap
  - chains interact and interpenetrate
- Above c*
  - coils become entangled and form a network of mesh ξ
  - ξ is the distance between two entanglement points

Semidilute Solutions

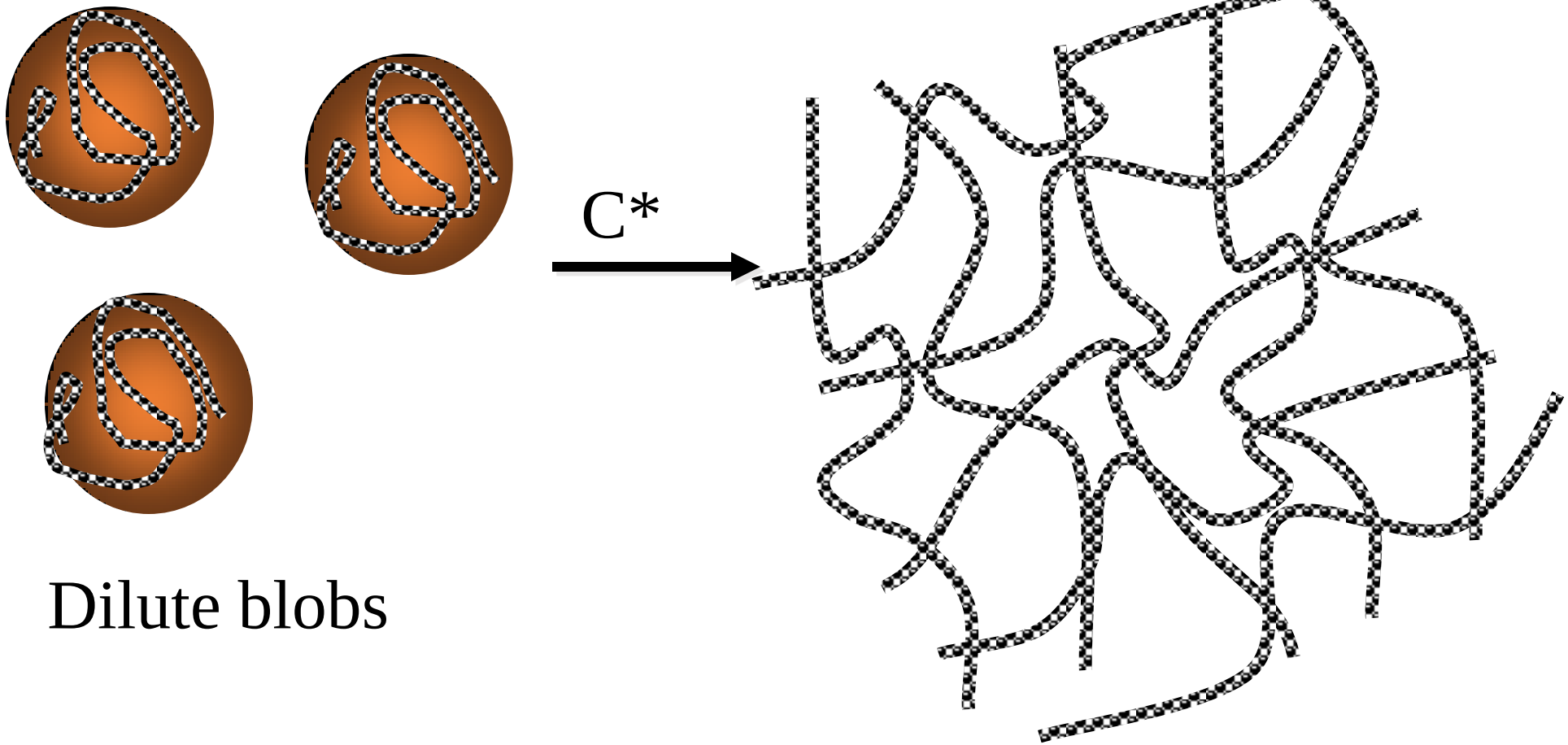

Semidilute Solutions

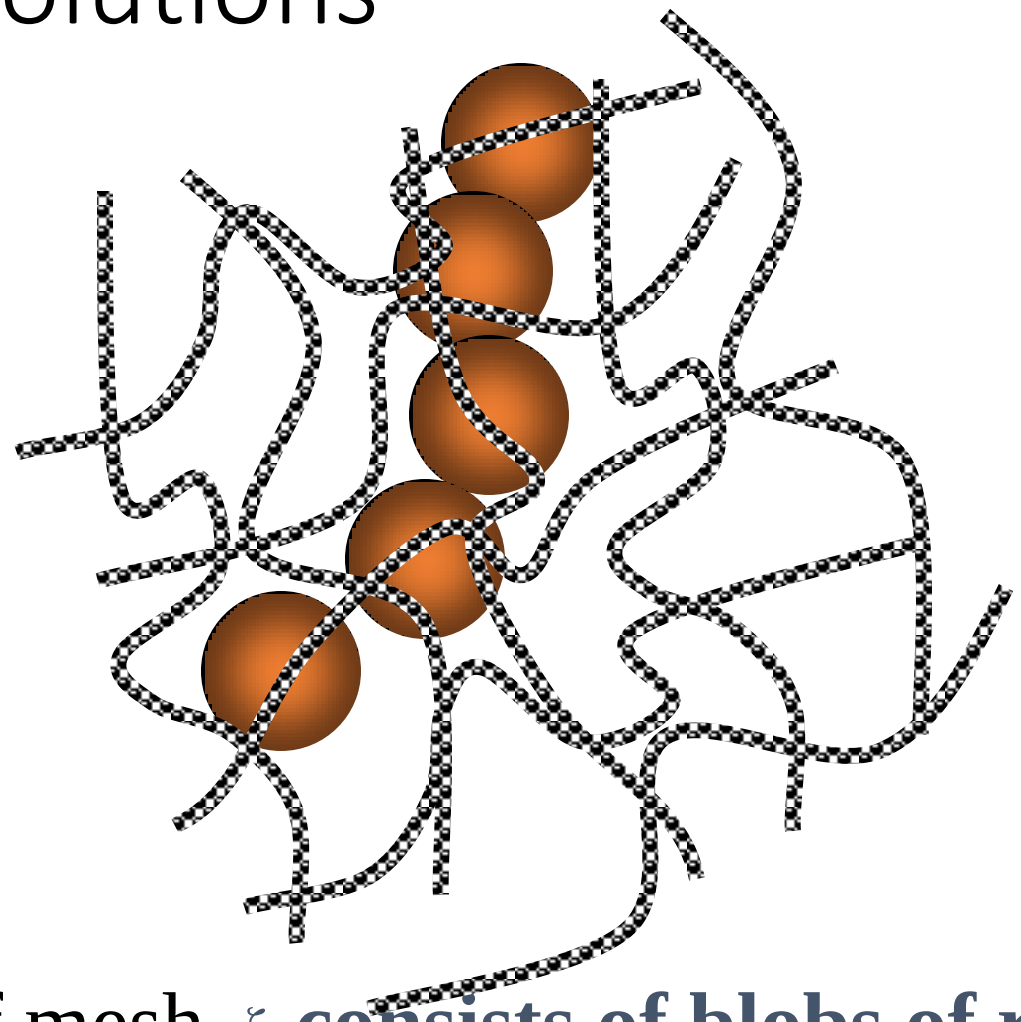

Network of mesh ξ **consists of blobs of radius r=** ξ

Polymers in good solvent in semi-dilute solution

For r> ξ

that is outside the blob

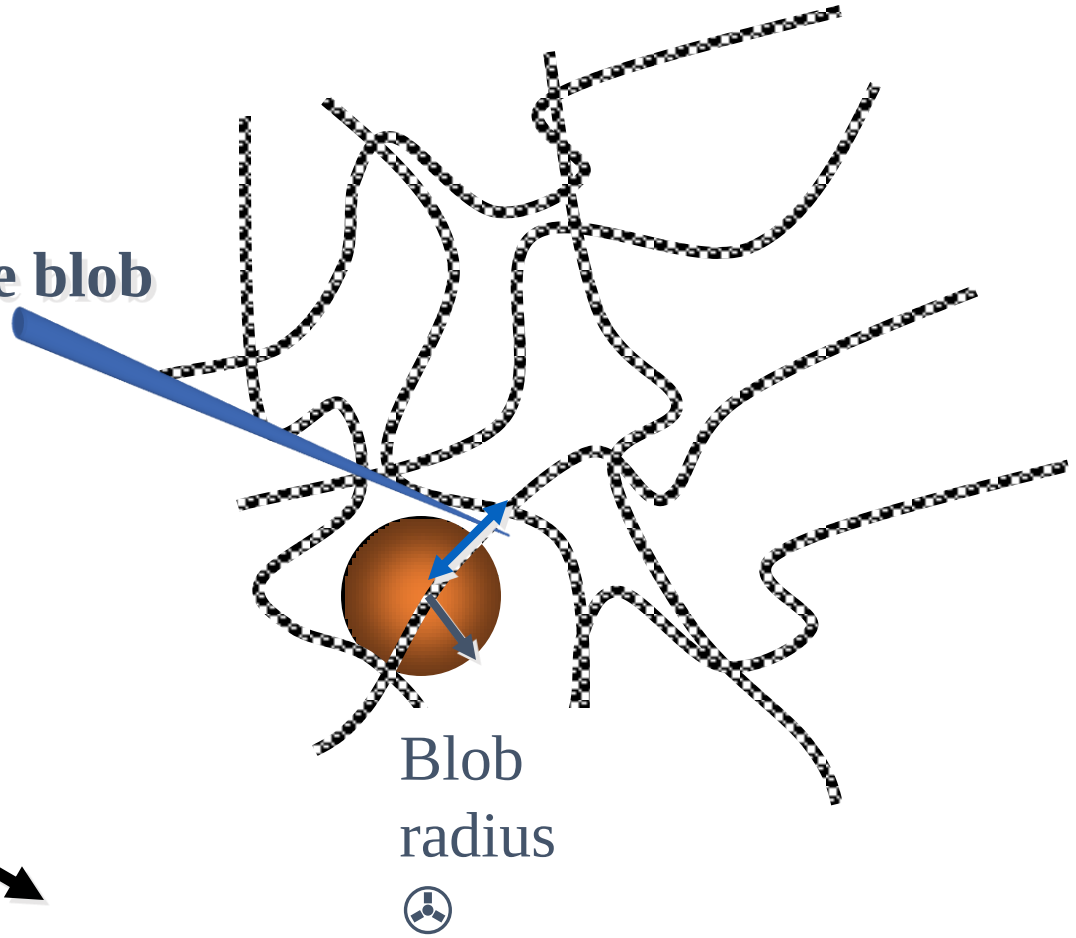

The repulsive interactions between monomers are screened out

The blobs connect in a random flight

Summary

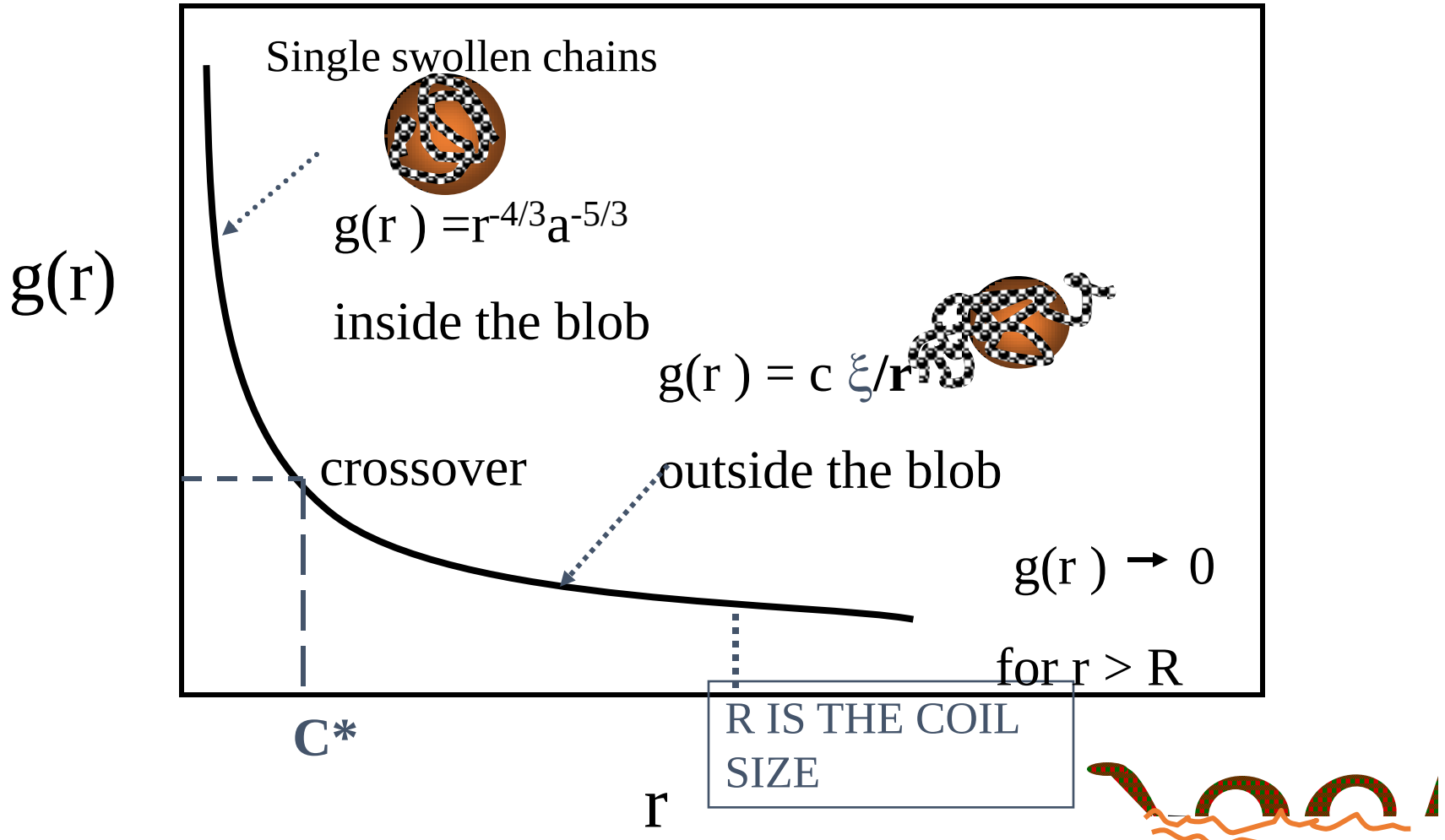
g(r)
Single swollen chains
g(r) =r-4/3a-5/3
inside the blob
g(r) = c ξ/r
crossover
outside the blob
g(r) → 0
for r > R
C*
r
R IS THE COIL SIZE

DILUTE SOLUTION VISCOSITY

Polymer Solution Viscosity

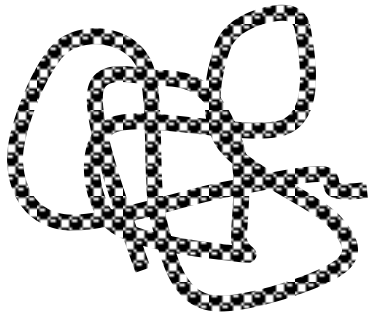

The viscosity of a solution depends upon the propensity of the solvent to flow

In a polymer solution, the polymer molecule ‘slows’ the flow of the solvent

Polymer Solution Viscosity

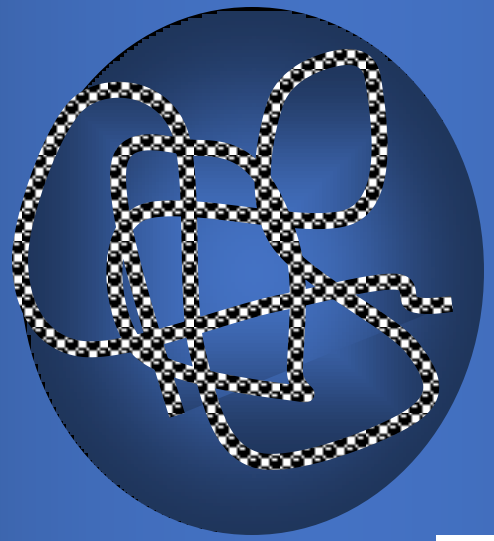

IF THE SOLVENT DOES NOT FLOW THROUGH THE COIL – IT IS CALLED A NON-FREE DRAINING COIL

Polymer Solution Viscosity

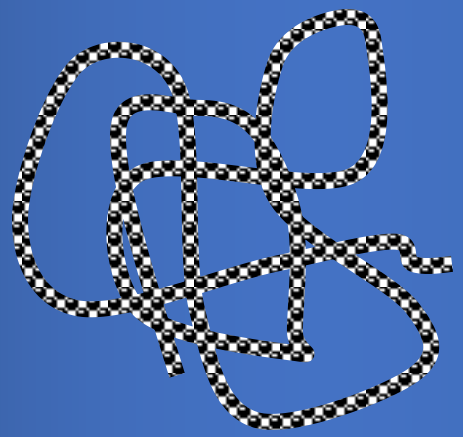

IF THE SOLVENT FLOWS THROUGH THE COIL – IT IS CALLED A FREE DRAINING COIL

Viscosity

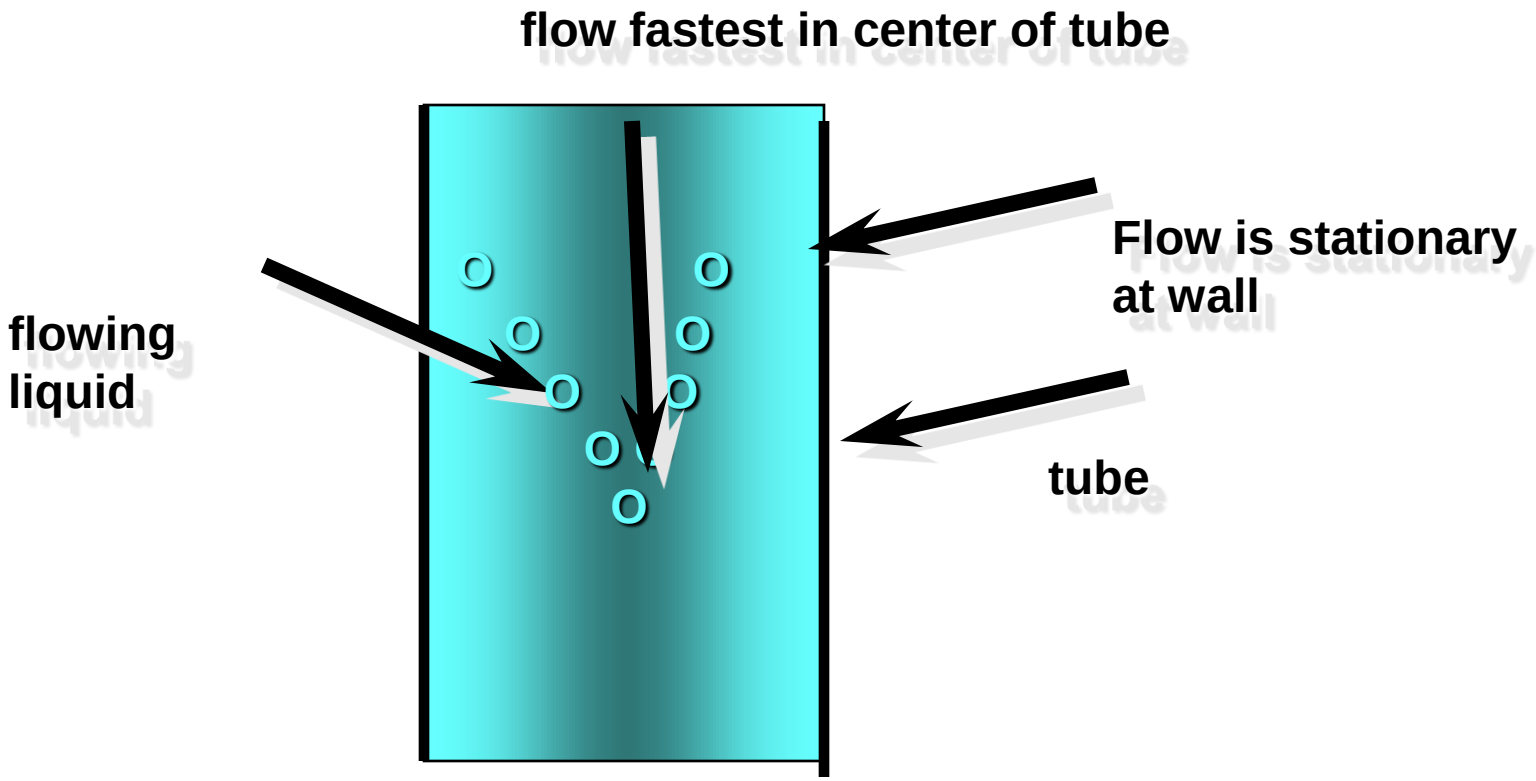

Polymer Solution Viscosity

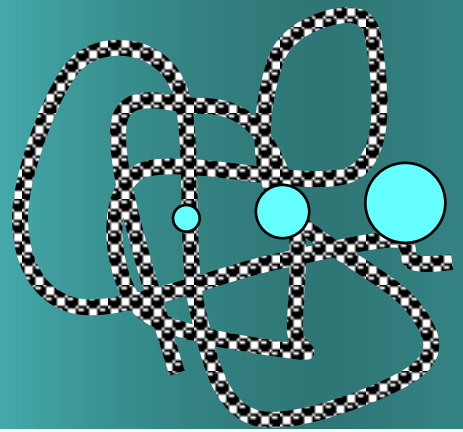

[η] is the hydrodynamic size of the polymer molecule in solution (dl/g)

The Mark-Houwink Equation

Intrinsic Viscosity, $[\eta] = K M^a$

A factor that depends upon the 'swollen' size of the polymer molecule

a = 0.5 for non-free draining
a = 1.0 for Free draining
For Gaussian Chains

Measurement of Viscosity

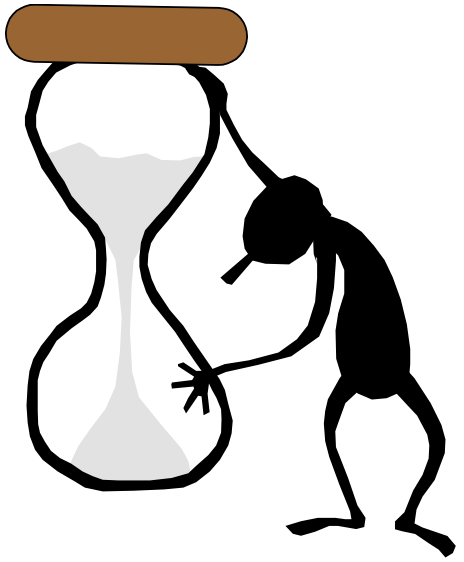

Measure time of solvent flow through viscometer t_o

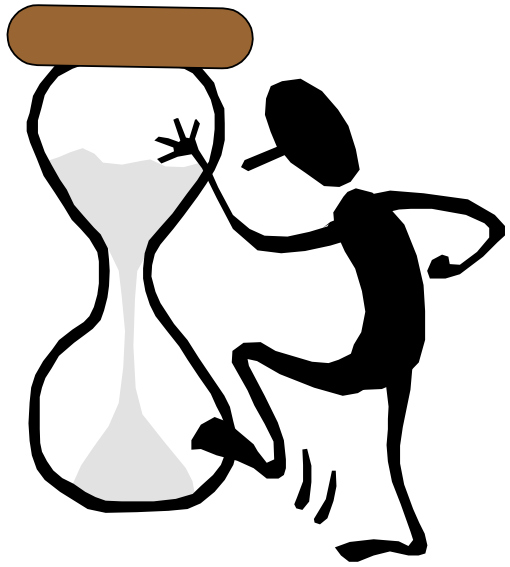

Measure time of solution flow through viscometer t

Viscosity

- We measure solution (η) and solvent (η_o) viscosity separately
- Relative Viscosity = $(\eta/\ \eta_o) = \eta_r$
  - that reveals how much more viscous the solution is compared to the solvent
- Specific Viscosity = $[(\eta - \eta_o)/\ \eta_o] = \eta_r - 1$
  - η_{sp}
  - removes the solvent viscosity

Determining the Intrinsic Viscosity

- Time the flow of solvent and polymer solutions through a capillary
- The specific reduced viscosity,

$$\eta_{sp}/c = (\eta - \eta_o)/\eta_o c$$

- Measure the (η_{sp}/c) for a series of dilute polymer solutions

What is the Intrinsic Viscosity?

- The units are decilitre/gram
  - volume per unit weight
  - The intrinsic viscosity gives the volume occupied by one gram of polymer in solution

- $[\eta].M$ = the volume occupied by one mole of polymer in solution

Reduced Specific Viscosity

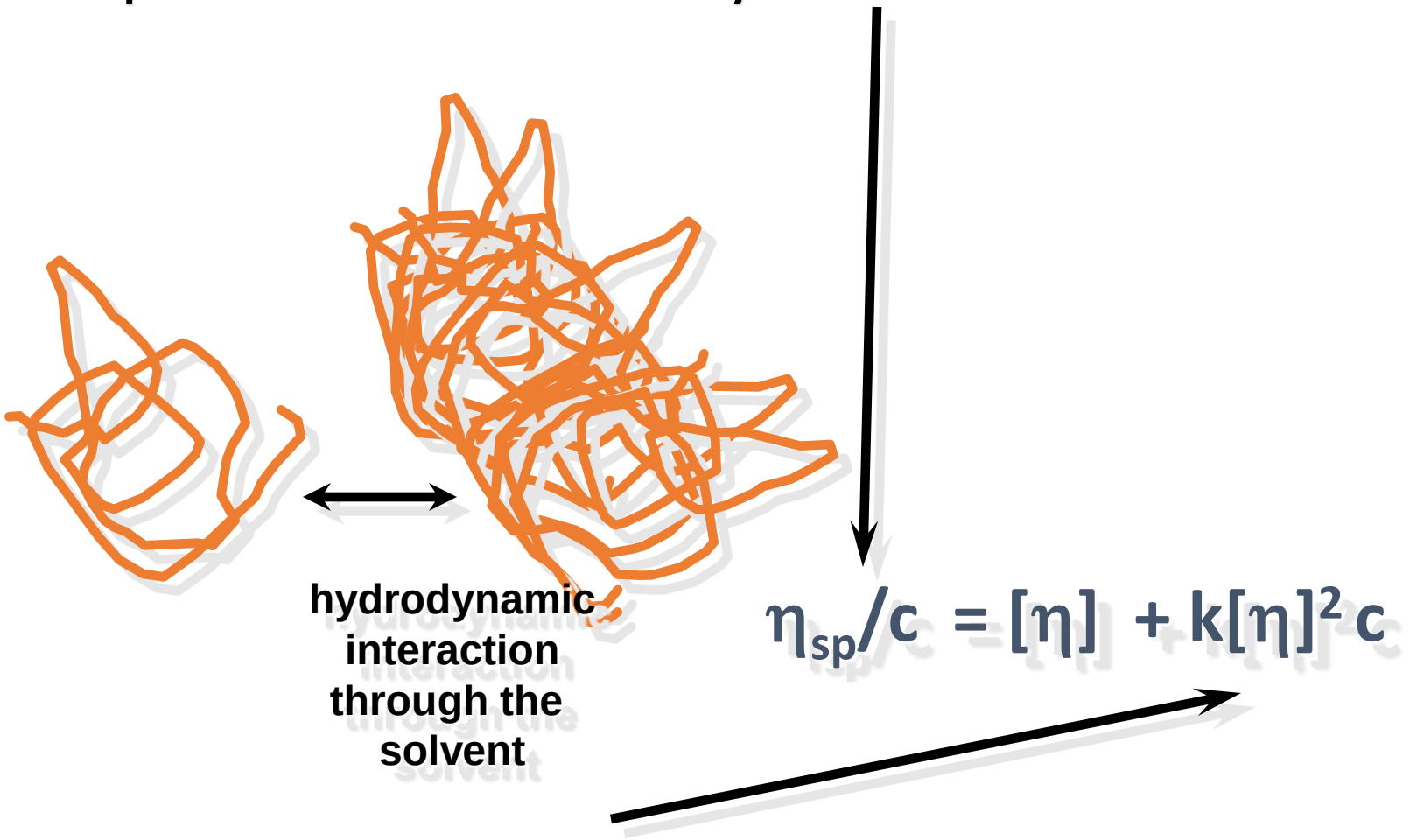

Viscosity

- Reduced Specific Viscosity = η_{sp}/c
  - a measure of the specific capacity of the polymer to increase the relative viscosity
  - But it contains the hydrodynamic interaction contribution
- Remove this contribution by extrapolating to infinite dilution

Determining the Intrinsic Viscosity

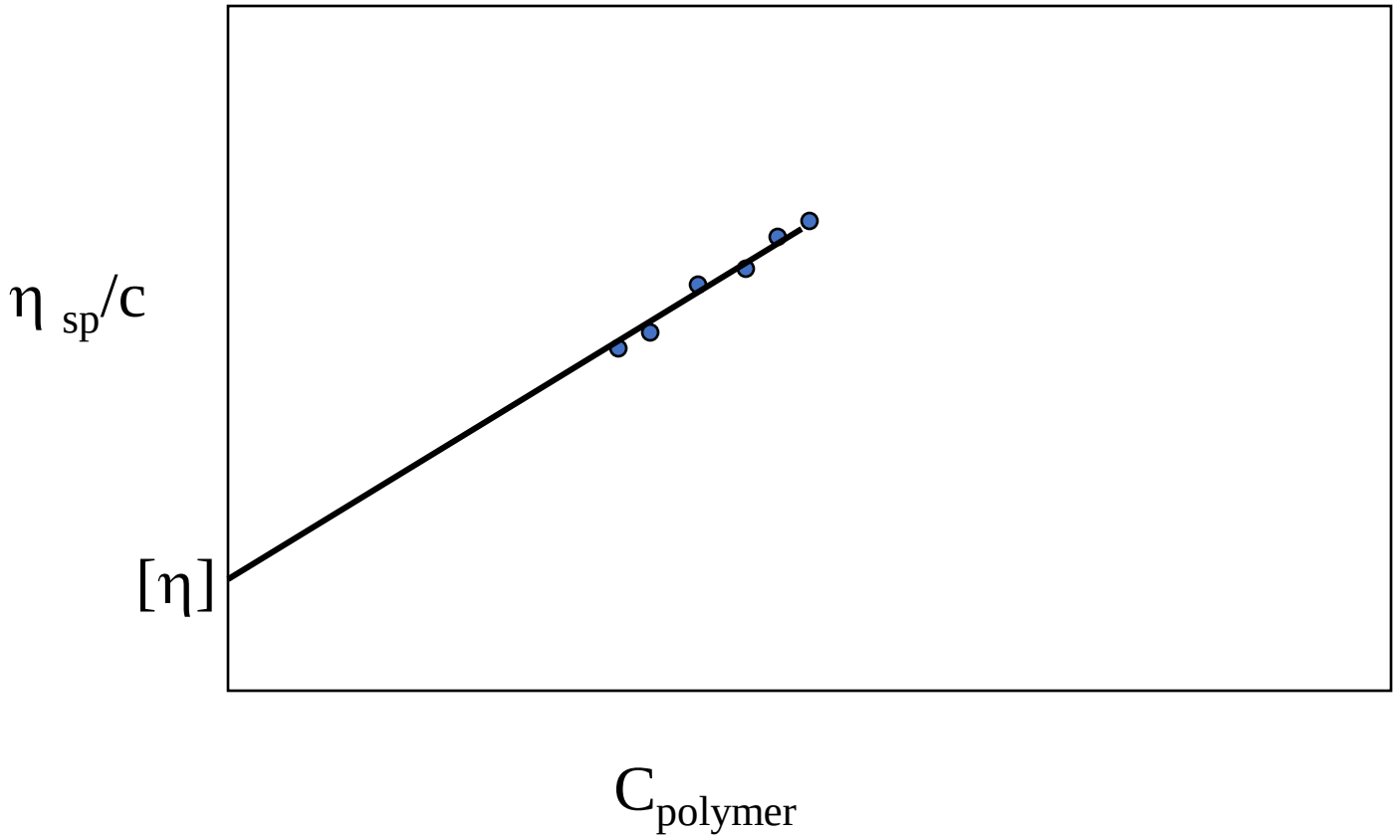

Viscosity –Huggins Plot

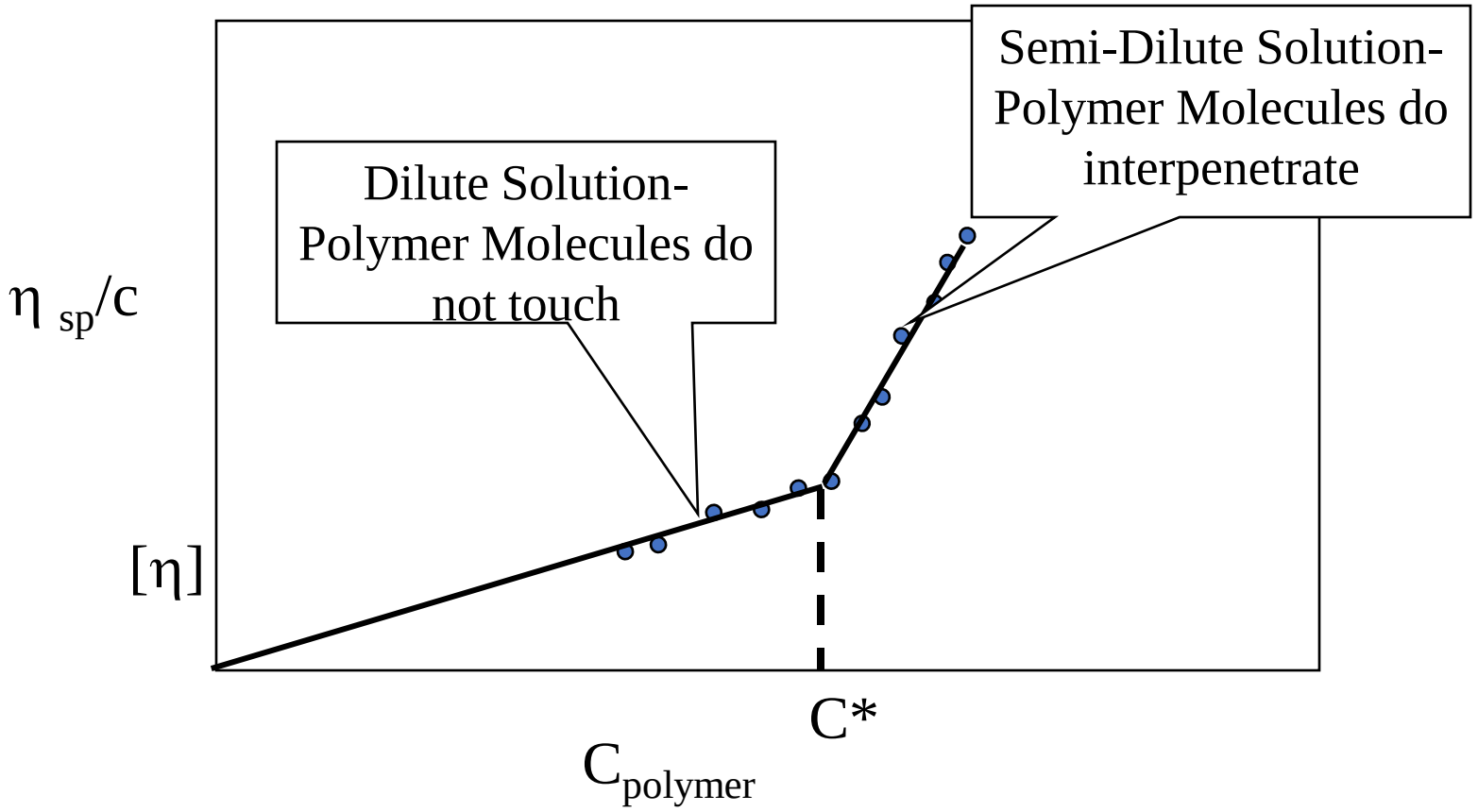

Reptation

- Above the chain entanglement threshold
  - The polymer molecules wriggle past each other
  - Like a snake moving along a tube made up of snakes
- Viscosity = $(\text{concn})^{2.2 - 3.4}$

The Glass Transition Temperature, Tg

- Below the Tg,
  - Chains have insufficient energy to reptate past each other
- Above the Tg
  - Polymer chains ‘wriggle’ and have enough excluded volume to wriggle past each other
- Plasticizers are small molecules that lower the Tg of a polymer or polymer system

Plasticization

- Small molecules interspersed between the polymer molecules can assist repatation
  - This is plasticization
- There is a time element
  - If the applied force must last long enough for the polymers to move
  - If the force is of short duration, elastic deformation and recovery will occur
    - Debra Number

The Mark Houwink-Sakurada Equation

$$[\eta] = KM^a$$

Rheology of Polymer solutions

Thermal Behavior of Gels

Example 1: A cold viscous solution maintains (partly) viscosity upon heating, e.g. guar gum, xanthan gum and CMC. Compared to the other gums, xanthan gum's viscosity is least effected by temperature increase.

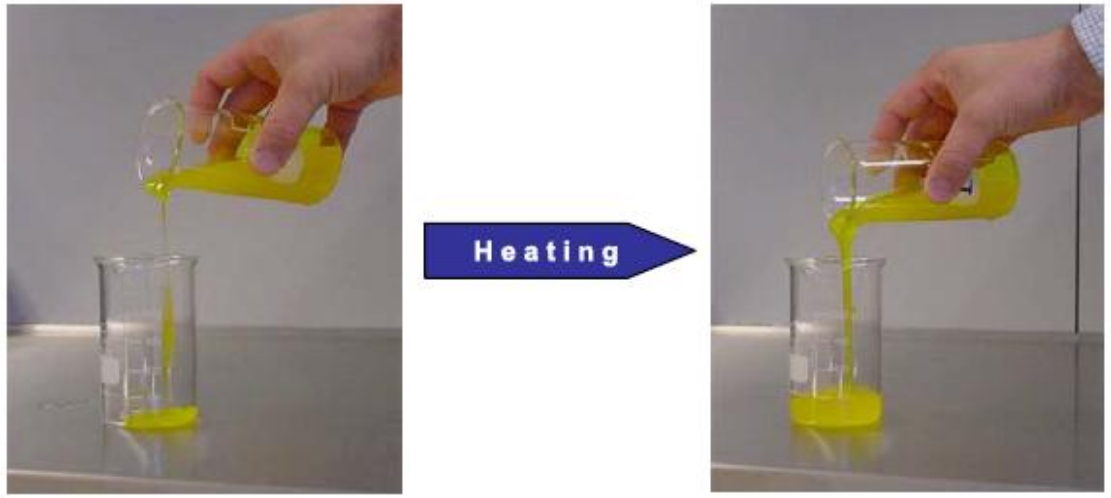

http://www.brenntag-specialties europe.com/en/downloads/Food_press_review/TB_Hydrocolloids_FNFN201009.pdf

Thermal Behavior of Gels

Example 2: A formed gel which melts upon heating, is known as a thermo-reversible gel. Gelatin is the most common example, although pectins and carrageenans can also form thermo-reversible gels.

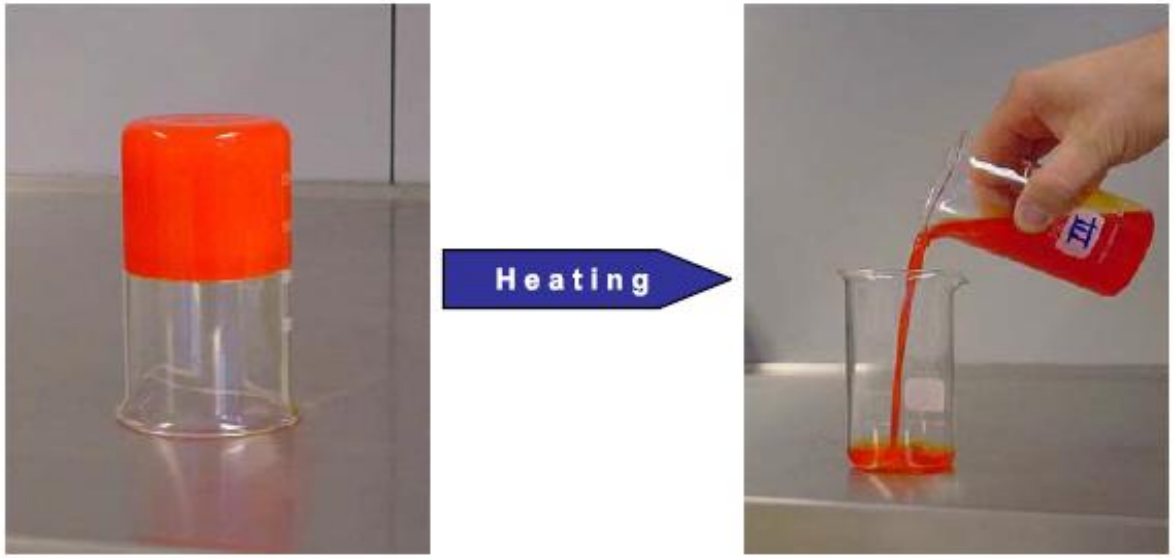

http://www.brenntag-specialties europe.com/en/downloads/Food_press_review/TB_Hydrocolloids_FNFN201009.pdf

Thermal Behavior of Gels

Example 3: A formed gel which does not melt upon heating, is known as a thermo-stable or thermo-irreversible gel. Alginates form thermo-stable gels, plus pectins can be formulated to become thermo-stable.

http://www.brenntag-specialties europe.com/en/downloads/Food_press_review/TB_Hydrocolloids_FNFN201009.pdf

Thermal Behavior of Gels

Example 4: A cold solution which gels on heating. This property is seen when cooking egg-white. The only hydrocolloids showing this thermo-gelling functionality are the cellulosic products MC and HPMC.

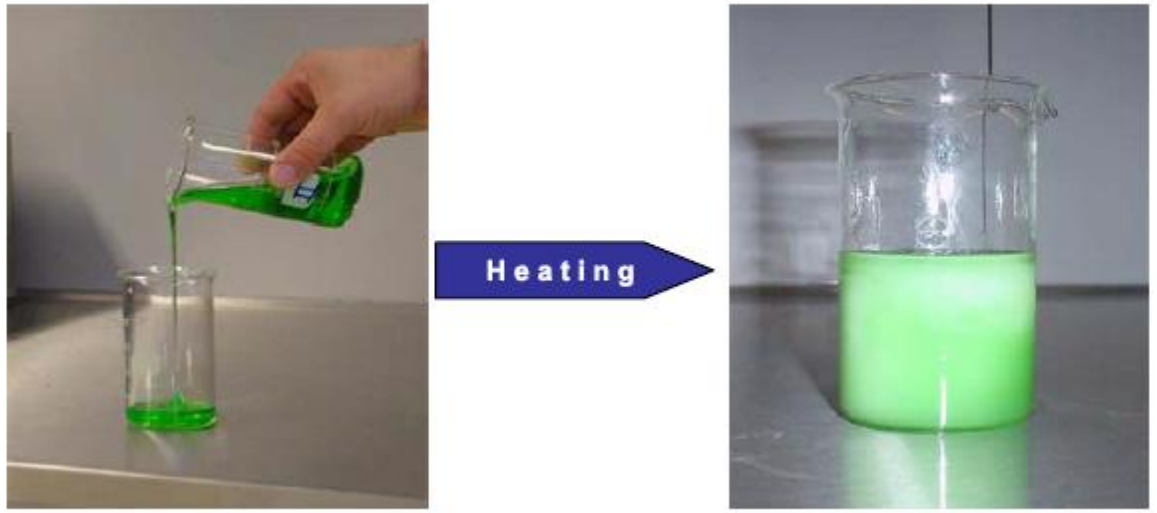

http://www.brenntag-specialties europe.com/en/downloads/Food_press_review/TB_Hydrocolloids_FNFN201009.pdf

RHEOLOGY

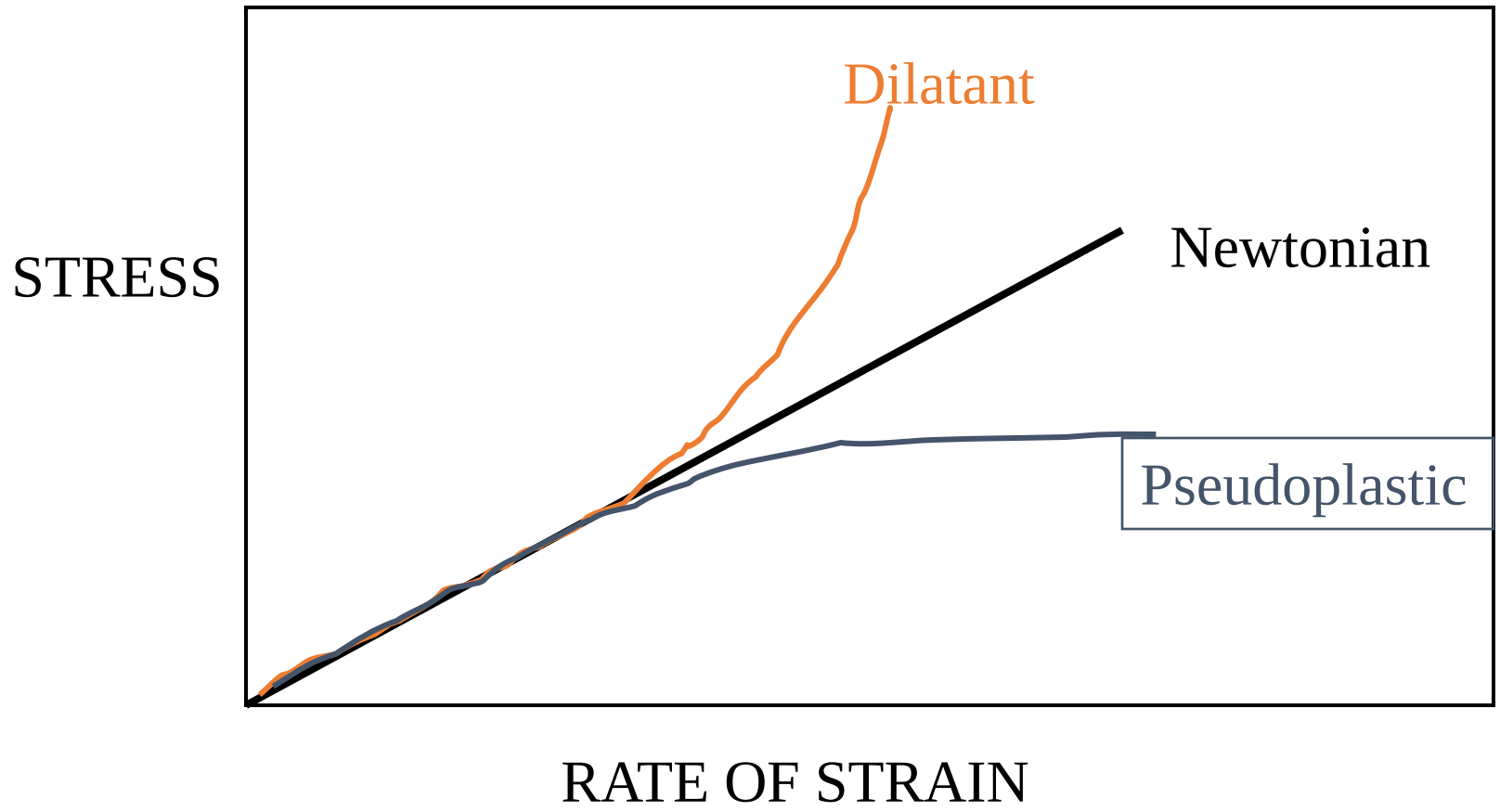

Rheology

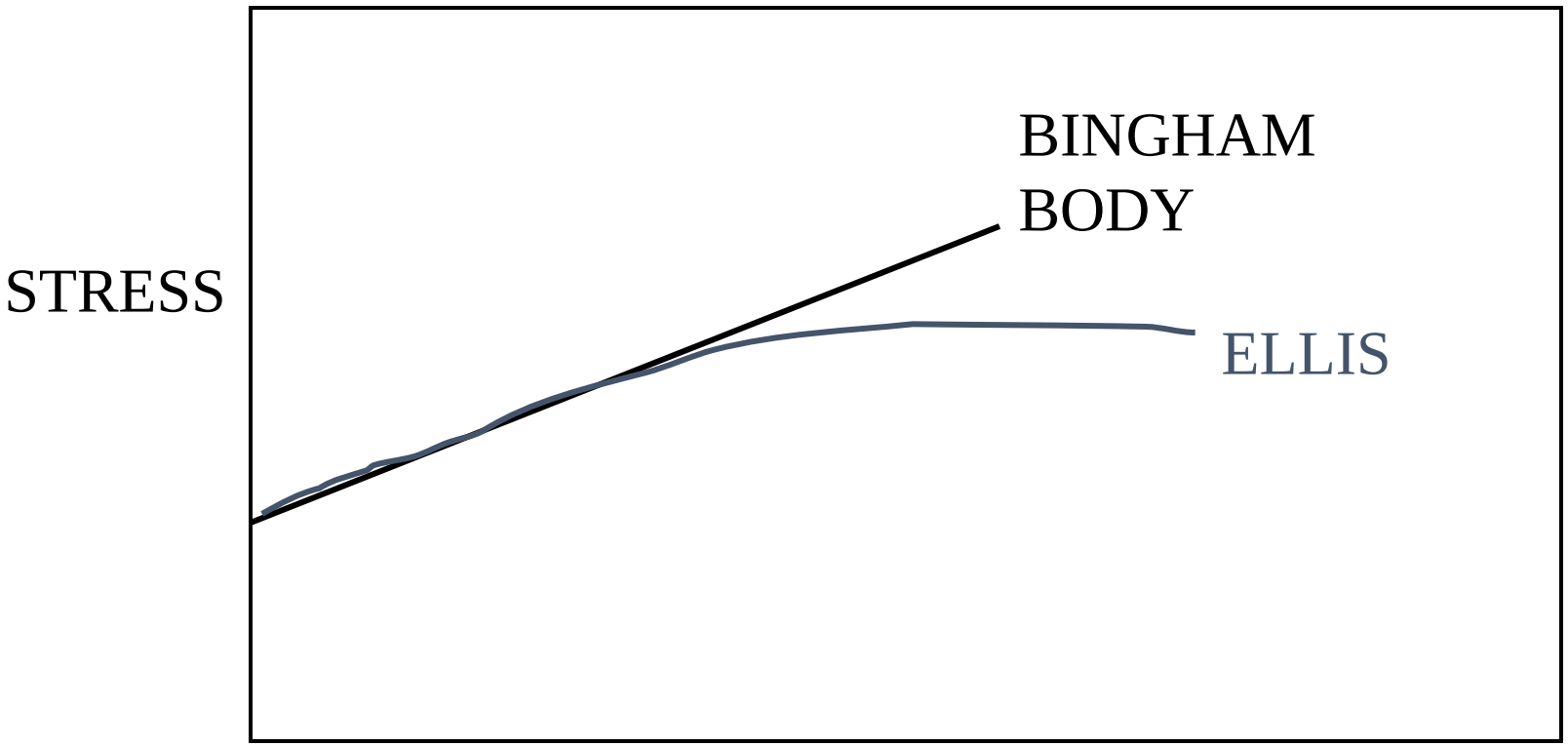

Thixotropy

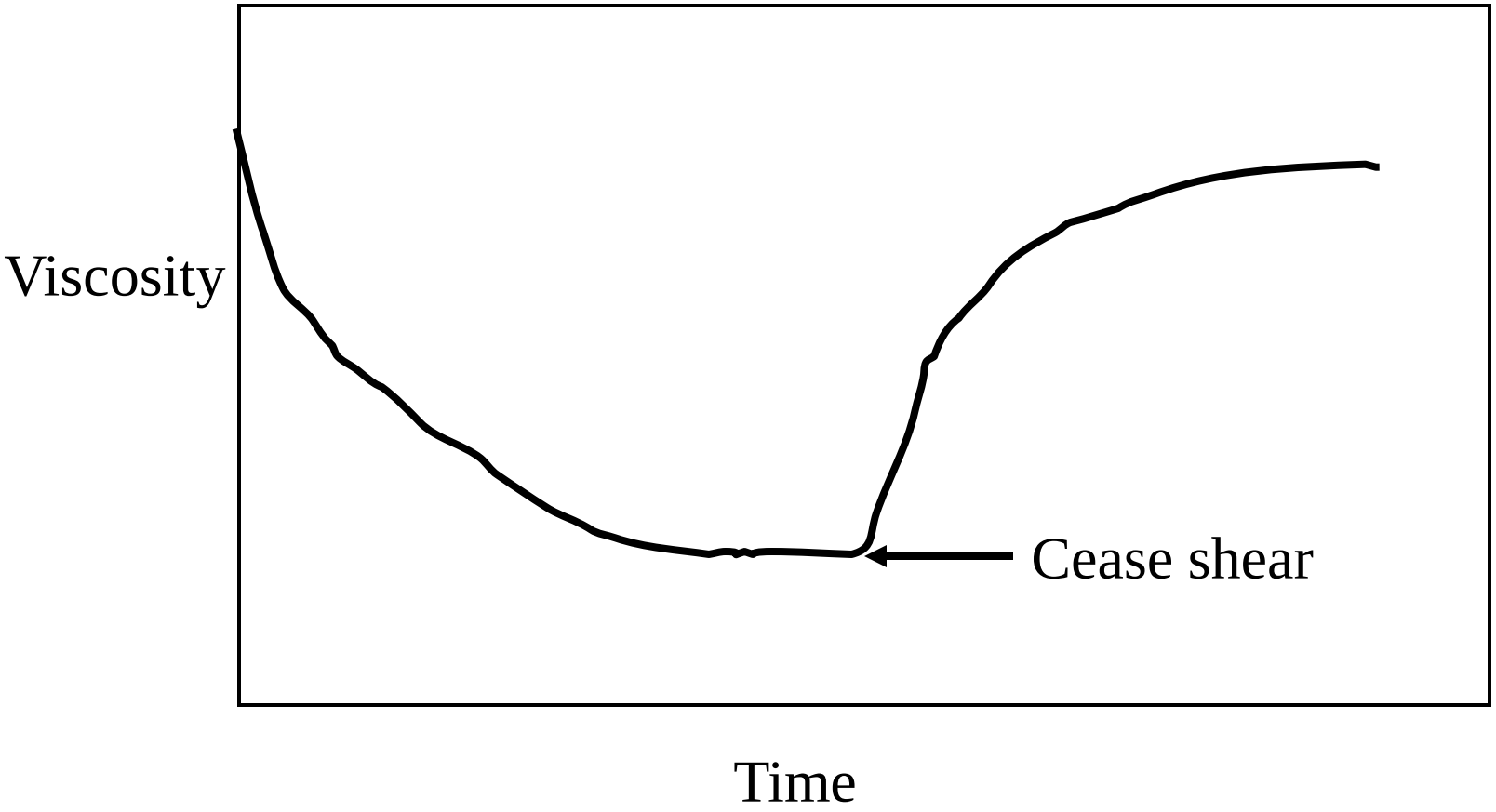

Rheopexy

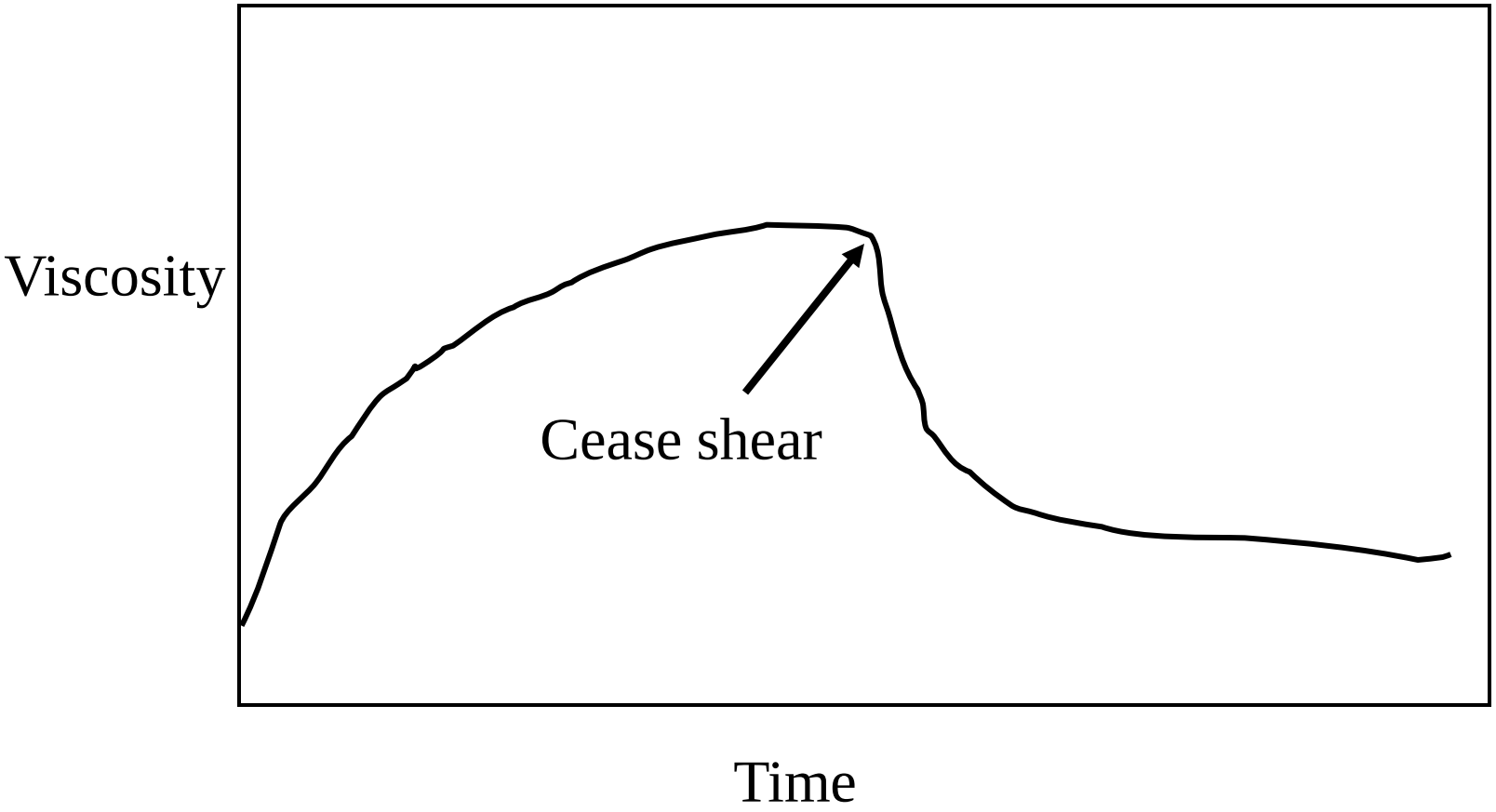

Elastic and Viscous

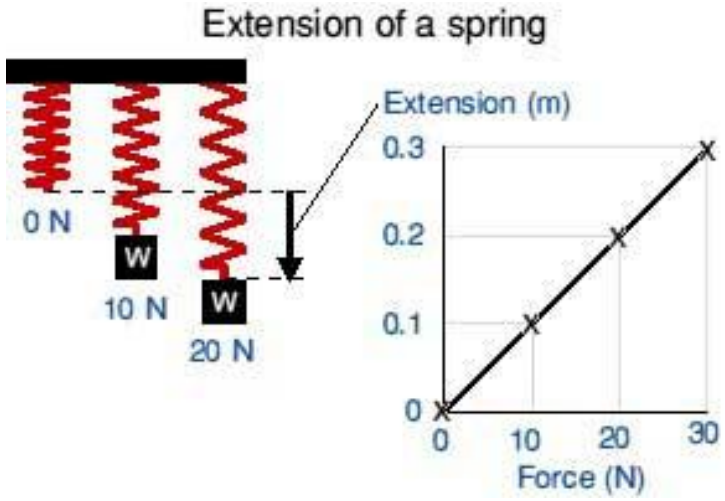

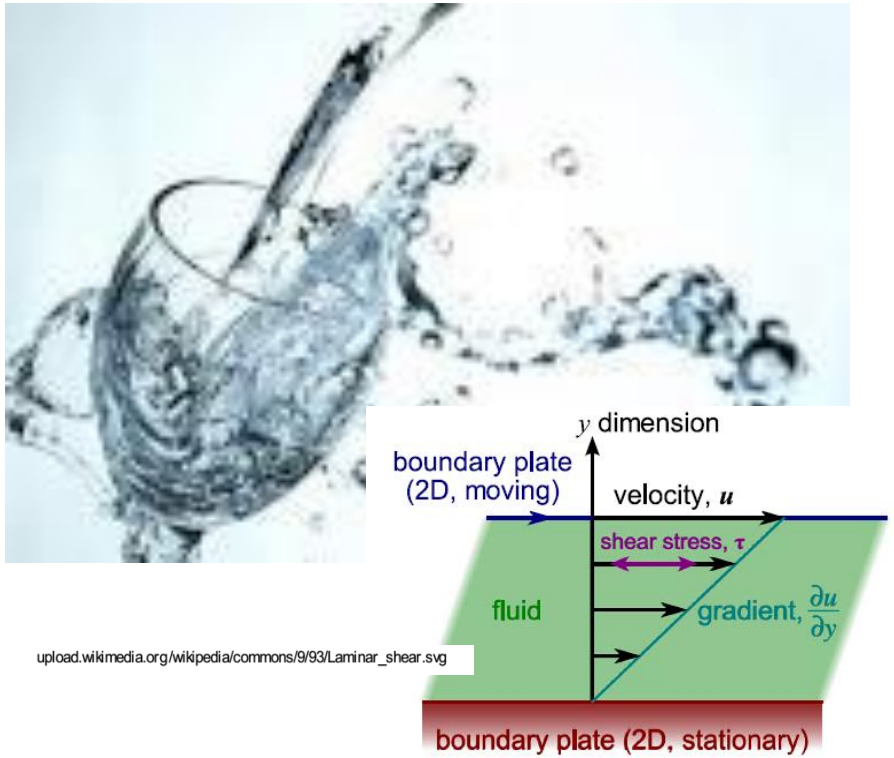

A Spring is an elastic solid

Hooke's law

$$F = kx,$$

For a Newtonian Liquid:

$$F = \mu A \frac{u}{y}$$

http://www.jeron.je/anglia/learn/sec/science/forcemot/page08.htm

http://fineartamerica.com/featured/pouring-liquid-tomislav-

Viscoelasticity

- Polymers are viscoelastic materials
- Purely elastic materials deform when stress is applied and completely recover their original shape when the stress is removed.
- Purely viscous liquids deform when a stress is applied but remain deformed when the stress is removed
  - The higher the stress, the greater the rate of strain
  - The viscosity is the proportionality factor that relates the magnitude of the applied stress to the rate of strain.

Viscoelasticity

- if the stress is held constant, the strain increases with time (creep);
- if the strain is held constant, the stress decreases with time (relaxation);
- the effective stiffness depends on the rate of application of the load; http://www.youtube.com/watch?v=f2XQ97XHjVw
- if cyclic loading is applied, hysteresis (a phase lag) occurs, leading to a dissipation of mechanical energy;

Viscoelasticity

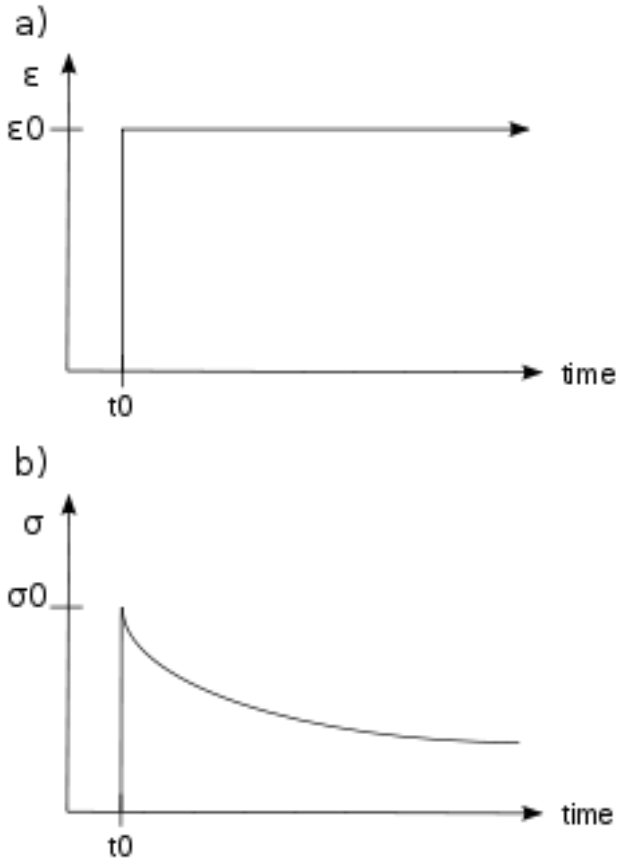

Linear viscoelasticity

$$\epsilon(t) = \frac{\sigma(t)}{E_{\text{inst,creep}}} + \int_0^t K(t-t')\dot{\sigma}(t')dt'$$

Applied stress

Immediate strain

Creep

$$\sigma(t) = E_{\text{inst,relax}}\epsilon(t) + \int_0^t F(t-t')\dot{\epsilon}(t')dt'$$

Applied strain

Immediate stress

Relaxation

•*t* is time, $\epsilon(t)$ is stress , $\sigma(t)$ is strain

• $E_{\text{inst,creep}}$ *is* instantaneous elastic moduli for creep, *I* $E_{\text{inst,relax}}$ *s* instantaneous elastic moduli for relaxation

•*K(t)* is the creep function, *F(t)* is the relaxation function

Storage and Loss Moduli

$$G = G' + iG''$$

Storage Modulus (the elastic component)

Loss Modulus (the viscous component)

$$\sigma = E\varepsilon$$

The elastic component can be modeled as a spring of spring constant E

$$\sigma = \eta \frac{d\varepsilon}{dt}$$

The viscous component can be modeled as a dashpot having a liquid of viscosity η

Springs and Dashpots

- The Maxwell Model

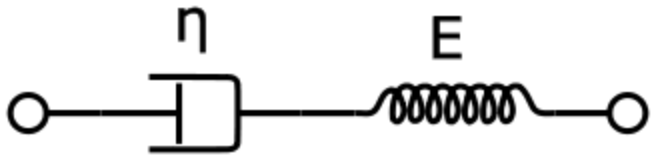

$$\frac{d\epsilon_{Total}}{dt} = \frac{d\epsilon_D}{dt} + \frac{d\epsilon_S}{dt} = \frac{\sigma}{\eta} + \frac{1}{E}\frac{d\sigma}{dt}$$

Predicts strain increasing with time for constant stress
.. But real polymers usually show strain rate decreasing with time

- The Kelvin-Voigt Model

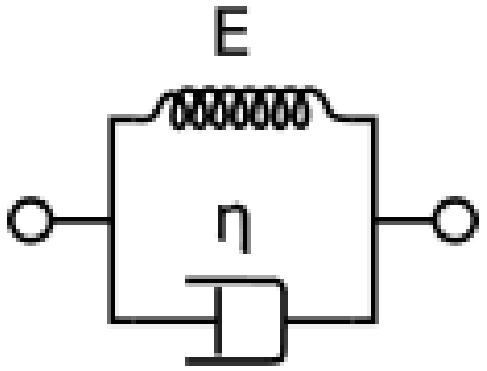

$$\sigma(t) = E\varepsilon(t) + \eta\frac{d\varepsilon(t)}{dt}$$

Good for modeling creep
Not so good for modeling relaxation

http://upload.wikimedia.org/wikipedia/commons/d/db/Maxwell_diagram.svg

Springs and Dashpots

- The Standard Linear Solid Model

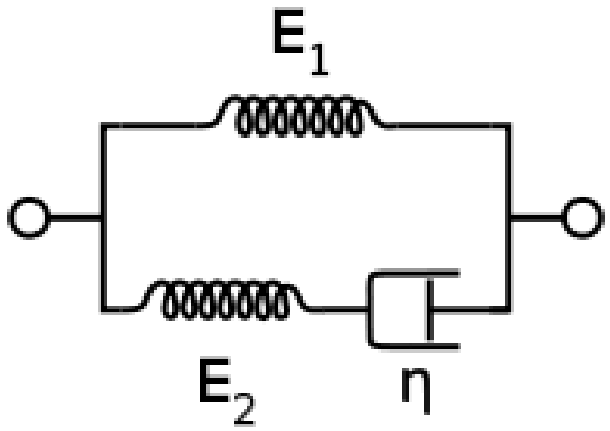

$$\frac{d\varepsilon}{dt} = \frac{\frac{E_2}{\eta}\left(\frac{\eta}{E_2}\frac{d\sigma}{dt} + \sigma - E_1\varepsilon\right)}{E_1 + E_2}$$

More accurate than Maxwell and Kelvin-Voigt for material resonses

…… but inaccurate for specific loads

http://upload.wikimedia.org/wikipedia/commons/d/db/Maxwell_diagram.svg

In Reality there is a Distribution of Relaxation Times

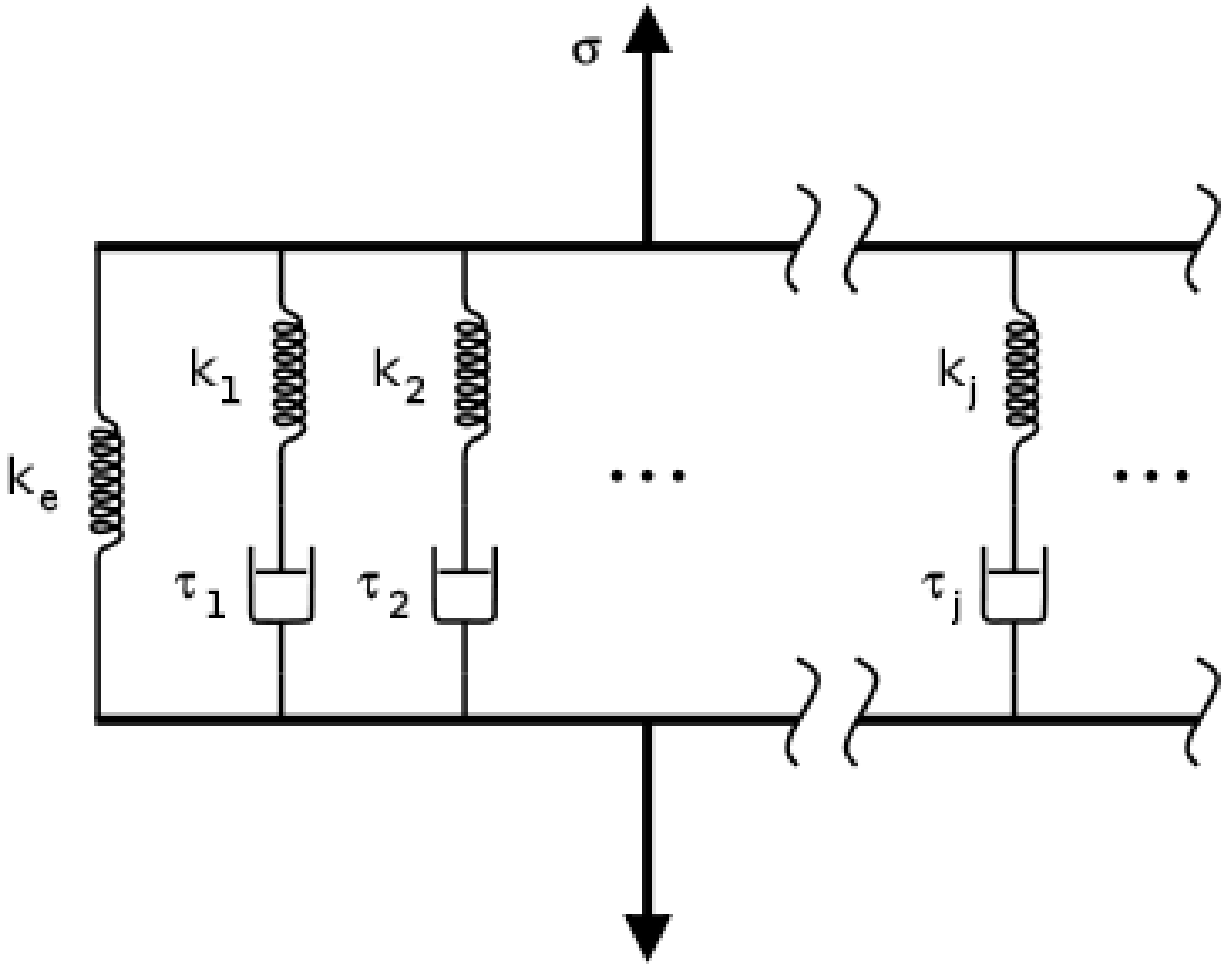

http://upload.wikimedia.org/wikipedia/commons/d/db/Maxwell_diagram.svg

Gel and thickened solution hierarchical structures

- Personal Care thickeners,rheology modifiers and gellants
  - generally function by constructing hierarchical structures

- This is especially true for ‘natural’ thickeners

Particulate Gels

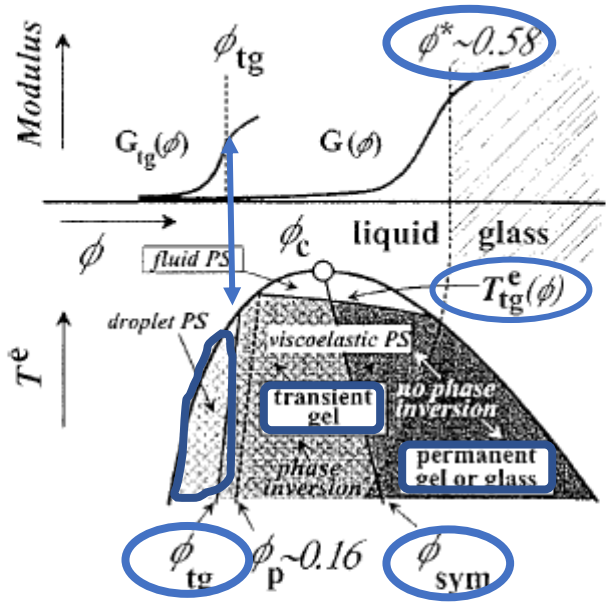

FIG. 10. Schematic diagram showing relationship between thermodynamics and rheology of a colloidal system exhibiting phase separation (PS) and transient gelation (tg). The plot of shear modulus G against volume fraction ϕ represents the rapid change in rheology caused by rapid quenching to low effective temperature T^e well inside the two-phase region. Various characteristic volume fractions can be identified: ϕ_{tg}, gelation threshold; ϕ_c, critical point; ϕ_p, percolation threshold; ϕ_{sym}, line of symmetry of phase coexistence; ϕ^*, glass transition point. (Reprinted with permission from Ref. 90. Copyright 1999 by the American Physical Society.)

Structure and Rheology of Simulated Gels Formed from Aggregated Colloidal Particles

Journal of Colloid and Interface Science **225**, 2–15 (2000)

Eric Dickinson

Procter Department of Food Science, University of Leeds, Leeds LS2 9JT, U.K.

Rheology of 'gel' structures at equilibrium

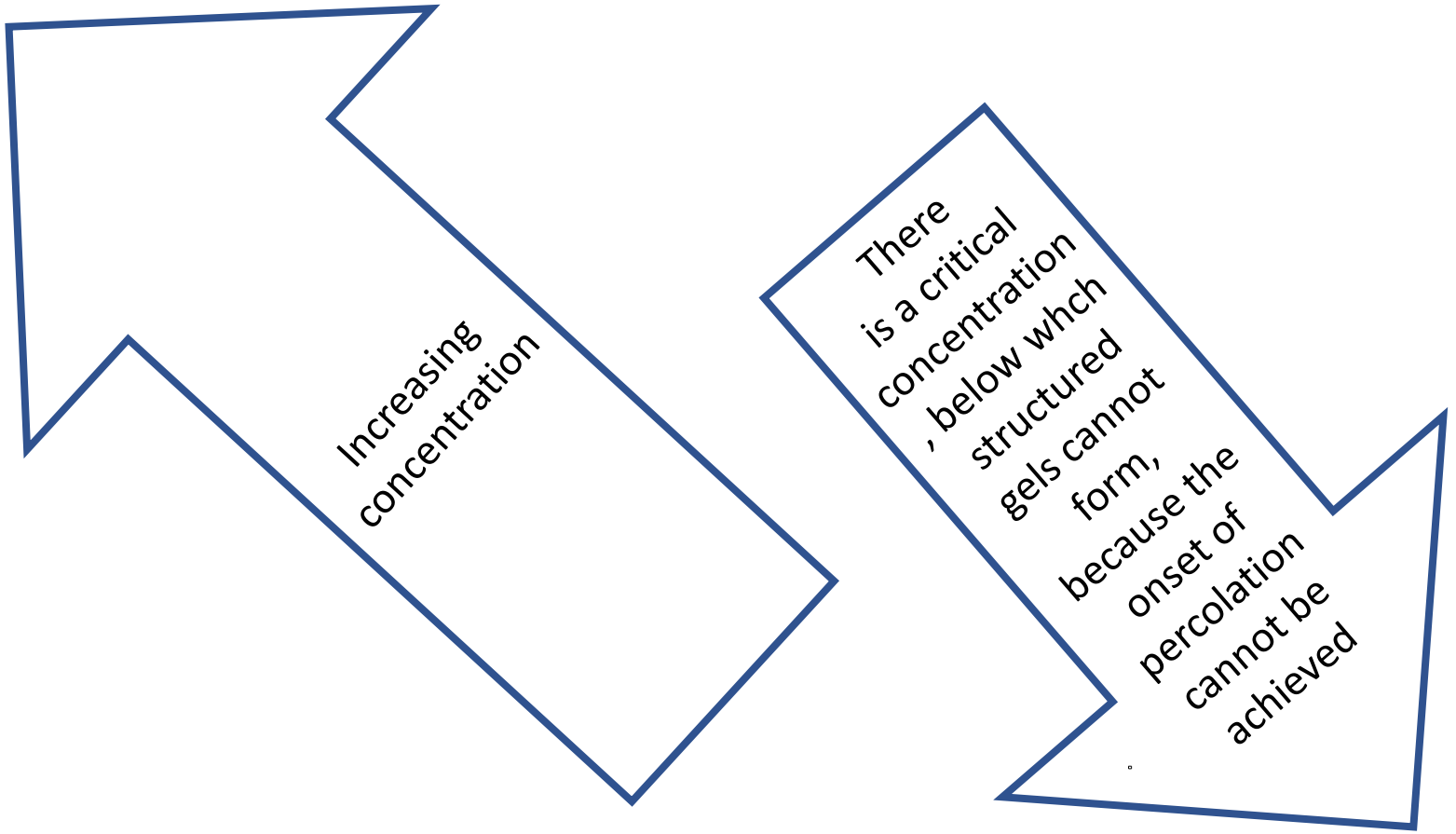

Yield Stress Fluids and failure of the Cox-Merz Rule

- At low strains , the structured ‘gels’ show elastic recovery
  - That is, they behave like elastic solids
- However, under steady shear, these gels flow like liquids
  - Whereas solids would fracture
- Therefore, structured gels behave like solids at low strains
  - Above a certain stress (yield stress) they flow like liquids.

- The empirical Cox-Merz rule states that the viscosity/rate of strain behavior is comparable to the complex viscosity/frequency behavior
  - The Cox –Merz rule is obeyed for many solutions
  - However, structured gels usually disobey the Cox-Merz rule
    - Because they cease to be flowable fluids below the yield stress

CONSIDER A POLYMER AS A STICKY PARTICLE

The Rheology of Aqueous Solutions of Hydroxyethylcellulose

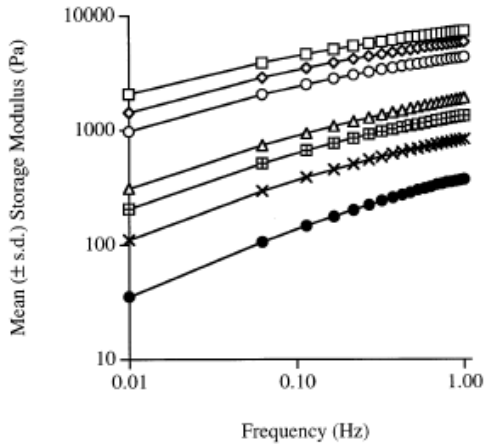

Fig. 1. The effects of polymer concentration (% w/w) and oscillatory frequency on the storage modulus (G′) of gels composed of hydroxyethylcellulose. Key: 3% w/w (●), 4% w/w (☆), 5% w/w (⊠), 6% w/w (△), 8% w/w (○), 10% w/w (◇) and 12% w/w (□). Each datum represents the mean (±S.D.) of at least three replicate measurements.

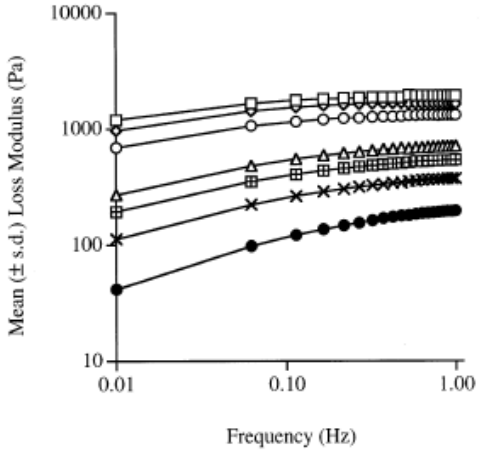

Fig. 2. The effects of polymer concentration (% w/w) and oscillatory frequency on the loss modulus (G″) of gels composed of hydroxyethylcellulose. Key: 3% w/w (●), 4% w/w (☆), 5% w/w (⊠), 6% w/w (△), 8% w/w (○), 10% w/w (◇) and 12% w/w (□). Each datum point represents the mean (±S.D.) of at least three replicate measurements.

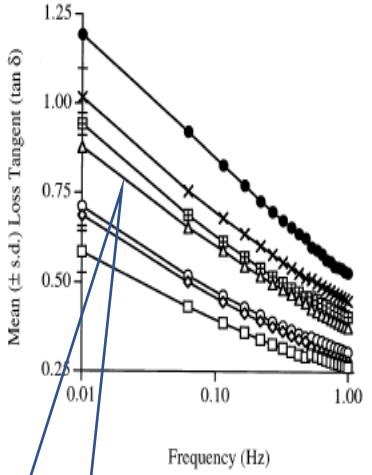

Fig. 3. The effects of polymer concentration (% w/w) and oscillatory frequency on the loss tangent (tan δ) of gels composed of hydroxyethylcellulose. Key: 3% w/w (●), 4% w/w (☆), 5% w/w (⊠), 6% w/w (△), 8% w/w (○), 10% w/w (◇) and 12% w/w (□). Each datum point represents the mean (±S.D.) of at least three replicate measurements.

ELSEVIER

International Journal of Pharmaceutics 151 (1997) 223–233

international journal of pharmaceutics

Textural, viscoelastic and mucoadhesive properties of pharmaceutical gels composed of cellulose polymers

David S. Jones *, A. David Woolfson, Andrew F. Brown

The Pharmaceutical Devices Group, School of Pharmacy, The Queen's University of Belfast, Medical Biology Centre, 97, Lisburn Road, Belfast BT9 7BL, United Kingdom

Received 1 December 1996; accepted 24 January 1997

Tanδ is G”/G’. Therefore all HEC solutions >3% are more elastic than viscous

The Rheology of Aqueous Solutions of Hydroxyethylcellulose

All formulations examined in this study exhibited wide ranges of viscoelastic properties that were dependent both on the concentration of the constituent polymers, i.e. HEC and Na CMC, and also on the oscillatory frequency. In all cases, the storage modulus increased as the frequency of oscillation increased, indicating a greater elastic character. This is consistent with the Maxwellian description of the response of viscoelastic materials to oscillatory stresses (Barry, 1974). Thus, at high frequencies, sufficient time is available to enable spring elongation and contraction under the imposed oscillatory shear, however, there is insufficient time available to allow for dashpot movement. Consequently, at these frequencies, the gels behaved as an elastic solid. As the oscillatory frequency is decreased, there is more time available to allow for dashpot extension and thus the materials exhibit properties characteristic of both solids and liquids. Ultimately, the storage modulus of all materials should approach zero, however, this was not observed in any of the gel systems.

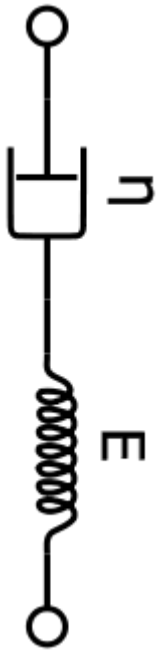

Slow viscous response

Fast elastic response

Relaxation:

Process A:

$$\tau_A = \frac{1}{6\pi^2}\frac{\zeta_0 b^2}{kT}N_e^2$$

$$G(t) = \frac{\rho RT}{M_e}\frac{1}{\langle|Eu|\rangle}\sum_{p=1}^{n_1}\exp\left(-\frac{tp^2}{\tau_A}\right)$$

Process B

$$\tau_B = \frac{\zeta_0 b^2 N^2 N_e^2}{3\pi^2 kT}$$

$$G(t) = \frac{\rho RT}{M_e}\sum_{p=1}^{N}\frac{1}{N}\exp\left(-\frac{p^2 t}{\tau_B}\right)$$

Process C:

$$\tau_C = \frac{1}{\pi^2}\frac{\zeta_0 a^2 N_e N^3}{kT}$$

$$G(t) = \frac{\rho RT}{M_e}\sum_{p\ \mathrm{odd}}\frac{8}{p^2\pi^2}\exp\left(-\frac{p^2 t}{\tau_C}\right)$$

ELSEVIER International Journal of Pharmaceutics 151 (1997) 223–233

international journal of pharmaceutics

Textural, viscoelastic and mucoadhesive properties of pharmaceutical gels composed of cellulose polymers

David S. Jones *, A. David Woolfson, Andrew F. Brown

The Pharmaceutical Devices Group, School of Pharmacy, The Queen's University of Belfast, Medical Biology Centre, 97, Lisburn Road, Belfast BT9 7BL, United Kingdom

Received 1 December 1996; accepted 24 January 1997

The slow viscous response arises from:

The longest Rouse-Zimm Modes

The coil would be expected to stretch under shear (De Gennes). The 'dashpot' relaxation in this case would be the stretching and re-formation of the coil.

Reptation is probably not significant in dilute solution. It may be important in concentrated solutions.

Rheology and Sensorial Attributes

- For Hydrogels, gel-like suspensions/emulsions
  - Rheological parameters that can be correlated with sensory perception include
    - Yield stress
    - Thixotropy
    - Wall slip
    - Shear banding
- These all should be measured for correlation of rheology with sensorial properties

S. Ozkan, T. W. Gillece, L. Senak and D. J. Moore, Characterization of yield stress and slip behaviour of skin/hair care gels using steady flow and LAOS measurements and their
correlation with sensorial attributes , International Journal of Cosmetic Science, 2012, 34, 193–201

Extension of coils and rods

ELSEVIER

International Journal of Biological Macromolecules 40 (2007) 327–335

INTERNATIONAL JOURNAL OF Biological Macromolecules STRUCTURE, FUNCTION AND INTERACTIONS

www.elsevier.com/locate/ijbiomac

Hydrodynamic properties of DNA and DNA–lipid complex in an elongational flow field

Naoki Sasaki [a,*], Hidetomo Ashitaka [b], Kenji Ohtomo [a], Akimasa Fukui [a]

[a] *Division of Biological Sciences, Graduate School of Science, Hokkaido University, Kita-ku, Sapporo 060-0810, Japan*
[b] *Chitose Institute of Science and Technology, 758-65, Bibi, Chitose 066-8655, Japan*

Received 22 May 2006; received in revised form 21 August 2006; accepted 29 August 2006
Available online 4 October 2006

A cooperative coil-rod transition occurs at a critical elongational shear rate

There is no critical shear rate for rods --- they show increasing alignment with the shear field as the shear rate increases

Ordered structures show up as birefringent shear bands

The alignment shows up as a generalized birefringence in the high shear regions of the 4-roll mill

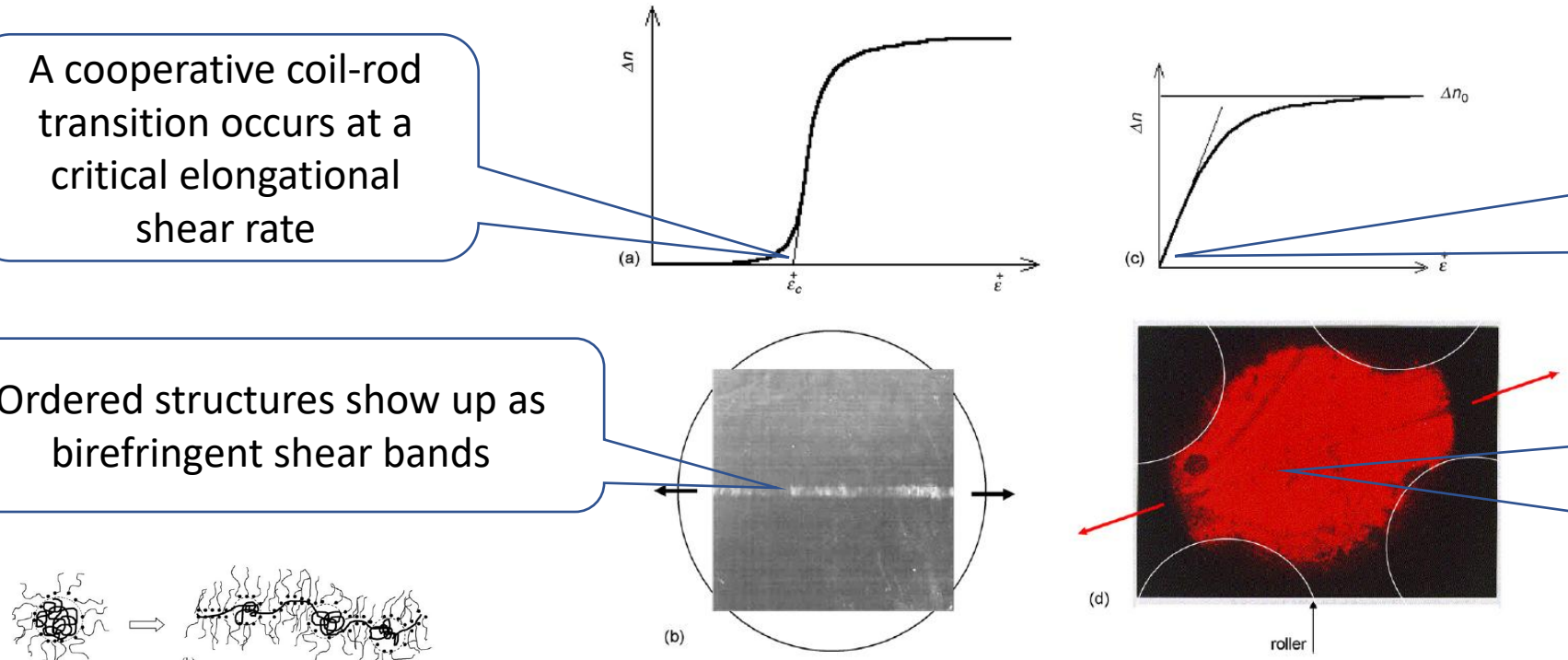

Fig. 2. (a) Schematic drawing of elongational flow-induced birefringence of flexible polymers as a function of strain rate $\dot{\varepsilon}$. $\dot{\varepsilon}_c$ is the critical strain rate for the coil–stretch transition. (b) Flow-induced birefringence pattern of a flexible polymer solution (high-molecular-weight polyethylene oxide (PEO) in low-molecular-weight PEO aqueous solution). Arrows indicate flow directions and a circle represents an optical microscopic field. (c) Schematic drawing of elongational flow-induced birefringence of rigid rod-like molecules as a function of strain rate $\dot{\varepsilon}$. (d) Flow-induced birefringence pattern of rigid rod-like polymer solution (poly(γ-methyl-D-glutamate) in chloroform). White circles indicate four rollers. Arrows show flow directions.

Cellulosic thickeners: Hydroxypropylcellulose HPC

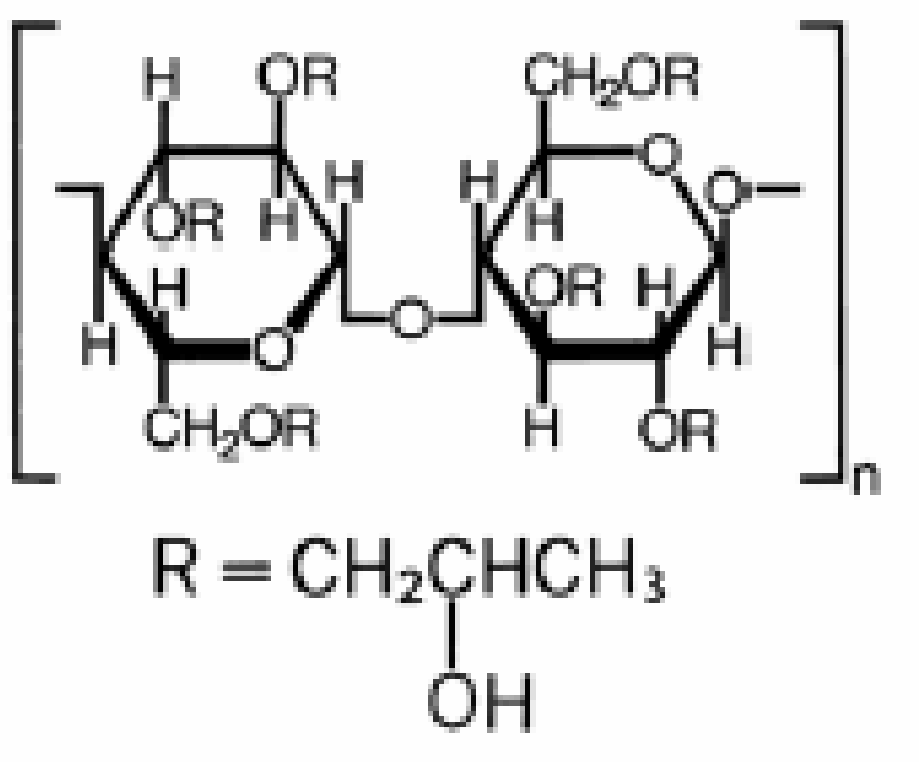

- Degree of Substitution (0-3) and Molar substitution
- Nonionic thickener
- Shear-thinning Rheology
- Low LCST (40C)

Rheological Studies on the Phase Separation of Hydroxypropylcellulose Solution Systems

SYUJI FUJII, NAOKI SASAKI, MITSUO NAKATA

Department of Biological Sciences, Graduate School of Science, Hokkaido University, Kita-ku, Sapporo 060-0810, Japan

T_{max} and T_{min} arise from change in chain flexibility with temperature

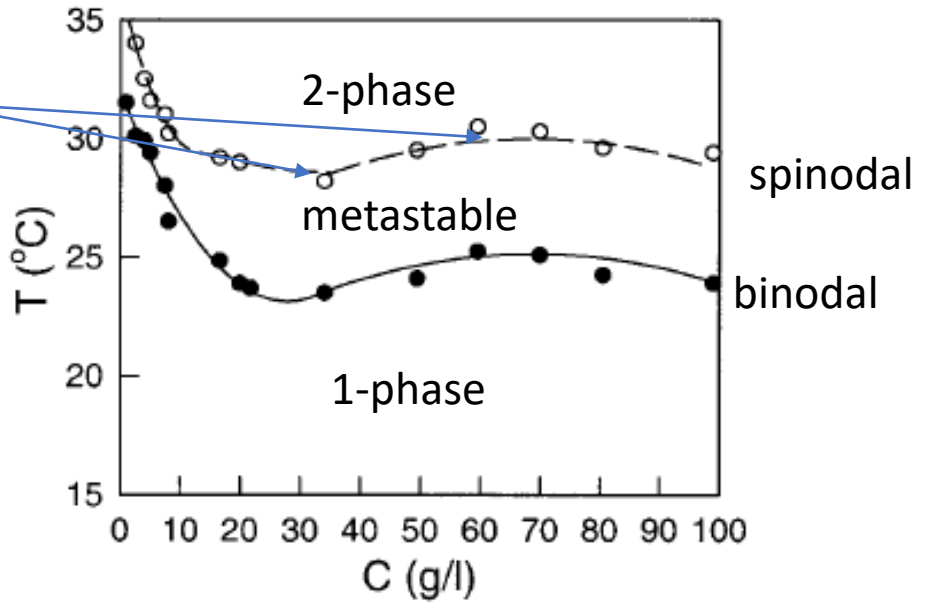

Figure 1. Phase diagram of HPC in a mixed solvent of 33.6 wt % of glycerol aqueous solution. Solid and dashed curves coincide with a cloud point T_p (●) and an apparent spinodal point temperature T_s (○), respectively.

experiments. The addition of glycerol to the water made the solvent very viscous. Because an increase in the solvent viscosity η_s slows down the relaxation of a polymer, it is possible to measure the flow birefringence even if the polymer concentration is low.

The Master Curve for Relaxation under extensional flow for Hydroxypropylcellulose

Normalize w.r.t, Debra Number

$$r = (\dot{\varepsilon} - \dot{\varepsilon}_c)/\dot{\varepsilon}_c$$

$$= D_e - 1$$

$$\mathrm{De} = \frac{t_c}{t_p} = \frac{\text{Stress relaxation time}}{\text{Time of observation}}$$

Below Tp
Same relaxation process at different temps.

Above Tp
Different relaxation processes: the curves do not fit on a single master curve

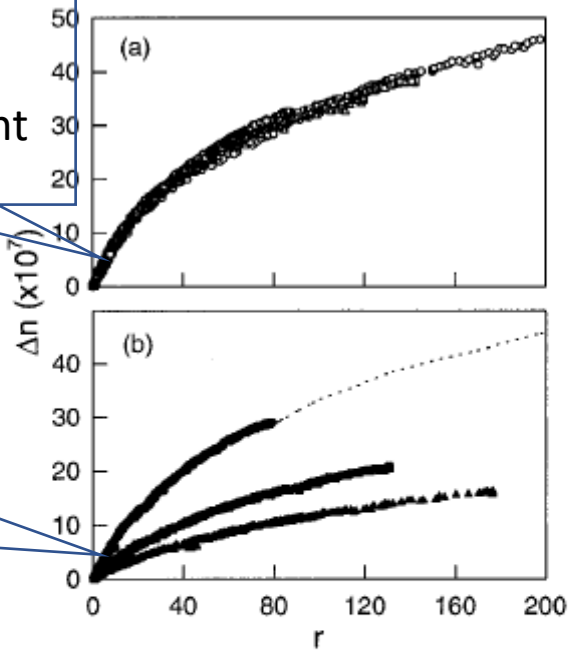

Figure 3. Elongational flow-induced birefringence Δn as a function of reduced strain rate, r. (a) In the one-phase region, a master curve was constructed. (b) In the two-phase region, the dotted line is the master curve constructed in the one-phase region in (a). The open and filled symbols indicate the birefringence before and after the phase separation, respectively. Here, the data sets in Figure 2 were replotted.

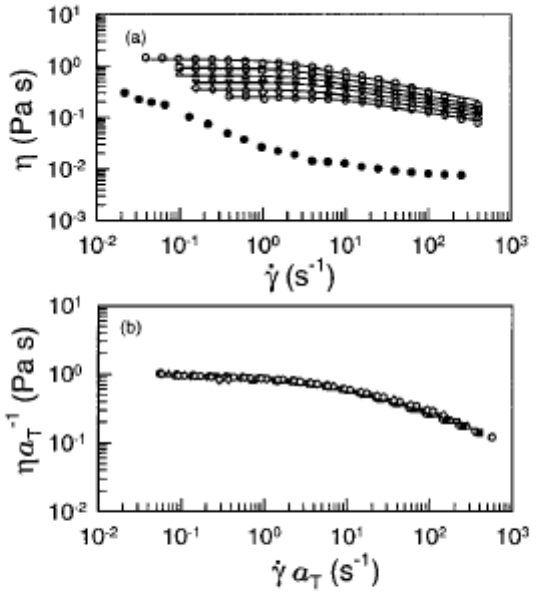

Figure 7. (a) Shear viscosity as a function of shear rate for HPC of 19.99 g/L at various temperatures: 5 (○), 10 (□), 15 (△), 20 (▽), 25 (◇), 30 (○), and 35 °C (●). (b) Shear viscosity multiplied by the inverse of a shift factor plotted as a function of shear rate multiplied by the shift factor. The reference temperature is 10 °C.

Master curve wrt shear rate indicates same relaxation process at different temperatures

Hydroxypropylcellulose

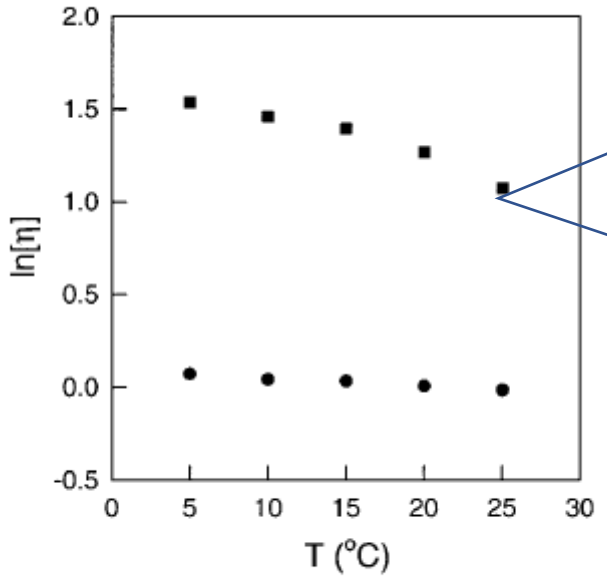

The hydrodynamic volume decreases with T increase (below Tp) *i.e.* the Kuhn length gets shorter

Figure 4. Intrinsic viscosity in (dL/g) as a function of the temperature for HPC of molecular weight 89,000 (●) and 437,000 (■) in a mixed solvent of glycerol and water.

Birefringence due to coil-rod transition during extension

Rheological Studies on the Phase Separation of Hydroxypropylcellulose Solution Systems

SYUJI FUJII, NAOKI SASAKI, MITSUO NAKATA

Department of Biological Sciences, Graduate School of Science, Hokkaido University, Kita-ku, Sapporo 060-0810, Japan

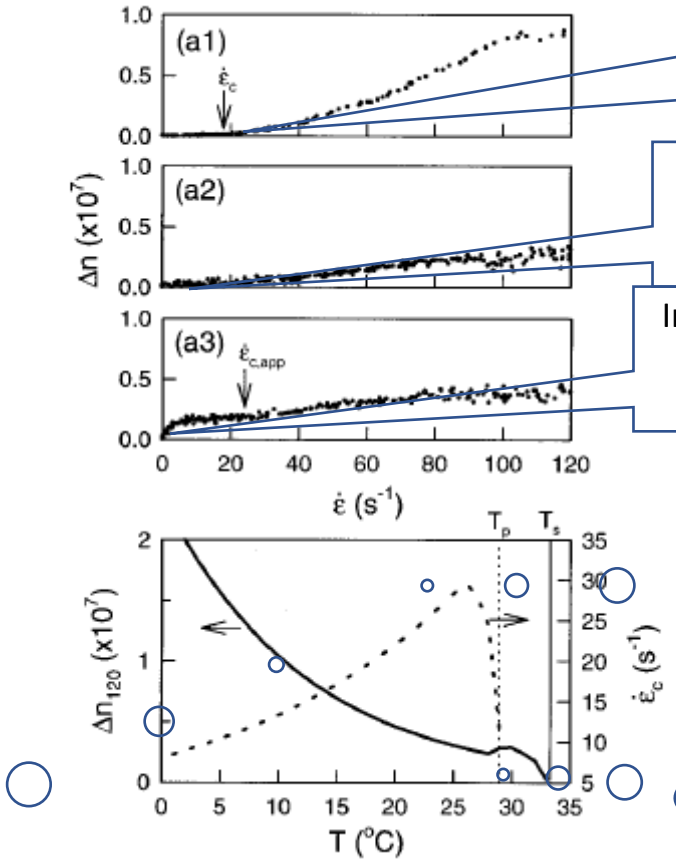

Critical strain rate indicates coil-rod transition below Tp

Transition to rod alignment *i.e.* rods present prior to shear in metastable region

In two phase region above Tp, the rod alignment is more prominent

The critical strain rate increases with T until the phase transition (Kuhn Length Decreasing)

The critical strain rate disappears at the binodal temp (the polymer becomes rod-like)

Figure 6. Temperature evolution of the birefringence pattern as a function of elongational strain rate from the one-phase region (near the phase boundary) to the two-phase region. (a1) A coil-stretch transition-like pattern with critical strain rate observed in the one-phase region. (a2) Intermediate pattern from the coil-stretch transition-like to mixed pattern. (a3) Mixed pattern of rigid rodlike and flexible-like responses in the two-phase region. (b) Temperature dependence of the birefringence intensity at 120 s^{-1}, Δn_{120}, and critical strain rate, ε_c. Vertical dotted and solid lines correspond to T_p and the apparent spinodal point T_s. Each diagram is based on the results of $C = 4.98$ g/L in our previous article.[20]

Zipper mode l for the formation of junction zones

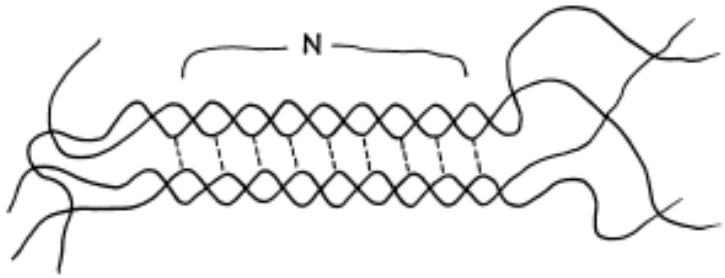

Fig. 1. — A single zipper with N links. Links can be opened from both ends. If the links 1, 2, ..., p are all open, the energy required to open the p + 1st link is E. Helices may not necessarily be double helices ; they may be single helices or triple helices. Here, double helices represent the association of somewhat ordered structure symbolically.

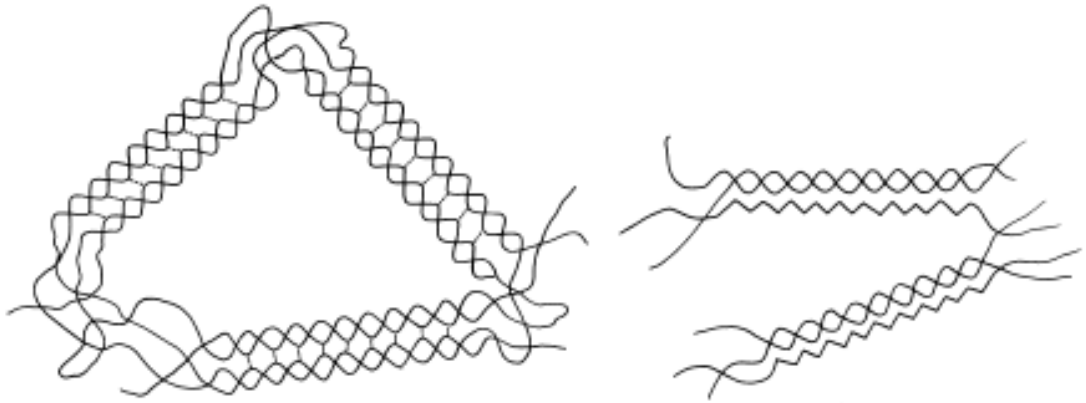

Fig. 2. — (a) Gels consisting of zippers of one kind. Gels consist of microcrystalline regions and amorphous regions. The former is called junction zones, and consist of association of molecules with ordered structure. (b) Gels consisting of zippers of one kind. Schematic representation of a mixed gel of galactomannan whose backbone is shown by a zigzag and xanthan shown by a double helix (proposed by Dea).

J. Phys. France **51** (1990) 1759-1768 15 AOÛT **1990,** PAGE 1759

Classification
Physics Abstracts
44.50 — 61.90 — 82.70

A zipper model approach to the thermoreversible gel-sol transition

K. Nishinari ([1, *]), S. Koide ([2]), P. A. Williams ([1]) and G. O. Phillips ([1])

([1]) Polymer and Colloid Chemistry Group, The North East Wales Institute, Connah's Quay, Deeside, Clwyd CH5 4BR, G.B.
([2]) President, Yamanashi University, Takeda 4, Kofu, Yamanashi, Japan

(*Received on January 19, 1990, revised on April 24, 1990, accepted on April 26, 1990*)

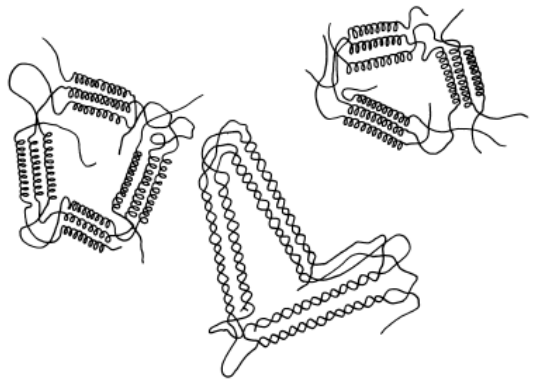

Fig. 3. — Gels consisting of various zippers (phase separated). When two gel-forming macromolecules are mixed, and form a gel, the gel consists of separated two regions if these two macromolecules do not interact so strongly.

Zipper model for the formation of junction zones

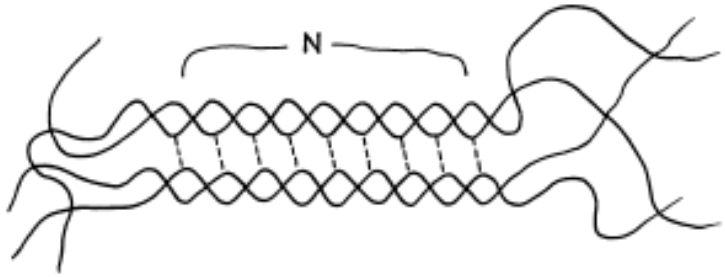

Fig. 1. — A single zipper with N links. Links can be opened from both ends. If the links 1, 2, ..., p are all open, the energy required to open the $p + 1$st link is E. Helices may not necessarily be double helices ; they may be single helices or triple helices. Here, double helices represent the association of somewhat ordered structure symbolically.

J. Phys. France **51** (1990) 1759-1768 15 AOÛT **1990,** PAGE 1759

Classification
Physics Abstracts
44.50 — 61.90 — 82.70

A zipper model approach to the thermoreversible gel-sol transition

K. Nishinari ([1, *]), S. Koide ([2]), P. A. Williams ([1]) and G. O. Phillips ([1])

([1]) Polymer and Colloid Chemistry Group, The North East Wales Institute, Connah's Quay, Deeside, Clwyd CH5 4BR, G.B.
([2]) President, Yamanashi University, Takeda 4, Kofu, Yamanashi, Japan

(*Received on January 19, 1990, revised on April 24, 1990, accepted on April 26, 1990*)

The partition function for such a single zipper is given by

$$\zeta = \sum_{p=0}^{N-1} (p+1)\, G^p \exp(-pE/\tau) \tag{1}$$

where $\tau = kT$. If the chain is long enough, the terminal contribution may be ignored and

$$\zeta = [1 - (N+1)\, x^N + N x^{N+1}]/(1-x)^2 \tag{2}$$

$$x = G \exp(-E/\tau)$$

is easily obtained from equation (1).

Now, we consider a system consisting of $\mathcal{N}$ single zippers each of which has N links. The partition function Z of this system is given by

$$Z = (\zeta)^{\mathcal{N}}. \tag{3}$$

Since the heat capacity C of this system is given by

$$C = kT^2 \frac{\partial^2}{\partial T^2} \log Z + 2\, kT \frac{\partial}{\partial T} \log Z \tag{4}$$

the substitution of (2), (3) into (4) leads to

$$\frac{C}{k} = \mathcal{N} \left(\log \frac{G}{x} \right)^2 \left[\frac{2x}{1-x} + \frac{N(N+1)\, x^N [-x^{N+1} + (N+1)\, x - N]}{[1 - (N+1)\, x^N + N x^{N+1}]^2} \right]. \tag{5}$$

Zipper model for the formation of junction zones

J. Phys. France **51** (1990) 1759-1768 15 AOÛT **1990,** PAGE 1759

Classification
Physics Abstracts
44.50 — 61.90 — 82.70

A zipper model approach to the thermoreversible gel-sol transition

K. Nishinari ([1, *]), S. Koide ([2]), P. A. Williams ([1]) and G. O. Phillips ([1])

([1]) Polymer and Colloid Chemistry Group, The North East Wales Institute, Connah's Quay, Deeside, Clwyd CH5 4BR, G.B.
([2]) President, Yamanashi University, Takeda 4, Kofu, Yamanashi, Japan

(*Received on January 19, 1990, revised on April 24, 1990, accepted on April 26, 1990*)

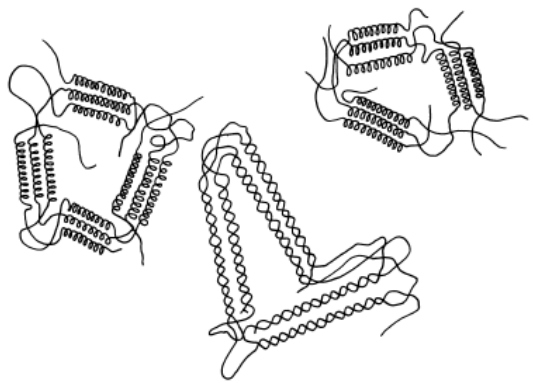

Fig. 3. — Gels consisting of various zippers (phase separated). When two gel-forming macromolecules are mixed, and form a gel, the gel consists of separated two regions if these two macromolecules do not interact so strongly.

When the interaction among different components is not strong as in the case of blend gels of agarose and gelatin, the gels formed on cooling may be thought as a phase separated gel as shown in figure 3. We consider here the case in which junction zones consist of associations with n different kinds of (not molecules but) zippers. Then, n is not necessarily equal to the number of molecular species. Let $N_1, N_2, \ldots, N_n$ be the number of links of single zippers of various kinds 1, 2, ..., n respectively. We assume that a gel consists of $\mathcal{N}_1$ single zippers of the kind 1 and $\mathcal{N}_2$ single zippers of the second kind 2, and so on. The heat capacity of such a system is written as

$$\frac{C}{k} = \sum_i C_i \qquad (6)$$

where C_i is given by equation (5).

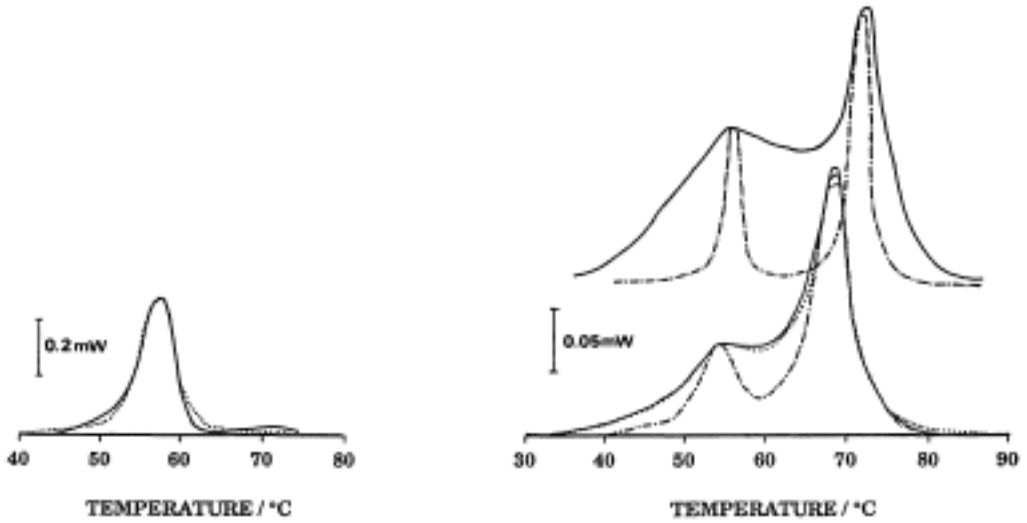

K-CARRAGEENAN

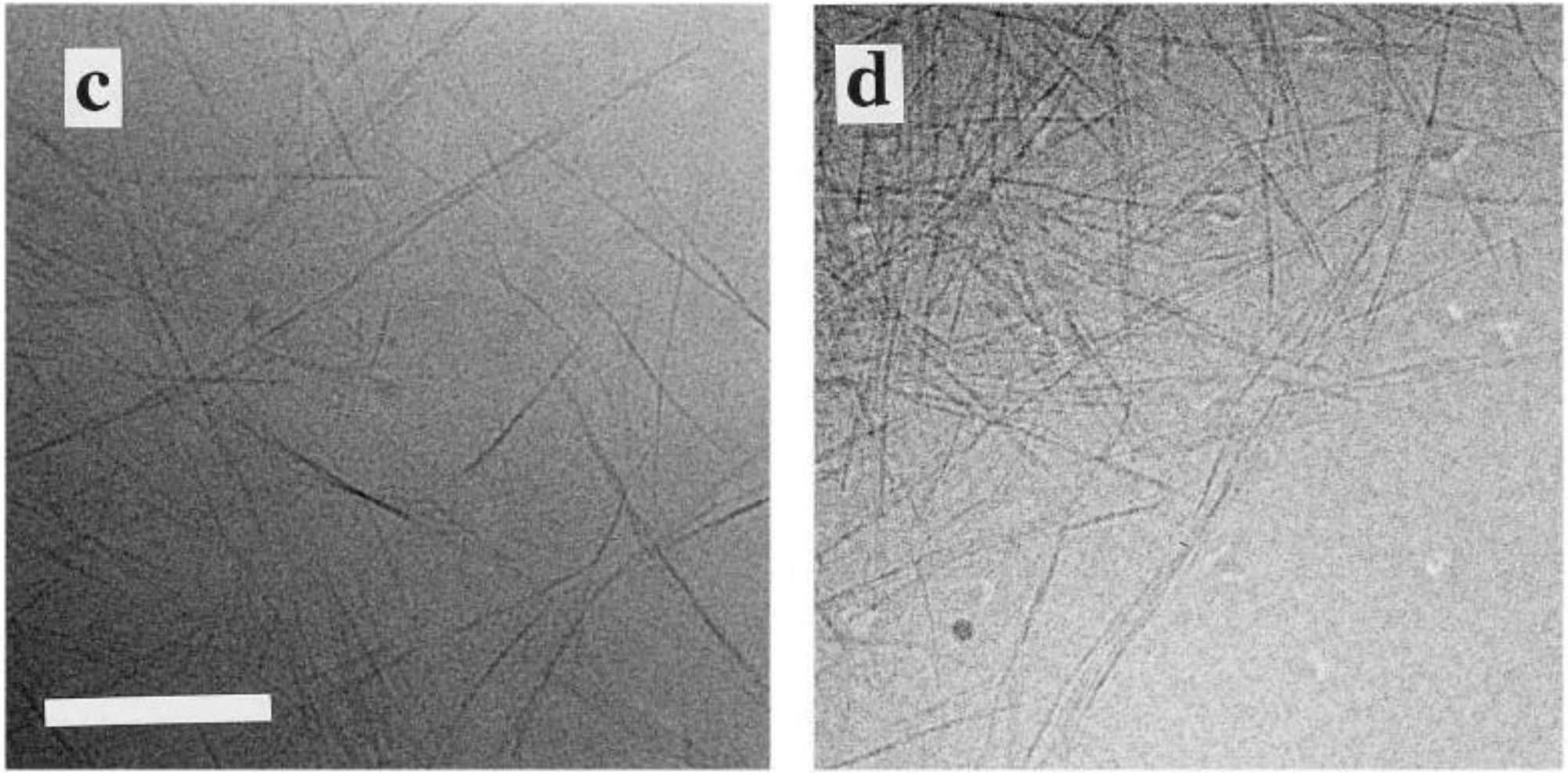

Fig. 3. Cryo-TEM images of vitrified 0.1% degraded κ-carrageenan in 0.1 M mixed salt solutions at $x_{Cs} = 0.3$ (a), 0.4 (b), 0.6 (c
and 1 (d). Scale bar = 100 nm. The samples were equilibrated at 25–30°C before vitrification. See [15] for detailed experimenta
nformation

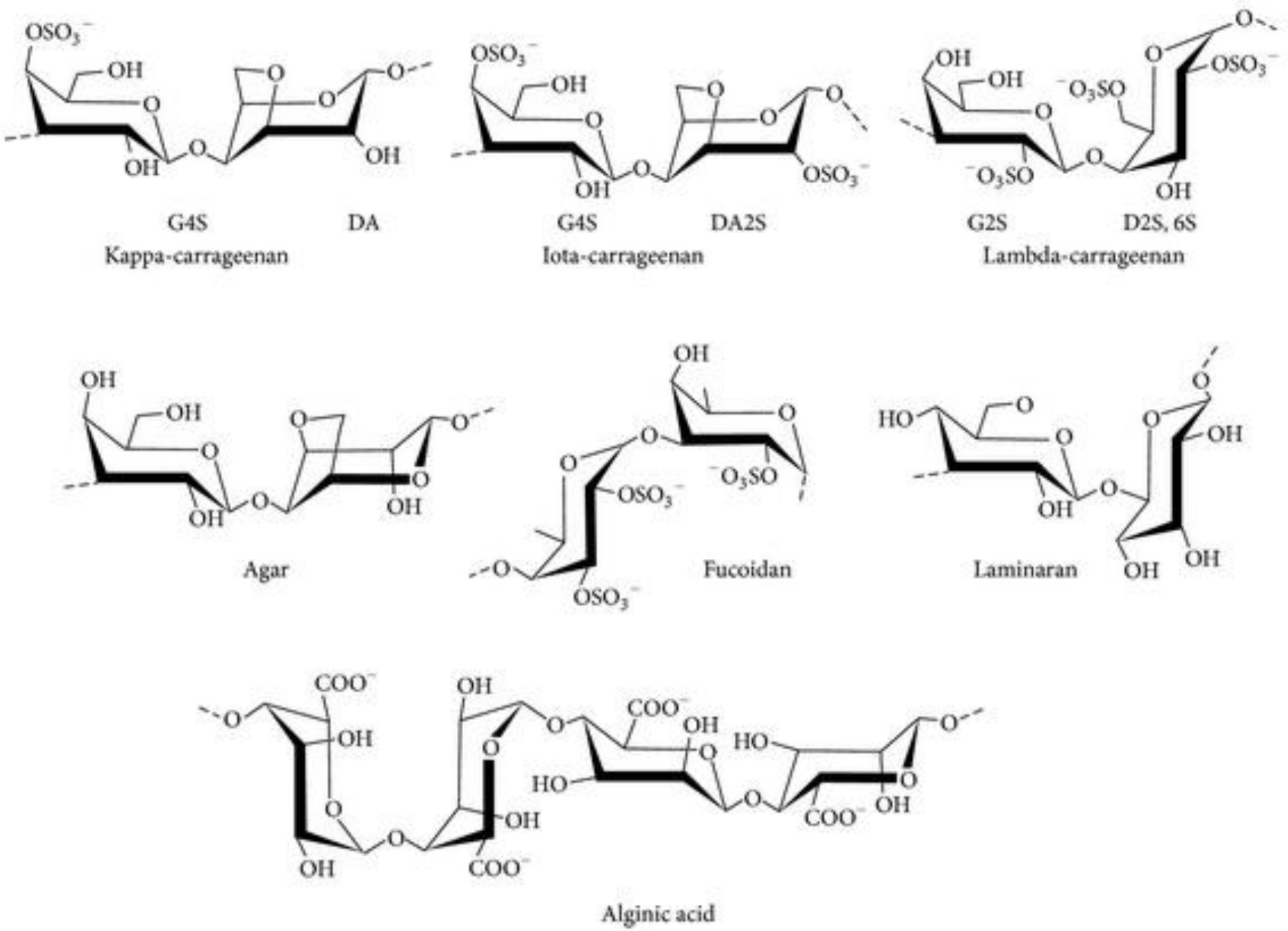

Carrageenan AFM

Andrew R. Kirby
A. Patrick Gunning
Victor J. Morris
Institute of Food Research
Norwich Laboratory
Norwich Research Park
Colney, Norwich NR4 7UA, UK

Imaging Polysaccharides by Atomic Force Microscopy

Biopolymers, Vol. 38, 355–366 (1996)

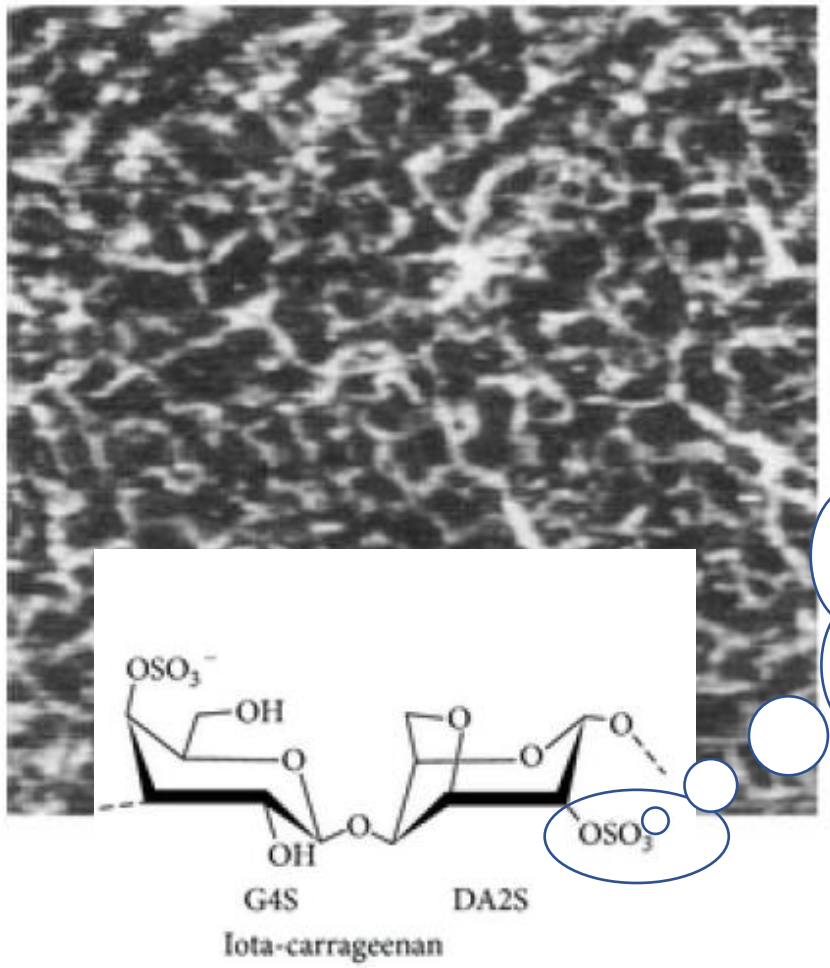

2-sulfate prevents crystallization of the double helices

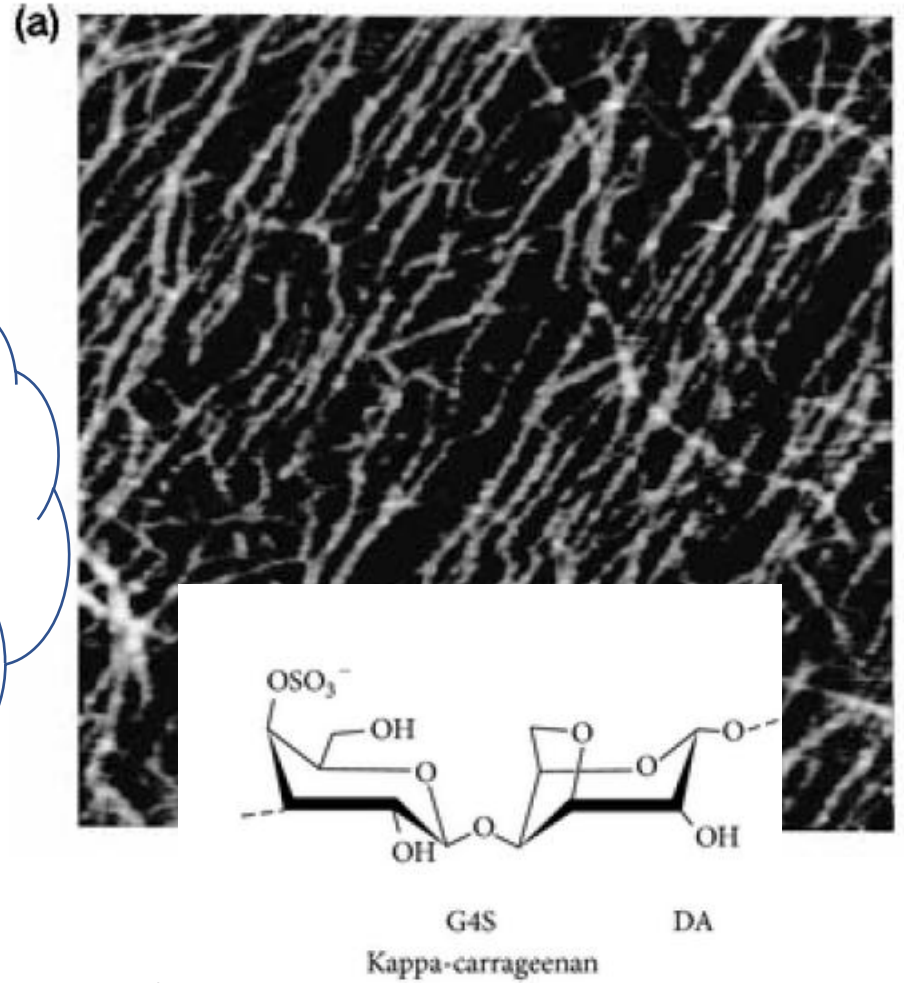

Carrageenan – the role of ions in hierarchical structure formation

ELSEVIER

International Journal of Biological Macromolecules
20 (1997) 35–41

INTERNATIONAL JOURNAL OF Biological Macromolecules STRUCTURE, FUNCTION AND INTERACTIONS

- Ability to form gels follows the sequence:

$$Li^+, Na^+, NR_4^+ \ll NH_4^+ < K^+, Cs^+ < Rb^+$$

These seem to be specific structuring ions

On the specific role of coions and counterions on κ-carrageenan conformation

Marina Ciancia *, Michel Milas, Marguerite Rinaudo

Centre de Recherches sur les Macromolécules Végétales, CERMAV-CNRS, affiliated with the University Joseph Fourier, BP 53,

<u>Helix formation can be followed by measuring specific optical rotatory power</u>

No hysteresis/no gel with NaCl – but helices form!

Hysteresis between gelling and melting – aggregation of helices.

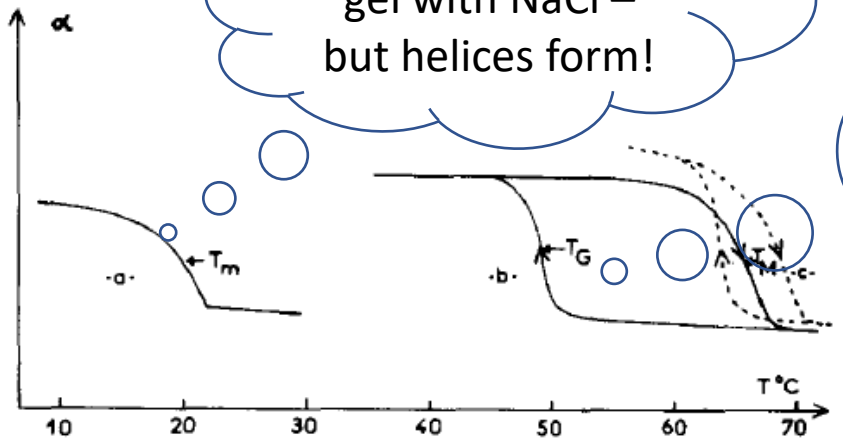

Fig. 1. [α] (T) for κ-carrageenan in the presence of 0.2 M NaCl (a), 0.1 M KCl (b), and 0.1 M KI (c). T_m is the conformational transition temperature, $T_G = T_m$ is the gelling temperature and T_M the melting temperature of the gel.

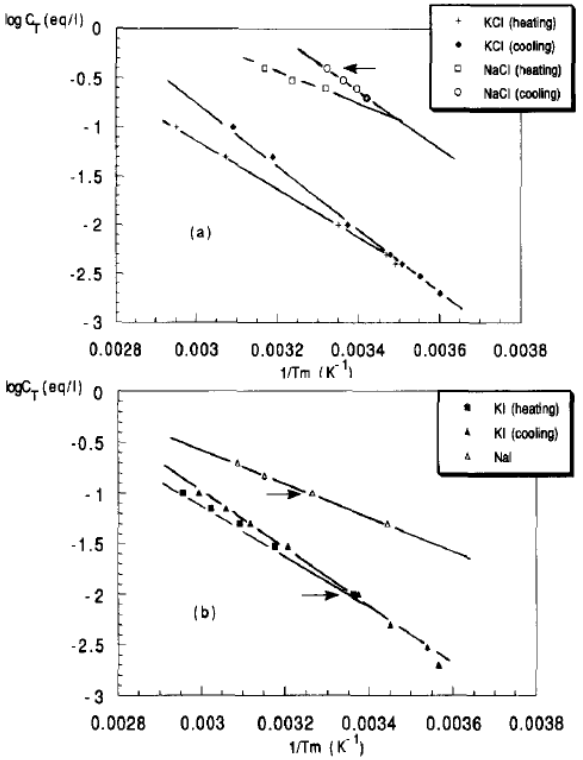

Fig. 2. Log $C_T(1/T_m)$ for κ-carrageenan in the presence of different electrolytes (a) KCl and NaCl, (b) NaI and KI. The arrows indicate the conditions for the microcalorimetry experiments.

Specific ion effects. – see next slide

Carrageenan – the role of ions in hierarchical structure formation

ELSEVIER

International Journal of Biological Macromolecules
20 (1997) 35–41

INTERNATIONAL JOURNAL OF Biological Macromolecules STRUCTURE, FUNCTION AND INTERACTIONS

On the specific role of coions and counterions on κ-carrageenan conformation

Marina Ciancia *, Michel Milas, Marguerite Rinaudo

Centre de Recherches sur les Macromolécules Végétales, CERMAV-CNRS, affiliated with the University Joseph Fourier, BP 53, 38041 Grenoble Cedex 9, France

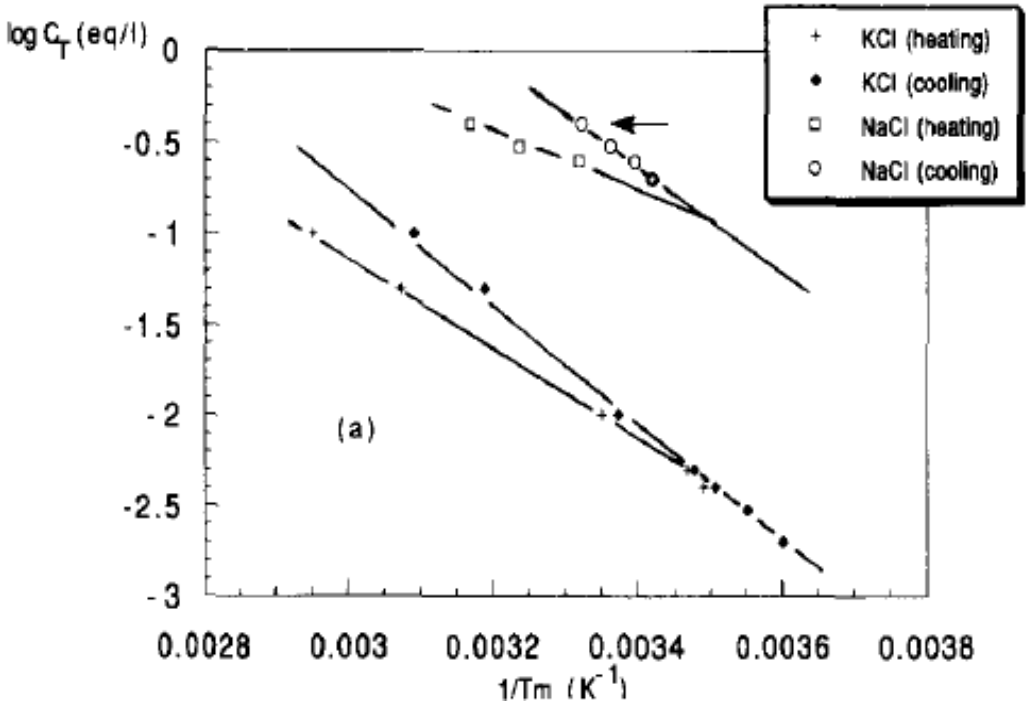

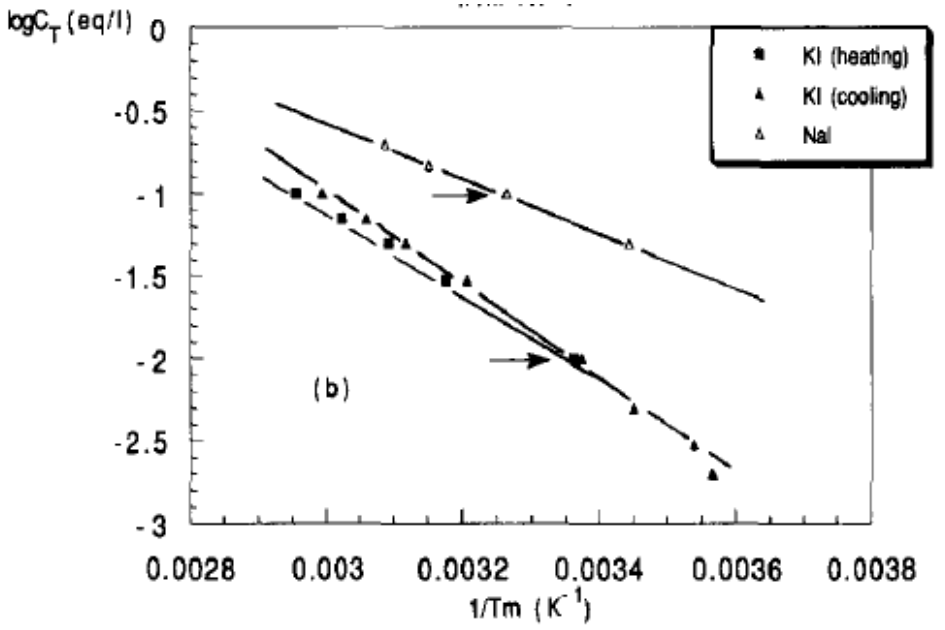

Fig. 2. Log $C_T(1/T_m)$ for κ-carrageenan in the presence of different electrolytes (a) KCl and NaCl, (b) NaI and KI. The arrows indicate the conditions for the microcalorimetry experiments.

Carrageenan – the role of ions in hierarchical structure formation

ELSEVIER

International Journal of Biological Macromolecules
20 (1997) 35–41

INTERNATIONAL JOURNAL OF Biological Macromolecules STRUCTURE, FUNCTION AND INTERACTIONS

On the specific role of coions and counterions on κ-carrageenan conformation

Marina Ciancia *, Michel Milas, Marguerite Rinaudo

Centre de Recherches sur les Macromolécules Végétales, CERMAV-CNRS, affiliated with the University Joseph Fourier, BP 53, 38041 Grenoble Cedex 9, France

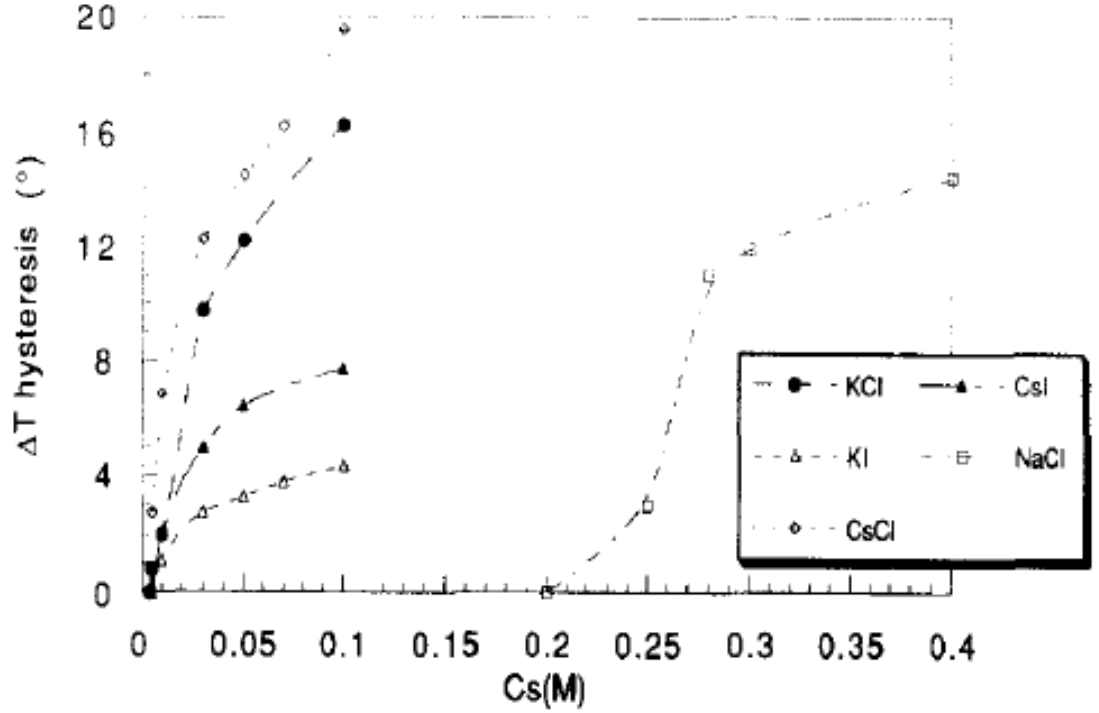

Fig. 3. $\Delta T_{hysteresis}$ (C_S) for κ-carrageenan in the presence of different electrolytes.

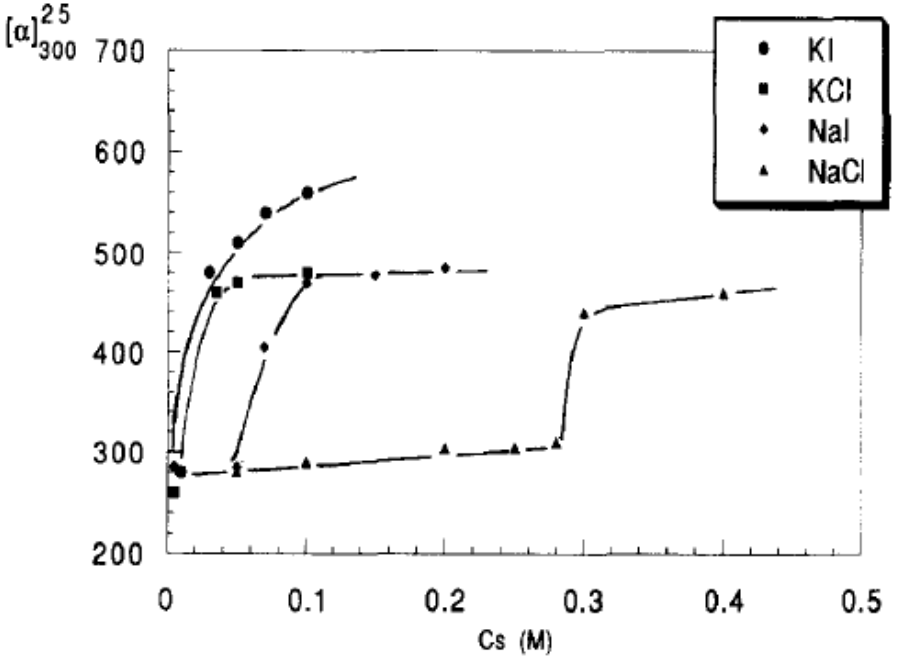

Fig. 4. Variation of the specific optical rotation at 25°C for κ-carrageenan as a function of the added salt.

POLYELECTROLYTES & INTERACTION BETWEEN IONIC ION ASSOCIATION PROPERTIES

Polyelectrolyte Model

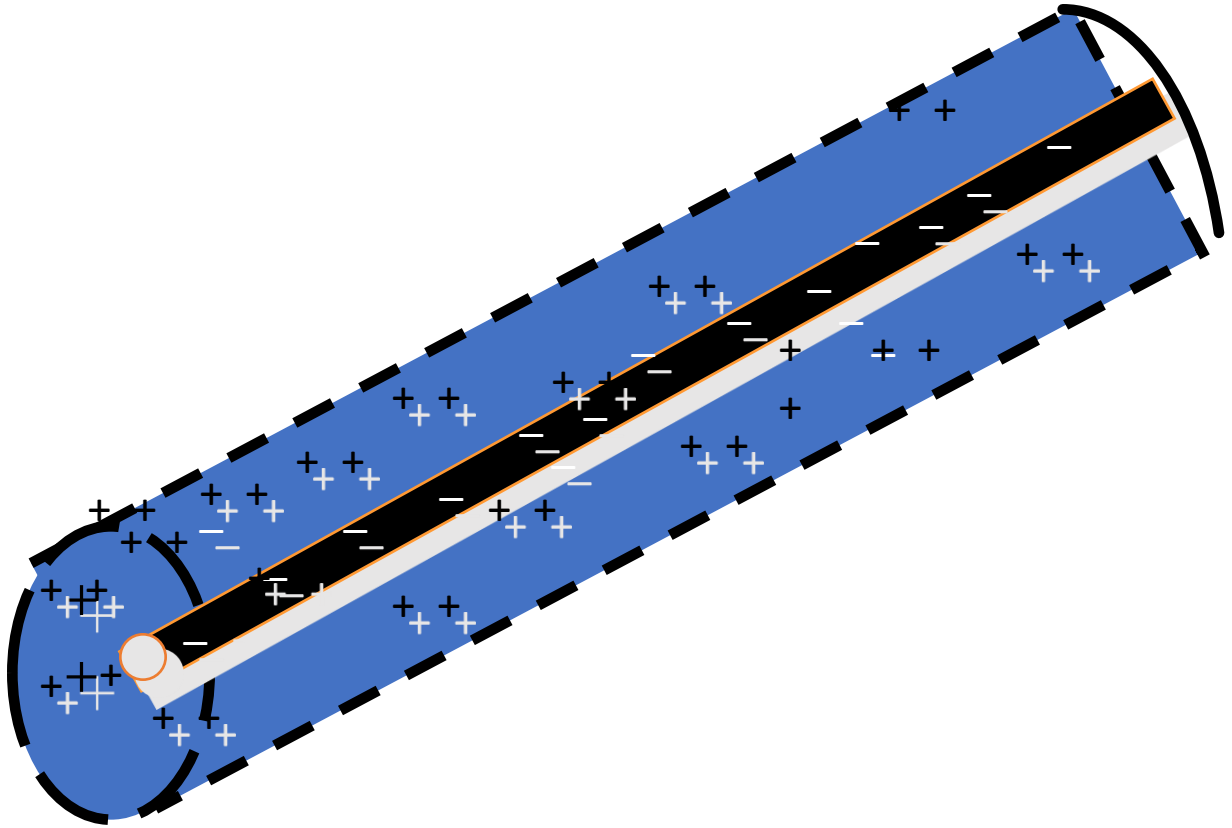

Fuoss, R.M.; Katchalsky, A.; Lifson, S.; *Proc. Nat. Acad Sci.* **1951,** *37,* 579
Manning, G.S.; *Quarterly Reviews of Biophysics,* **1978,** *2,* 179
Gao, J.Y.; Dubin, P.L.; Sato, T.; Morishima, Y.; *J. Chromatography, A;* **1997,** *766,*236

Counterion Distribution

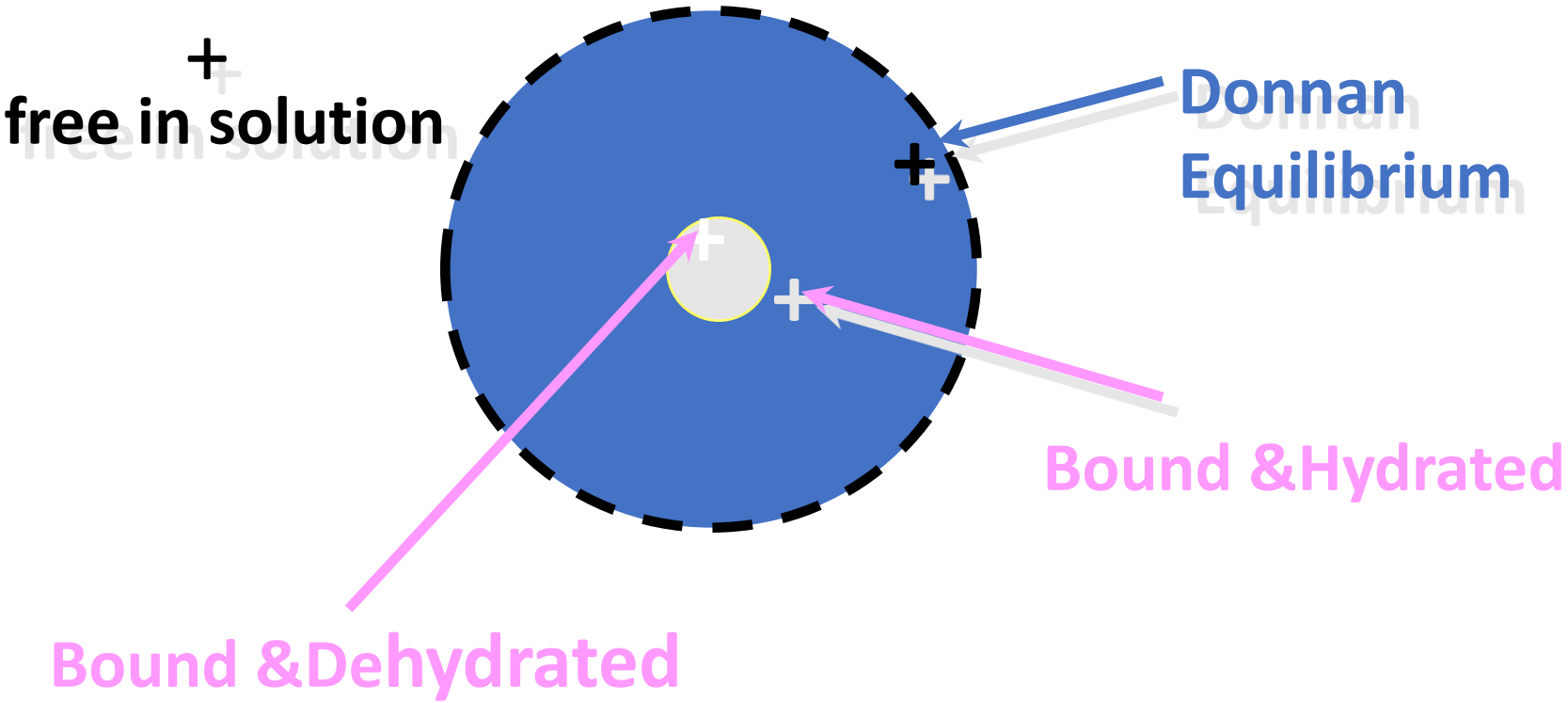

Oosawa, F.; Polyelectrolytes, Marcel Dekker Co.; NY.; 1971

Polyelectrolyte-Counterion Interaction

- Two theories:
  - Cell Theory (Poisson-Boltzmann)
  - Manning theory (Counterion Condensation)

Poisson-Boltzmann Model

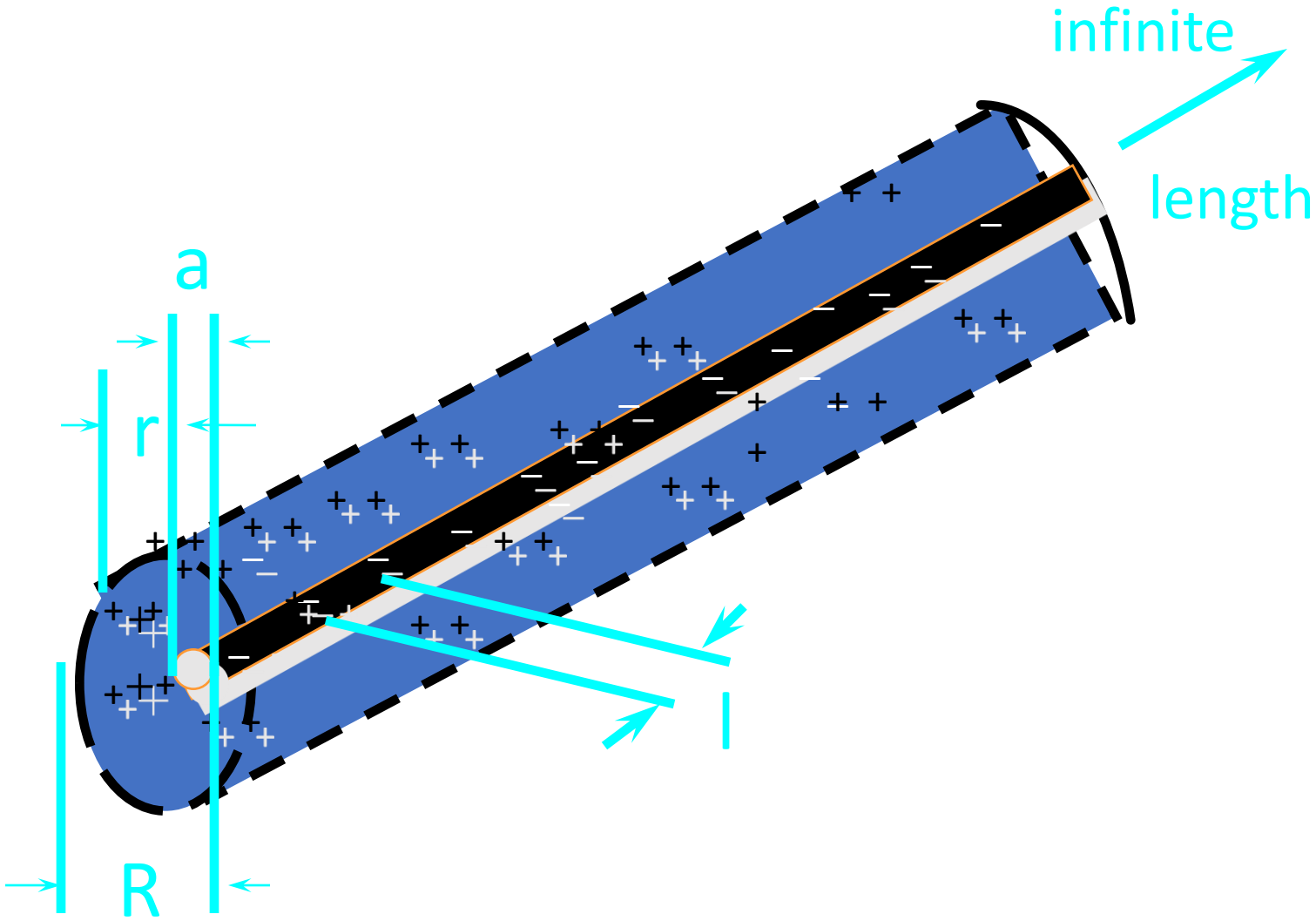

Poisson-Boltzmann Model

- Infinitely long rod, radius ‘a’
- medium of constant dielectric
- fixed polyion charge spread evenly along the rod
- counterions contained within a concentric cylinder, radius ‘R’

Manning Theory

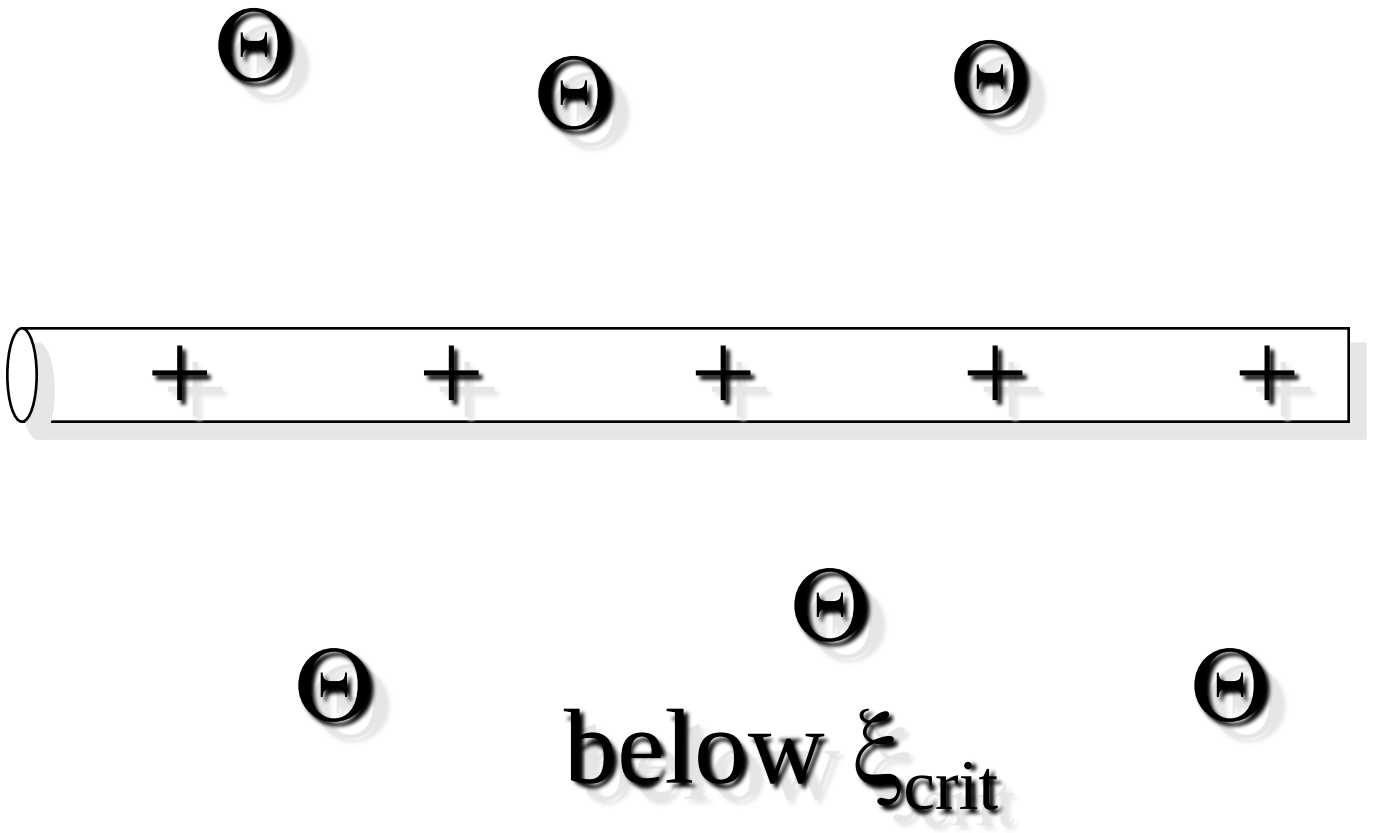

Manning Theory

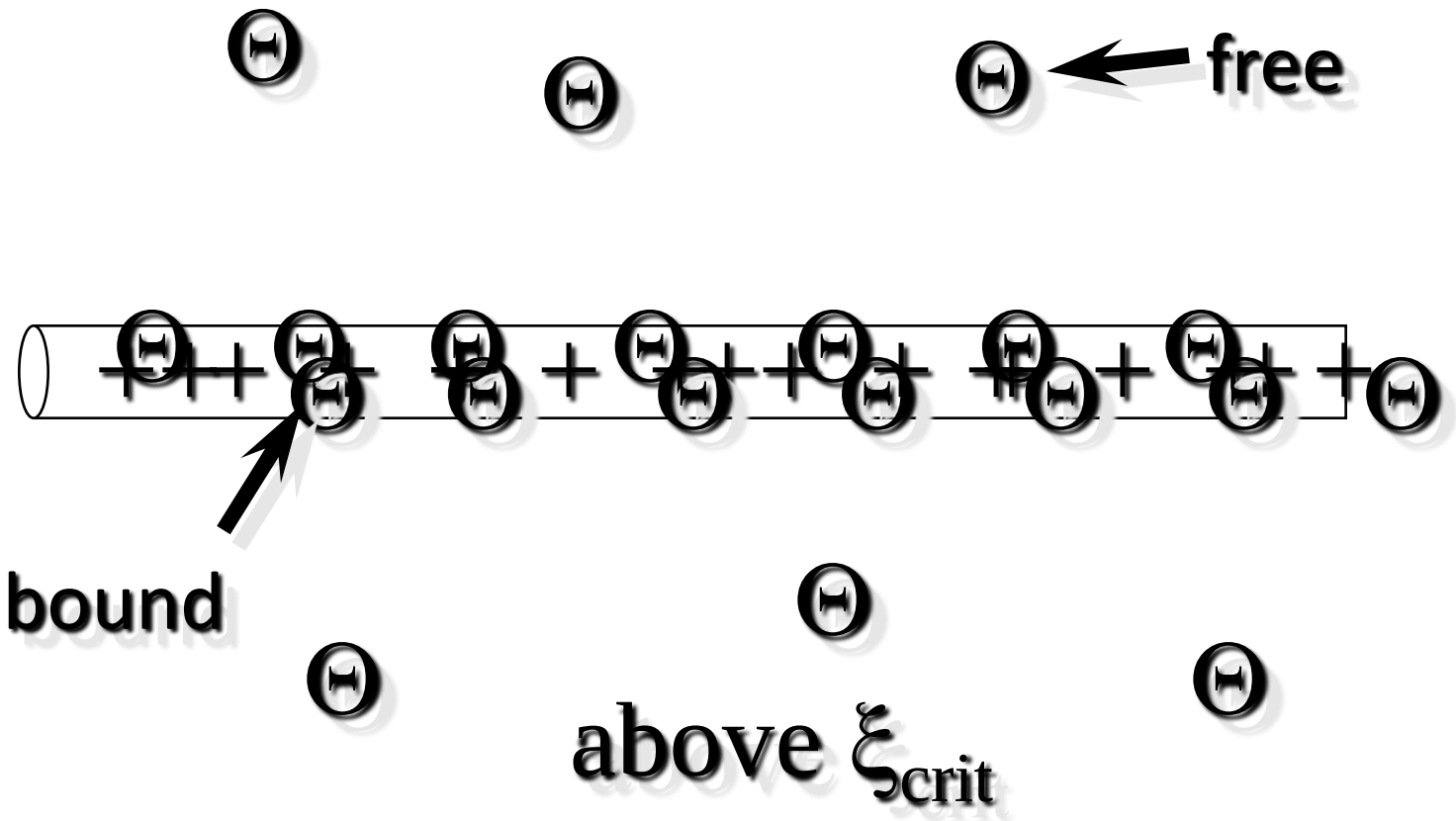

Manning Theory

- Two-state theory
  - counterions free or bound
- Dimensionless charge density is reduced to unity by counterion condensation

$$\xi = \frac{\alpha\mu^2}{\varepsilon kTlz}$$

Manning Theory

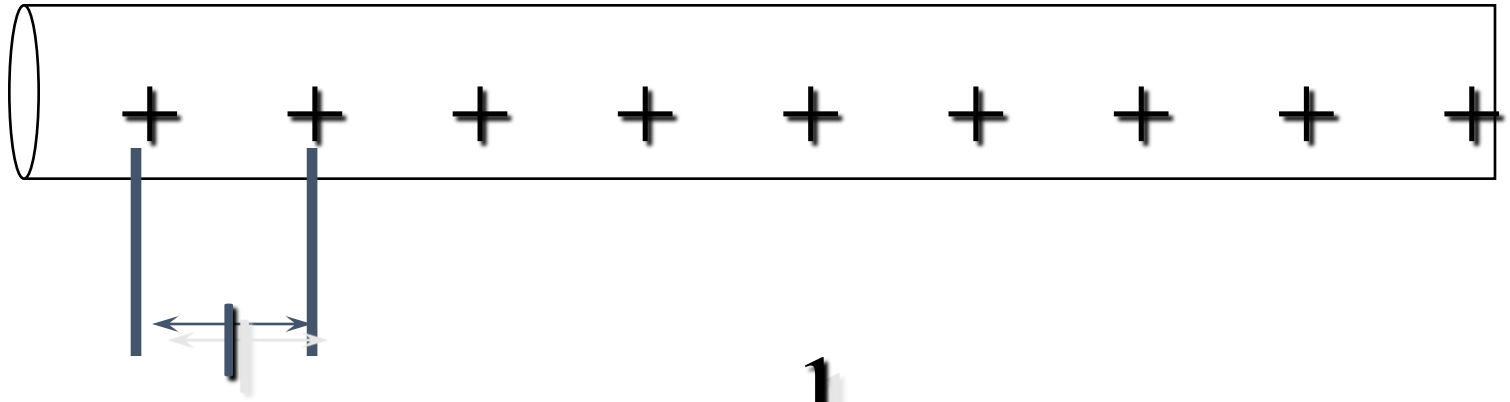

$$\xi_{crit} = \frac{1}{z_i}$$

Manning Theory

- For vinyl monomer homopolyelectrolytes:
  - l = 0.25nm
  - $P_b = 1-(\frac{1}{z\xi})$
    - 65% of monovalent ions condense
      - 82% of divalent ions condense

- Counterion-polyion interaction can cause natural polyelectrolytes to form spectacular heirarchical structures
  - That can confer stimuli-responsive behavior
  - The hierarchical structures can change on storage
    - Anticipatory knowledge is required to avoid ‘surprises’

Gel/network formation from helical junction zones

In order to from a gel, helical 'junction zones' must be connected into a effective network; Two possible network structures are shown below.

Macromolecules **1994,** *27,* 4160–4166

On the Mechanism of Gelation of Helix-Forming Biopolymers

Christer Viebke,* Lennart Piculell, and Svante Nilsson†

Physical Chemistry 1, Chemical Center, Lund University, S-221 00 Lund, Sweden

Received January 25, 1994®

Intramolecular helices

- the junction zone is formed by a double helix between two chains;
- The branching is formed at 'kinks' in the chain that cannot be wound into the helical structure

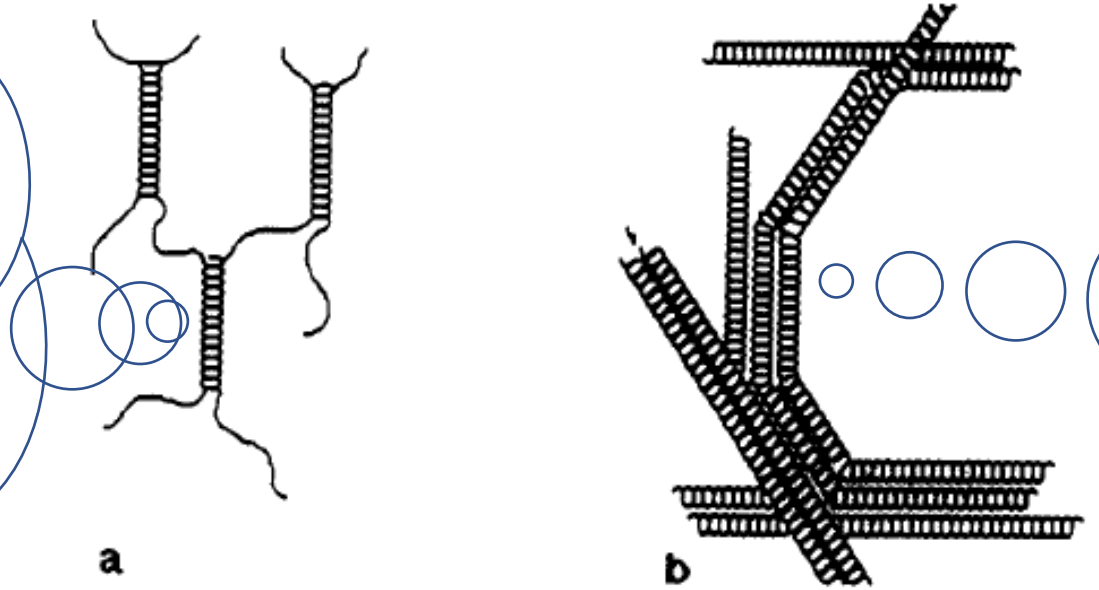

Figure 1. Schematic drawings of possible mechanisms of network formation in helical gels: gelation on the helical (a) and superhelical (b) levels.

Aggregation of fully developed helices

- branching is formed by bending of the helices to form junctions between the aggregated 'junction zones'

Evidence for Gelling by Helix Aggregation

Macromolecules **1994,** *27,* 4160–4166

On the Mechanism of Gelation of Helix-Forming Biopolymers

Christer Viebke,* Lennart Piculell, and Svante Nilsson†

Physical Chemistry 1, Chemical Center, Lund University, S-221 00 Lund, Sweden

Received January 25, 1994®

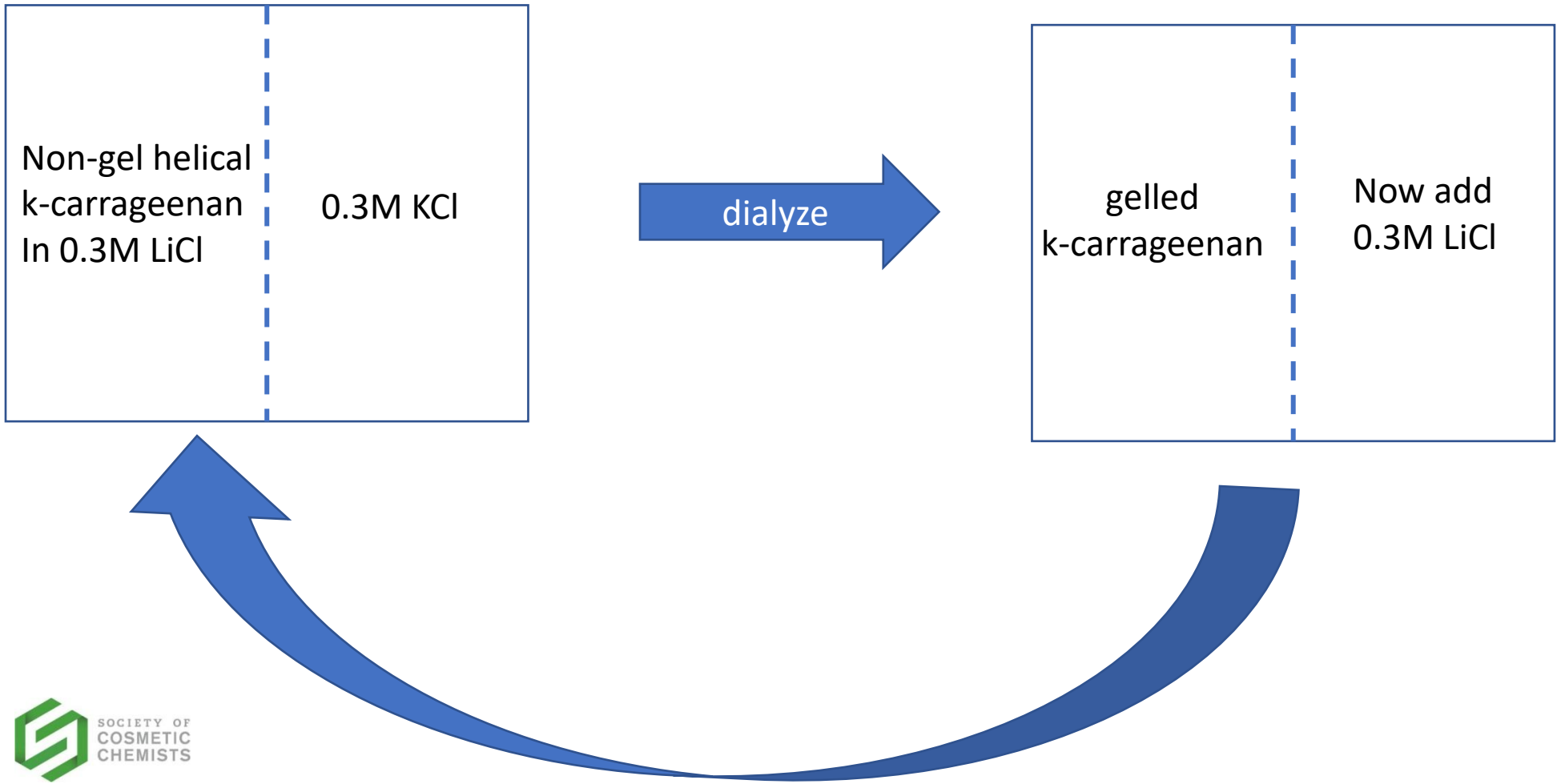

‘State Diagram’ for K-Carrageenan

Degraded k-carrageenan

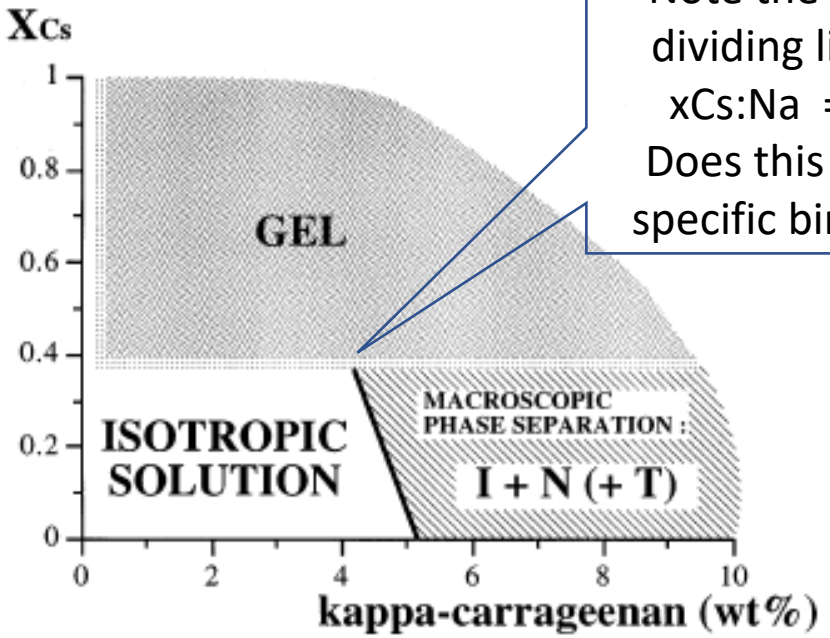

Note the sharp dividing line at xCs:Na = 0.4
Does this imply specific binding?

Fig. 1. Schematic ‘state diagram’ showing the various states displayed by helical samples of ultrasonically degraded (M_w = 50–100 kDa) κ-carrageenan in 0.1 M mixed salt solutions of NaI and CsI at 25°C. I + N (+ T) refers to phase separated samples containing one isotropic and one nematic phase or (at the highest concentrations) turbid samples.

ELSEVIER
International Journal of Biological Macromolecules
21 (1997) 141–153
INTERNATIONAL JOURNAL OF Biological Macromolecules STRUCTURE, FUNCTION AND INTERACTIONS

Organisation and association of κ-carrageenan helices under different salt conditions

e c
l, Sweden
1 2AW, UK

Intact k-carrageenan

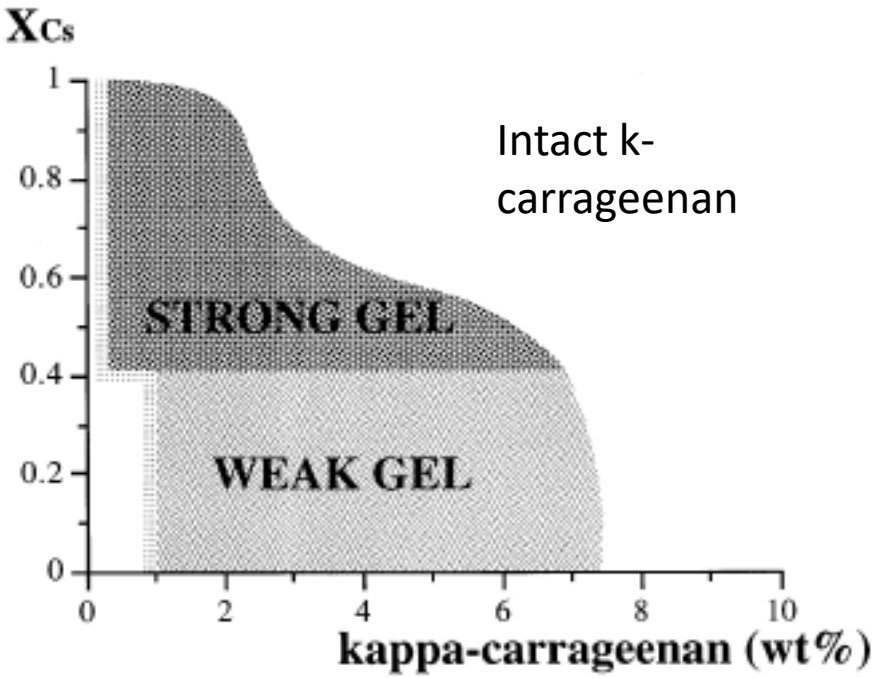

Fig. 8. Schematic ‘state diagram’ showing states displayed by helical samples of intact (M_w = 300–400 kDa) κ-carrageenan in 0.1 M mixed salt solutions of NaI and CsI at 25°C.

Specific site binding of ions on K-Carrageenan?

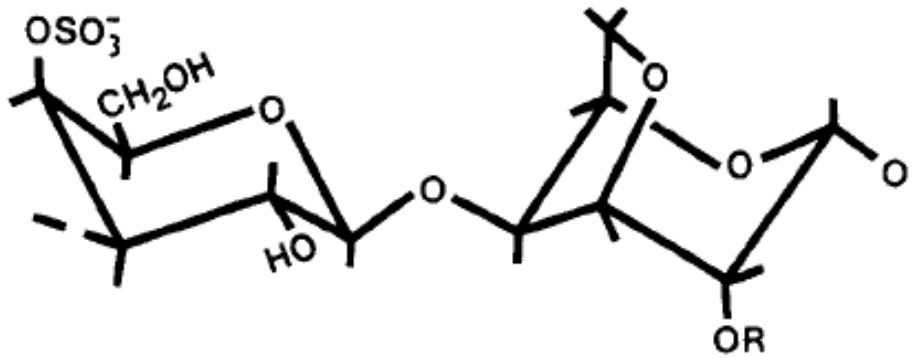

Figure 1. Repeating disaccharide structures of κ- (R = H) and ι- (R = SO_3^-) carrageenan.

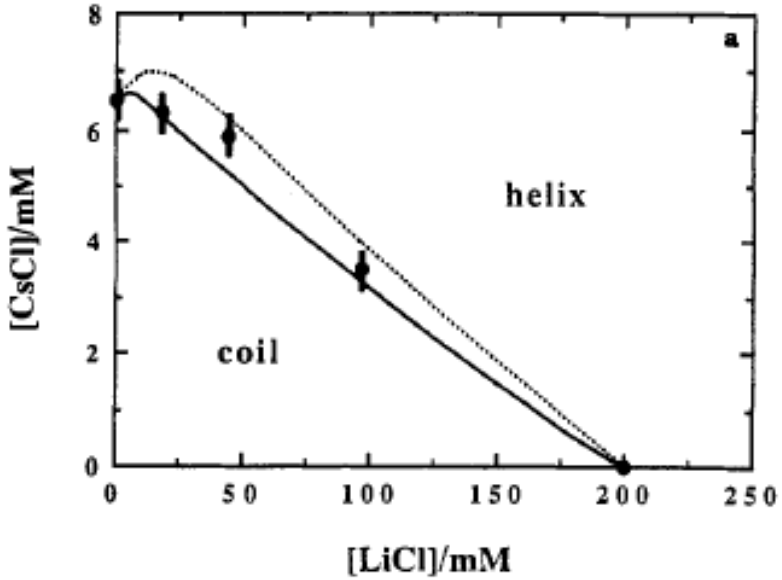

Macromolecules 1991, *24*, 3804–3811

Helix–Coil Transitions of Ionic Polysaccharides Analyzed within the Poisson–Boltzmann Cell Model. 4. Effects of Site-Specific Counterion Binding

S. Nilsson* and L. Piculell

Physical Chemistry 1, University of Lund, Chemical Center, Box 124, S-221 00 Lund, Sweden

Received October 19, 1990; Revised Manuscript Received January 23, 1991

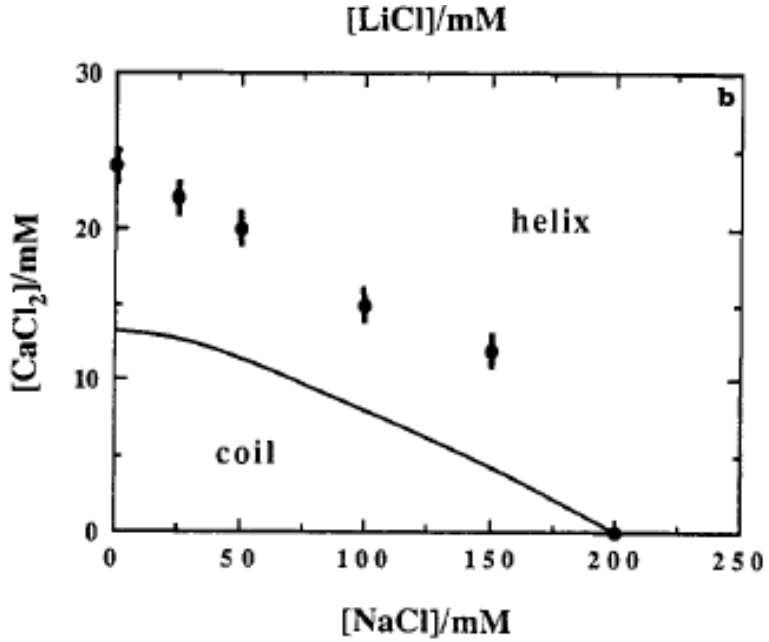

Figure 2. Conformational stability diagrams (see text) for κ-carrageenan (sample 1) in mixed electrolyte solutions: (a) 3.8 mM carrageenan in LiCl/CsCl at 17 °C. The molar ratios of the cesium and lithium forms of carrageenan are the same as the molar ratios of the salts. Points indicates experimental data; lines are model predictions (see text) for $n = 1$, $K_{0,\text{helix}} = 1.86\ M^{-1}$ (dotted line) and for $n = 2$, $K_{0,\text{helix}} = 5.0\ M^{-1}$ (solid line). (b) 5 mM carrageenan in NaCl/$CaCl_2$ at 18 °C. The solid line is calculated (see text) for purely electrostatic polyion–counterion interactions.

Specific site binding of ions on K-Carrageenan?

Helix–Coil Transitions of Ionic Polysaccharides Analyzed within the Poisson–Boltzmann Cell Model. 4. Effects of Site-Specific Counterion Binding

S. Nilsson* and L. Piculell

Physical Chemistry 1, University of Lund, Chemical Center, Box 124, S-221 00 Lund, Sweden

Received October 19, 1990; Revised Manuscript Received January 23, 1991

Table II
Thermodynamic Interaction Parameters for Specific Ions

	$K_{0,helix}$ (M^{-1}) at 290 K		$\Delta H^0_{binding}$, kJ/mol		ΔH_{cal},[a] kJ/mol	
ion	$n = 1$	$n = 2$	$n = 1$	$n = 2$	$n = 1$	$n = 2$
Rb^+	3.42	9.85	24.5	24.6	23.0	21.6
Cs^+	1.86	5.0	23.1	24.4	21.5	20.4

[a] Refers to pure salt forms.

Cf 12.7kJ/mol for non-specific salts

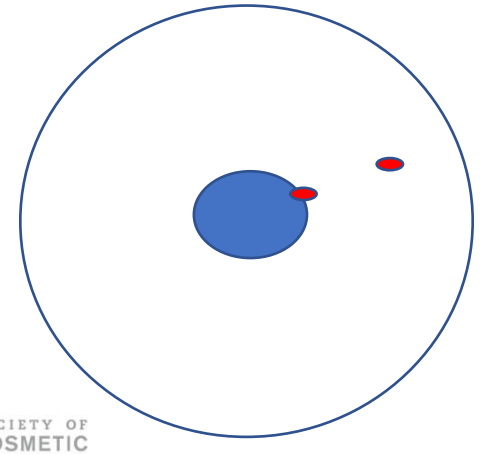

Use Poisson-Boltzmann Cell theory and law of Mass Action to calculate the chemical potential of polyions free and bound to coil and helix– calculate the enthalpy and entropies of binding

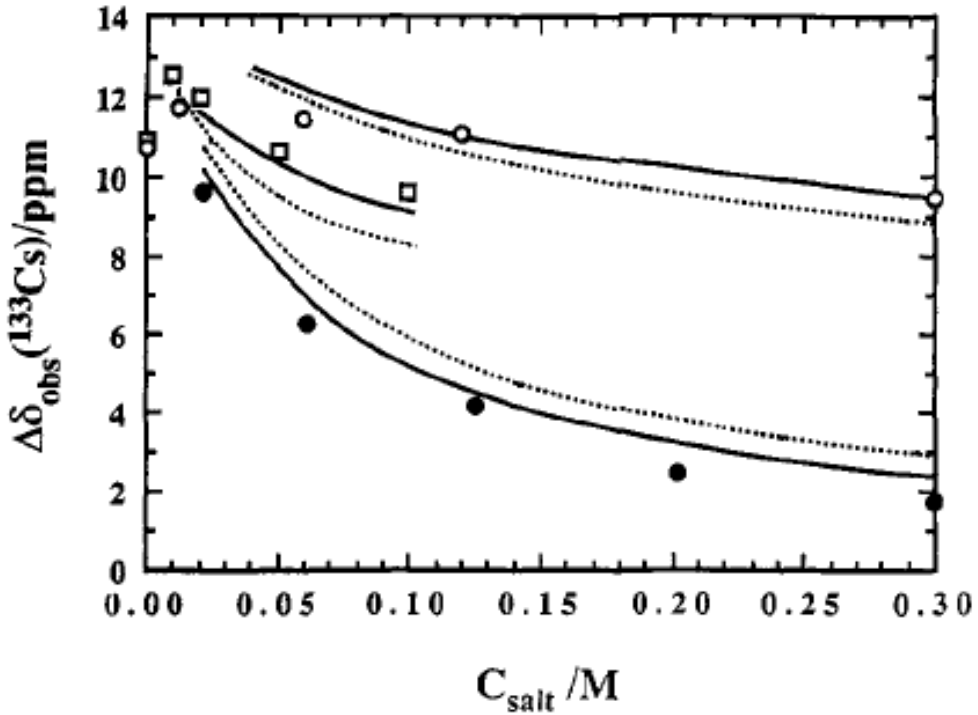

Figure 5. Variation in ^{133}Cs NMR shift with concentration of NaCl (○), $CaCl_2$ (□), or CsCl (●) added to 48 mM Cs–κ-carrageenan at 25 °C. Experimental data are from ref 8. Lines are calculated for $n = 1$, $\Delta\delta_b = 36.4$ ppm and $K_{0,helix} = 1.6\ M^{-1}$ (dotted) and for $n = 2$, $\Delta\delta_b = 41.5$ ppm and $K_{0,helix} = 4.1\ M^{-1}$ (solid).

Specific site binding of ions on K-Carrageenan?

3804 *Macromolecules* 1991, *24*, 3804–3811

Helix–Coil Transitions of Ionic Polysaccharides Analyzed within the Poisson–Boltzmann Cell Model. 4. Effects of Site-Specific Counterion Binding

S. Nilsson* and L. Piculell

Physical Chemistry 1, University of Lund, Chemical Center, Box 124, S-221 00 Lund, Sweden

Received October 19, 1990; Revised Manuscript Received January 23, 1991

Table II
Thermodynamic Interaction Parameters for Specific Ions

	$K_{0,helix}$ (M^{-1}) at 290 K		$\Delta H^0_{binding}$, kJ/mol		ΔH_{cal},[a] kJ/mol	
ion	$n = 1$	$n = 2$	$n = 1$	$n = 2$	$n = 1$	$n = 2$
Rb^+	3.42	9.85	24.5	24.6	23.0	21.6
Cs^+	1.86	5.0	23.1	24.4	21.5	20.4

[a] Refers to pure salt forms.

Cf 12.7kJ/mol for non-specific salts

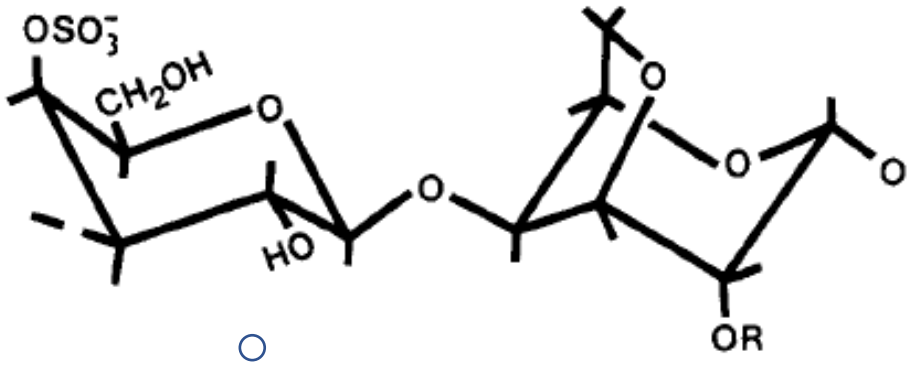

Figure 1. Repeating disaccharide structures of κ- (R = H) and ι- (R = SO_3^-) carrageenan.

The OH groups on k-Carrageenan are not well configured to complex with the counterions– However, in a double-helical conformation, the OH groups would be configured correctly and the double helical conformation would be stiff.

Conclude that aggregation (and gelling) is caused by specific binding of ions to the assembled helix (rather than to the coil)

Zipper Model

Alginates and Pectin

Alginates

2456 J. Phys. Chem. B 2007, 111, 2456−2462

Multiple Steps and Critical Behaviors of the Binding of Calcium to Alginate

Yapeng Fang,*,† Saphwan Al-Assaf,† Glyn O. Phillips,†,‡ Katsuyoshi Nishinari,†,§ Takahiro Funami,|| Peter A. Williams,⊥ and Liangbin Li#

Glyn O. Phillips Hydrocolloid Research Center, North East Wales Institute, Plas Coch, Mold Road, Wrexham LL11 2AW, UK, Phillips Hydrocolloid Research Ltd., 45 Old Bond Street, London W1S 4AQ, UK, Department of Food and Human Health Sciences, Graduate School of Human Life Science, Osaka City University, Sugimoto, Sumiyoshi, Osaka 558-8585, Japan, Hydrocolloid Laboratory, San-Ei Gen F.F.I., Inc., 1-1-11 Sanwa-cho, Toyonaka, Osaka 561-8588, Japan, Centre for Water-Soluble Polymers, North East Wales Institute, Plas Coch, Mold Road, Wrexham LL11 2AW, UK, and National Synchrotron Radiation Laboratory and Department of Polymer Science and Engineering, University of Science and Technology of China, Anhui, 230026, China

- Exopolysaccharides extracted from brown seaweeds and some bacteria
- Linear block copolymers of mannuronate and guluronate linked with alternating residues

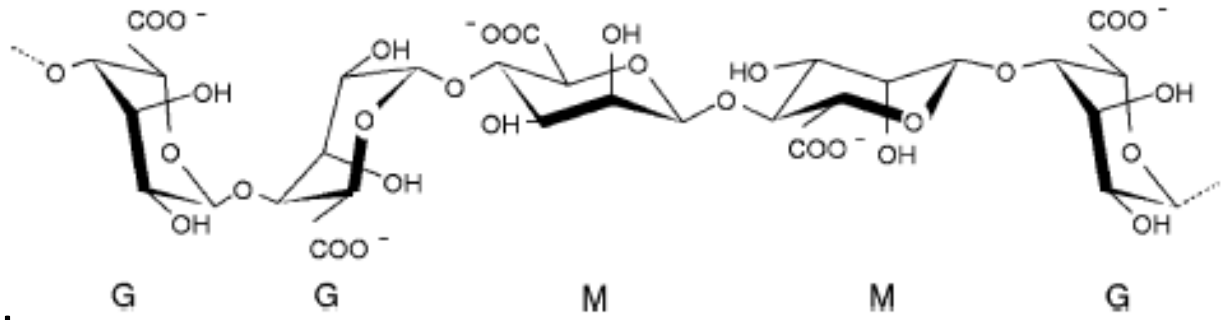

- Biosynthesis Pathway
  - Mannuronan is polymerized and then post-modified by epimerase enzymes which convert mannuronate to guluronate
  - Epimerase enzymes are now being used industrially to create alginates with optimum properties for specific applications.

Alginates

- The guluronate residues selectively bind alkaline earth metals
- The egg- box model*:
  - The G-blocks form a 2/1 helical conformation and divalent cations are coordinated within the cavities formed thereby
  - The ‘egg-box’ dimer sequences associate laterally
    - To form junction zones

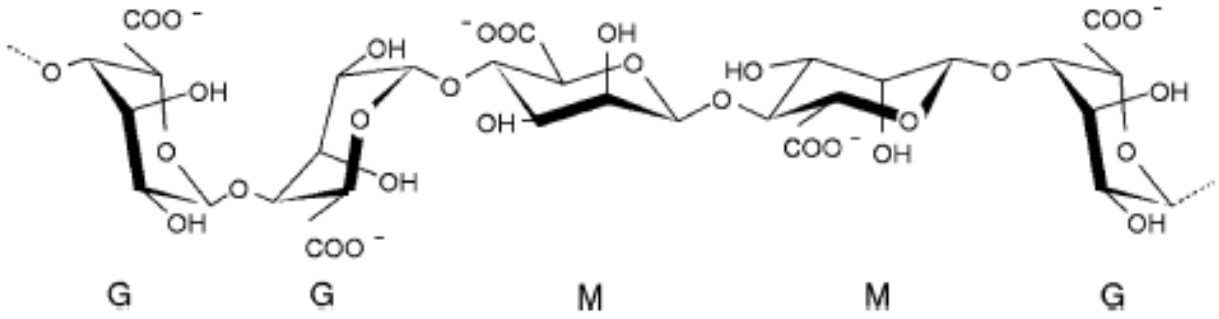

(9) Grant, G. T.; Morris, E. R.; Rees, D. A.; Smith, P. J. C.; Thom, D. *FEBS Lett.* **1973**, *32*, 195.

2456 *J. Phys. Chem. B* **2007**, *111*, 2456–2462

Multiple Steps and Critical Behaviors of the Binding of Calcium to Alginate

Yapeng Fang,*,† Saphwan Al-Assaf,† Glyn O. Phillips,†,‡ Katsuyoshi Nishinari,†,§ Takahiro Funami,|| Peter A. Williams,⊥ and Liangbin Li#

Glyn O. Phillips Hydrocolloid Research Center, North East Wales Institute, Plas Coch, Mold Road, Wrexham LL11 2AW, UK, Phillips Hydrocolloid Research Ltd., 45 Old Bond Street, London W1S 4AQ, UK, Department of Food and Human Health Sciences, Graduate School of Human Life Science, Osaka City University, Sugimoto, Sumiyoshi, Osaka 558-8585, Japan, Hydrocolloid Laboratory, San-Ei Gen F.F.I., Inc., 1-1-11 Sanwa-cho, Toyonaka, Osaka 561-8588, Japan, Centre for Water-Soluble Polymers, North East Wales Institute, Plas Coch, Mold Road, Wrexham LL11 2AW, UK, and National Synchrotron Radiation Laboratory and Department of Polymer Science and Engineering, University of Science and Technology of China, Anhui, 230026, China

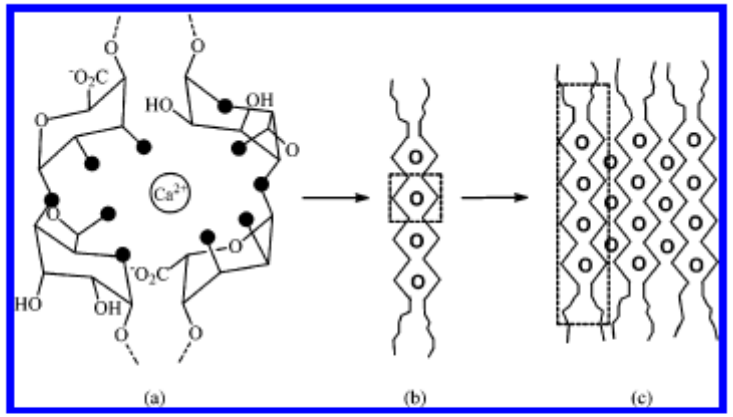

Figure 1. Schematic representation of the hierarchical structure of egg-box junction zones in alginate/calcium gels: (a) coordination of Ca^{2+} in a cavity created by a pair of guluronate sequences along alginate chains; (b) egg-box dimer, and (c) laterally associated egg-box multimer. The black solid circles represent the oxygen atoms possibly involved in the coordination with Ca^{2+}. The open circles represent Ca^{2+} ions.

SOCIETY OF COSMETIC CHEMISTS *

Alginates

2456 J. Phys. Chem. B 2007, 111, 2456–2462

Multiple Steps and Critical Behaviors of the Binding of Calcium to Alginate

Yapeng Fang,*,† Saphwan Al-Assaf,† Glyn O. Phillips,†,‡ Katsuyoshi Nishinari,†,§ Takahiro Funami,|| Peter A. Williams,⊥ and Liangbin Li#

Glyn O. Phillips Hydrocolloid Research Center, North East Wales Institute, Plas Coch, Mold Road, Wrexham LL11 2AW, UK, Phillips Hydrocolloid Research Ltd., 45 Old Bond Street, London W1S 4AQ, UK, Department of Food and Human Health Sciences, Graduate School of Human Life Science, Osaka City University, Sugimoto, Sumiyoshi, Osaka 558-8585, Japan, Hydrocolloid Laboratory, San-Ei Gen F.F.I., Inc., 1-1-11 Sanwa-cho, Toyonaka, Osaka 561-8588, Japan, Centre for Water-Soluble Polymers, North East Wales Institute, Plas Coch, Mold Road, Wrexham LL11 2AW, UK, and National Synchrotron Radiation Laboratory and Department of Polymer Science and Engineering, University of Science and Technology of China, Anhui, 230026, China

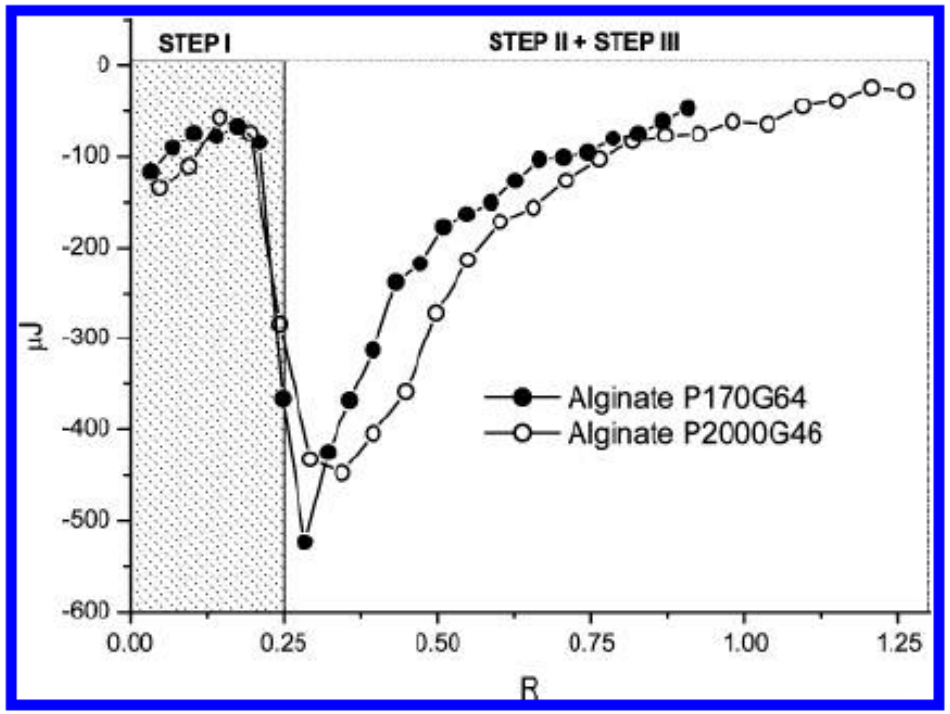

Figure 4. Assignment of different steps in the binding isotherms of P170G64 and P2000G46 according to R (= Ca/G ratio). Note that Step II and Step III are indistinguishable here; the illustration is to maintain consistency with Figures 5 and 6.

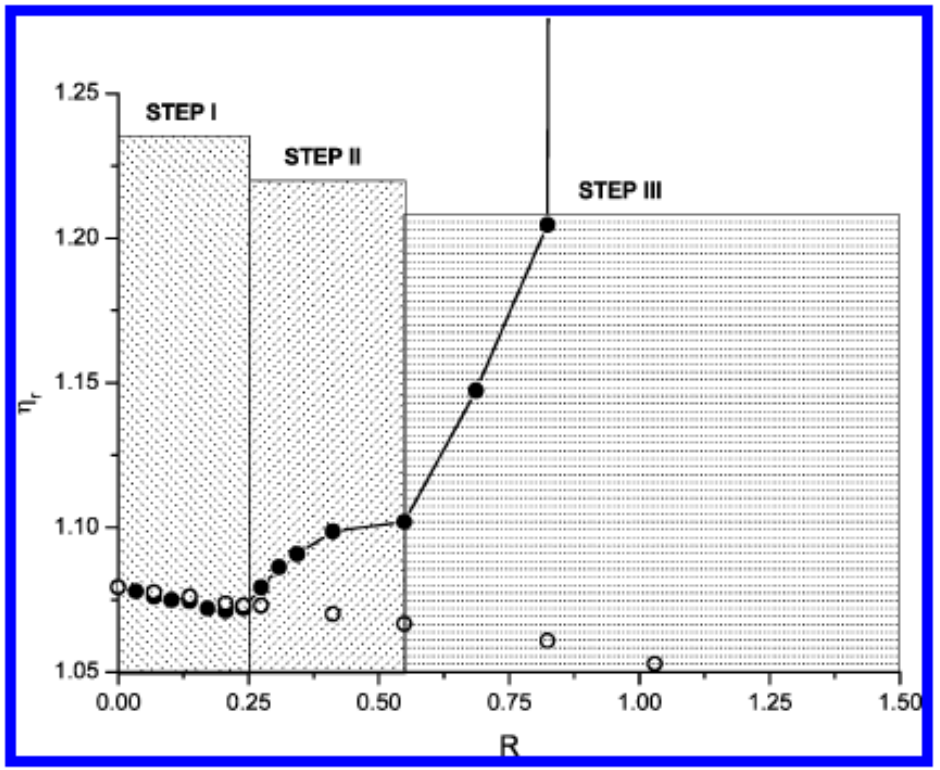

Figure 5. The change of relative viscosity η_r with R (= Ca/G ratio) during the titration of 7.5 mM $CaCl_2$ into 0.052% (w/w) P170G64. The open circles show the relative viscosity for control samples titrated with buffer solvent.

Alginates

2456 J. Phys. Chem. B 2007, 111, 2456−2462

Multiple Steps and Critical Behaviors of the Binding of Calcium to Alginate

Yapeng Fang,*,† Saphwan Al-Assaf,† Glyn O. Phillips,†,‡ Katsuyoshi Nishinari,†,§ Takahiro Funami,|| Peter A. Williams,⊥ and Liangbin Li#

Glyn O. Phillips Hydrocolloid Research Center, North East Wales Institute, Plas Coch, Mold Road, Wrexham LL11 2AW, UK, Phillips Hydrocolloid Research Ltd., 45 Old Bond Street, London W1S 4AQ, UK, Department of Food and Human Health Sciences, Graduate School of Human Life Science, Osaka City University, Sugimoto, Sumiyoshi, Osaka 558-8585, Japan, Hydrocolloid Laboratory, San-Ei Gen F.F.I., Inc., 1-1-11 Sanwa-cho, Toyonaka, Osaka 561-8588, Japan, Centre for Water-Soluble Polymers, North East Wales Institute, Plas Coch, Mold Road, Wrexham LL11 2AW, UK, and National Synchrotron Radiation Laboratory and Department of Polymer Science and Engineering, University of Science and Technology of China, Anhui, 230026, China

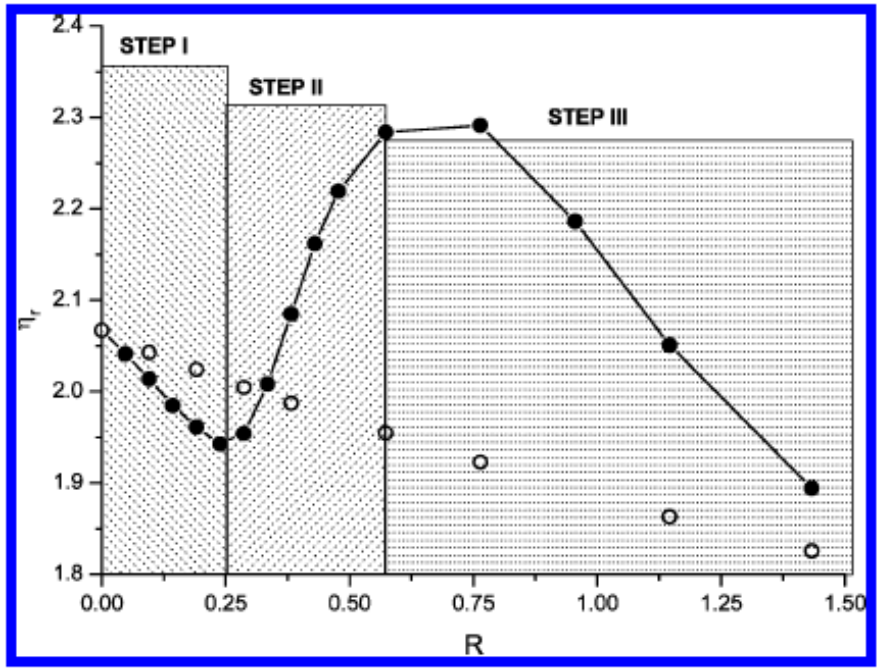

Figure 6. The change of relative viscosity η_r with R (= Ca/G ratio) during the titration of 7.5 mM $CaCl_2$ into 0.052% (w/w) P2000G46. The open circles show the relative viscosity for control samples titrated with buffer solvent.

Alginates

2456 J. Phys. Chem. B 2007, 111, 2456–2462

Multiple Steps and Critical Behaviors of the Binding of Calcium to Alginate

Yapeng Fang,*,† Saphwan Al-Assaf,† Glyn O. Phillips,†,‡ Katsuyoshi Nishinari,†,§ Takahiro Funami,|| Peter A. Williams,⊥ and Liangbin Li#

Glyn O. Phillips Hydrocolloid Research Center, North East Wales Institute, Plas Coch, Mold Road, Wrexham LL11 2AW, UK, Phillips Hydrocolloid Research Ltd., 45 Old Bond Street, London W1S 4AQ, UK, Department of Food and Human Health Sciences, Graduate School of Human Life Science, Osaka City University, Sugimoto, Sumiyoshi, Osaka 558-8585, Japan, Hydrocolloid Laboratory, San-Ei Gen F.F.I., Inc., 1-1-11 Sanwa-cho, Toyonaka, Osaka 561-8588, Japan, Centre for Water-Soluble Polymers, North East Wales Institute, Plas Coch, Mold Road, Wrexham LL11 2AW, UK, and National Synchrotron Radiation Laboratory and Department of Polymer Science and Engineering, University of Science and Technology of China, Anhui, 230026, China

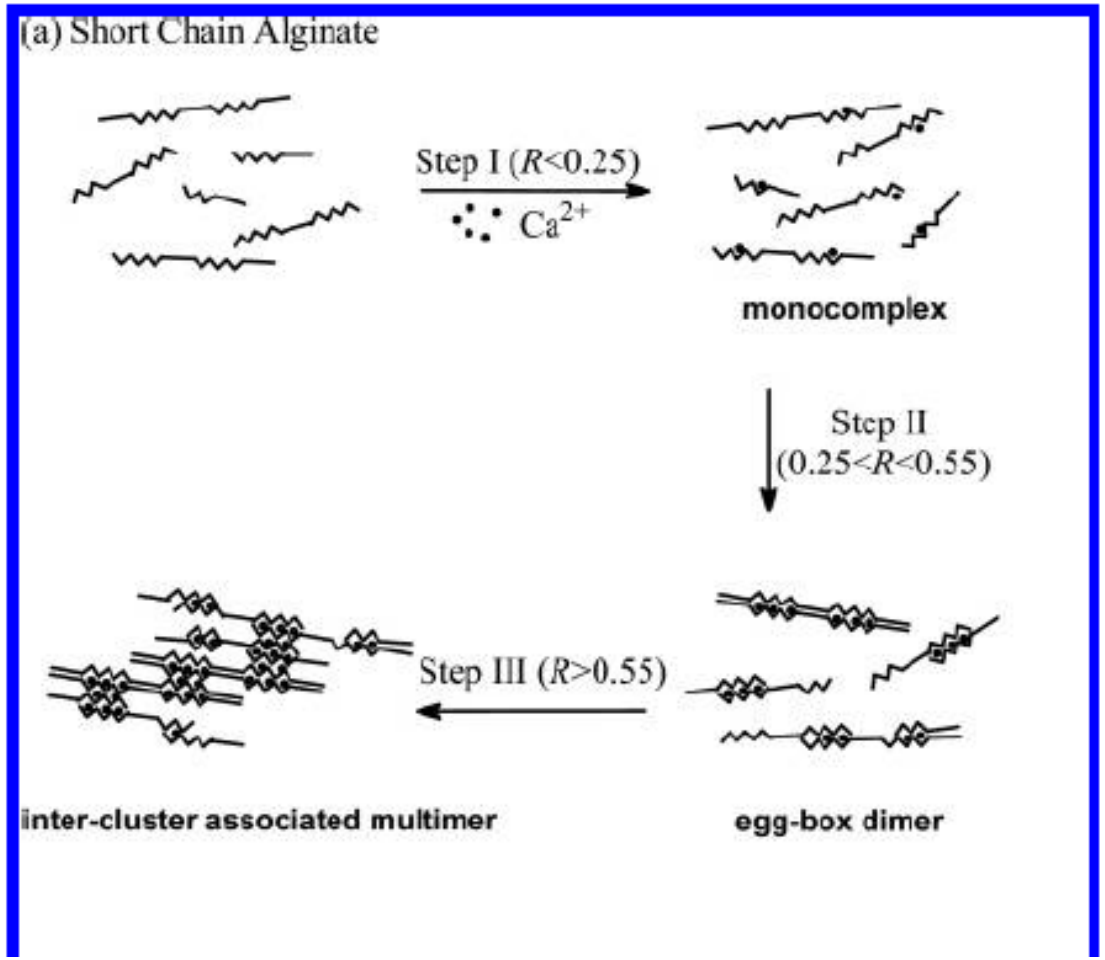

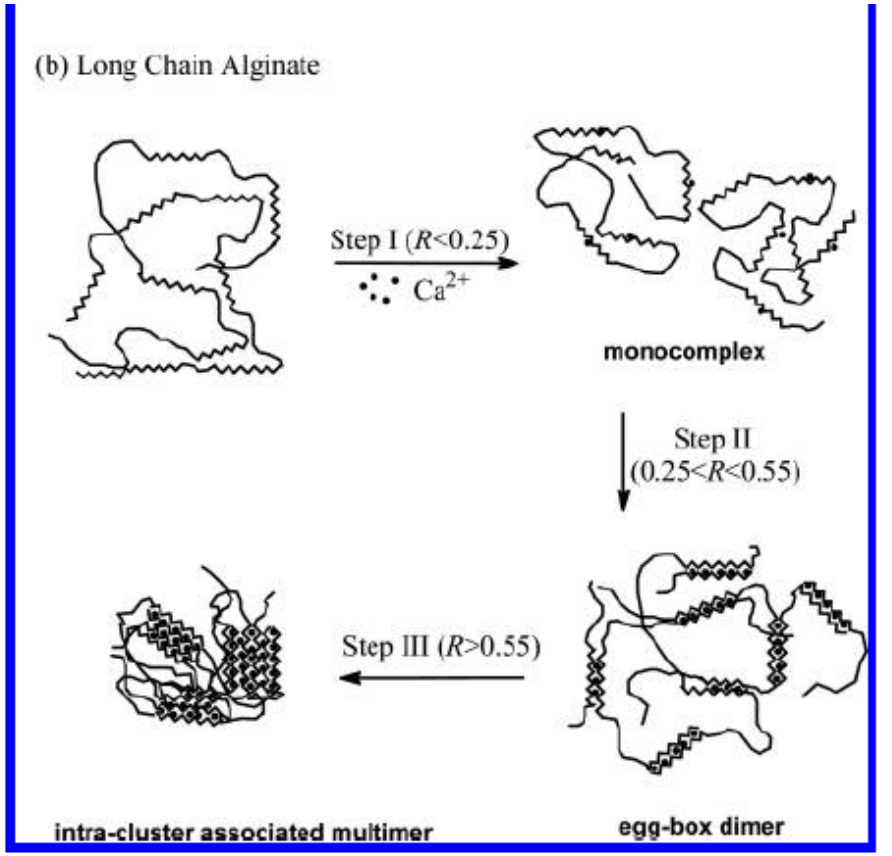

Figure 8. Schematic illustration of the multiple-step binding of Ca^{2+} to alginate: (a) short-chain alginate, and (b) long-chain alginate. The zigzag lines, smooth lines, and dots stand for G blocks, M blocks, and calcium ions, respectively. *R* is the feeding ratio of Ca^{2+} to G residue.

Alginates

New Hypothesis on the Role of Alternating Sequences in Calcium−Alginate Gels

Ivan Donati,*,† Synnøve Holtan,† Yrr A. Mørch,† Massimiliano Borgogna,‡ Mariella Dentini,§ and Gudmund Skjåk-Bræk†

Institute of Biotechnology, Norwegian University of Science and Technology, Sem Sælands V. 6/8, 7491 Trondheim, Norway, Department of Biochemistry, Biophysics and Macromolecular Chemistry, University of Trieste, Via Licio Giorgieri 1, 34127 Trieste, Italy, Department of Chemistry, University of Rome "La Sapienza", Rome, Italy

Scheme 1. Conversion of M Residues in Alternating Sequences Performed by AlgE4

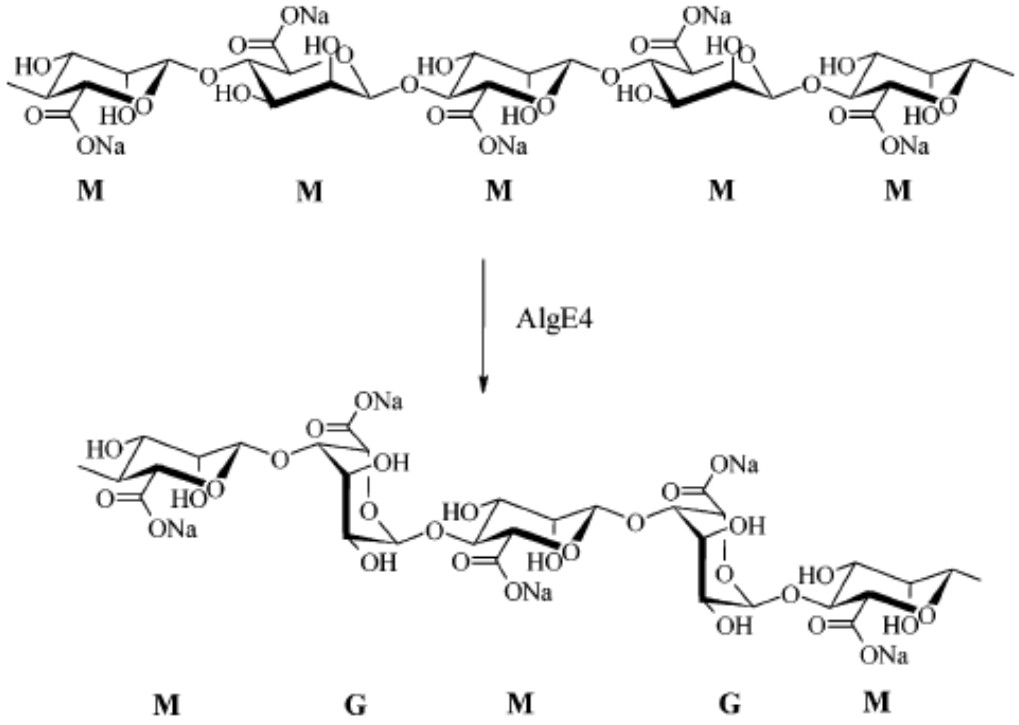

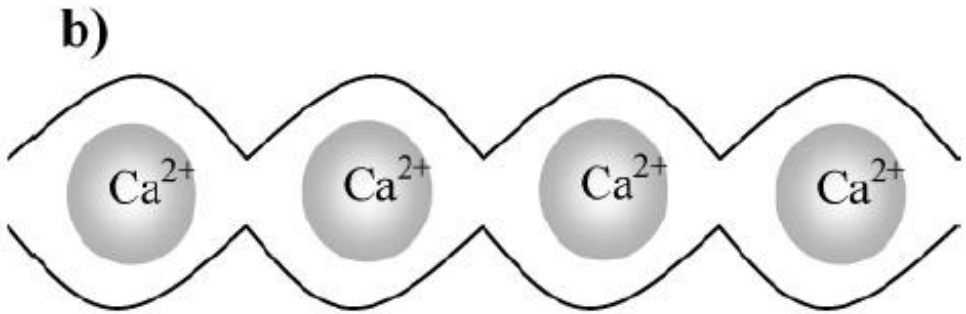

Pectins

- Pectin is composed of long sequences of partially methyl esterified (1-4)-linked α-D-glacturonate residues
- Galacturonate is structurally the mirror image of guluronate
- Therefore, similar egg-box structures to alginate may be expected

Available online at www.sciencedirect.com
ScienceDirect
Carbohydrate Polymers 72 (2008) 334–341
ELSEVIER
Carbohydrate Polymers
www.elsevier.com/locate/carbpol

Binding behavior of calcium to polyuronates: Comparison of pectin with alginate

Yapeng Fang [a,*], Saphwan Al-Assaf [a], Glyn O. Phillips [a,b], Katsuyoshi Nishinari [a], Takahiro Funami [c], Peter A. Williams [d]

[a] Glyn O. Phillips Hydrocolloid Research Center, North East Wales Institute, Plas Coch, Mold Road, Wrexham LL11 2AW, UK
[b] Phillips Hydrocolloid Research Ltd., 45 Old Bond Street, London W1S 4AQ, UK
[c] Hydrocolloid Laboratory, San-Ei Gen F.F.I., Inc., 1-1-11 Sanwa-cho, Toyonaka, Osaka 561-8588, Japan
[d] Centre for Water-Soluble Polymers, North East Wales Institute, Plas Coch, Mold Road, Wrexham LL11 2AW, UK

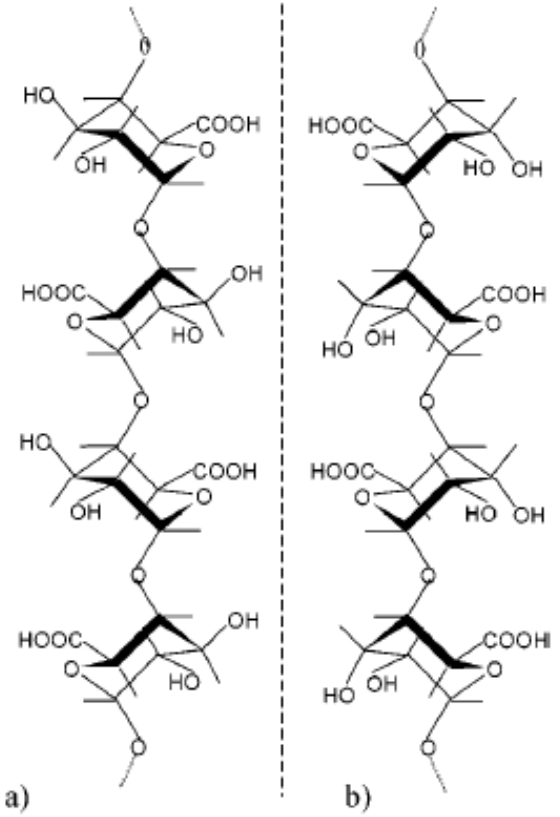

Figure 1. Schematic drawings of (a) galacturonate and (b) guluronate chains.

Pectins *c.f.* Alginates

Available online at www.sciencedirect.com
ScienceDirect
Carbohydrate Polymers 72 (2008) 334–341
Carbohydrate Polymers
www.elsevier.com/locate/carbpol

Binding behavior of calcium to polyuronates: Comparison of pectin with alginate

Yapeng Fang [a,*], Saphwan Al-Assaf [a], Glyn O. Phillips [a,b], Katsuyoshi Nishinari [a], Takahiro Funami [c], Peter A. Williams [d]

[a] Glyn O. Phillips Hydrocolloid Research Center, North East Wales Institute, Plas Coch, Mold Road, Wrexham LL11 2AW, UK
[b] Phillips Hydrocolloid Research Ltd., 45 Old Bond Street, London W1S 4AQ, UK
[c] Hydrocolloid Laboratory, San-Ei Gen F.F.I., Inc., 1-1-11 Sanwa-cho, Toyonaka, Osaka 561-8588, Japan
[d] Centre for Water-Soluble Polymers, North East Wales Institute, Plas Coch, Mold Road, Wrexham LL11 2AW, UK

Similar initial binding

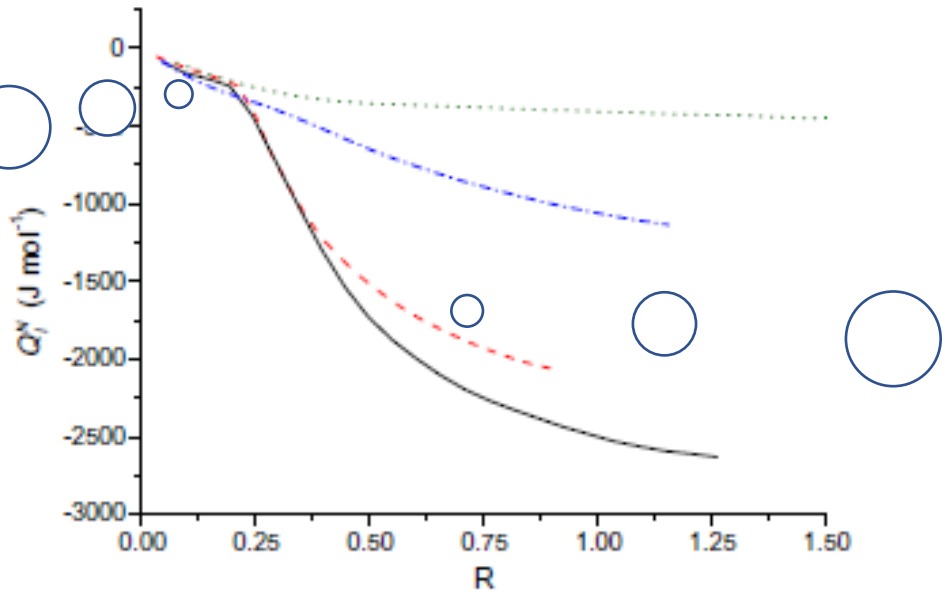

Fig. 5. Comparison of the normalized accumulative heat Q_i^N for the bindings of Ca to different polyuronates: LGA (solid line); HGA (dashed line); LMP (dash dotted line); and HMP (dotted line). Normalization is done on the basis of per mole of specific-binding sites, which refer to guluronate and free galacturonic acid units for alginate and pectin, respectively. R is defined as the molar ratio of Ca to the specific-binding sites. Note that the data for alginate was reproduced from the previous paper (Fang et al., 2007).

Secondary binding (egg-box) is much more energetically favorable for alginate (guluronate) than for pectin (galacturonate)

Pectins *c.f.* Alginates

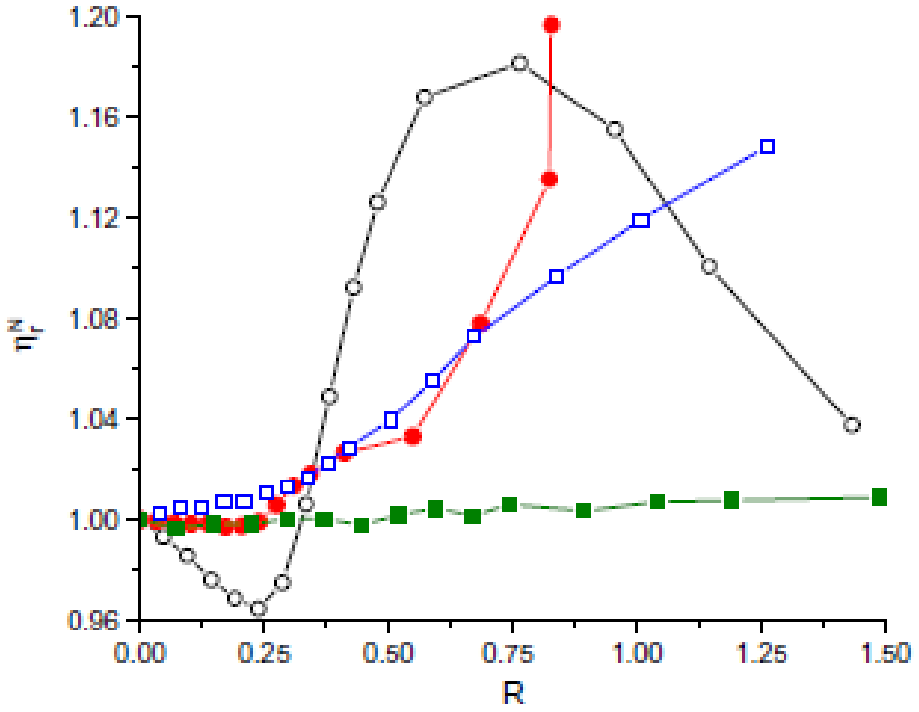

Fig. 6. Comparison of the changes of the normalized relative viscosity η_r^N for the bindings of Ca to different polyuronates: LGA (○); HGA (●); LMP (□); and HMP (■). *R* is the molar ratio of Ca to guluronate and free galacturonic acid units for alginate and pectin, respectively. The definition of η_r^N has been described in Section 2. Note that the viscosity data for alginate was reproduced from the previous paper (Fang et al., 2007).

ELSEVIER
Available online at www.sciencedirect.com
ScienceDirect
Carbohydrate Polymers 72 (2008) 334–341
Carbohydrate Polymers
www.elsevier.com/locate/carbpol

Binding behavior of calcium to polyuronates: Comparison of pectin with alginate

Yapeng Fang [a,*], Saphwan Al-Assaf [a], Glyn O. Phillips [a,b], Katsuyoshi Nishinari [a], Takahiro Funami [c], Peter A. Williams [d]

[a] Glyn O. Phillips Hydrocolloid Research Center, North East Wales Institute, Plas Coch, Mold Road, Wrexham LL11 2AW, UK
[b] Phillips Hydrocolloid Research Ltd., 45 Old Bond Street, London W1S 4AQ, UK
[c] Hydrocolloid Laboratory, San-Ei Gen F.F.I., Inc., 1-1-11 Sanwa-cho, Toyonaka, Osaka 561-8588, Japan
[d] Centre for Water-Soluble Polymers, North East Wales Institute, Plas Coch, Mold Road, Wrexham LL11 2AW, UK

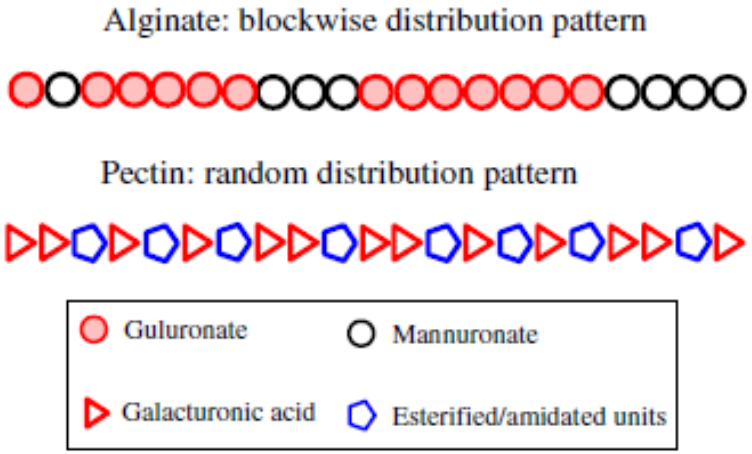

Fig. 7. Schematic illustration of the structural difference of alginate and pectin. Note that in reality the structure of pectin is much more complicated than is illustrated here, which is interrupted by many branched regions (so-called 'hairy' regions).

Chain Stiffness of Polysaccharides

Table 3
Calculated persistence length (L_p) and characteristic ratio (C_∞) for the four (1→4)-linked acidic polysaccharides

	α-D-Gal*p*A	α-L-Gul*p*A	β-D-Man*p*A	β-D-Glc*p*A
L_p (Å)	166	210	119	105
C_∞	72	91	43	41

1: glucuronan, 2: mannuronan, 3: guluronan, 4: galacturonan.

Modeling Gelation of Alginates

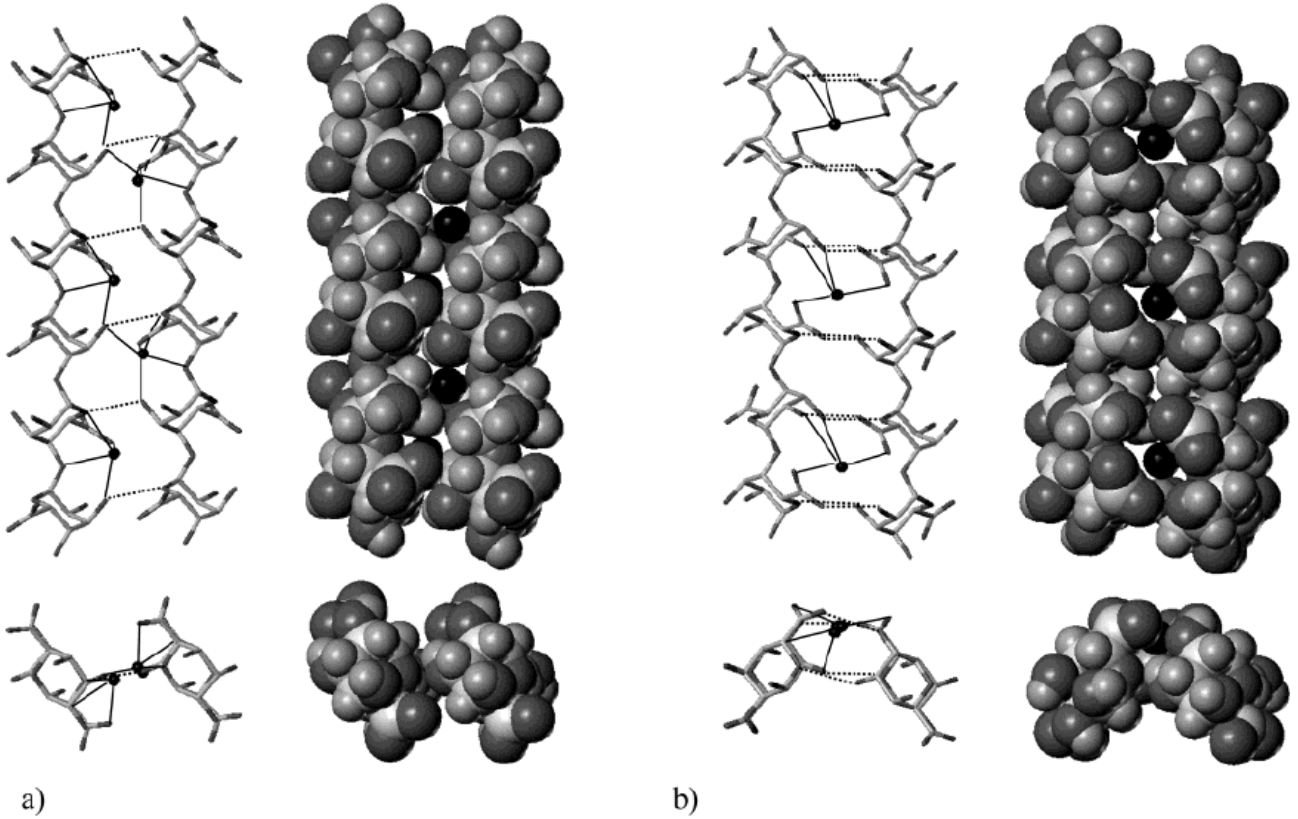

Figure 4. Representations (stick and van der Waals structures) of the best [chain–Ca^{2+}–chain] associations of 2-fold guluronate chains: (a) parallel arrangement; (b) antiparallel arrangement. Positions of calcium ions have been reoptimized with respect to the dimer structures. Dark circles represent calcium ions. Key: (—) calcium coordination; (- - -) hydrogen bonds.

The antiparallel chain pairing gave rise to an efficient hydrogen bond network with two complementary hydrogen bonds: O2âââO6, 2.73 Å (2.88 Å), and O3âââO5, 2.87 Å (2.91 Å). It also provided a unique periodic chelation site for calcium ions.

It is not possible to discriminate between the two forms of these chain pairings based on total energy; however, the antiparallel arrangement is probably favored in the gel since it has been reported that urea substantially weakens the gel.

The shape of this structure is close to that of the popular “egg box model”.

Calcium coordination: only four ligands from the chains, O2 and O6 of both chains

Braccini and Pérez *Biomacromolecules, Vol. 2, No. 4, 2001*

Modeling Gelation of Pectins

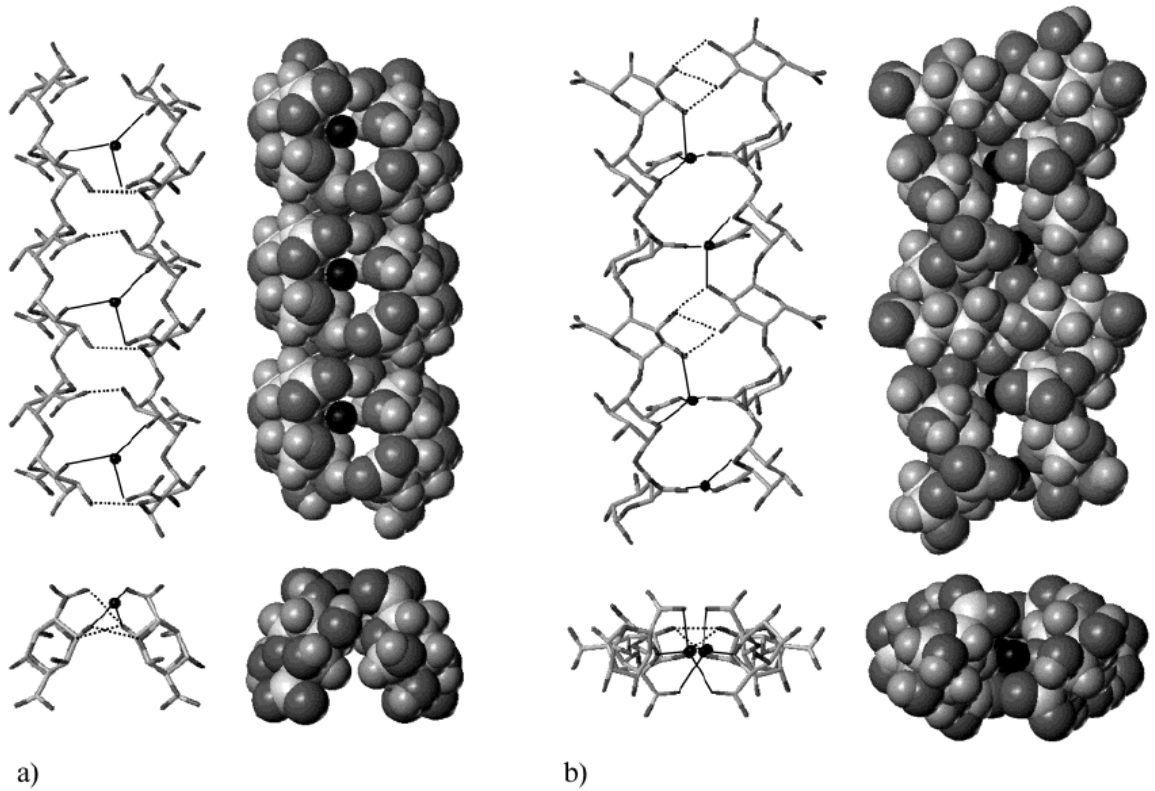

Figure 5. Representations (stick and van der Waals structures) of the best [chain−Ca^{2+}−chain] associations of antiparallel galacturonate chains: (a) $3_1$and (b) 2_1 helical conformations. Positions of calcium ions have been reoptimized with respect to the dimer structures. Dark

irrespective of the helical form, the antiparallel arrangement was the most favorable one.

this best antiparallel association is similar to the "egg box structure". But……

Braccini and Pérez *Biomacromolecules, Vol. 2, No. 4, 2001*

Modeling Gelation of Alginates and Pectins

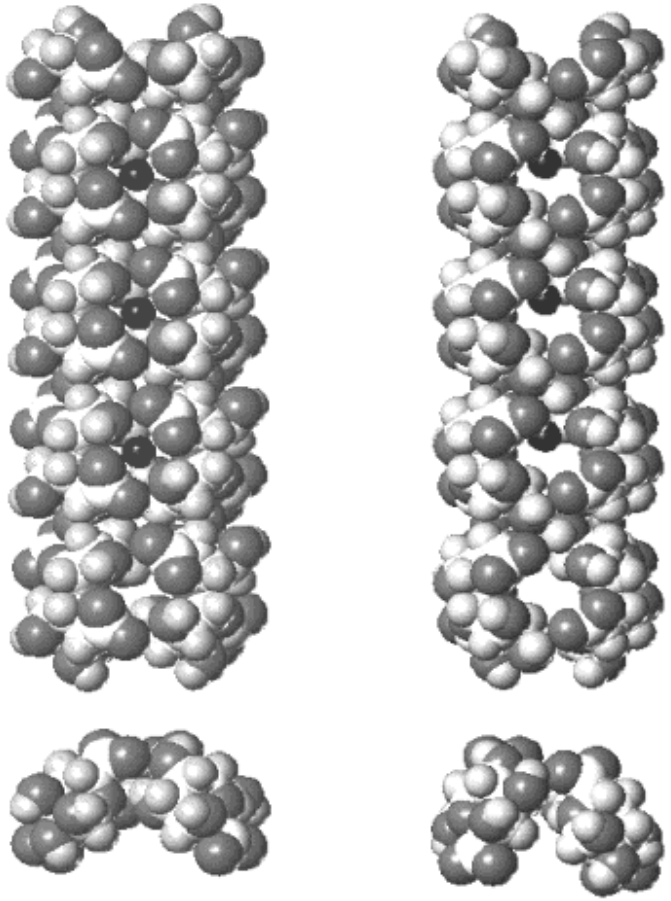

Figure 6. van der Waals representation of the calculated egg box models for (a) guluronate and (b) galacturonate chains, respectively. Dark circles represent the calcium ions.

For Pectate, the cavities formed by the joined chains do not have the proper size for calcium ions; they are far too large (Figure 6b).

The present calculations clearly demonstrate that the "egg box model" cannot correspond to the pairwise associations of pectate chains that form the junction zones in calcium pectate gels.

Braccini and Pérez *Biomacromolecules, Vol. 2, No. 4, 2001*

Stretching properties of xanthan, carob, modified guar and celluloses in cosmetic emulsions

Laura Gilbert, Vincent Loisel, Géraldine Savary, Michel Grisel, Céline Picard*

Université du Havre, URCOM, EA 3221, FR CNRS 3038, 25, rue Philippe Lebon B.P. 540, 76058 Le Havre Cedex, France

Carbohydrate Polymers 93 (2013) 644–650

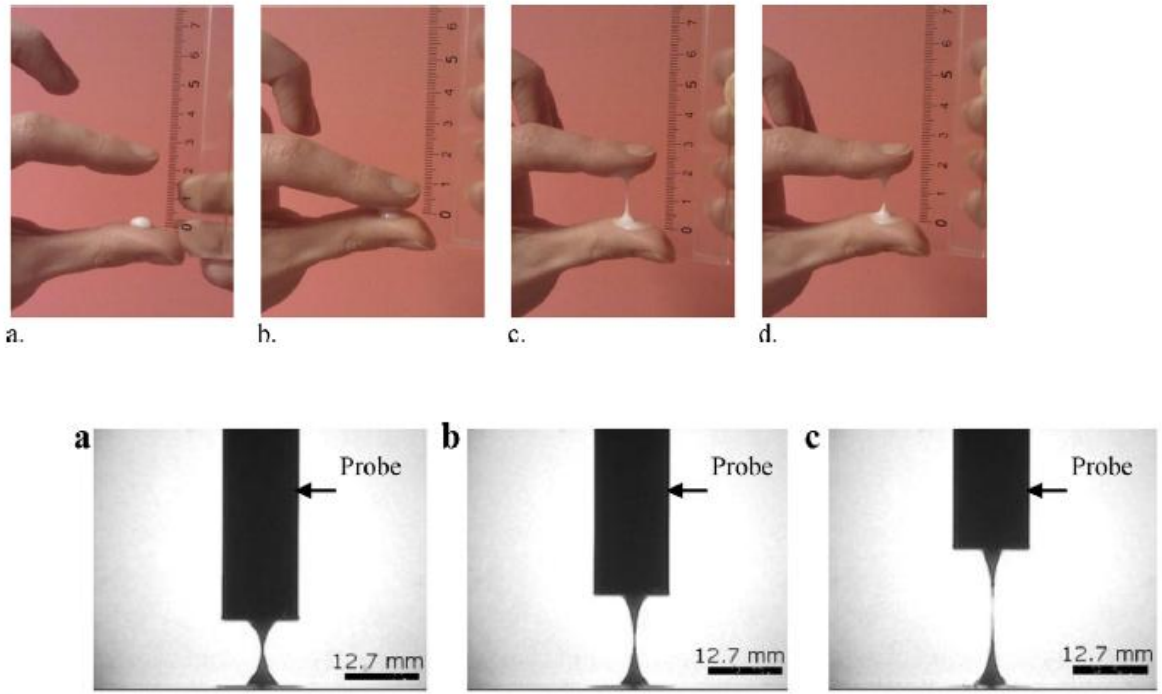

Fig. 6. Images of the stretching properties (L_{max}) of the Control (a), HPM cellulose (b) and HP guar (c) emulsions. Experiments were performed at 40 mm/s, with the P/0.5R probe and a gap of 0.8 mm over 1 cycle.

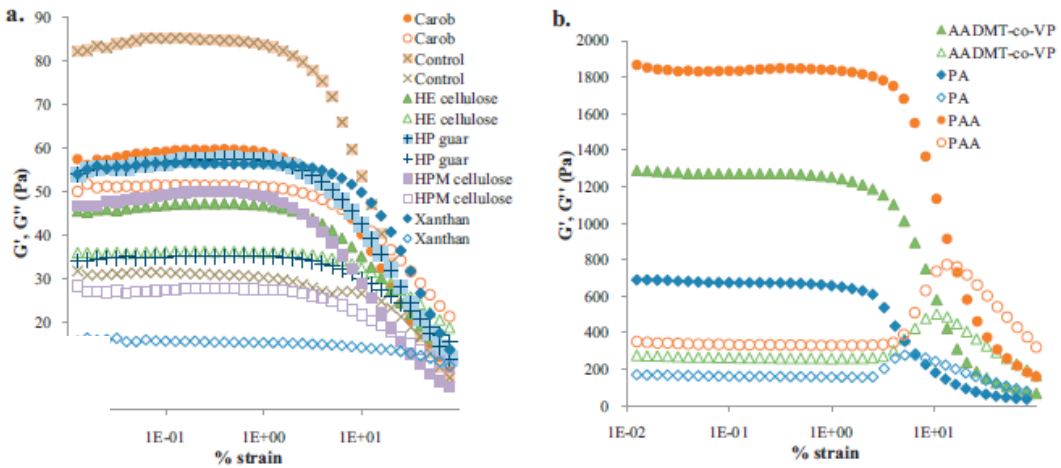

ization of the 9 O/W emulsions (codes detailed in Section 2.1.1) at 1 rad s^{-1}. Each curve presents the mean values over three tests. The standard n 5%, and are not shown for a better readability. Solid symbols: storage modulus, G'; hollow symbols: loss modulus G''. Part (a) corresponds to arbohydrate polymer and the control one; part (b) corresponds to the emulsions containing a synthetic polymer.

CaBER Extensional Rheometer

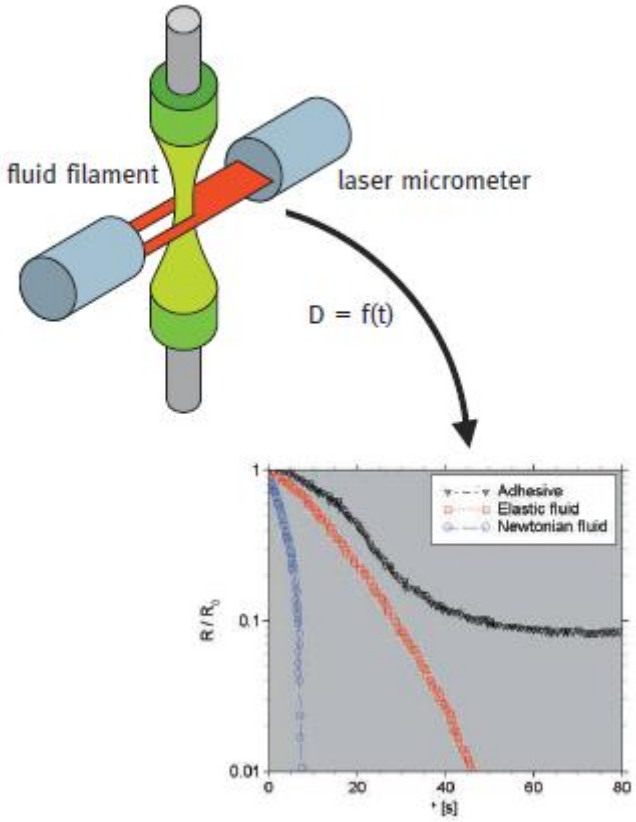

Glycol stretched in the CaBER.

http://www.campoly.com/files/8113/5216/6124/CaBER.pdf

Galactomannans

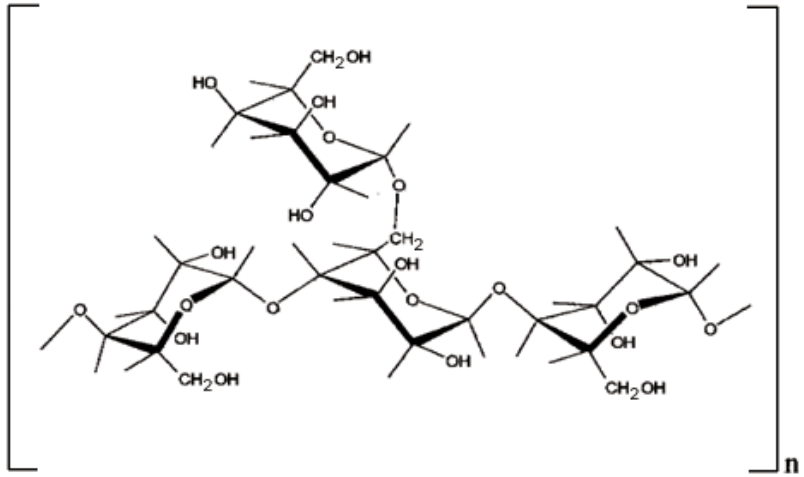

Figure 1. Proposed structure of a galactomannan of average 3:1 mannose to galactose ratio.

Galactomannan substitution levels

Ivory nut mannan	no galactose
Locust bean gum	1 galactose / 4 mannose
Tara Gum	1 galactose / 3 mannose
Guar Gum	1 galactose / 2 mannose
Fenugreek Gum	1 galactose / 1 mannose

- Guar gum forms viscous solutions with a long texture.
- Locust Bean Gum forms viscous, shear thinning solutions.
  - can form gels in combination with other hydrocolloids.
  - excellent in syneresis control

http://www.scielo.br/img/fbpe/jbchs/v12n6/a17fig01.gif

http://www.cybercolloids.net/library/carob/carob-and-locust-bean-gum-introduction

Guar Gum

- Guar is principally grown in India and Australia
- A nonionic hydrocolloid
- Guar gum is more soluble than locust bean gum
  - more galactose branch points = better stabilizer
  - it is not self-gelling (locust bean gum self-gels)
  - but calcium can crosslink guar gum to gel
  - not affected by ionic strength or pH over pH range 5-7
  - but will degrade at pH extremes at raised temperatures (e.g. pH 3 at 50 °C).[2]
  - Strong acids and alkalies hydrolyze gur gum
    - Lead to loss of viscosity
    - insoluble in most hydrocarbon solvents

Guar Gum

- Guar gum shows high low-shear viscosity
  - strongly shear-thinning.
  - Very thixotropic above 1% concentration,
  - below 0.3%, the thixotropy is small
  - Greater low-shear viscosity than locust bean gum,
  - shows viscosity synergy with Xanthan Gum
- Guar gum retards ice crystal growth
  - by slowing mass transfer across the solid/liquid interface.
  - It shows good stability during freeze-thaw cycles.[

Guar Gum

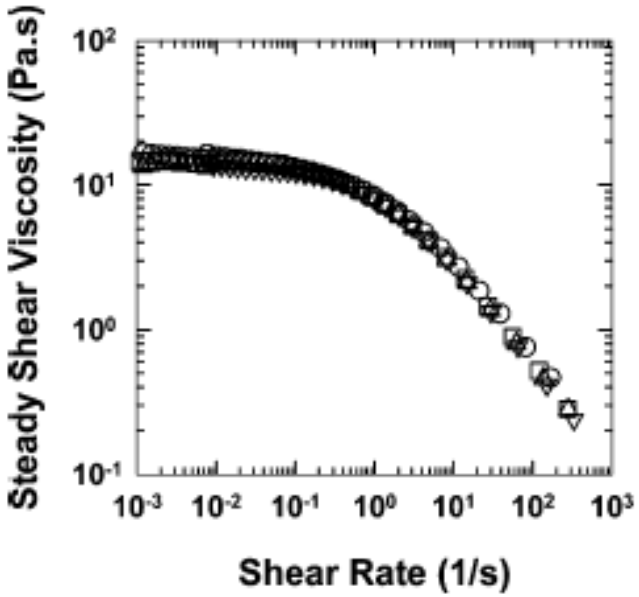

Figure 2. Steady shear behavior of a 1% guar solution. The figure shows the master curve obtained by time–temperature superposition of flow curves measured at 25 (○), 50 (□), 60 (△), and 75 °C (▽).

Shamsheer Mahammad, Donald A. Comfort, Robert M. Kelly, and Saad A. Khan,

Biomacromolecules **2007**, *8*, 949–956

Rheological Properties of Guar Galactomannan Solutions during Hydrolysis with Galactomannanase and α-Galactosidase Enzyme Mixtures

Locust Bean Gum

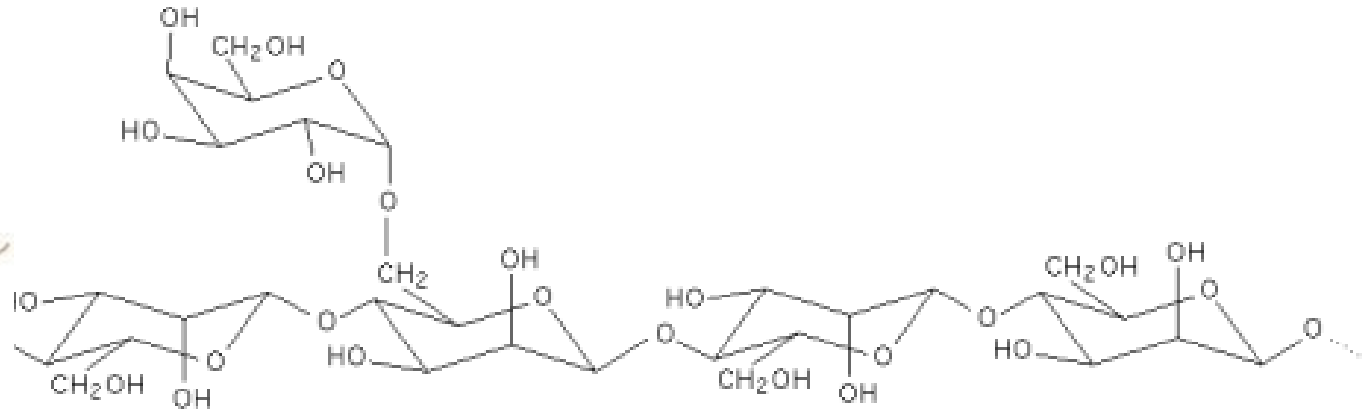

LBG is only partially soluble in cold water. The mannan sections of the polymer chain can bind together to form a crystalline region which is thermodynamically more stable than the solution state. Hence even when in solution at ambient temperature there is a tendency for the polymer chains to wish to aggregate

http://www.cybercolloids.net/library/carob/carob-and-locust-bean-gum-introduction

The aggregation can be increased by reductions in water activity and reduction in solution temperature which ultimately forms a 3D network and a gel. This is exactly what happens in ice cream during freezing. Their are two great advantages of this: firstly a weak gel structure does not impart a slimy or slippery mouth feel to the ice cream and more critically the formation of a weak gel on cooling imparts excellent meltdown resistance to the ice cream.

Gallactomannans - Cassia

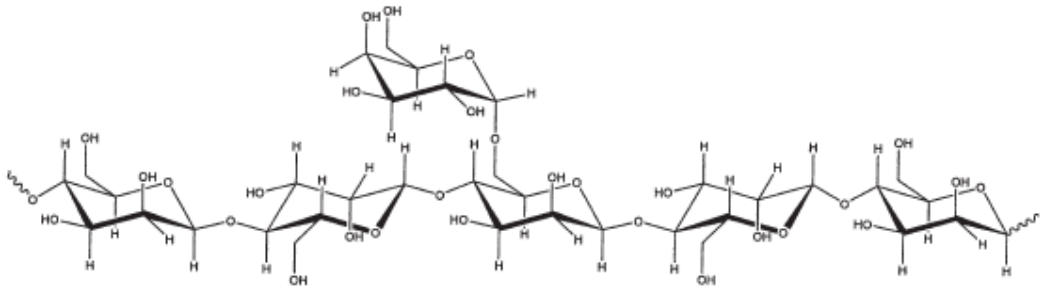

Figure 1. Average repeat unit for cassia.

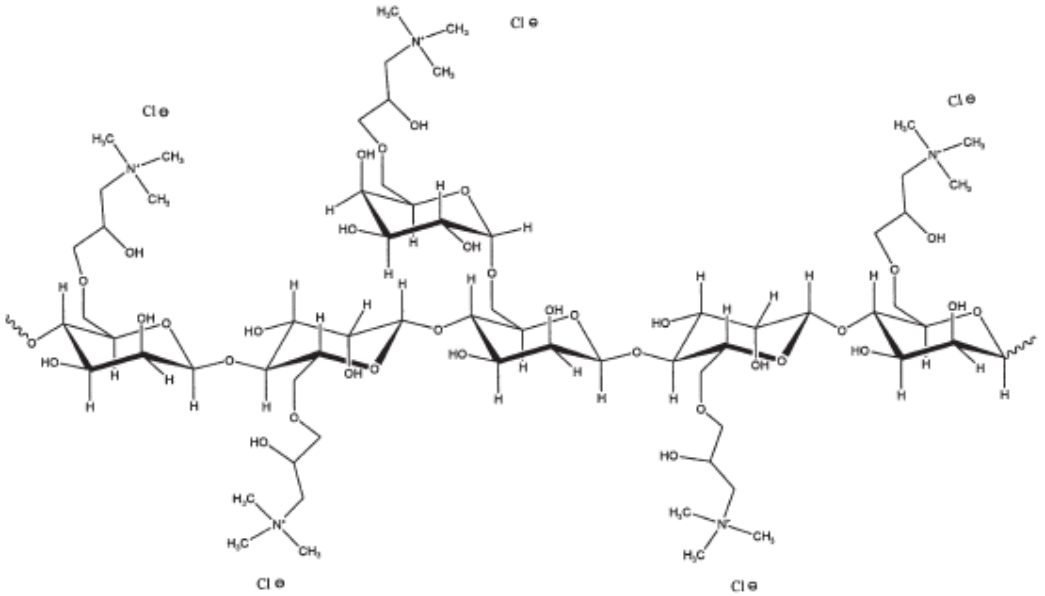

Figure 2. Average repeat unit for cassia hydroxypropyltrimonium chloride at a substitution level of 3.0 meq/g.

DENISE WADE RAFFERTY, JOSEPH ZELLIA, DANIEL HASMAN, and JOHN MULLAY **The mechanics of fi xatives as explained by polymer composite principles**, *J. Cosmet. Sci.*, ***60, 251–259 (March/April 2009)***

Polysaccharides Hydroxypropylguar

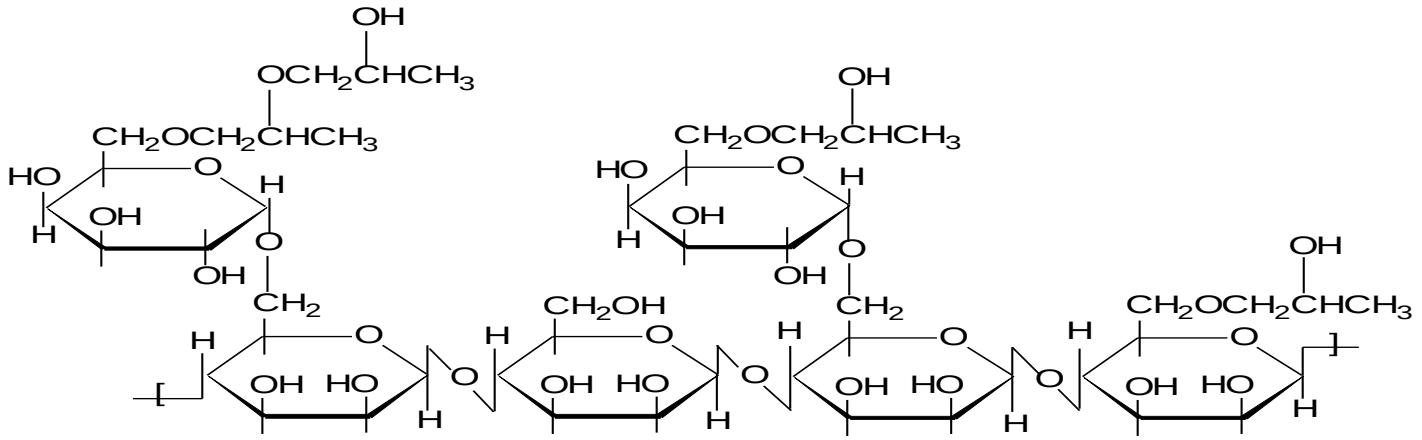

- Galactomannan
- pH range 4-8
- Compatible with surfactants
- Pseudoplastic

Xanthan Gum

- **Xanthan gum** is a polysaccharide secreted by the bacterium Xanthomonas Campestris
- Xanthan gum forms pseudo-plastic viscous solutions,
  - pH and temperature stable compared to other thickeners.
- Pseudo-plasticity
  - suitable as a stabilizer of suspensions, emulsions and foams

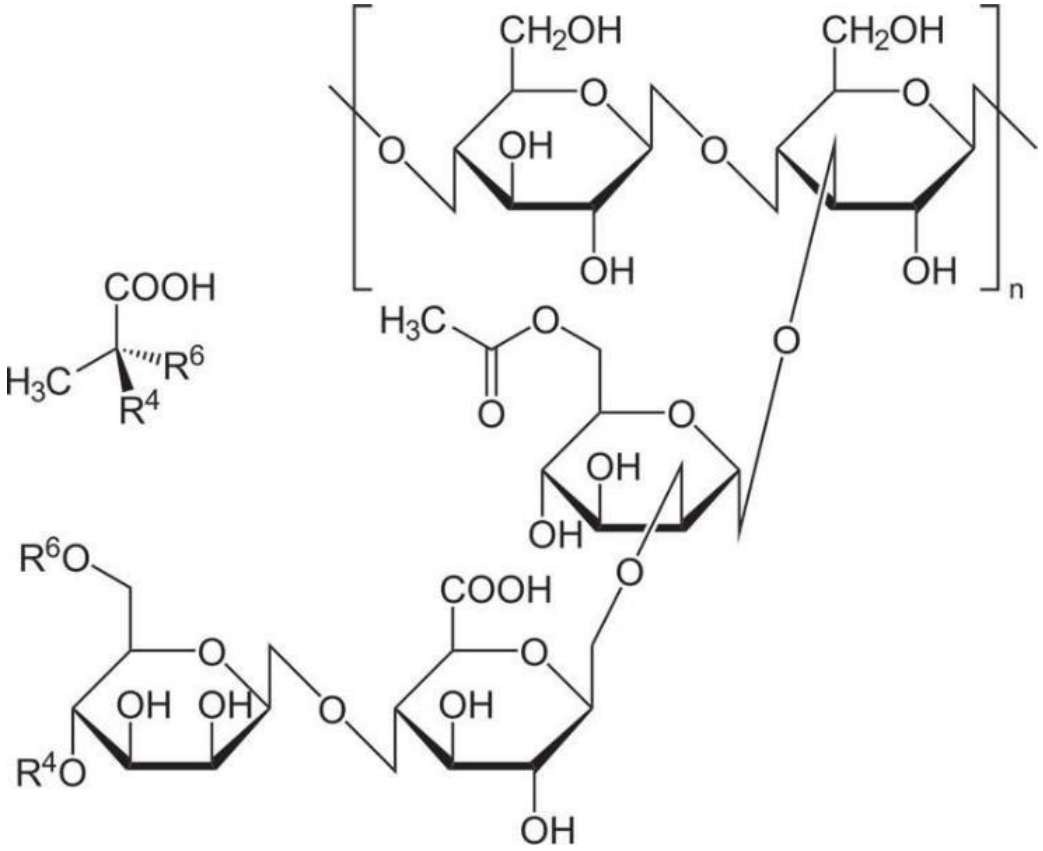

http://chemistry.about.com/od/factsstructures/ig/Chemical-Structures---X/Xanthan-Gum.htm

Polysaccharides-Xanthan Gum

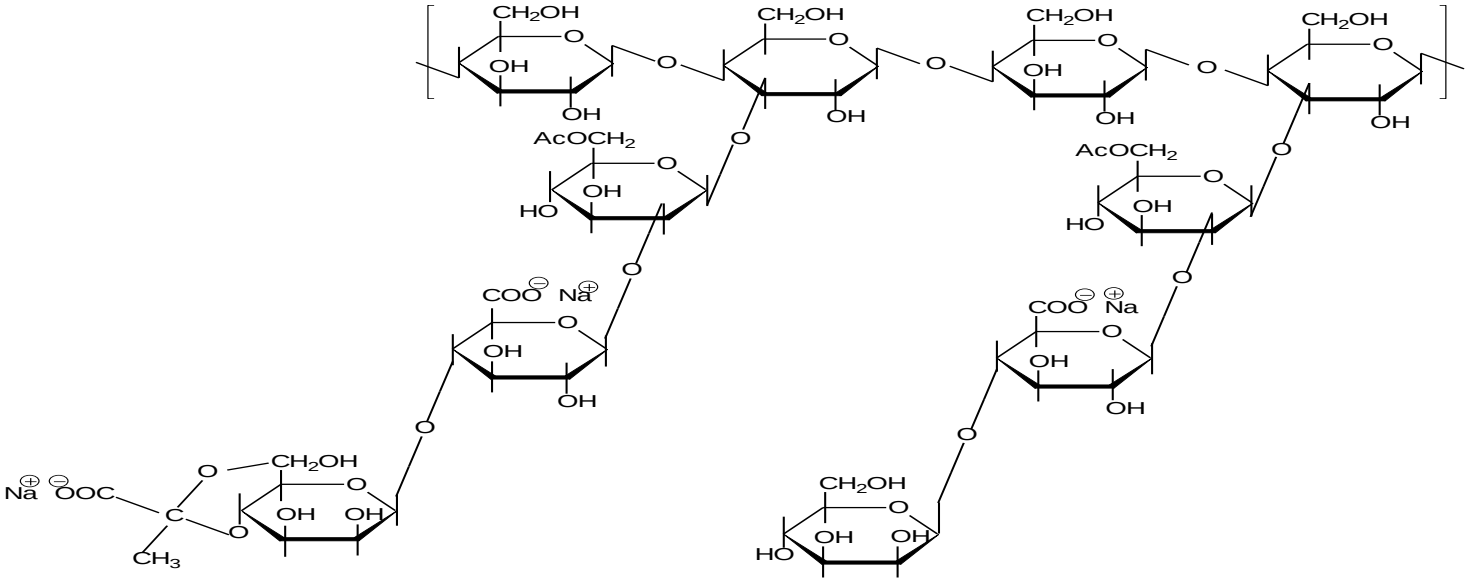

- Branched Polysaccharide produced by fermentation from *Xanthomonas campestris*
- Polymer repeat unit is Li amhydroglucose-with trisaccharide chain on C-3 on alternating rings
- Exists as single, double, or triple helices
- Helical matrix Imparts pseudoplasticity, suspending and instant recovery
- Salt-resistant

Xanthan Gum

Figure 2: Effect of Electrolyte on Xanthan Molecular Configuration

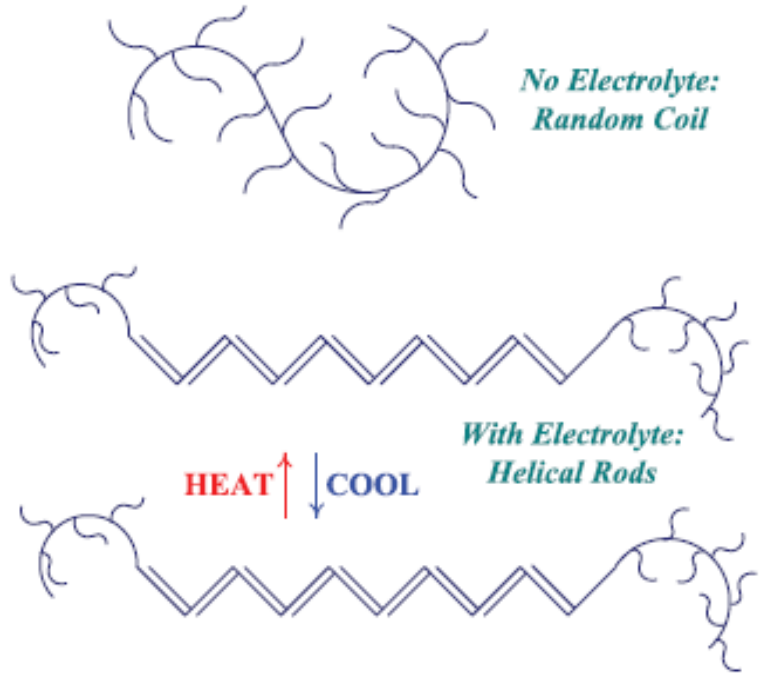

http://www.rtvanderbilt.com/vanzan.pdf

Xanthan Gum

Figure 3: Xanthan Gum Polymer Network

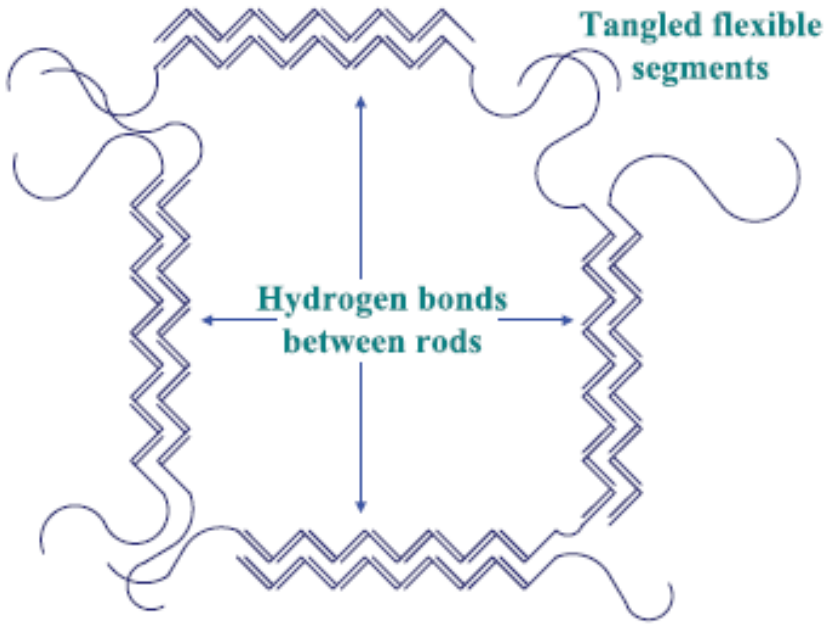

http://www.rtvanderbilt.com/vanzan.pdf

Xanthan Gum

Figure 3: Xanthan Gum Polymer Network

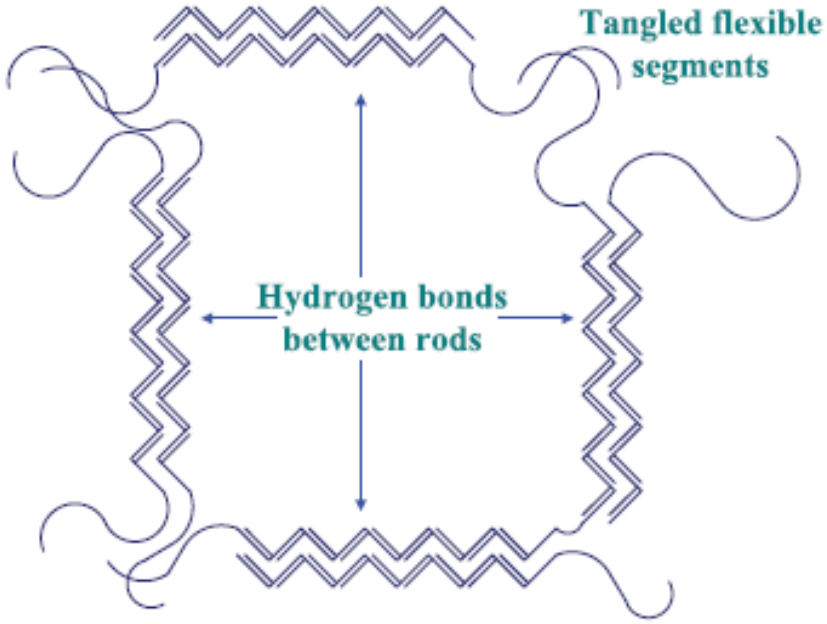

http://www.rtvanderbilt.com/vanzan.pdf

Particulate Thickeners

The Influence of Osmotic Pressure

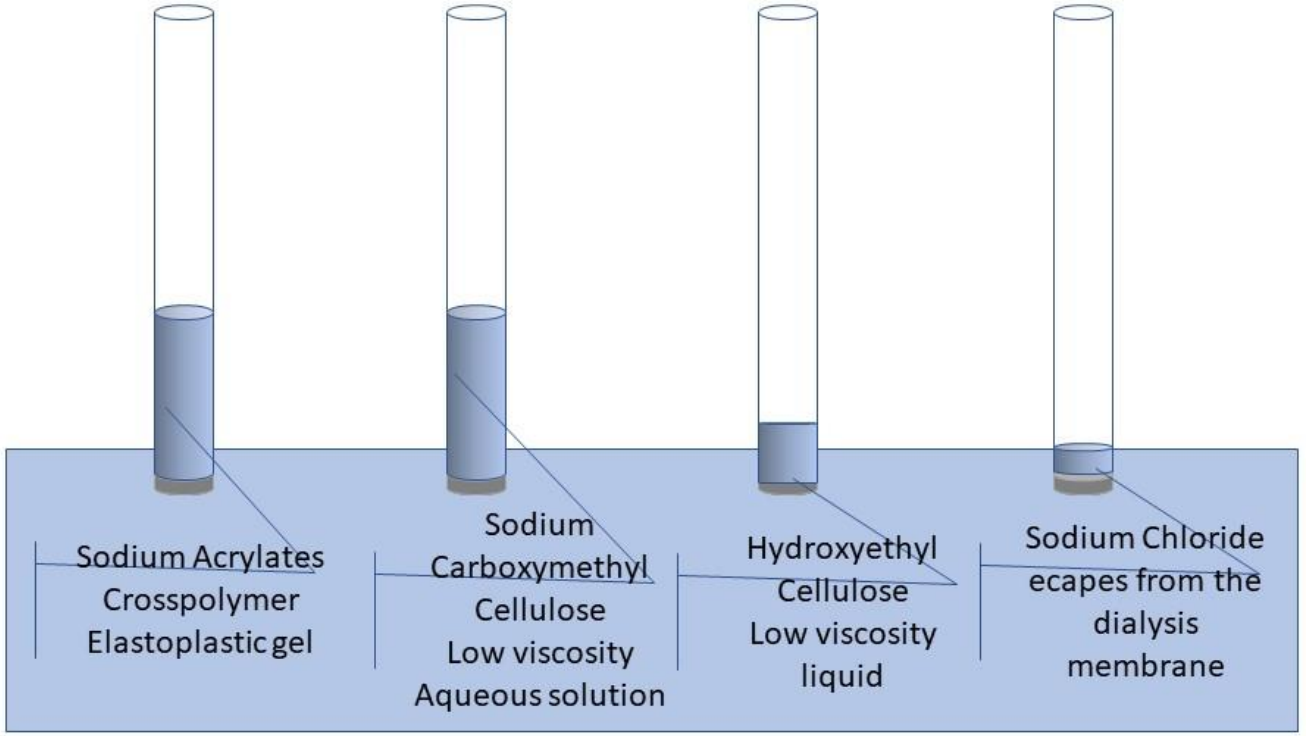

Figure 1: Schematic illustration of the effect of osmotic pressure on polymers entrapped in dialysis membranes which are dangled to just touch the water surface. Sodium Acrylates Crosspolymer osmotically 'sucks' in water to form an elastoplastic gel that rises far above the water surface. Similarly, the polyelectrolyte, sodium carboxymethylcellulose 'sucks' in water to form a non-viscous solution that rises far above the plane of the water surface. The nonionic polymer hydroxyethylcelllulose 'sucks' in a relatively small amount of water, whereas sodium chloride placed in the dialysis membrane escapes into the reservoir.

The Influence of Osmotic Pressure

Figure 2: The osmotic pressure experiment described in figure 1. The photograph was taken 48 hours after initially dangling the dialysis tubes into the water. From left to right the dialysis tubes contained 1 gram each of Sodium Acrylates Crosspolymer, Hydroxyethylcellulose, Sodium Carboxymethylcellulose, and common salt. The membrane with common salt collapsed as the salt diffused into the reservoir.

The Influence of Osmotic Pressure

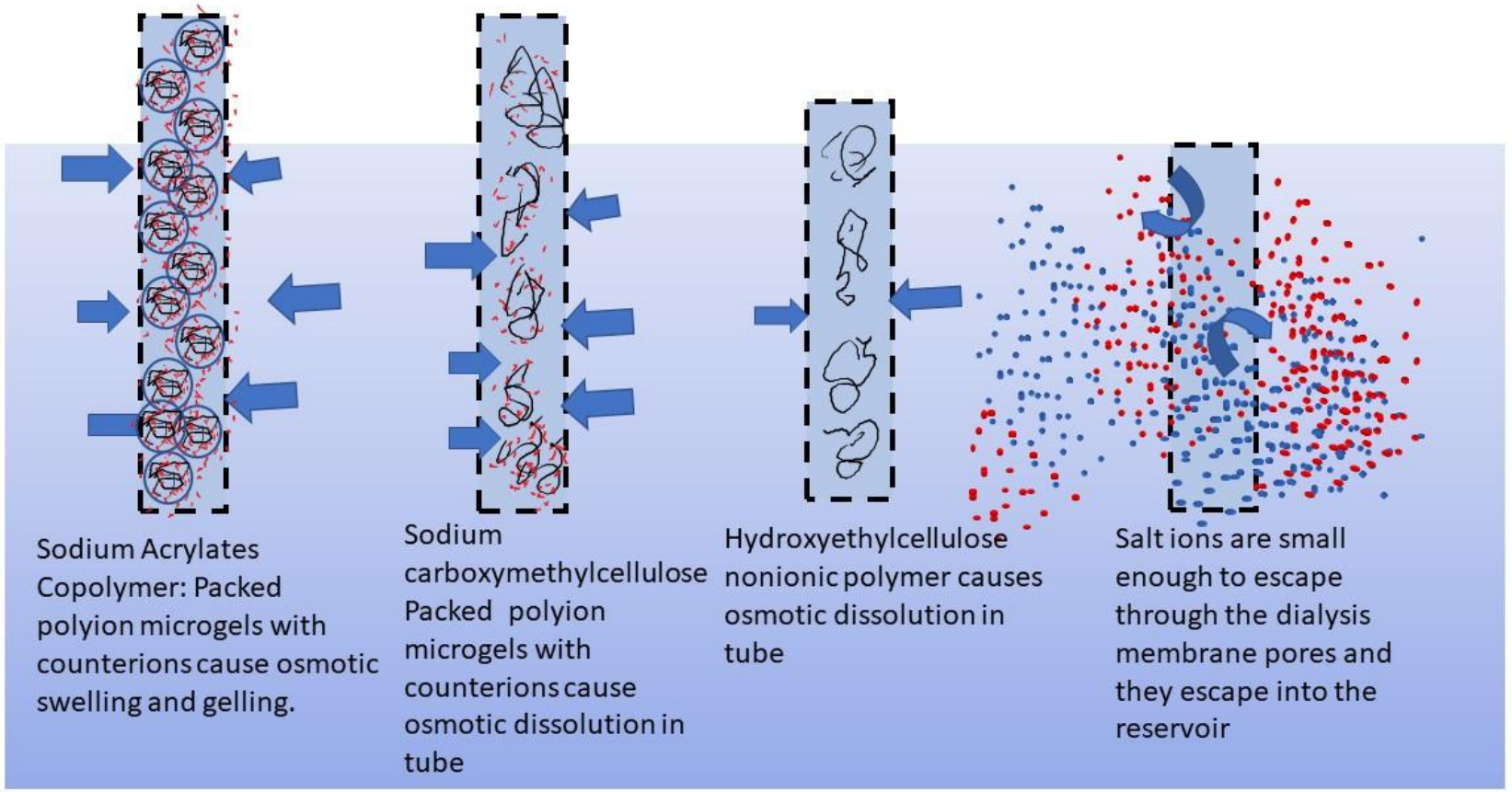

Figure 3: A schematic representation of the role of osmosis in the swelling and dissolution of polymers, polyions, and crosspolymer microgels. See text for explanation.

Critical Overlap and Critical Entanglement

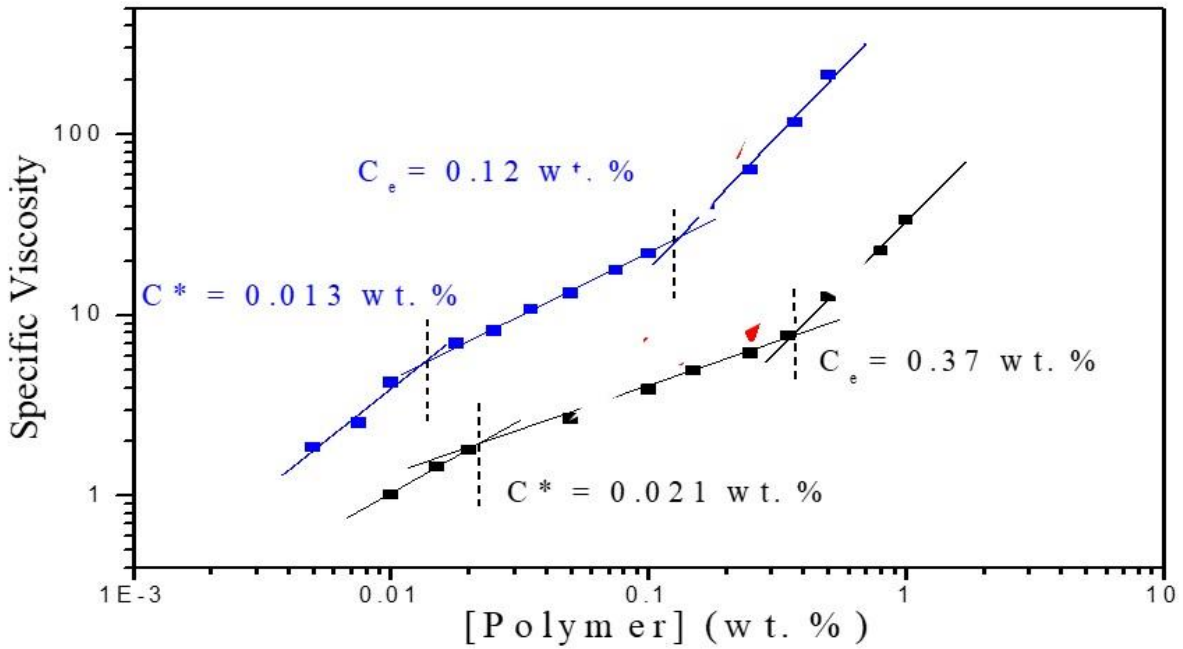

Figure 4: Viscometry can be used to find the critical overlap concentration (C*) and critical entanglement concentration (Ce) of polymers in solution.

Donnan Equilibrium

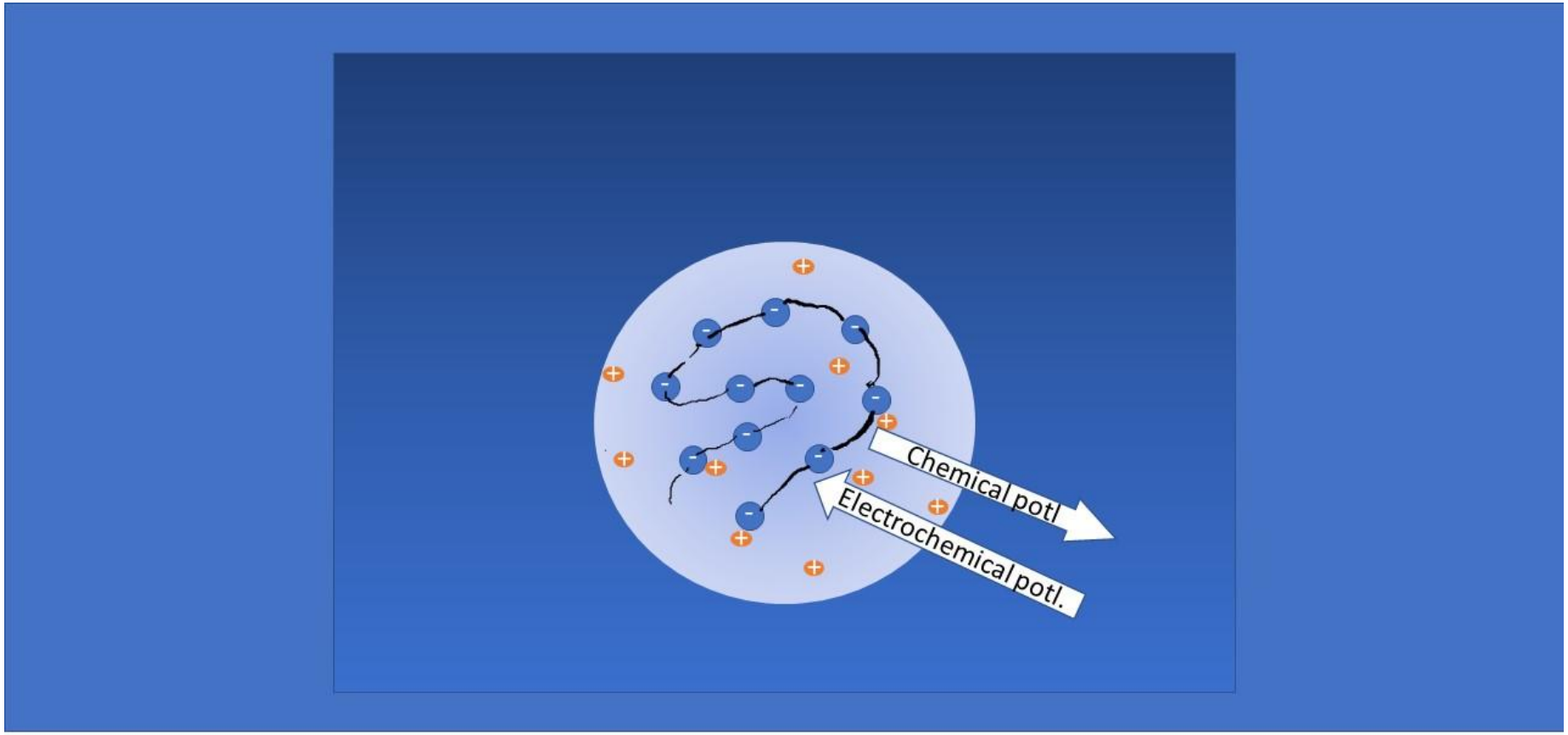

Figure : The Donnan Equilibrium in a polyelectrolyte; chemical potential tends to drive the counterions to form a homogenous solution but electrochemical potential attracts the counterions to the oppositely charge polyion. As a result, the counterions reside in a diffuse cloud around the polyion.

Donnan Equilibrium and Manning Condensation

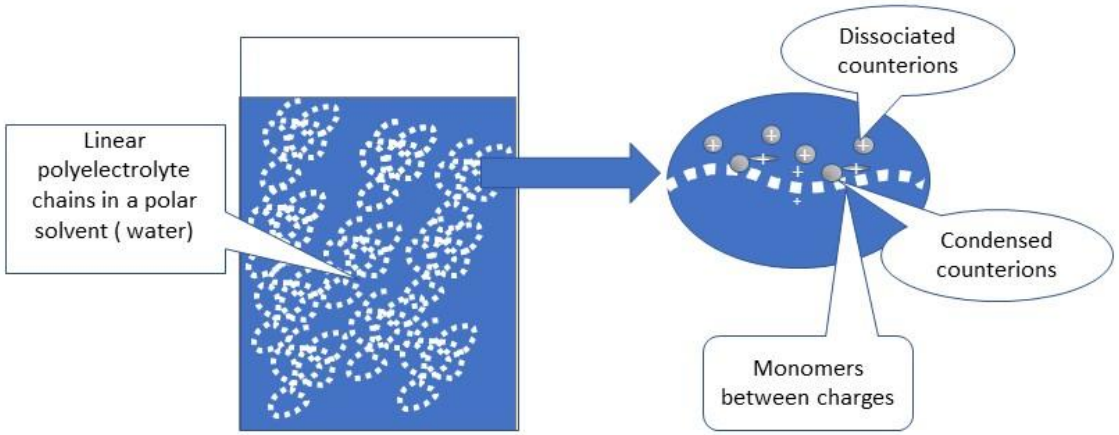

Figure 7 . There is a limit to the number of counterions that can be generated. According to Manning Theory, when the polyion attains a critical charge density, counterions condense on the polymer chain and the charge density of the chain and population of counterions remain constant. The counerions then exist in one of two states: either dissociated or condensed.. Figure adapted from M. Rubinstein, R.H. Colby, A.V Dobrynin, J-F Joanny.; Macromolecules, 1996, 29, 398.

Jamming Fluids

- Stir a Concentrated Dispersion of Corn Starch
  - If you stir fast enough it will become ‘solid’

- http://www.youtube.com/watch?v=f2XQ97XHjVw

Viscosity -Concentration Relationship

for suspension of
Non Interacting Particles

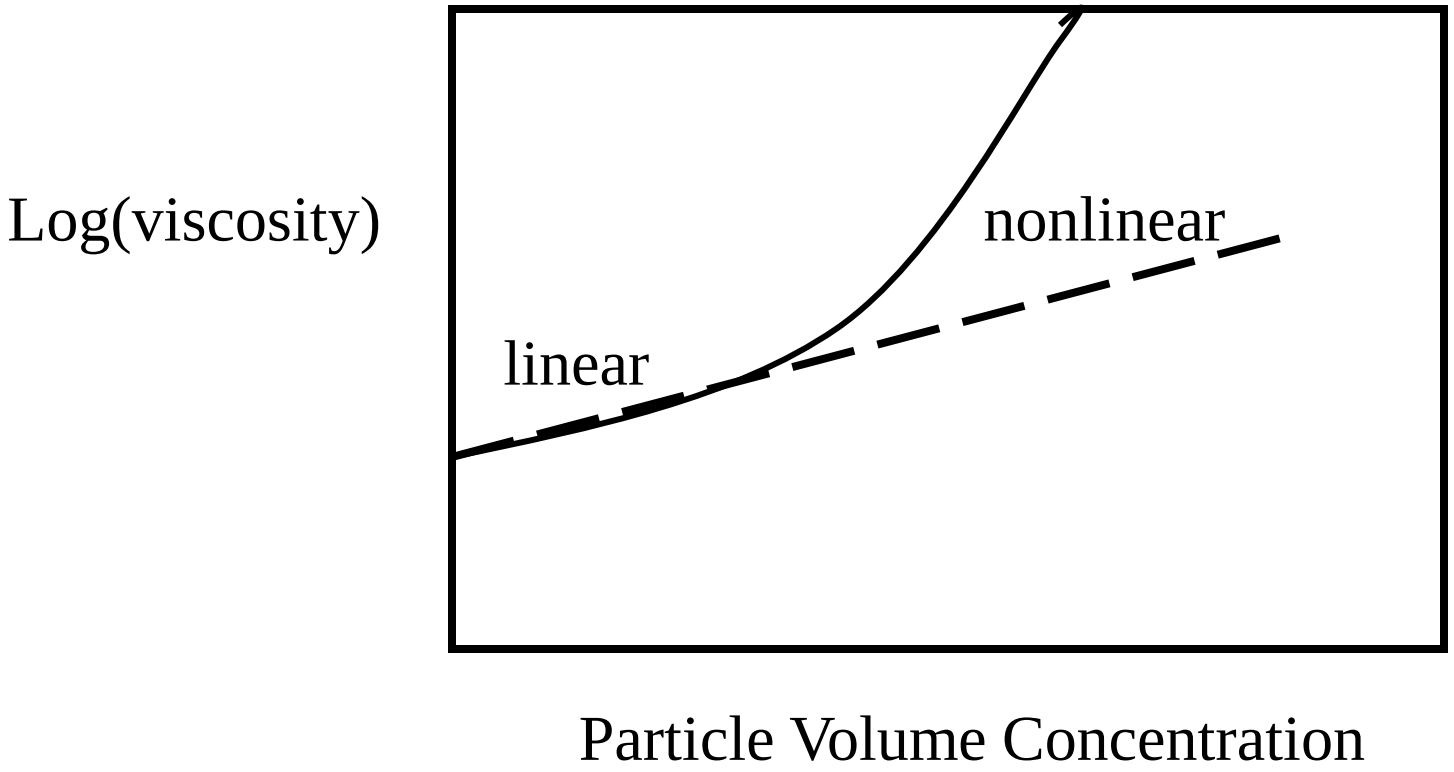

Viscosity -Concentration Relationship

for suspension of
Neglibly Interacting Particles

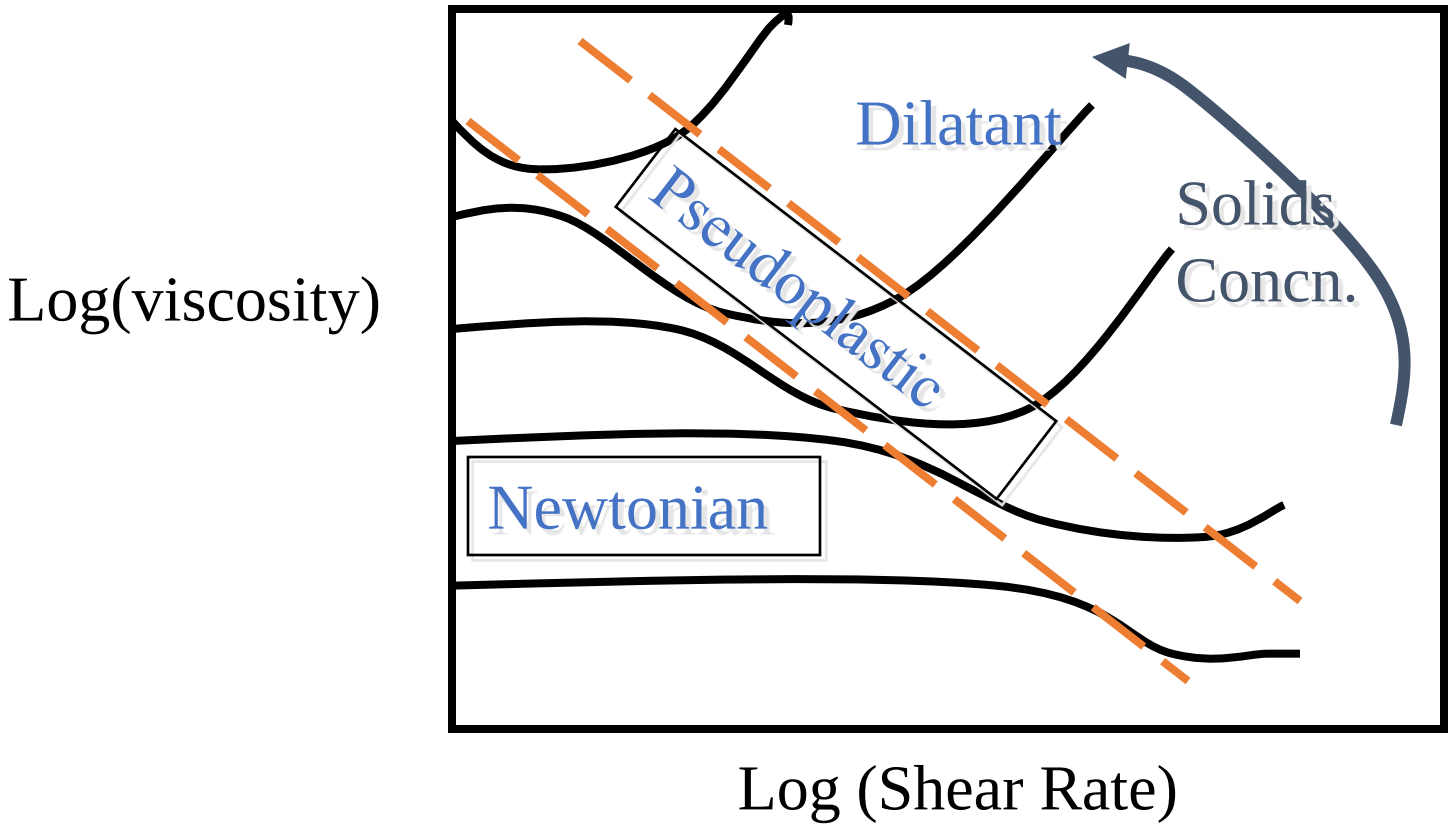

Rheological Behavior of Suspensions/Dispersions

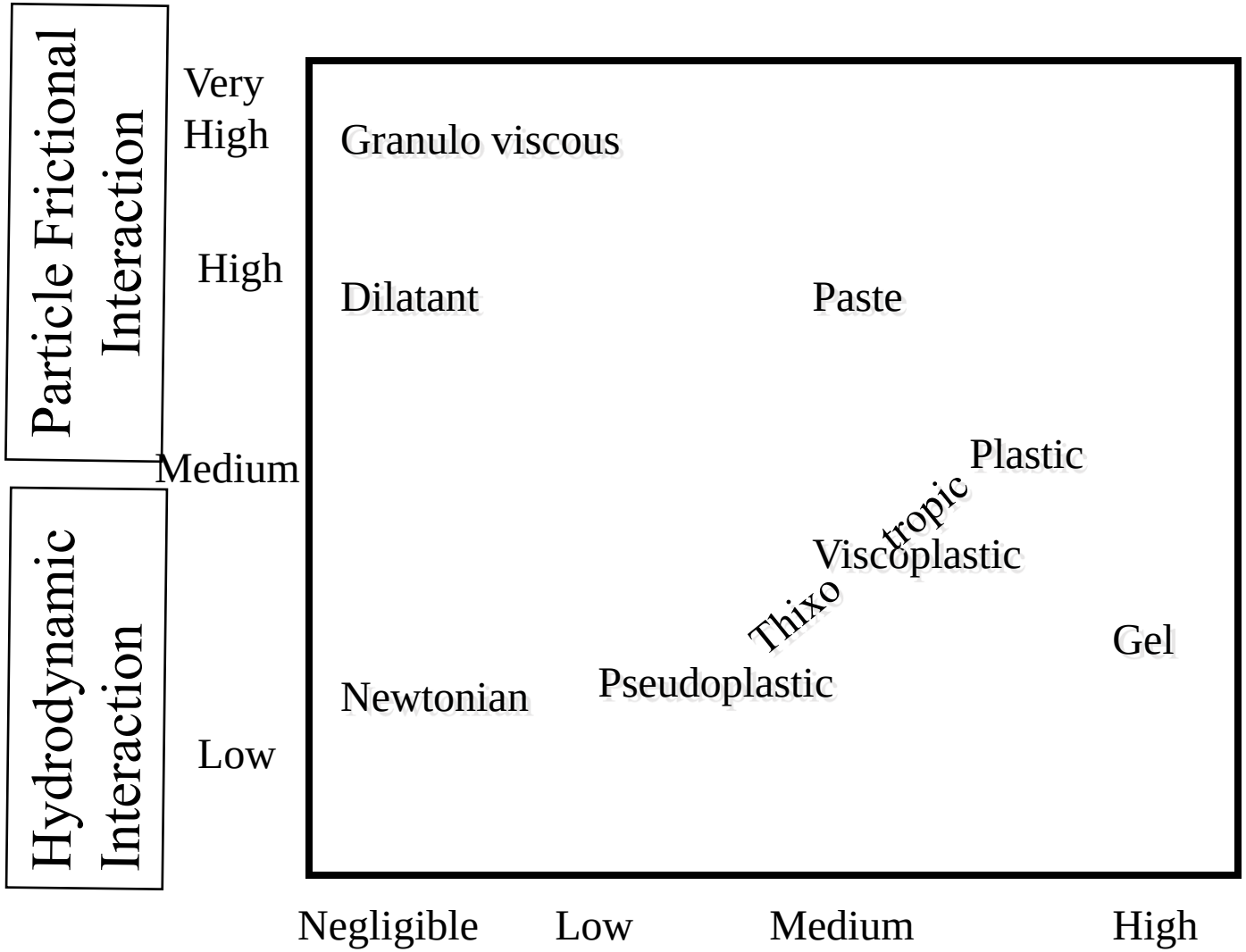

Jamming Fluids

- Incompatible loads cause transient rearrangements
  - Not steady flow!
- Even small perturbations can lead to ‘avalanches’
- General loadings in 3 dimensions require different orientations of force chains
  - Like a network or skeleton

Yield stress fluids

Yield stress fluids

- 2 Types:
  - Thixotropic yield stress fluids
  - Simple Yield stress fluids

Which is more viscous? Whipped cream or Syrup

- Upon stirring syrup give more resistance to flow
  - Conclude that syrup is more viscous
- But leave them standing
  - Syrup flattens and whipped cream keeps its shape
    - Therefore, it seems that whipped cream is more viscous than syrup.
- The conundrum is settled when one understands
  - Syrup is a Newtonian liquid
  - Whipped cream is solid below a critical applied
    - And flows when the stress exceeds that critical value.
- In fact whipped cream is a **yield stress fluid**

Yield Stress Fluids

- Yield stress fluids are characterized by a solidlike to liquidlike transition when the applied stress exceeds a yield stress.(1)
  - Creams, gels, structured shampoos
- 2 types of yield stress materials(2)
  - Simple yield stress materials
    - Foams, emulsions, Carbomer microgels
  - Thixotropic Yield Stress Materials
    - Avalanche fluids like clay dispersions

1. P. Coussot, H. Tabuteau, X. Chateau, L. Tocquer and G. Ovarlez, *J. Rheol.*, 2006, 50, 975–994
2. P. C. F. Møller, A. Fall, V. Chikkadi, D. Derks and D. Bonn, *Phil. Trans. R. Soc. Lond. A*, 2009, 367, 5139–5155.

Yield Stress Fluids

- Simple yield stress materials (1,2)
    - A finite critical shear rate
    - Instantaneous recovery after shear
- Thixotropic Yield Stress Materials (3,4)
    - Homogeneous flow at vanishingly small shear rates under controlled stress
    - Relatively long recovery times that correspond to the rebuilding of fluid structure

1. L. Becu, S. Manneville and A. Colin, *Phys. Rev. Lett.*, 2006, 96, 138302.
2. A. Ragouilliaux, G. Ovarlez, N. Shahidzadeh-Bonn, B. Herzhaft, T. Palermo and P. Coussot, *Phys. Rev. E*,2007, 76, 051408.
3. P. Coussot, L. Tocquer, C. Lanos and G. Ovarlez, *J.Non-Newtonian Fluid Mech.*, 2009, 158, 85–90.
4. G. Ovarlez, K. Krishan and S. Cohen-Addad, *Europhys. Lett.*, 2010, 91, 68005

The Herschel Bulkley Model of Yield Stress Fluids

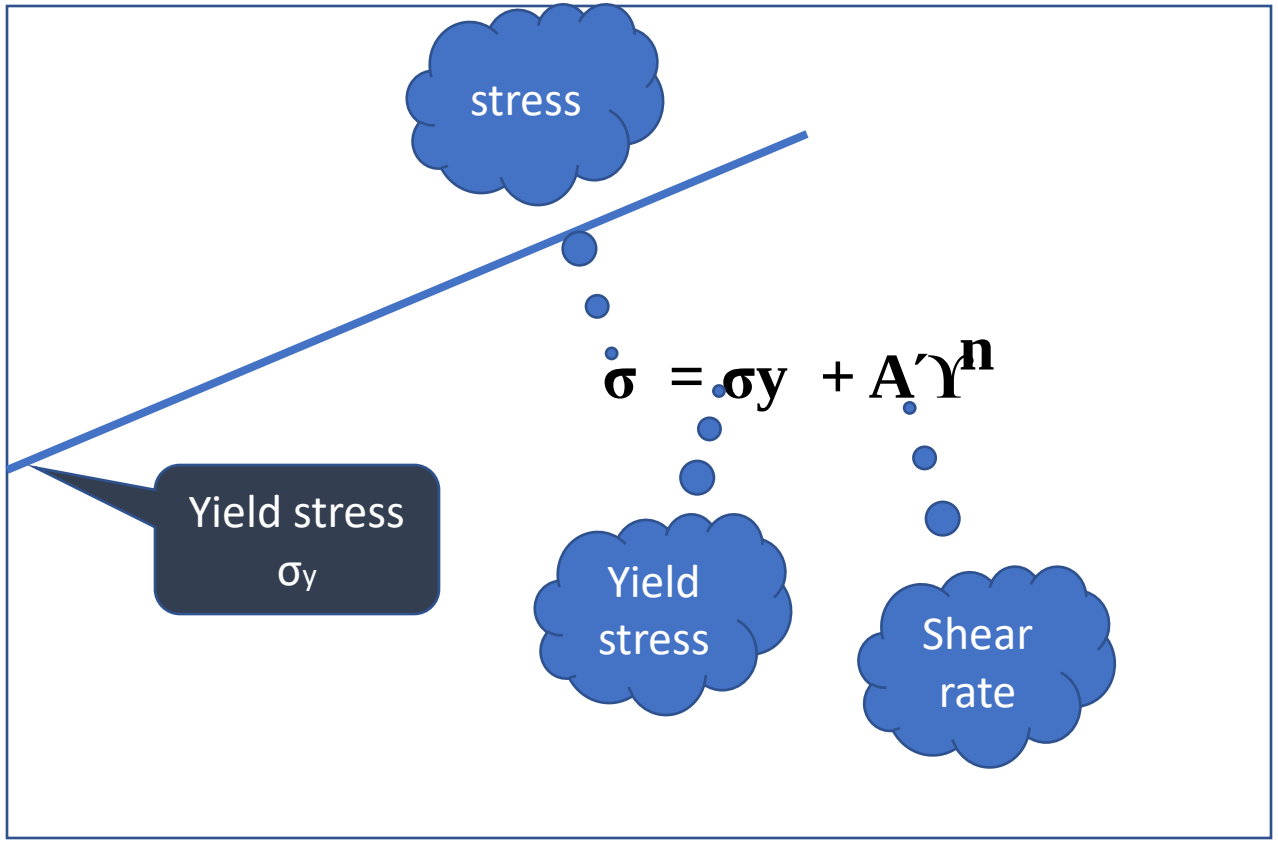

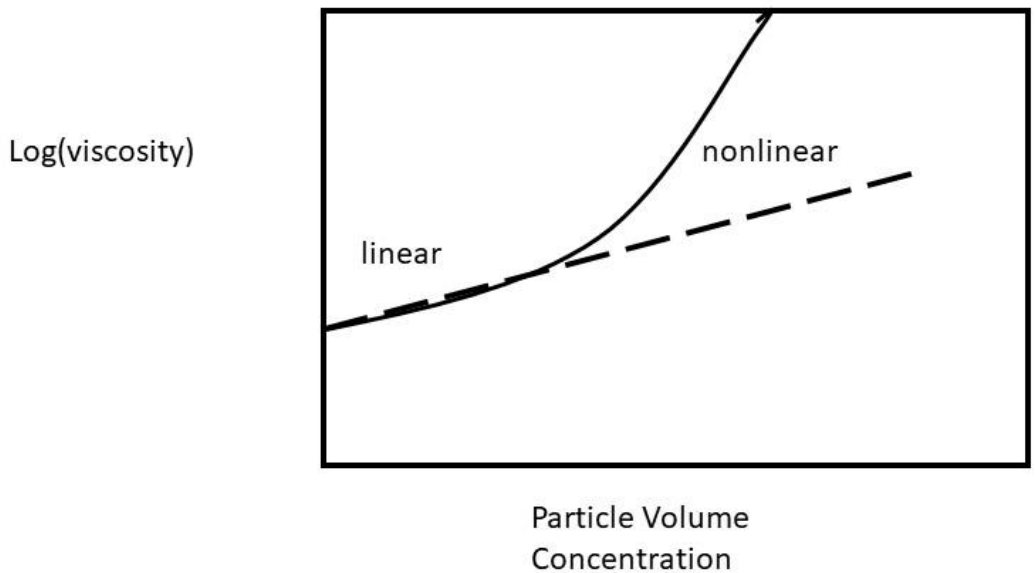

Figure 8: Viscosity -Concentration Relationship for suspensions of non Interacting Particles

1

Probing the Microstructure of Sodium Acrylates Crosspolymer

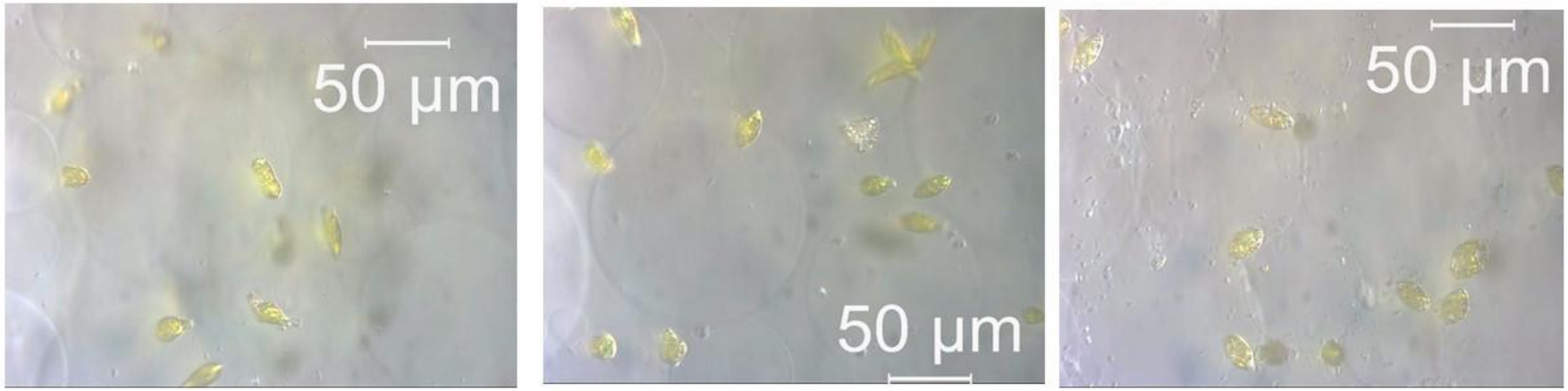

0.0625% Sodium Acrylates Crosspolymer. Euglena swim freely

0.125% Sodium Acrylates Crosspolymer. Euglena apparently swim through a maze

0.5 percent Sodium Acrylates Crosspolymer. Euglena trapped by their heads but flagellae can still move

Figure 10: The microstructure of polyelectrolyte crosspolymer gels can be probed by microscopic observation of the motion of Euglena micro-organisms

Slip at the wall

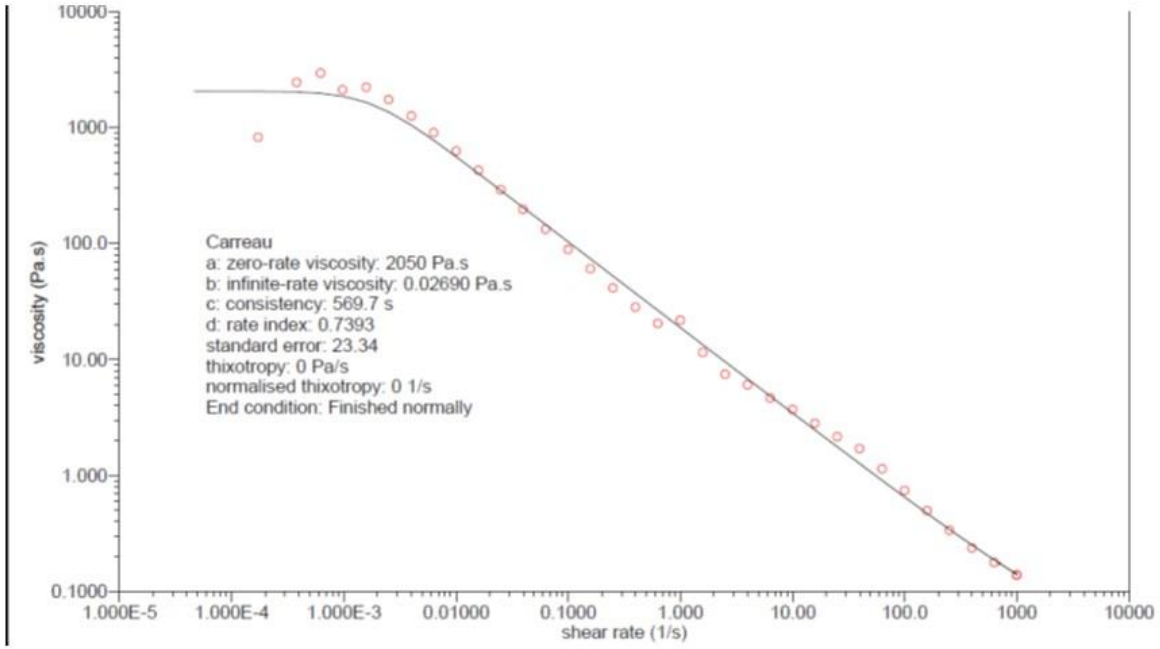

Figure 11: Controlled stress rheometry of a Sodium Acrylates Crosspolymer Gel. The low value of Viscosity for the measurement at the lowest shear rate is indicative of wall-slip or shear-banding prior to the yield stress. Note the pronounced shear-thinning after yield.

Avalanche Fluids

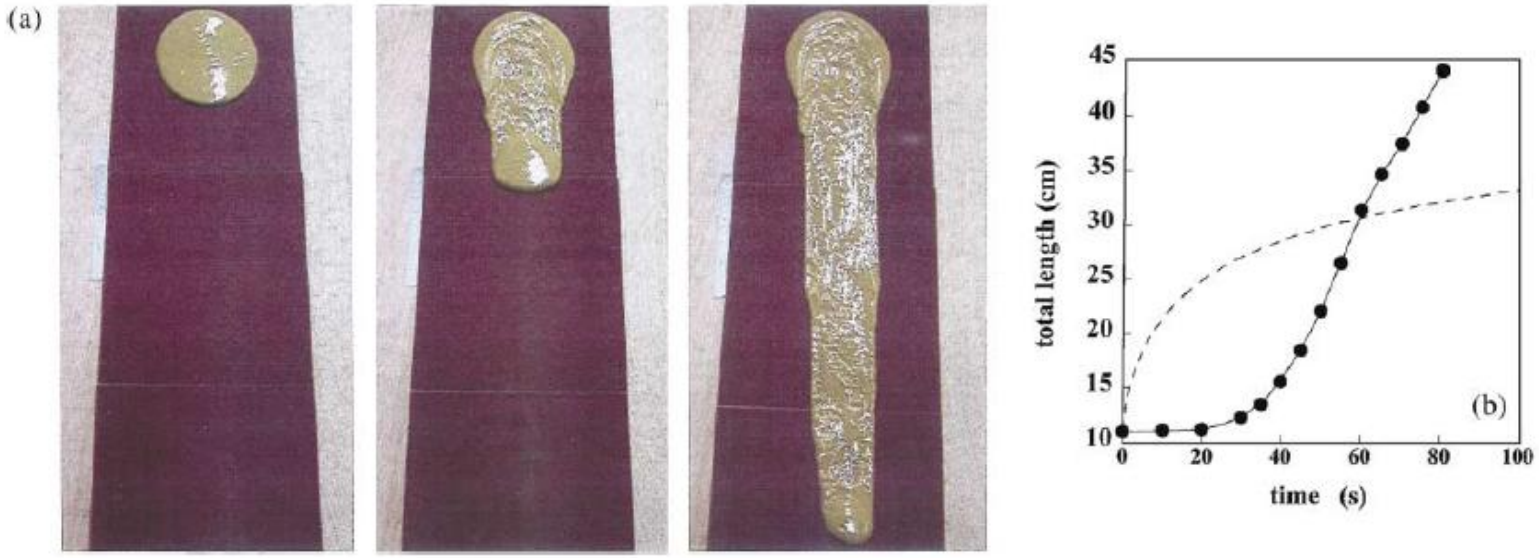

FIG. 2 (color). (a) Avalanche flow of a clay suspension over an inclined plane covered with sandpaper. The suspension was presheared and poured onto the plane, after which it was left at rest for 1 h. The pictures are taken at the critical angle for which the suspension just starts to flow visibly. (b) Distance traveled by the deposit as a function of time compared to that of a theoretical ideal yield stress fluid (dashed line).

Avalanche Fluids

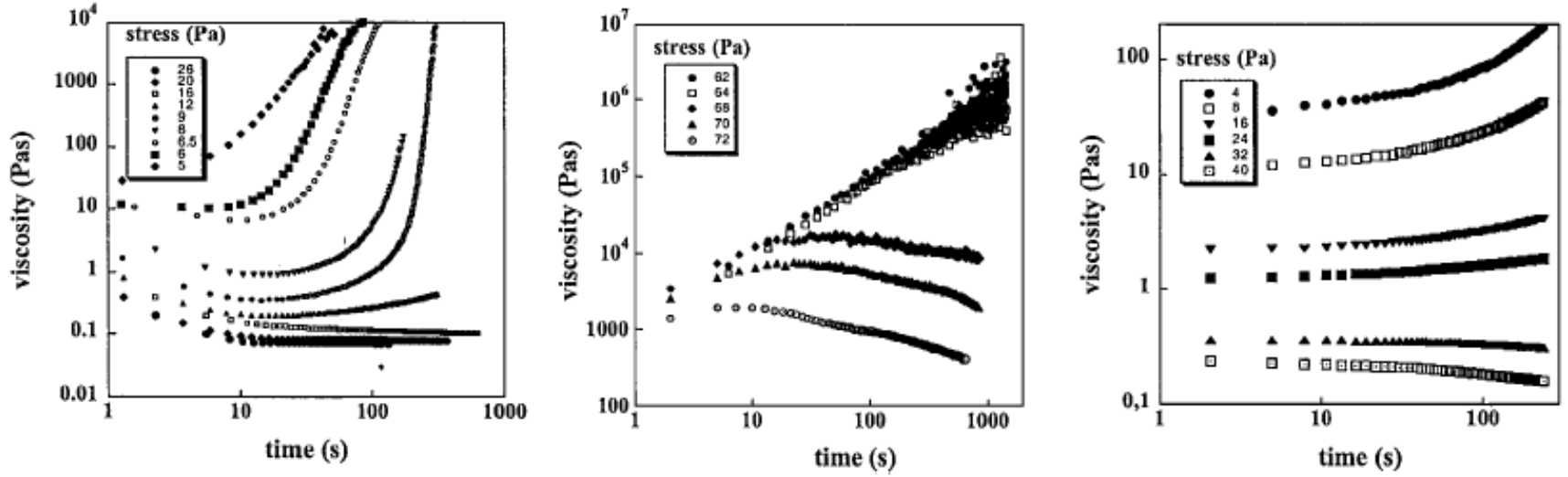

FIG. 3. Bifurcation in the rheological behavior: viscosity as a function of time for three completely different systems: from left to right, a weakly flocculated clay suspension: bentonite (solid fraction: 4%) in water; a polymer gel: a commercial hair gel (Vivelle dop) and a colloidal glass: 3% Laponite RD in water.

Bentonite structured clay suspension

Packed polymer microgels- hair gel

Colloidal Glass Laponite in water

Bentonite Clay

http://www.californiaearthminerals.com/media/09a-ionmin.jpg

http://www.rawell.co.uk/media/content/products_technical_information/what_is_bentonite/Platelet_Structure.jpg

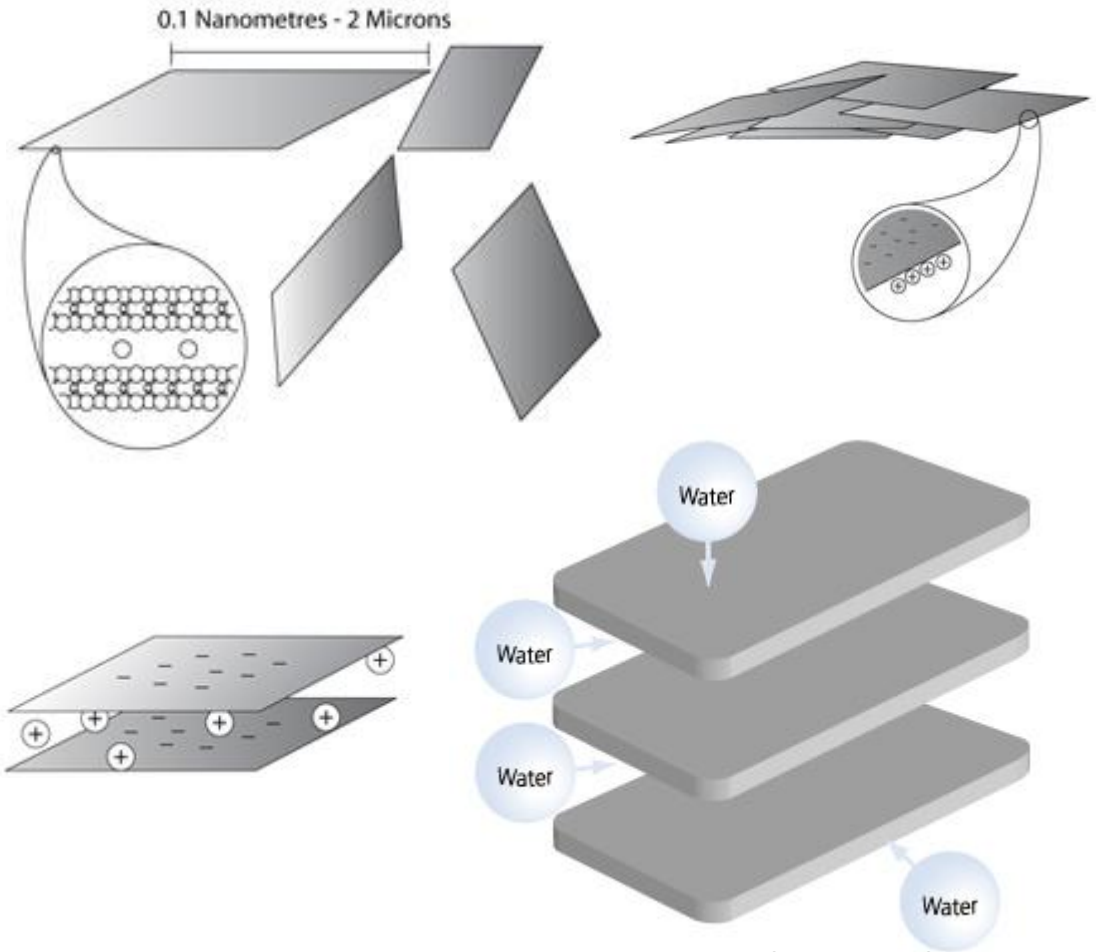

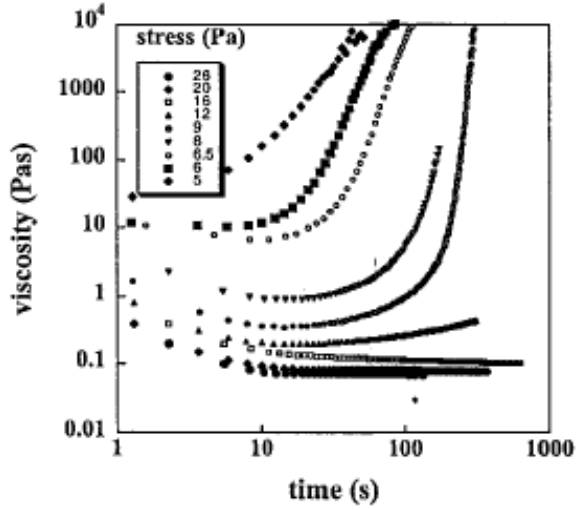

Laponite: Colloidal Glass

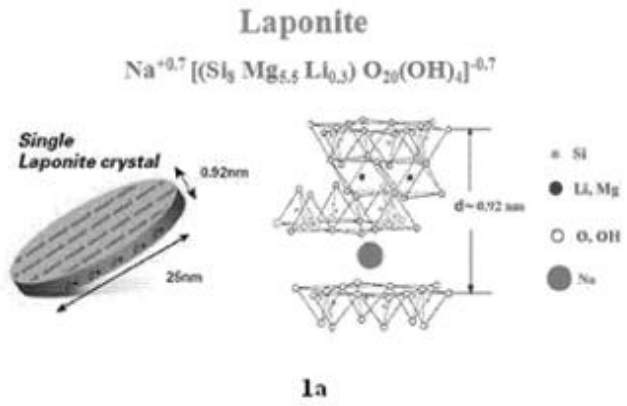

Chemical Structure of Laponite - image by F.L.O. Paula

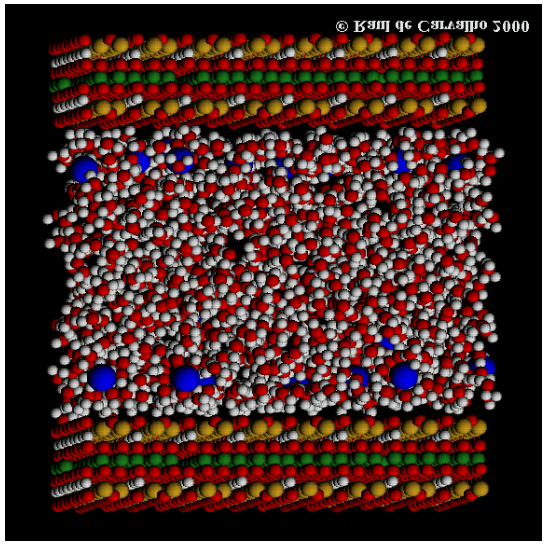

http://www.ucl.ac.uk/~ucapnsz/images/laponite.gif

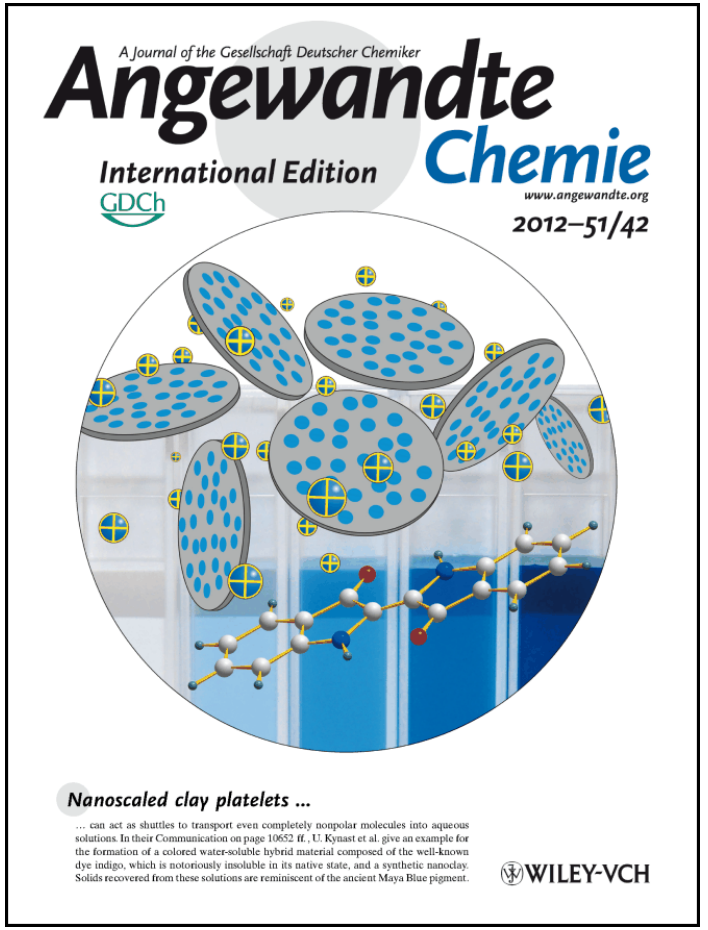

Laponite Blue: Dissolving the Insoluble, Dr. Marina M. Lezhnina, Tobias Grewe, Dr. Hardo Stoehr, Dr. Ulrich Kynast.

SOCIETY OF COSMETIC CHEMISTS

Laponite: Colloidal Glass

Barbara Ruzicka, Emanuela Zaccarelli, Laura Zulian, Roberta Angelini, Michael Sztucki,Abdellatif Moussaïd, Theyencheri Narayanan & Francesco Sciortino, Observation of empty liquids and equilibrium gels in a colloidal clay, *Nature Materials*, **10**, 56–60, (2011)

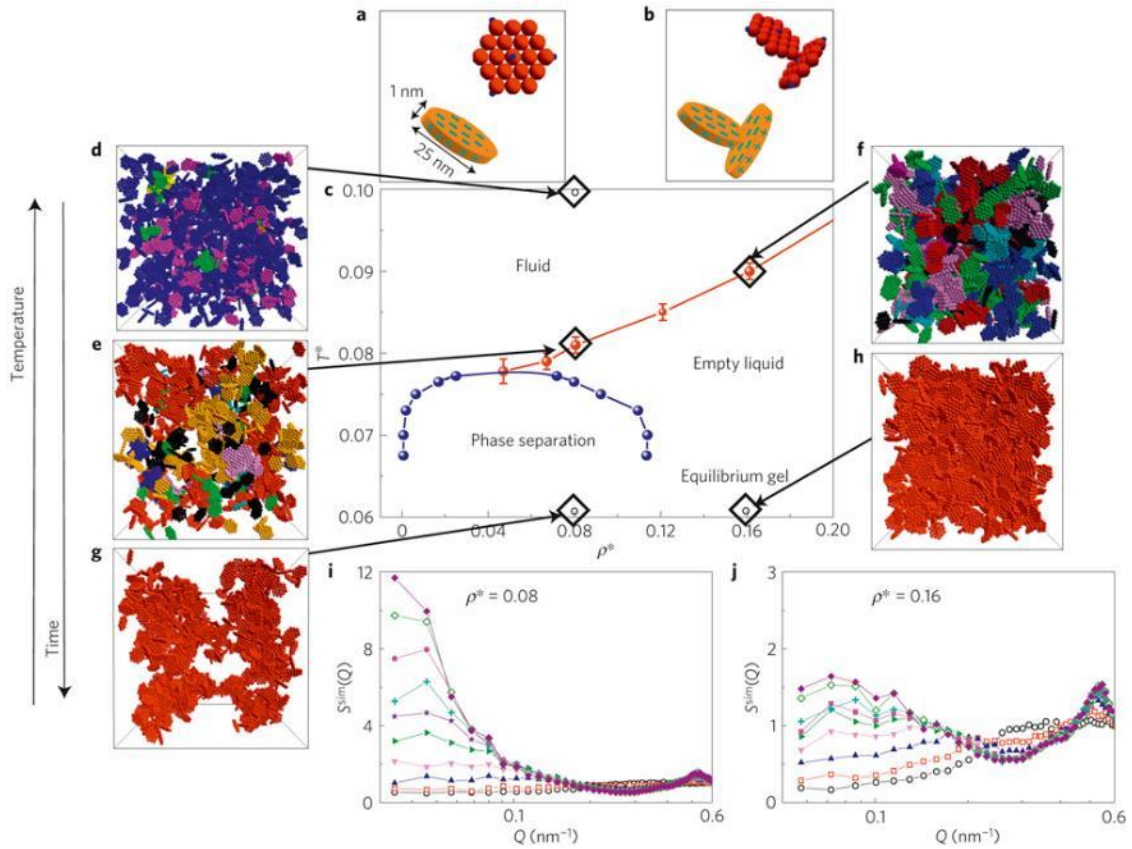

a, Cartoon of a Laponite platelet and its schematization as a rigid disc composed by 19 sites (red spheres) with five attractive patches (blue spheres), three located on the rim and one at the centre of each face. **b**, Cartoon representing a T-bonded configuration for two interacting Laponite platelets and its realization in simulations. **c**, Numerical phase diagram: binodal (blue curve) and percolation locus (red curve) in the ρ^*–T^* plane, where ρ^* is the number density scaled by the close-packing density and T^* is the thermal energy scaled by the strength of the bond (see Methods). **d**–**h**, Three-dimensional snapshots of MC simulations at different state points. Different colours correspond to different clusters, and the red colour is reserved for the percolating cluster. **d**, Equilibrium fluid phase atT^*=0.10 and $\rho^*\simeq$0.08. **e**,**f**, Equilibrium configuration at percolation for $\rho^*\simeq$0.08 and 0.16. **g**,**h**, Final gel configurations at T^*=0.06 inside ($\rho^*\simeq$0.08) and outside ($\rho^*\simeq$0.16) the phase-separation region. In these cases, platelets are connected into a single cluster (gel), which is clearly inhomogeneous (homogeneous) inside (outside) the binodal region. **i**,**j**, Evolution of the $S^{sim}(Q)$ after a quench at T^*=0.06 for $\rho^*\simeq$0.08 (inside the phase-separation region) and $\rho^*\simeq$0.16 (outside the phase-separation region). Waiting times are 10^2,1.2×10^5,5.7×10^5,1.6×10^6,3.6×10^6,6.1×10^6,10^7,2.2×10^7,4.9×10^7,1.1×10^8 in MC steps.

Laponite: Colloidal Glass

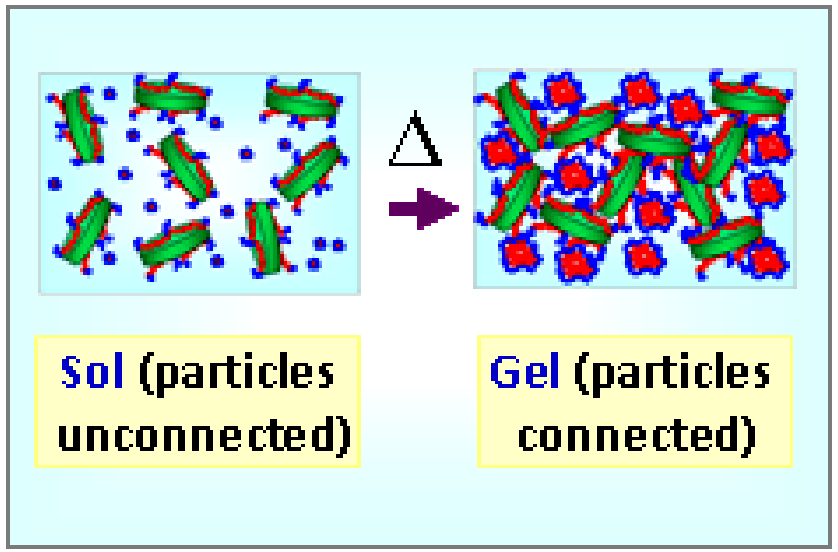

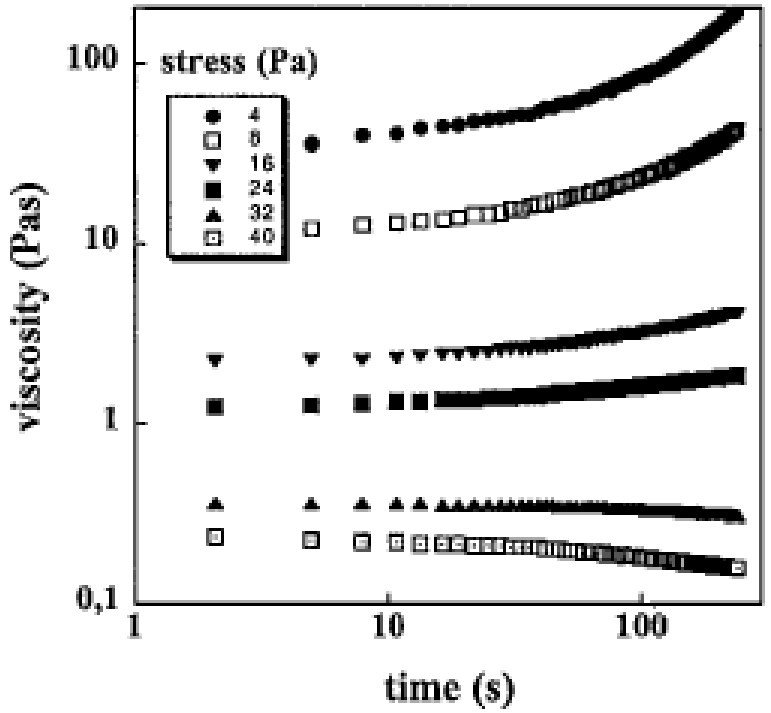

Thermogelling fluids containing low concentrations of Pluronic F127 and laponite nanoparticles.

K. Sun and S. R. Raghavan*

Langmuir, 26, 8015 (2010)

Rheophysical classification of suspensions and pastes

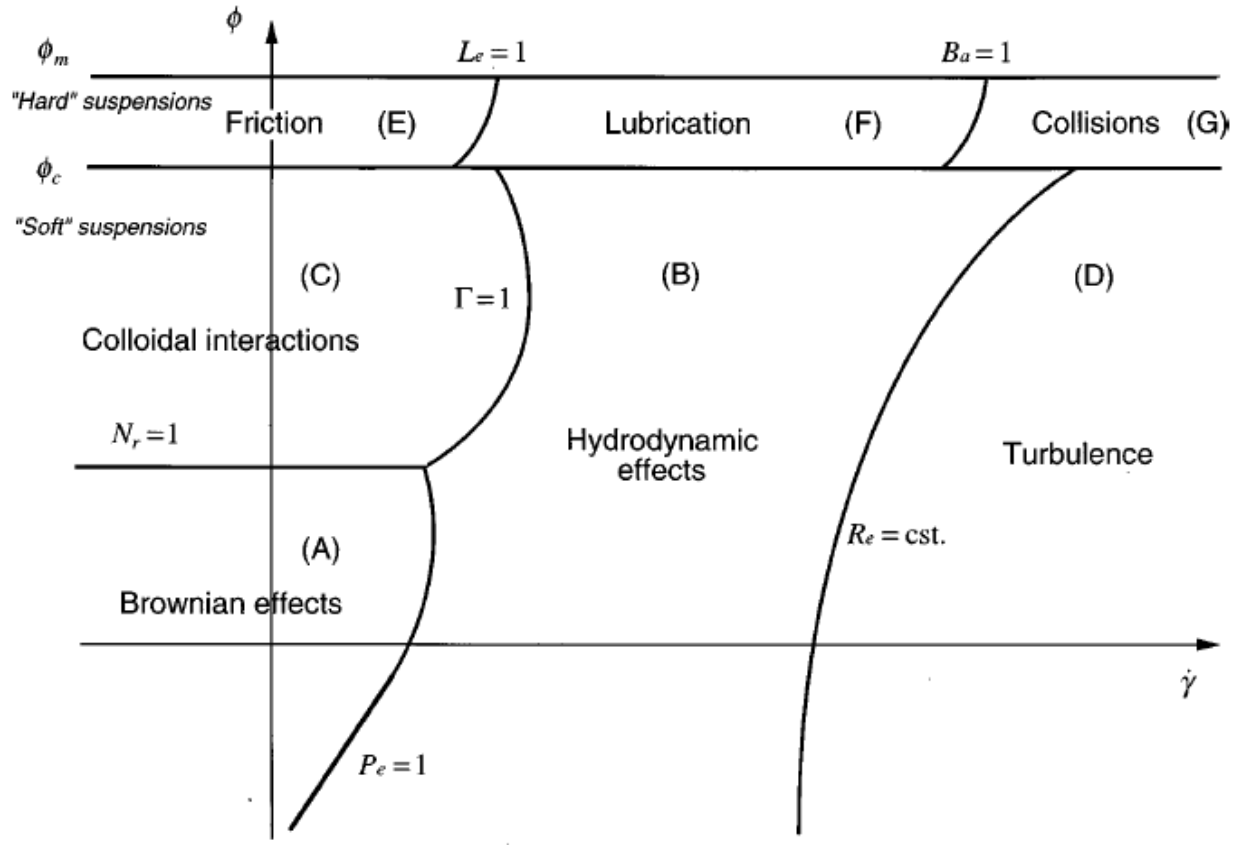

PHYSICAL REVIEW E VOLUME 59, NUMBER 4 APRIL 1999

Rheophysical classification of concentrated suspensions and granular pastes

P. Coussot[1,*] and C. Ancey[2]

Rheophysical classification of suspensions and pastes

Each Particle is in a potential energy minimum created by the interaction of neighboring particles

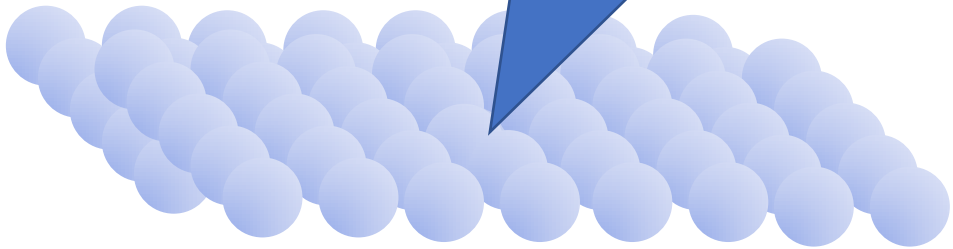

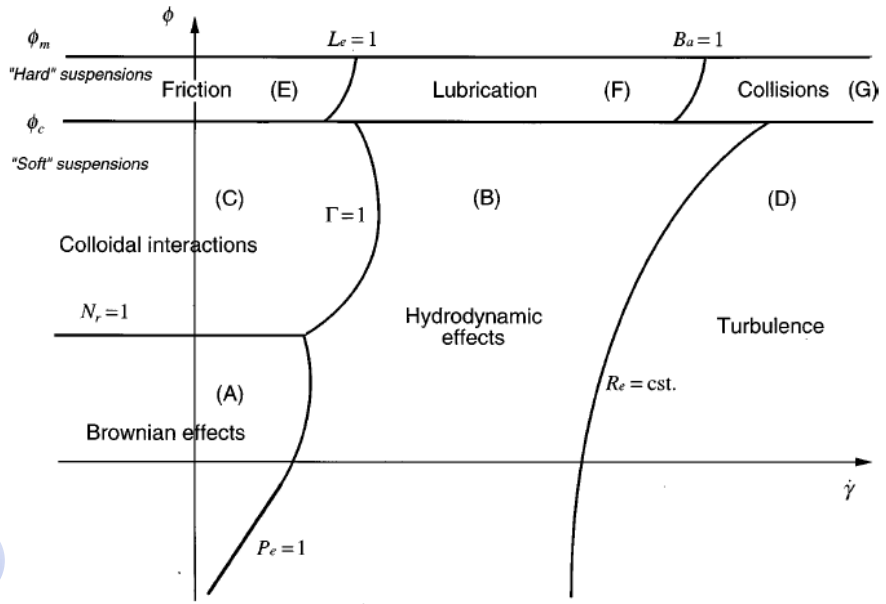

PHYSICAL REVIEW E VOLUME 59, NUMBER 4 APRIL 1999

Rheophysical classification of concentrated suspensions and granular pastes

P. Coussot[1,*] and C. Ancey[2]

Rheophysical classification of suspensions and pastes

A particle needs to exceed the activation energy, ϕ_0, to escape from its position in the particle assembly

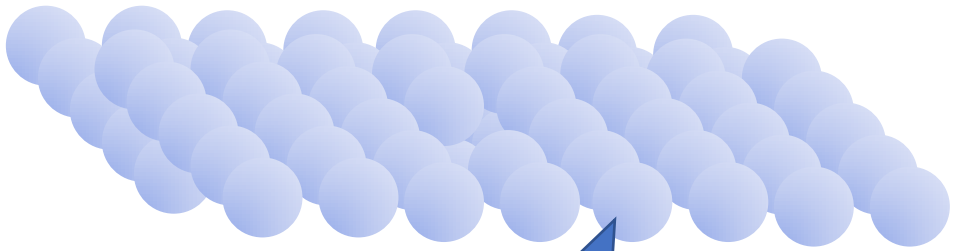

The available energy is kT

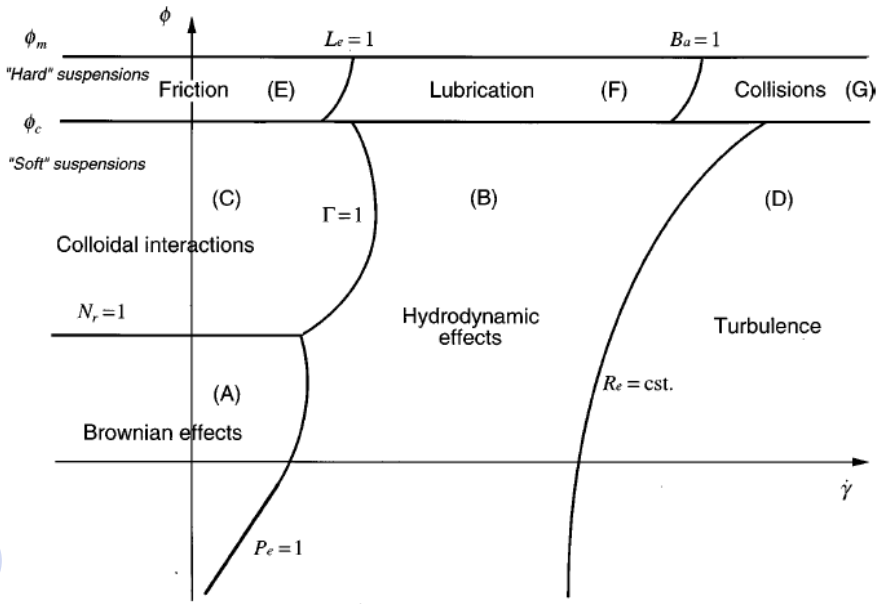

$$N_r = \frac{\Phi_0}{kT},$$

PHYSICAL REVIEW E VOLUME 59, NUMBER 4 APRIL 1999

Rheophysical classification of concentrated suspensions and granular pastes

P. Coussot[1,*] and C. Ancey[2]

Rheophysical classification of suspensions and pastes

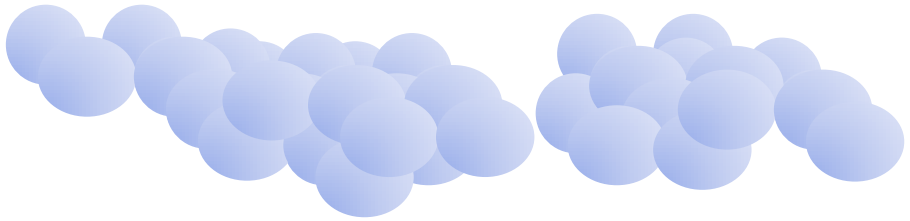

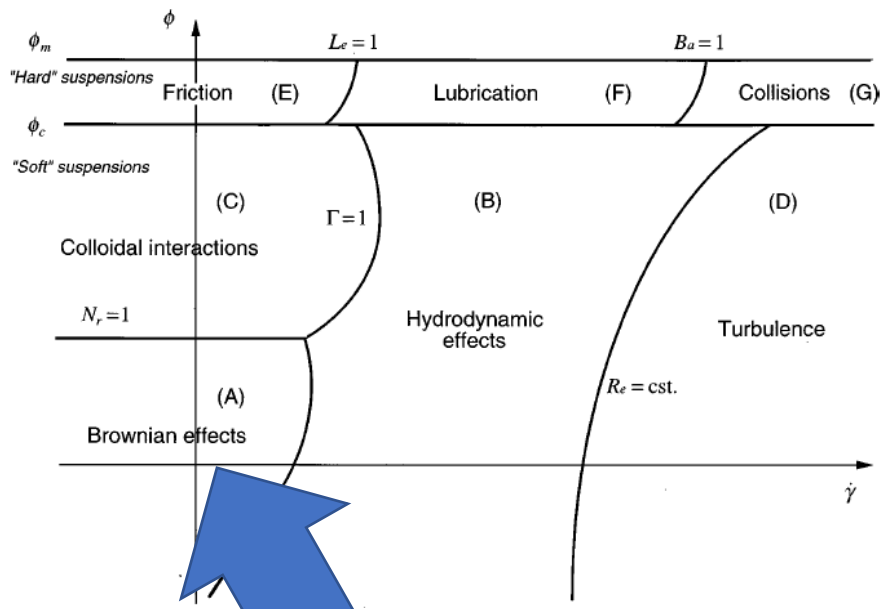

$$N_r = \frac{\Phi_0}{kT}, \quad < 1$$

PHYSICAL REVIEW E VOLUME 59, NUMBER 4 APRIL 1999

Rheophysical classification of concentrated suspensions and granular pastes

P. Coussot[1,*] and C. Ancey[2]

Rheophysical classification of suspensions and pastes

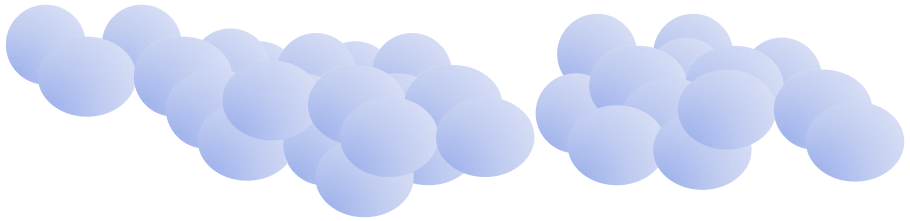

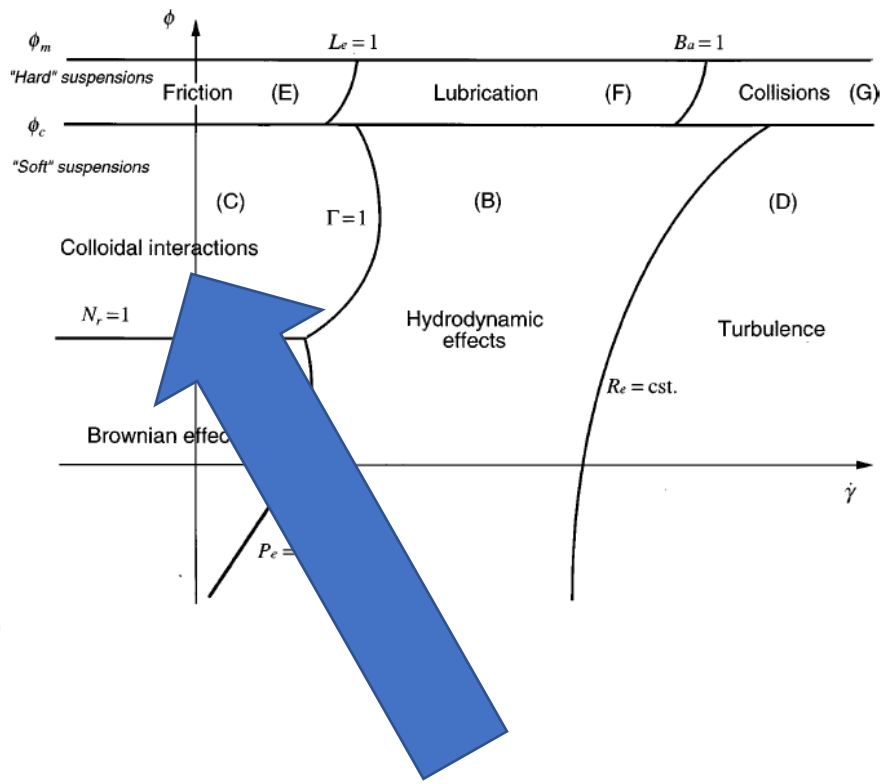

$$N_r = \frac{\Phi_0}{kT}, \quad < 1$$

PHYSICAL REVIEW E VOLUME 59, NUMBER 4 APRIL 1999

Rheophysical classification of concentrated suspensions and granular pastes

P. Coussot[1,*] and C. Ancey[2]

Rheophysical classification of suspensions and pastes

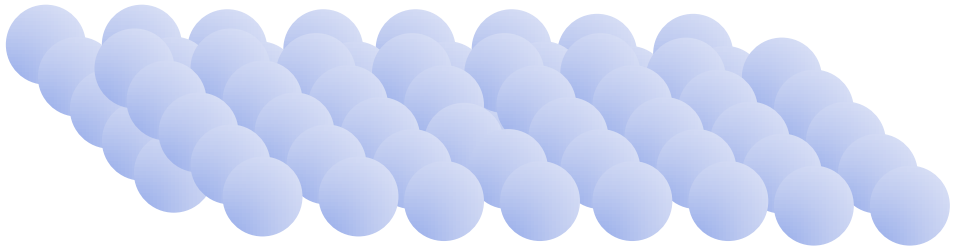

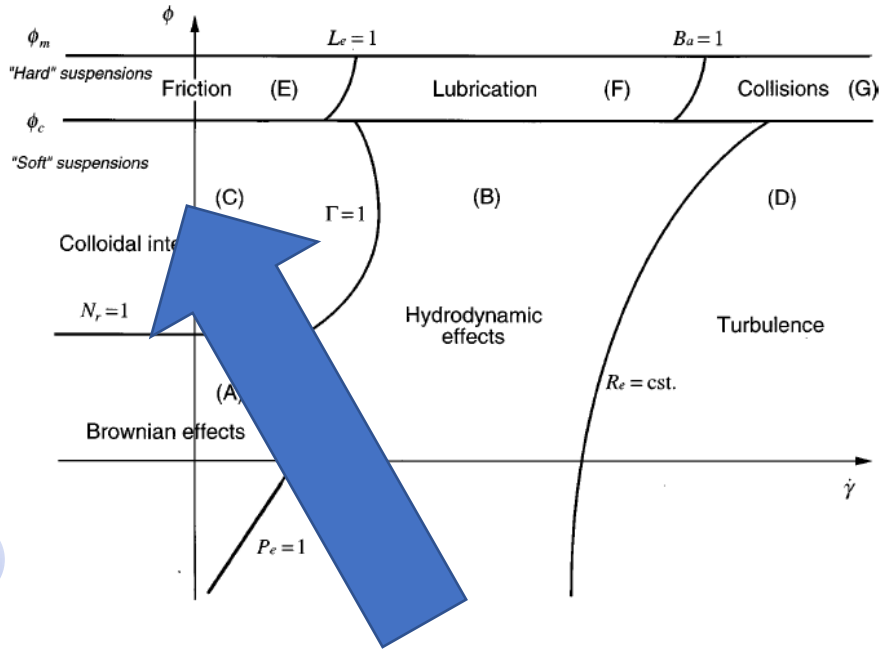

$$N_r = \frac{\Phi_0}{kT}, \qquad < 1$$

PHYSICAL REVIEW E VOLUME 59, NUMBER 4 APRIL 1999

Rheophysical classification of concentrated suspensions and granular pastes

P. Coussot[1,*] and C. Ancey[2]

Laponite: Colloidal Glass

Barbara Ruzicka, Emanuela Zaccarelli, Laura Zulian, Roberta Angelini, Michael Sztucki, Abdellatif Moussaïd, Theyencheri Narayanan & Francesco Sciortino,
Observation of empty liquids and equilibrium gels in a colloidal clay, *Nature Materials*, **10**, 56–60, (2011)

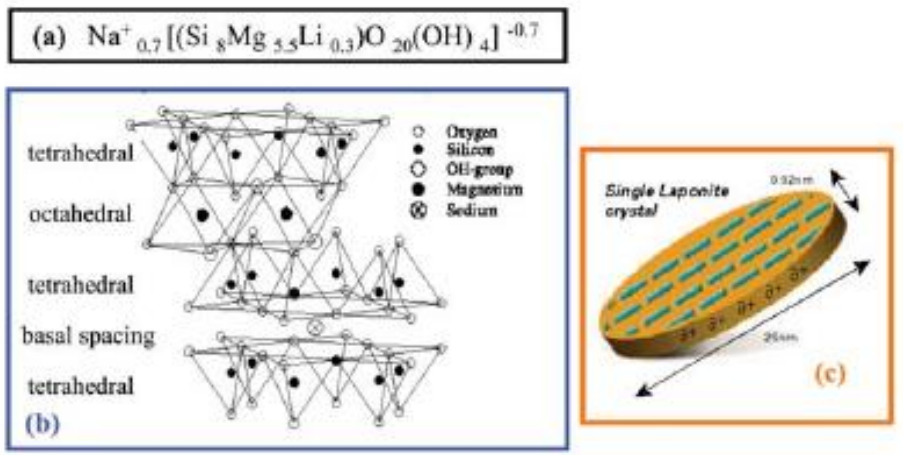

a, Cartoon of a Laponite platelet and its schematization as a rigid disc composed by 19 sites (red spheres) with five attractive patches (blue spheres), three located on the rim and one at the centre of each face. **b**, Cartoon representing a T-bonded configuration for two interacting Laponite platelets and its realization in simulations. **c**, Numerical phase diagram: binodal (blue curve) and percolation locus (red curve) in the ρ^*–T^* plane, where ρ^* is the number density scaled by the close-packing density and T^* is the thermal energy scaled by the strength of the bond (see Methods). **d**–**h**, Three-dimensional snapshots of MC simulations at different state points. Different colours correspond to different clusters, and the red colour is reserved for the percolating cluster. **d**, Equilibrium fluid phase at T^*=0.10 and $\rho^* \simeq 0.08$. **e**,**f**, Equilibrium configuration at percolation for $\rho^* \simeq 0.08$ and 0.16. **g**,**h**, Final gel configurations at T^*=0.06 inside ($\rho^* \simeq 0.08$) and outside ($\rho^* \simeq 0.16$) the phase-separation region. In these cases, platelets are connected into a single cluster (gel), which is clearly inhomogeneous (homogeneous) inside (outside) the binodal region. **i**,**j**, Evolution of the $S^{sim}(Q)$ after a quench at T^*=0.06 for $\rho^* \simeq 0.08$ (inside the phase-separation region) and $\rho^* \simeq 0.16$ (outside the phase-separation region). Waiting times are 10^2,1.2×10^5,5.7×10^5,1.6×10^6,3.6×10^6,6.1×10^6,10^7,2.2×10^7,4.9×10^7,1.1×10^8 in MC steps.

Laponite: Colloidal Glass

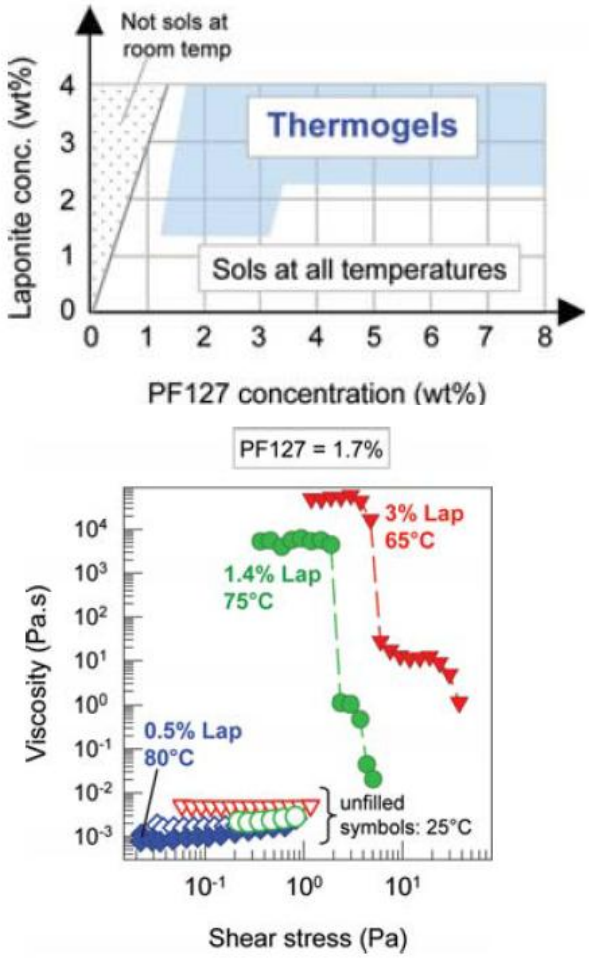

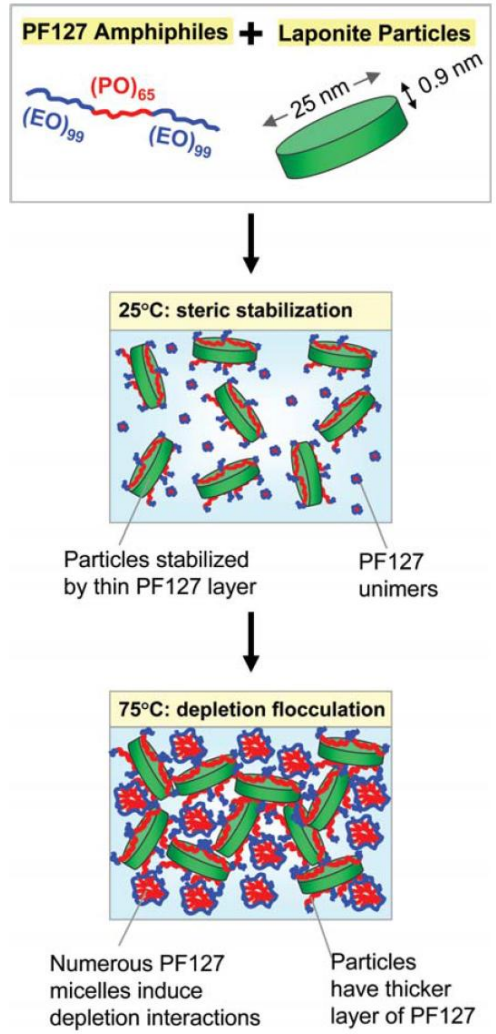

[Thermogelling fluids containing low concentrations of Pluronic F127 and laponite nanoparticles.](#)
K. Sun and S. R. Raghavan* ***Langmuir***, 26, 8015 (2010)

MICROGEL THICKENERS

Carbomer Gel Structure

- The structure of Carbomer dispersions can be described in terms of polydisperse glasses made of individual swollen hydrophylic elastic sponges
- They display elastoplasticity, and significant dissipation both below and above their yield stress

J.M. Piau, Carbopol gels: Elastoviscoplastic and slippery glasses made of individual swollen sponges Meso- and macroscopic properties, constitutive equations and scaling laws; J. Non-Newtonian Fluid Mech. 144 (2007) 1–29

Microgels

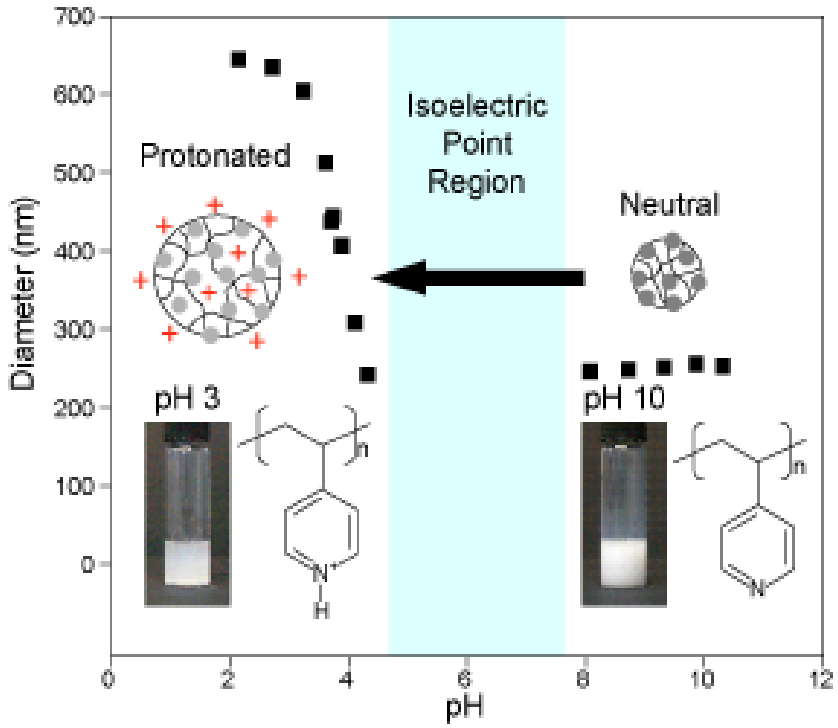

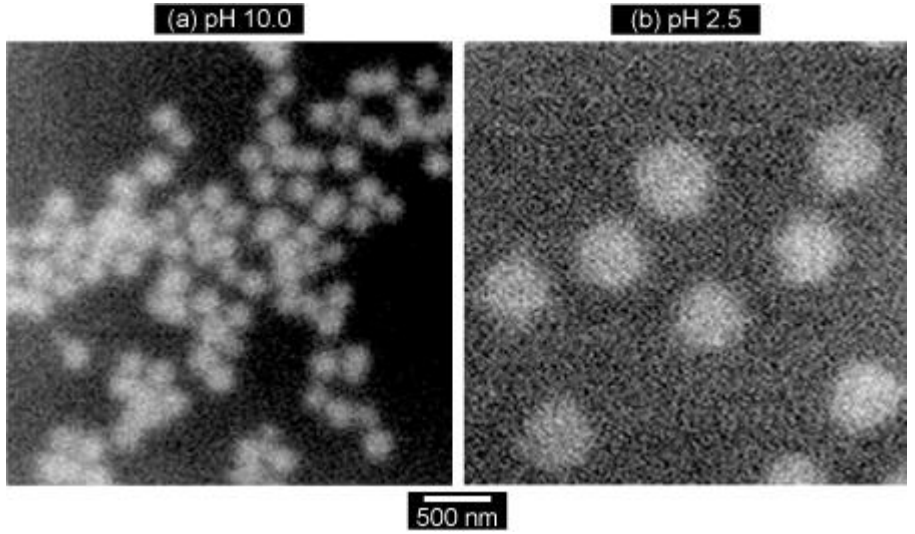

BERKELEY LAB
LAWRENCE BERKELEY NATIONAL LABORATORY
U.S. DEPARTMENT OF ENERGY | Office of Science
A-Z INDEX | PHONE BOOK | JOBS | SEARCH

Advanced Light Source
An Office of Science User Facility

http://www-als.lbl.gov/index.php/contact/261-first-direct-imaging-of-swollen-microgel-particles.html

Microgels

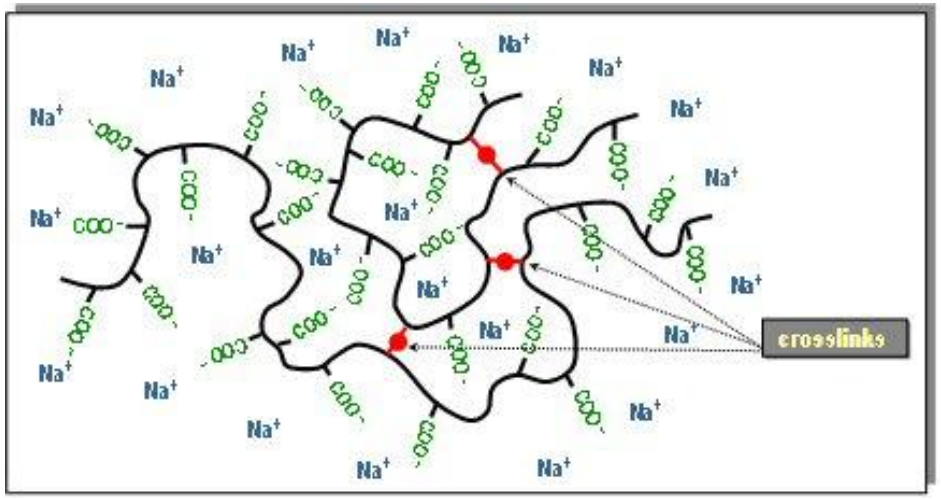

http://www.lubrizol.com/CorporateResponsibility/ProductStewardship/Carbopol.html

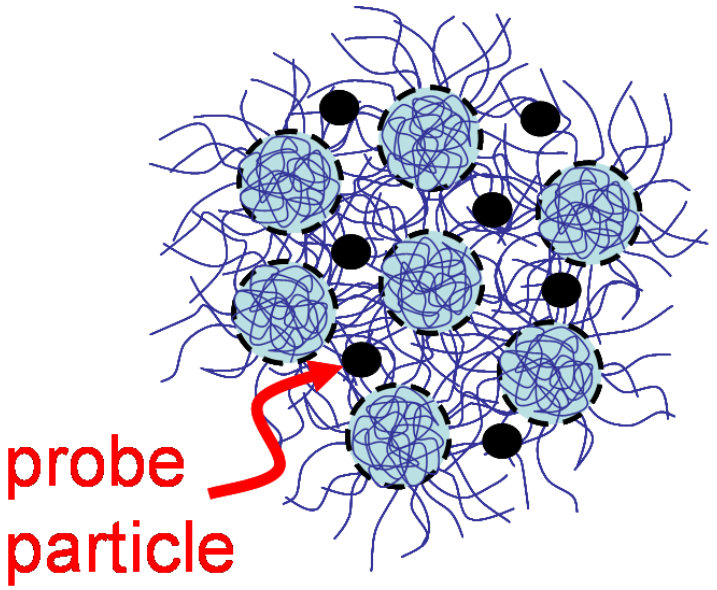

Conceptual Drawing of Carbopol® Particles.

http://www.sfu.ca/

Carbomer

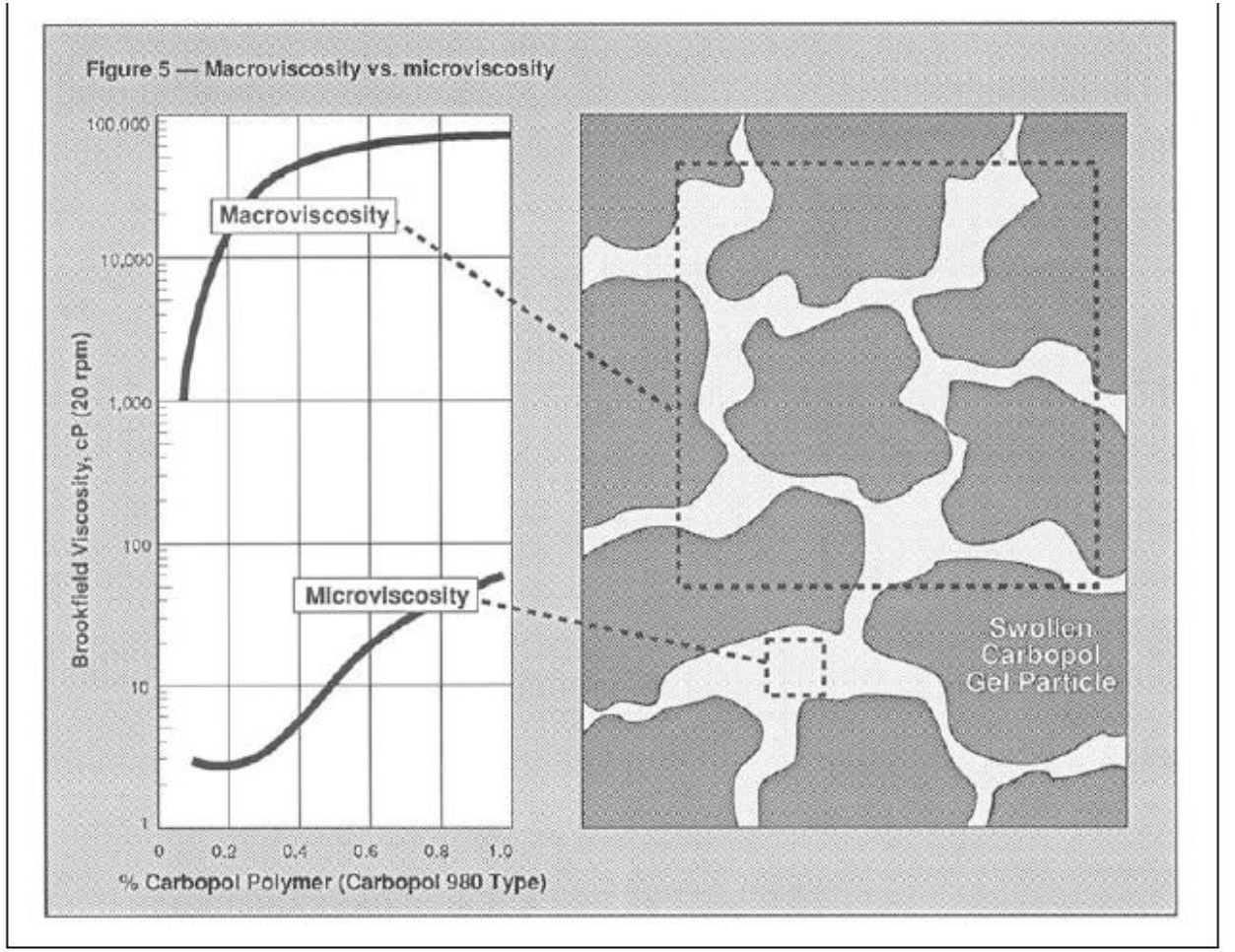

Lubrizol

TDS-180

Flow and Suspension Properties of Carbopol® Polymers

Microrheology and Structure of Carbomer Gels

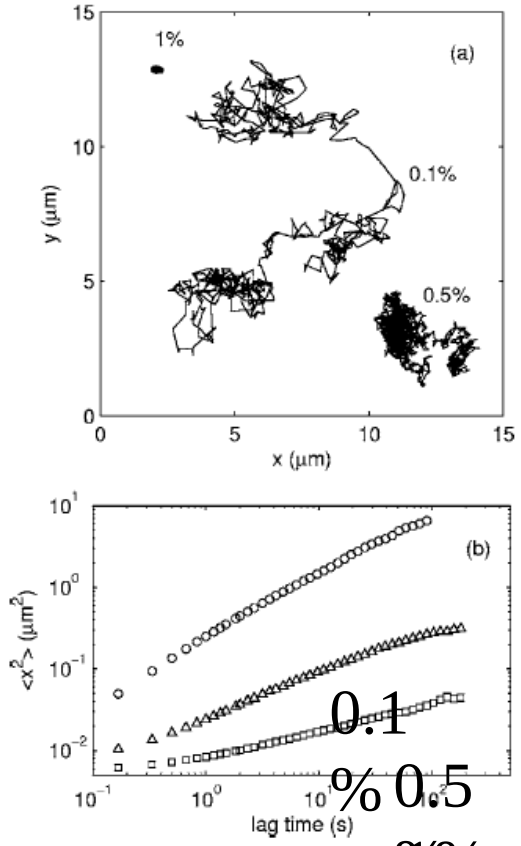

FIG. 2. (a) Typical trajectories of 0.49-μm fluorescent particles suspended in carbopol solutions, measured by fluorescence microscopy particle tracking. Trajectories for three different concentrations are shown. (b) The mean-squared displacement $\langle x^2(\tau) \rangle$ determined from analysis of the x components of the trajectories of many particles. The symbols indicate different concentrations as in Fig. 1.

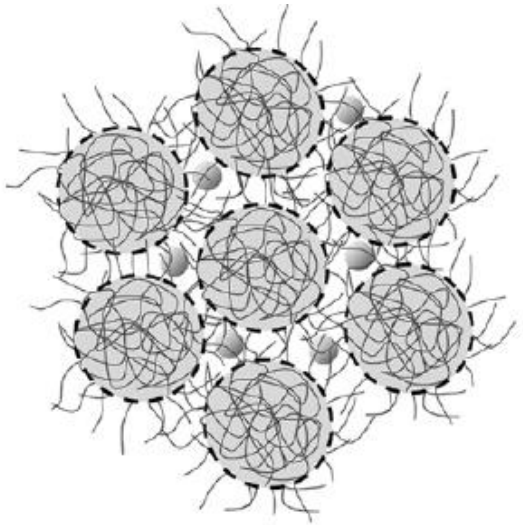

FIG. 10. A schematic illustration of the structure of Carbopol gels showing the highly cross-linked cores of the microgel particles surrounded by a viscous medium containing polymer chains (after Ref. [9]). The small probe particles diffuse in the pores of viscous fluid between the gel particles.

Felix K. Oppong,[1,2] Laurent Rubatat,[3] Barbara J. Frisken,[3] Arthur E. Bailey,[3,4] and John R. de Bruyn, **Microrheology and structure of a yield-stress polymer gel;** PHYSICAL REVIEW E **73**, 041405 2006

Carbomer – Shear thinning

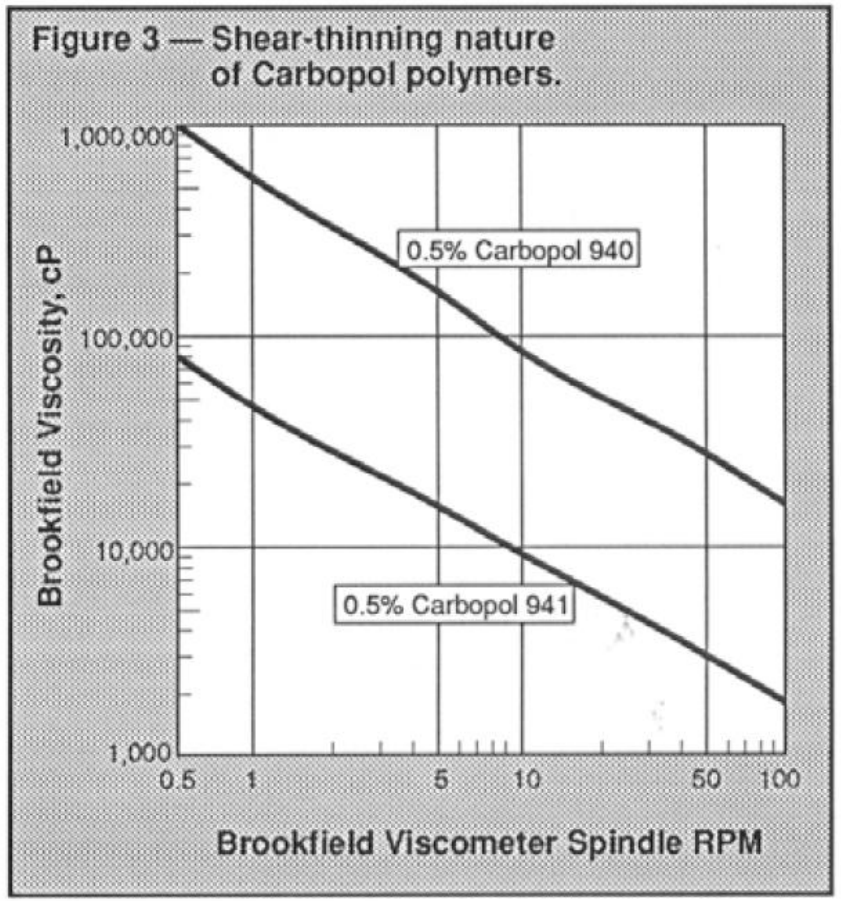

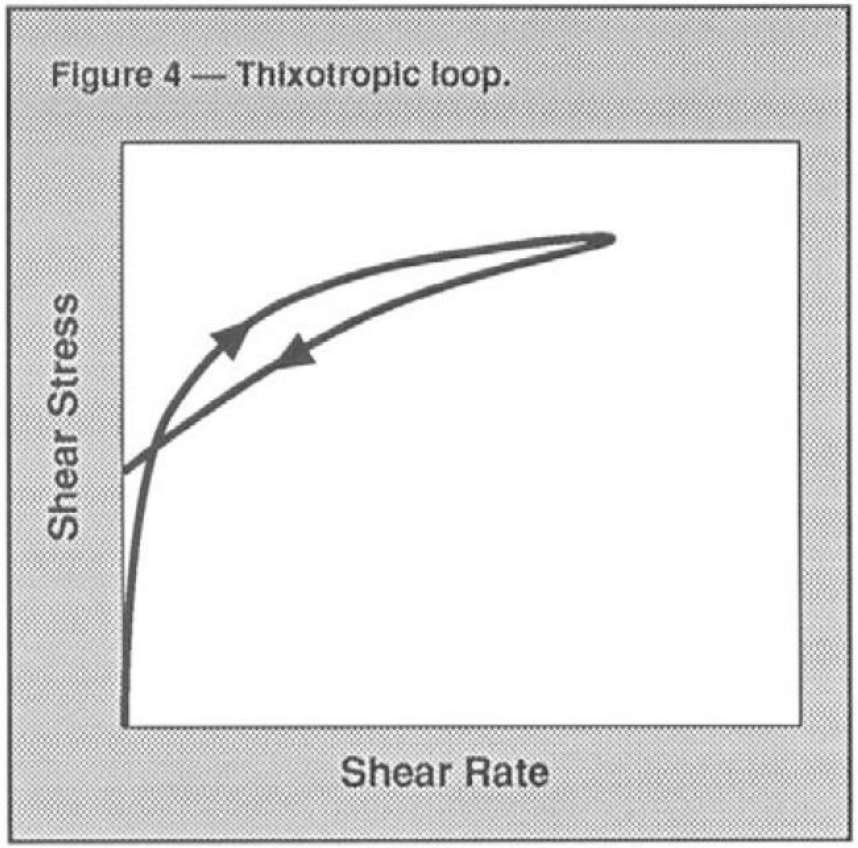

TDS1-80
Flow and Suspension Properties of Carbopol® Polymers

Carbomer Yield Stress

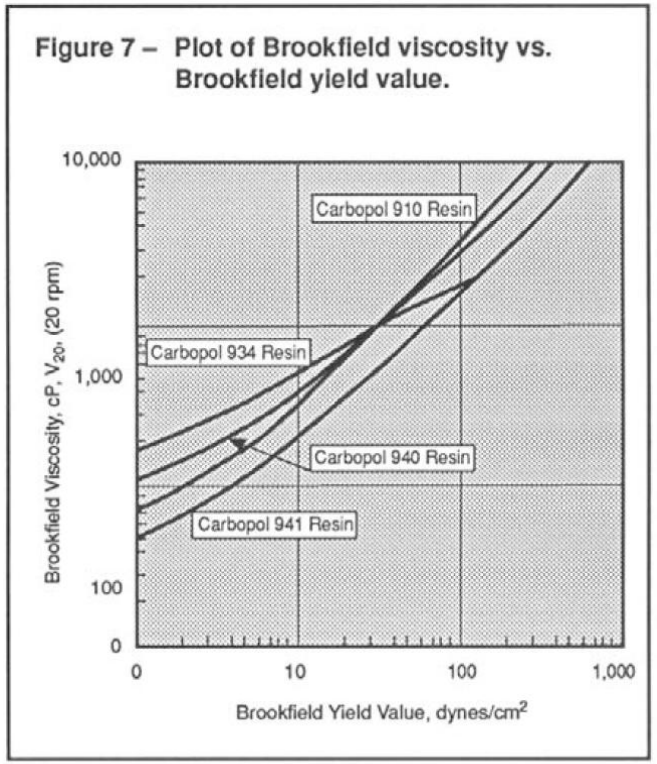

Brookfield Yield Value =

(Apparent Viscosity at 0.5 rpm - Apparent Viscosity at 1 rpm) / 100

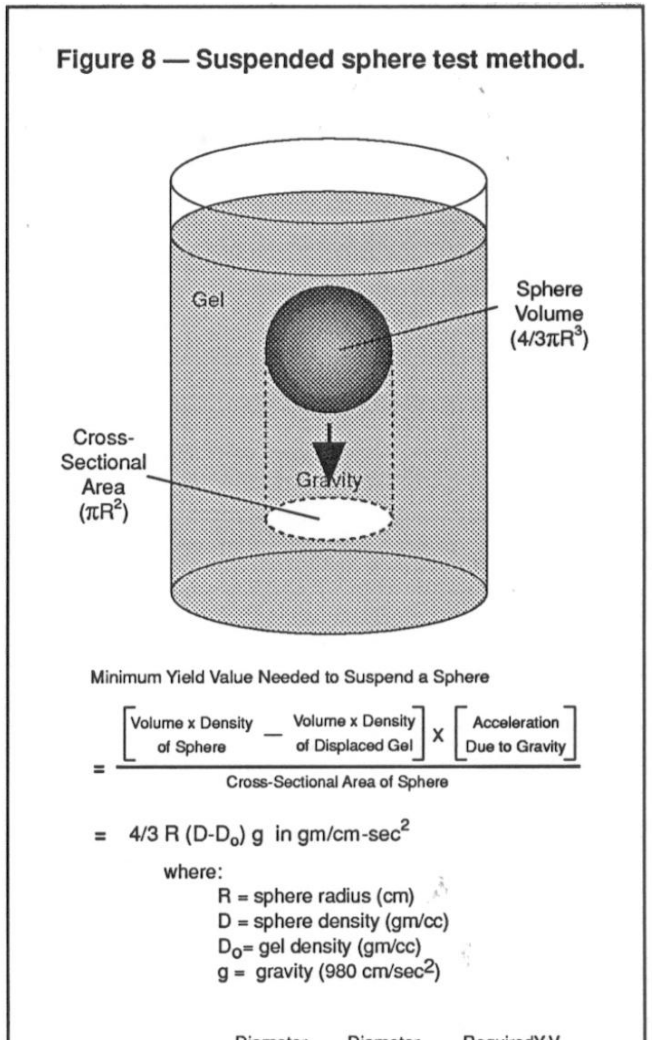

SOCIETY OF COSMETIC CHEMISTS

Lubrizol

TDS1-80

Flow and Suspension Properties of Carbopol® Polymers

Fluid Rheology

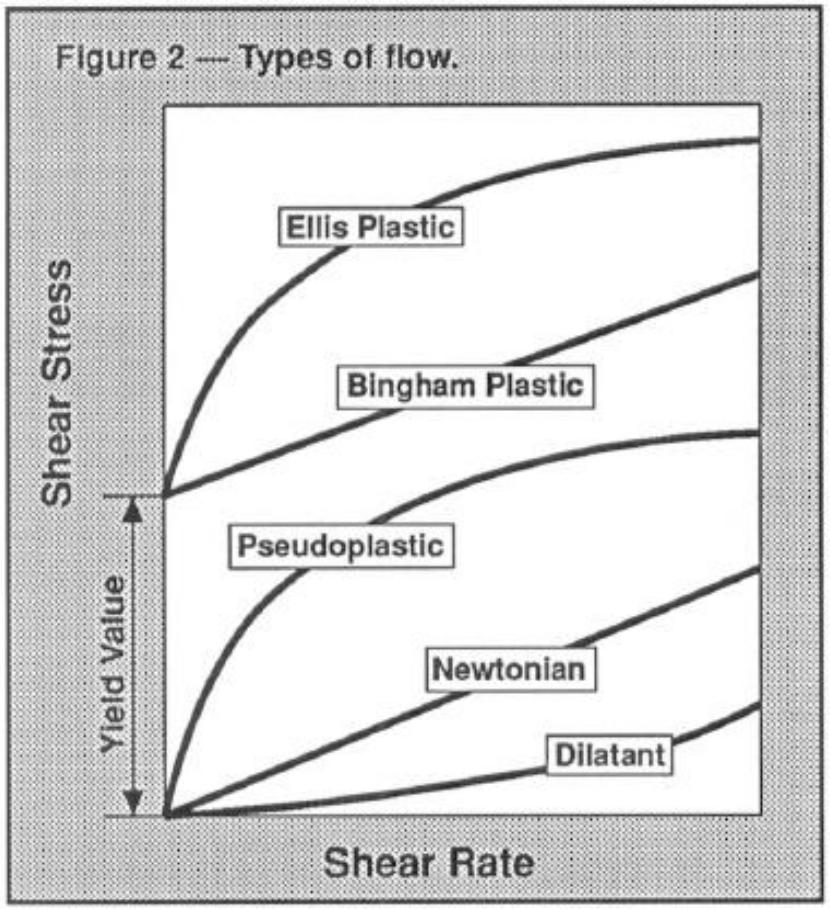

http://www.lubrizol.com/Personal-Care/Documents/Technical-Data-Sheets/TDS-180-Flow-and-Suspension-Properties-of-Carbopol%C2%AE-Polymers.pdf

Viscosity / yield stress comparison

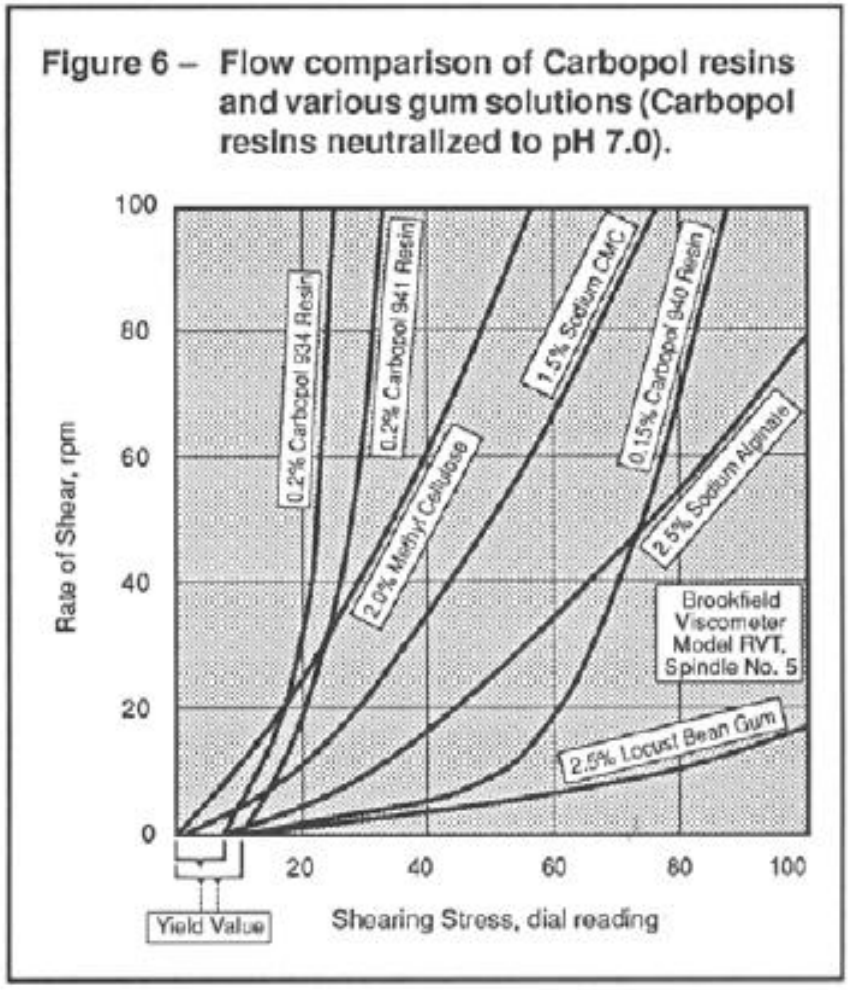

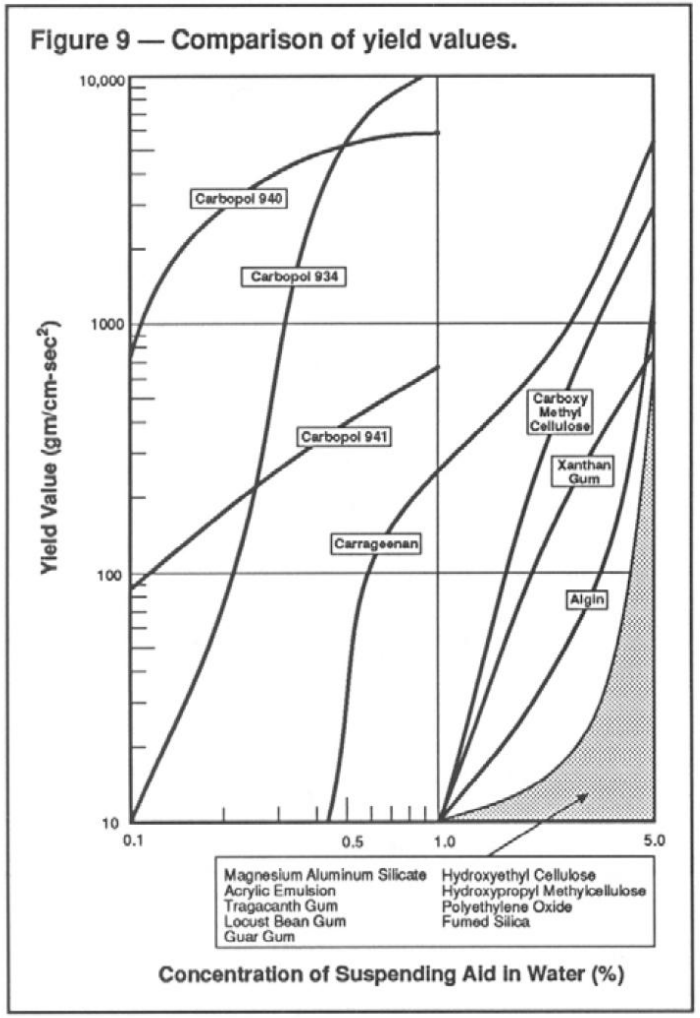

SOCIETY OF COSMETIC CHEMISTS

Lubrizol

TDS1-80
Flow and Suspension Properties of Carbopol® Polymers

Carbomer Gel Structure

- Physical gels have complex macroscopic properties because of their different creep, elastic, viscous, plastic and thixotropic characteristics, and their specific mesoscopic physicochemistry. Like other plastic materials, they are prone to localized deformation and slip. Consequently, it is far more difficult to perform rheometry measurements on physical gels than on better known viscous or viscoelastic polymer solutions [2]. Purely phenomenological approaches, which may be misleading in rheology, become much more so in the case of plastic and/orthixotropic materials. Moreover, the corresponding models have received less attention than the much-researched polymer models.
- The associated physico- and biochemical mechanisms generally still need to be identified or understood better. Hence, when experimental and theoretical difficulties are overcome for a particular gel, the results can be used to understand certain other systems which share similar mesoscopic properties.

J.M. Piau, Carbopol gels: Elastoviscoplastic and slippery glasses made of individual swollen sponges Meso- and macroscopic properties, constitutive equations and scaling laws; J. Non-Newtonian Fluid Mech. 144 (2007) 1–29

Carbomer Gels

- Details of sample preparation and rheometry tests may influence the yield stress values measured.
- Variations of up to 100% may result from the cumulated difficulties
  - neutralization and mixing of concentrated gels,
  - changes in resin properties from batch to batch and over different periods of manufacture,
  - resin aging
  - humidity,
  - poor control of ionic strengths,
  - sufficiently correct but approximate rheometrical procedures. by a factor of 10 or more are reported they can result
- The rheometry of complex materials is much more demanding than the rheometry of polymer solutions.

J.M. Piau, Carbopol gels: Elastoviscoplastic and slippery glasses made of individual swollen sponges Meso- and macroscopic properties, constitutive equations and scaling laws;
J. Non-Newtonian Fluid Mech. 144 (2007) 1–29

Shear Rheometry Artefacts and Errors

- Evaporation
- Navier linear slip at the wall $\tau = kus$ can be misinterpreted as an apparent viscosity
- instabilities in the bulk can result in the localization of deformation along a surface within the bulk of the sample.
- Poor angular resolution creep test for a linear elastic material
- *Logarithmic stress sweep test for a linear elastic material with stepped time increments of strain;*
  - *A spurious viscosity appears to be measured*
- *Stress sweep test for a non-linear elastic material*
- *Apparent and real shear rates in a scissometer with a rough cup*
- *Air bearing torque drifts for a fixed shaft position*
- During creep tests at a constant reference stress the shaft of rheometers may vibrate considerably.

J.M. Piau, Carbopol gels: Elastoviscoplastic and slippery glasses made of individual swollen sponges Meso- and macroscopic properties, constitutive equations and scaling laws;
J. Non-Newtonian Fluid Mech. 144 (2007) 1–29

The Herschel Bulkley Model of Yield Stress Fluids

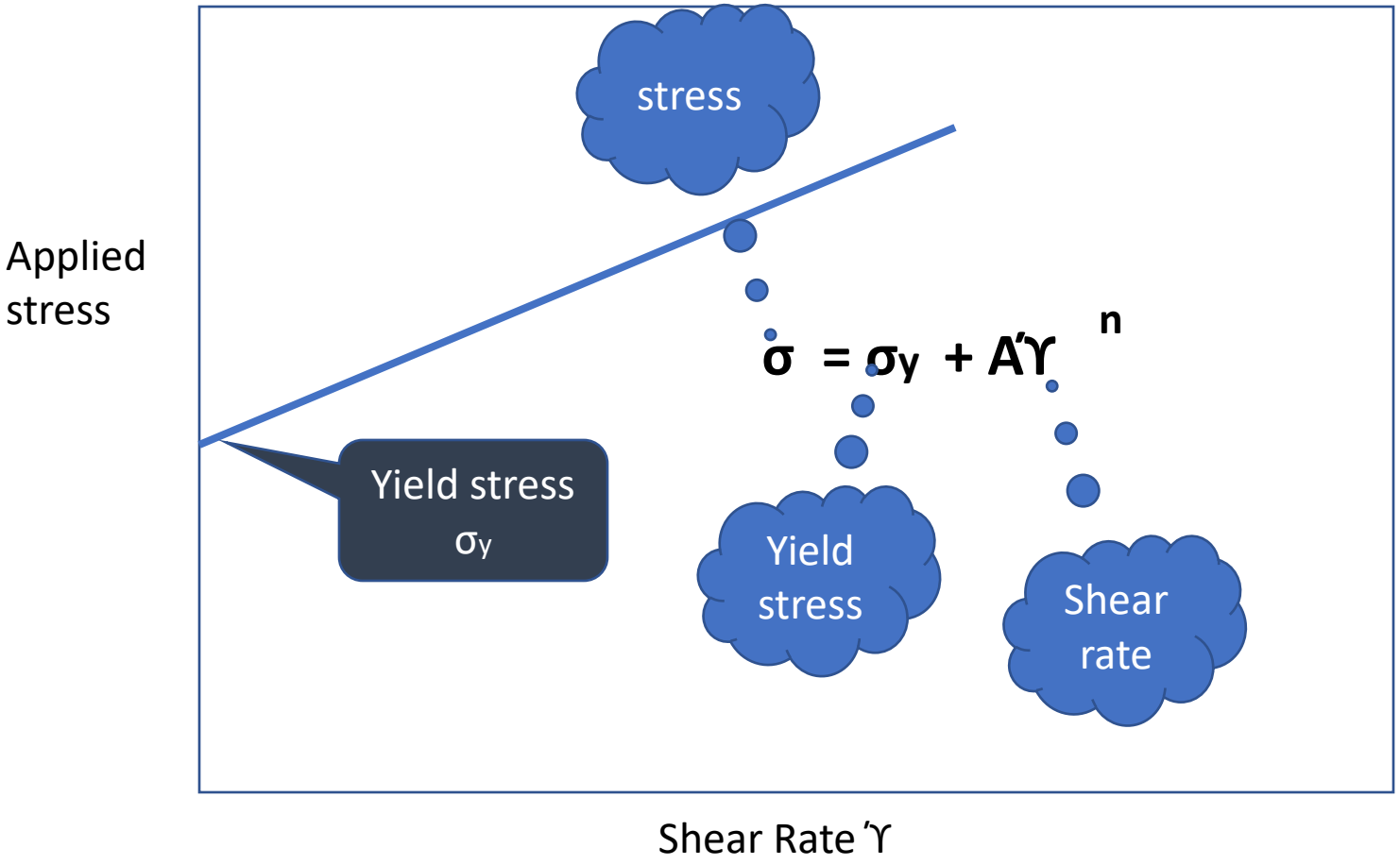

Microrheology and Structure of Carbomer Gels

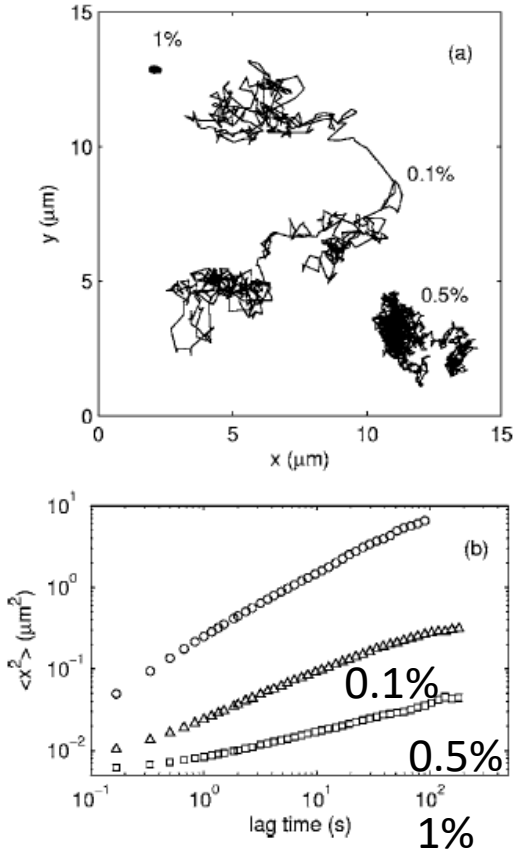

FIG. 2. (a) Typical trajectories of 0.49-μm fluorescent particles suspended in carbopol solutions, measured by fluorescence microscopy particle tracking. Trajectories for three different concentrations are shown. (b) The mean-squared displacement $\langle x^2(\tau)\rangle$ determined from analysis of the x components of the trajectories of many particles. The symbols indicate different concentrations as in Fig. 1.

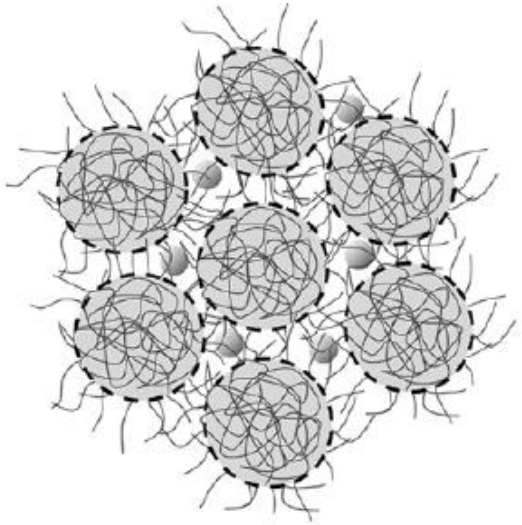

FIG. 10. A schematic illustration of the structure of Carbopol gels showing the highly cross-linked cores of the microgel particles surrounded by a viscous medium containing polymer chains (after Ref. [9]). The small probe particles diffuse in the pores of viscous fluid between the gel particles.

Felix K. Oppong,[1,2] Laurent Rubatat,[3] Barbara J. Frisken,[3] Arthur E. Bailey,[3,4] and John R. de Bruyn, **Microrheology and structure of a yield-stress polymer gel;** PHYSICAL REVIEW E **73**, 041405 2006

Repulsion Networks
The Electrical Double Layer

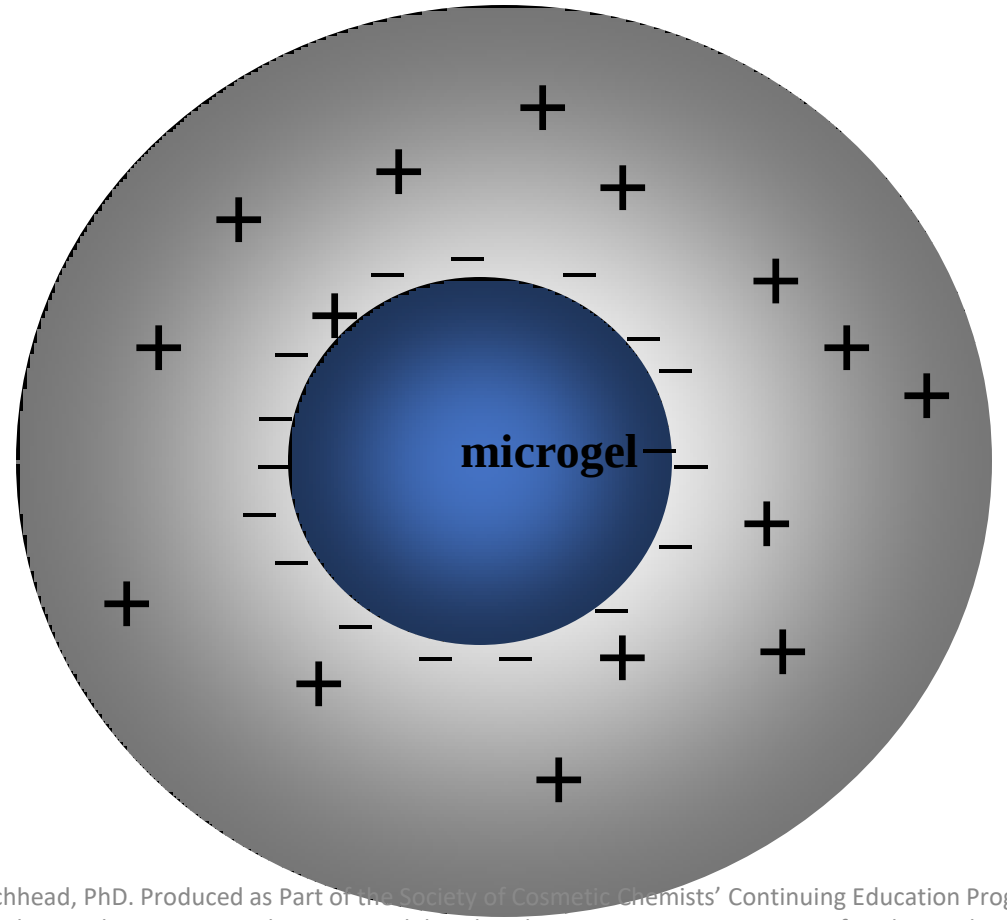

Stabilization by the Electric Double Layer

Repulsion as the double layers overlap

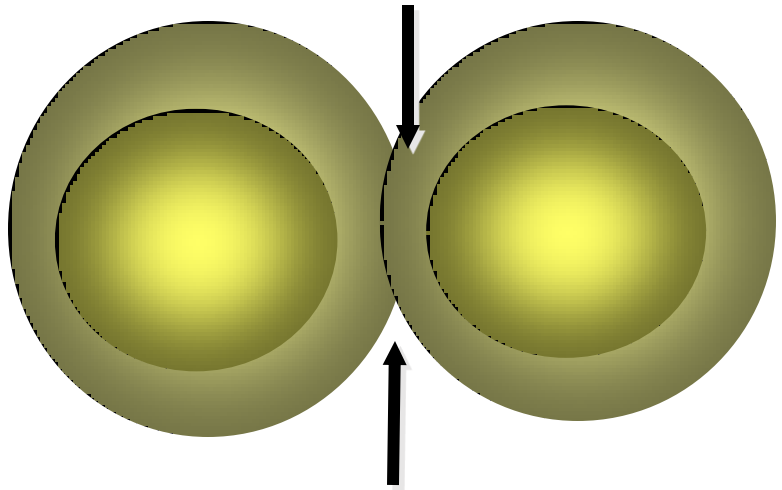

Microgel rheology in quiescent state

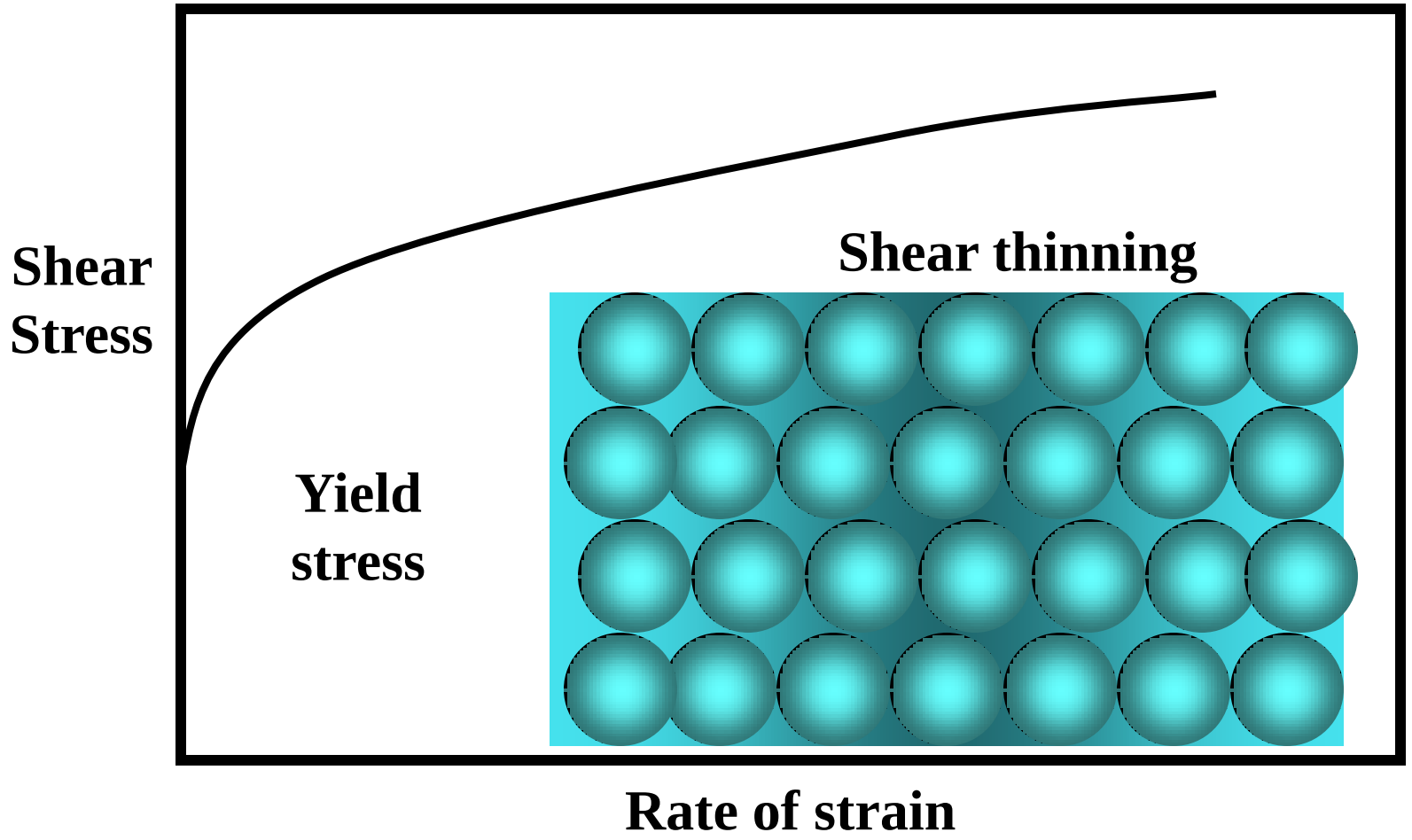

Microgel rheology in flow

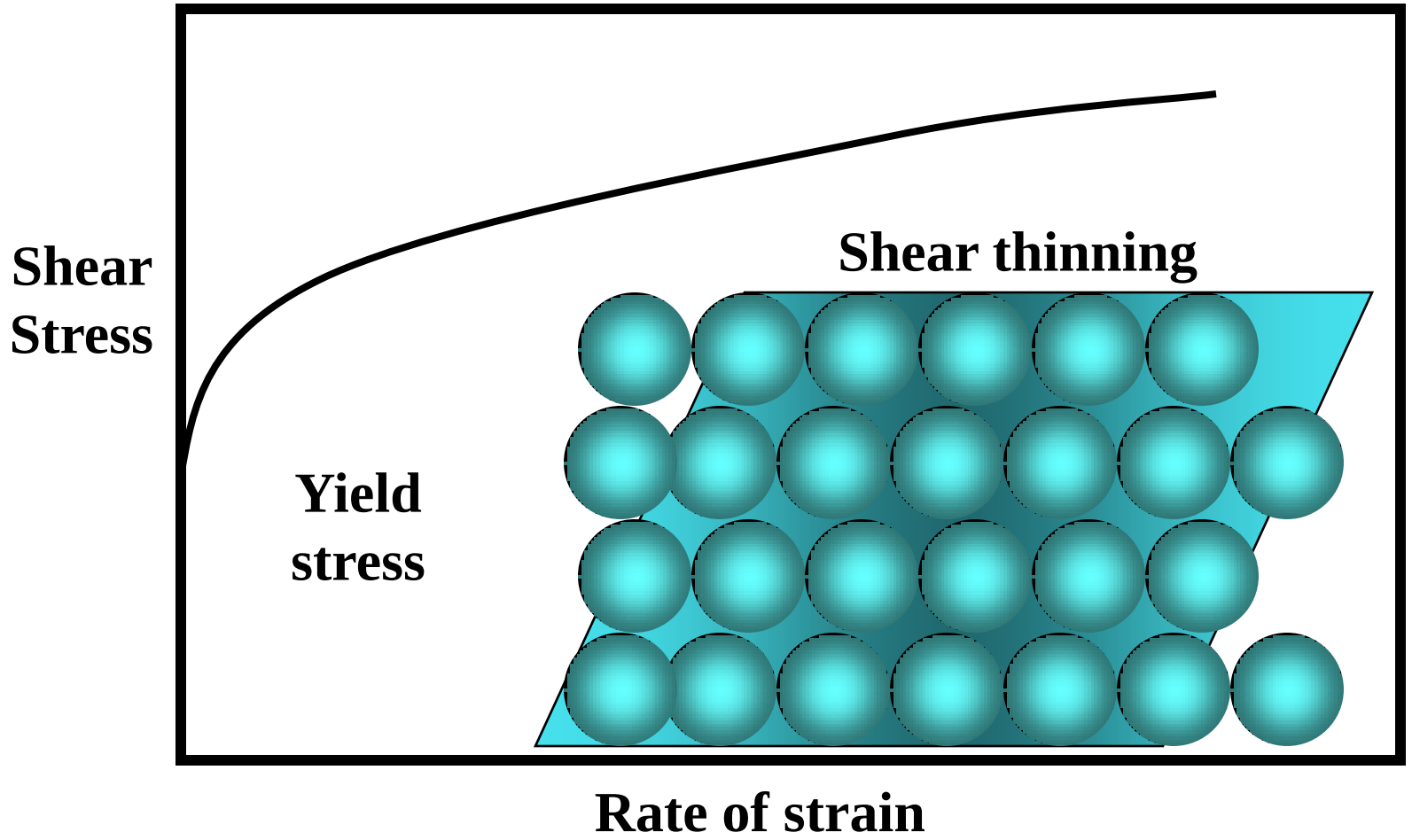

Microgel rheology inflow

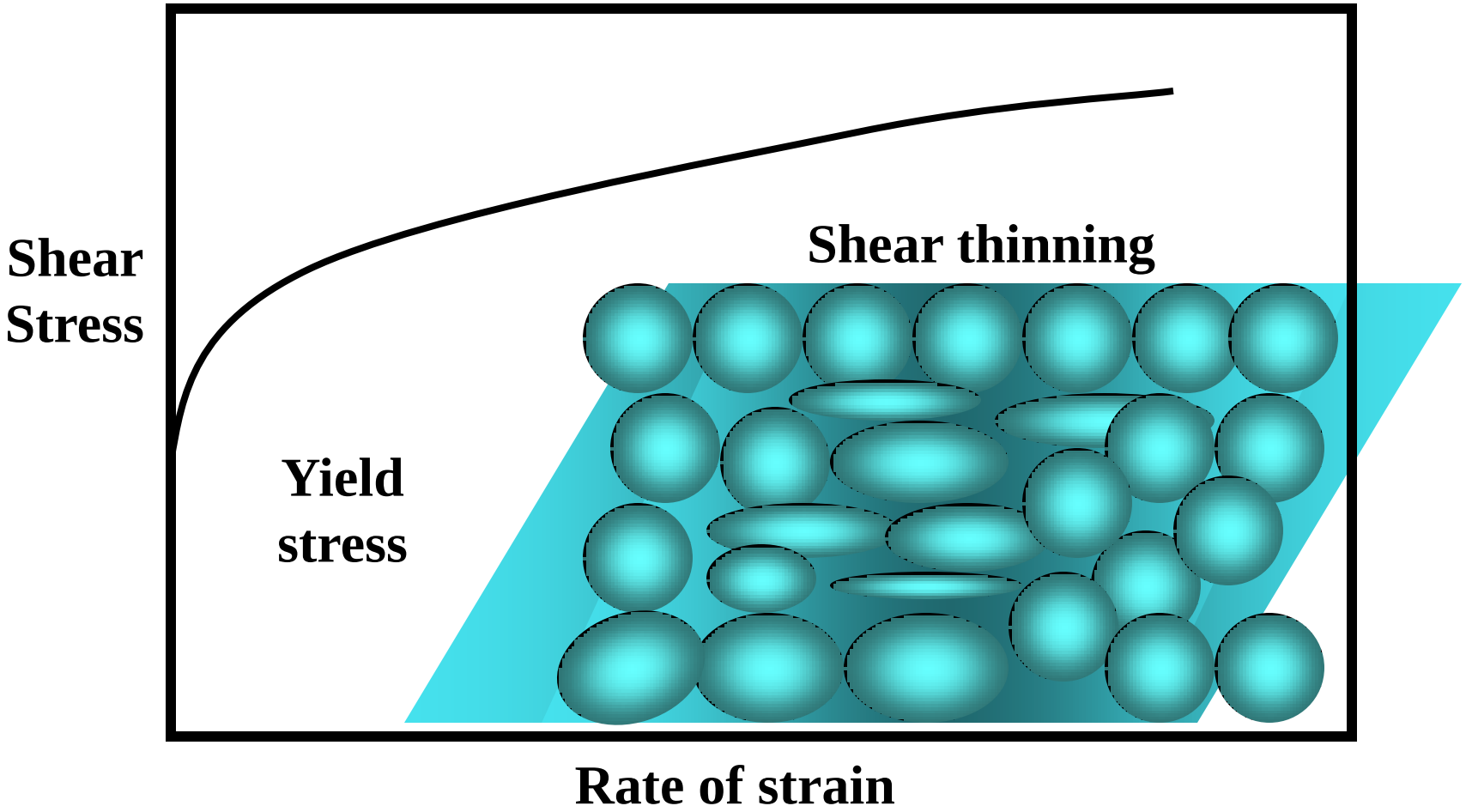

Microgel rheology when flow ceases

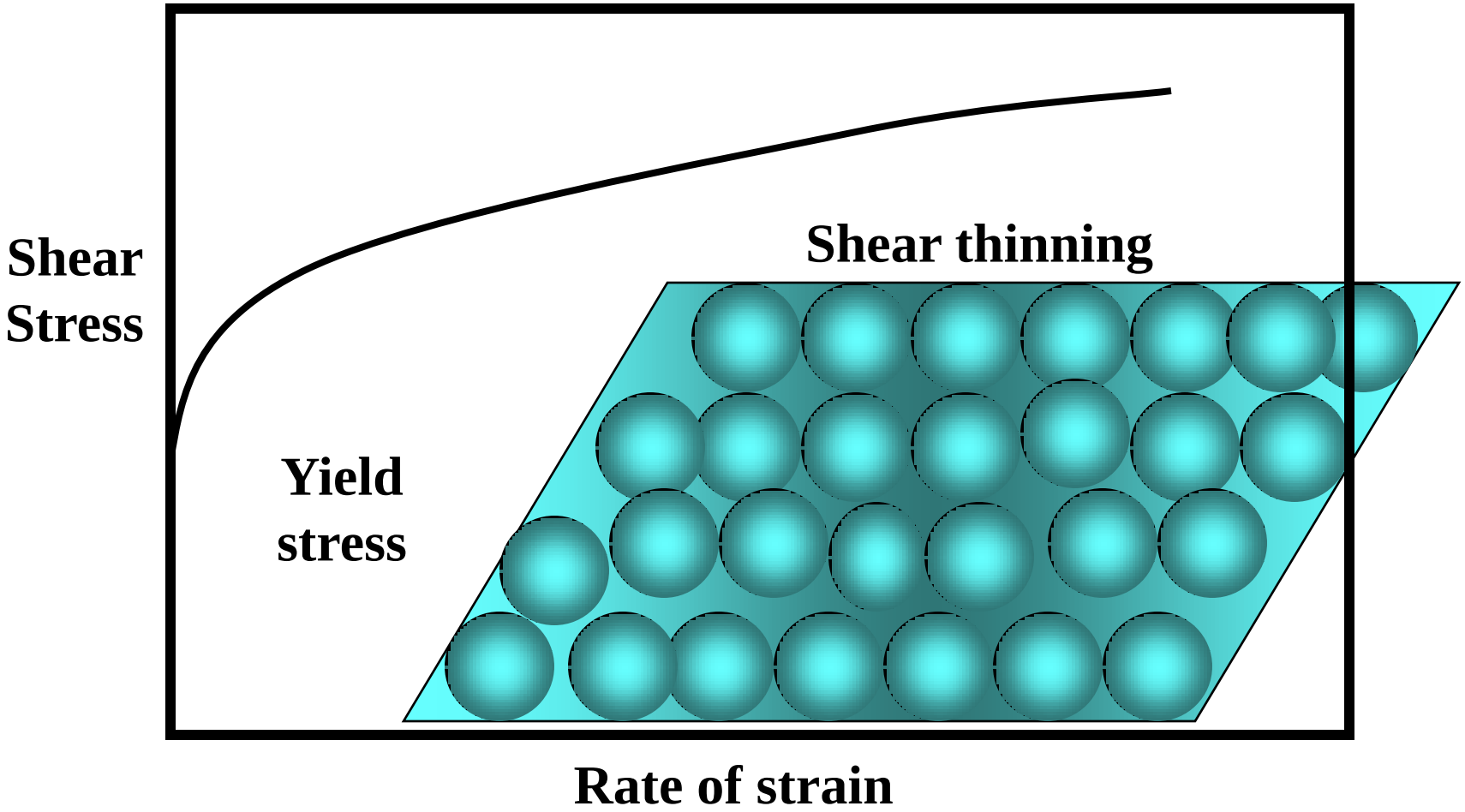

…Microgel thickeners can be used to stabilize against creaming and sedimentation

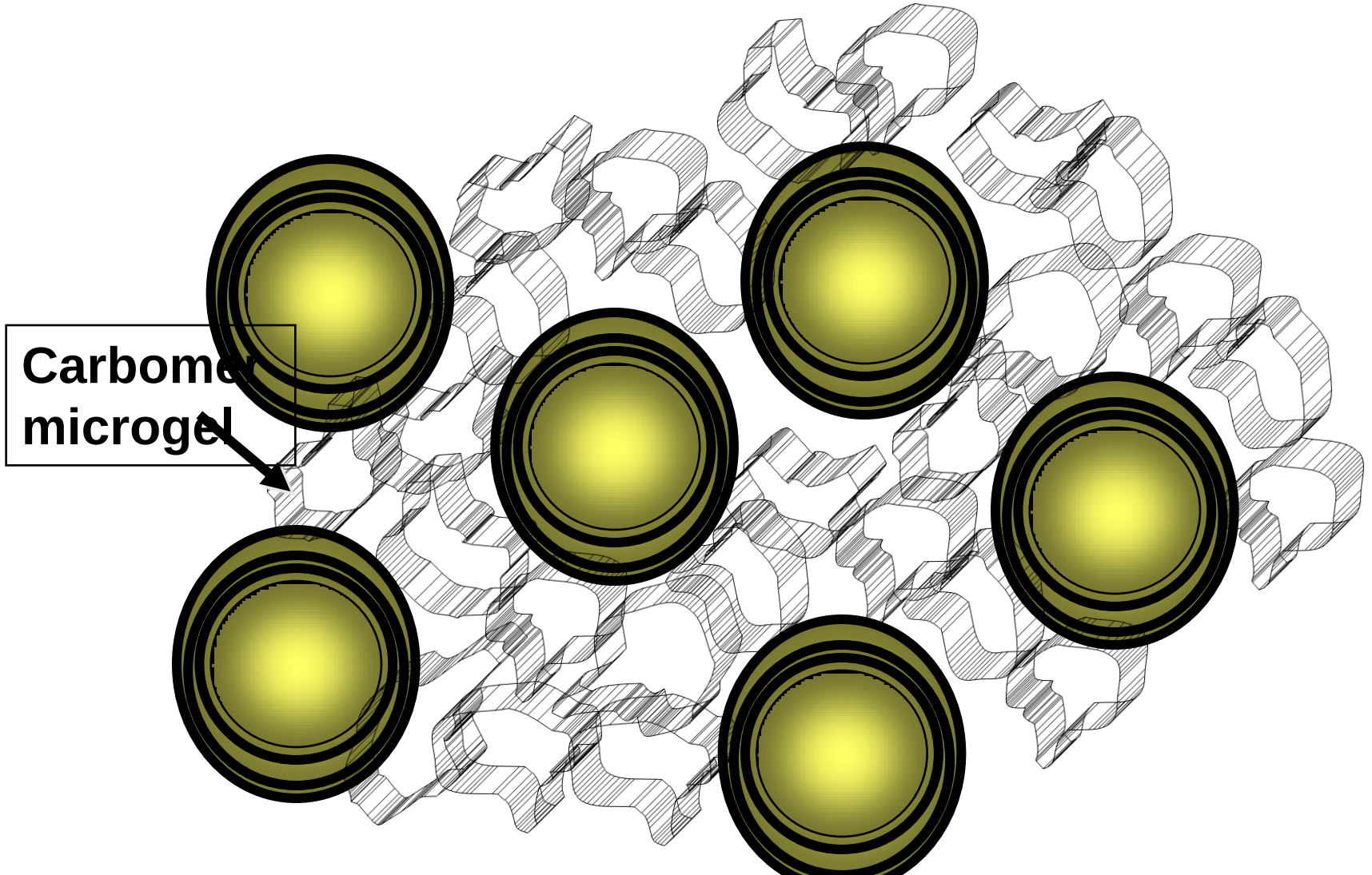

Carbomer

- Oil Droplets are trapped in place by the Microsponges
- and the system flows

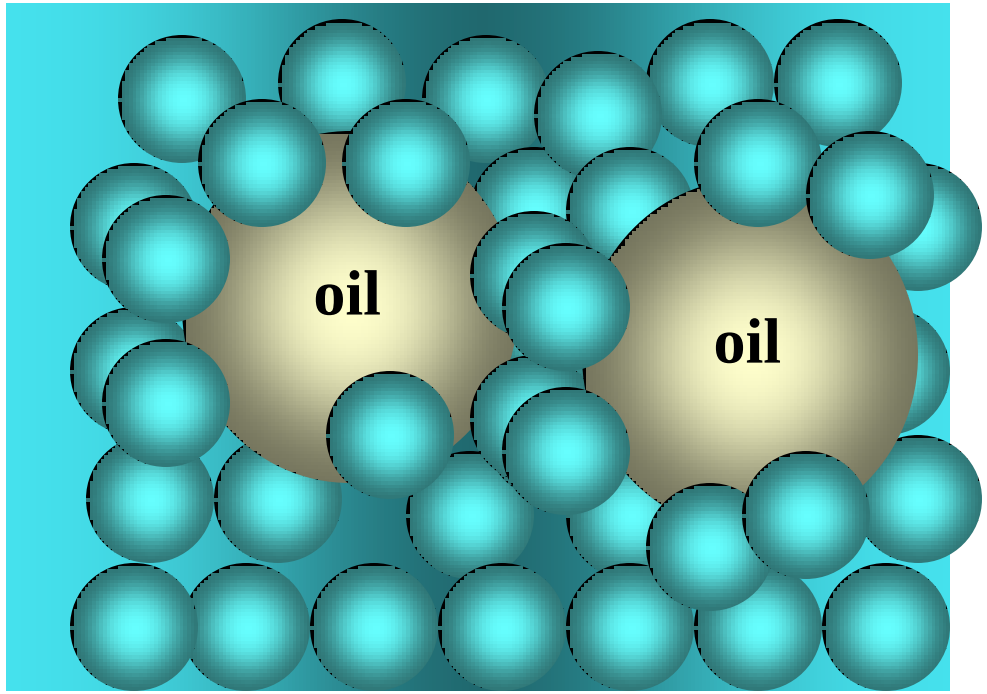

SimpleYield Stress Fluid
Carbomer Mucilage

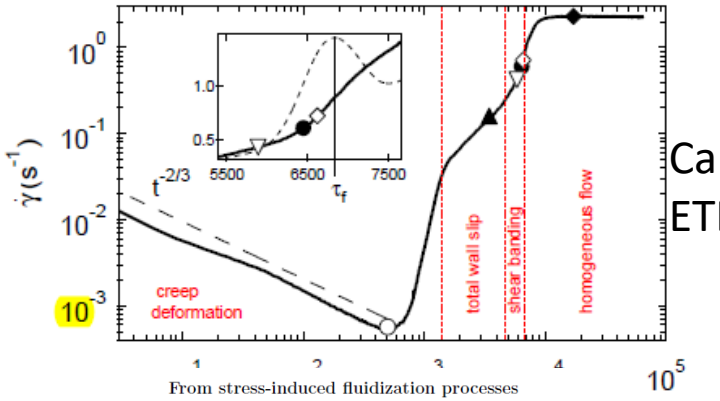

Carbopol®
ETD 2050

From stress-induced fluidization processes
to Herschel-Bulkley behaviour in simple yield stress fluids

Thibaut Divoux,[1] Catherine Barentin,[2] and Sébastien Manneville[1,3]

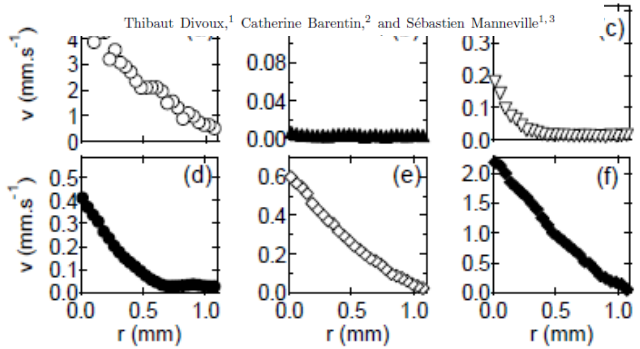

FIG. 1: Top: Shear-rate $\dot{\gamma}$ vs time t for a shear stress $\sigma = 37$ Pa applied at $t = 0$ (batch 1, rough BC). Inset: zoom on the shear-banding regime. The dashed curve shows $d\dot{\gamma}(t)/dt$ whose maximum corresponds to τ_f. Bottom: velocity profiles $v(r)$, where r is the distance to the rotor, at different times [symbol, time (s)]: (◯, 500), (▲, 3460), (▽, 5890), (●, 6450), (◇, 6620), (♦, 17349). On each profile, the upper value of the velocity scale is set to the current rotor velocity v_0 so that the slip velocity v_s at the rotor can be read directly as $v_s = v_0 - v(r = 0)$.

Thibaut Divoux, Catherine Barentin, and Sebastien Manneville, From stress-induced fluidization processes to Herschel-Bulkley behaviour in simple yield stress fluids, June 30, 2011

SimpleYield Stress Fluid Carbomer Mucilage

Carbopol® ETD 2050

Batch 1

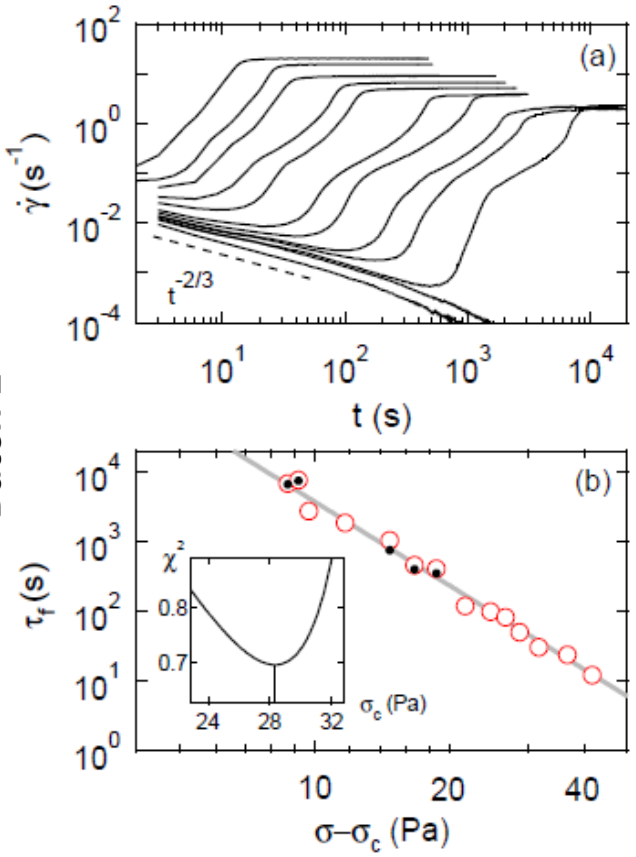

FIG. 2: (a) Shear rate $\dot{\gamma}$ vs time for $\sigma = 35$, 36, 37, 38, 40, 43, 45, 50, 55, 60, 65, and 70 Pa (from bottom to top) for batch 1 and rough BC. (b) Fluidization time τ_f extracted from the second inflection point of $\dot{\gamma}(t)$ (○) and from USV (•) vs the reduced shear stress $\sigma - \sigma_c$ with $\sigma_c = 28.3$ Pa. The gray line corresponds to the best fit $\tau_f = B/(\sigma - \sigma_c)^\beta$ with $B = (3.77 \pm 0.07) \cdot 10^7$ and $\beta = 4.0 \pm 0.1$. The inset shows the least square determination of σ_c (see text).

Batch 2

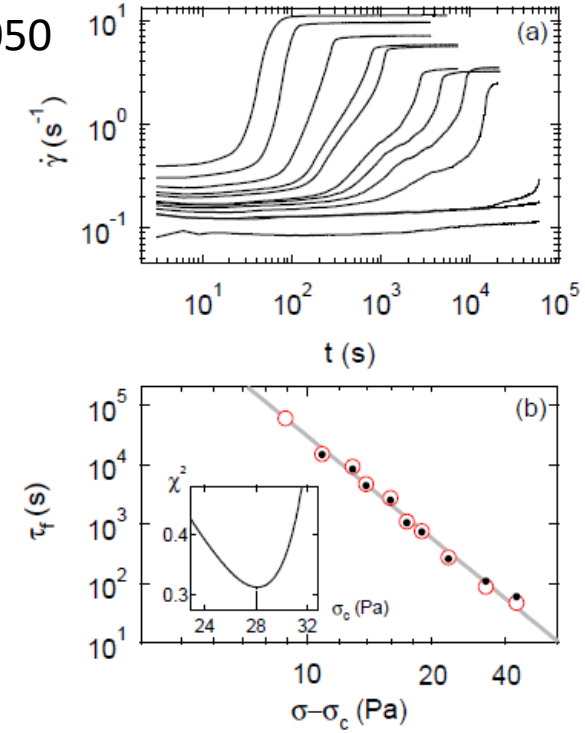

FIG. 3: (a) Shear rate $\dot{\gamma}$ vs time for $\sigma = 32$, 36, 37, 39, 41, 42, 44, 45.5, 47, 50, 55, and 60 Pa (from bottom to top) for batch 2 and smooth BC. (b) Fluidization time τ_f extracted from the second inflection point of $\dot{\gamma}(t)$ (○) and from USV (•) vs the reduced shear stress $\sigma - \sigma_c$ with $\sigma_c = 28.1$ Pa. The gray line corresponds to the best fit $\tau_f = B/(\sigma - \sigma_c)^\beta$ with $B = (1.74 \pm 0.04) \cdot 10^{10}$ and $\beta = 5.75 \pm 0.15$. The inset shows the least square determination of σ_c (see text).

Thibaut Divoux, Catherine Barentin, and S´ebastien Manneville, From stress-induced fluidization processes to Herschel-Bulkley behaviour in simple yield stress fluids, June 30 2011

SimpleYield Stress Fluid- Carbomer Mucilage

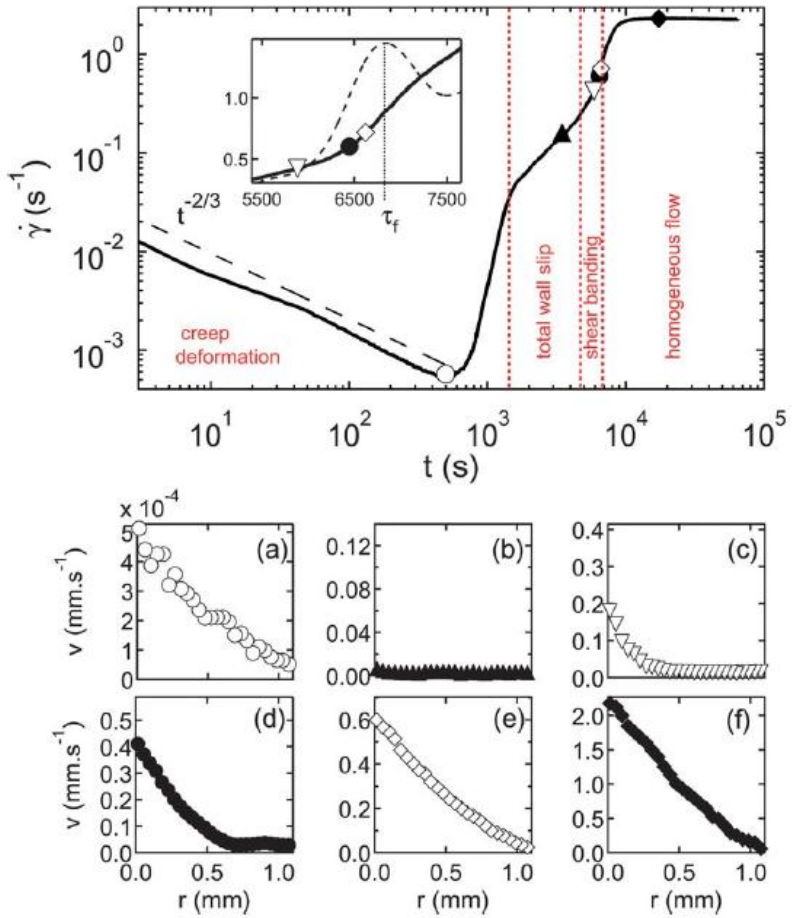

Fig. 1 Top: Shear-rate $\dot{\gamma}$ vs time t for a shear stress $\sigma = 37$ Pa applied at $t = 0$ (batch 1, rough BC). Inset: zoom on the shear-banding regime. The dashed curve shows $d\dot{\gamma}(t)/dt$ whose maximum corresponds to τ_f. Bottom: velocity profiles $v(r)$, where r is the distance to the rotor, at different times [symbol, time (s)]: (○, 500), (▲, 3460), (▽, 5890), (●, 6450), (◇, 6620), (◆, 17349). On each profile, the upper value of the velocity scale is set to the current rotor velocity v_0 so that the slip velocity v_s at the rotor can be read directly as $v_s = v_0 - v(r = 0)$.

Carbopol® ETD 2050

Thibaut Divoux, Catherine Barentin, and S´ebastien Manneville, From stress-induced fluidization processes to Herschel-Bulkley behaviour in simple yield stress fluids, June 30 2011

Shear Banding in Yield Stress Fluids

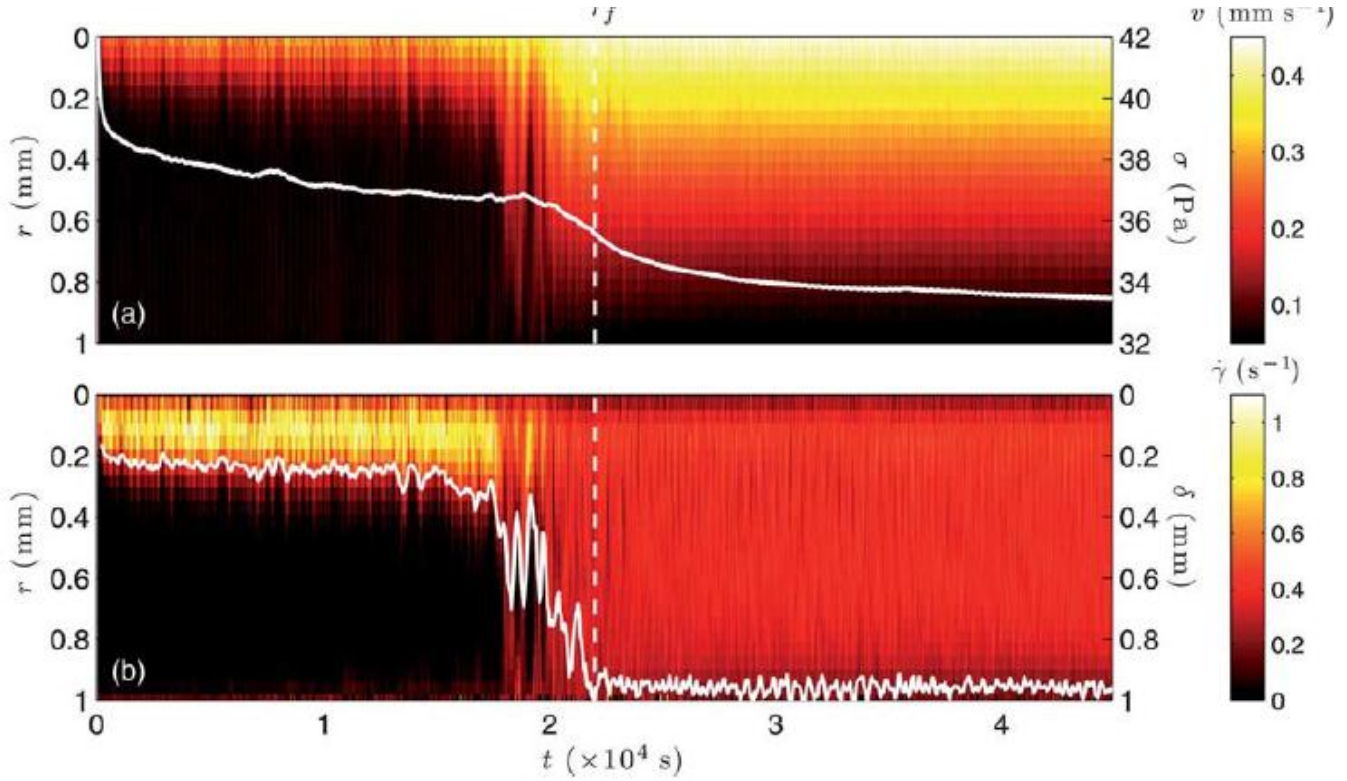

Fig. 3 (a) Spatiotemporal diagram of the velocity data $v(r,t)$ as a function of position r and time t. A constant shear rate $\dot{\gamma} = 0.5\ s^{-1}$ is applied at time $t = 0$ to a 1% w/w carbopol microgel seeded with 0.5% w/w hollow glass spheres in a smooth Couette cell of gap width 1 mm. The radial position r (left vertical axis) is measured from the rotating inner wall. Also shown with a white line is the stress response $\sigma(t)$ (right vertical axis). (b) Spatiotemporal diagram of the local shear rate $\dot{\gamma}(r,t)$. The white line shows to the position $\delta(t)$ of the interface between the fluidized band and the solid-like region. The vertical dashed line indicates the fluidization time τ_f, *i.e.* the time at which the shear rate field becomes homogeneous.

Thibaut Divoux, Catherine Barentin, and S´ebastien Manneville, From stress-induced fluidization processes to Herschel-Bulkley behaviour in simple yield stress fluids, June 30, 2011

SOCIETY OF COSMETIC CHEMISTS

SHEAR BANDING

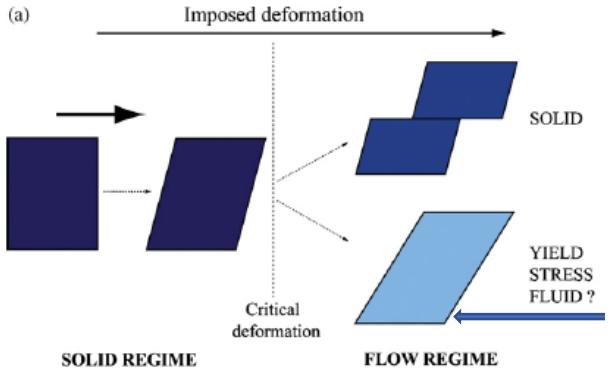

Fig. 1. Typical aspects of the deformation field inside a sample undergoing an apparent deformation. For a solid the induced deformation is homogeneous up to a critical value, then a shear-banding develops. For a (theoretical) yield stress fluid the induced deformation field is homogeneous up to a critical value in the solid regime, then the material flows homogeneously in its liquid regime (a). In practice it seems that a more appropriate frame for some yield stress fluids is that described in (b) in which the transition from the solid to the liquid regime is progressive, i.e. with a shear-banding at low apparent shear rates and a homogeneous flow beyond a critical shear rate.

P. Coussot et al. / J. Non-Newtonian Fluid Mech. xxx (2008) xxx–xxx

CARBOMER

WEAKLY FLOCCULATED GELS

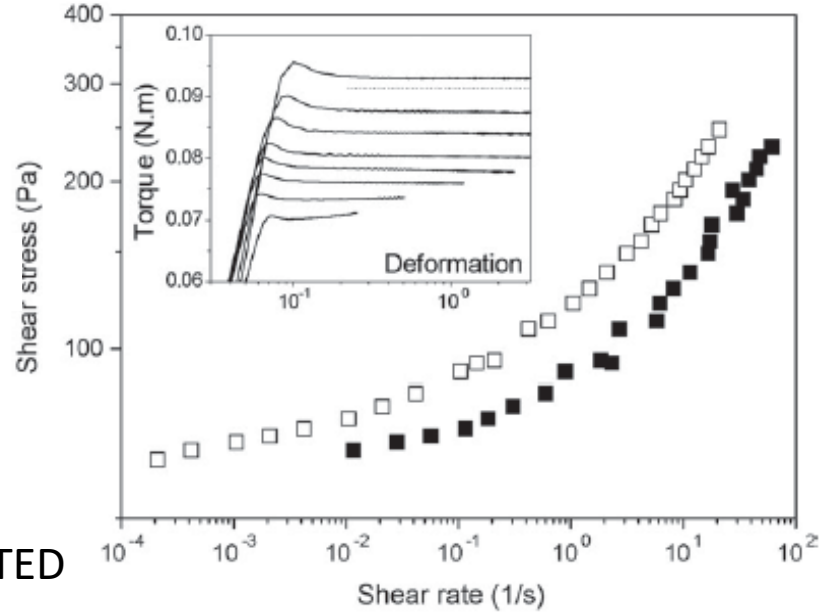

Fig. 7. Steady-state data for a Carbopol gel obtained from wide-gap Couette geometry under controlled rotation velocity (see text). The empty squares correspond to the apparent shear rates ($\dot{\gamma}_{app}$) and shear stresses (τ_{app}) associated with the plateau levels (see inset). The filled squares correspond to the effective shear rates and shear stresses values determined from a complete analysis of the data (see text, Eq. (4)). The inset shows the evolution of the torque as a function of the apparent deformation (i.e. $\int_t \dot{\gamma}_{app}\, dt$) induced for the lowest levels of rotation velocity (from top to bottom: 2×10^{-1}, 10^{-1}, 5×10^{-2}, 2×10^{-2}, 10^{-2}, 5×10^{-3}, 2×10^{-3} and 10^{-3} rpm).

SOCIETY OF COSMETIC CHEMISTS

Shear Velocity in Emulsion in Couette Flow

G. Ovarlez, S. Rodts, A. Ragouilliaux, P. Coussot, J. Goyon, A. Colin, Wide-gap Couette flows of dense emulsions: local concentration measurements, and comparison between macroscopic and local constitutive law measurements through magnetic resonance imaging, Phys. Rev. E 78 (2008) 036307.

No difference between macroscopic and local rheologies is interpreted to mean that these are simple yield stress materials.

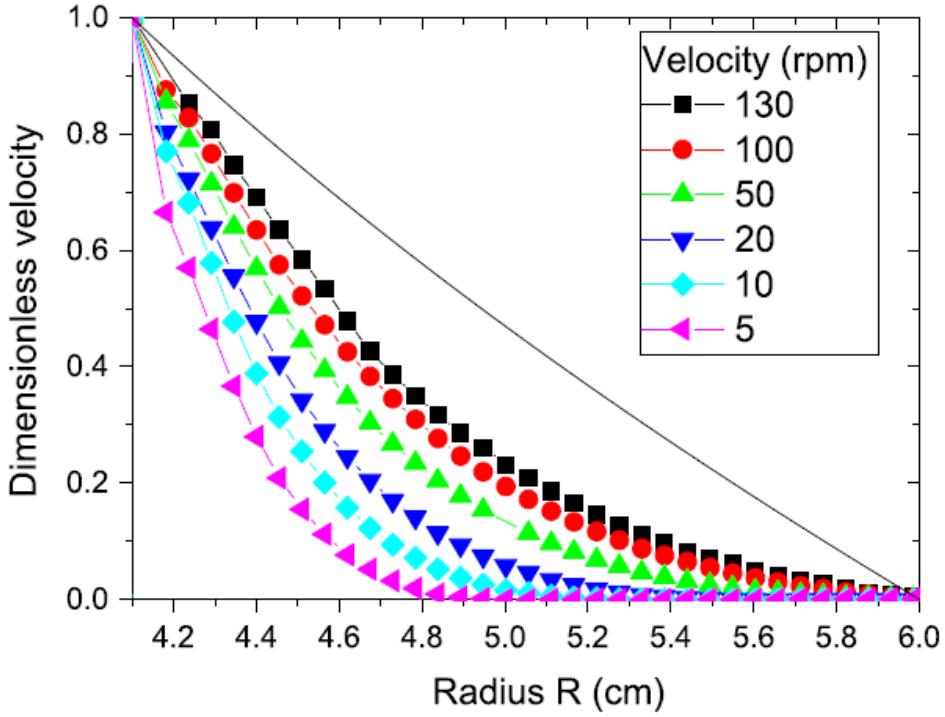

Fig. 5. Dimensionless velocity profiles $V(R)/V(R_i)$, measured by MRI techniques, for the steady flows of a concentrated emulsion in a wide gap Couette geometry, at various rotational velocities ranging from 5 to 130 rpm (see legend); the solid line is the theoretical profile for a Newtonian fluid. The emulsion is composed of 1 μm diameter silicone oil droplets dispersed at a 75% volume fraction in water stabilized by Sodium Dodecyl Sulfate at a 8.5 wt% concentration [32]. Figure from Ovarlez et al. [32].

Shear Velocity in Emulsion in Couette Flow

G. Ovarlez, S. Rodts, A. Ragouilliaux, P. Coussot, J. Goyon, A. Colin, Wide-gap Couette flows of dense emulsions: local concentration measurements, and comparison between macroscopic and local constitutive law measurements through magnetic resonance imaging, Phys. Rev. E 78 (2008) 036307.

No difference between macroscopic and local rheologies is interpreted to mean that these are simple yield stress materials.

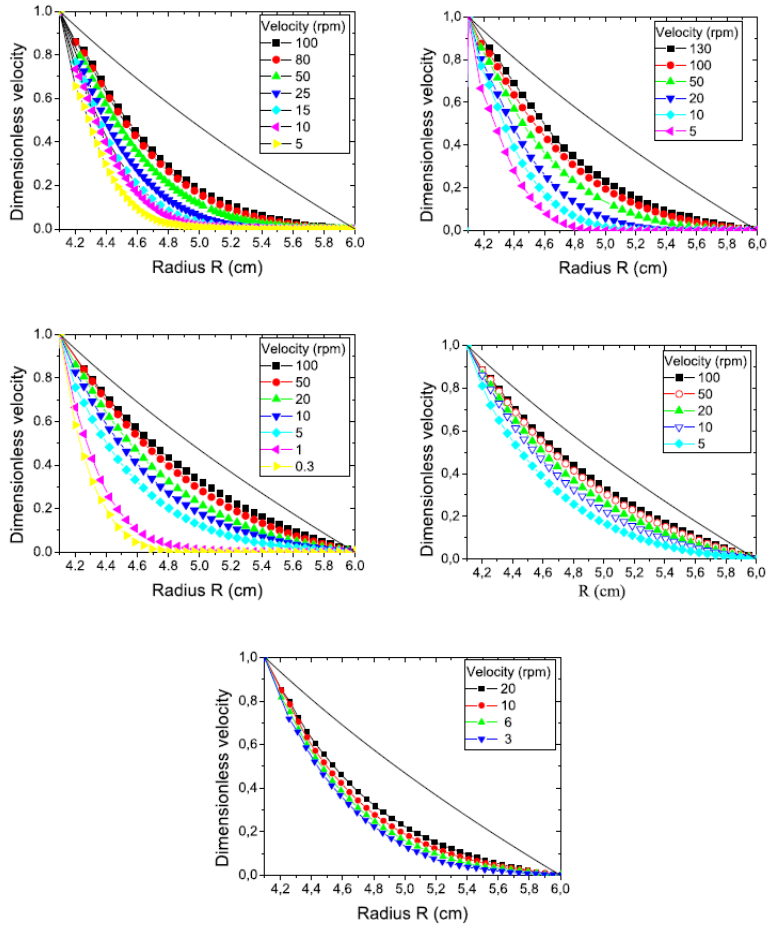

FIG. 2: (Color online) a) Dimensionless velocity profiles for the steady flows of a 0.3μm adhesive emulsion, at various rotational velocities ranging from 5 to 100rpm; the line is the theoretical dimensionless velocity profile for a Newtonian fluid. b) Same plot for a 1μm non-adhesive emulsion. c) Same plot for a 6.5μm adhesive emulsion. d) Same plot for a 6.5μm non-adhesive emulsion. e) Same plot for a 40μm non-adhesive emulsion.

Shear Banding in Yield Stress Fluids

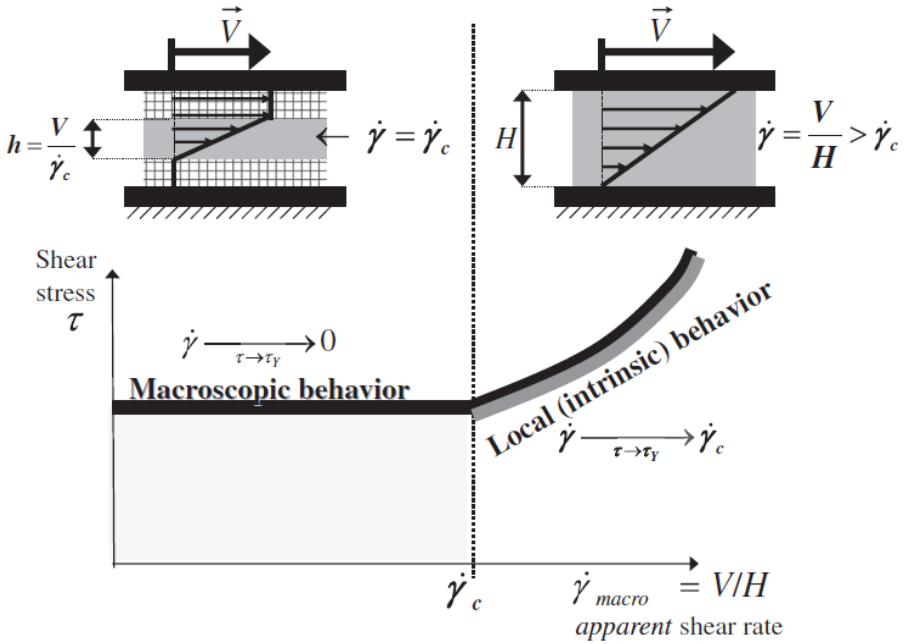

Fig. 1. Illustration of the difference between the material intrinsic constitutive law (grey line) and the flow curve measured macroscopically in a homogeneous stress field (black line) in a shear-banding material. At high macroscopic shear rate ($\dot{\gamma}_{macro} > \dot{\gamma}_c$), flow is homogeneous and the macroscopic flow curve matches the local behavior. At low macroscopic shear rate ($\dot{\gamma}_{macro} < \dot{\gamma}_c$), shear banding occurs: the local shear rate in the flowing material – $\dot{\gamma}_c$ – differs from the macroscopic shear rate and the macroscopic flow curve does not match the local behavior.

Emulsion, Foam, Carbomer Gel Simple Yield Stress Fluids

G. Ovarlez, S. Cohen-Addad, K. Krishan, J. Goyon, P. Coussot, On the existence of a simple yield stress fluid behavior, Journal of Non-Newtonian Fluid Mechanics, 193, 2013, 68

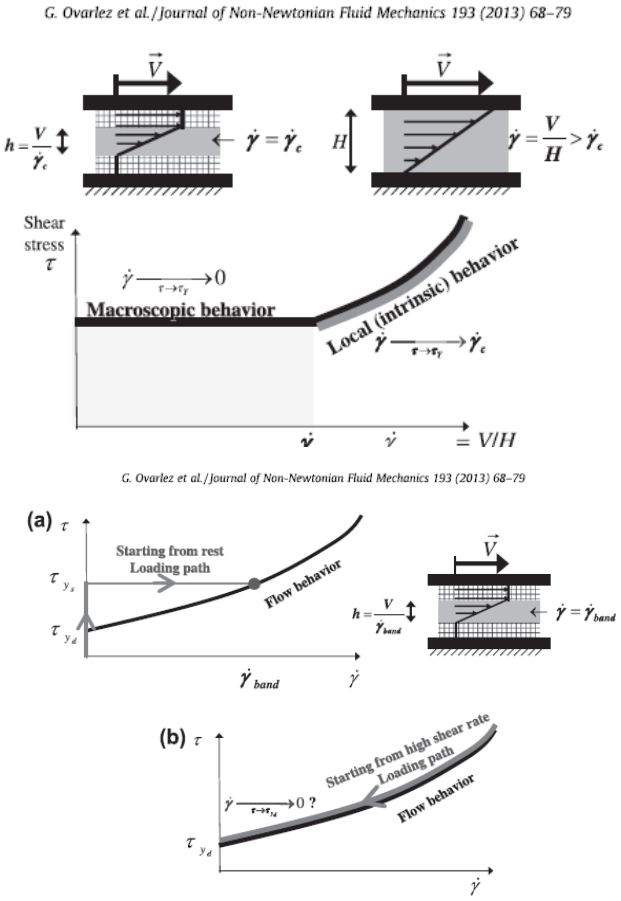

For soft particles- A BAND MAY OCCUR AT THE START OF FLOW THEN NORMAL DISSIPATION AS FLOW REACHES A STEADY STATE

Emulsion, Foam, Carbomer Gel Simple Yield Stress Fluids

G. Ovarlez, S. Cohen-Addad, K. Krishan, J. Goyon, P. Coussot, On the existence of a simple yield stress fluid behavior, Journal of Non-Newtonian Fluid Mechanics, 193, 2013, 68

For soft particles- a single constitutive equation in simple shear for emulsion, foam and Carbomer gel. Consistent with the Herschel Bulkeley Model.

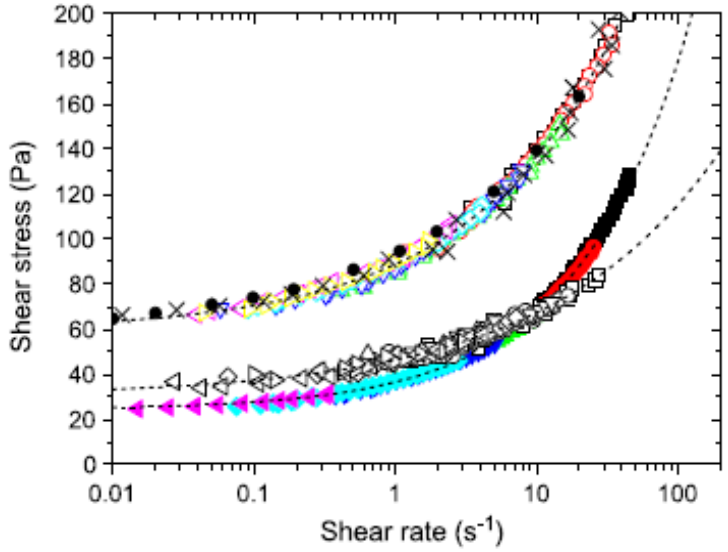

Fig. 9. Constitutive laws of (from bottom to top) a concentrated emulsion, a foam, and a Carbopol gel, measured locally in a wide gap Couette cell using MRI techniques. Macroscopic data measured in the Carbopol gel in the Couette geometry (crosses) and in a cone and plate geometry (filled circles) are also shown. The dotted lines are Herschel–Bulkley fits to the data $\tau = \tau_y + \eta_{HB}\dot{\gamma}^n$ with: $\tau_y = 24.3$ Pa, $\eta_{HB} = 12.3\,\text{Pa}\,\text{s}^{0.55}$, and $n = 0.55$ (emulsion); $\tau_y = 30.3$ Pa, $\eta_{HB} = 16.2\,\text{Pa}\,\text{s}^{0.36}$, and $n = 0.36$ (foam); $\tau_y = 59.3$ Pa, $\eta_{HB} = 29.6\,\text{Pa}\,\text{s}^{0.42}$, and $n = 0.42$ (Carbopol gel). The emulsion is composed of 6.5 μm diameter silicone oil droplets dispersed at a 75% volume fraction in a mixture of 50 wt% glycerine and 50 wt% water stabilized by Brij and trimethyl tetradecyl ammonium bromide at a 1 wt% concentration [32]. The foam is composed of 45 μm diameter bubbles at a 92% volume fraction in a SLES foaming solution described in [34]. The gel is a hair gel (Vivelle Dop, France), which is mainly made up of Carbopol in water [49].

SimpleYield Stress Fluid Carbomer Mucilage

Carbopol® ETD 2050

- No shear banding means Carbomer is a Simple Yield Stress Fluid
- Insignificant thixotropy loop means Carbomer is a Simple Yield Stress Fluid

Thibaut Divoux, Catherine Barentin, and S´ebastien Manneville, From stress-induced fluidization processes to Herschel-Bulkley behaviour in simple yield stress fluids, June 30 2011

FIRST DIRECT IMAGING OF SWOLLEN MICROGEL PARTICLES

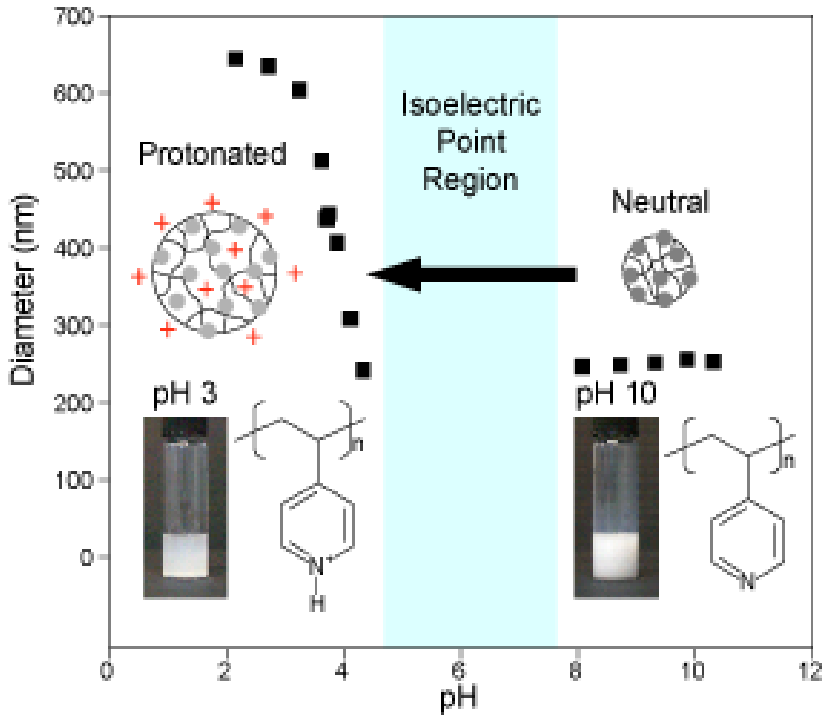

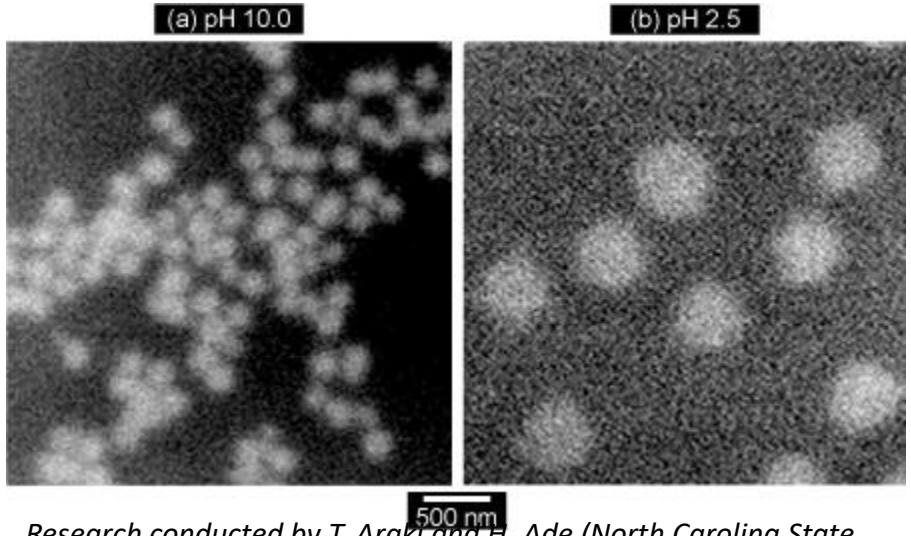

Research conducted by T. Araki and H. Ade (North Carolina State University) and S. Fujii and S.P. Armes (University of Sheffield, U.K.). Research funding: U.S. Department of Energy, Office of Basic Energy Sciences (BES); Royal Society/Wolfson Research Merit Award; and Engineering and Physical Sciences Research Council (EPSRC). Operation of the ALS is supported by BES.
Publication about this research: S. Fujii, S.P. Armes, T. Araki, and H. Ade, "Direct imaging and spectroscopic characterization of stimulus-responsive microgels," J. Am. Chem. Soc. ***127****, 16808 (2005).*

SimpleYield Stress Fluid Carbomer Mucilage

Carbopol® ETD 2050

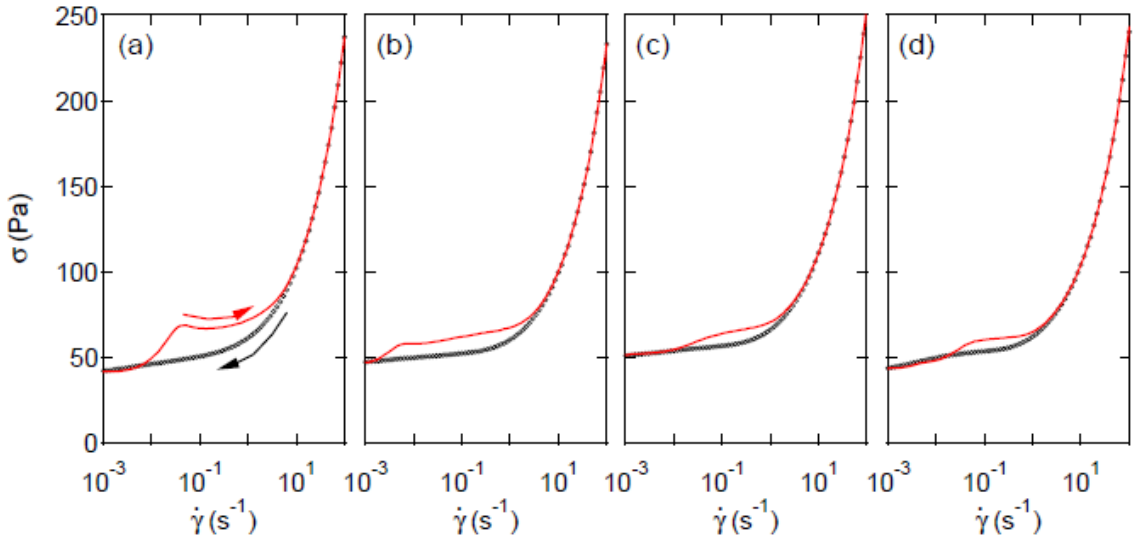

FIG. 8: Flow curves, shear stress σ vs shear rate $\dot{\gamma}$, obtained by decreasing $\dot{\gamma}$ from 100 to 10^{-3} s^{-1} ($\circ$) and then increasing $\dot{\gamma}$ from 10^{-3} to 100 s^{-1} (red line) for various waiting times per point: (a) $t_w = 2$ s, (b) $t_w = 10$ s, (c) $t_w = 30$ s, and (d) $t_w = 70$ s. Note that the hysteresis loop for $\dot{\gamma} \lesssim 1$ s^{-1} decreases for increasing waiting times. The total duration of the longest measurements shown in (d) is $2.1 \cdot 10^4$ s. Experiments performed in a plate-plate geometry ($e = 1$ mm) with rough BC ($\delta = 46$ μm) on a 1 % wt. carbopol microgel without any seeding glass spheres.

Insignificant thixotropy loop means Carbomer is a Simple Yield Stress Fluid

Thibaut Divoux, Catherine Barentin, and S´ebastien Manneville, From stress-induced fluidization processes to Herschel-Bulkley behaviour in simple yield stress fluids, June 30 2011

Un-Neutralized Carbomer in PEG 400

G. Bonacucina et al. / International Journal of Pharmaceutics 282 (2004) 115–130

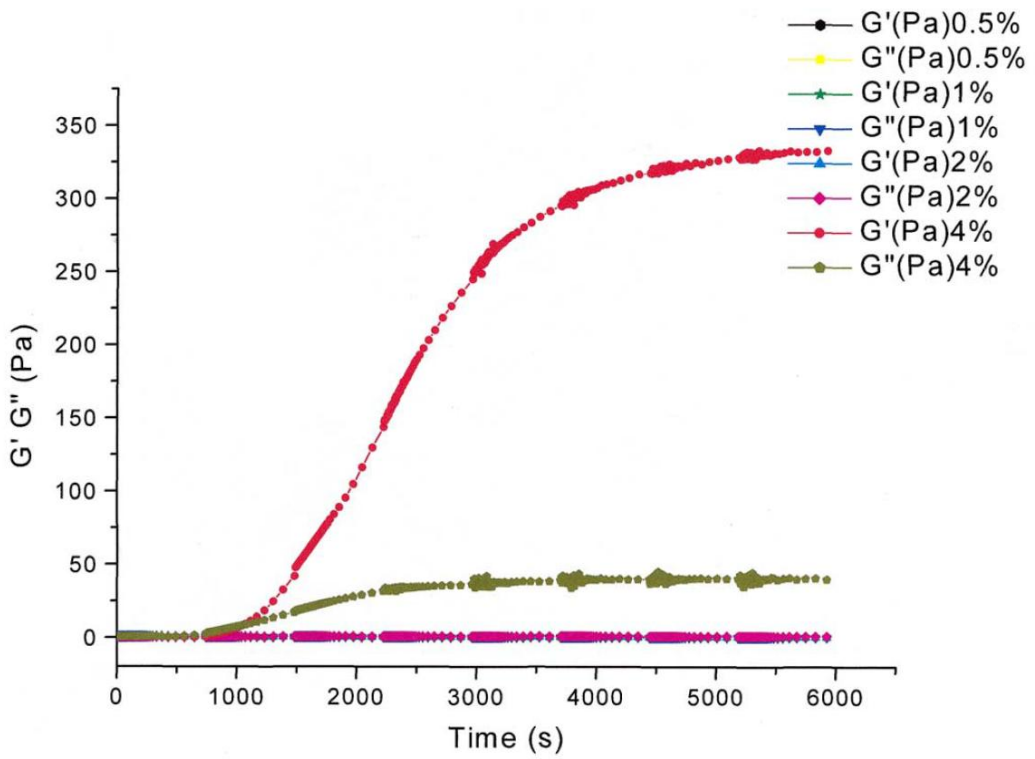

Un-Neutralized Carbomer in PEG 400

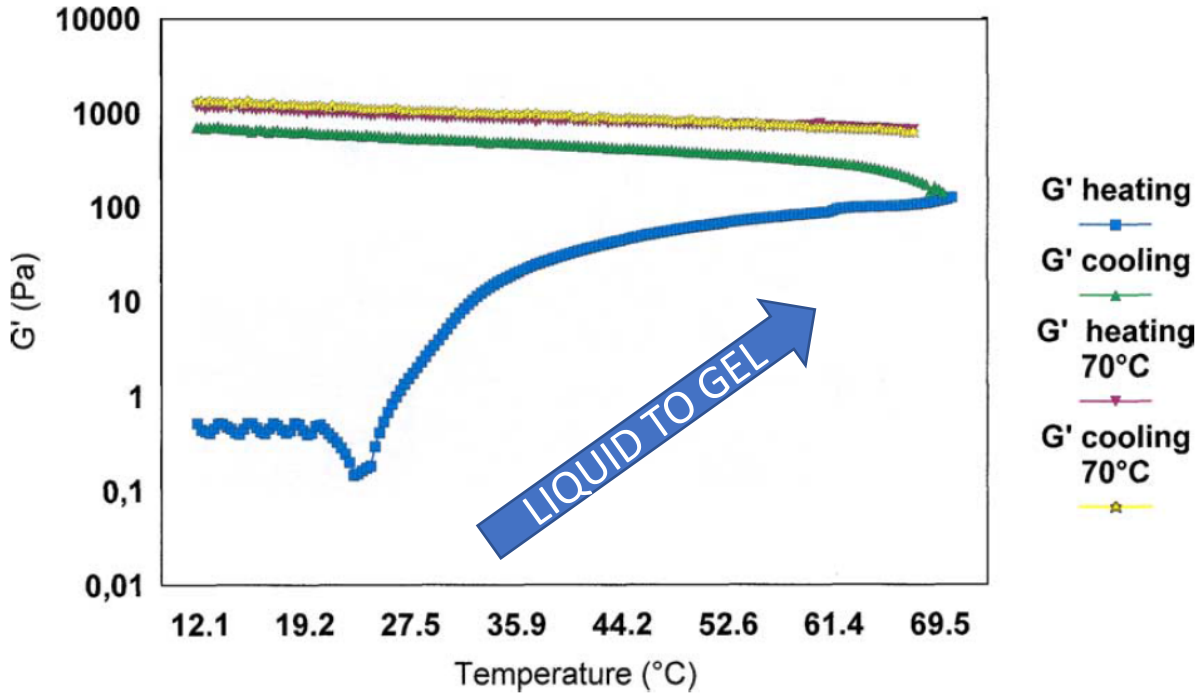

Fig. 2. Temperature sweep of Carbopol 974 in PEG 400.

G. Bonacucina et al. / International Journal of Pharmaceutics 282 (2004) 115–130

Un-Neutralized Carbomer in PEG 400

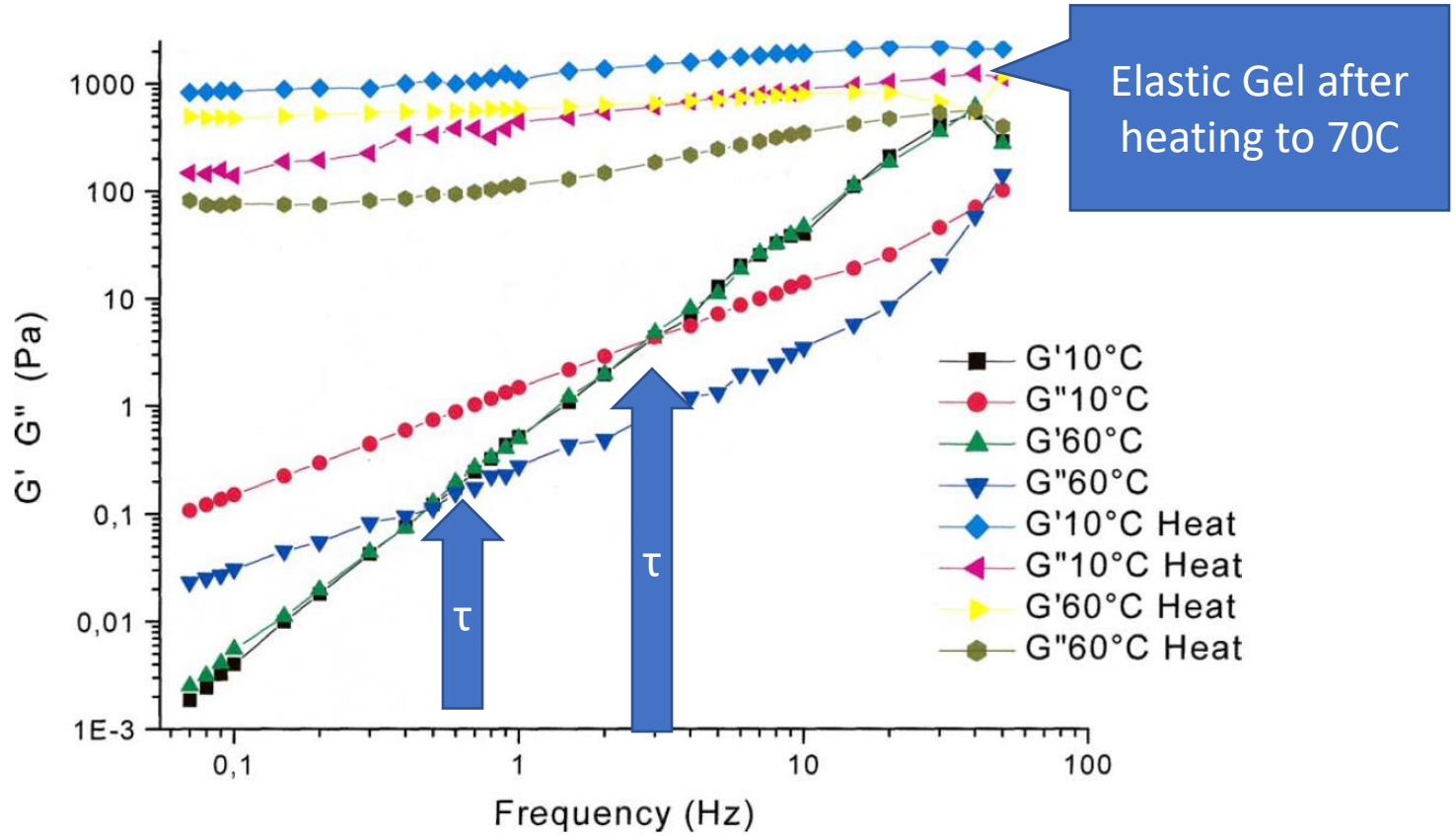

Fig. 3. Frequency sweep of Carbopol 974 gels in PEG 400 prepared at room temperature (I method) and at 70 °C (II method).

G. Bonacucina et al. / International Journal of Pharmaceutics 282 (2004) 115–130

Yield stress fluids

- The yield stress measured in one situation is often different from that in another situation
  - Lab measurements often do not correlate with real world observations

Relating Rheology to Sensory Attributes

Slip

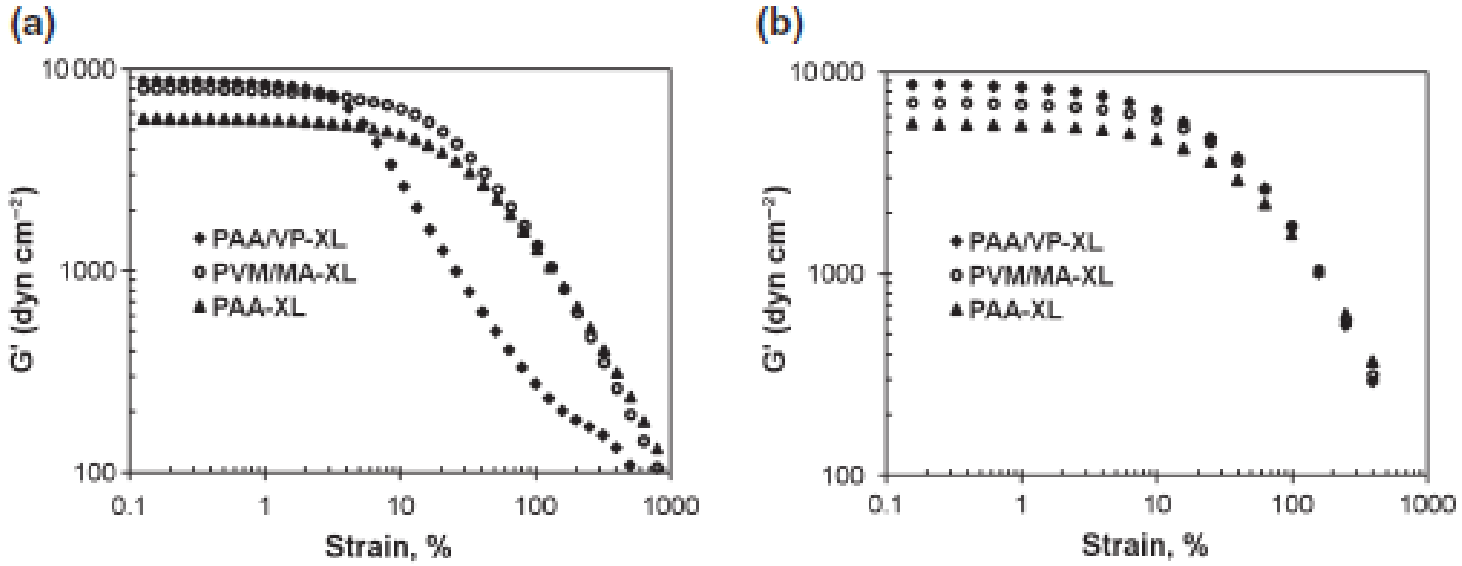

Figure 1 Strain amplitude dependency of the storage modulus (G' (dyn cm^{-2})) at 1 rps using smooth surface fixtures (a) and rough surface fixtures (b).

S. Ozkan, T. W. Gillece, L. Senak and D. J. Moore, Characterization of yield stress and slip behaviour of skin/hair care gels using steady flow and LAOS measurements and their correlation with sensorial attributes, International Journal of Cosmetic Science, 2012, 34, 193–201

Shear Stress/ Shear Rate Profiles

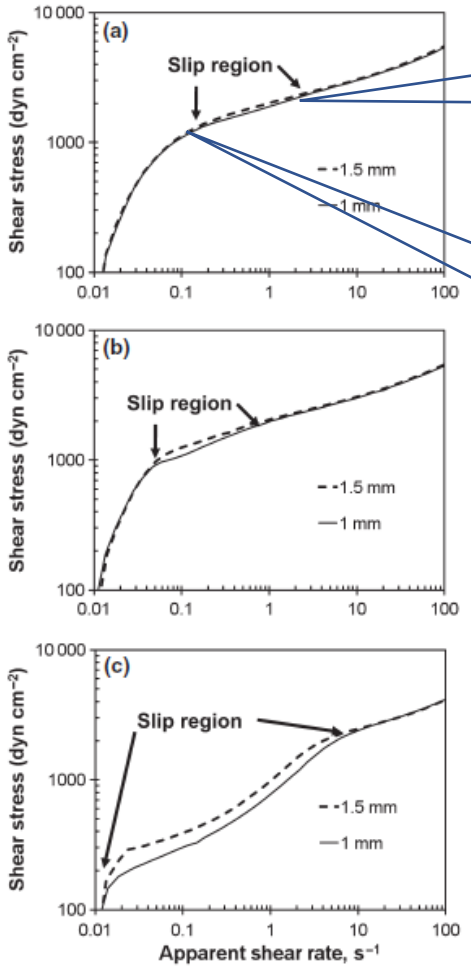

Yield starts here

Slip starts here

Figure 2 Continuous shear rate ramp results at 1.5-mm and 1.0-mm gap openings for (a) PAA-XL, (b) PVM/MA-XL and (c) PAA/VP-XL.

Table V Herschel–Bulkley model parameters and Navier's slip coefficients

	1% PAA/VP-XL	1% PVM/MA-XL	1% PAA-XL
τ_0, Pa	161.5	168.5	123.7
m, Pa $s^{1/n}$	12	22.8	41.5
n	0.54	0.52	0.43
β, m (Pa $s^{1/nb}$)^{nb}	0.0033	0.141	0.024
s_b	1.07	0.35	0.43

S. Ozkan, T. W. Gillece, L. Senak and D. J. Moore, Characterization of yield stress and slip behaviour of skin/hair care gels using steady flow and LAOS measurements and their correlation with sensorial attributes, International Journal of Cosmetic Science, 2012, 34, 193–201

SOCIETY OF COSMETIC CHEMISTS

Principle Component Analysis

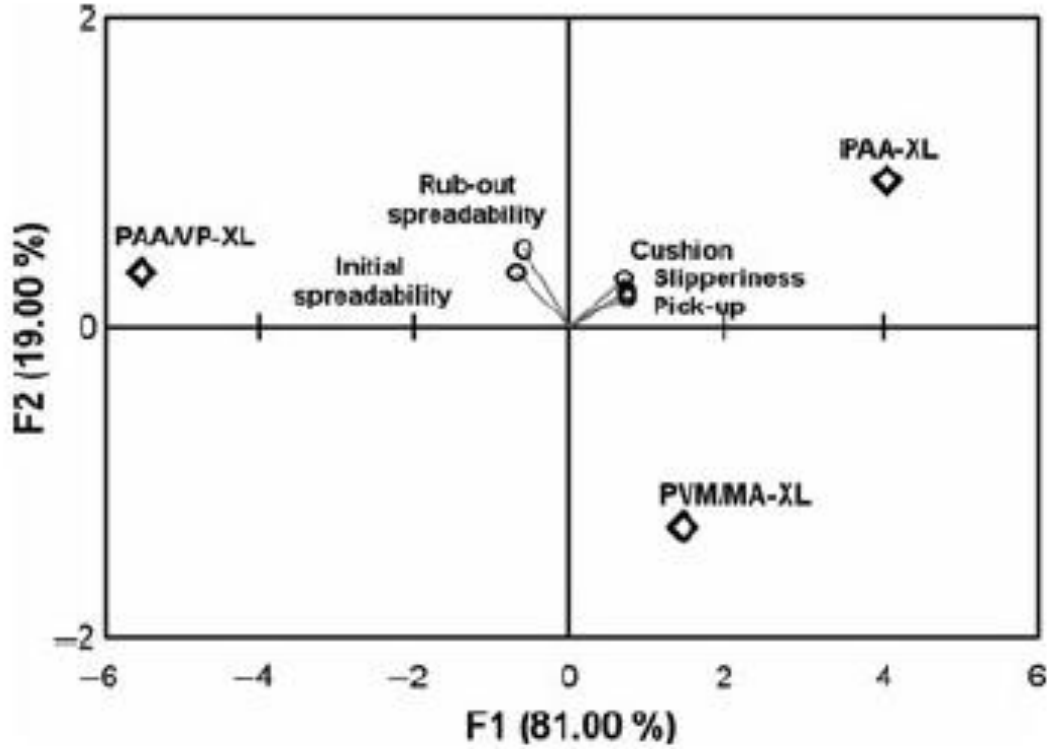

Figure 4 Sensory data: Principle component analysis.

S. Ozkan, T. W. Gillece, L. Senak and D. J. Moore, Characterization of yield stress and slip behaviour of skin/hair care gels using steady flow and LAOS measurements and their correlation with sensorial attributes, International Journal of Cosmetic Science, 2012, 34, 193–201

Principle Component Analysis of Conventional Rheology and Sensory Data

Elastic Modulus and HB n

Shear and extensional viscosity

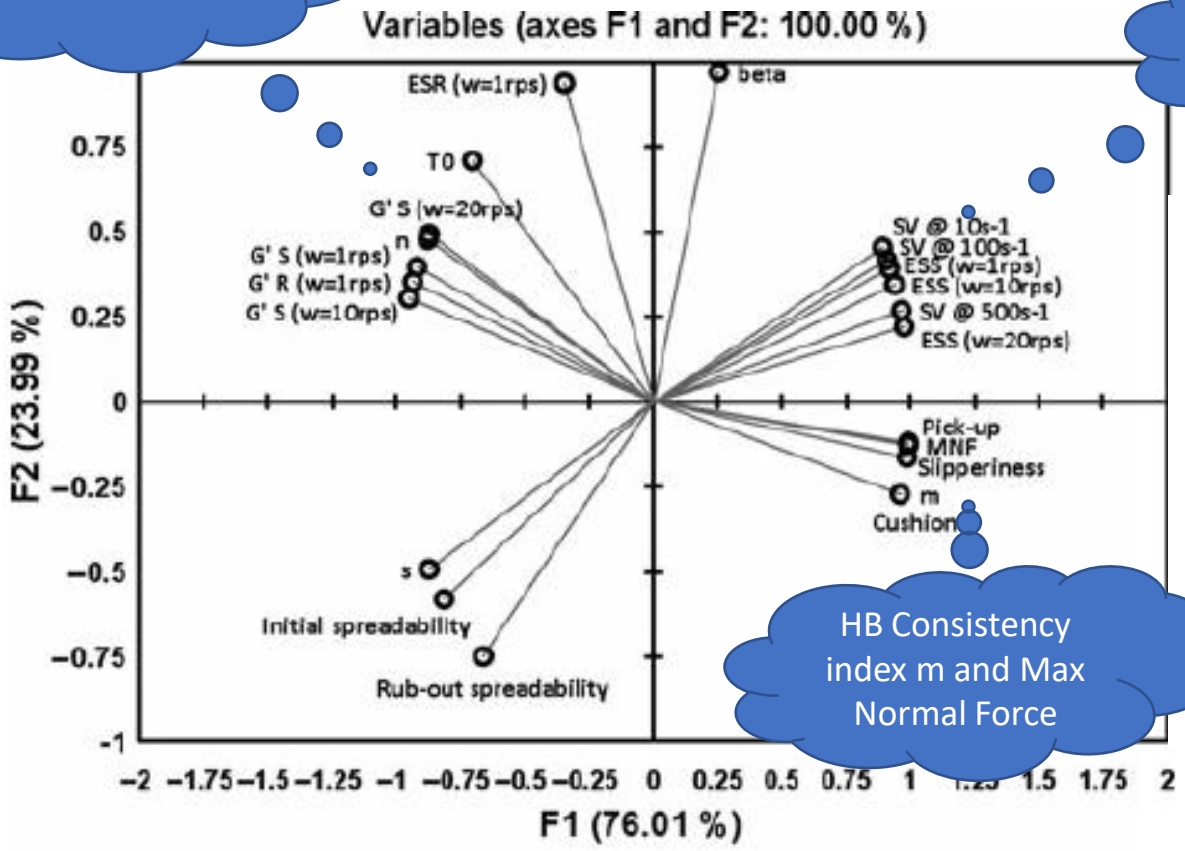

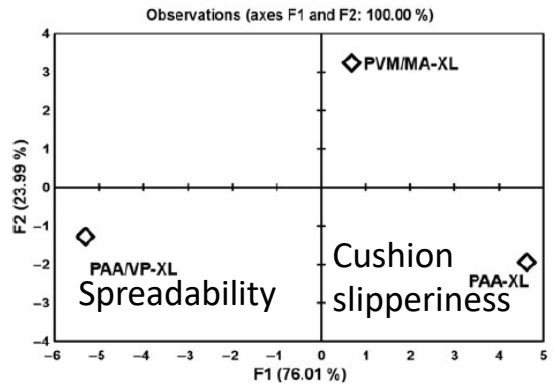

HB Consistency index m and Max Normal Force

$$\tau = \tau_0 + m\dot{\gamma}^n$$

S. Ozkan, T. W. Gillece, L. Senak and D. J. Moore, Characterization of yield stress and slip behaviour of skin/hair care gels using steady flow and LAOS measurements and their correlation with sensorial attributes, International Journal of Cosmetic Science, 2012, 34, 193–201

Principle Component Analysis of LAOS Rheology and Sensory Data

Shear viscosity

Alternate Modulus at 400% Strain

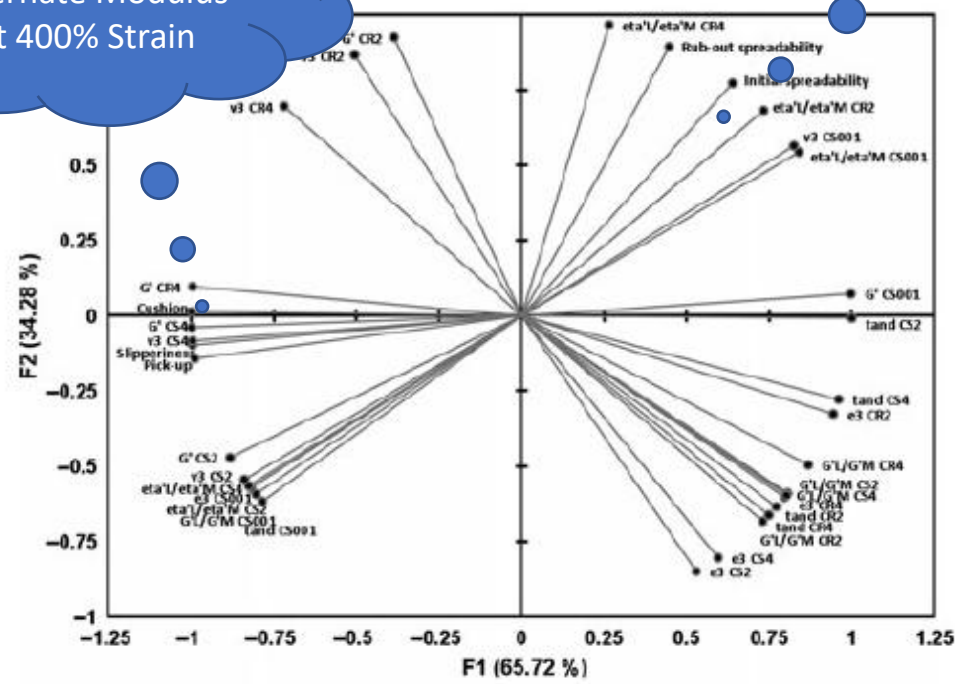

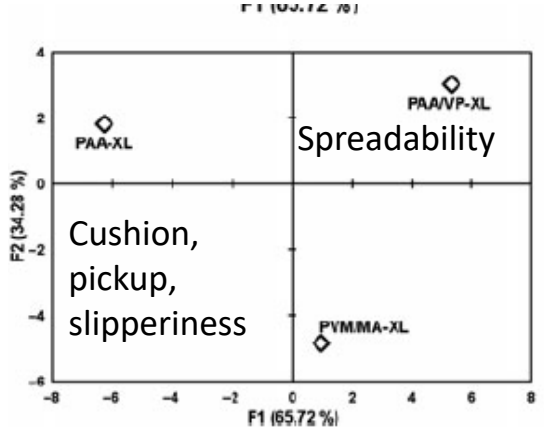

$$\tau = \tau_0 + m\dot{\gamma}^n$$

S. Ozkan, T. W. Gillece, L. Senak and D. J. Moore, Characterization of yield stress and slip behaviour of skin/hair care gels using steady flow and LAOS measurements and their correlation with sensorial attributes, International Journal of Cosmetic Science, 2012, 34, 193–201

Shear Viscosity and Extensional Viscosity

- A fluid can be shear-thinning under regular shear
  - But strain thickening under extension

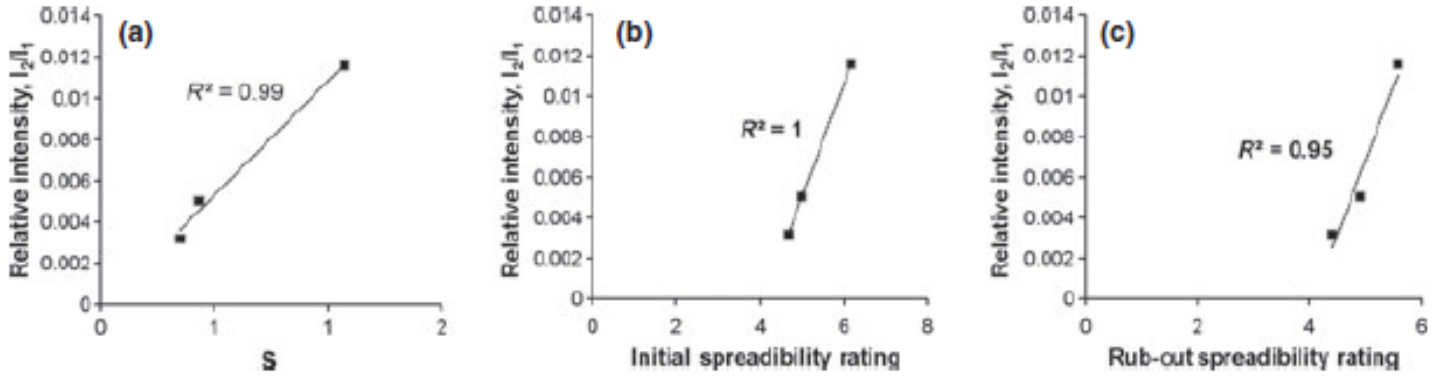

Figure 7 Linear regression fit for relative intensity (I_2/I_1) vs. slip velocity coefficient, s, collected with smooth surfaces at 400% strain (a), and sensory ratings vs. relative intensity (I_2/I_1) data collected with smooth surfaces at 400% strain (b and c).

S. Ozkan, T. W. Gillece, L. Senak and D. J. Moore, Characterization of yield stress and slip behaviour of skin/hair care gels using steady flow and LAOS measurements and their correlation with sensorial attributes, International Journal of Cosmetic Science, 2012, 34, 193–201

SOCIETY OF COSMETIC CHEMISTS

Hydrophobically-Modified Hydrophilic Polymers

- Outline
  - Hydrophilic polymers modified by hydrophobic moieties
  - Combination of surfactant and polymer properties in one molecule
  - Self-associate in aqueous solution to form complex micellar structures

Polymeric Emulsifiers

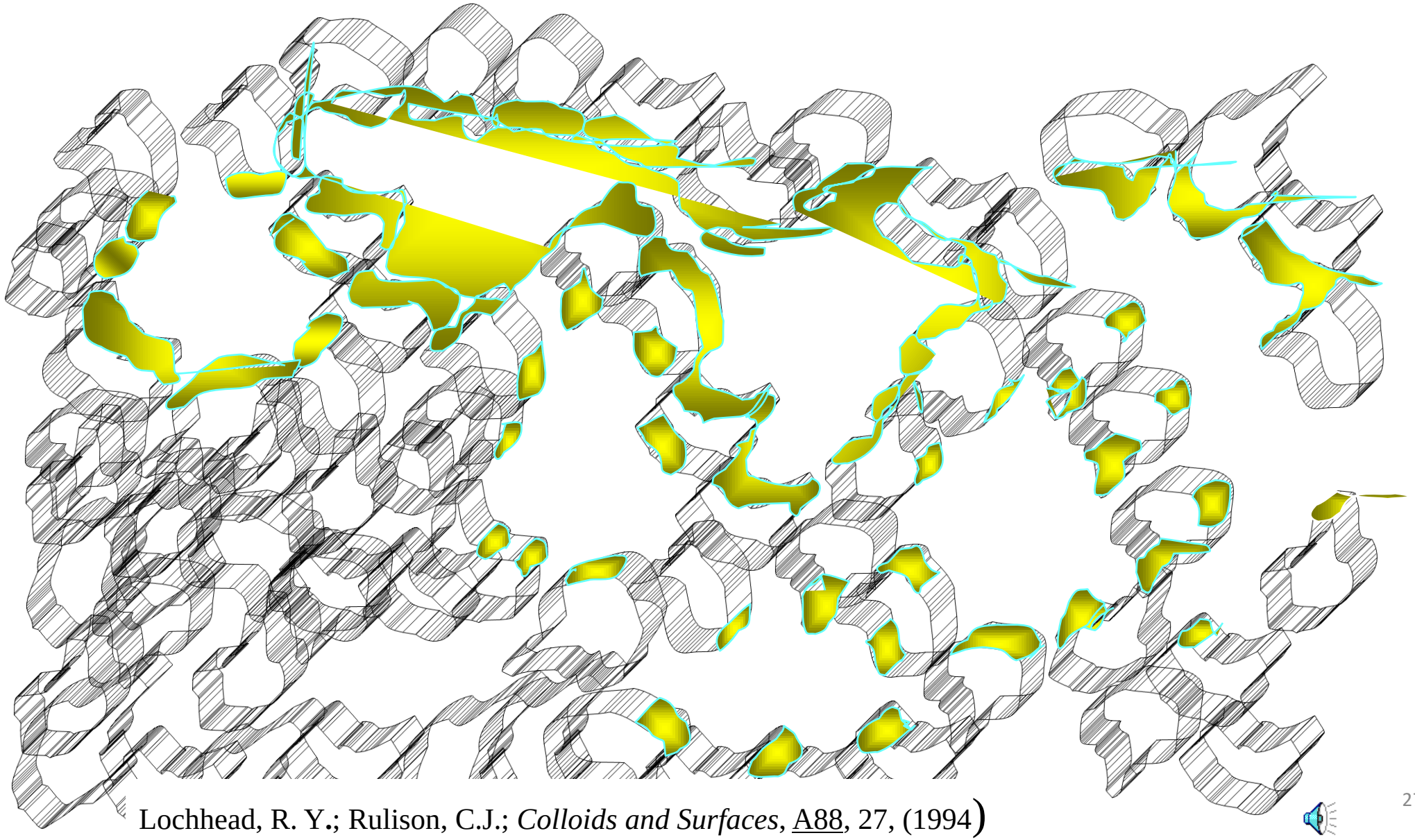

Lochhead, R. Y.; Rulison, C.J.; *Colloids and Surfaces*, A88, 27, (1994)

Polymeric Emulsifiers

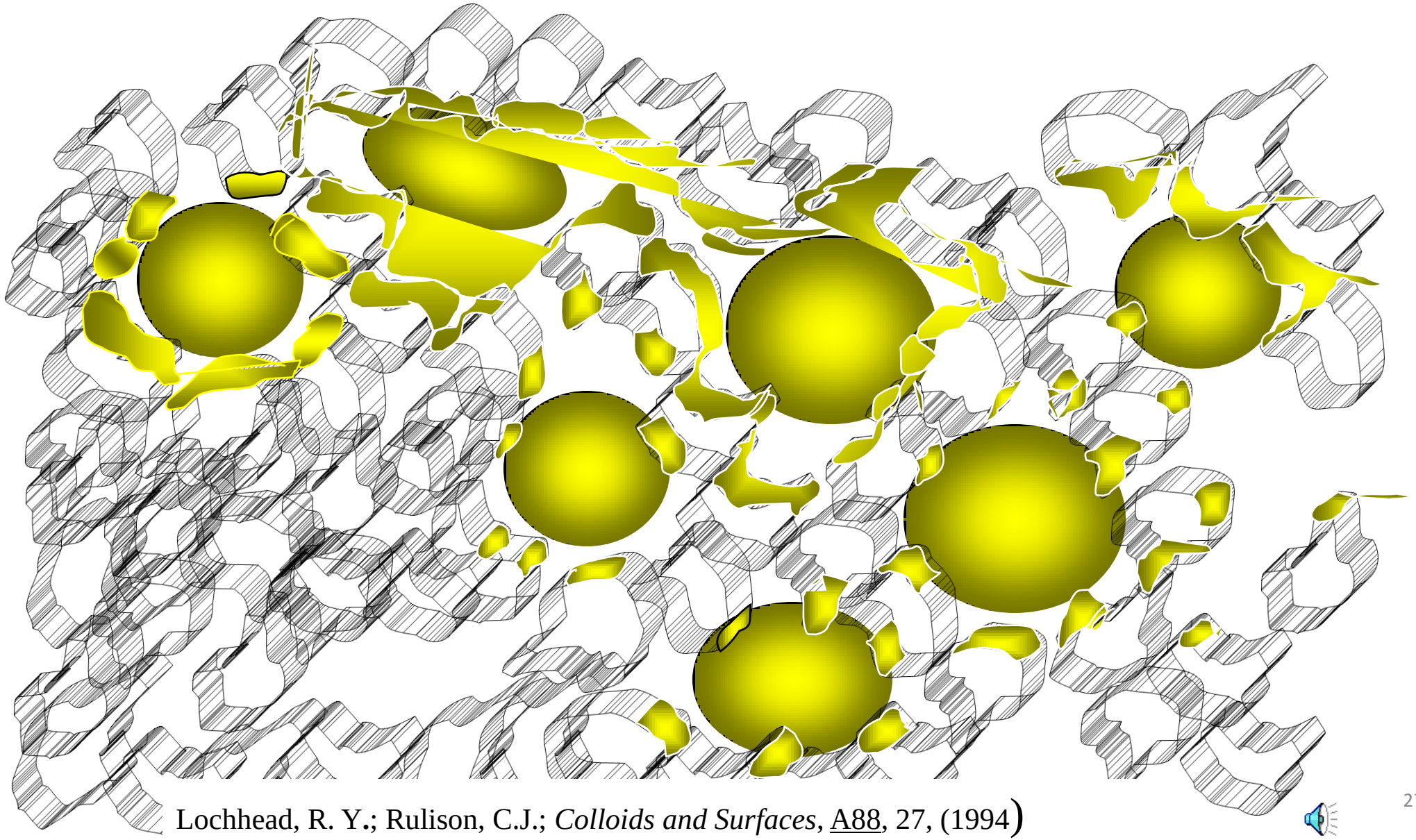

Lochhead, R. Y.; Rulison, C.J.; *Colloids and Surfaces*, A88, 27, (1994)

Displacement Flocculation and Coagulation

- Adsorbed polymer can be displaced by:
  - Surfactant
  - Dispersant
  - Defoamer
  - Antifreeze
  - Coalescing Aids
  - Competing surfaces such as amorphous silica

HYDROPHOBICALLY MODIFIED HYDROXYETHYL CELLULOSE

- Mol wt. = 300,000
- One cetyl group
- per 143 anhydroglucose residues
- Rigid backbone
- Huggins k = 2.63 indicates association eve in dilute solution
  - Nishikawa, Yekta, Pham Winnik, & Sau; *Langmuir, (Dec,* **1998), 14,** 7119

HYDROPHOBICALLY MODIFIED HYDROXYETHYL CELLULOSE

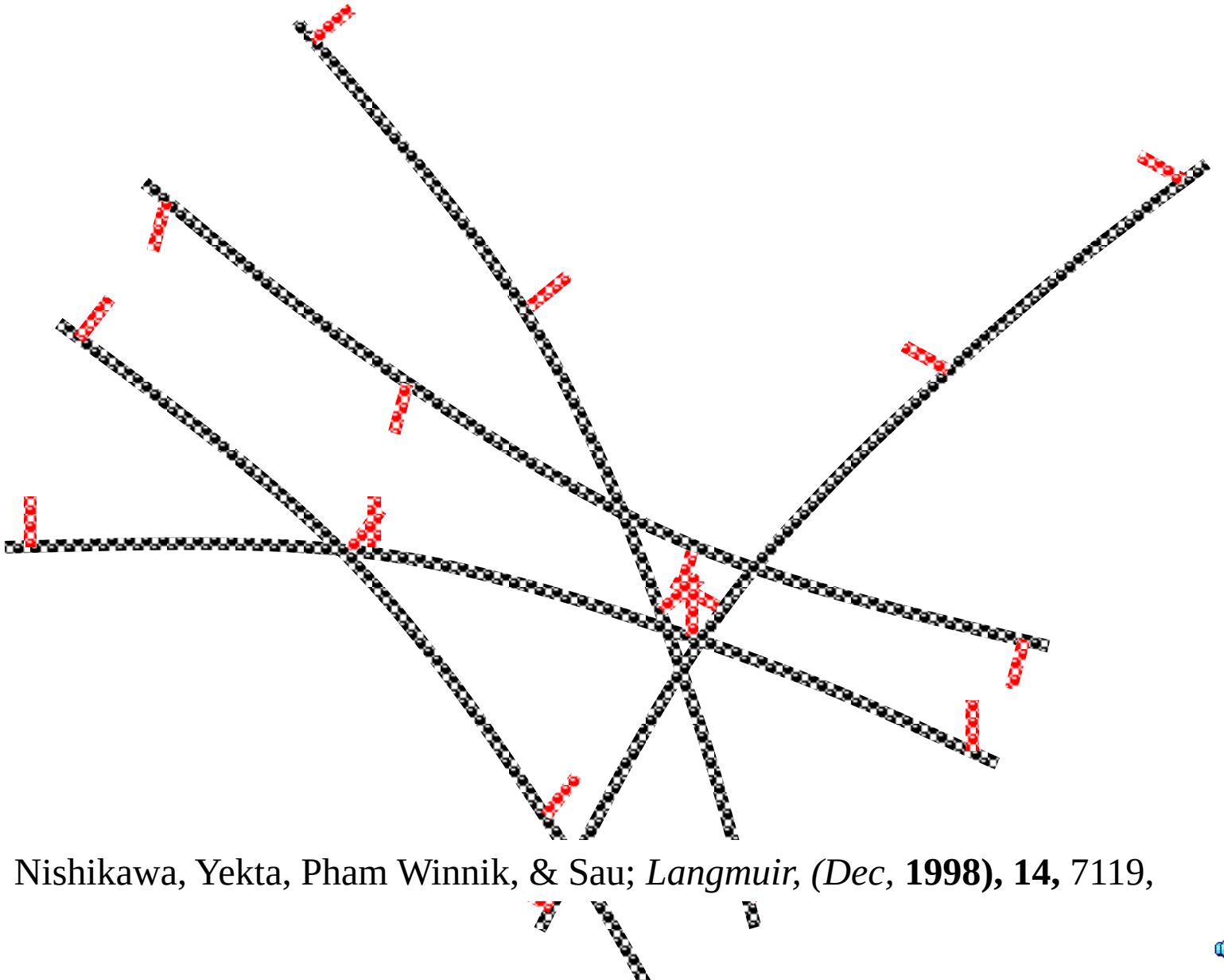

Nishikawa, Yekta, Pham Winnik, & Sau; *Langmuir, (Dec,* **1998), 14,** 7119,

HMHEC
EFFECT OF SDS

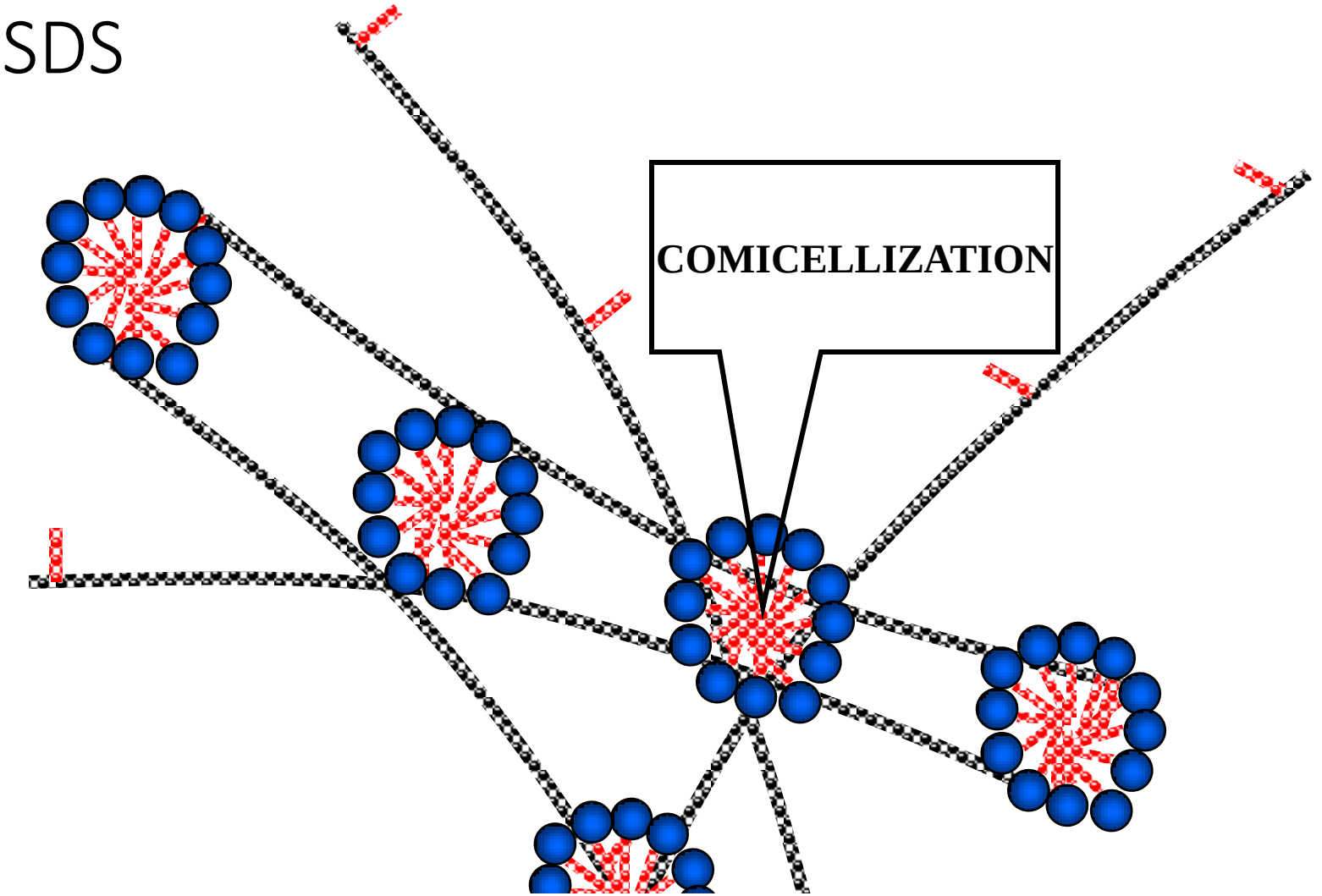

Nishikawa, Yekta, Pham Winnik, & Sau; *Langmuir, (Dec,* **1998), 14,** 7119,

HYDROPHOBICALLY MODIFIED HYDROXYETHYL CELLULOSE

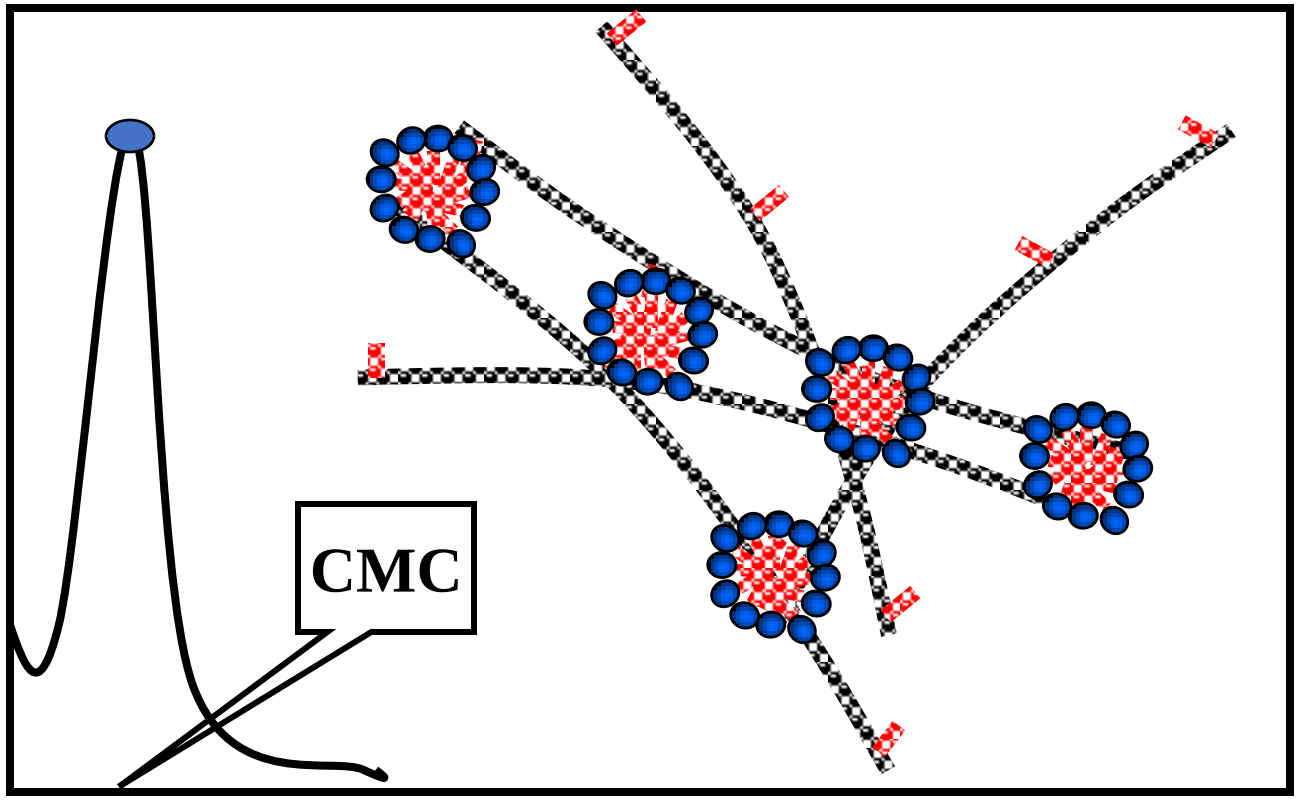

Landoll &Sau; ACS Adv. Chem Ser, 213; (1986) 343

HYDROPHOBICALLY MODIFIED HYDROXYETHYL CELLULOSE

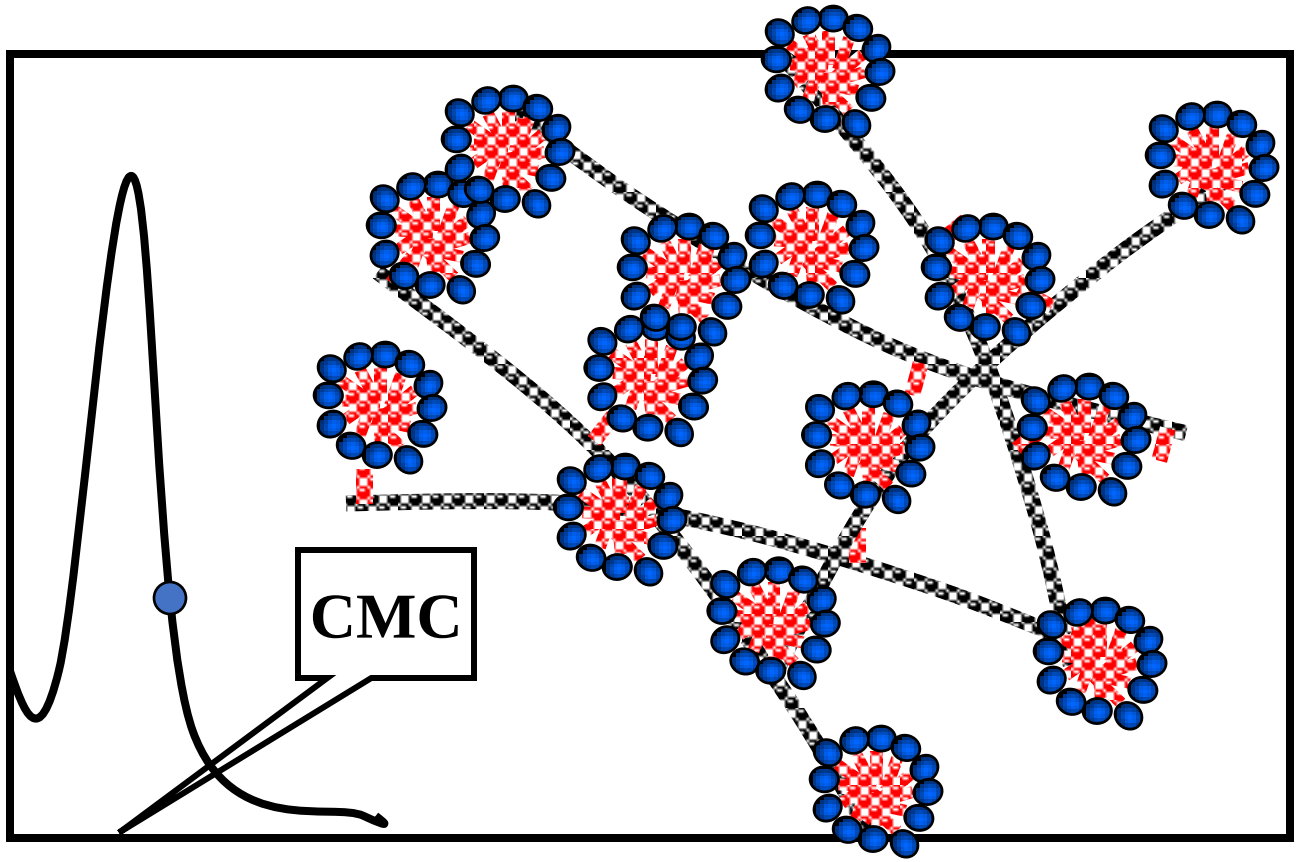

Landoll &Sau; ACS Adv. Chem Ser, 213; (1986) 343

HYDROPHOBICALLY MODIFIED HYDROXYETHYL CELLULOSE

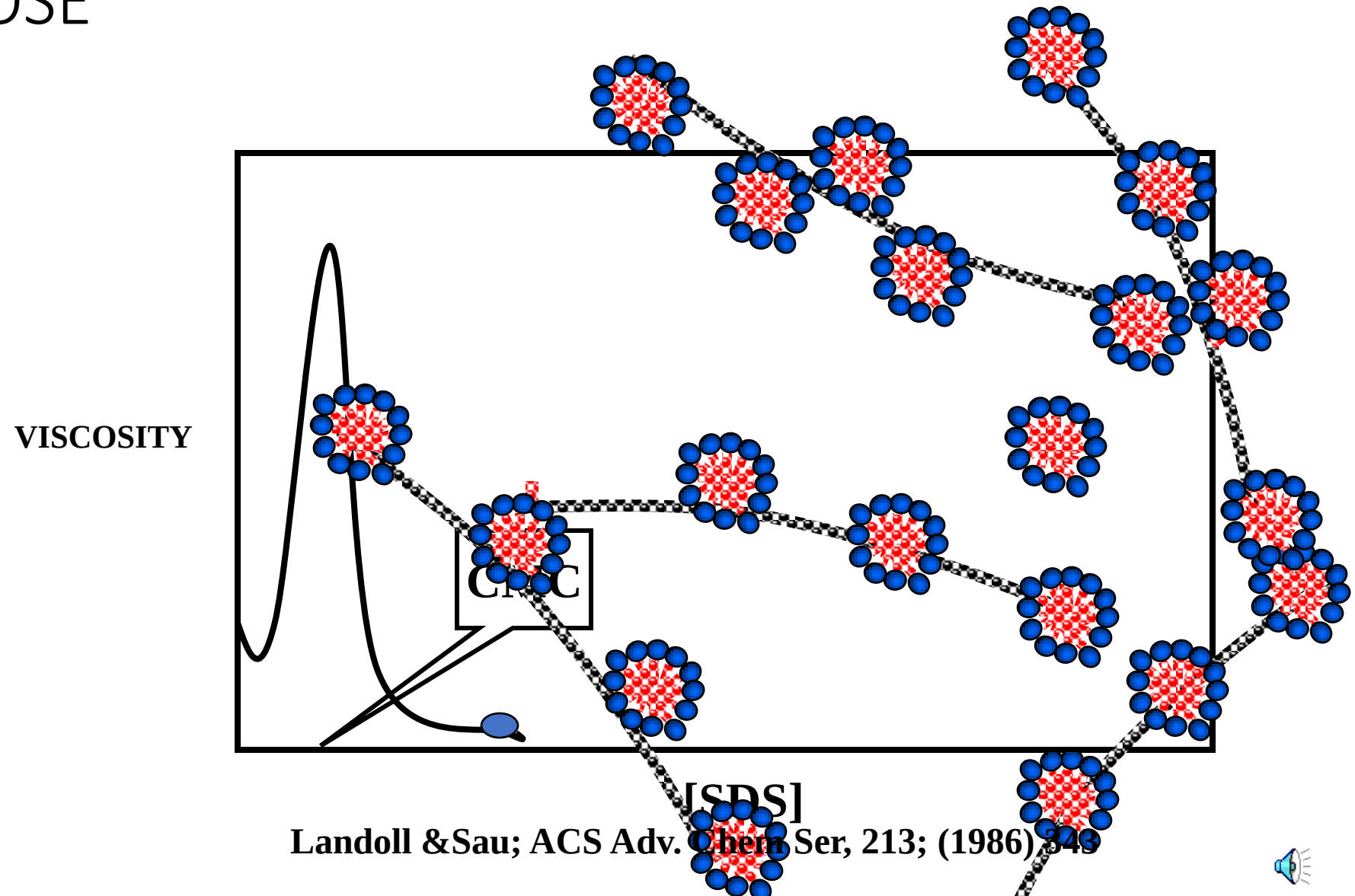

Landoll &Sau; ACS Adv. Chem Ser, 213; (1986) 343

Polymer-Surfactant Interaction

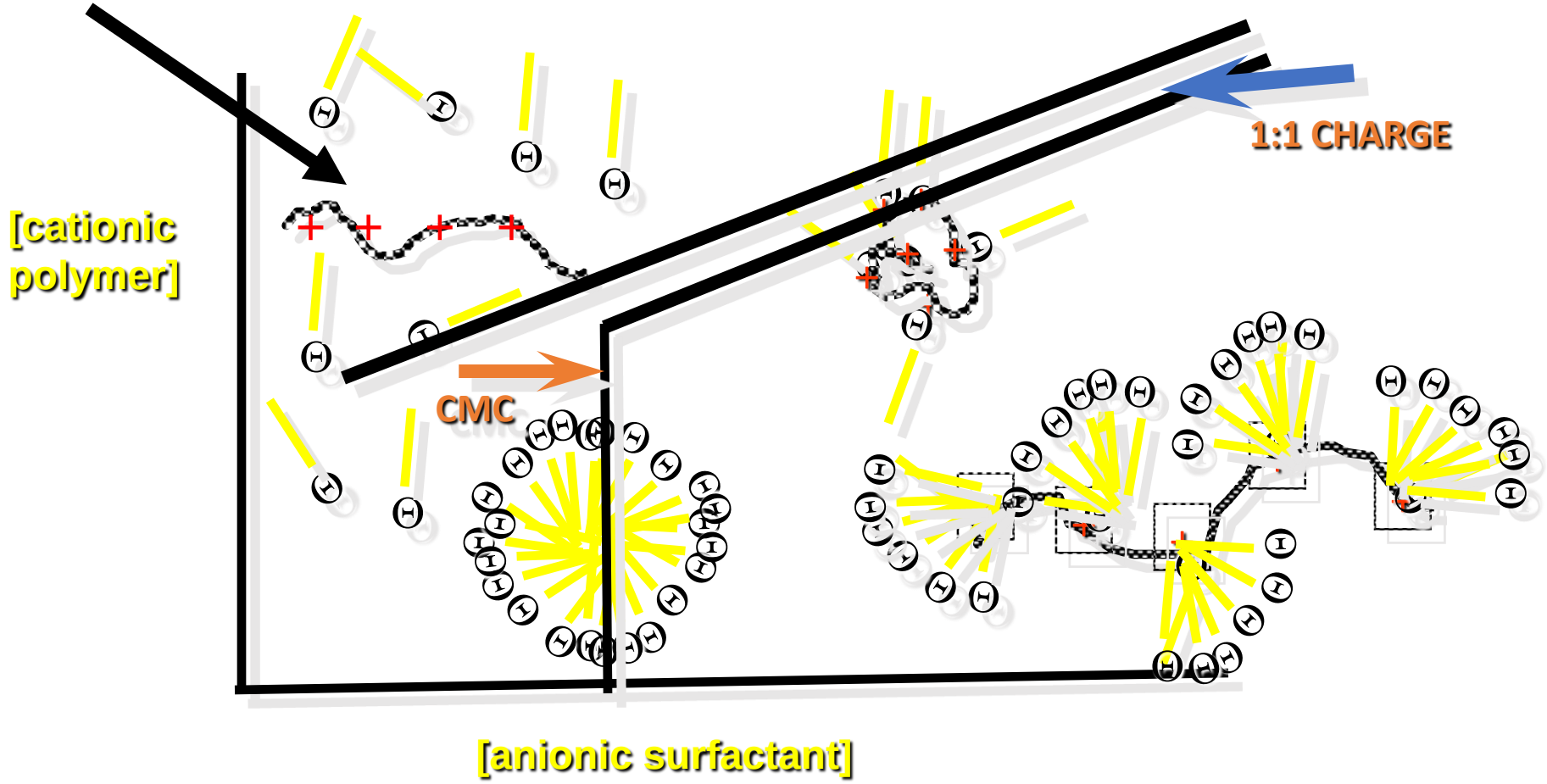

Polymer-Surfactant Interaction

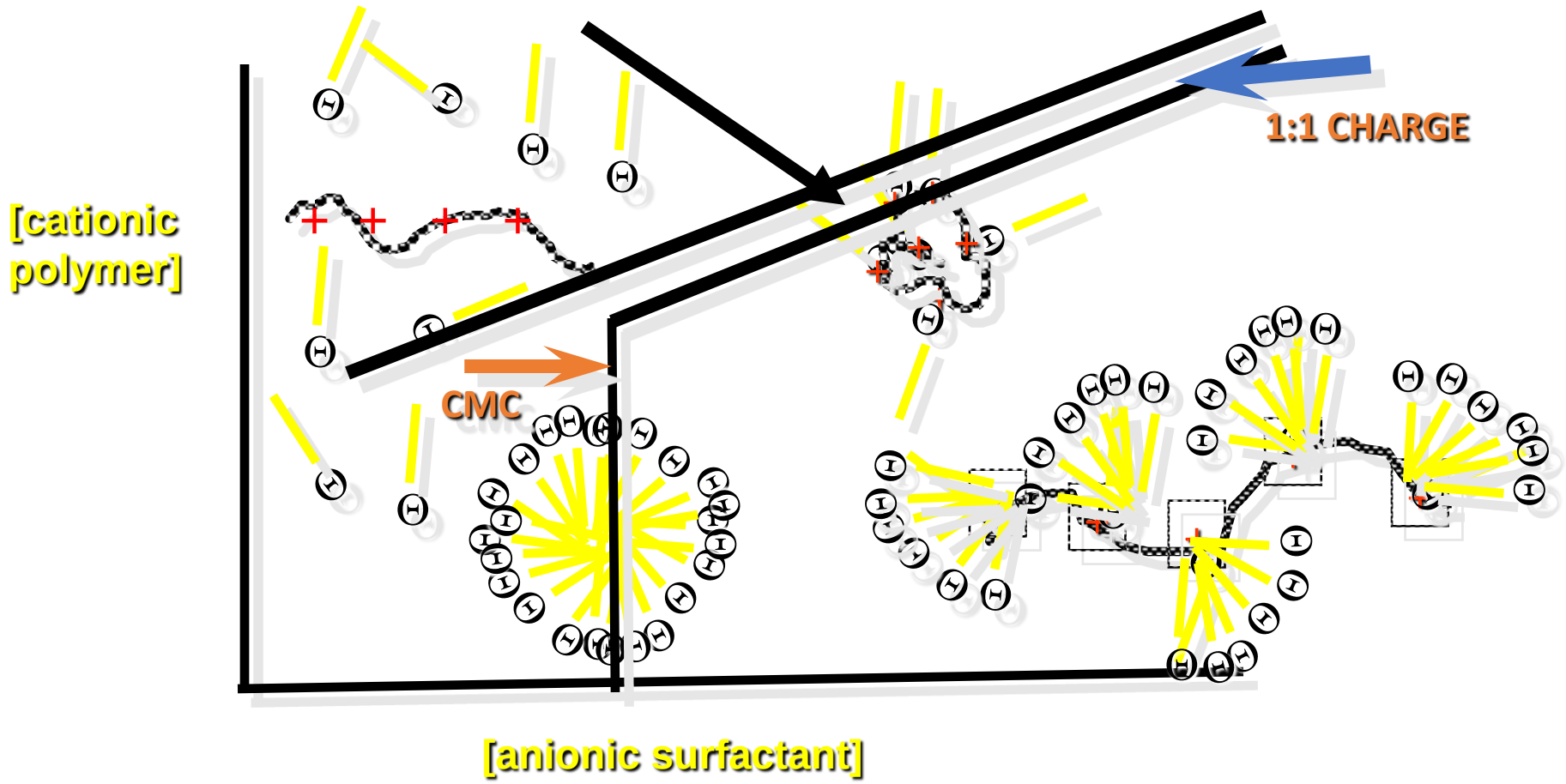

Polymer-Surfactant Interaction

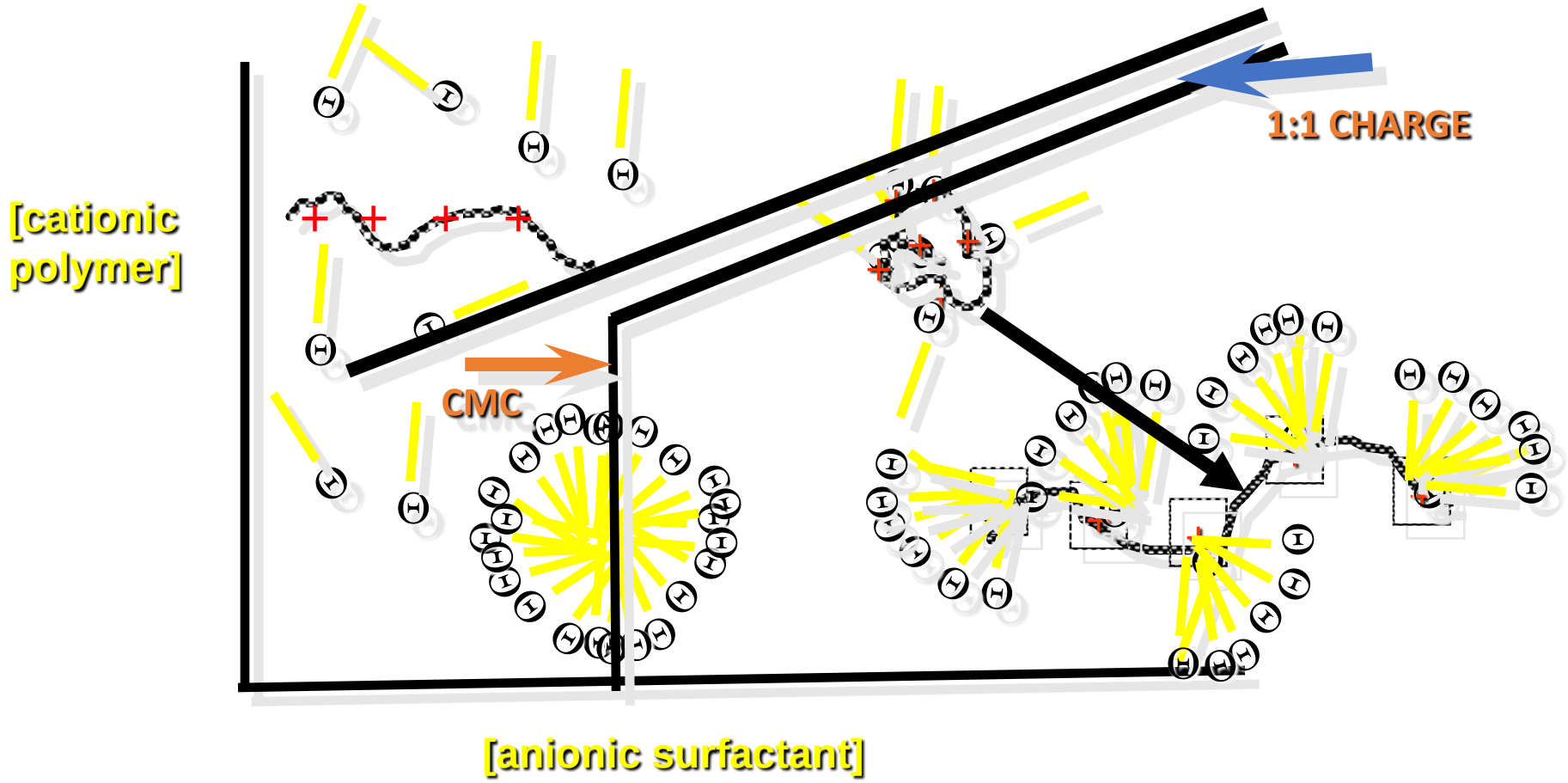

Proposed Mechanism

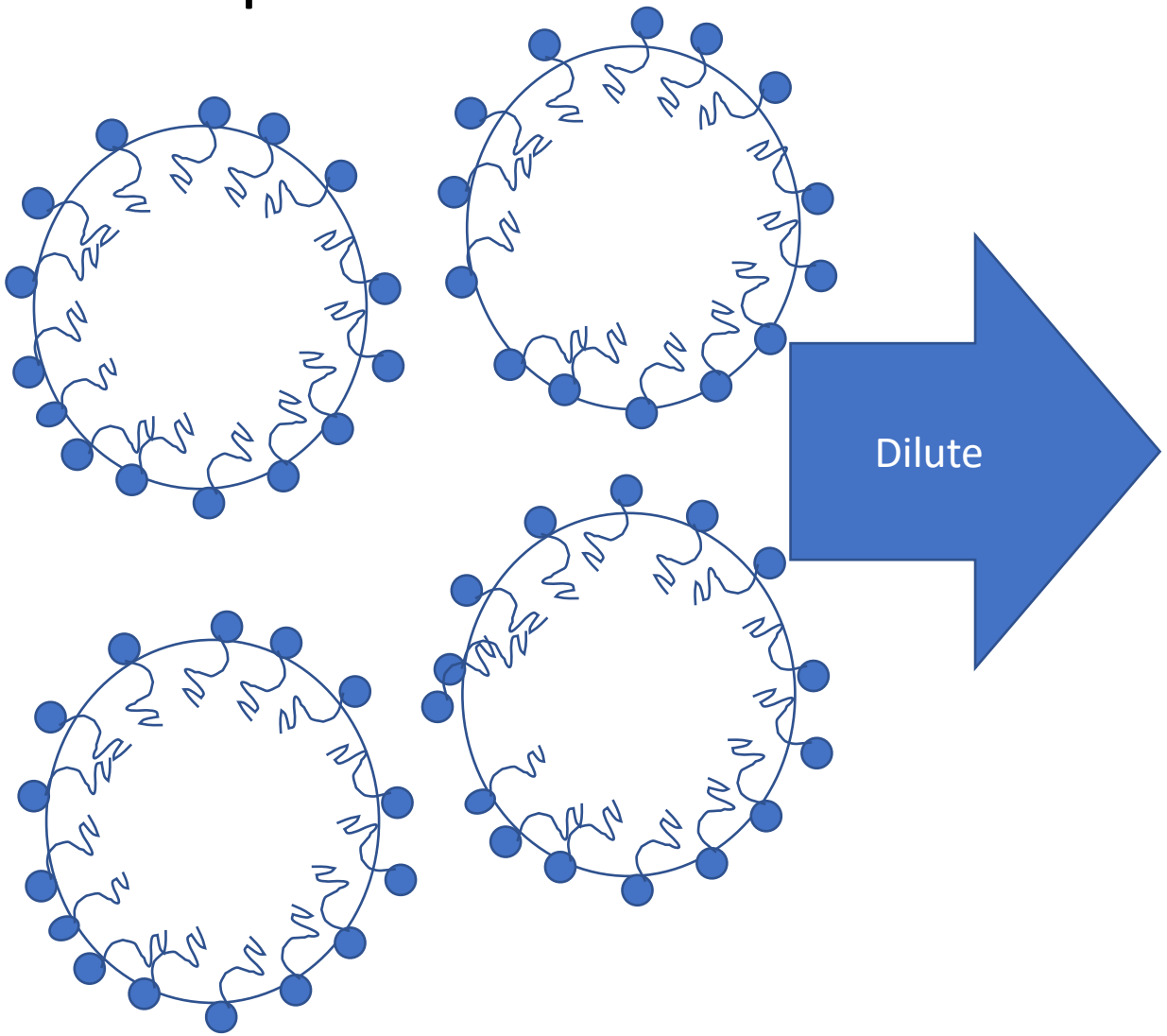

Proposed Mechanism

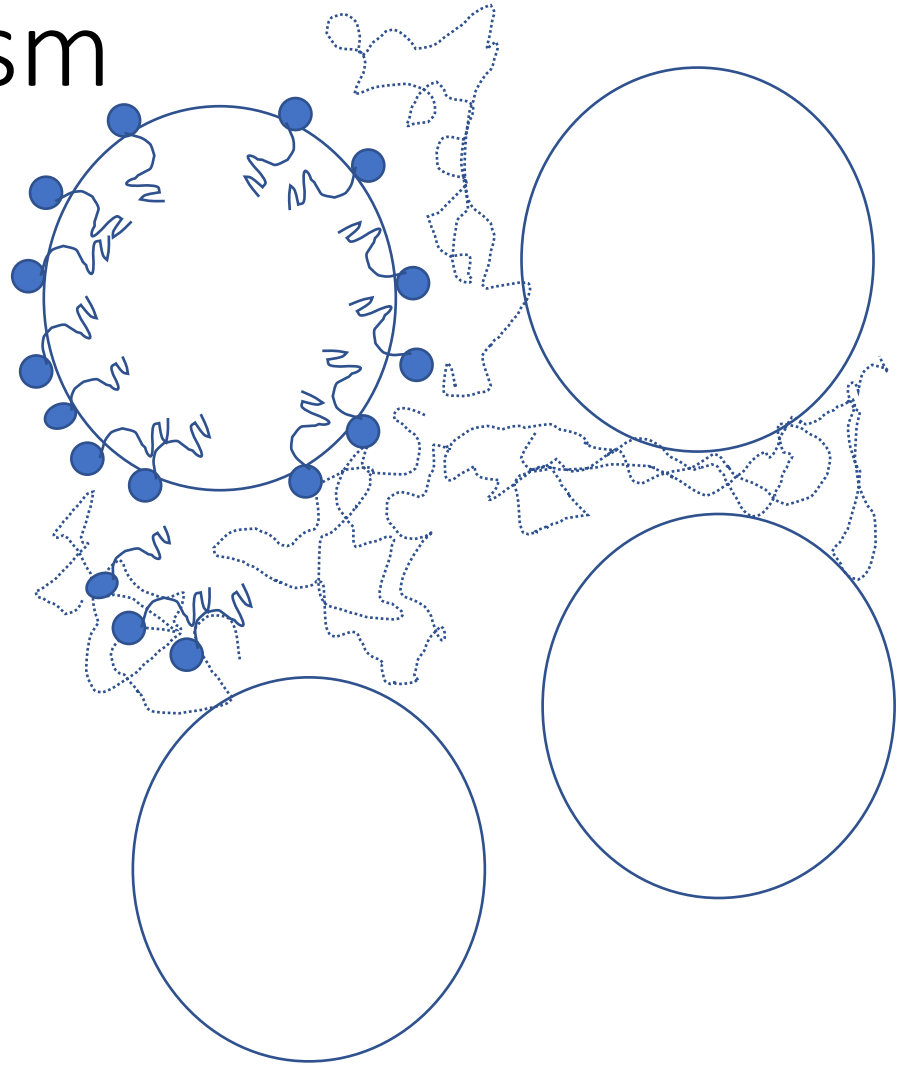

Coacervate Forms

Surfactant desorbed from foam interface

Fixatives and Films

Cosmetic Polymers

Desired Attributes of Hair Fixatives

- Hairstyle hold improvement
- Ease of application on wet hair
- Easy combing
- No sticky feel
- Quick drying
- Not powdery when groomed
- Ensures hair body and bounce
- Increased hair volume
- Hairs do not clump
- Non-hygroscopic film
- Better hair gloss
- No excessive stiffness

C. Zviak, ‘ The Science of Hair Care’

The Challenges

- Hairstyle hold improvement
  - This must be achieved with a minimal amount of fixative resin conveniently applied
    - Aerosol spray
    - Pump spray
    - Gel
    - Mousse

The Challenges

- Ease of application on wet hair
  - The solvent medium must be compatible with water
  - Also it must be generally recognized as safe
    - Ocular
    - Inhalation

The Challenges

- Easy combing
  - The cohesive strength of the polymer film must be less than the tensile strength and shear strength of the hair
  - The adhesive bond of the film to the hair must be weaker than the shear strength of the hair

Hairspray Components

- Fixative Polymer
- Solvent
- Propellants
- Adjuvants
- Valve System

Hairspray Mechanism

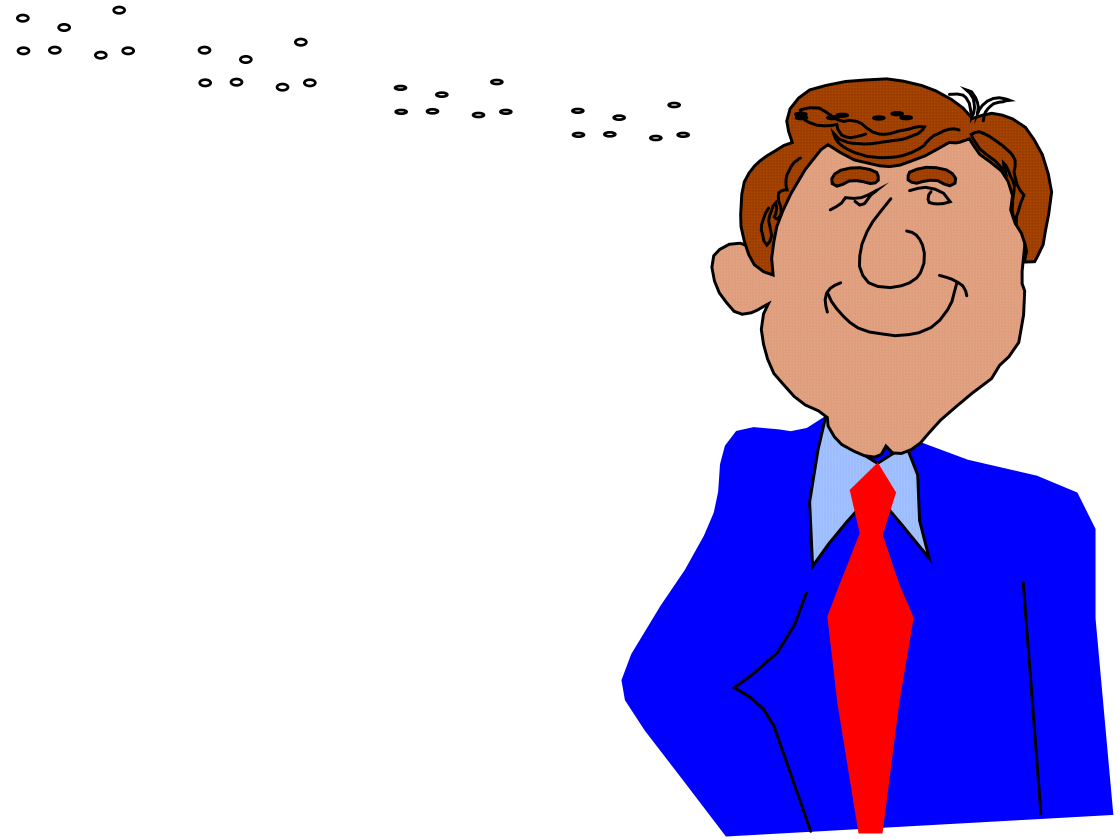

Rayleigh Instability

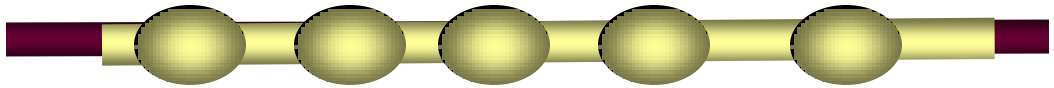

Hairspray Mechanism

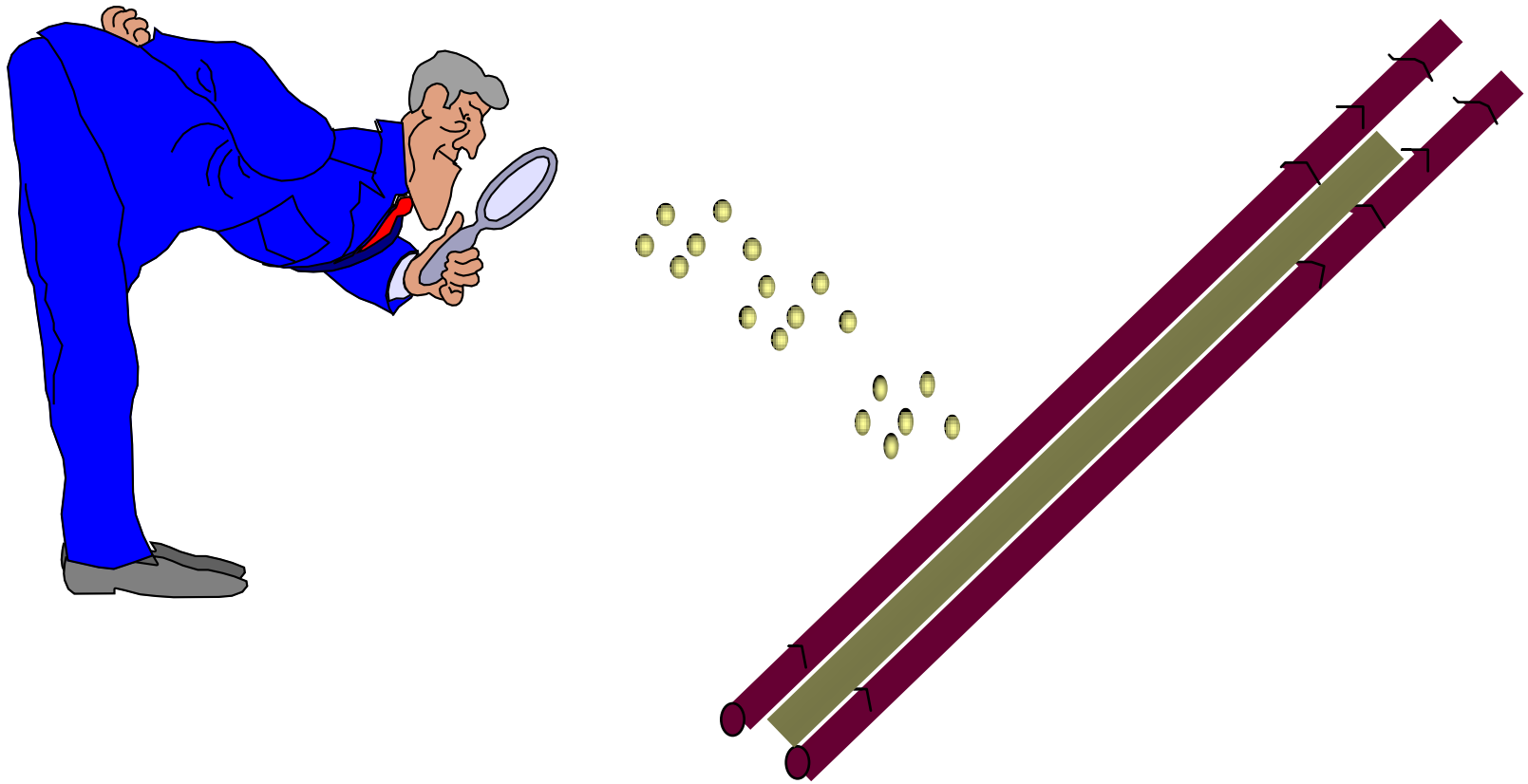

Hairspray Mechanism

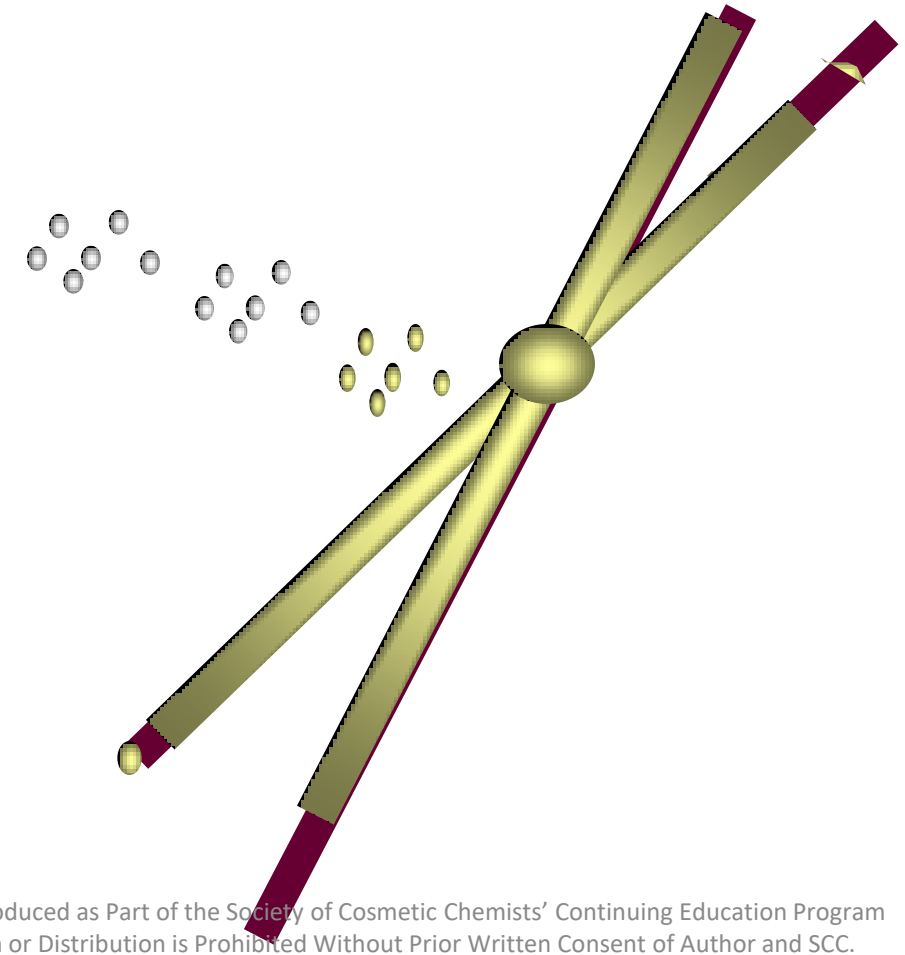

Hairspray Mechanism

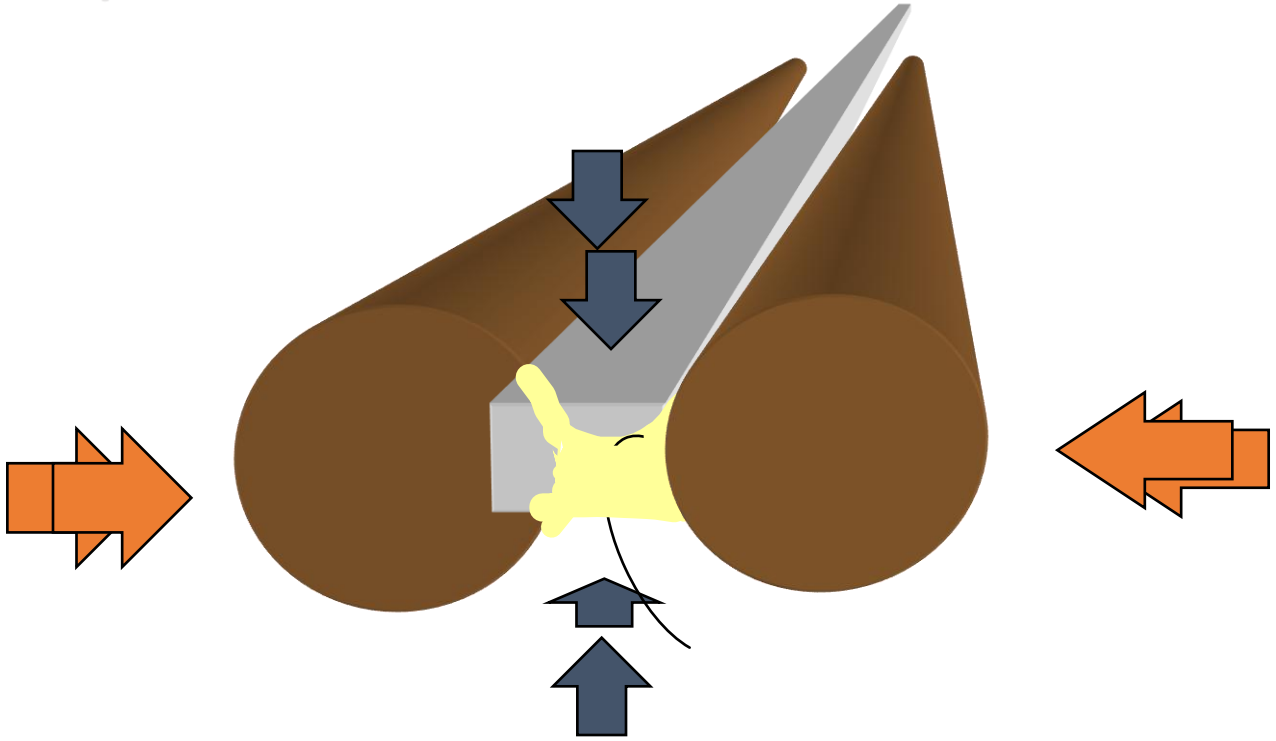

Laplace Pressure

Causes Hair to be driven together

Hairspray Mechanism

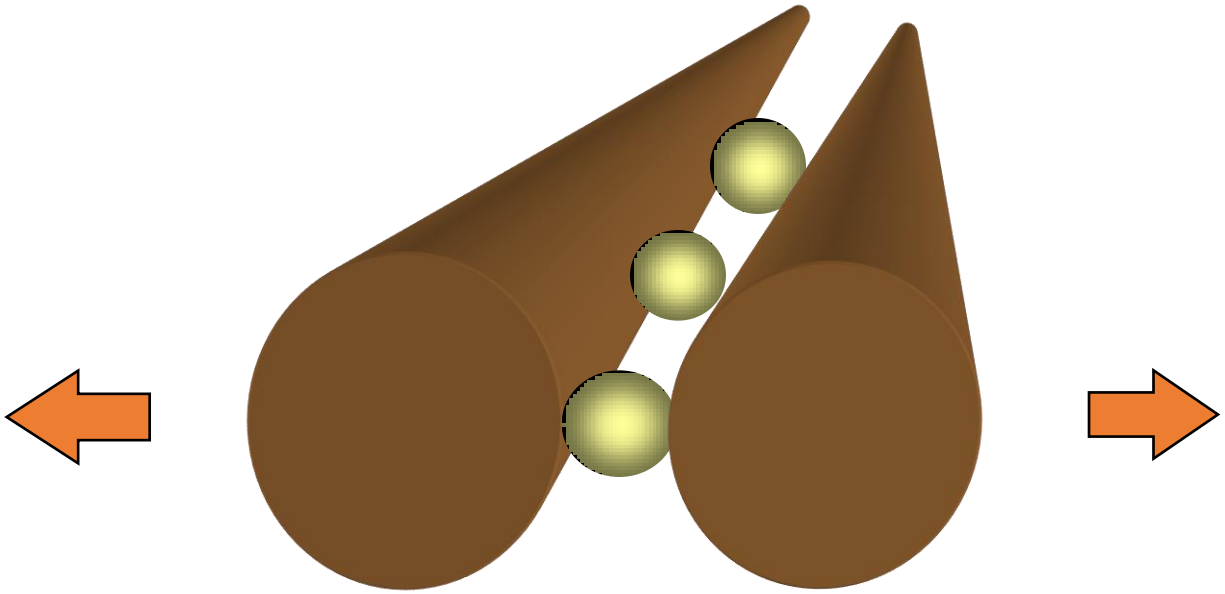

Contact Angle > 90^{o} causes the fibers to be pushed apart

Strength and Toughness

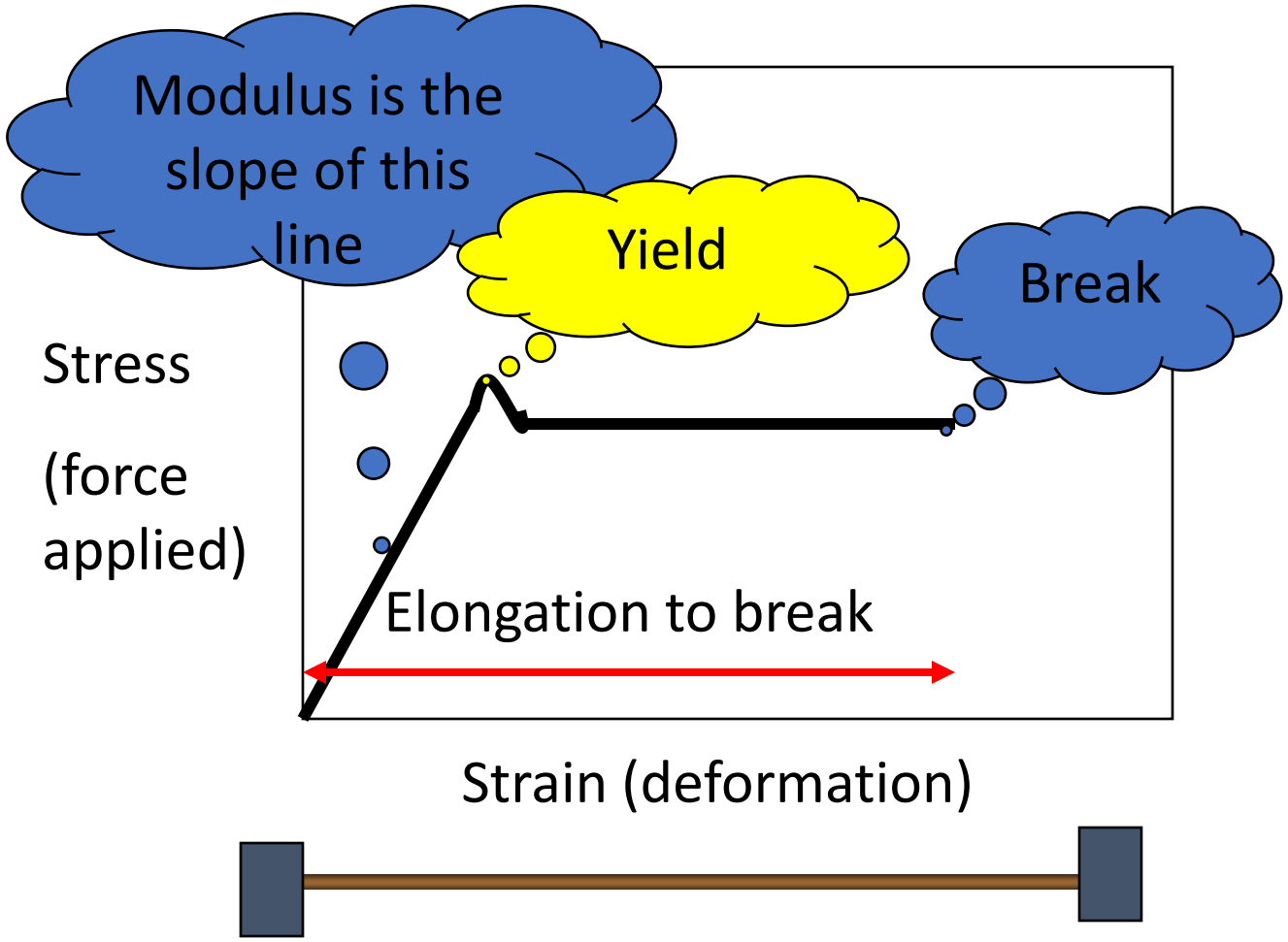

Reptation

- Above the chain entanglement threshold
  - The polymer molecules wriggle past each other
  - Like a snake moving along a tube made up of snakes
- Viscosity = $(concn)^{2.2 - 3.4}$

Plasticization

- Small molecules interspersed between the polymer molecules can assist repatation
  - This is plasticization
- There is a time element
  - If the applied force must last long enough for the polymers to move
  - If the force is of short duration, elastic deformation and recovery will occur
    - Debra Number

Strength and Toughness

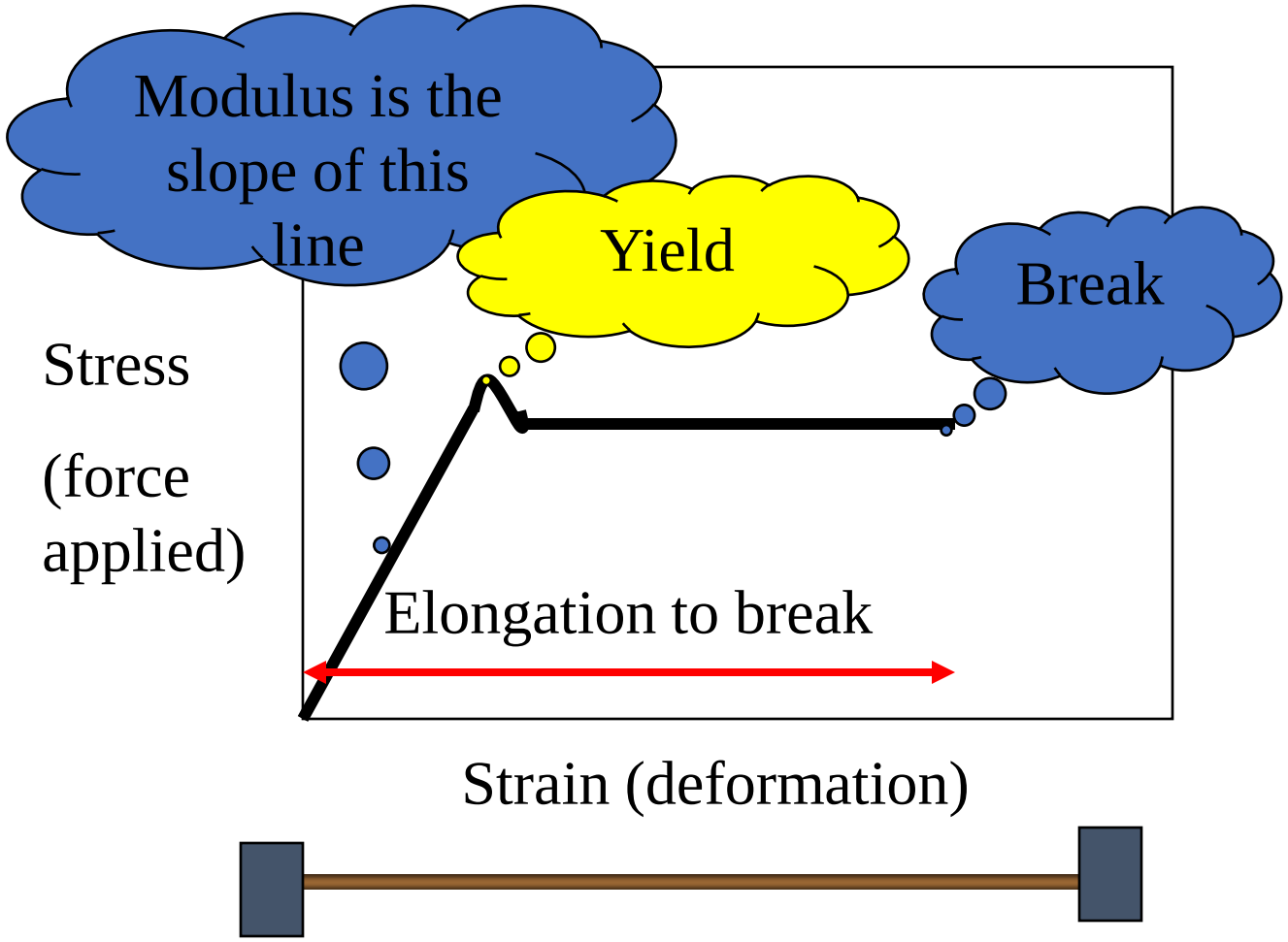

Strength and Toughness

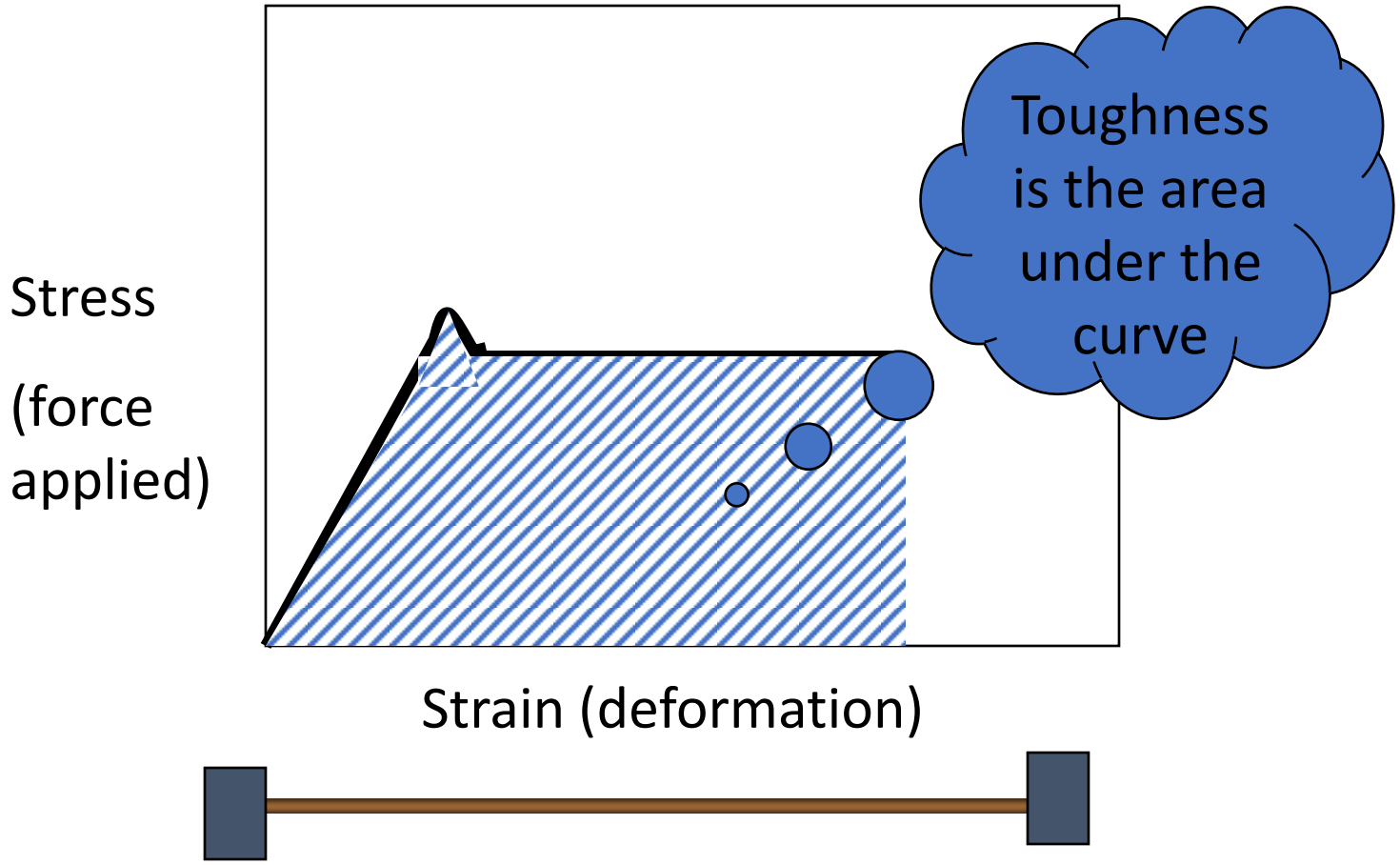

Strength and Toughness

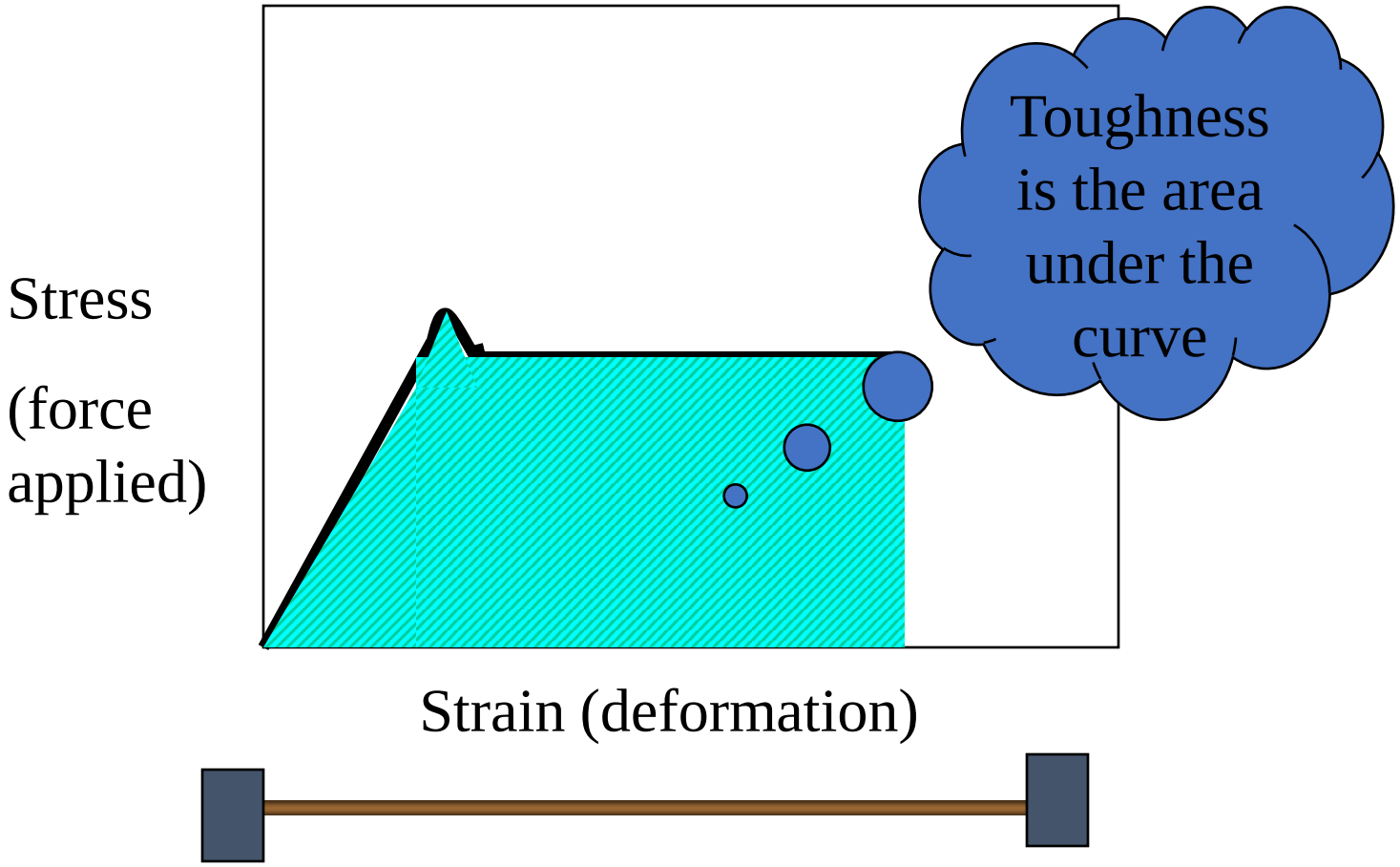

No Sticky Feel

- The polymer in the dried film should be immobile during the time of ‘touch’ and should have insufficient time to interact with the stratum corneum of the fingertips
- Quick Drying
  - volatile solvent and propellant
  - gellant

Mechanical Property Aesthetics

- Ensures hair body and bounce
- Increased hair volume
- Hairs do not clump
- No excessive stiffness

- The polymer film must ‘crosslink’ the hair matrix in place, rather than coat the hair

Non-hygroscopic Film

- The reason for this is to avoid plasticization of the film by absorbed water vapor
- This begs the question “ what is plasticization?”
  - It merely means that small molecules within the polymer matrix make it easier for the polymer chains to wriggle past each other
  - This lowers Tg and makes the polymer ‘softer’

Desired Properties of a Hairspray

- Better hair gloss
  - This means that the polymer system must show no phase separation during the process of film formation

Poly(vinylpyrrolidone) [PVP]

- 1950's -Hairstyles ascend
- Hairspray becomes necessary
- Shellac is used as the fixative polymer
  - but shellac is insoluble in water
  - cannot be removed by shampoos

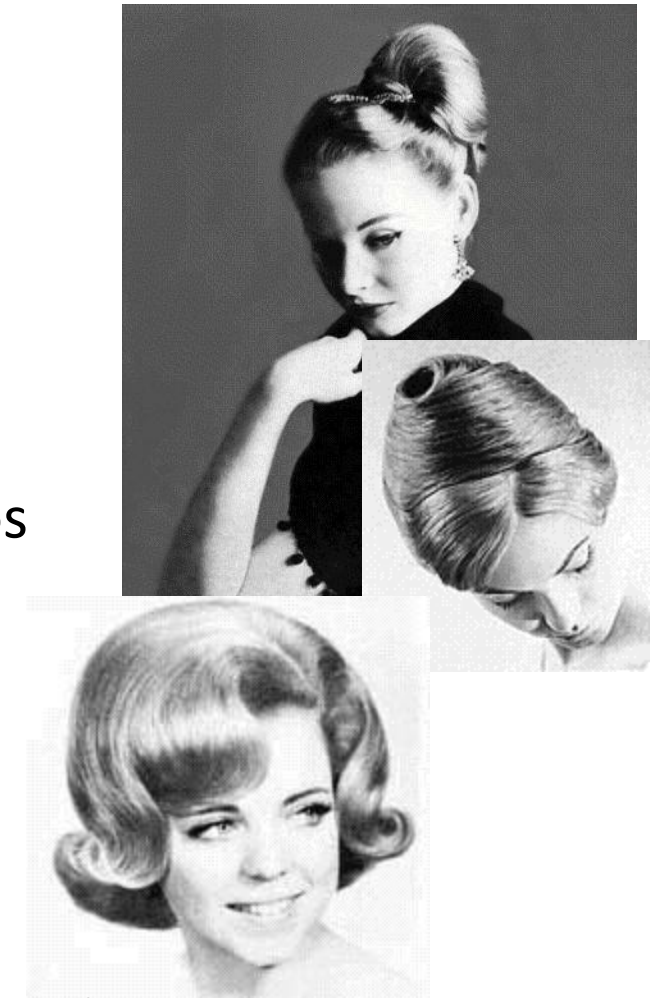

Poly(vinylpyrrolidone) [PVP]

- PVP IS WATER SOLUBLE
- PVP IS SUBSTANTIVE TO KERATIN
- THEREFORE THE MODERN HAIRSPRAY WAS BORN
  - USING PVP AS FIXATIVE
- PVP WAS SAVED AS A COMMERCIAL MATERIAL

Poly(vinylpyrrolidone) [PVP]

- PVP is provided as K15, K30, K60, K90 etc.
- The Firkentscher ‘K’ value
  - An early measure of polymer molecular weight
  - $\eta_{sp}/c = [(75\ k^2)/(1+1.5kc)] + k$
    - Where K = 1000k

Poly(vinylpyrrolidone) [PVP]

- However, PVP was plasticized by atmospheric humidity
  - p.m. ‘hairstyle droop’ on humid days

- Copolymers were introduced to provide the desired properties

Poly(N-2-vinylpyrrolidone)
PVP

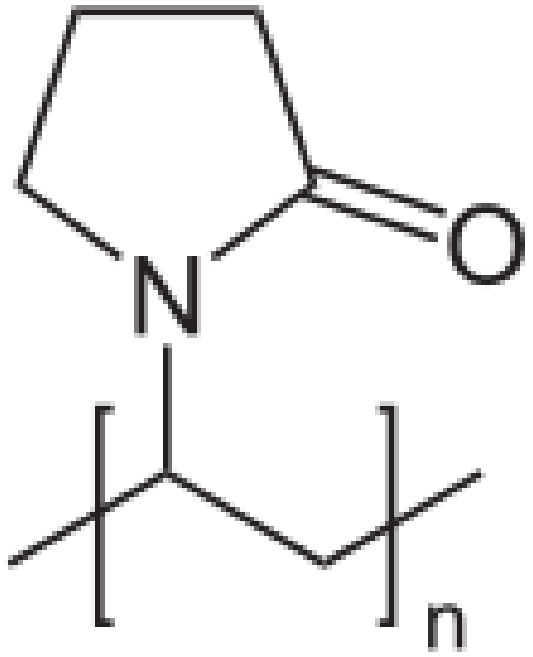

Copolymers

- Random copolymers consist of two monomers randomly positioned along the chain.
  - True random copolymers display ‘weighted average’ properties
- The properties of interest for early hairsprays were:
  - Hardness or softness (translated as low Tg or high Tg)
  - Polar or Nonpolar (for control of sensitivity to humidity)

PVP/VA

(*PVP/VA from ISP; Luviskol from BASF*)

- Polyvinylpyrrolidine/vinyl acetate copolymer
  - PVP is polar and ‘hard’ (Tg below room temperature)
  - VA is nonpolar and ‘soft’(Tg above room temperature)
- Introduced to overcome the extreme moisture sensitivity of PVP homopolymer.
- VA content of commercial resins varies from 30 to 70 percent
  - Hairsprays 70% VA
  - Hairgels 30% VA

PVP/VA

- Below pH 4.5, PVP forms and insoluble, hydrogen-bonded complex with poly(acrylic acid)
  - Carbomer Gels need special care
  - Clarity is best obtained at pH neutral

PVP/VA

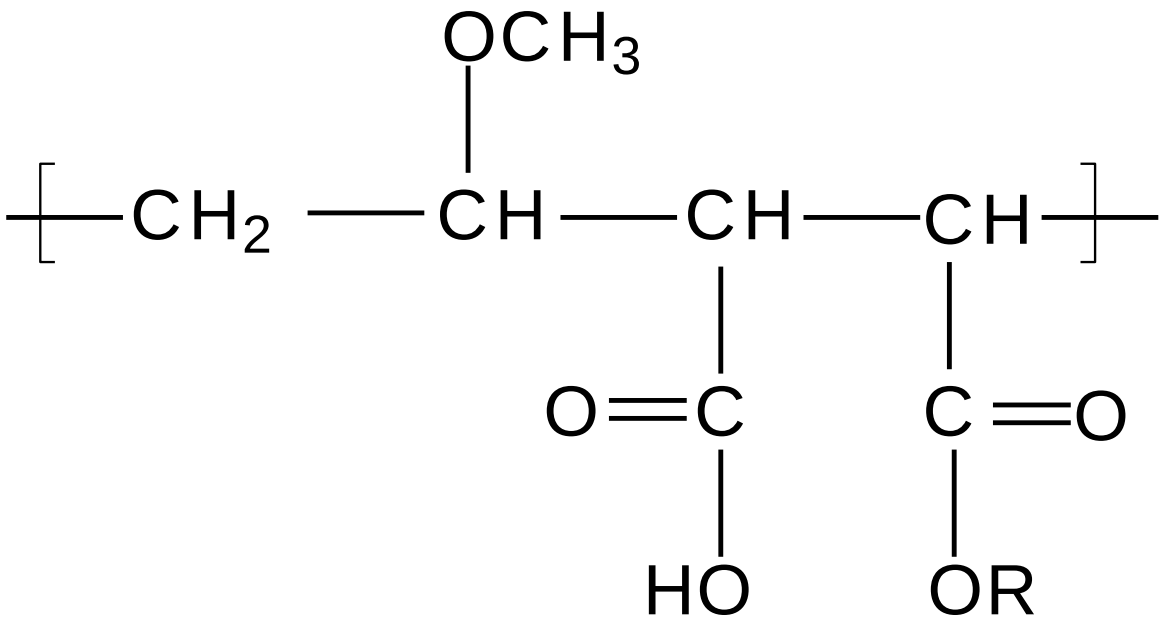

R=ethyl, isopropyl,butyl

Evolution of Hair Fixative Resins from PVP/VA

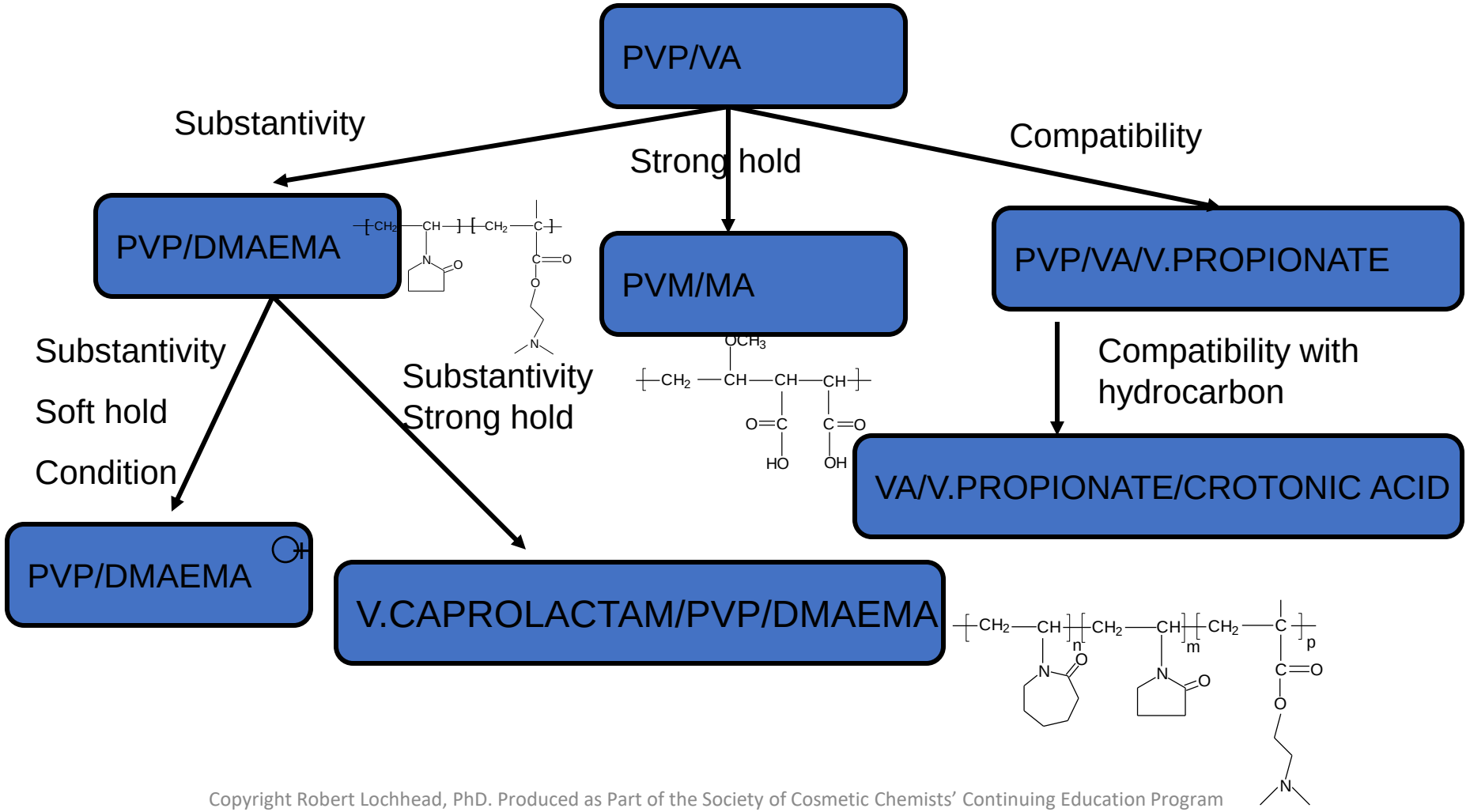

Evolution of Hair Fixative Resins from VA/Crotonic Acid

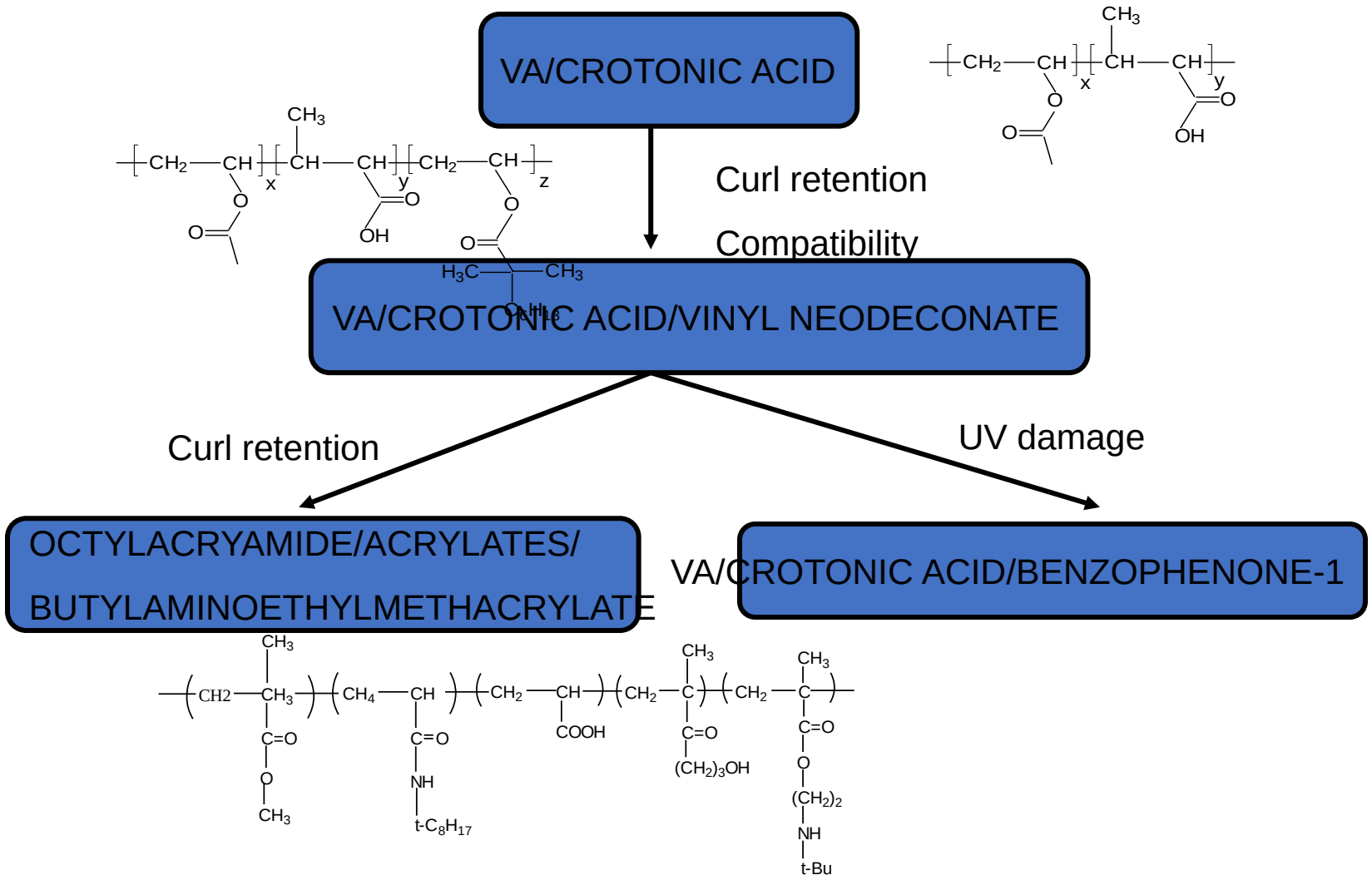

Conditioning Polymers

Electrical Charges Associated with Surfaces

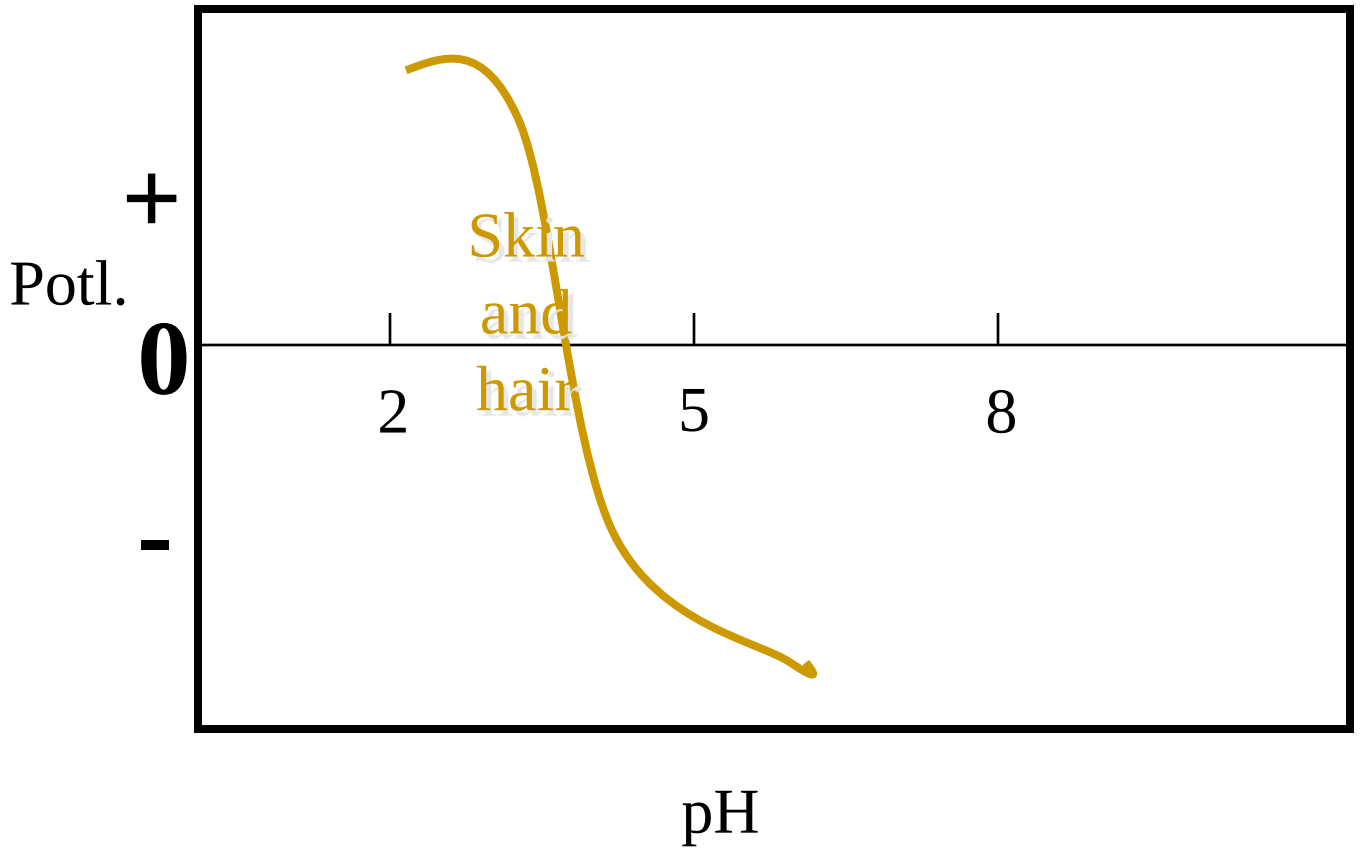

Every material surface possesses a characteristic Point of Zero Charge

Surfactants and Conditioning

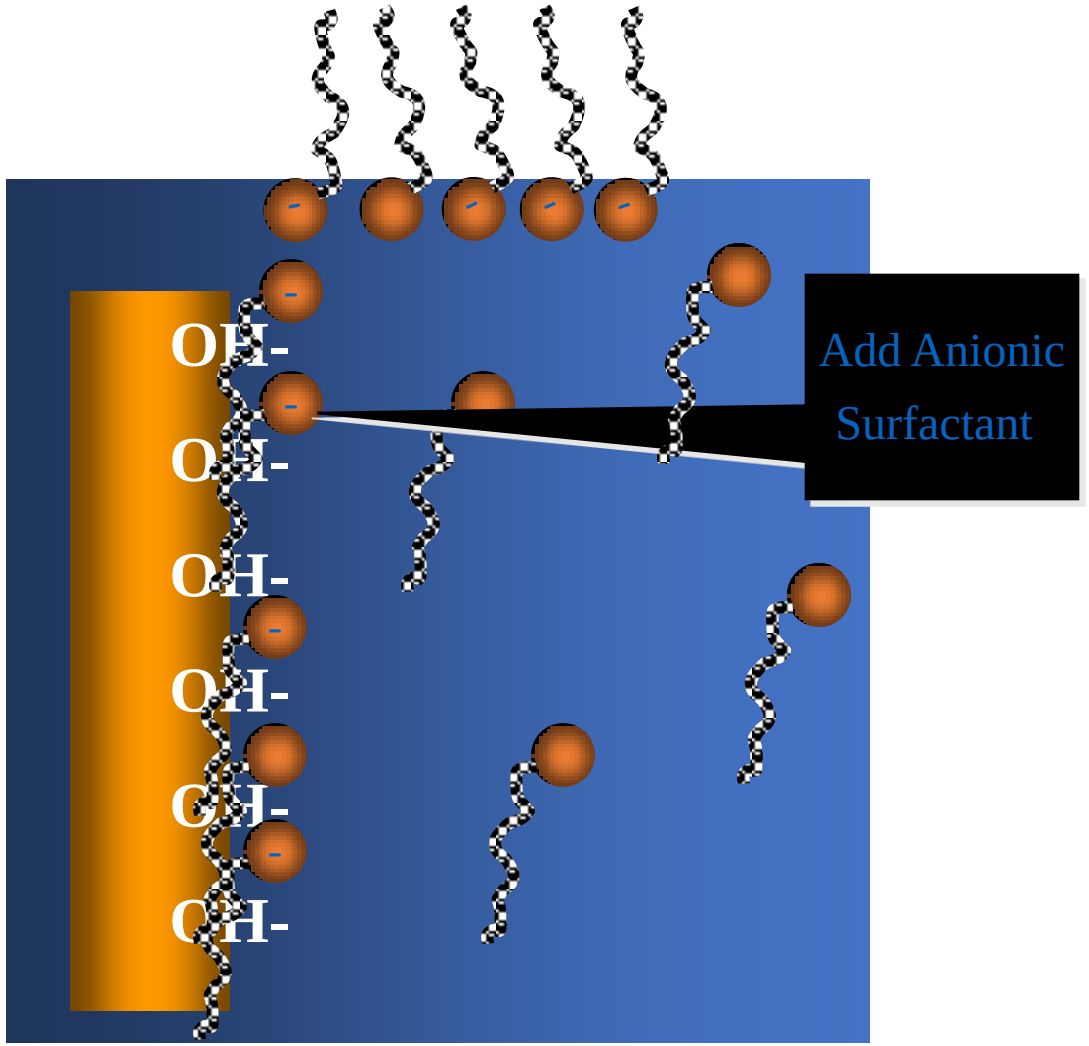

Adsorption at liquid/vapor interface reduces $\gamma_{s/l}$.

Adsorption on Hair enhances wetting

Surfactants and Dispersion

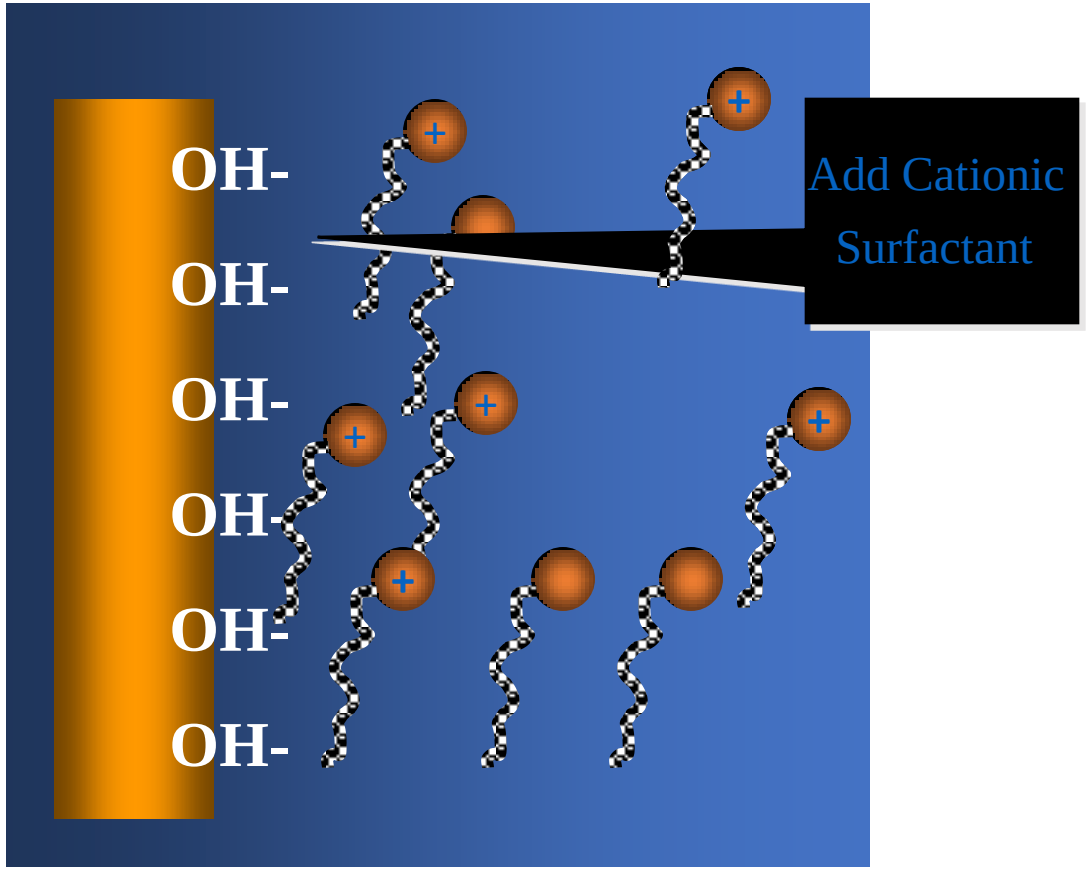

Electrical Charges Associated with Surfaces

- When immersed in aqueous solution, all surfaces interact with the hydrogen ions or hydroxyl ions of the water and also with other ions in solution
- These ions can adsorb or desorb and an electrical potential is conferred on the surface

Electrical Charges Associated with Surfaces

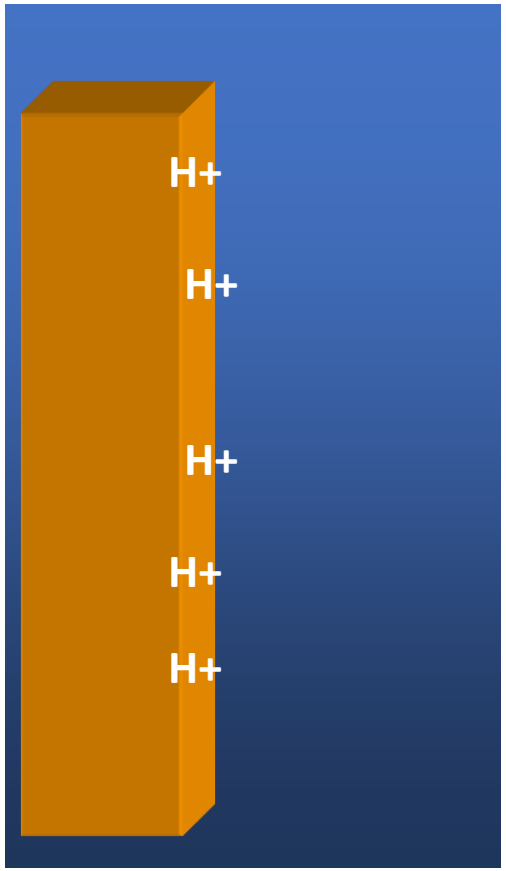

Adsorbed Cations confer positive surface potential

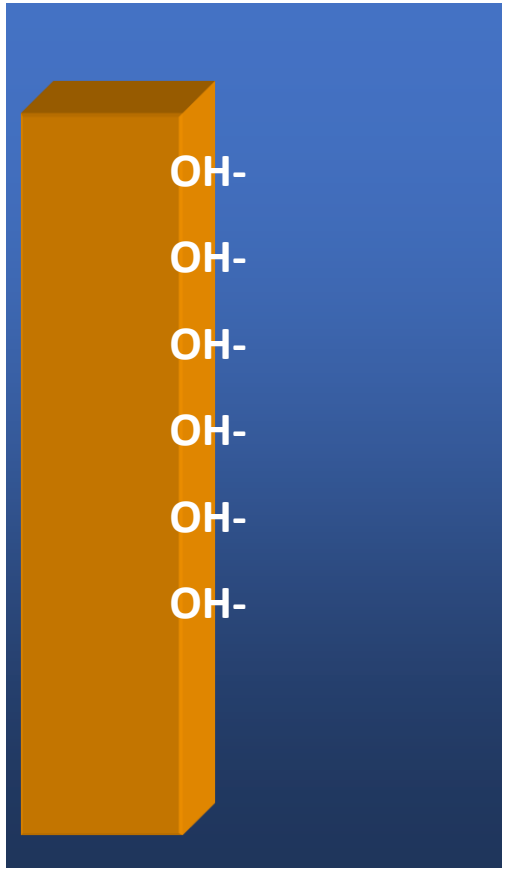

Adsorbed Anions confer negative surface potential

Electrical Charges Associated with Surfaces

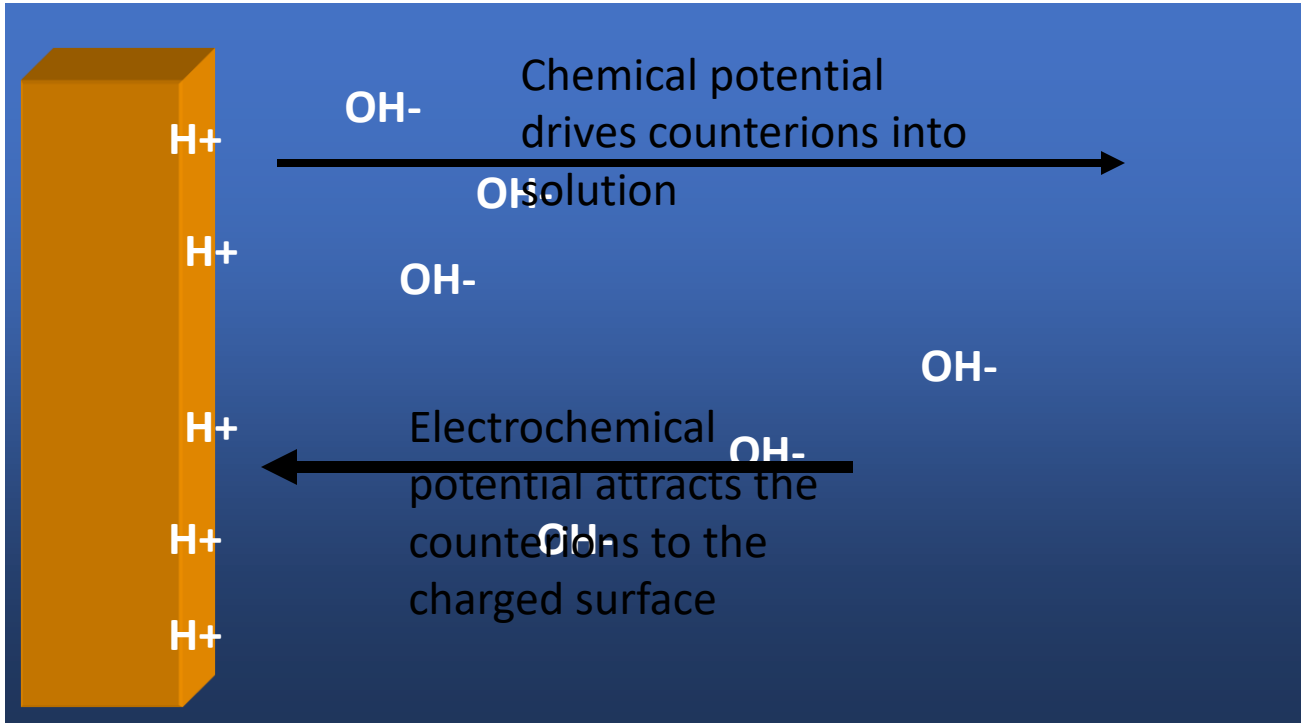

Adsorbed Cations confer positive surface potential

and soluble counterions diffuse from the surface but are held in proximity by the need for electrical neutrality

Electrical Charges Associated with Surfaces

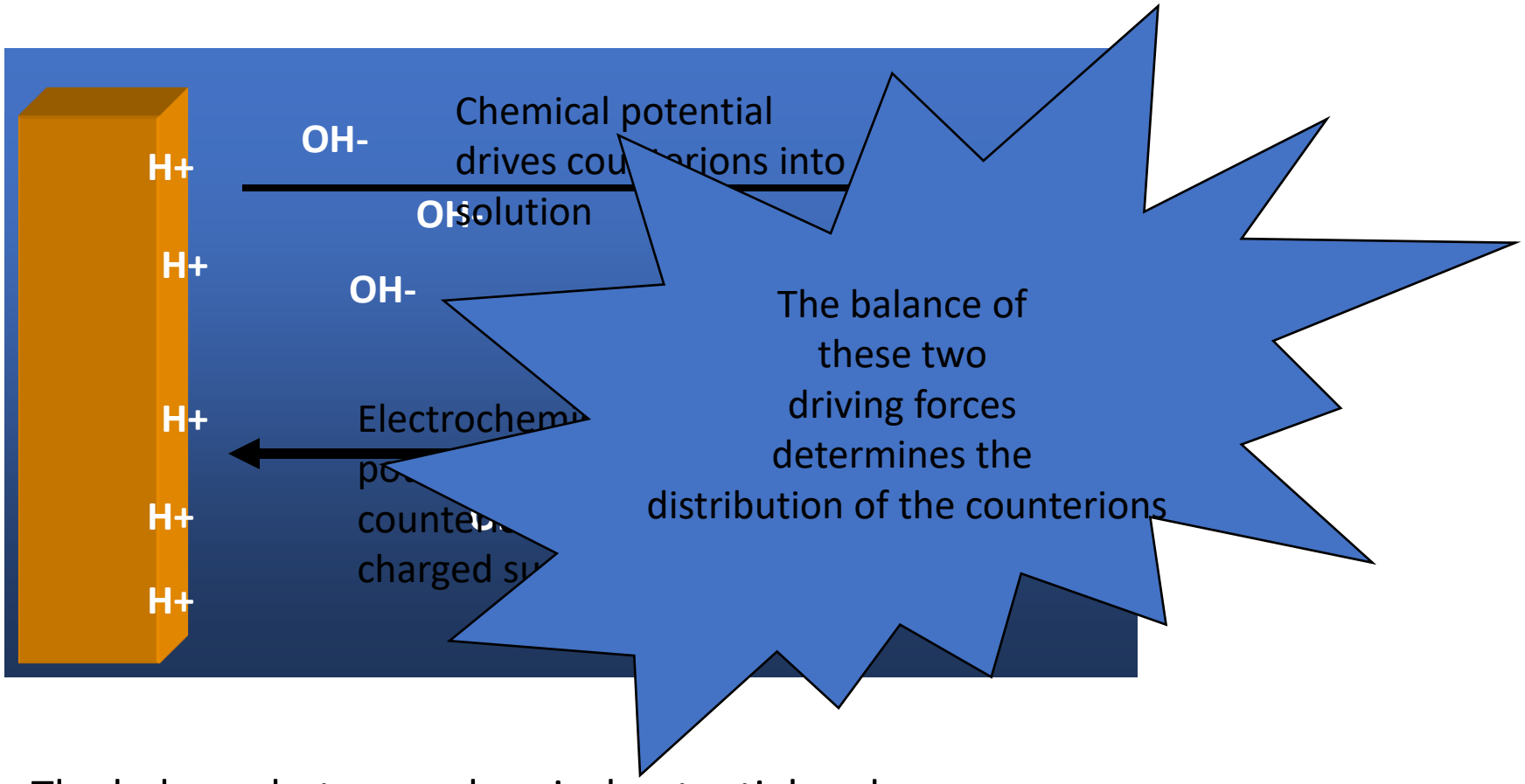

The balance between chemical potential and electrochemical potential establishes a Donnan Equilibrium

Electrical Charges Associated with Surfaces

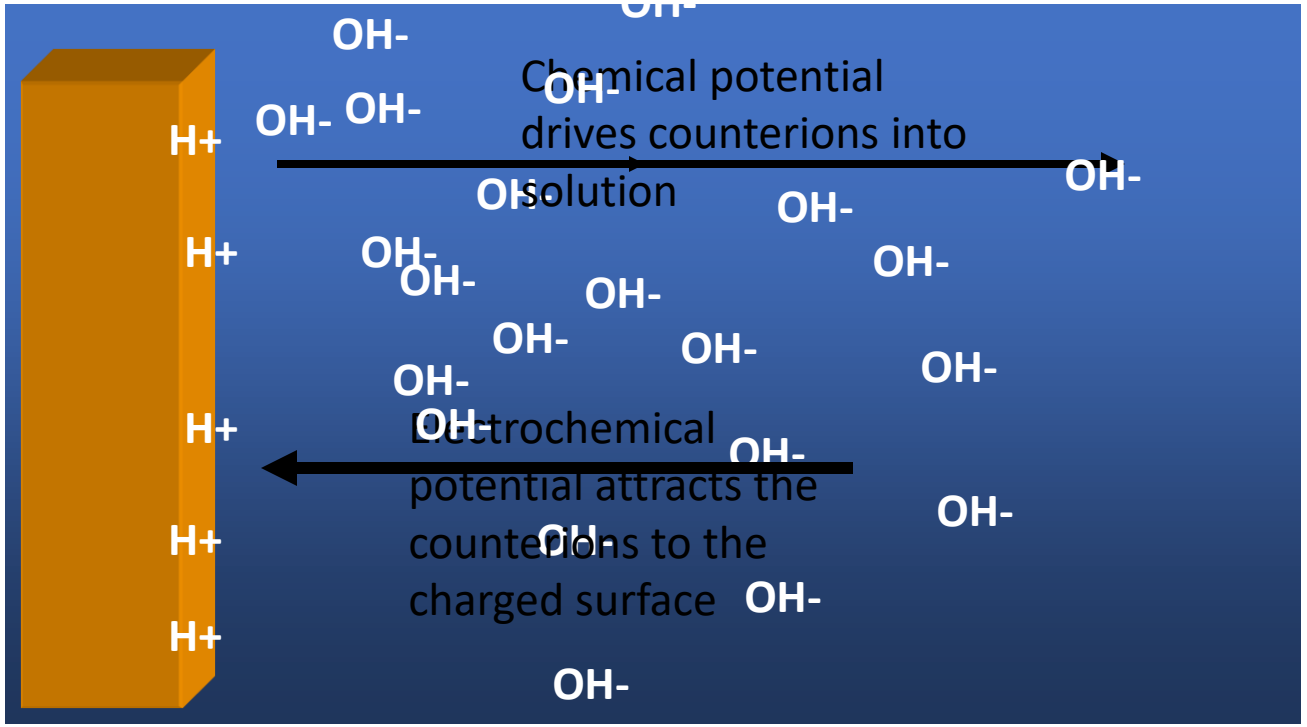

If the pH is raised by adding more hydroxyl ions, the chemical potential drive is decreased and the distribution of counterions favors more electroneutralization of the surface potential

Electrical Charges Associated with Surfaces

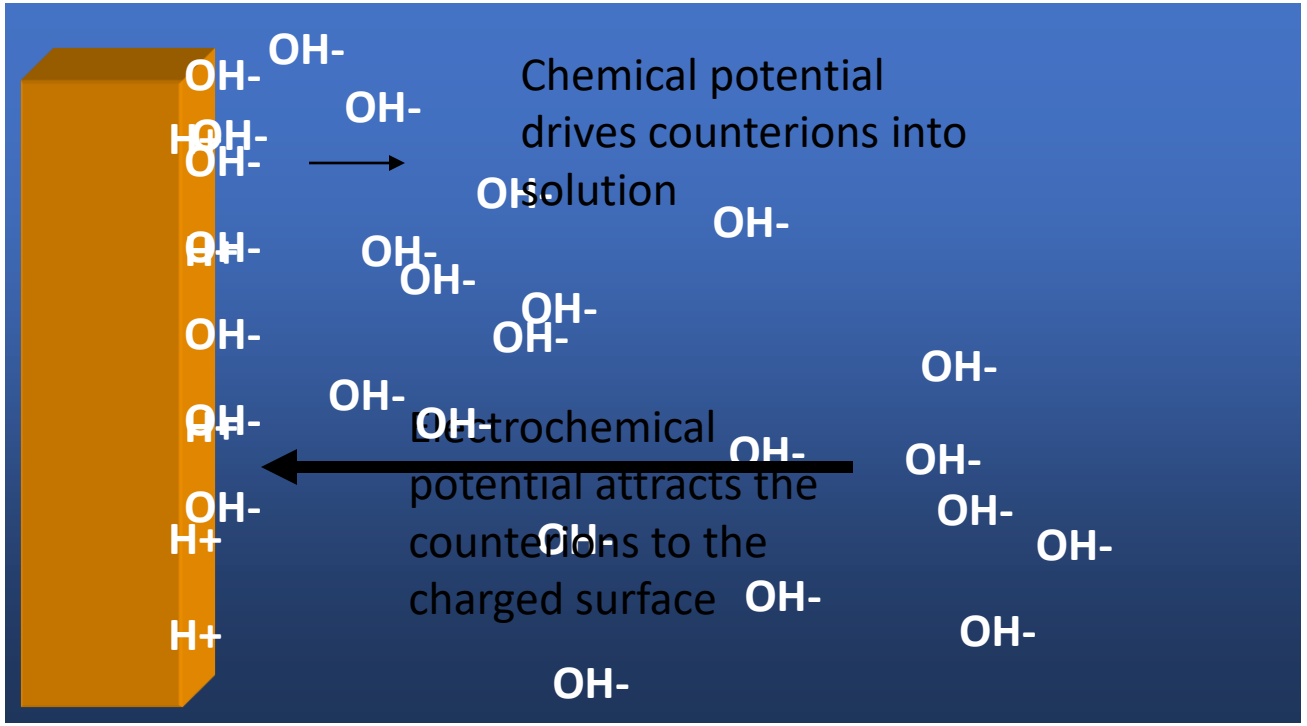

If excess base is added, the surface charge will reverse in sign, from positive to negative

Electrical Charges Associated with Surfaces

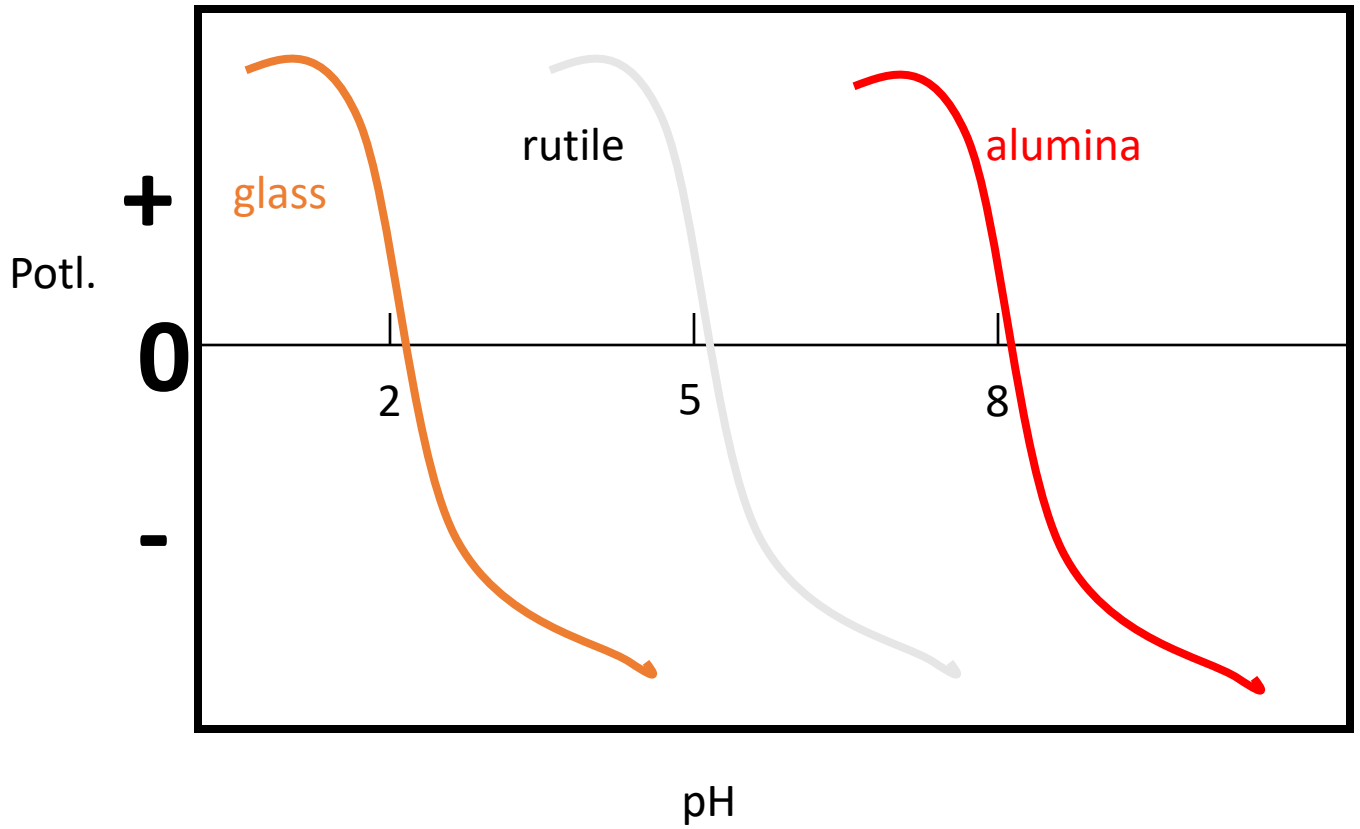

Every material surface possesses a characteristic Point of Zero Charge

Dispersion Instability

- Attractive Energy
- Repulsive Energy
- Total Energy
  - Sum of Attractive and Repulsive Forces

Attractive Forces

- Sources of attractive forces
  - Permanent dipole
  - Dipole-induced dipole
  - Induced dipole-induced dipole
- Forces vary inversely with intermolecular distance^{6}
- Dependent on the polarizability and density of atoms and solvent
- Attraction for particles decreases in water
- Attraction weakest when dispersed molecules are chemically similar to solvent

Theory of London Attraction

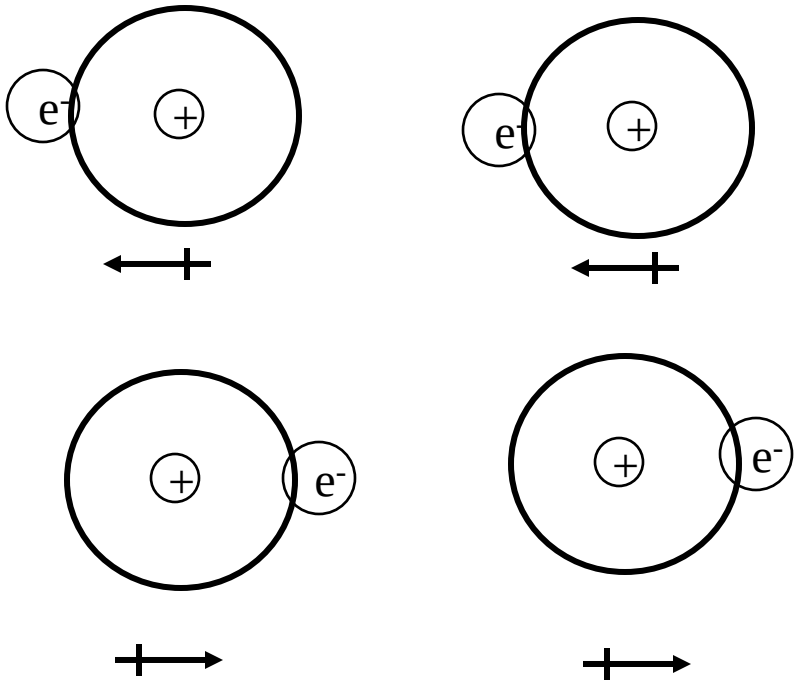

Summation of transitory dipoles leads to zero net permanent dipole moment, however, in both configurations, the atoms are mutually attractive

Van der Waals Forces Between Colloidal Particles

- For a colloidal particle, each atom or molecule of one particle attracts every atom in the other particle
- Each particle has 10^6-10^{10} atoms

Net effect of adding a myriad of possible atomic interactions is a generation of long range attraction (5-10 nm) between particles that is of considerable strength

Electrical Colloidal Stability of Latexes

- Provided by surfactants
  - anionic, cationic, nonionic
  - surfactants can interfere with coating performance
- Copolymerization with ionic monomers
  - water-soluble products are made in this process and they remain in the latex
- Interfacially adsorbed polyelectrolyes
  - excellent stability and little effect on the coatings performance
  - sometimes polyelectrolyte is desorbed (under shear) causing poor deposition of film (competition for interface)

What Forms the Repulsive Barrier?

1. Electrical Double Layer

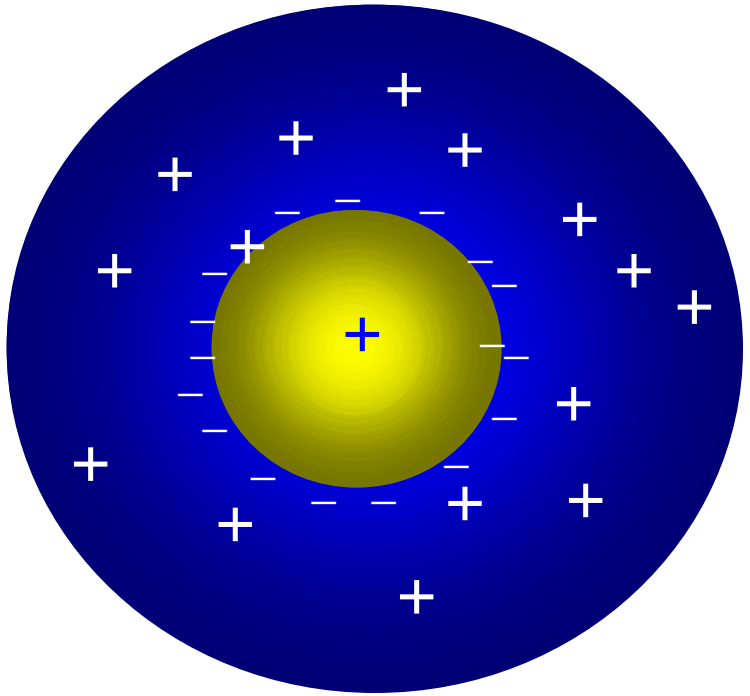

Electrical Double Layer

- Composed of two layers
  - An inner layer that may include adsorbed ions
  - Diffuse layer
    - Thermal energy
    - Electrical forces
- Thickness of double layer
    - Concentration of ions

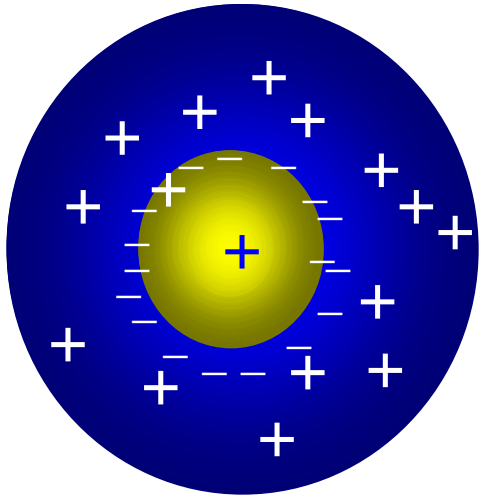

Example of Double Layer Thickness

- Double layer thickness decreases with increasing ion strength
- Ionic strength given by

$$I = \frac{1}{2} \cdot \sum_i c_i \cdot z_i^2$$

Where c_i-concentration

z_i-ion charge

Example:

For $I=10^{-1}$M, DLC=1nm

For $I=10^{-3}$M, DLC =10nm

Electrical Colloidal Stability of Latexes

- Provided by surfactants
  - anionic, cationic, nonionic
  - surfactants can interfere with coating performance
- Copolymerization with ionic monomers
  - water-soluble products are made in this process and they remain in the latex

What Forms the Repulsive Barrier?
Electron Double Layer

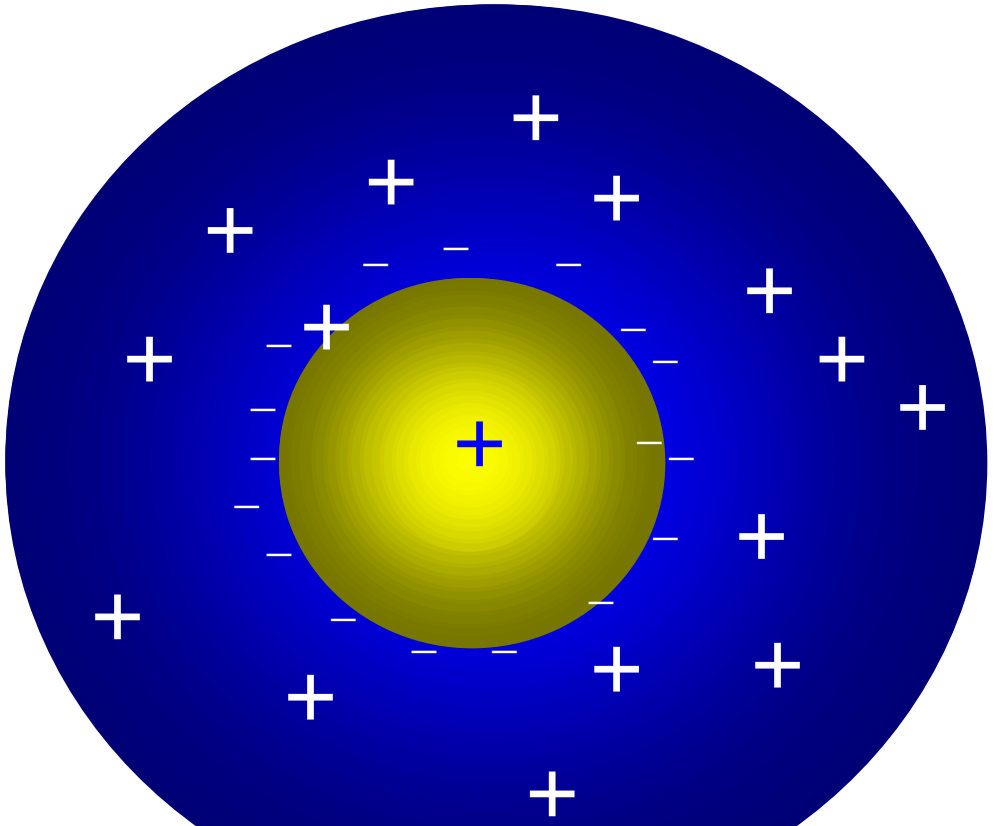

Electrical Double Layer

- Composed of two layers
  - An inner layer that may include adsorbed ions
  - Diffuse layer
    - Thermal energy
    - Electrical forces
- Thickness of double layer
  - Concentration of ions

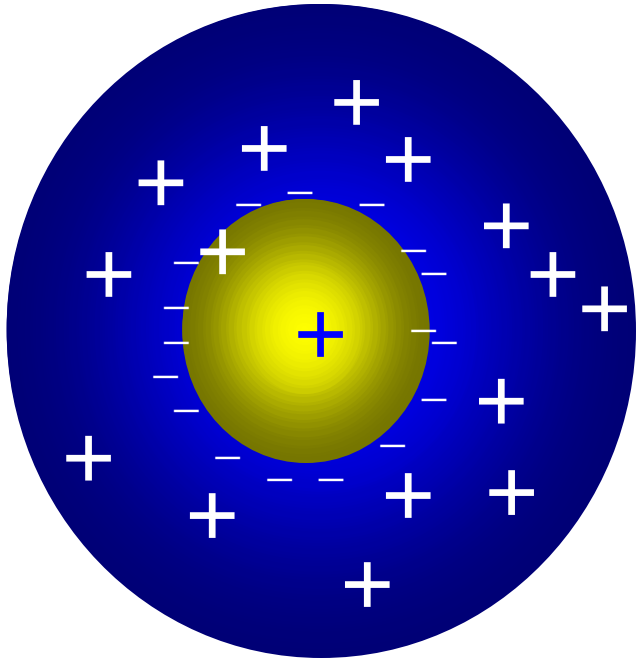

Example of Double Layer Thickness

- Double layer thickness (κ^{-1}) decreases with increasing ion strength
- Ionic strength given by

$$I = \frac{1}{2} \cdot \sum_i c_i \cdot z_i^2$$

Where c_i-concentration

z_i-ion charge

Example:

For I=10^{-1}M, κ^{-1}=1nm

For I=10^{-3}M, κ^{-1}=10nm

Schramm, L. Emulsions: Fundamentals and Applications in the Petroleum Industry. Chapter 1. (Schramm, L. L. Ed.) American Chemical Society, Washington D.C. 1992.

Electrical Colloidal Stability of Latexes

- Provided by surfactants
  - anionic, cationic, nonionic
  - surfactants can interfere with coating performance
- Copolymerization with ionic monomers
  - water-soluble products are made in this process and they remain in the latex

DLVO STABILITY

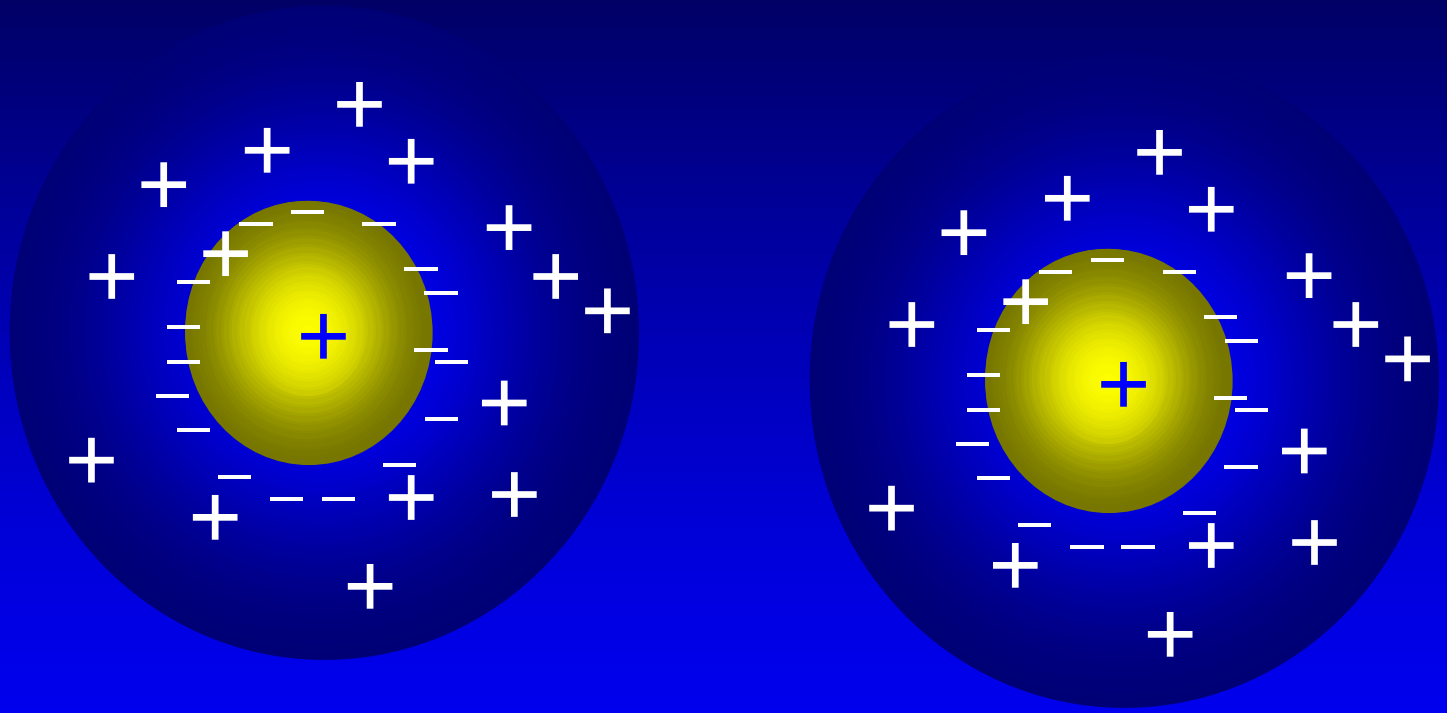

Stabilization by the Electric Double Layer

Repulsion as the double layers overlap

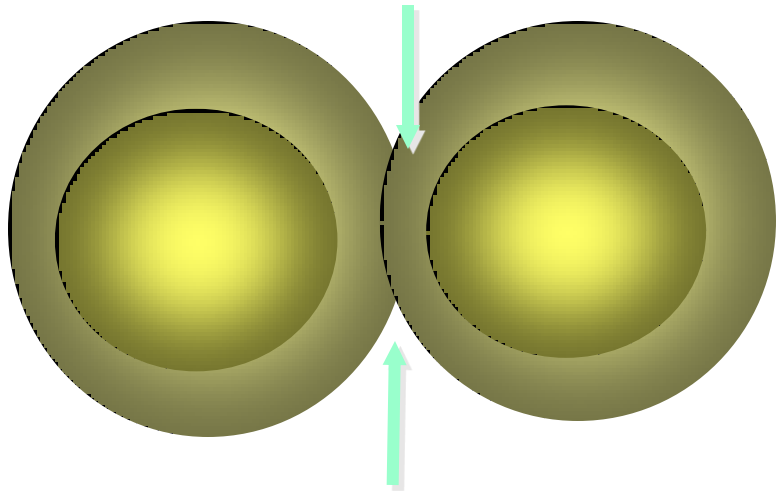

Stability of dispersions

- Complex:
  - attractive and repulsive forces act simultaneously
    - depend on physical conditions
    - pH, ionic strength, temperature, concentration
  - usually thermodynamically unstable
  - kinetically stable

DLVO THEORY

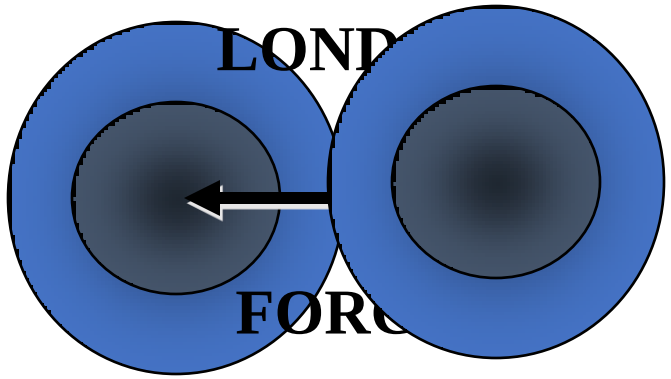

ISE THEORY

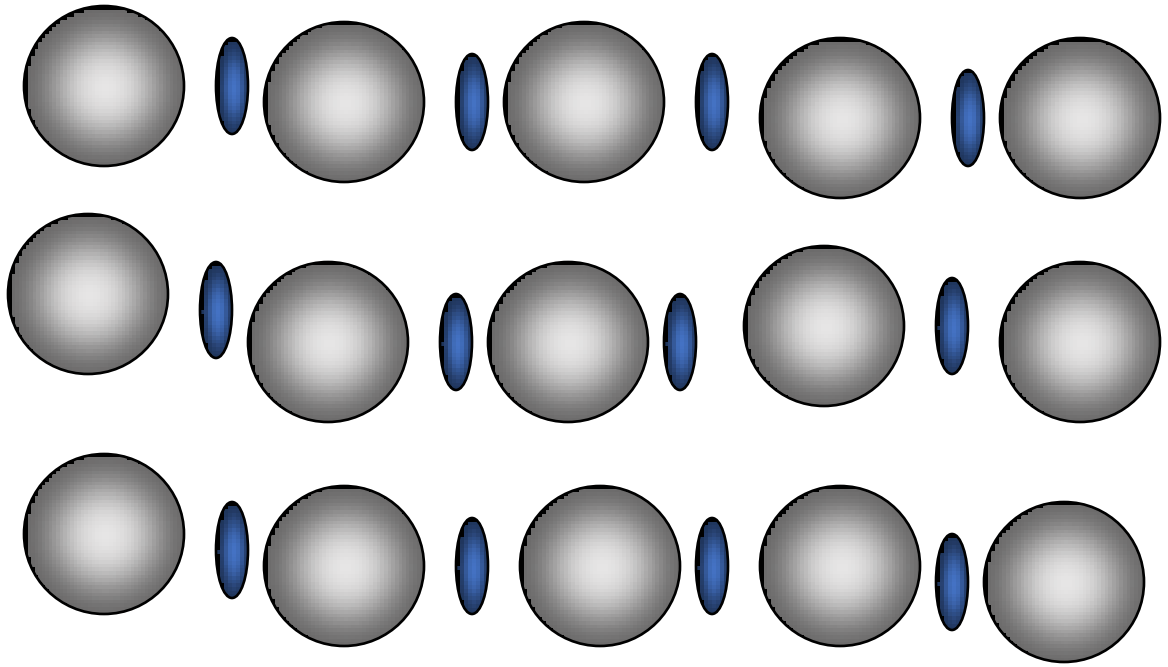

Surfactants and Conditioning

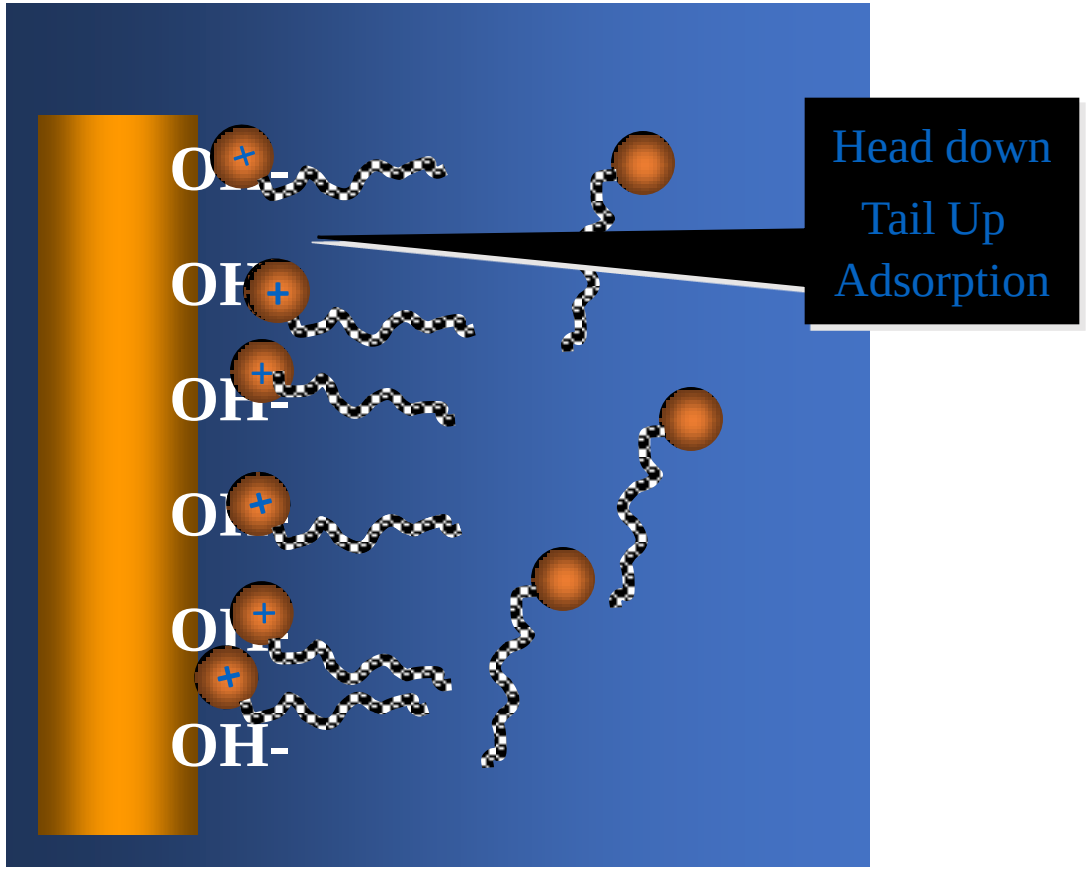

Surfactants and Conditioning

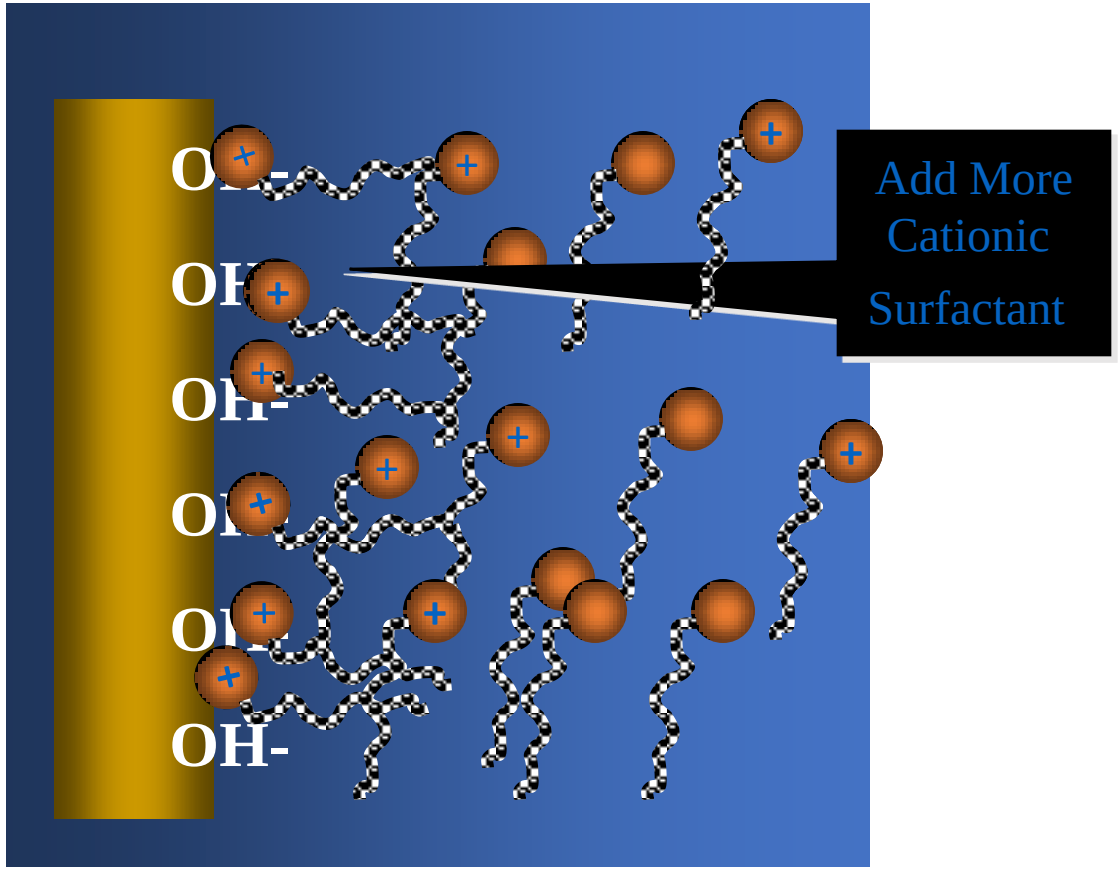

Surfactants and Conditioning

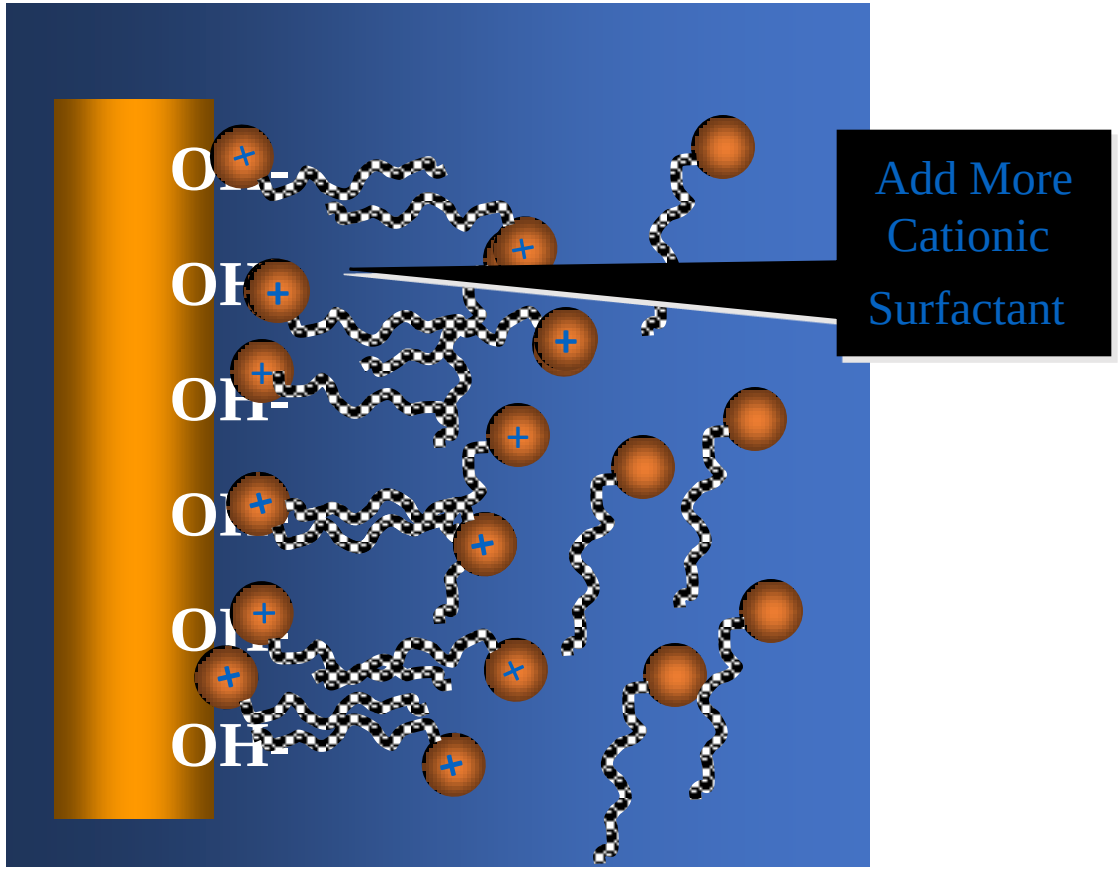

Surfactants and Conditioning

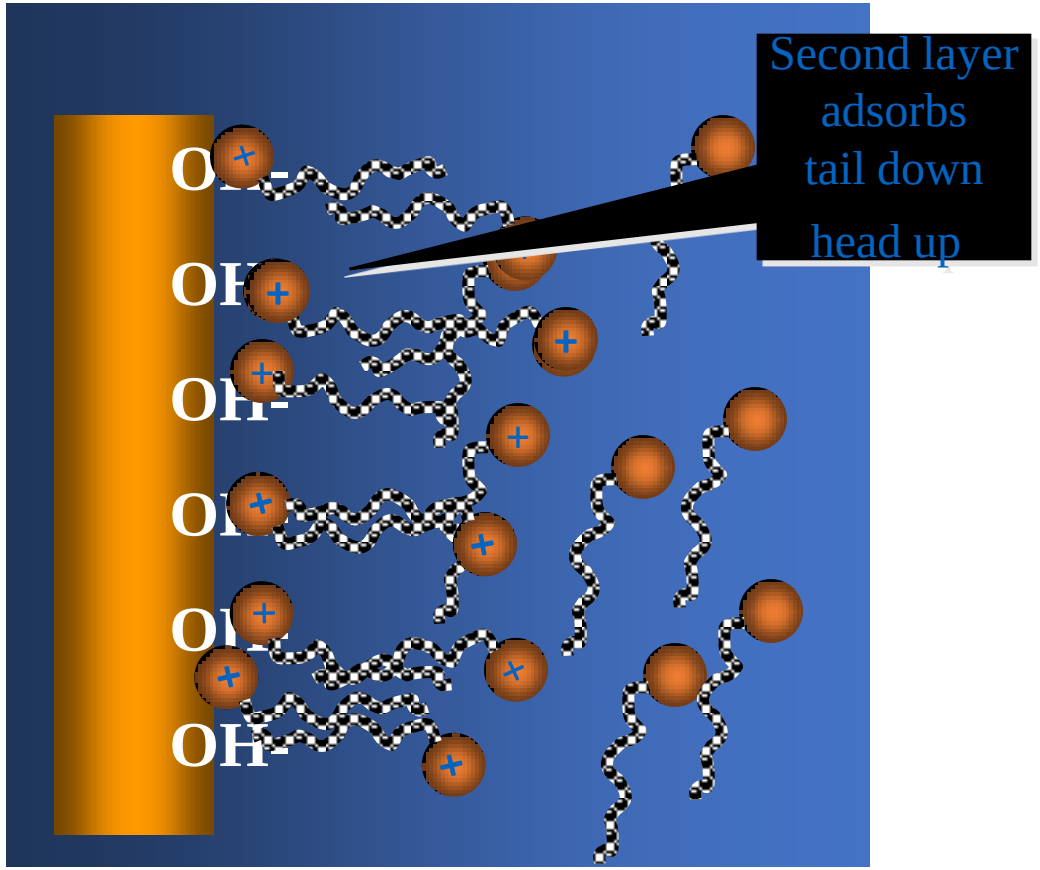

WATER -SOLUBLE AND SWELLABLE POLYMERS AT INTERFACES

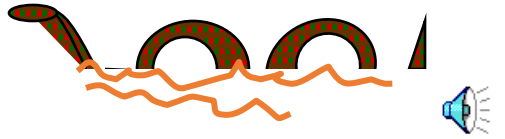

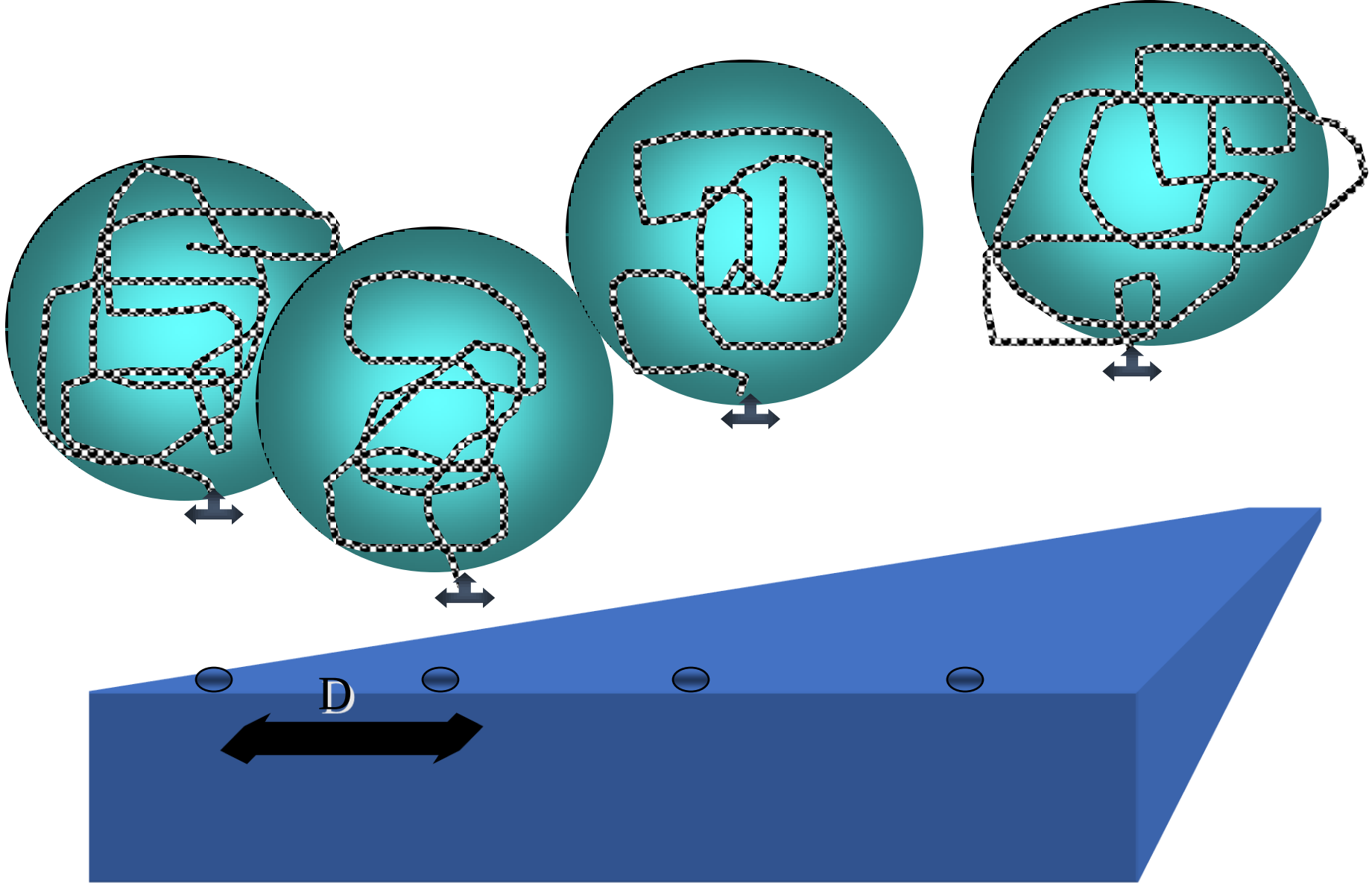

ADSORPTION AS MUSHROOMS

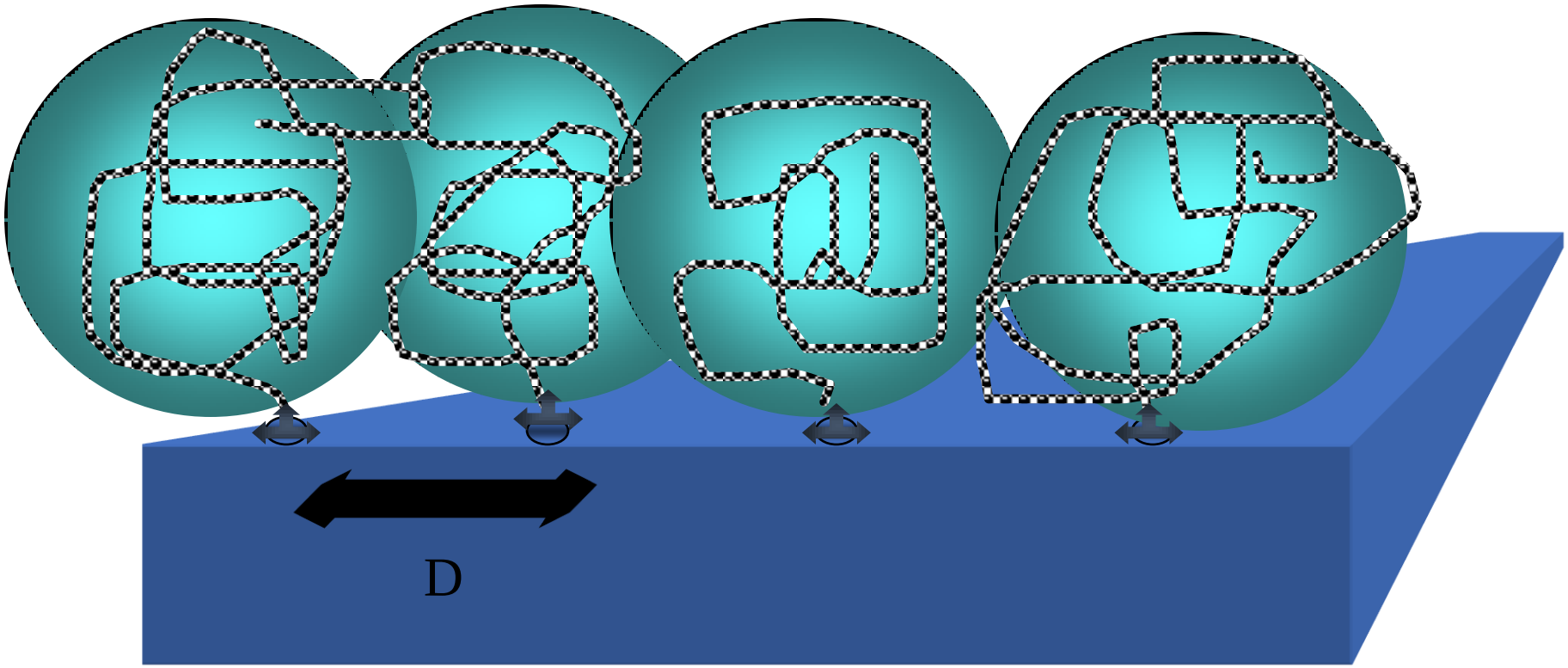

ADSORPTION AS MUSHROOMS

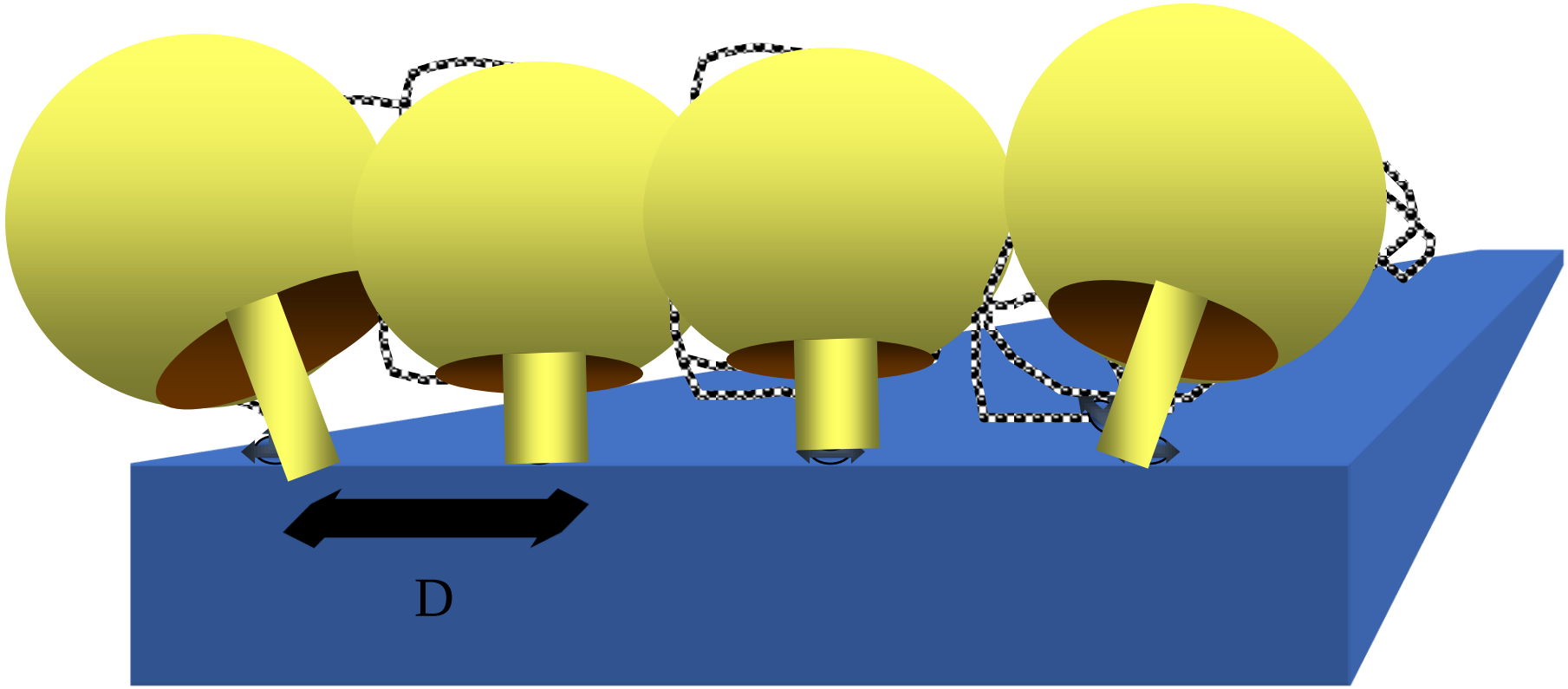

ADSORPTION AS MUSHROOMS

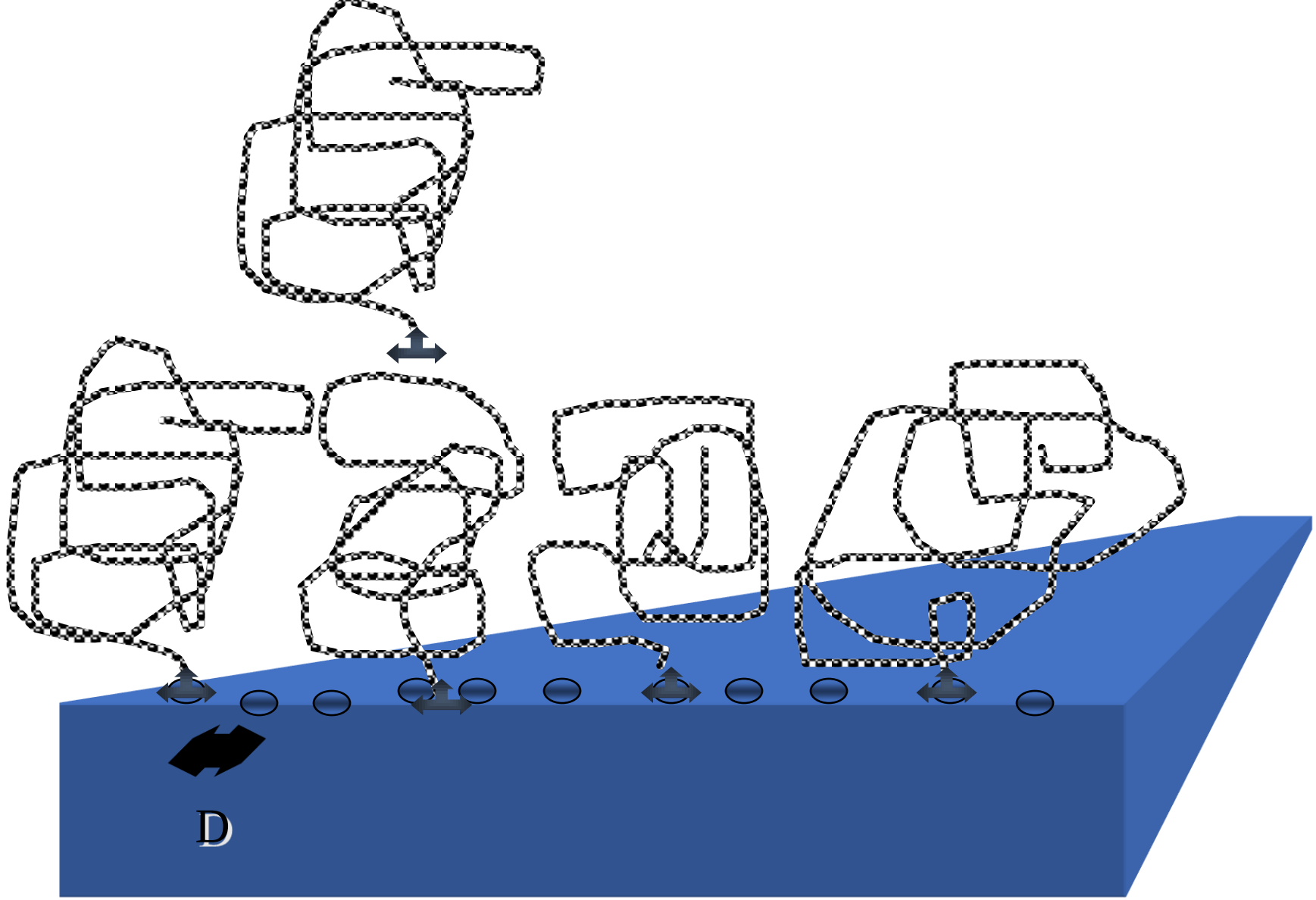

ADSORPTION AS MUSHROOMS

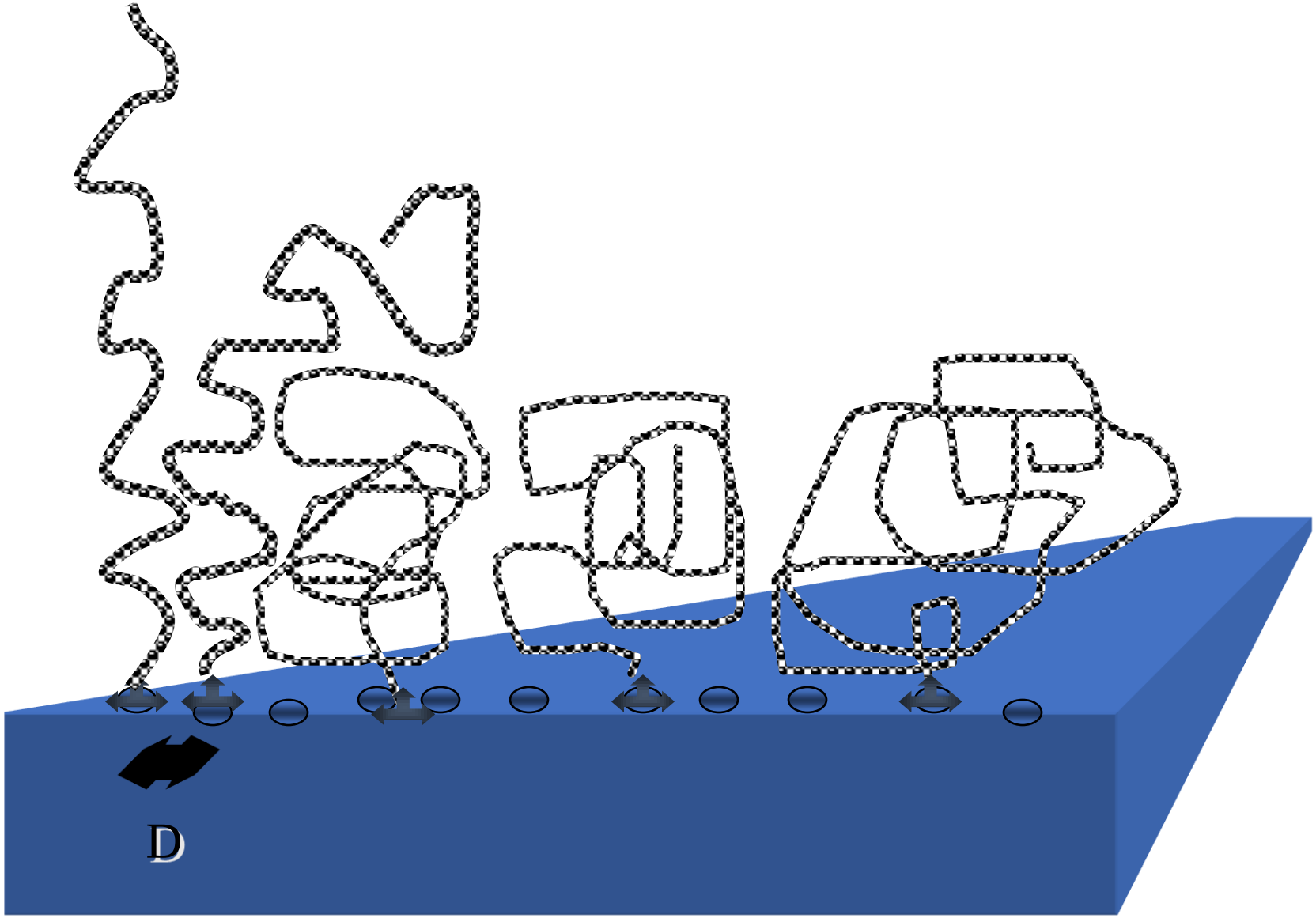

ADSORPTION AS BRUSHES

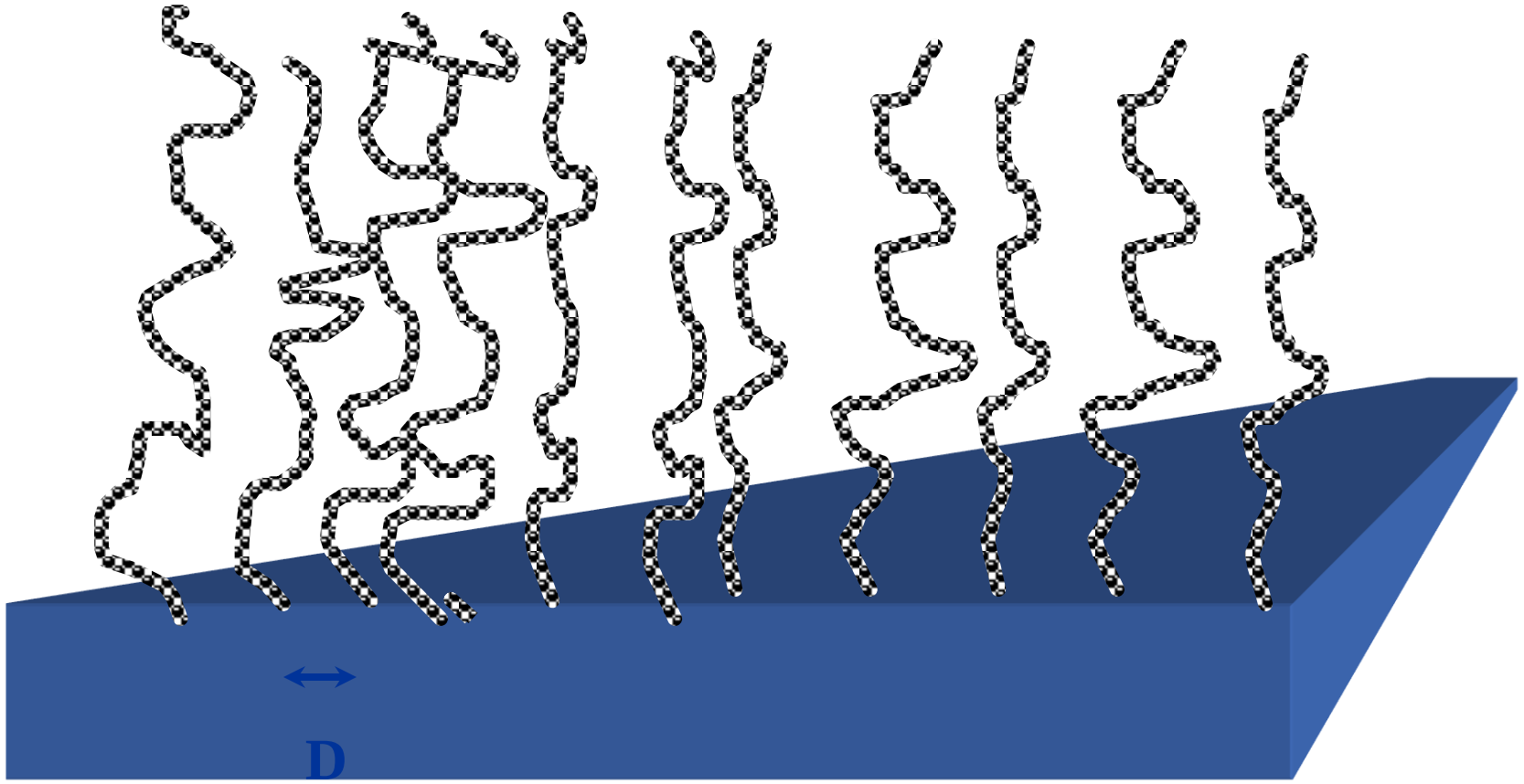

ADSORPTION AS BRUSHES

LOOPS, TRAINS & TAILS

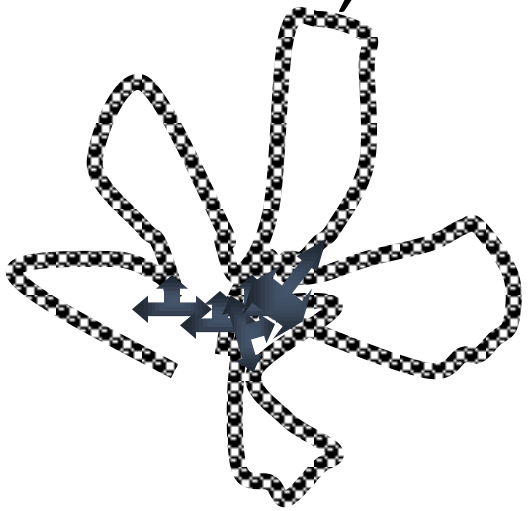

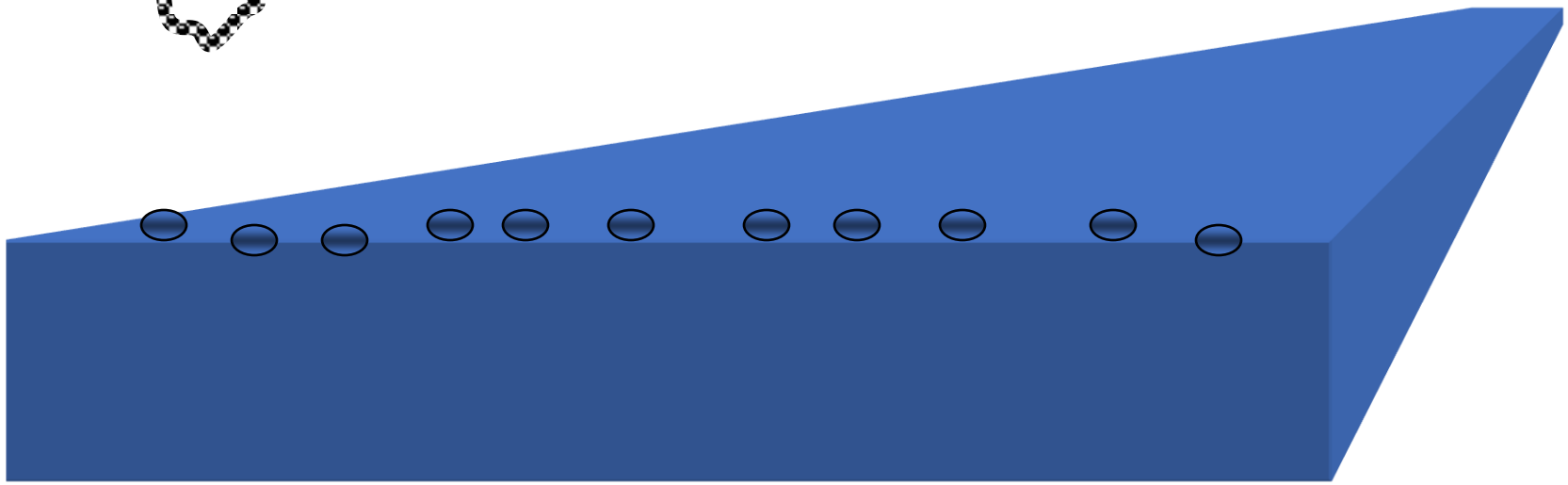

LOOPS, TRAINS & TAILS

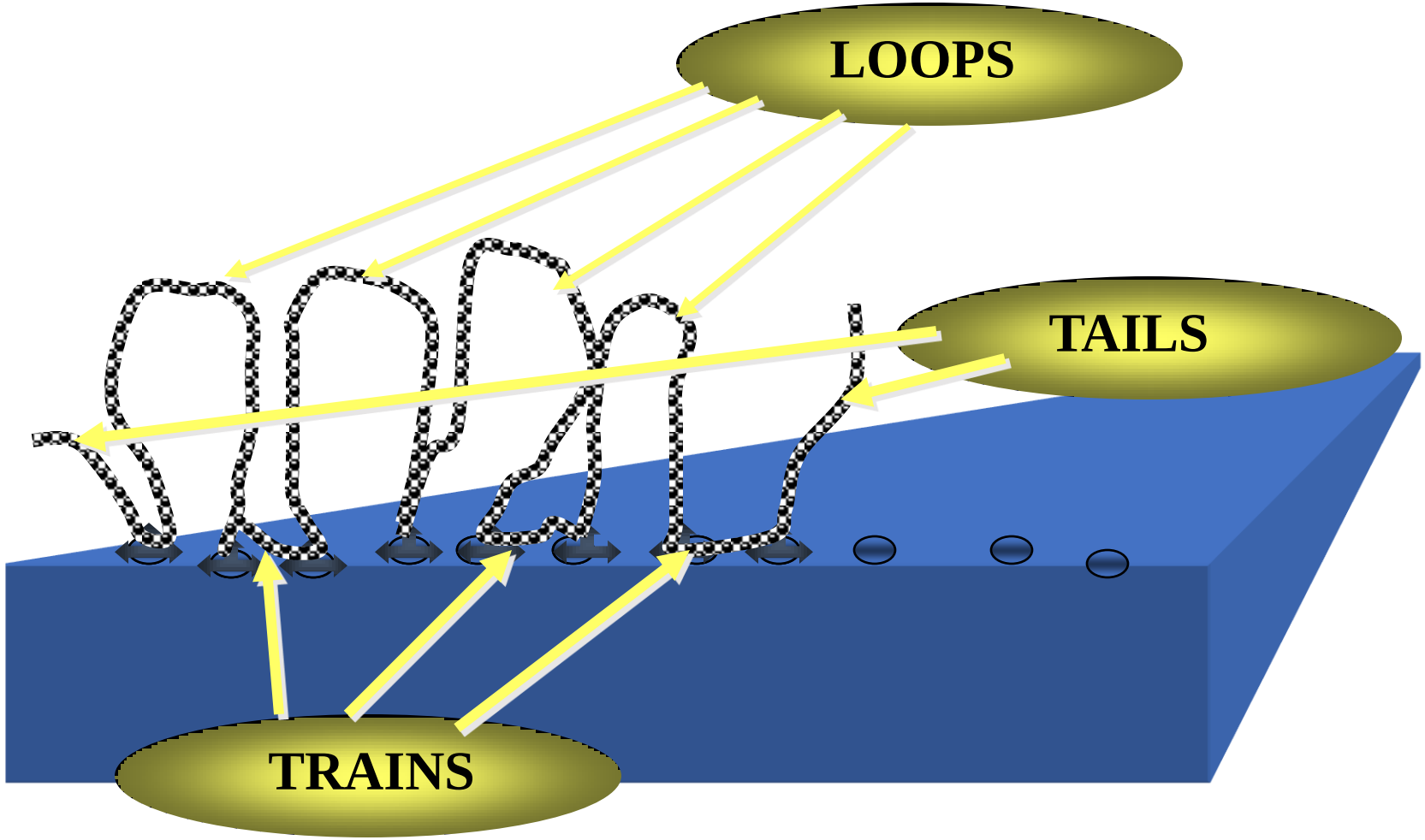

Strong Interaction

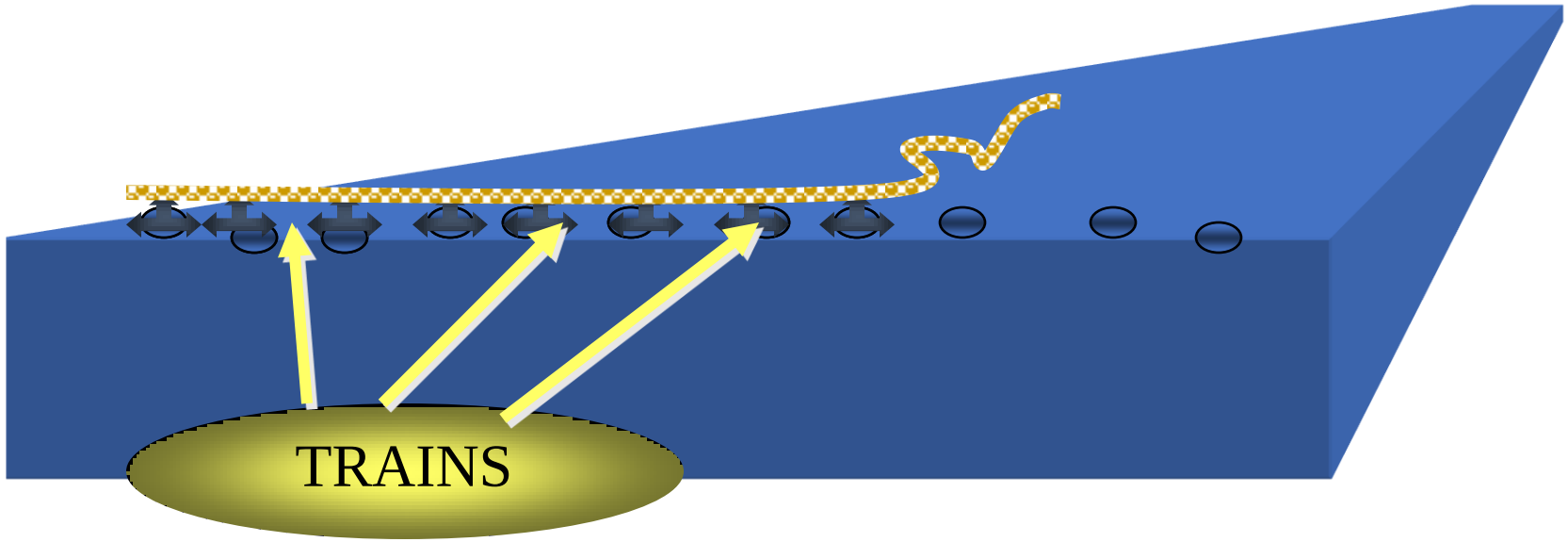

Vinylpyrrolidone/dimethylaminoethylmethacrylate Copolymer

- The isoelectric point of hair is ~pH 5
- Cationic polymers show enhanced substantivity to hair
- Control ionic repulsion at hair surface
- Note:
  - Flyaway arises from triboelectric charging

QUATERNIZED PVP/DIMETHYLAMINOETHYL METHACRYLATE COPOLYMER *(Polyquaternium 11)*

- Quaternization assures substantivity to hair under alkaline conditions-Important when formulating high pH cold wave lotions
- Cationic polymers used in conditioning and soft-setting formulations:
  - Aid in detangling during combing of wet hair
  - Easily removed by shampoo

QUATERNIZED PVP/DIMETHYLAMINOETHYL METHACRYLATE COPOLYMER *(Polyquaternium 11)*

- Ideally suited for styling lotions (commonly called glazes), gels and aerosol foams (mousses) because of good wet combing and easy setting
- When dry, they can give a crisp shiny curl (wet look)
  - These curls can be combed out with minimum of flaking, resulting in a conditioned styled look
- Improve condition of damaged hairs. Making their surfaces smooth and increasing strength

Polyquaternium-6
(Merquat 100 –Nalco)

- Polydiallyldimethylammonium chloride
- Excellent substantivity to skin and hair
  - Confers conditioning benefits
- Does not form films
- Poor compatibility with anionic ingredients

Polyquaternium-7
(Merquat 550 & S –Nalco)

- Poly(acrylamide-*co*-diallyldimethylammonium chloride)
- Excellent substantivity to skin and hair
  - Confers conditioning benefits
- Forms films
- Good compatibility with anionic surfactants

Steric Stabilization

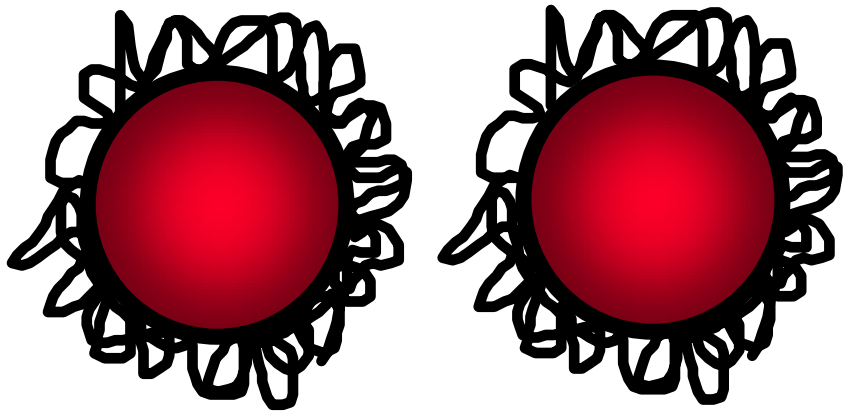

The stabilization of emulsions by polymer adsorbed at the interface between the dispersed and continuous phases

Napper, D.H.; *Polymeric Stabilization of Colloidal Dispersions*, Academic Press, 1983
Vincent, B.; Whittington, S.; In *Colloid and Surface Science*; Matijevic, E., Ed.; Plenum: 1982

Mechanisms of Steric Stabilization

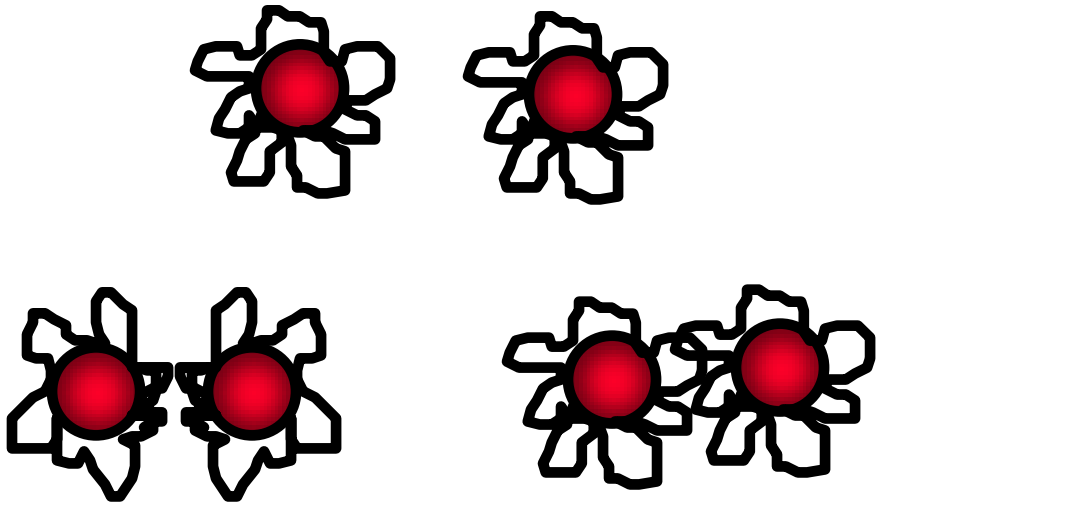

Entropic restriction

Overlap of polymer extended coils

Mechanisms of Steric Stabilization

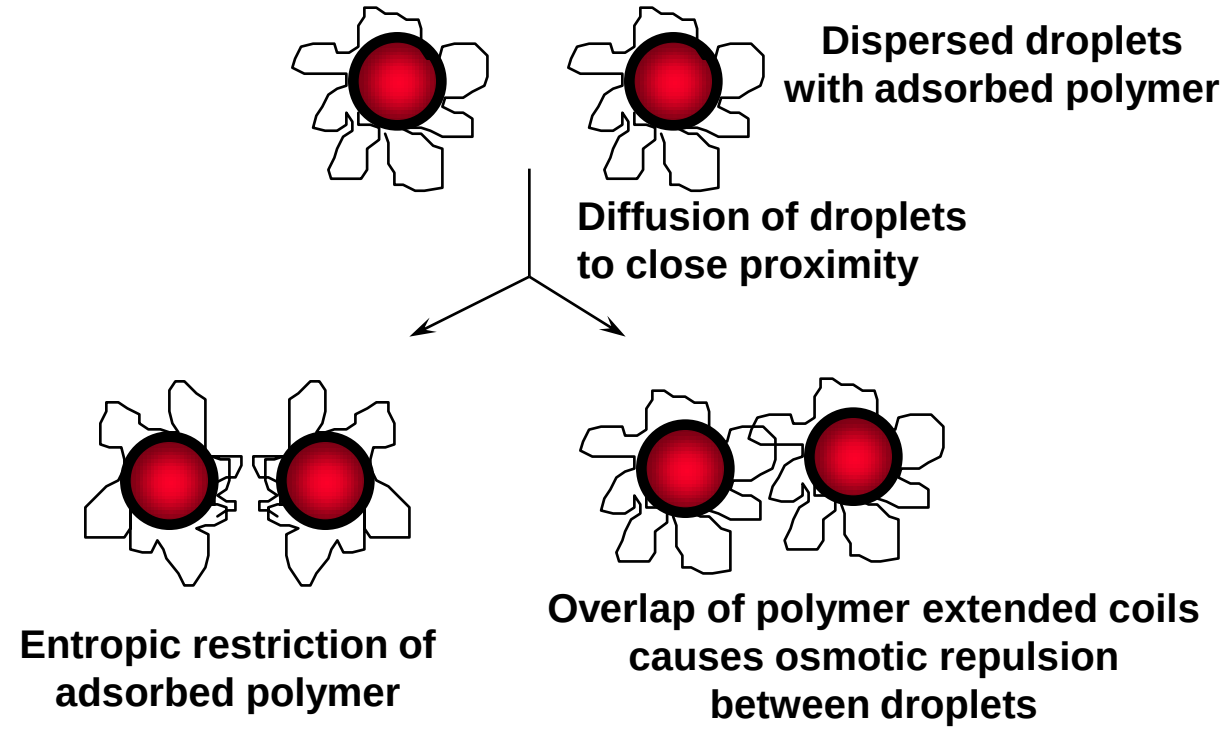

…but Steric Stabilization Does Not Stabilize Against Creaming or Sedimentation

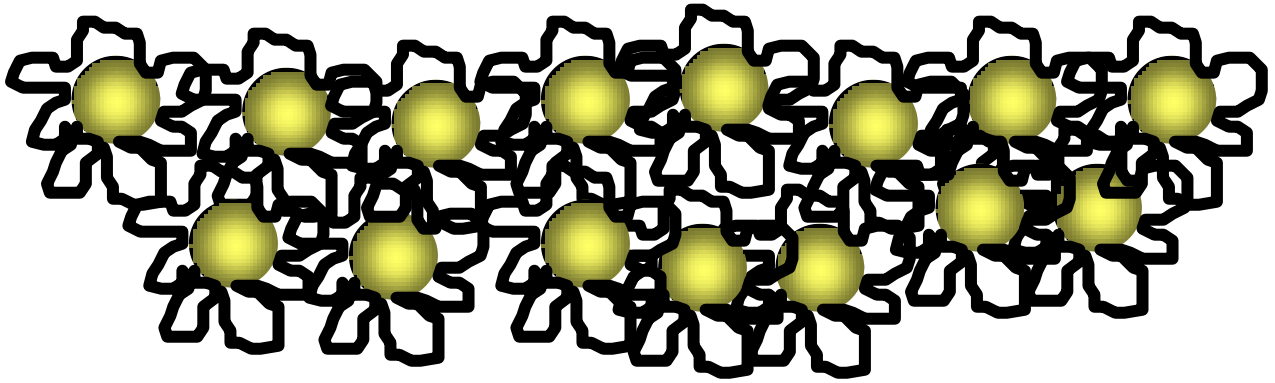

…Microgel Thickeners Can Be Used to Stabilize Against Creaming

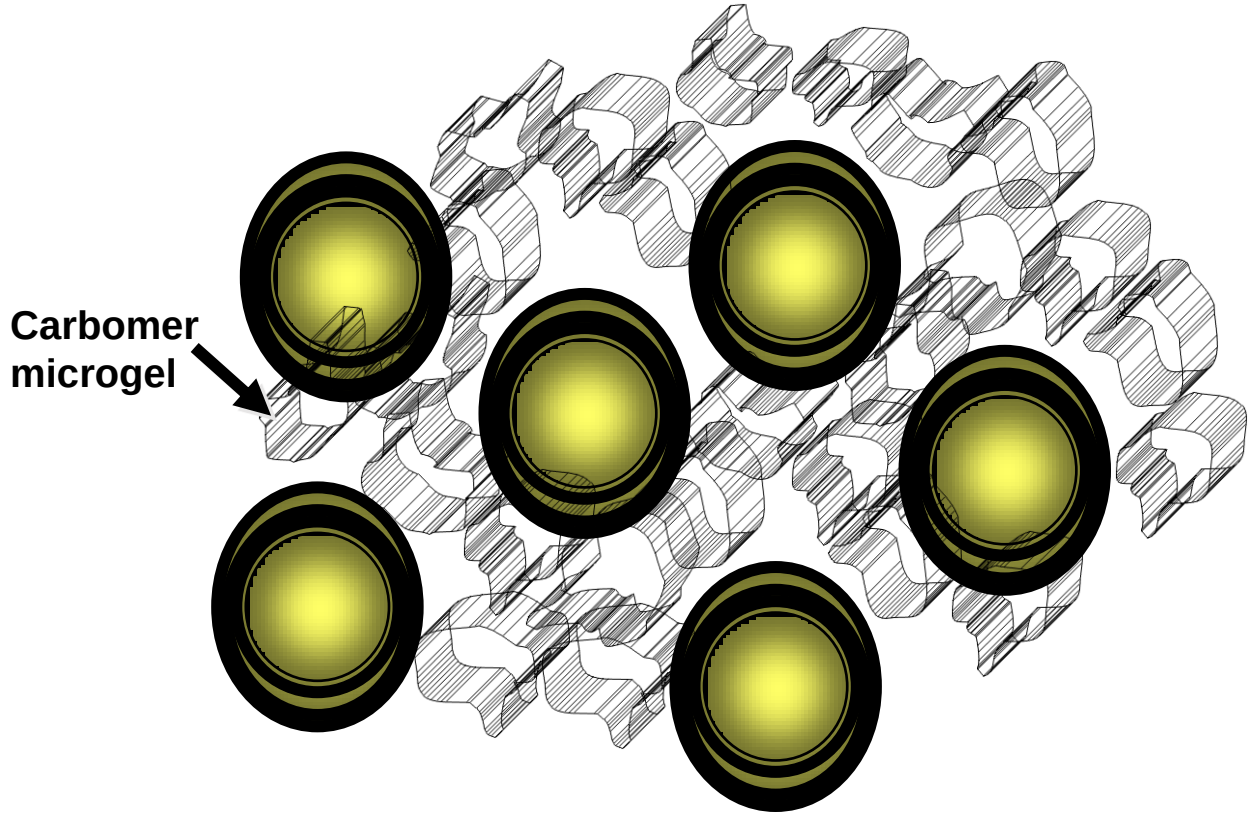

Polymeric Emulsifiers

The Consequence of Critical Overlap on Steric Stabilization

Polymer Concn.

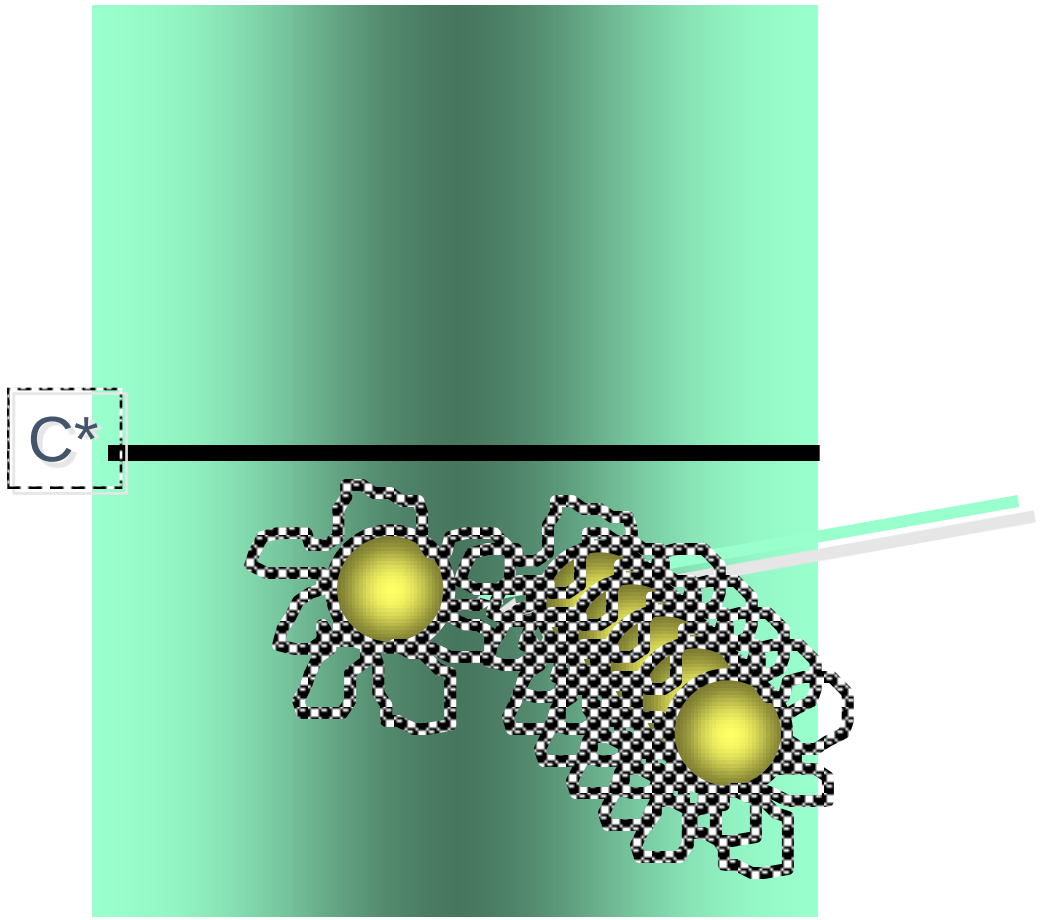

Intrusion of solvent forces droplets apart

The Consequence of Critical Overlap on Steric Stabilization

Polymer Concn.

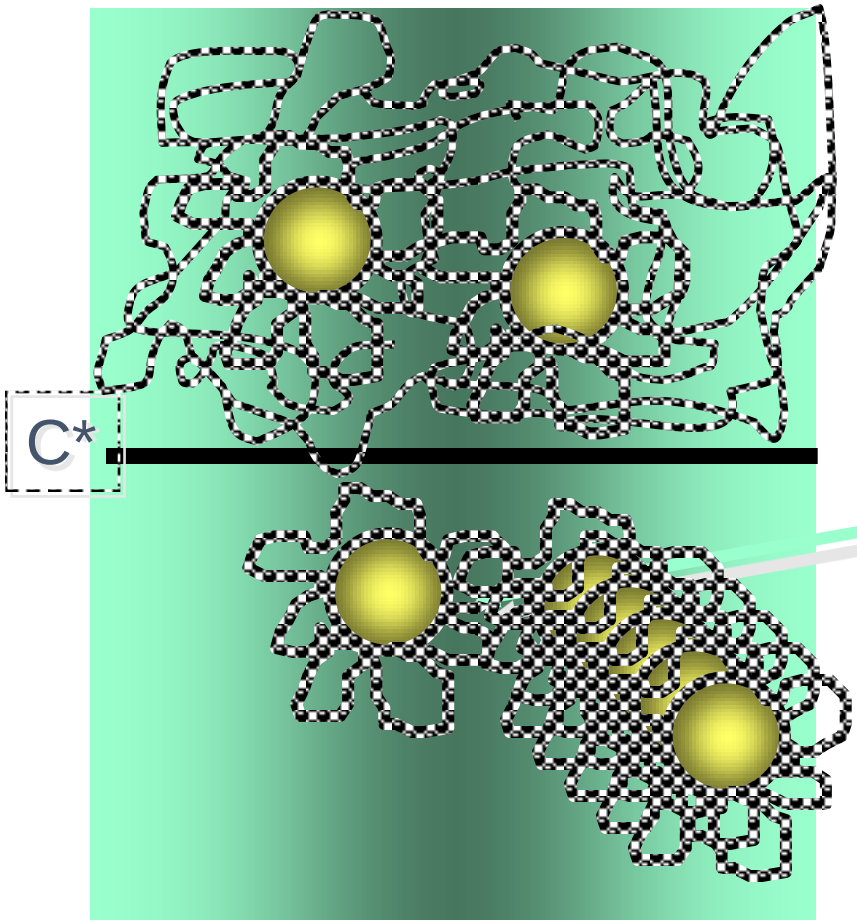

Intrusion of solvent forces droplets apart

HUGGIN'S PLOT BY CONTRAVES FOR AQUEOUS HMPAA AT pH = 5.5

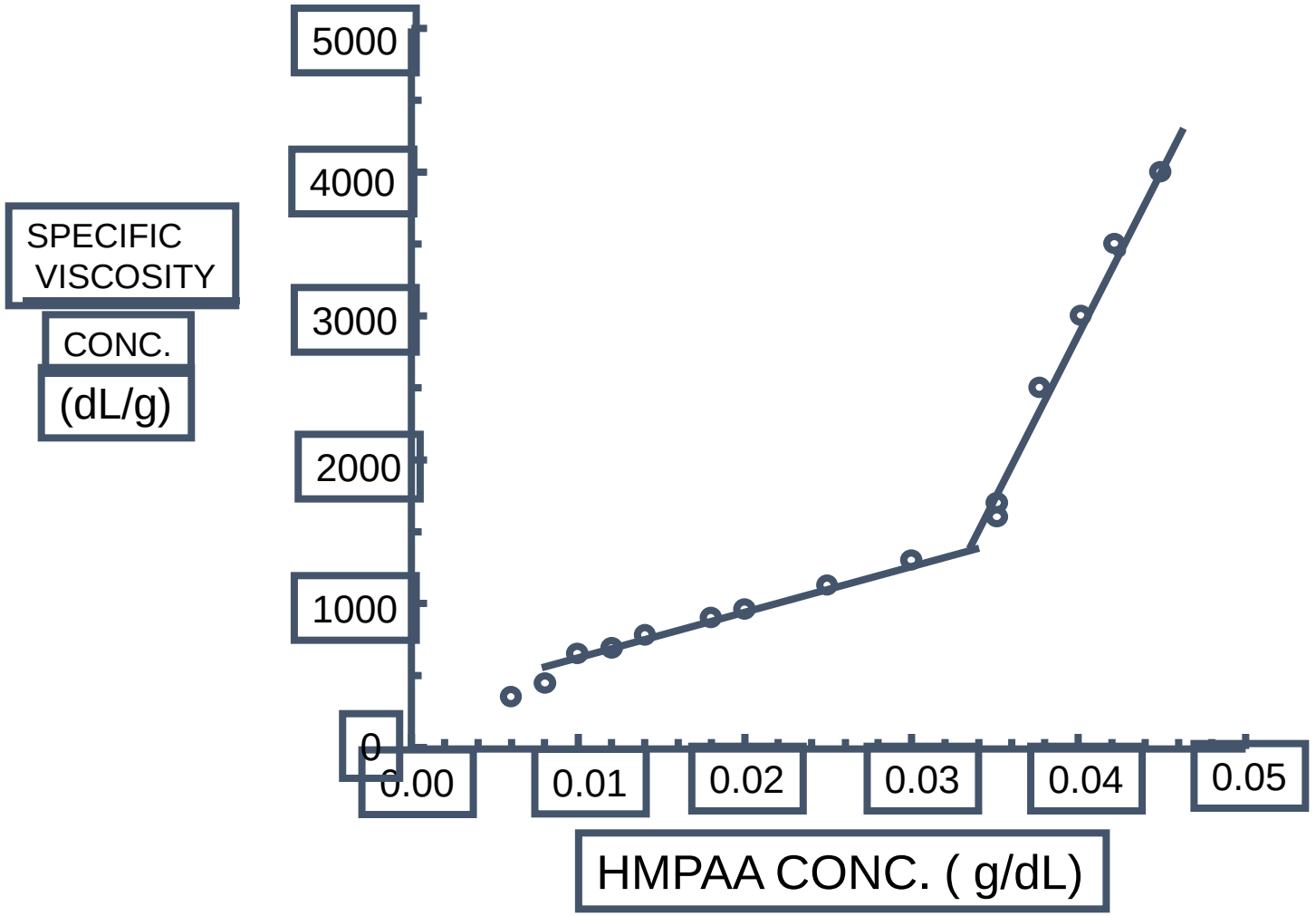

Depletion Flocculation

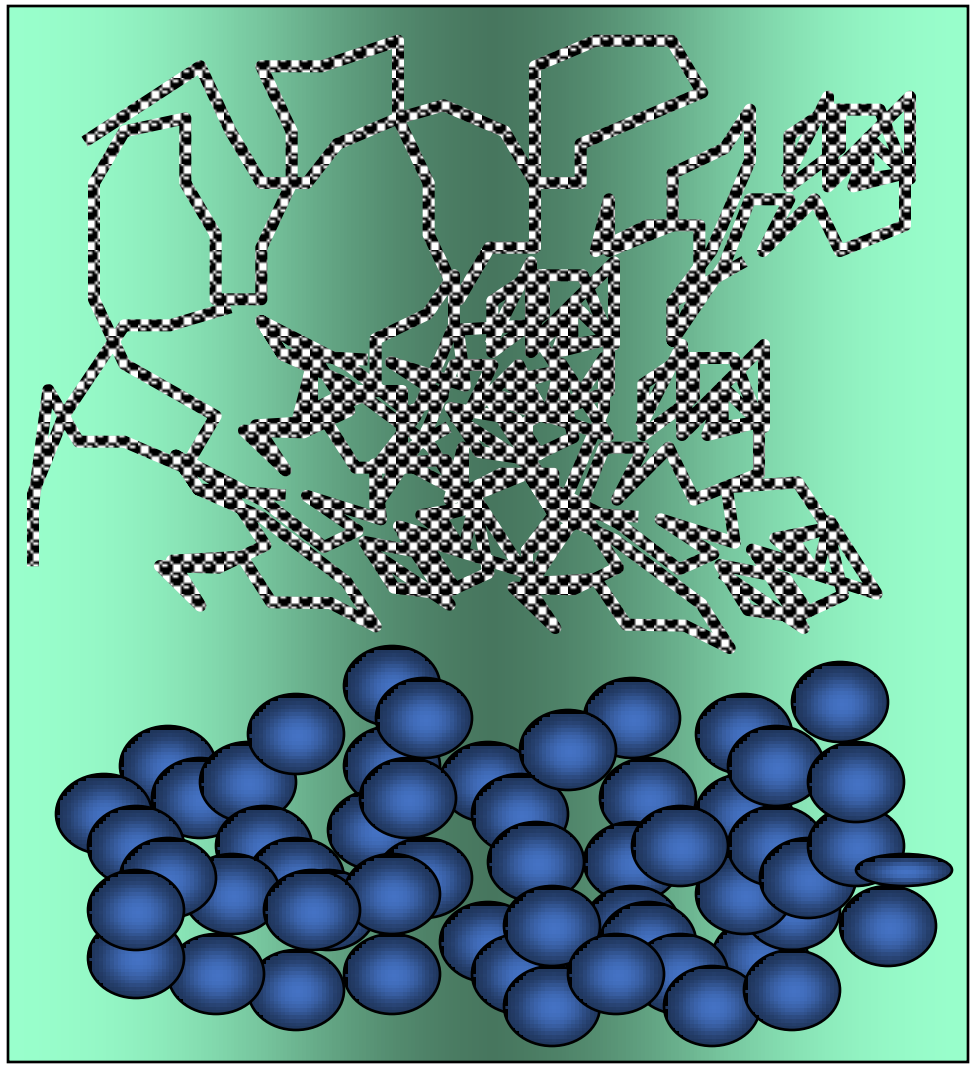

Polymeric Emulsifiers

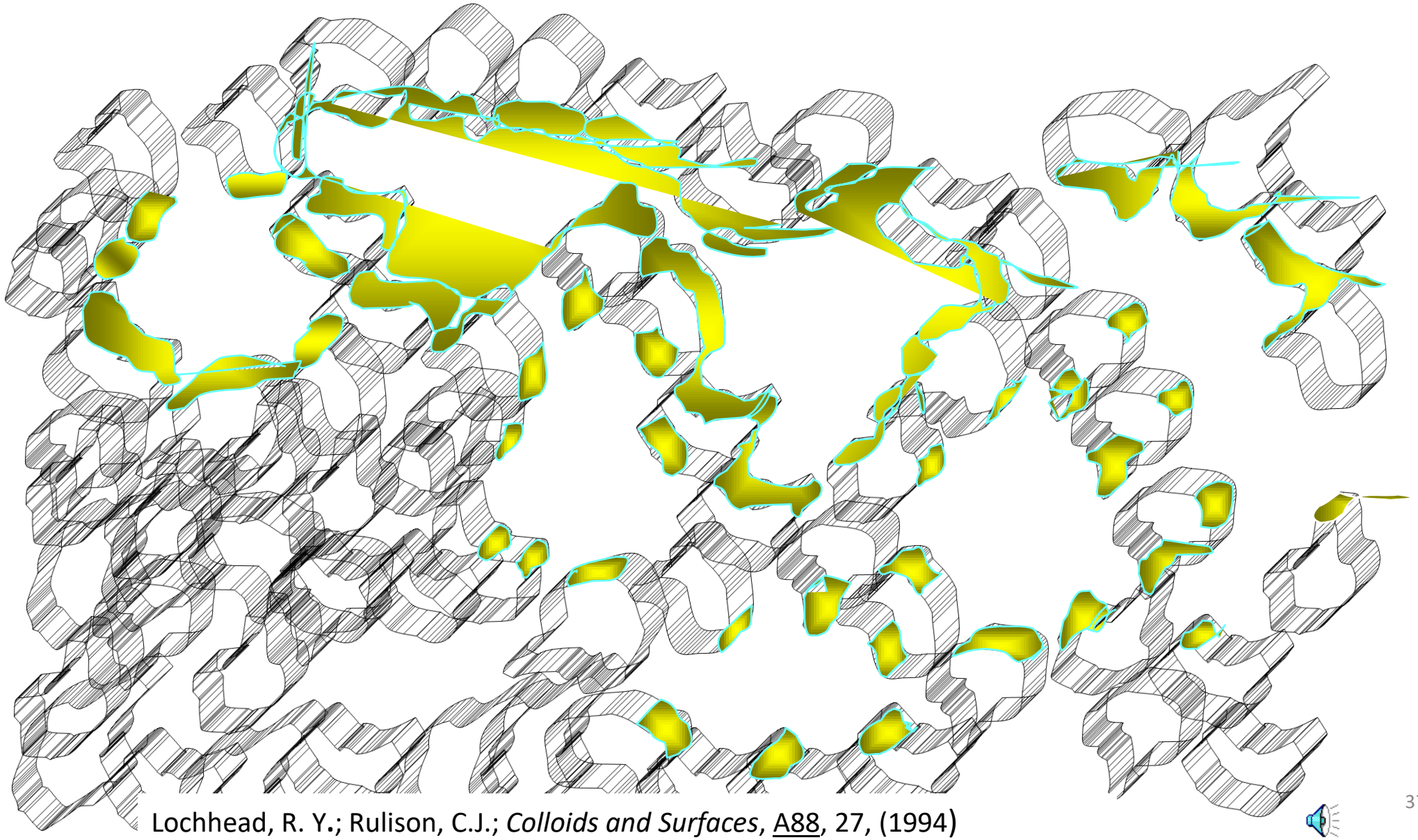

Lochhead, R. Y.; Rulison, C.J.; *Colloids and Surfaces*, A88, 27, (1994)

Polymeric Emulsifiers

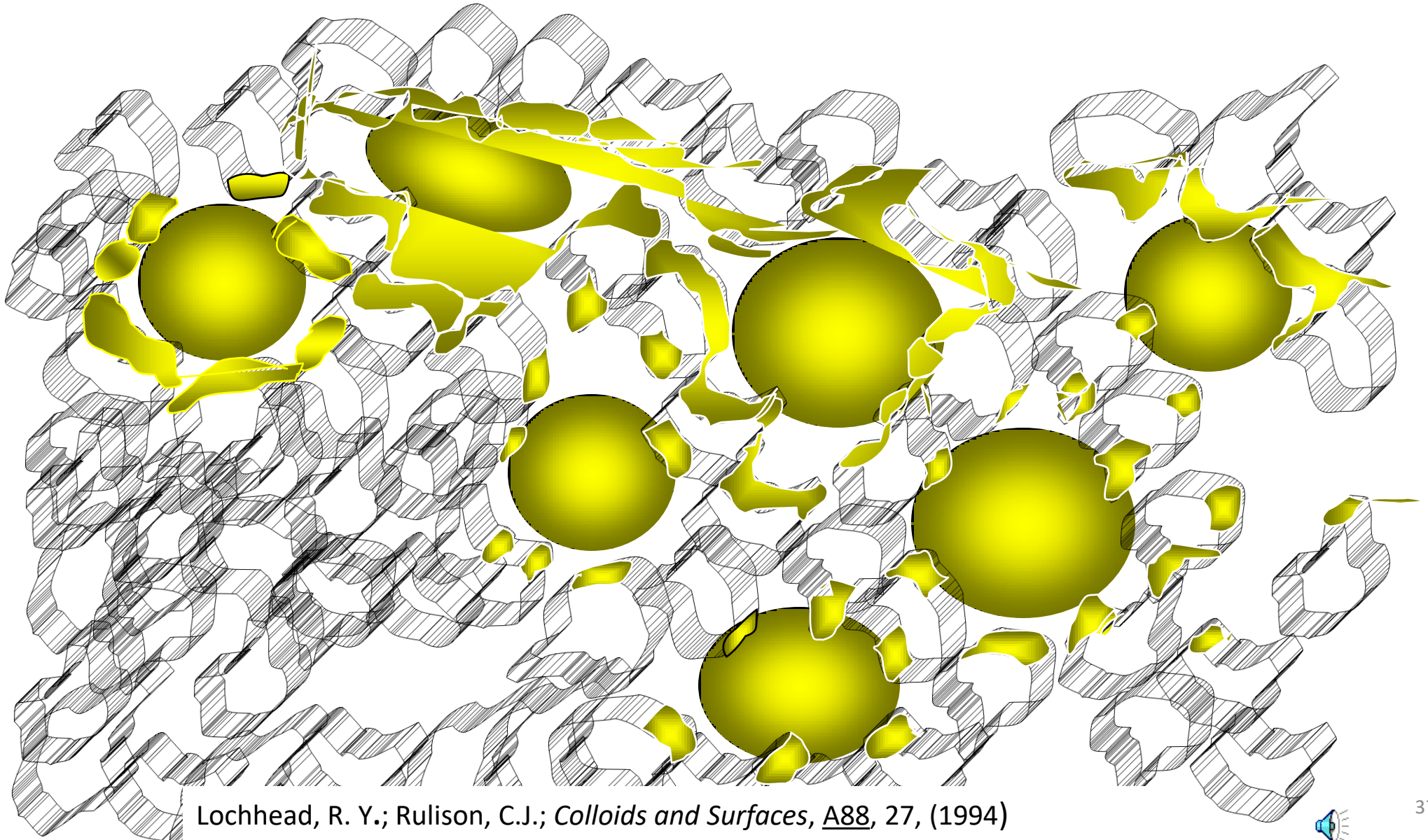

Lochhead, R. Y.; Rulison, C.J.; *Colloids and Surfaces*, A88, 27, (1994)

Acrylates C10-30 Alkyl Acrylate Crosspolymer

- Benefits
  - HLB balancing
  - Long-term stability
  - Triggered release of oil phase
  - ‘Waterproofing’ of substrate
- Disadvantages
  - Difficult/slow processing
  - Poor skin feel

Alkyl Taurate – Acrylamide Crosspolymers

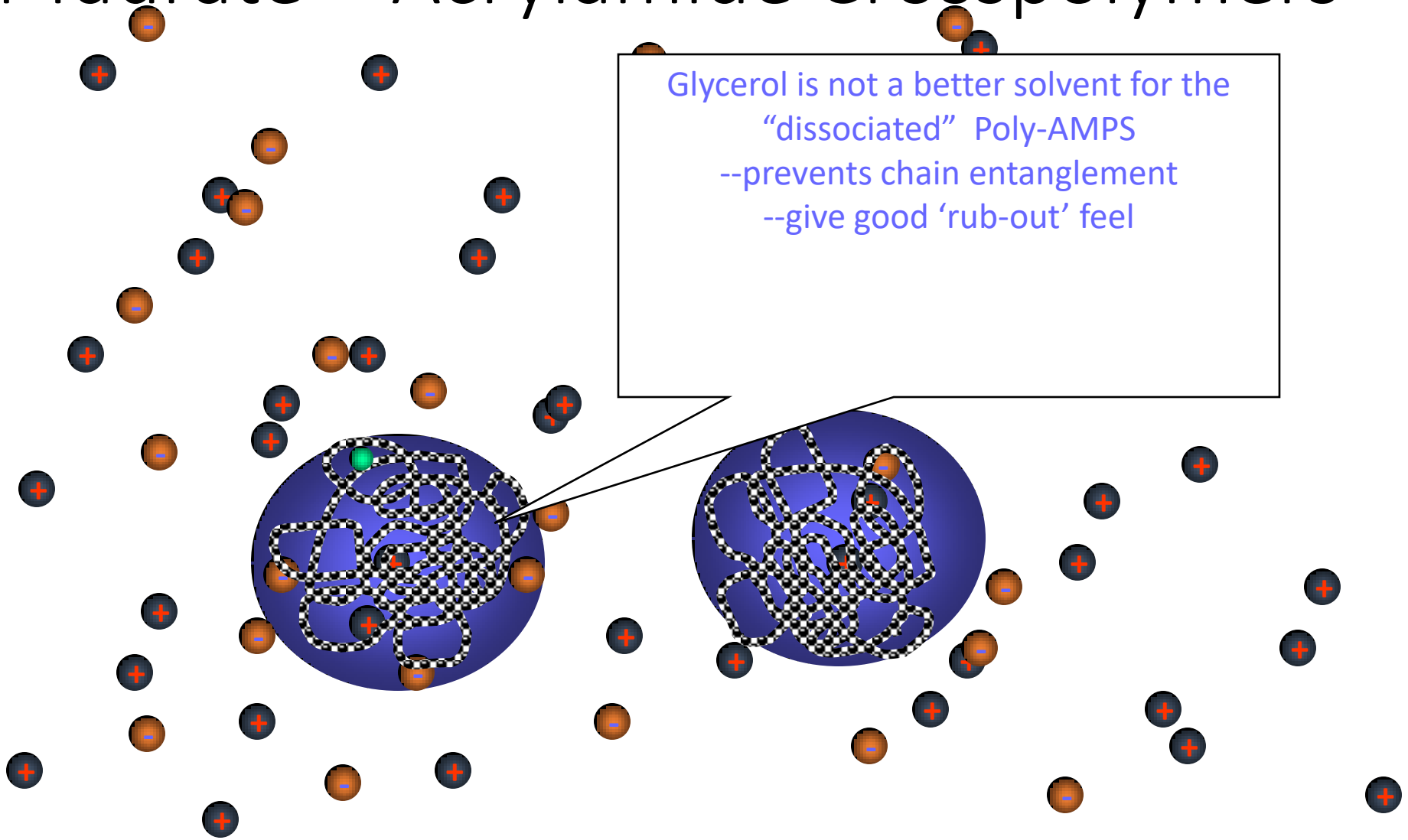

Hydrophobically Modified,

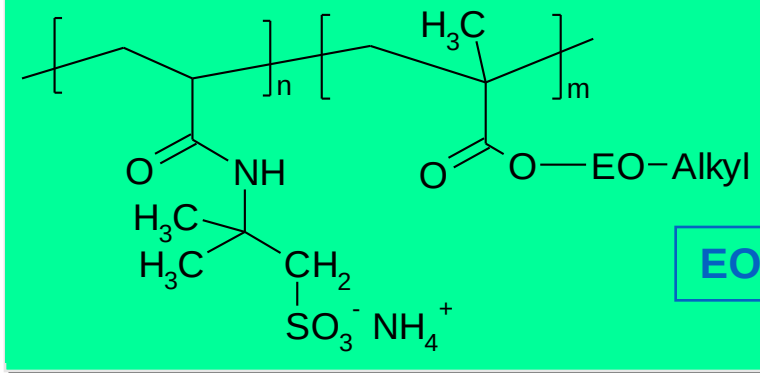

EO = $(CH_2\text{-}CH_2\text{-}O)_{25}$ and Alkyl = $C_{22}H_{45}$

Chemical composition	» Polymeric sulfonic acid, hydrophobically modified
INCI designation	» Ammonium Acryloyldimethyl-taurate/Beheneth-25 Methacrylate Copolymer
Physical form	» white powder
pH-value	» 4.0 - 6.0 (1% in dist. water)

Depletion Segregation

Depletion Flocculation

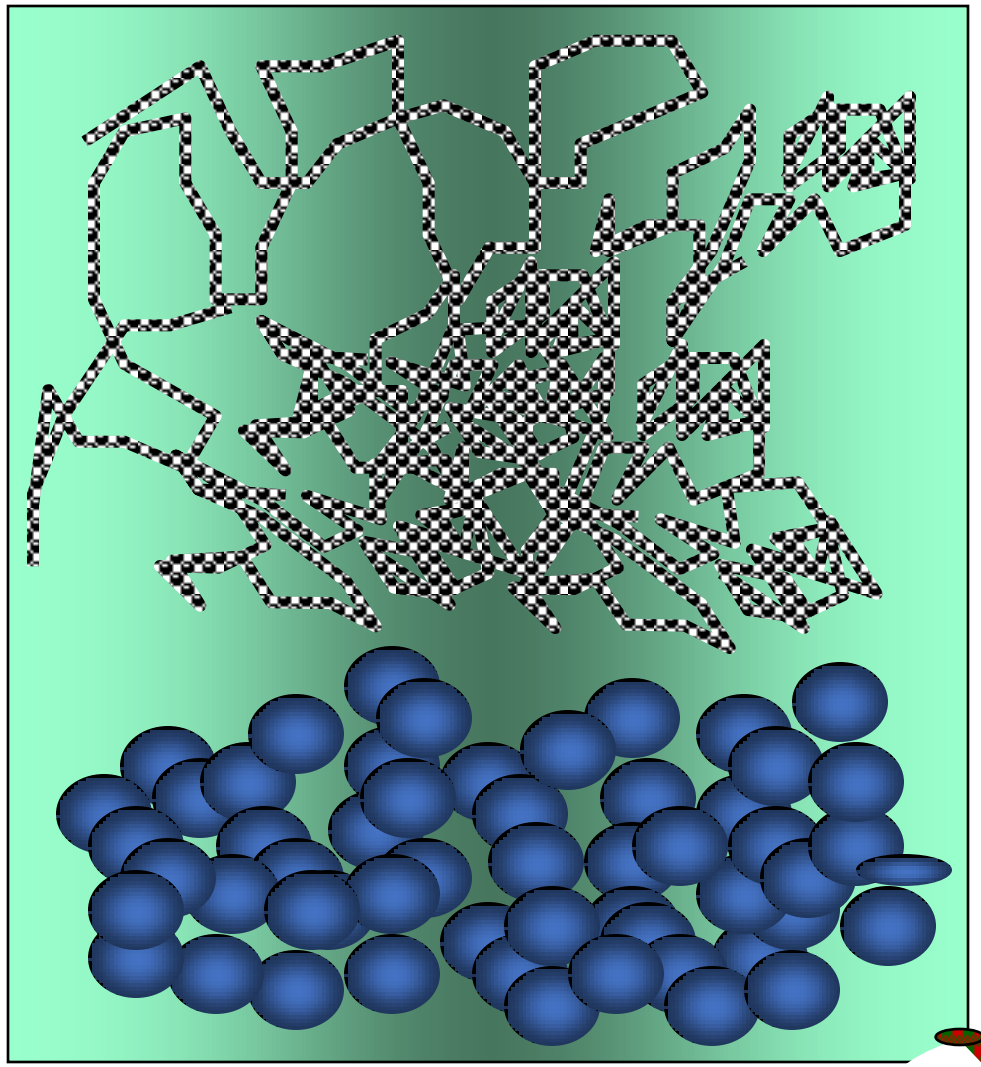

Depletion Flocculation by Particle Crowding

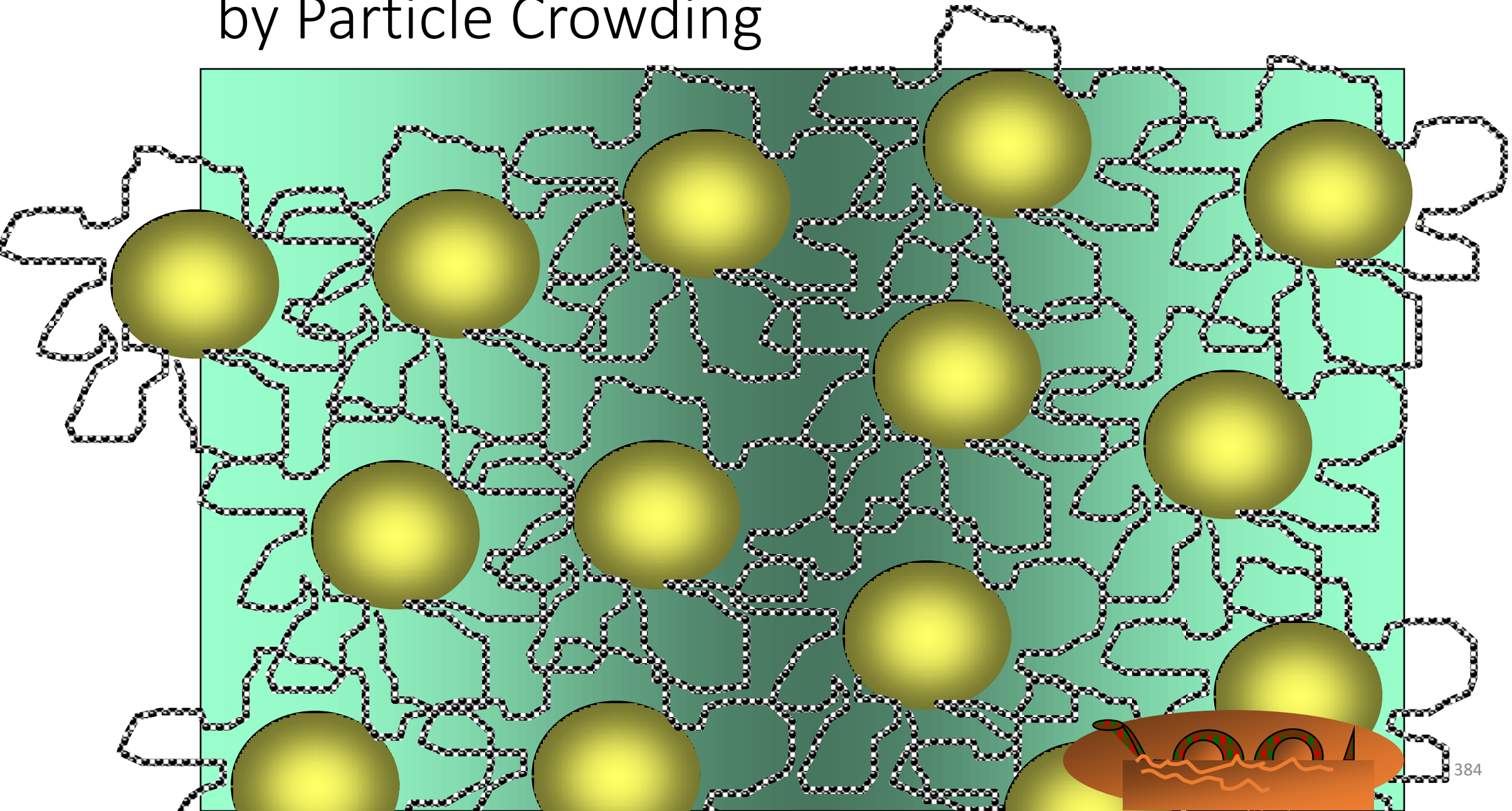

Depletion Flocculation by Particle Crowding

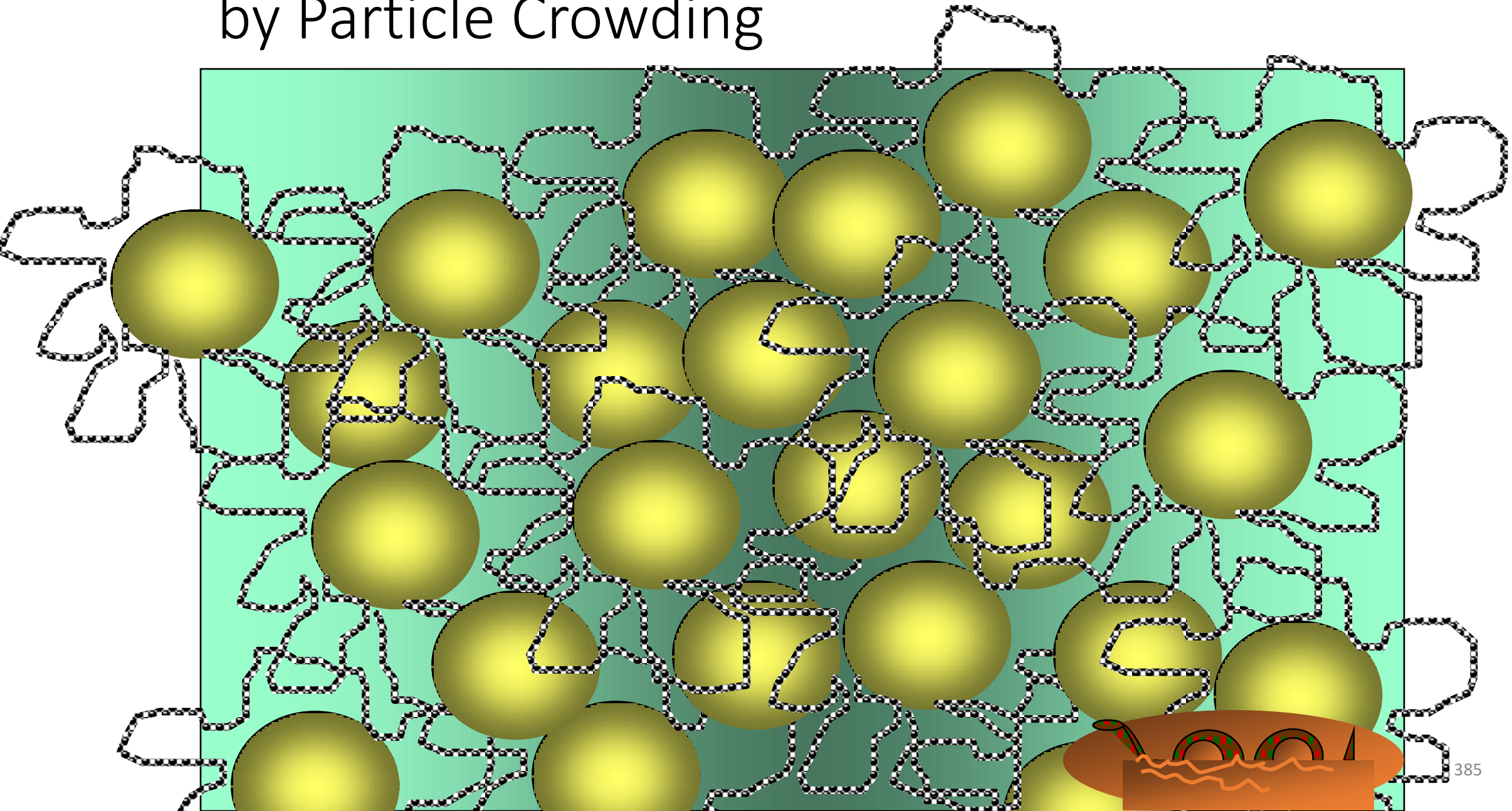

Depletion Flocculation by Particle Crowding

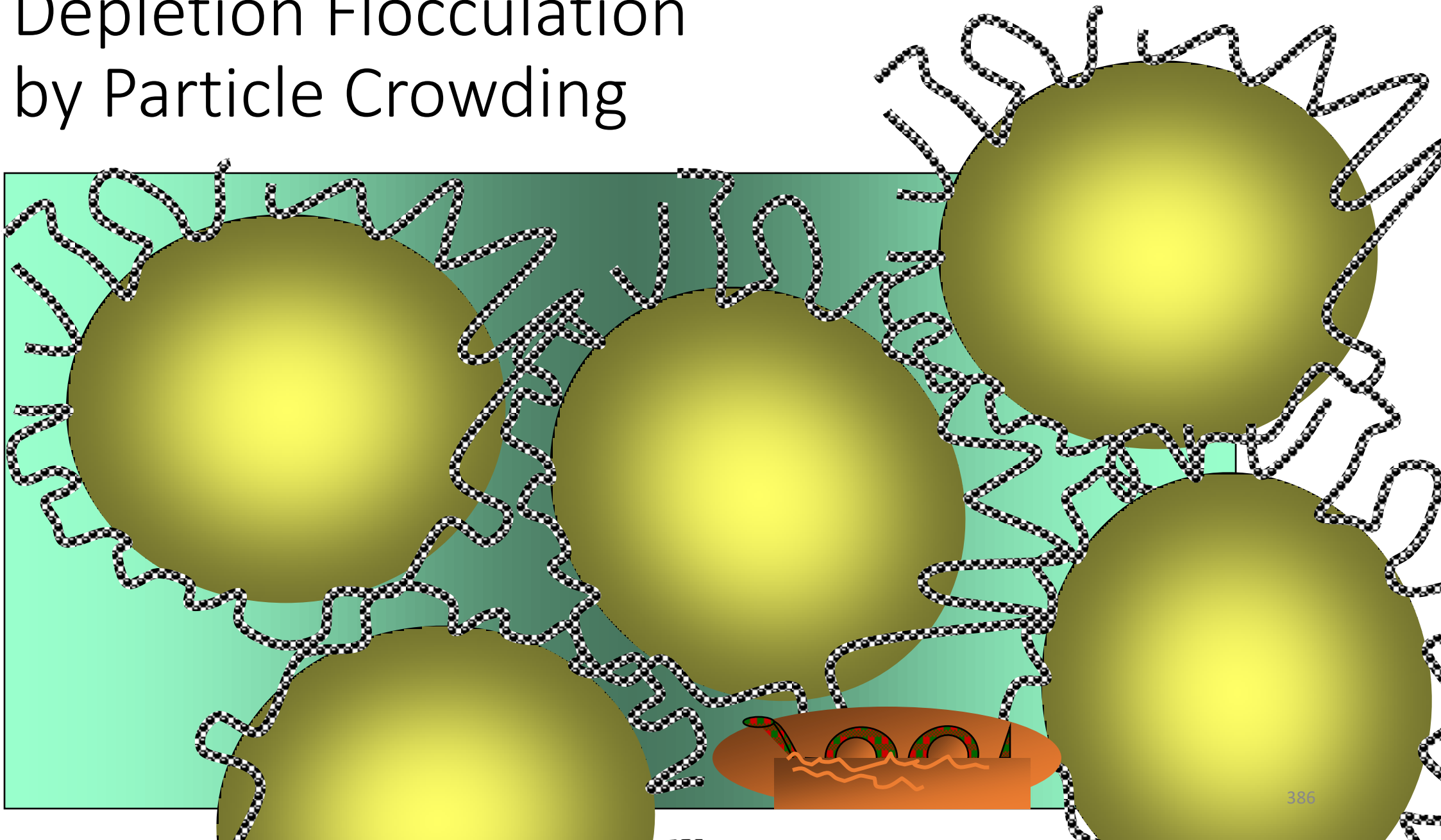

Depletion Flocculation by Particle Crowding

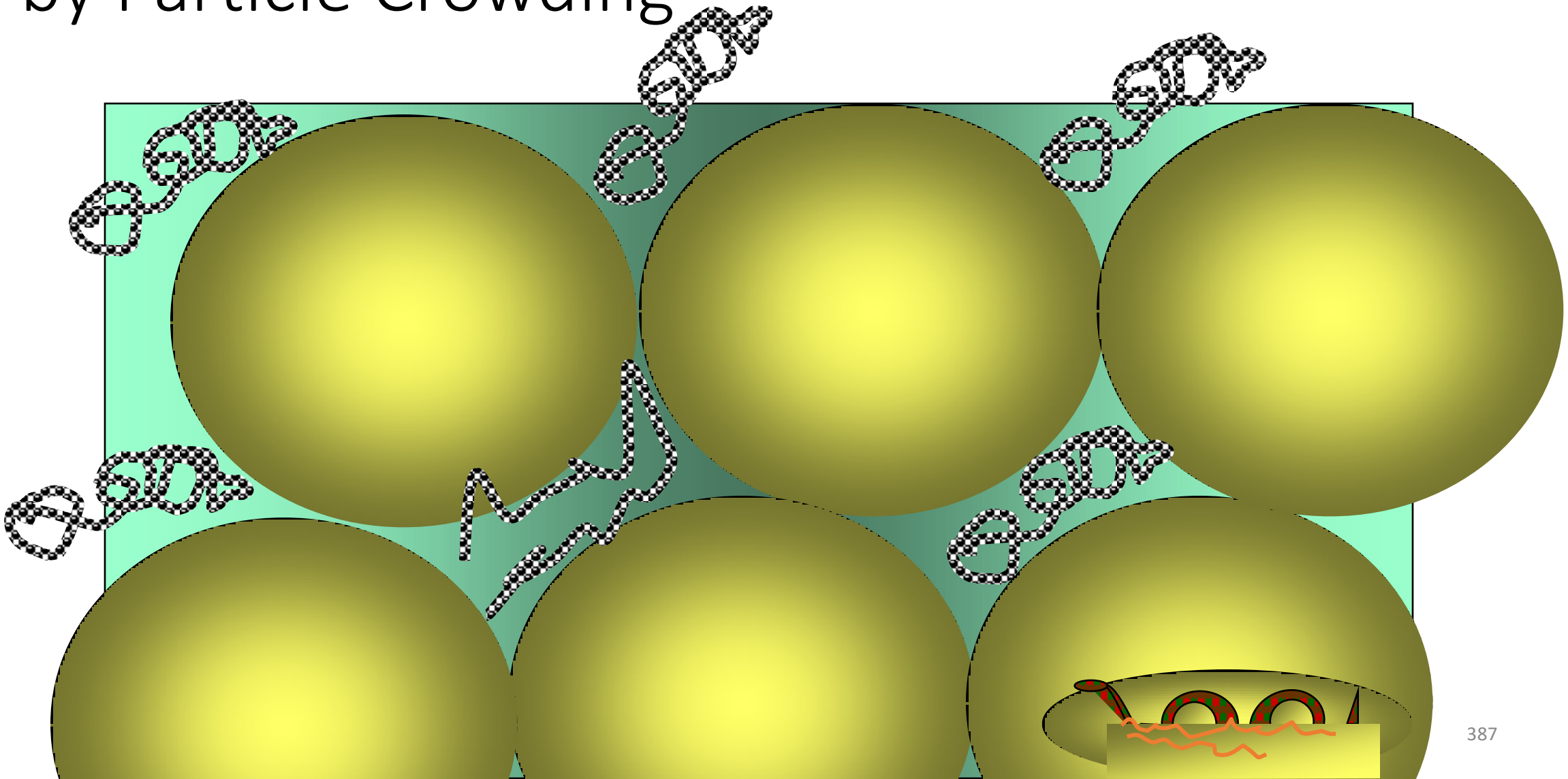

Depletion Flocculation

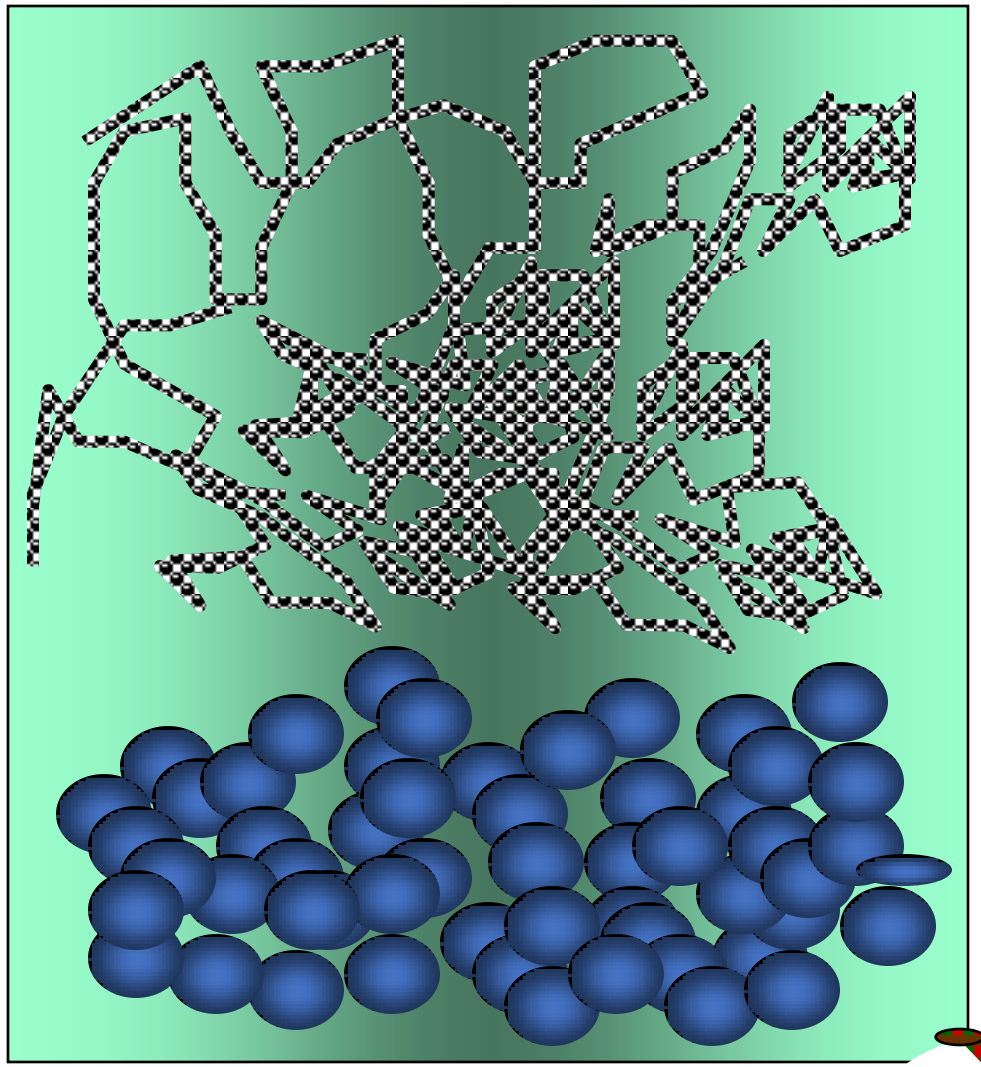

Depletion Stabilization

Depletion Stabilization

- Two particles in solution will be attracted to each other by London Dispersion Forces

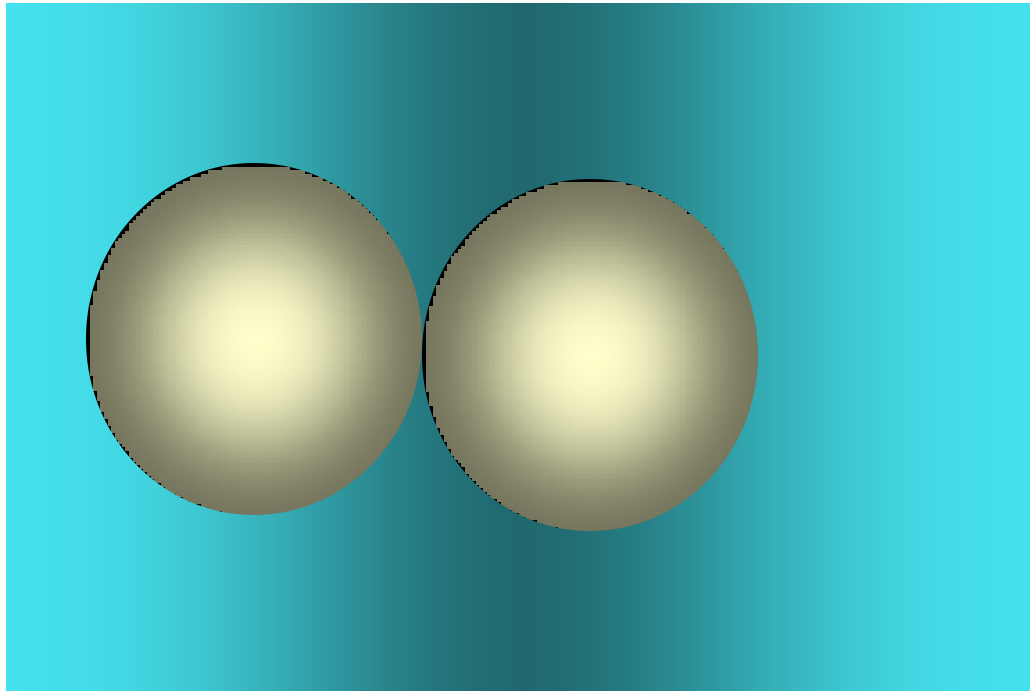

Depletion Stabilization

- The flocculation of particles can be prevented by the presence of dissolved, nonadsorbing polymer.

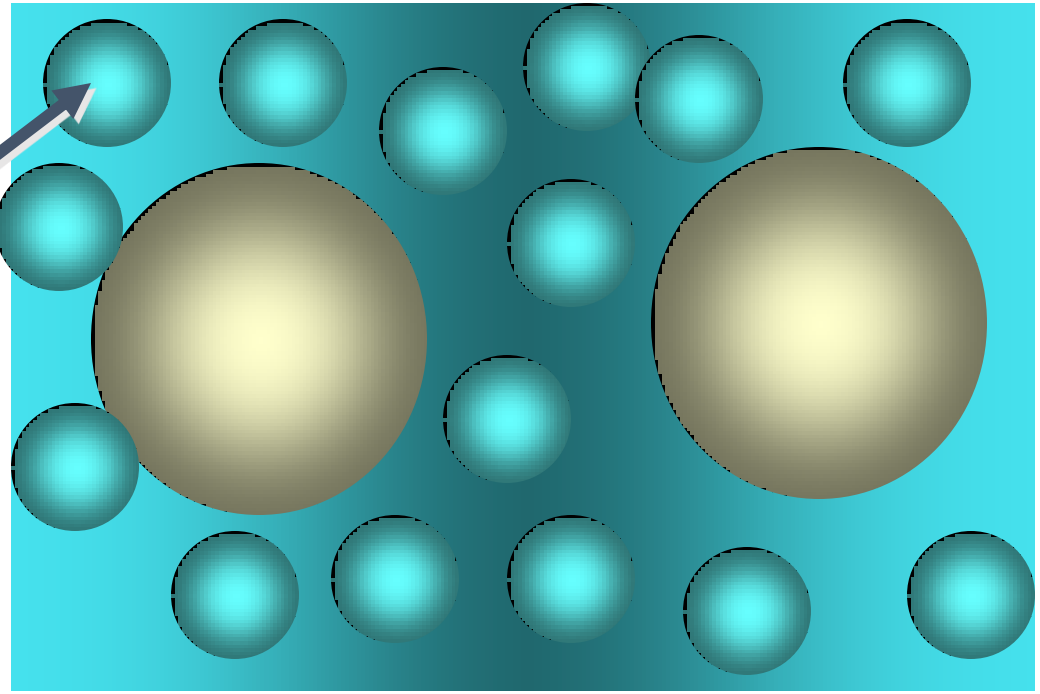

Depletion Interaction
Walz/Sharma Model

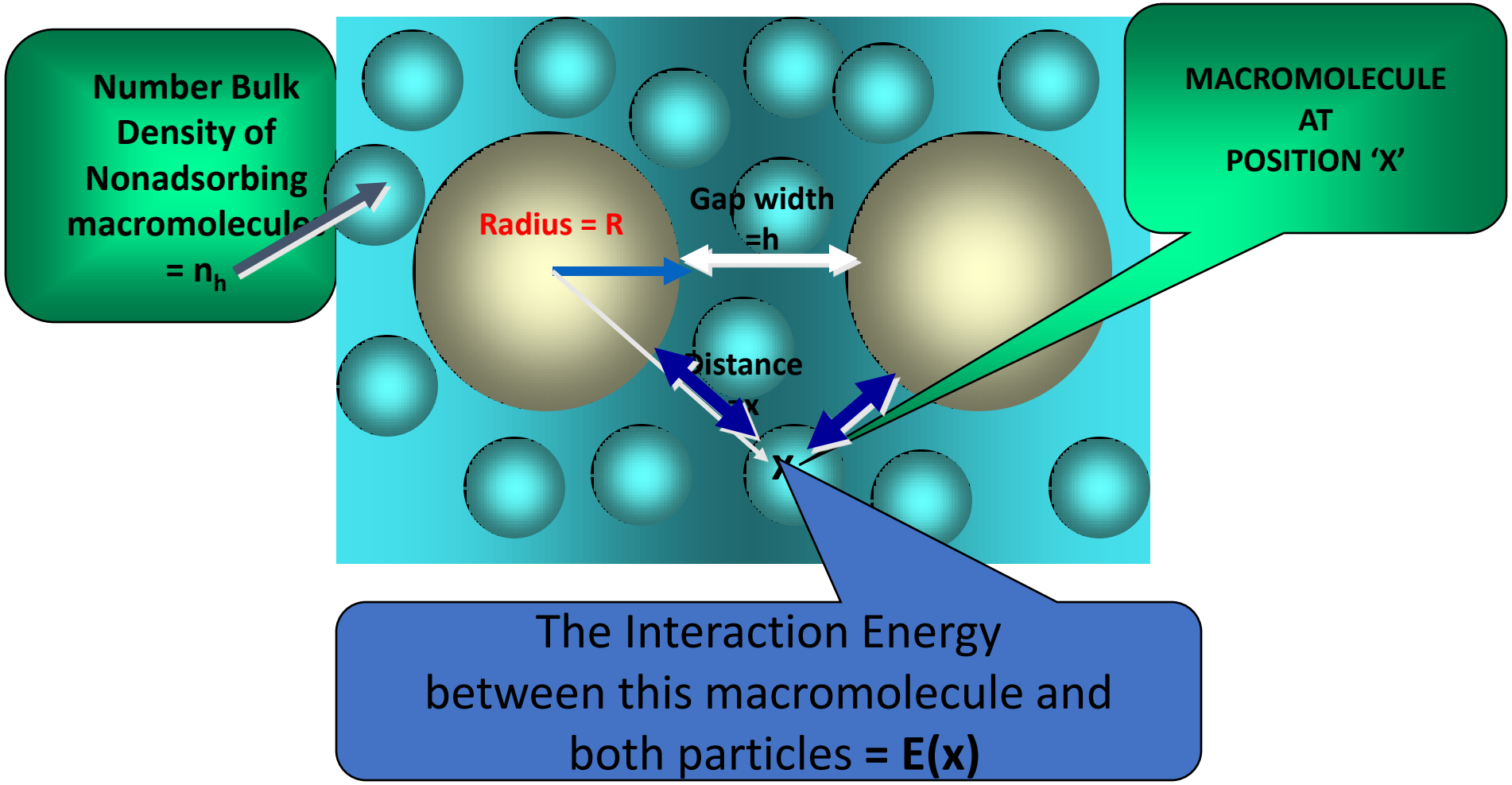

Depletion Interaction
Walz/Sharma Model

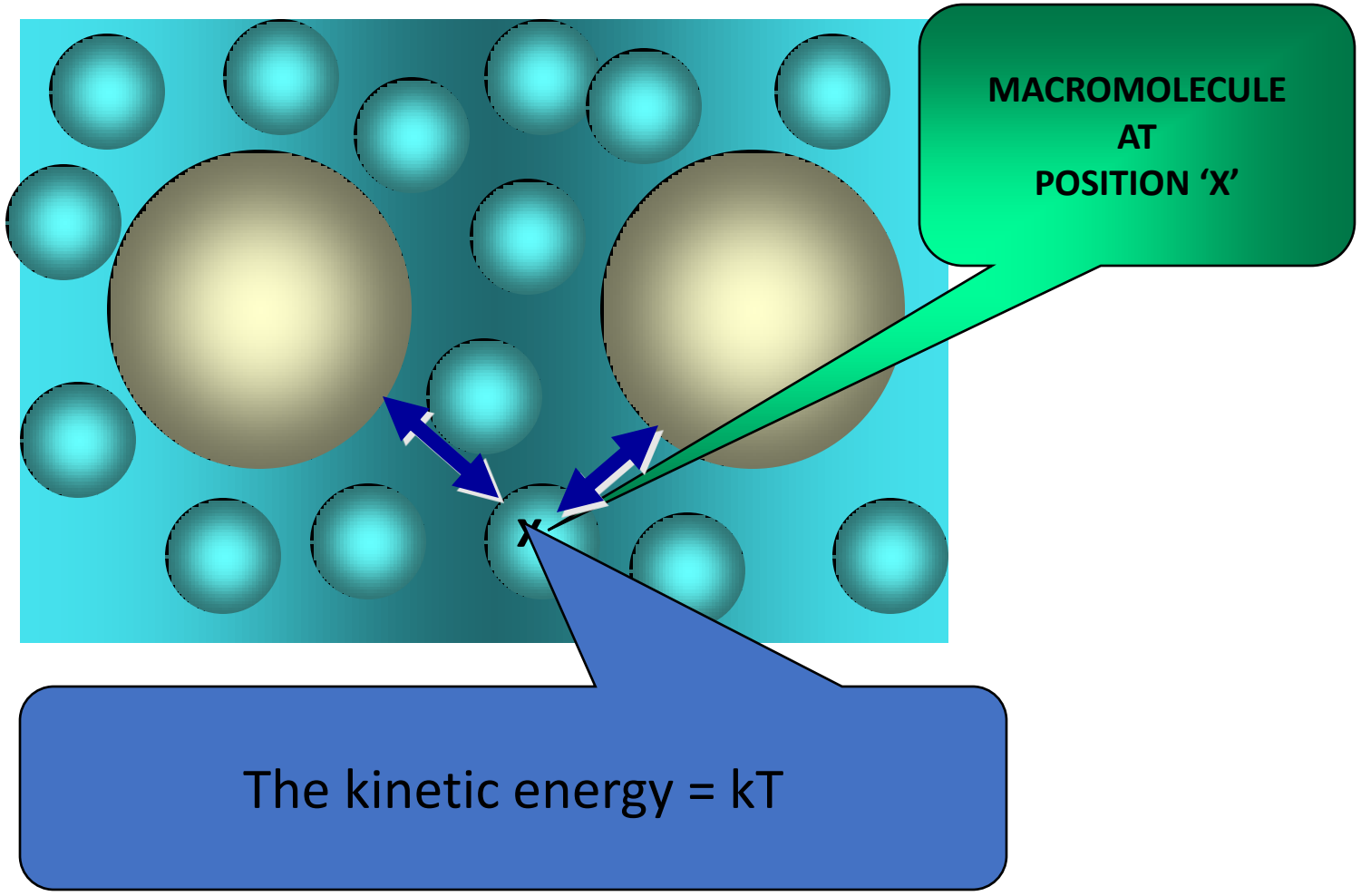

Depletion Interaction
Walz/Sharma Model

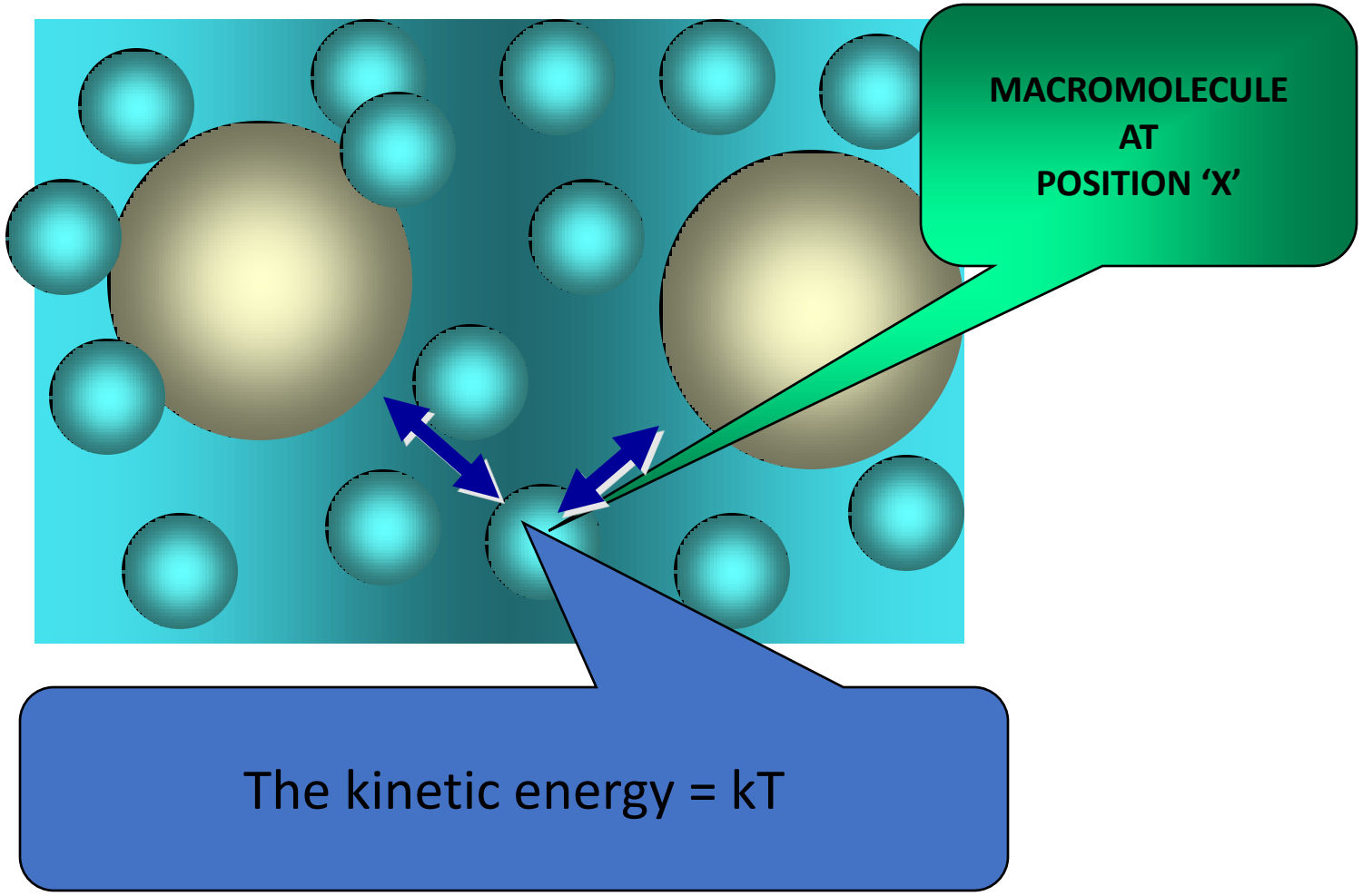

Depletion Interaction
Walz/Sharma Model

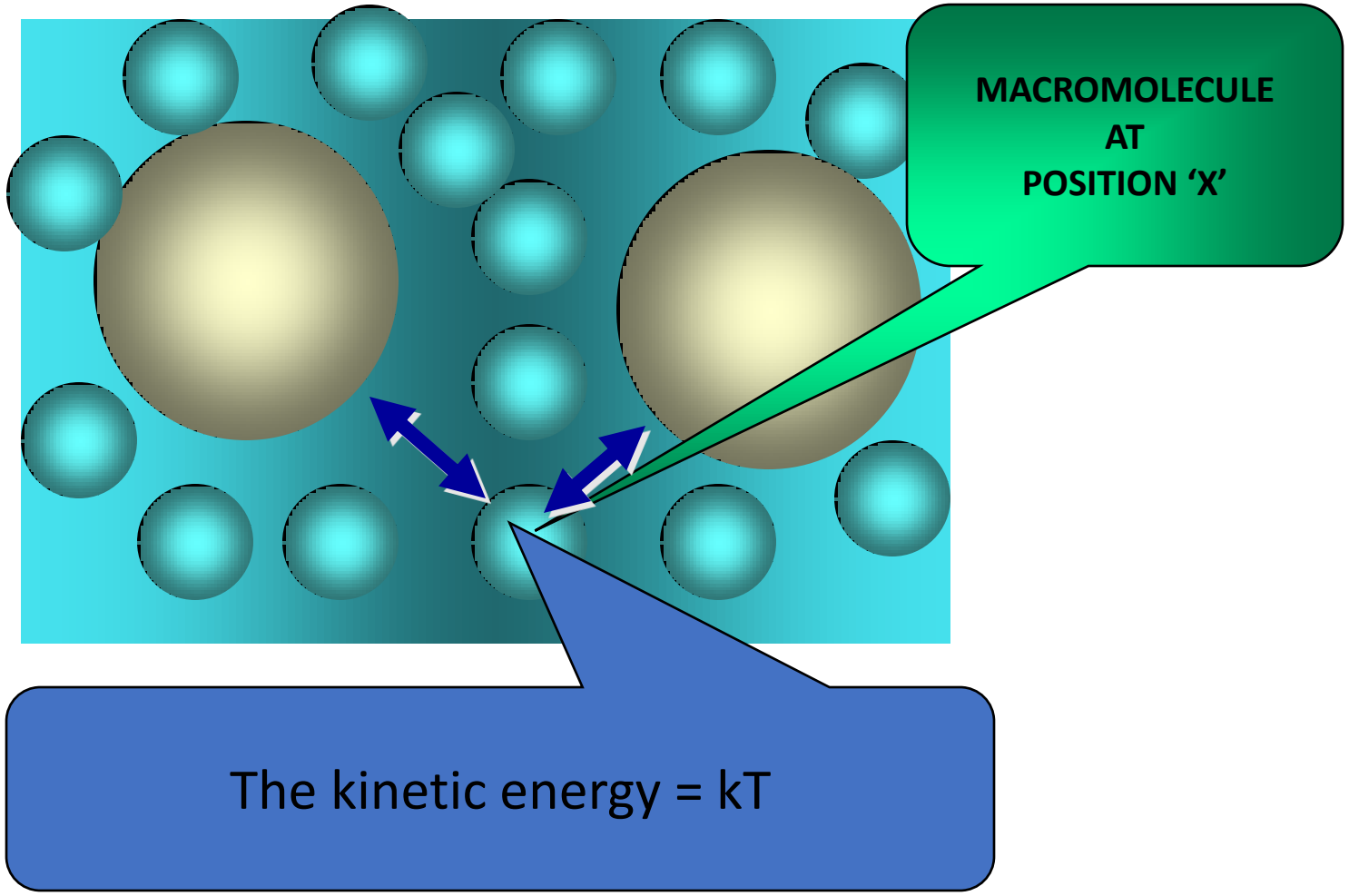

Depletion Interaction
Walz/Sharma Model

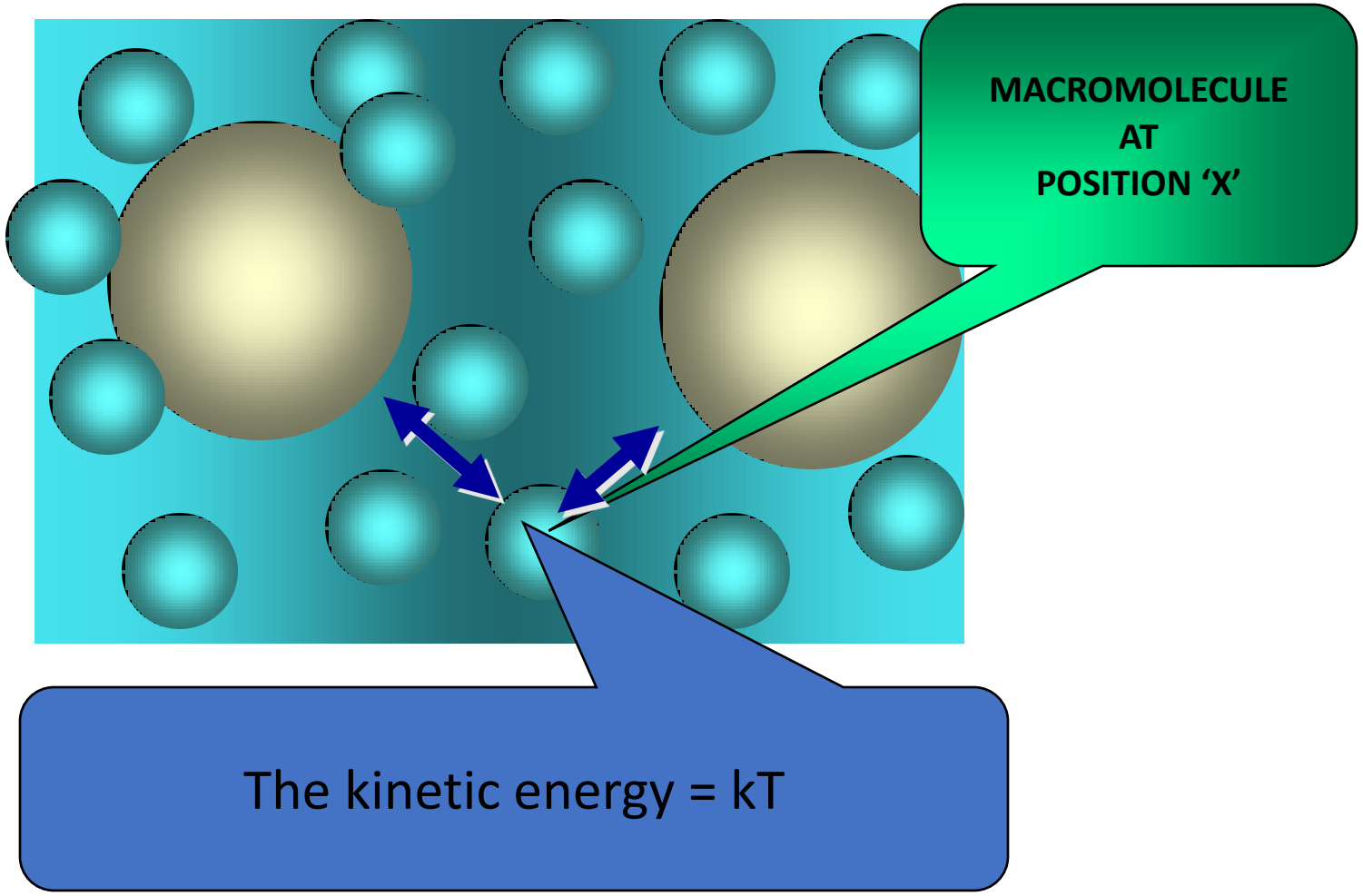

Depletion Interaction
Walz/Sharma Model

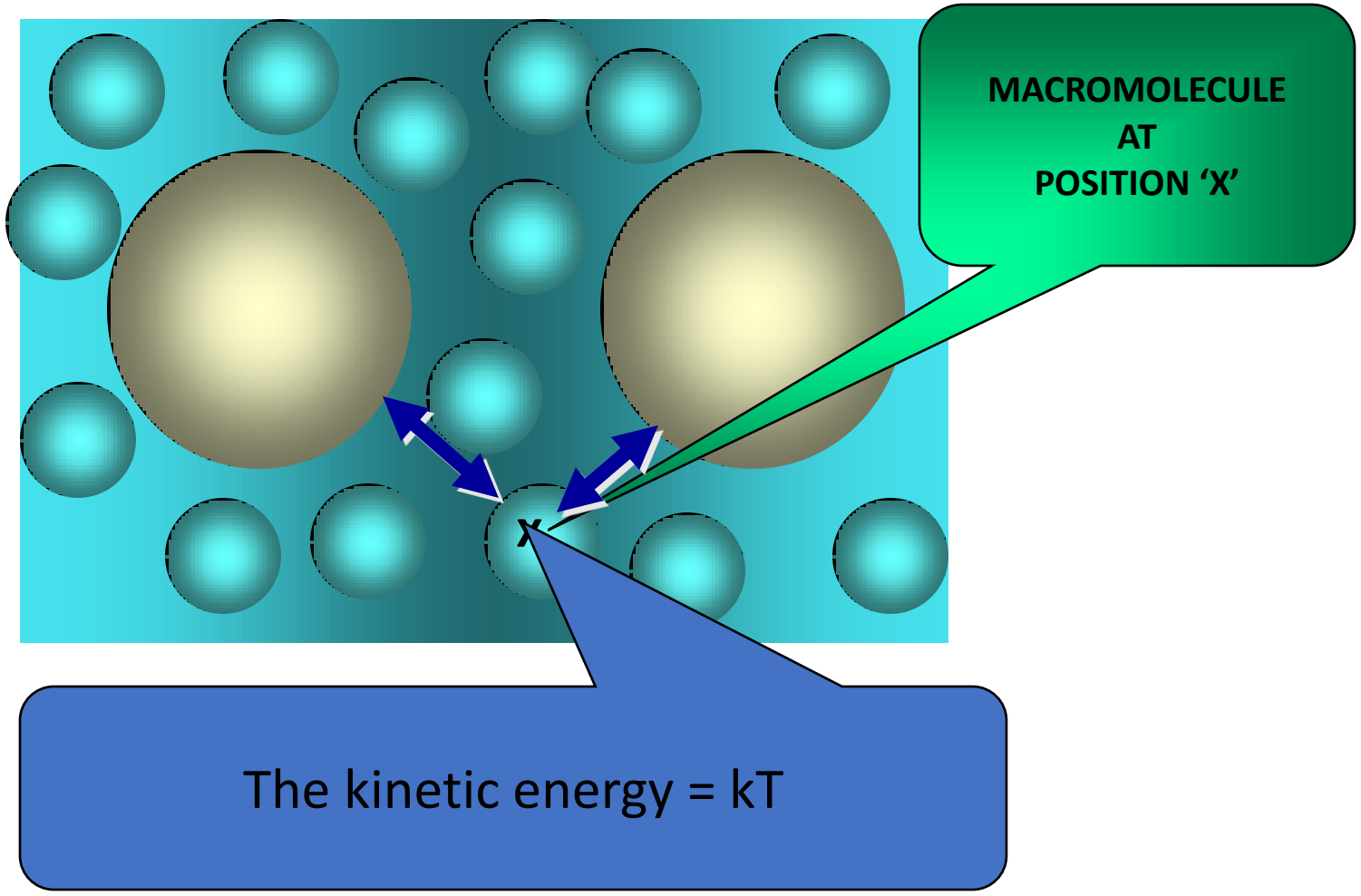

Depletion Interaction
Walz/Sharma Model

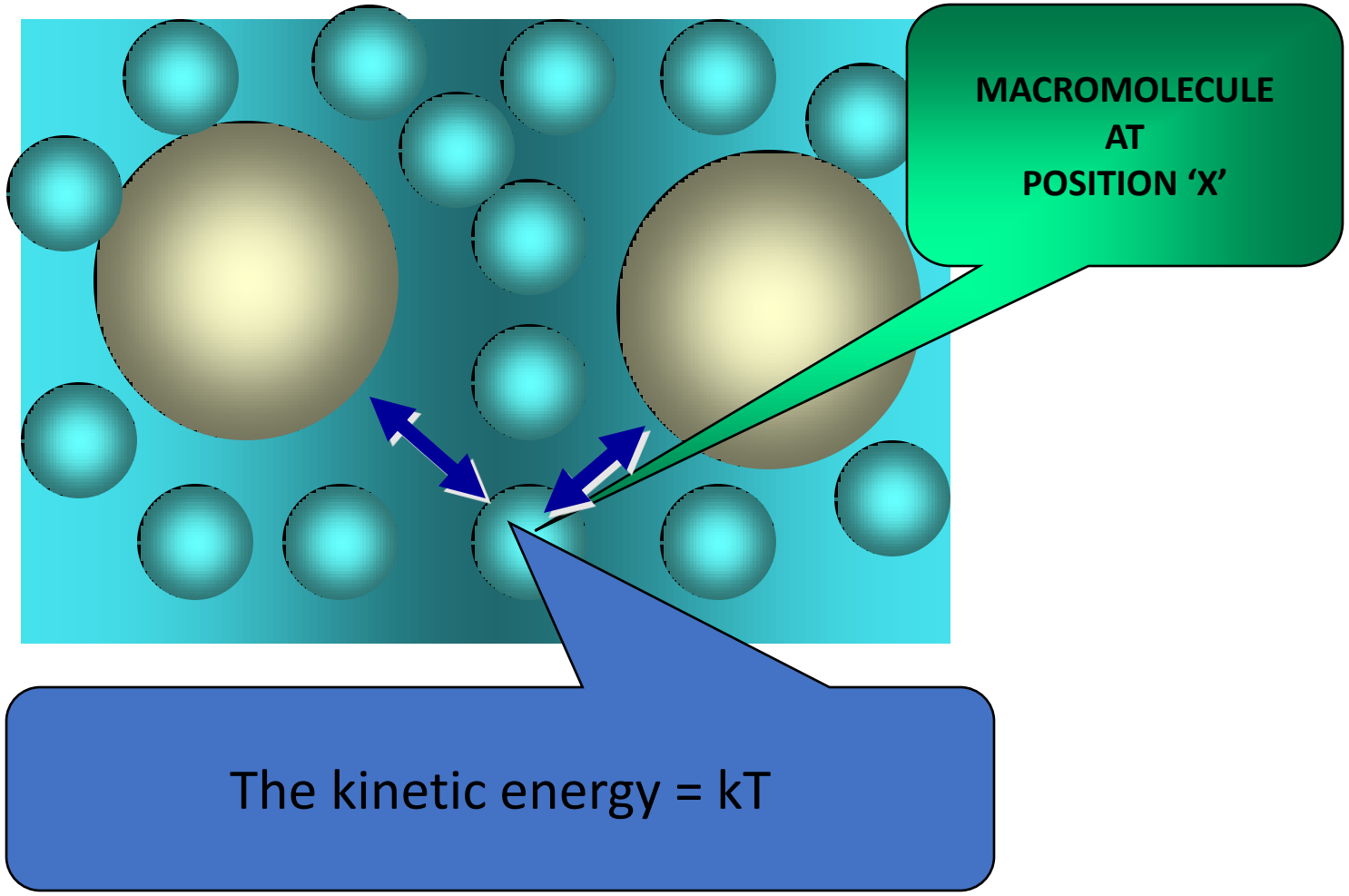

Depletion Interaction
Walz/Sharma Model

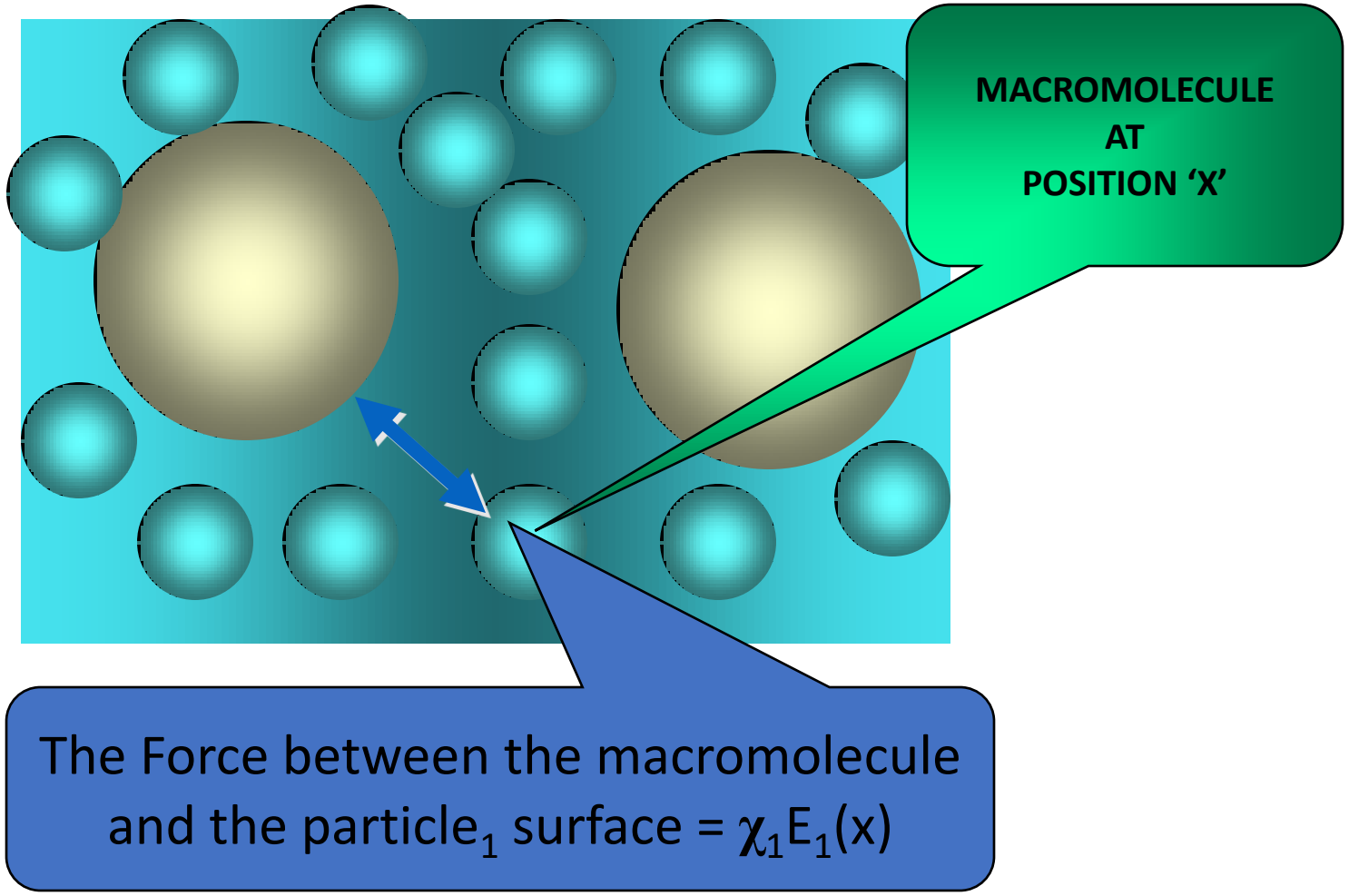

Depletion Interaction Walz/Sharma Model

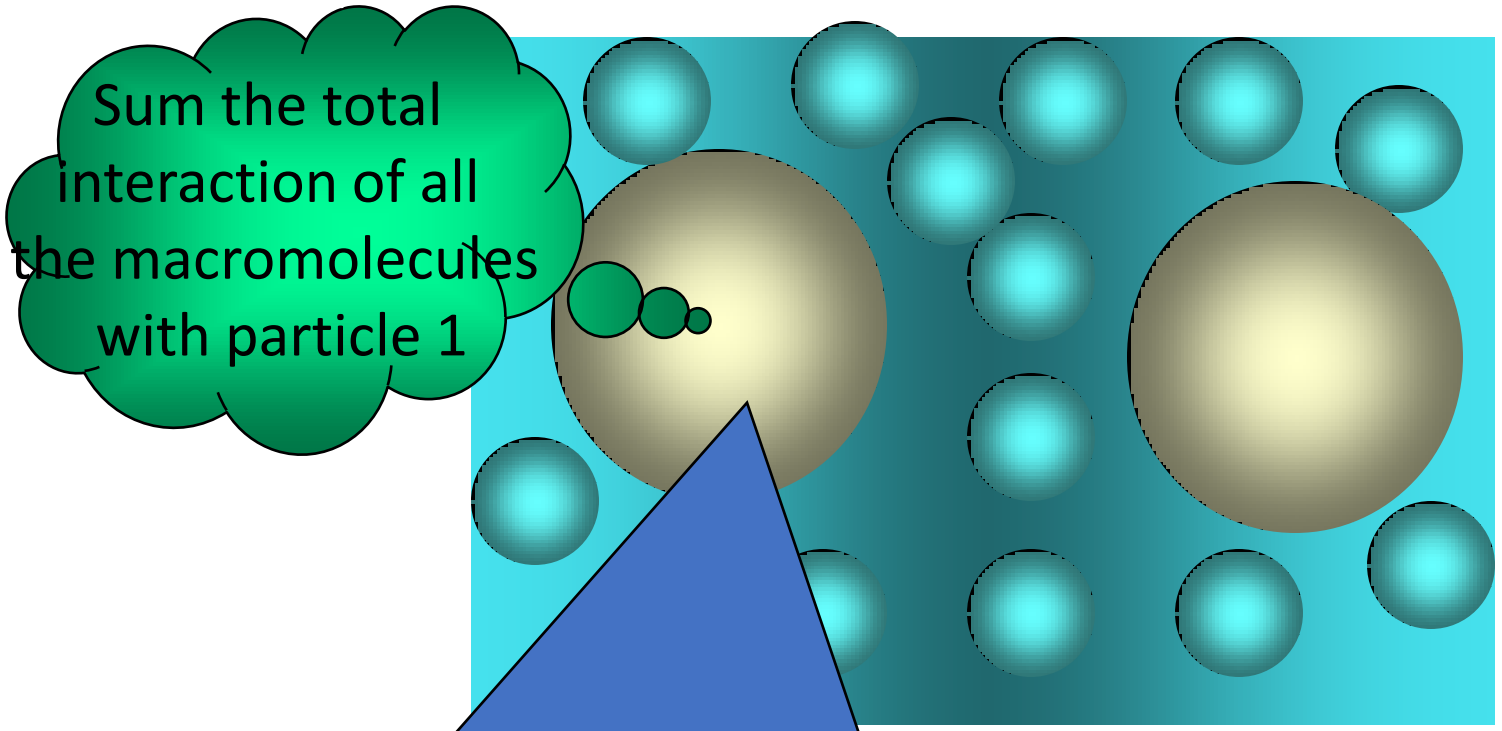

The Force exerted on Particle$_1$ = $\mathbf{A}\mathbf{n}_b \exp\{\frac{E(x)}{kT}\} \chi_1 E_1(x)\, dx$

Depletion Interaction Walz/Sharma Model

The Depletion Energy can be calculated from the depletion force on particle 1

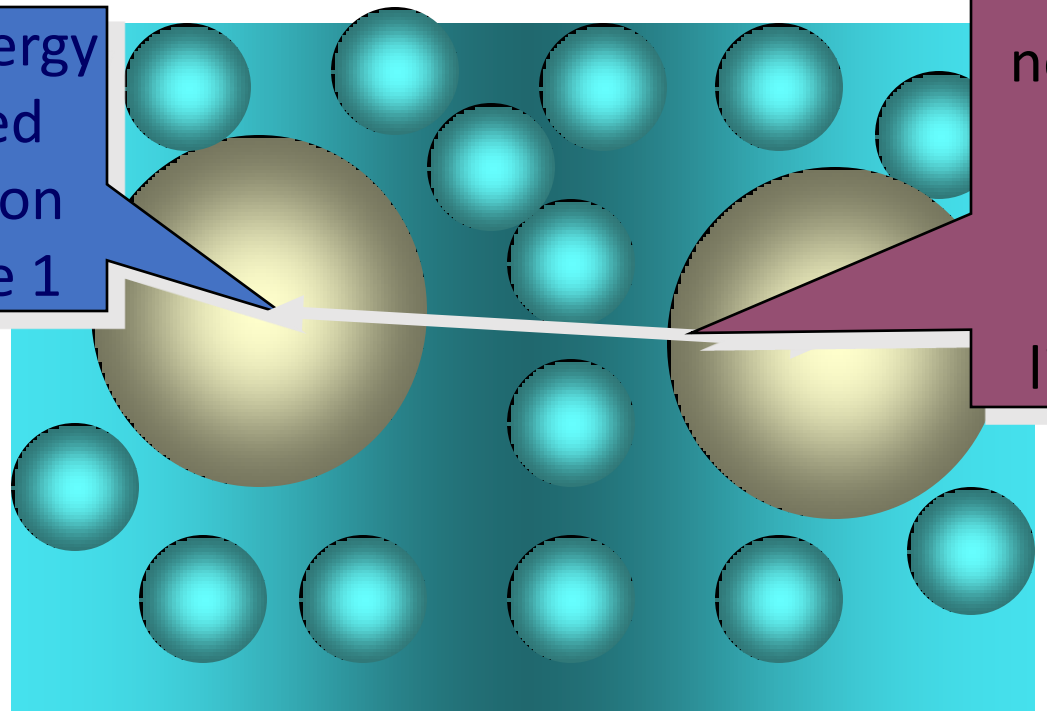

$F_1(h)$ is the net force acting between the particles along the line of centers

Emulsions Stabilized by Particles

- Solid stabilized emulsions
  - encountered in nature
  - Major problem in crude and synthetic fuels
  - Food emulsions

Tambe, D.E.; Sharma, M.M.; *J. Colloid Interface Sci.,* **157,** 244, (1993)

Particles as Emulsion Stabilizers

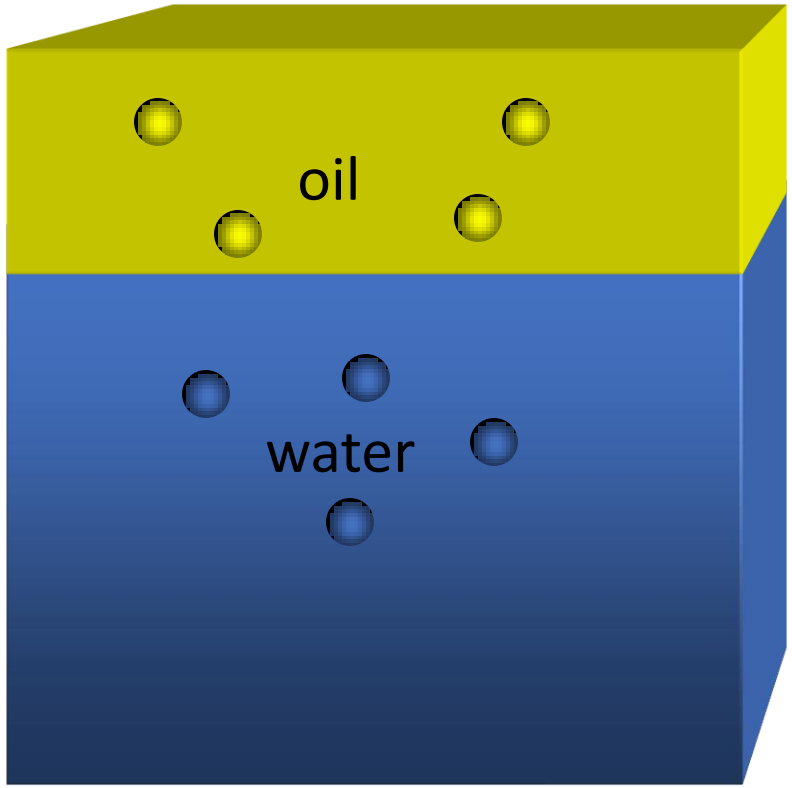

Hydrophobic Particles will seek the oil phase

Hydrophilic Particles will seek the aqueous phase

Particles of Intermediate Hydrophobicity

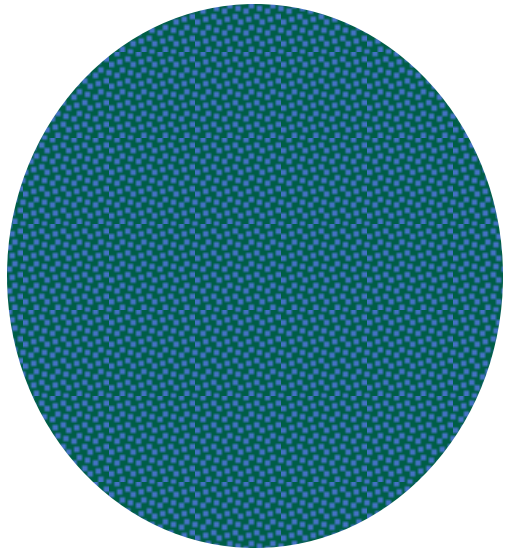

These particles possess different ratios of surface hydrophobic and hydrophilic groups

Particles of Intermediate Hydrophobicity

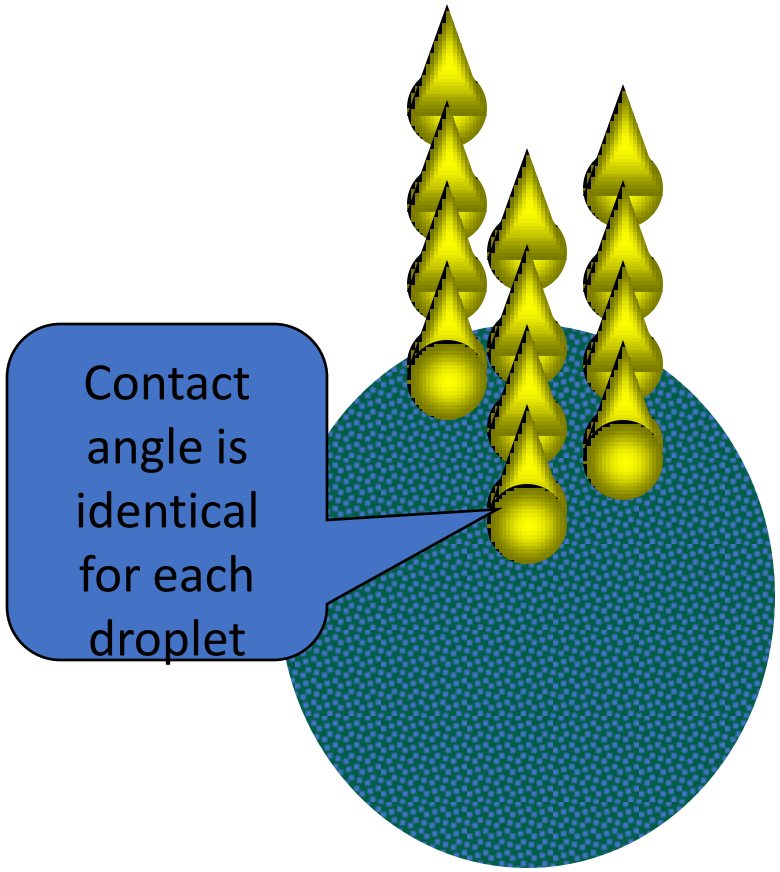

These particles possess different ratios of surface hydrophobic and hydrophilic groups—But they wet uniformly

Particles as Emulsion Stabilizers

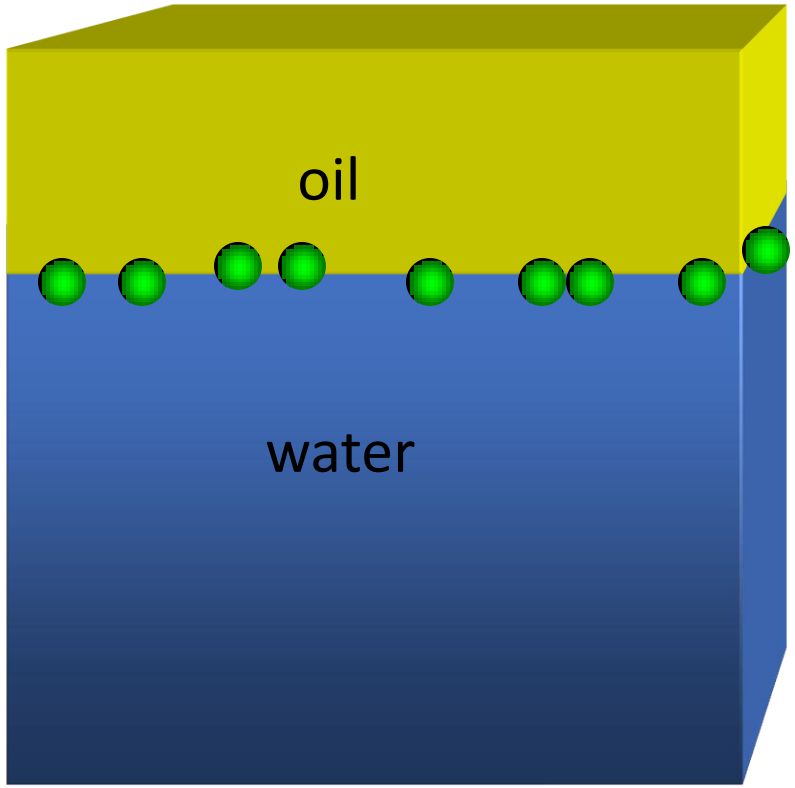

Particles of intermediate hydrophobicity will seek the oil water interface

Particles as Emulsion Stabilizers

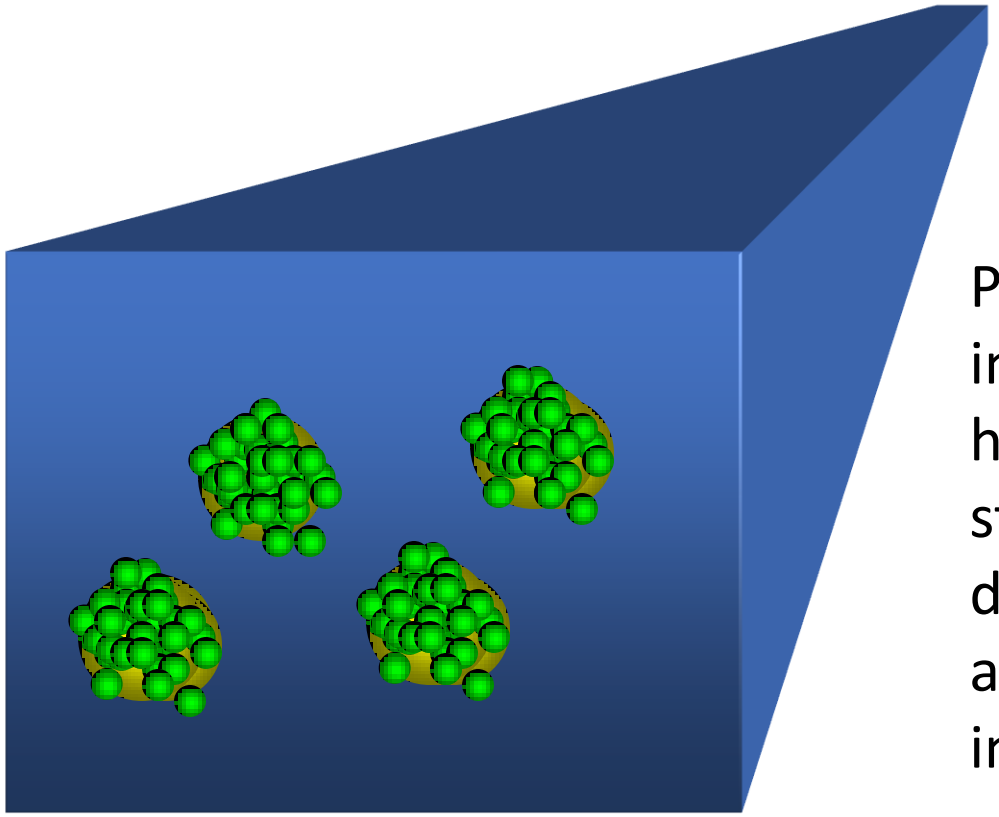

Particles of intermediate hydrophobicity stabilize emulsion droplets by adsorbing at the oil/water interface

Binks, B.P.; Lumsden, S.O.; *Langmuir,* **2000,** *16,* 2539

Pickering Emulsions

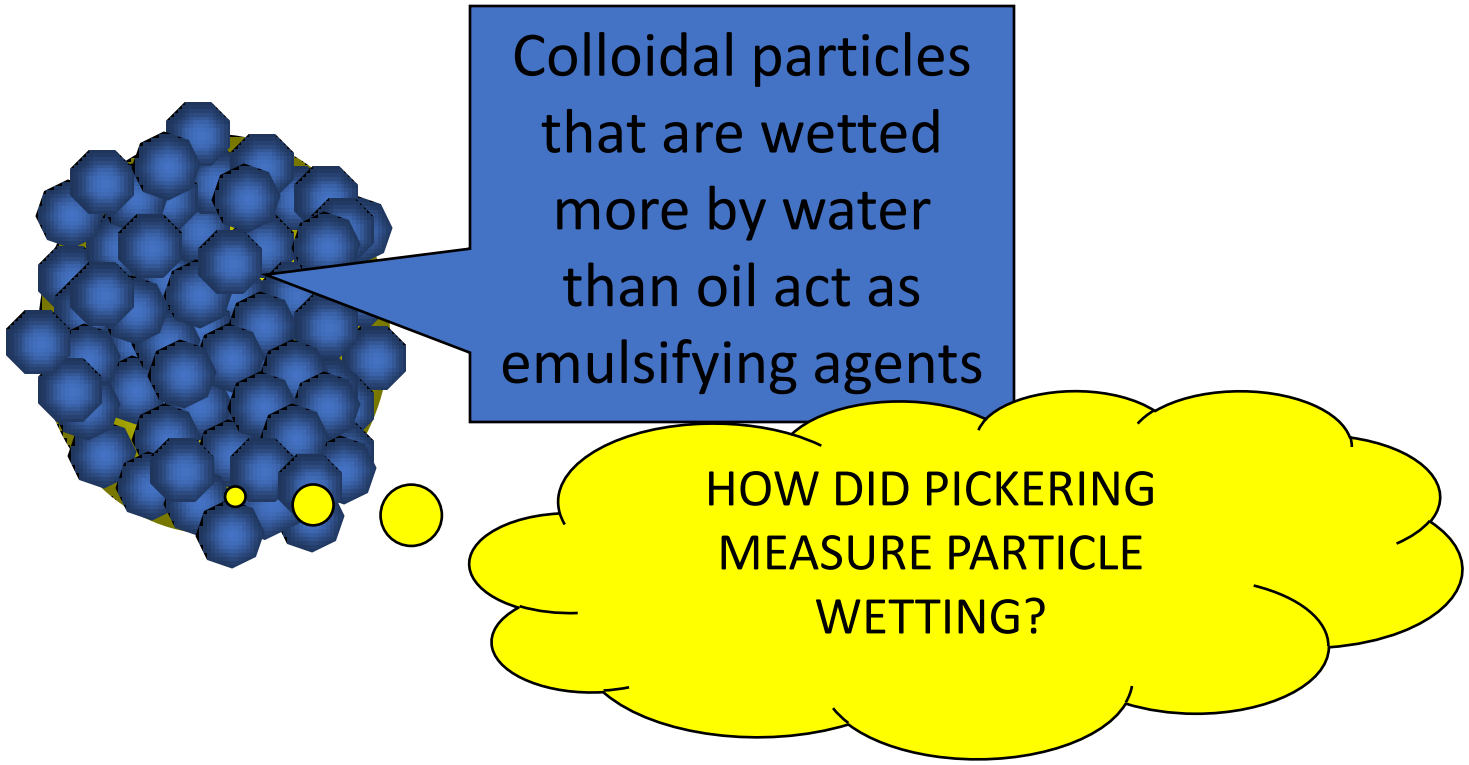

Pickering, S.U.; *J. Chem. Soc.*, **91,** 2001, (1907)

Pickering Emulsions

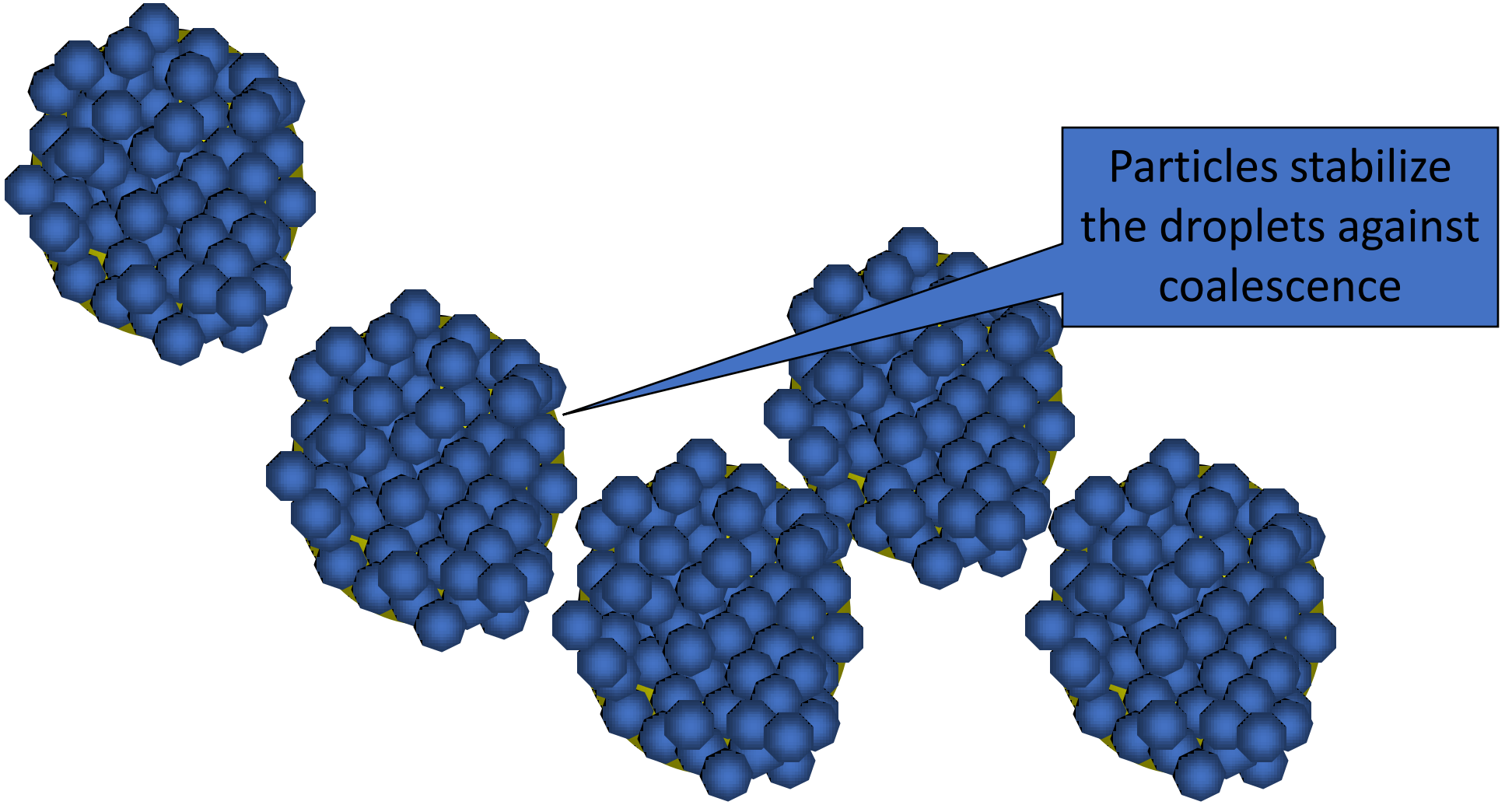

Pickering, S.U.; *J. Chem. Soc.*, **91,** 2001, (1907)

Colloid -Stabilized Emulsions

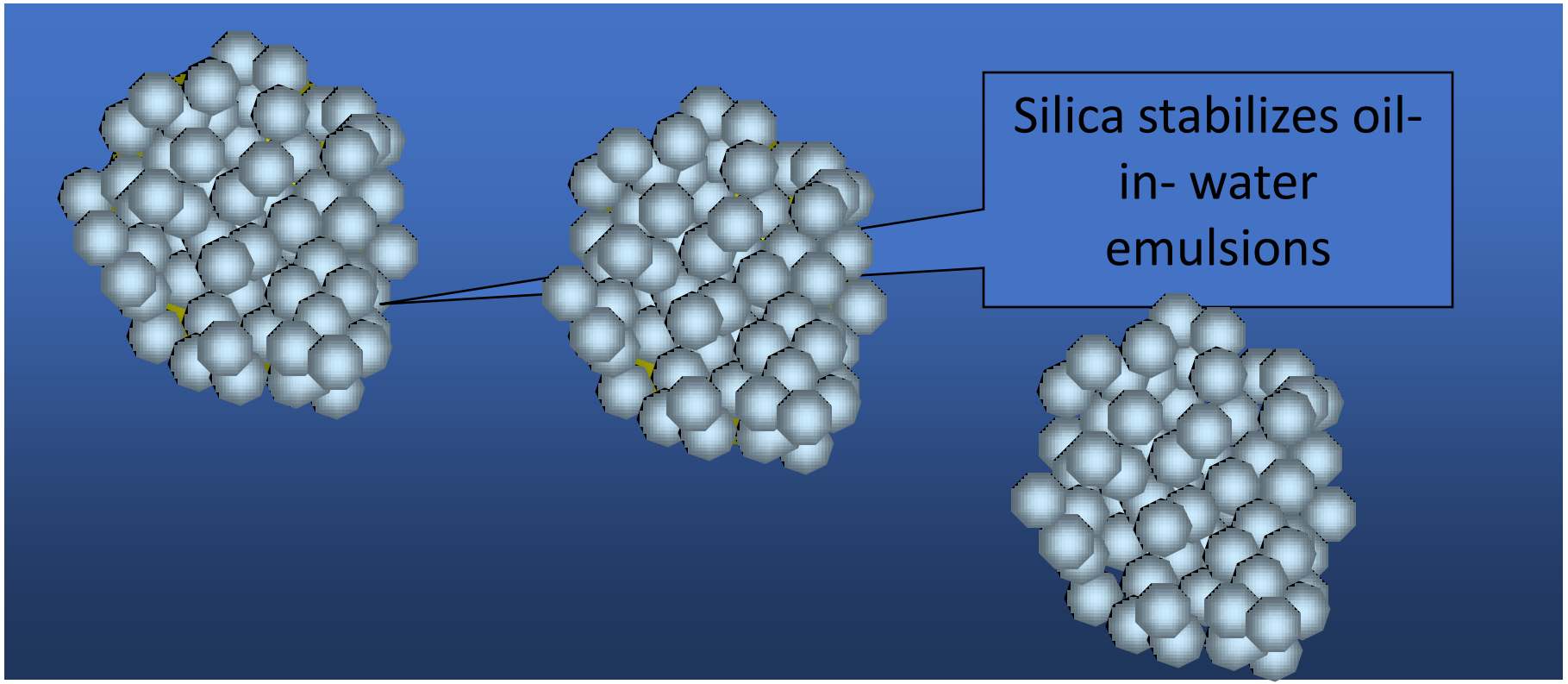

Briggs, T.R.; *Ind. Eng. Chem.;* **13,** (11), 1008, (1921)

Water-wet particles stabilize water-in-oil emulsions

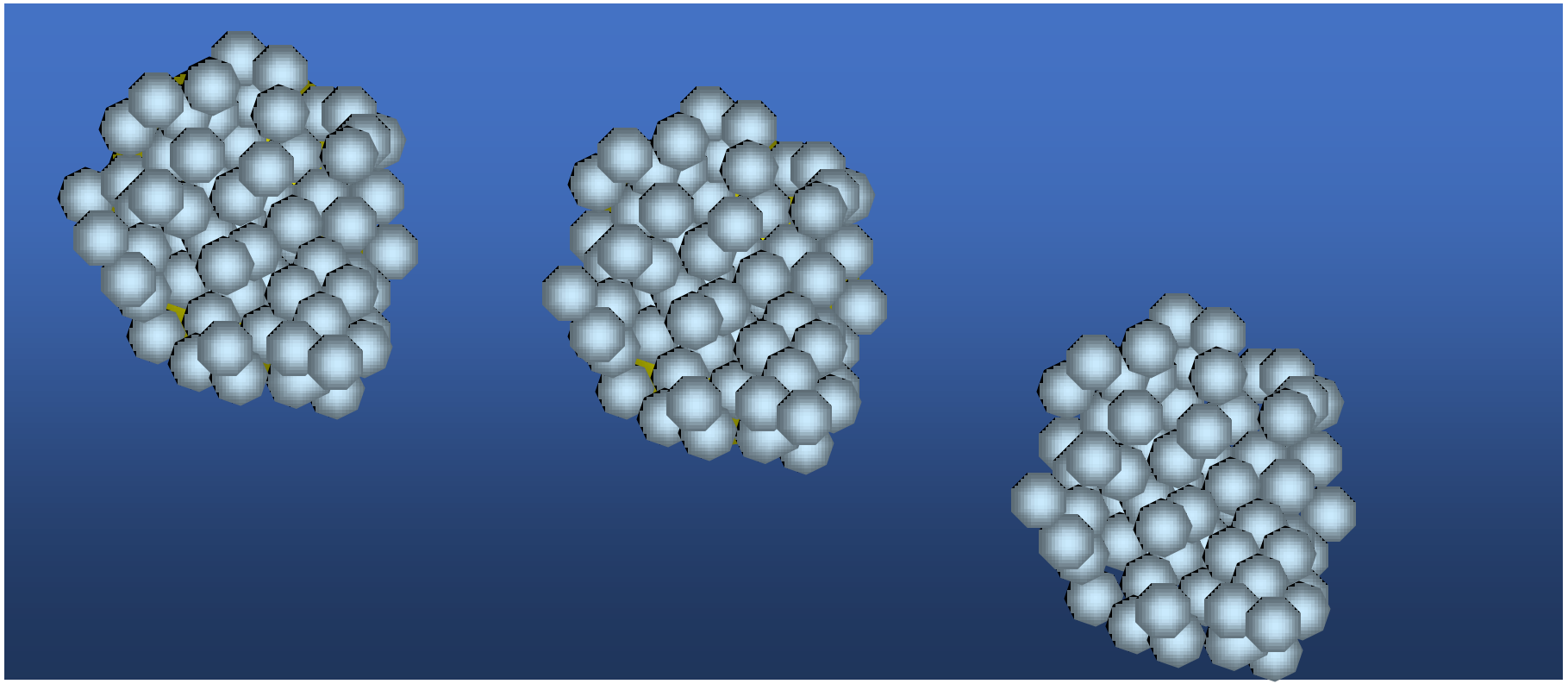

Finkle, P.; Draper, D.; Hildebrand, J.H.; *J. Amer. Chem. Soc.,* **45,** 2780**,** (1923)

Colloid -Stabilized Emulsions

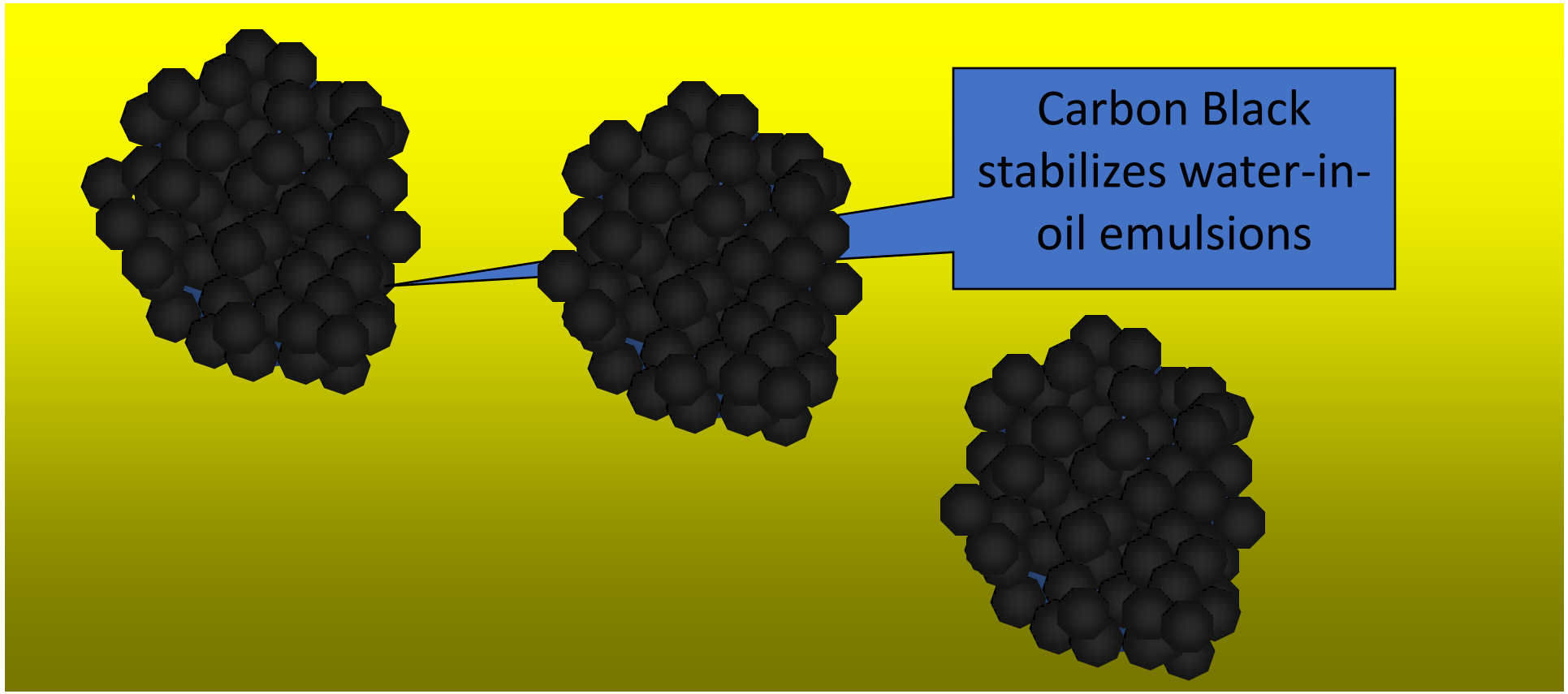

Briggs, T.R.; *Ind. Eng. Chem.;* **13,** (11), 1008, (1921)

Oil-wet particles stabilize water-in-oil emulsions

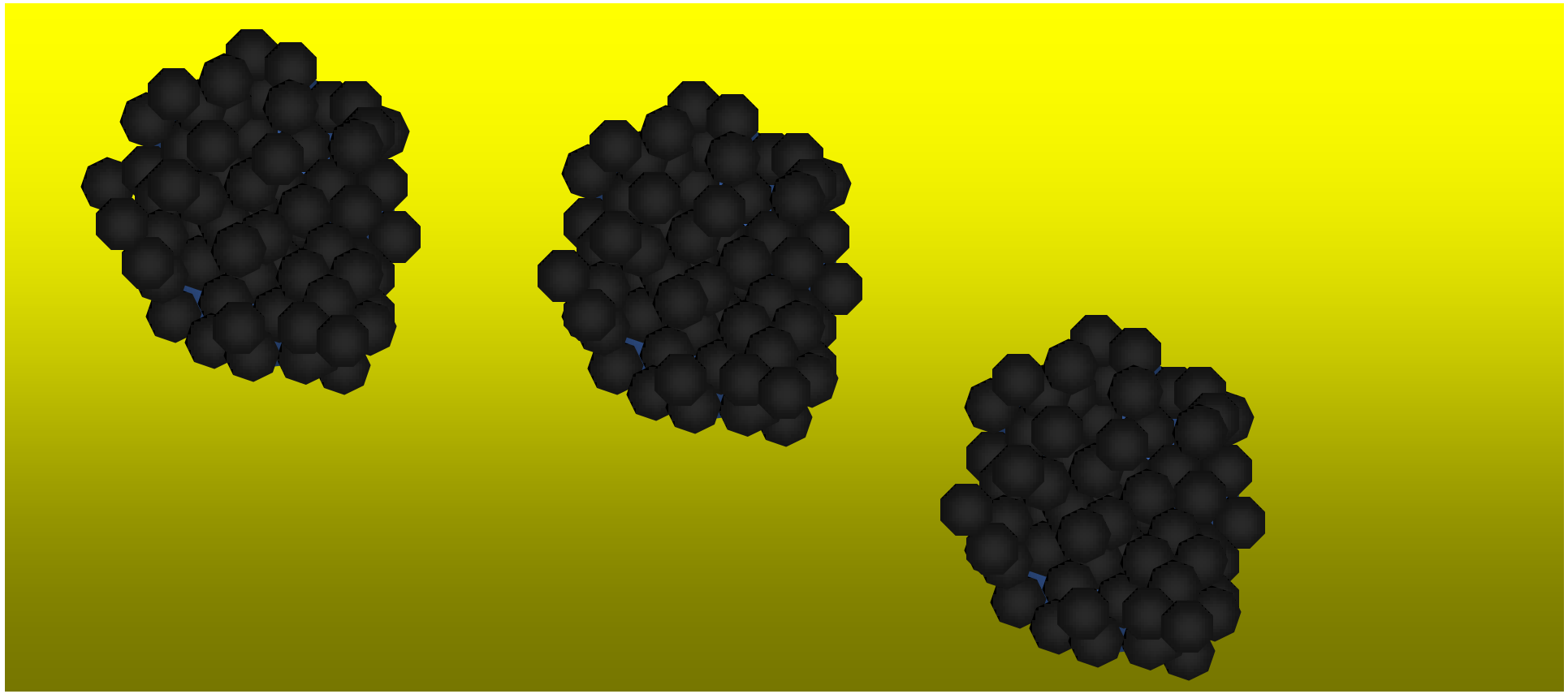

Finkle, P.; Draper, D.; Hildebrand, J.H.; *J. Amer. Chem. Soc.,* **45,** 2780**,** (1923)

Colloid -Stabilized Emulsions
Mixtures of C Black and Silica

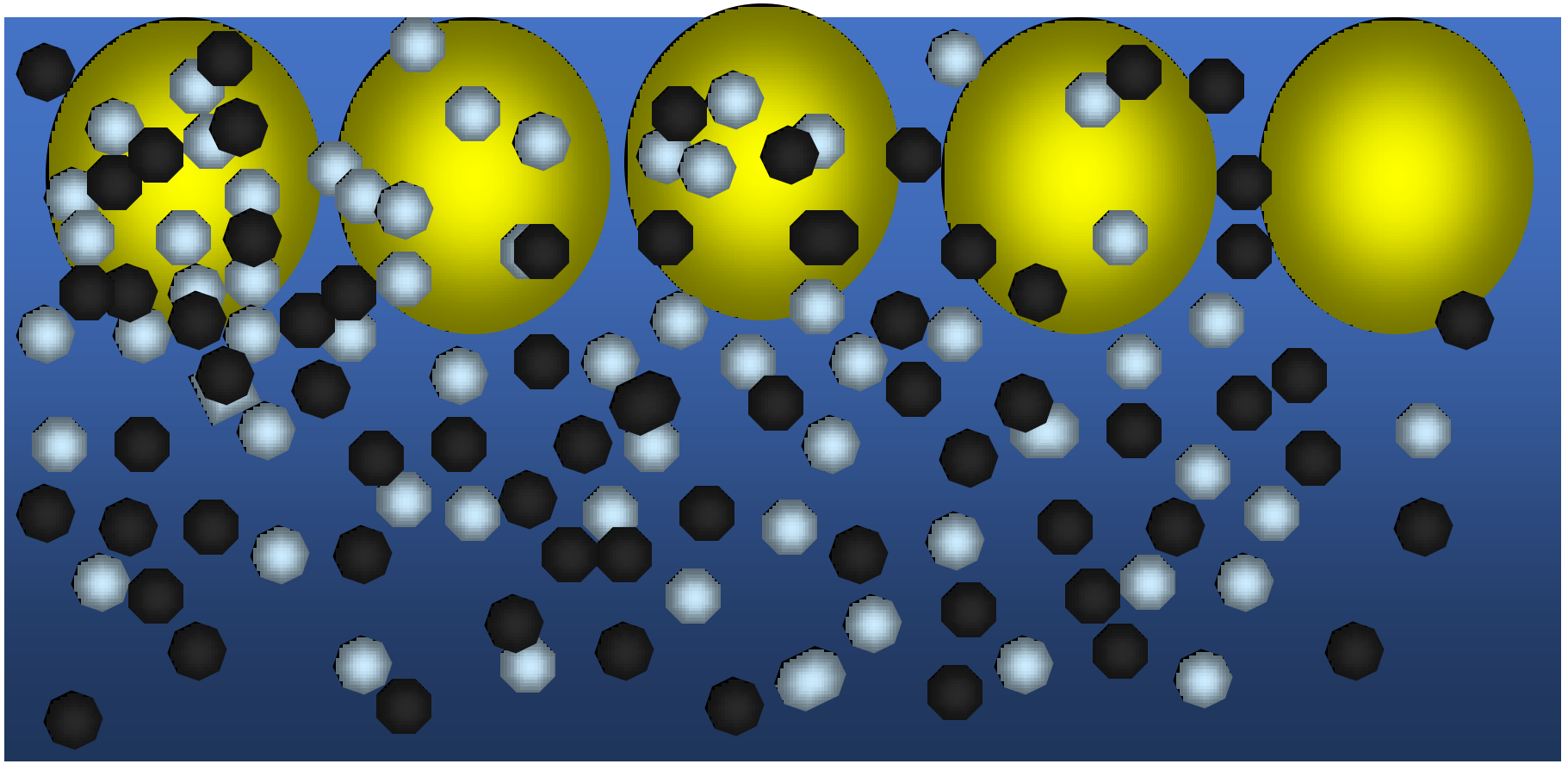

Briggs, T.R.; *Ind. Eng. Chem.;* **13,** (11), 1008, (1921)What is the effect of crystalline ferric oxide?

Colloid -Stabilized Emulsions
Mixtures of C Black and Silica

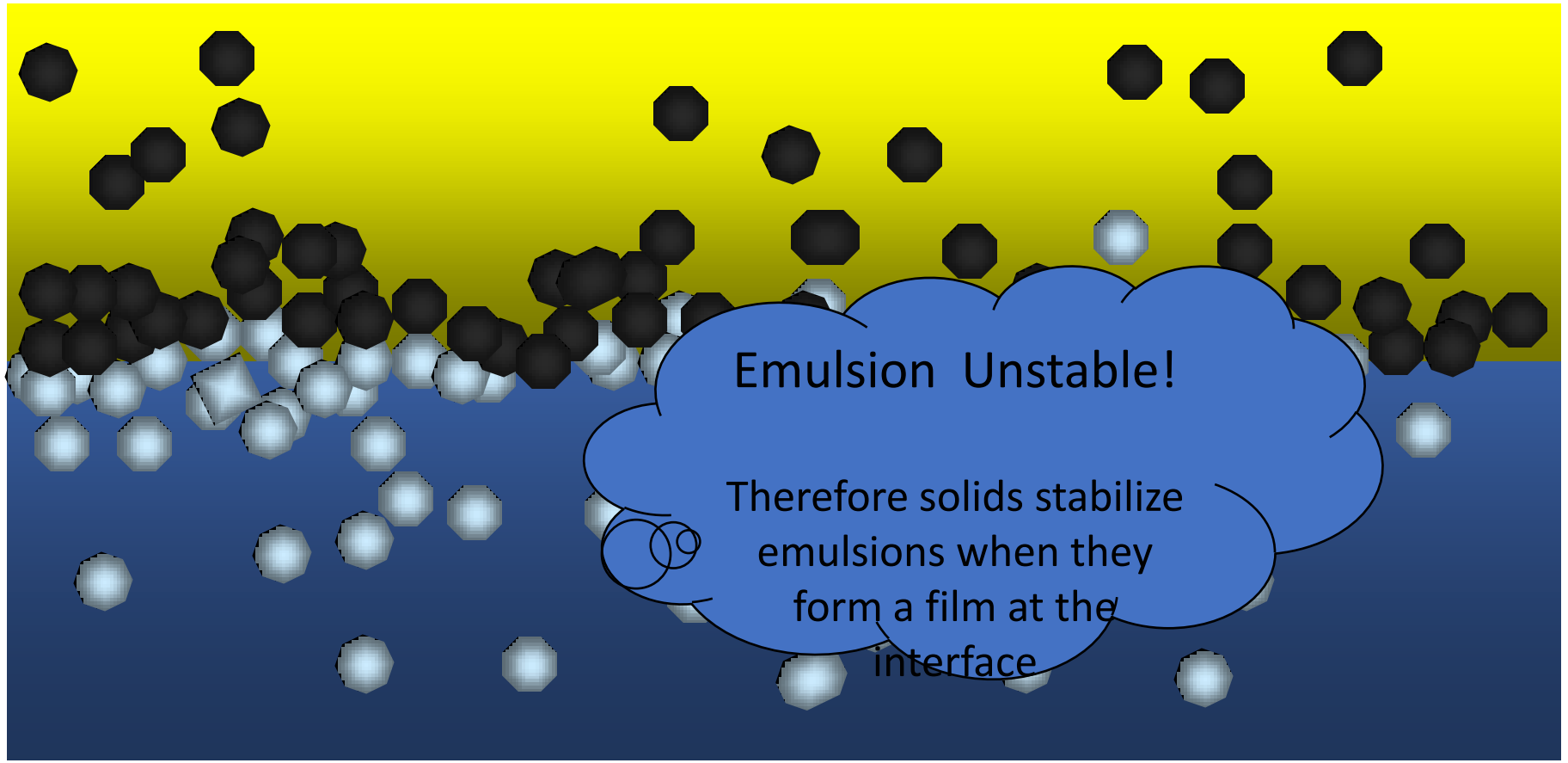

Briggs, T.R.; *Ind. Eng. Chem.;* **13,** (11), 1008, (1921)

Emulsion destabilized by crystals in the oil phase

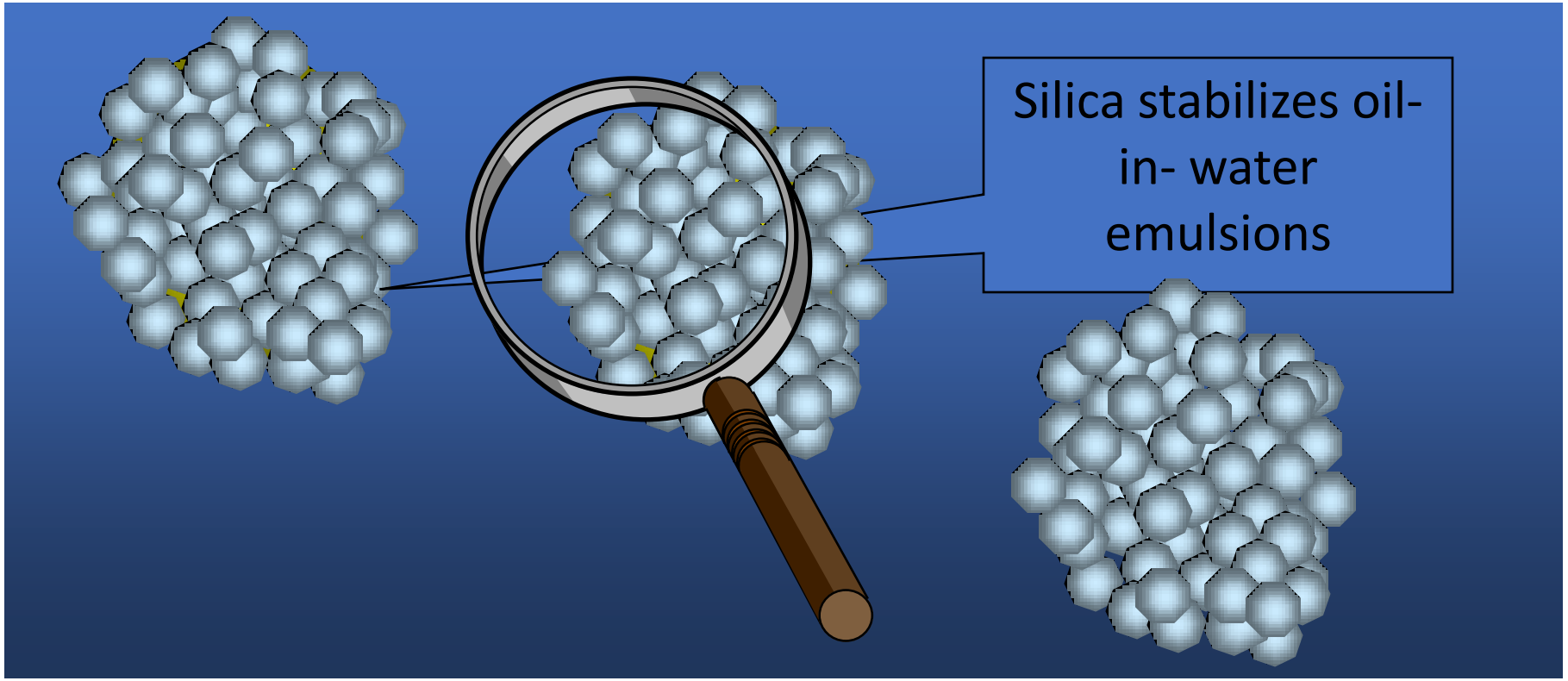

Van Boekel, M.A.; Walstra, P.; *Colloids Surf.,* **3,** 109, (1981)

Emulsion destabilized by crystals in the oil phase

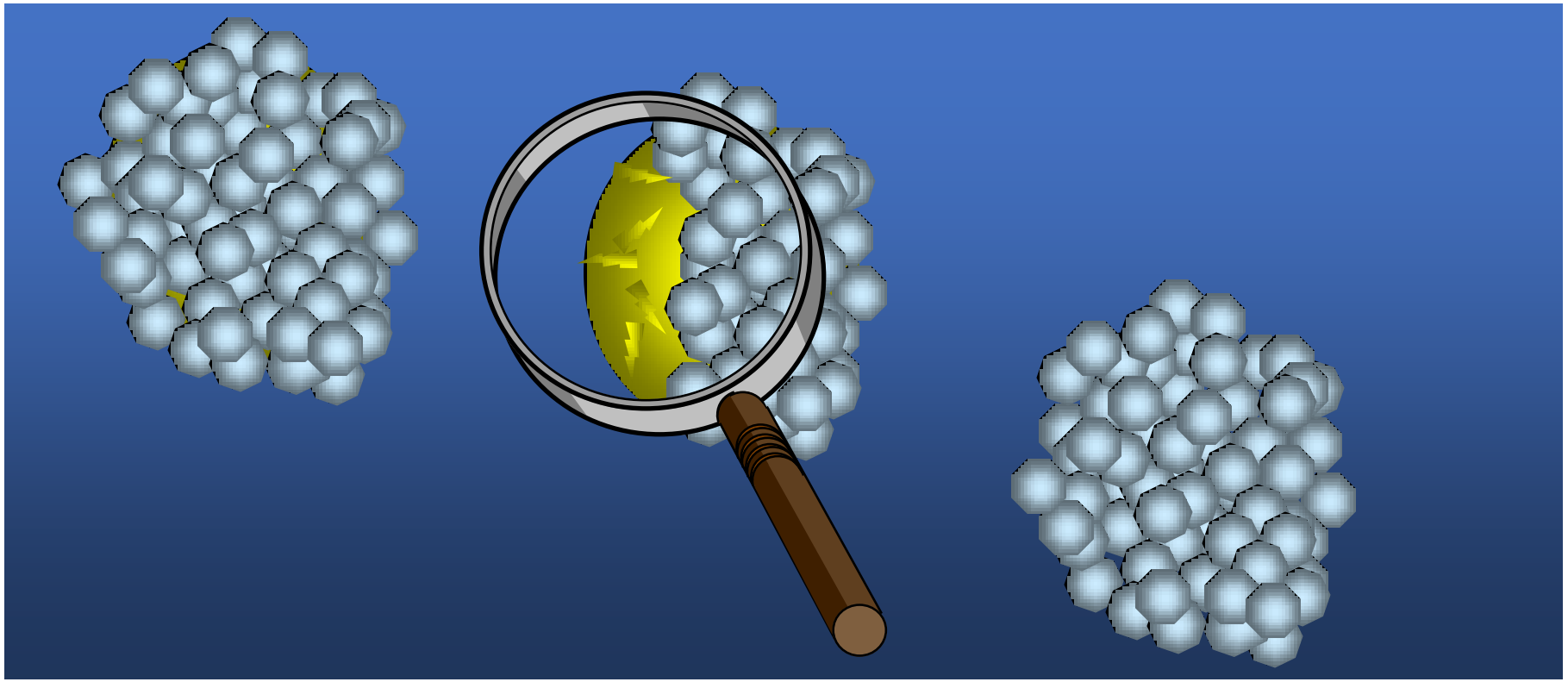

Van Boekel, M.A.; Walstra, P.; *Colloids Surf.,* **3,** 109, (1981)

Colloid -Stabilized Emulsions
Mixtures of C Black and Silica

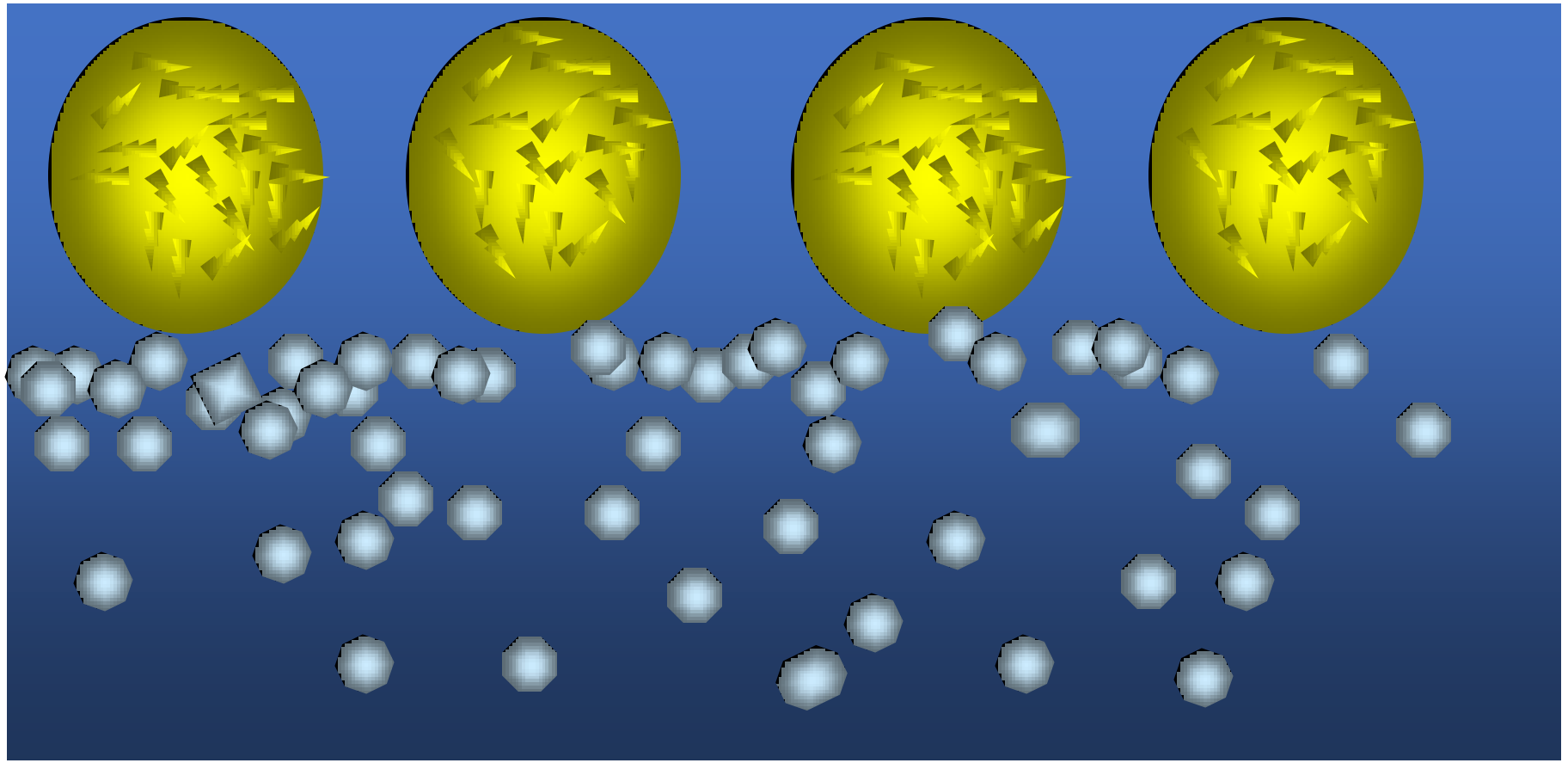

Van Boekel, M.A.; Walstra, P.; *Colloids Surf.,* **3,** 109, (1981)

Emulsion destabilized by crystals in the oil phase

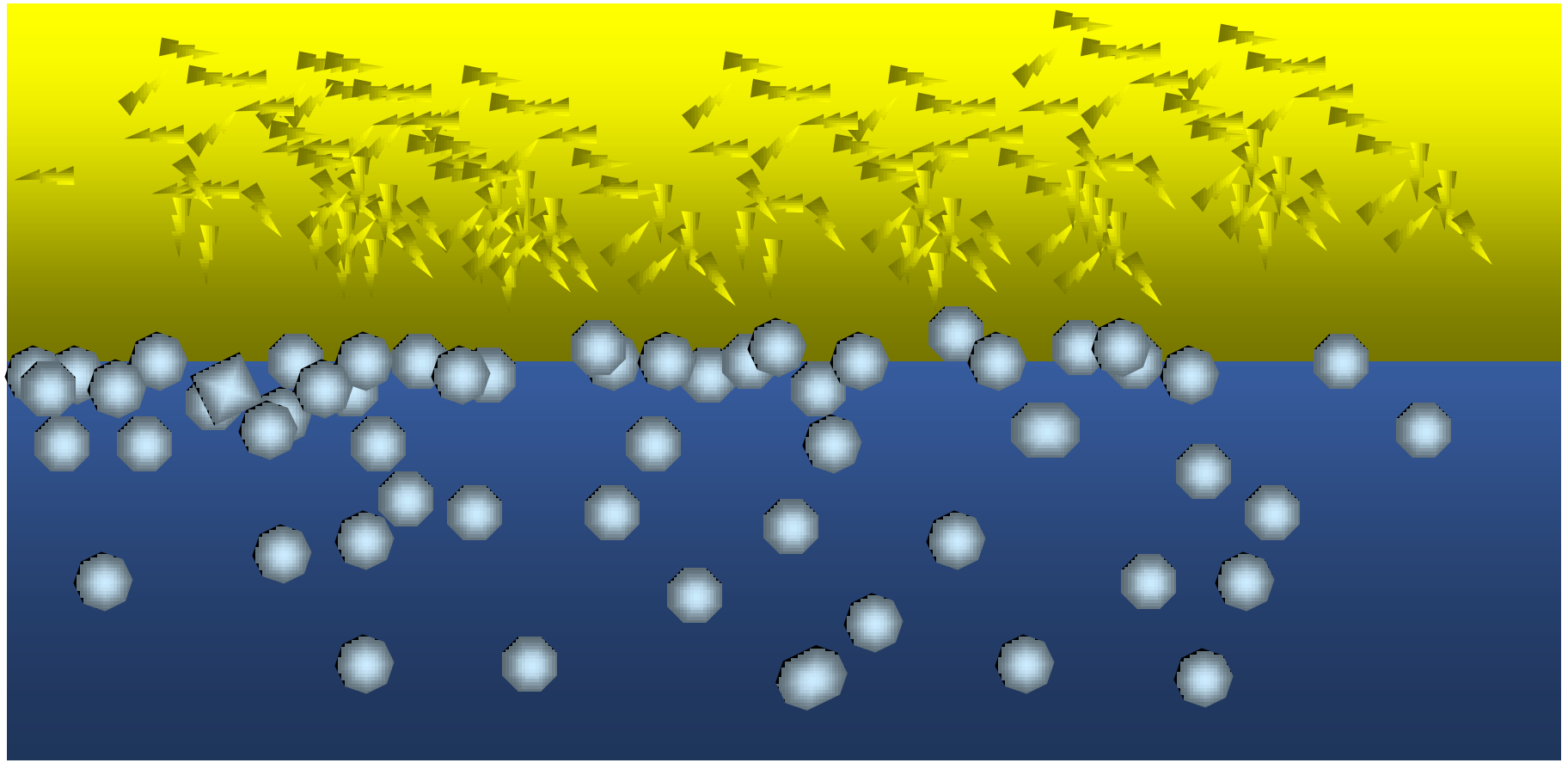

Van Boekel, M.A.; Walstra, P.; *Colloids Surf.,* **3,** 109, (1981)

Emulsion Stabilization with Powders

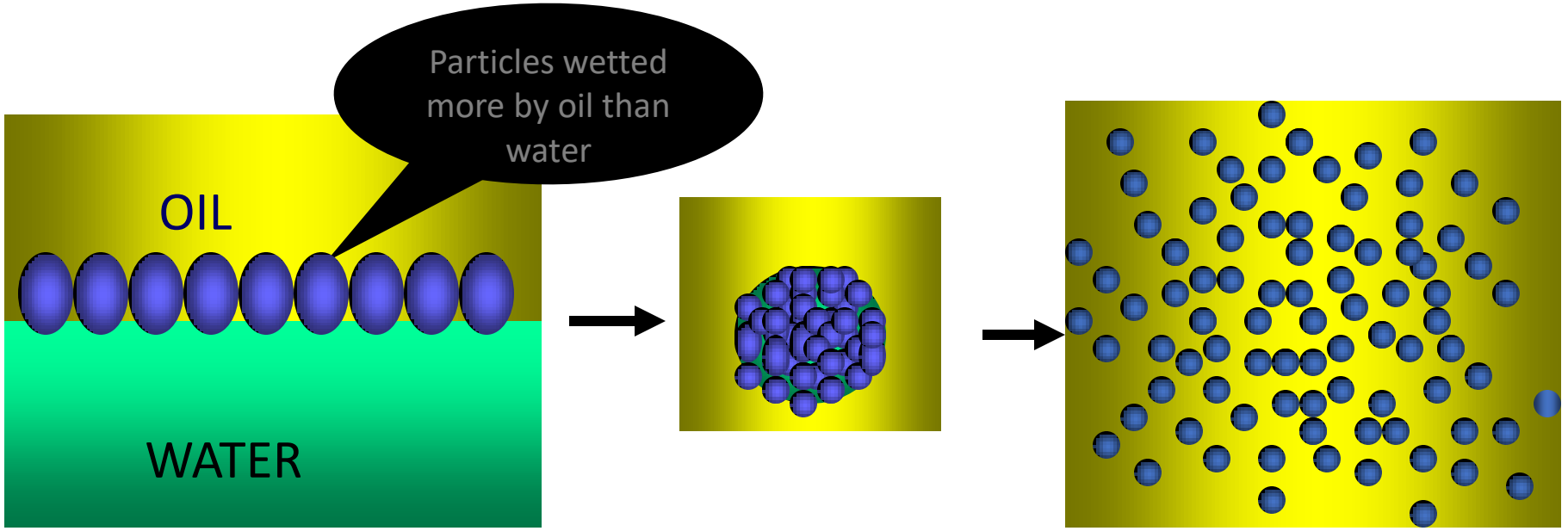

Water-in-oil emulsion

Finkle, Draper and Hildebrand, *J. Amer. Chem. Soc, (*1923), **45,** 2780

Summary

- A Brief (not all-inclusive) review of polymers in cosmetics
- Fixatives and Films
  - Hairsprays
  - Polymer Solution Physics
- Conditioning Polymers
- Gels and Rheology Modifiers
- Polymer-surfactant interaction

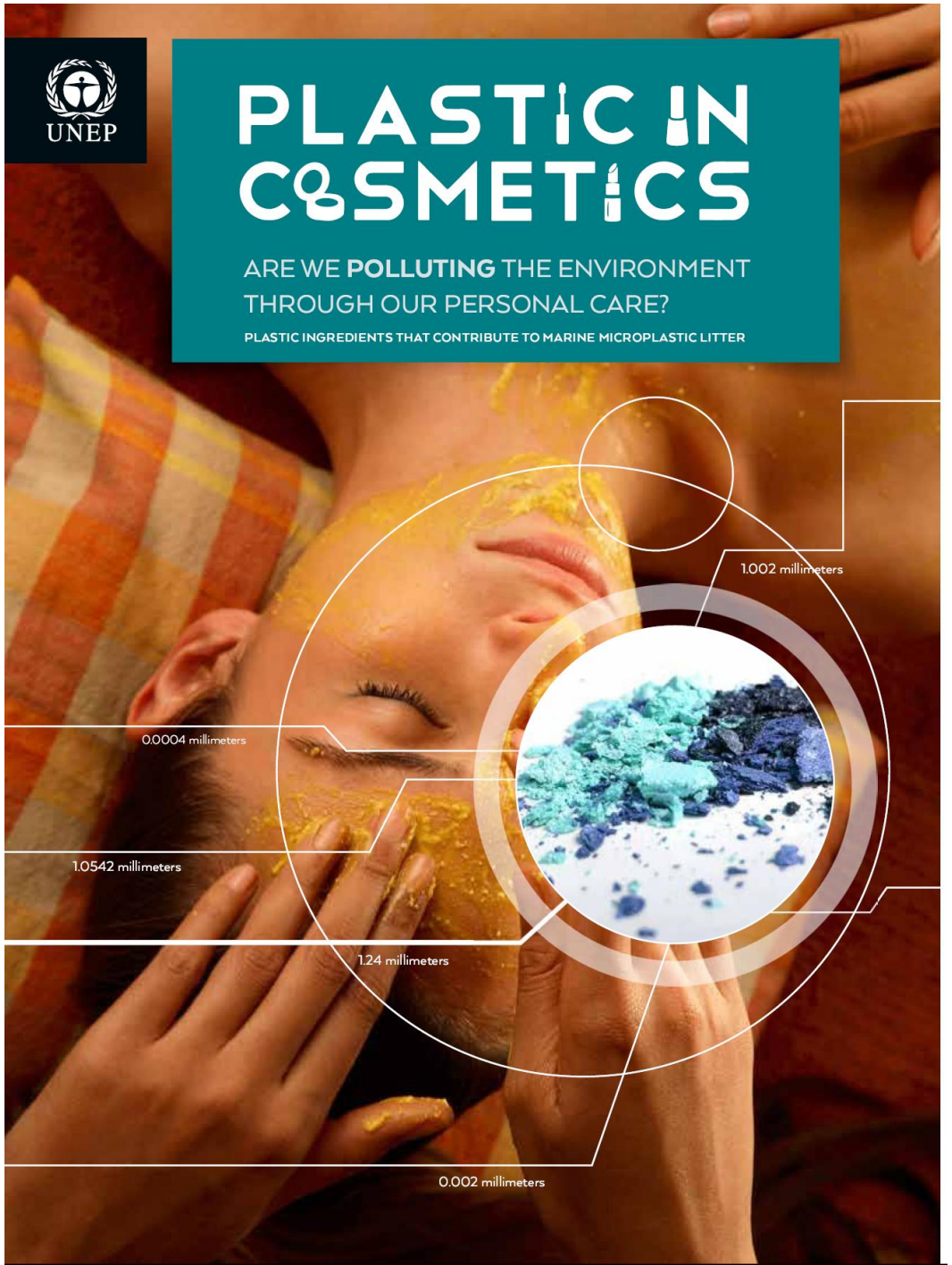

POLYMER	EXAMPLES OF FUNCTIONS IN PCCP FORMULATIONS
Nylon-12 (polyamide-12)	Bulking, viscosity controlling, opacifying (e.g. wrinkle creams)
Nylon-6	Bulking agent, viscosity controlling
Poly(butylene terephthalate)	Film formation, viscosity controlling
Poly(ethylene isoterephthalate)	Bulking agent
Poly(ethylene terephthalate)	Adhesive, film formation, hair fixative; viscosity controlling, aesthetic agent, (e.g. glitters in bubble bath, makeup)
Poly(methyl methylacrylate)	Sorbent for delivery of active ingredients
Poly(pentaerythrityl terephthalate)	Film formation
Poly(propylene terephthalate)	Emulsion stabilizing, skin conditioning
Polyethylene	Abrasive, film forming, viscosity controlling, binder for powders
Polypropylene	Bulking agent, viscosity increasing agent
Polystyrene	Film formation
Polytetrafluoroethylene (Teflon)	Bulking agent, slip modifier, binding agent, skin conditioner
Polyurethane	Film formation (e.g. facial masks, sunscreen, mascara)
Polyacrylate	Viscosity controlling
Acrylates copolymer	Binder, hair fixative, film formation, suspending agent
Allyl stearate/vinyl acetate copolymers	Film formation, hair fixative
Ethylene/propylene/styrene copolymer	Viscosity controlling
Ethylene/methylacrylate copolymer	Film formation
Ethylene/acrylate copolymer	Film formation in waterproof sunscreen, gellant (e.g. lipstick, stick products, hand creams)
Butylene/ethylene/styrene copolymer	Viscosity controlling
Styrene acrylates copolymer	Aesthetic, coloured microspheres (e.g. makeup)
Trimethylsiloxysilicate (silicone resin)	Film formation (e.g. colour cosmetics, skin care, sun care)

The #CleanSeas Campaign

UN Environment launch of the Clean Seas campaign in Bali, Indonesia.
Photo Credit: UN Environment/Shawn Heinrichs

U.N. INITIATIVE TO TRANSFORM,

- Habits, Practices, standards and policies
- TO CUT OFF WASTE PLASTIC STREAM FROM THE ENVIRONMENT

http://www.cleanseas.org/

UN environment

Exploring the potential for adopting alternative materials to reduce marine plastic litter

SOCIETY OF COSMETIC CHEMISTS


UNEP
BIODEGRADABLE
PLASTICS
& MARINE LITTER
MISCONCEPTIONS, CONCERNS AND IMPACTS
ON MARINE ENVIRONMENTS

Conclusions

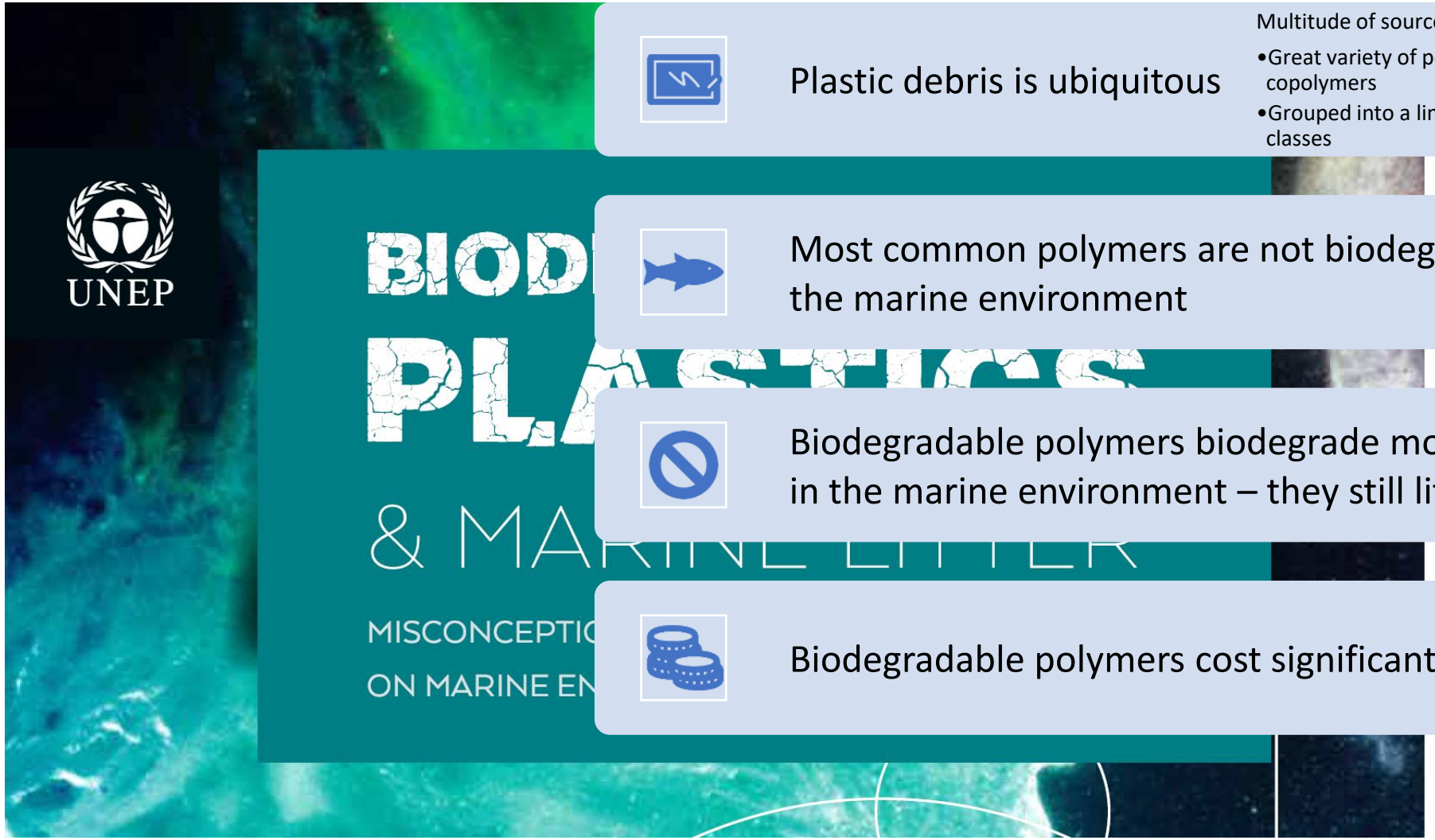

Plastic debris is ubiquitous

Multitude of sources

- Great variety of polymers and copolymers
- Grouped into a limited number of classes

Most common polymers are not biodegradable in the marine environment

Biodegradable polymers biodegrade more slowly in the marine environment – they still litter

Biodegradable polymers cost significantly more

Conclusions

- Oxo-degradable polymers add to microplastic in oceans
  - Fragment slowly in the environment
- Biodegradation claims are influenced by commercial rather than data supported
- The term ‘biodegradable’ induces public to litter more

Table 2.1 SWOT analysis (Strengths, Weaknesses, Opportunities and Threats) of conventional synthetic polymers.

S1. Improved human health outcomes from medical applications S2. Packaging reduces food wastage from field to market and market to consumer S3. Lower water and energy consumption in production S4. Novel applications where there are no equivalents S5. Lower fuel consumption in aviation and vehicular transport S6. Packaging reduces damage to goods during transport S7. Convenience to consumers, including for 'take-away' or 'fast-food' applications	W1. Utilises fossil fuels and is not carbon neutral W2. Risk to human health during production due to exposure to chemicals, including endocrine-disrupting chemicals W3. Risk to human health, social and economic well-being and the environment during use and end-of-life phases W4. Very limited biodegradation in the environment, especially in the ocean, leading to rapid accumulation W5. Waste management solutions are grossly inadequate in most countries W6. Circular production patterns are rarely implemented
O1. Development of new polymers and composites for diverse applications O2. Redesign of products to allow lower material use, product re-use and improved recycling potential, in a circular or closed-loop production cycle O3. Utilisation of intrinsically lower risk chemicals in production and as additives to maintain performance	T1. Continuing accumulation of plastics and microplastics in the environment T2. Long term consequences for human reproductive and developmental health T3. Long term consequences for social and economic well-being due to impact of plastic waste

PLASTICS ENTER THE OCEANS VIA RIVERS

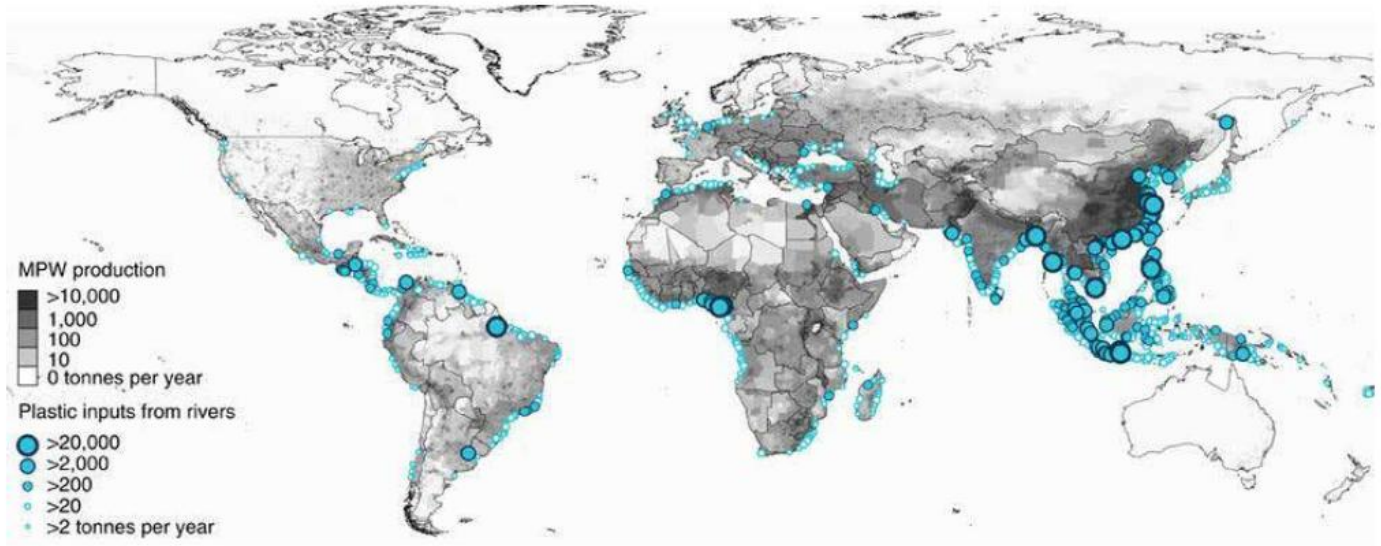

Figure 3.1 Estimated annual mass (tonnes) of plastic entering the oceans via rivers. River contributions are derived from individual watershed characteristics such as: population density (inhabitants km-2); per capita mismanaged plastic waste (MPW) production (kg d-1) and monthly averaged run-off (mm d-1). The model is calibrated against river plastic concentration measurements from Europe, Asia, North and South America (reproduced from Lebreton *et al.* 2017 under a Creative Commons Attribution 4.0 International License).

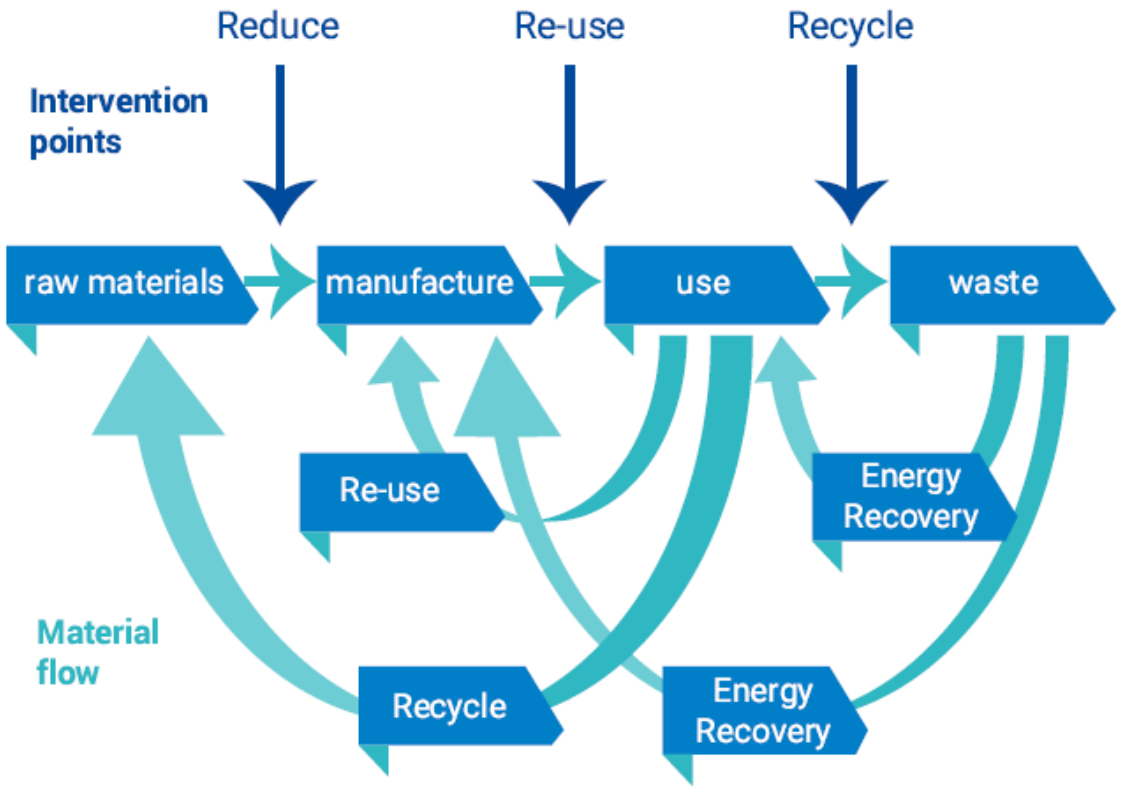
Reduce
Re-use
Recycle
Intervention points
raw materials
manufacture
use
waste
Re-use
Energy Recovery
Material flow
Recycle
Energy Recovery

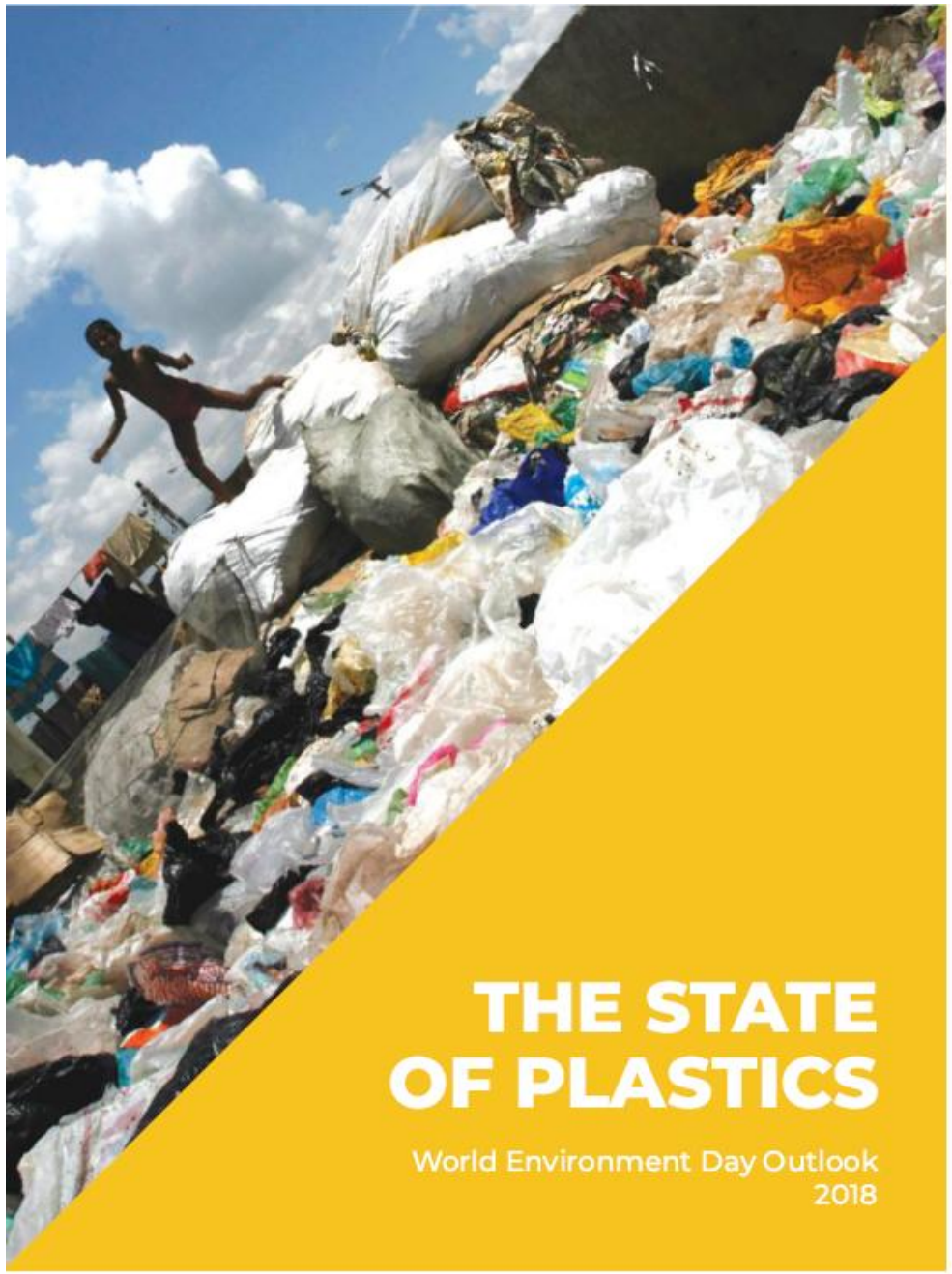

THE STATE OF PLASTICS

World Environment Day Outlook 2018

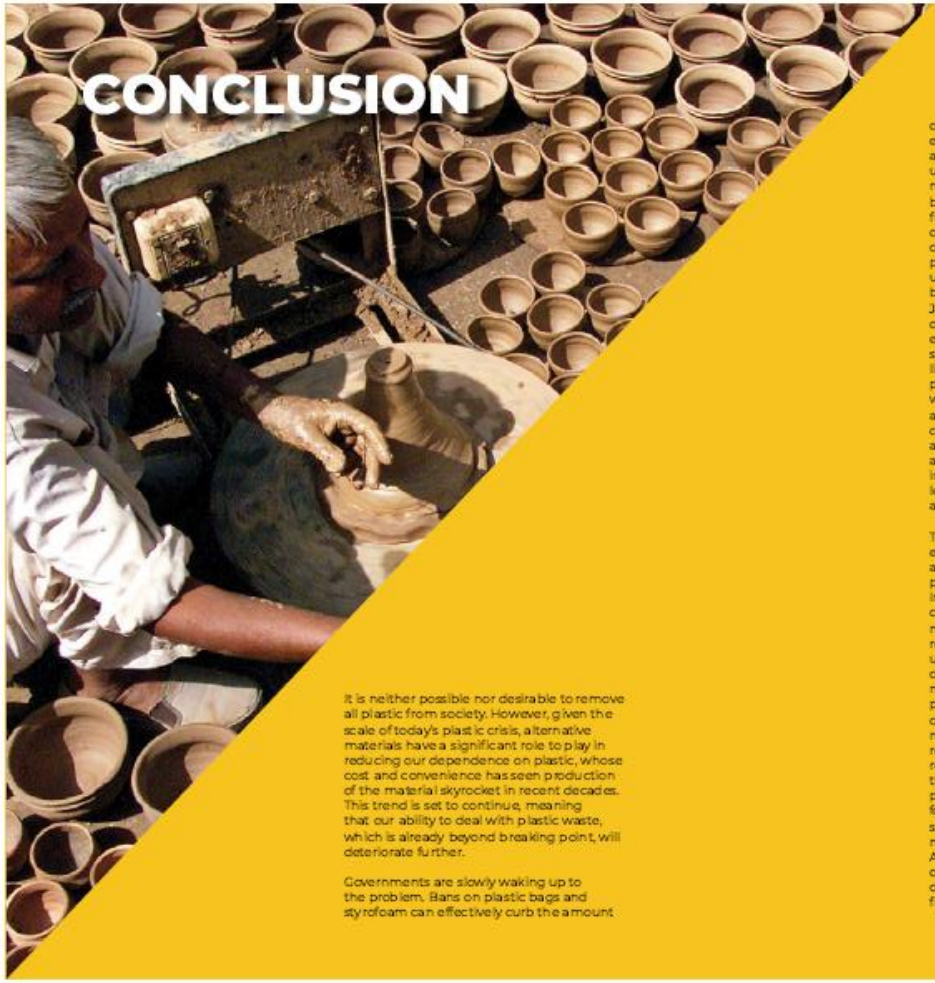

CONCLUSION

It is neither possible nor desirable to remove all plastic from society. However, given the scale of today's plastic crisis, alternative materials have a significant role to play in reducing our dependence on plastic, whose cost and convenience has seen production of the material skyrocket in recent decades. This trend is set to continue, meaning that our ability to deal with plastic waste, which is already beyond breaking point, will deteriorate further.

Governments are slowly waking up to the problem. Bans on plastic bags and styrofoam can effectively curb the amount of plastic waste dumped in our environment. They also create an incentive to promote the use of bags constructed from natural materials while providing businesses with an opportunity to fill the gap. But the enforcement of government regulations has often been poor. Single-use plastic bags continue to be widely used and mismanaged despite bans and levies. In contrast, in Japan, where no bans are in place on single-use plastic, a highly effective waste management system accounts for relatively limited leakages of single-use plastics in the environment. By working together with industries and consumers, governments can support the development and promotion of sustainable alternatives by building infrastructure, drawing up new legislation and funding research and development.

Transitioning to more environmentally suitable alternatives to conventional plastics will be a lengthy process. In the meantime, strengthening circular thinking and waste management systems will help reduce plastic pollution. The use of alternatives must be part of a broader strategy towards more sustainable production, particularly of packaging and other single-use items. This will mean redesigning products, reducing waste and improving recycling. We must also balance the aim of reducing plastic packaging waste with reducing food waste. Scaling up potential solutions to support a mass market remains a big barrier. Addressing issues like the supply of raw material, the availability of appropriate skills, access to financing, infrastructure and the level of current technology will be key. Businesses must take a close look at how their products are designed and disposed of as they seek to develop environmentally friendly products that are easier to recycle. They must be held to account for the impact their products have on the environment.

Biomass-based biopolymers such as PLA, PHA and TPS show great potential as alternatives, especially for packaging and other single-use items, provided they are used in closed loop-systems. But their promotion as a "greener" alternative is unjustified without industrial composting or anaerobic digestion facilities. They are not suitable for dispensing "fast food" in uncontrolled public spaces. Nor will the increasing use of PLA, PHA and TPS and similar biopolymers reduce the amount of plastic waste reaching the ocean or ending up in landfill. In addition, there is a risk that such polymers will contaminate recycling waste streams. The use of natural materials, either directly or as a biomass source, depends on prices in the agricultural and horticultural sectors. These can be highly variable and unpredictable. Building in flexibility in the selection of different materials will be an advantage.

Moving towards more closed-loop, carbon-neutral production cycles, including the use of industrial composting and anaerobic digestion, will demonstrate the beneficial use of waste, and should promote more effective waste management and wider acceptance among the public. Natural alternatives to conventional plastics, and the use of biomass-based biopolymers,

Journal of Cleaner Production 193 (2018) 491–505

Contents lists available at ScienceDirect

Journal of Cleaner Production

journal homepage: www.elsevier.com/locate/jclepro

Review

Food packaging in the circular economy: Overview of chemical safety aspects for commonly used materials

Birgit Geueke*, Ksenia Groh, Jane Muncke

Food Packaging Forum Foundation, Staffelstrasse 8, 8045 Zurich, Switzerland